AN INVESTIGATION INTO THE EFFECTS OF THE EPSTEIN-BARR VIRUS-ENCODED NUCLEAR PROTEIN, EBNA1, ON THE TGFβ AND BMP SIGNALLING PATHWAYS IN HUMAN EPITHELIAL CELLS

By

Kathryn Louise Date

A thesis submitted to The University of Birmingham

for the degree of

DOCTOR OF PHILOSOPHY

School of Cancer Sciences

College of Medical and Dental Sciences

The University of Birmingham

September 2011

ABSTRACT

In addition to its essential roles in the maintenance, replication and transcription of the EBV genome, EBNA1 has more recently been shown to influence the transcription of cellular genes and to modulate the activity of key cellular signalling pathways. EBNA1 has previously been shown to abrogate TGFβ signalling in carcinoma cell lines, although the exact mechanism remains to be elucidated. This study has endeavoured to further dissect this observation, whilst revealing a novel function for EBNA1 in the activation of the closely-related BMP signalling pathway. The observed abrogation of canonical TGFβ signalling is now proposed to be the result of an EBNA1-mediated induction of negative regulators, while a concomitant increase in secreted TGFβ, in combination with a shift towards linker region phosphorylation of the R-Smad proteins in EBNA1-expressing cells conceivably constitutes a method of promoting pro-tumourigenic TGFβ-mediated effects, such as cellular migration. In addition, results demonstrating the activation of BMP signalling upon the expression of EBNA1, and in EBV-positive cell lines, are also indicative of a role in the promotion of migration, and potentially metastasis. In this way, EBNA1 may mediate effects that contribute to the development of EBV-associated tumours.

ACKNOWLEDGEMENTS

I would like to gratefully acknowledge the Medical School Scientific Projects Committee for funding my research, and I would like to thank Professor Lawrence Young for giving me the opportunity to work within the group and for the intellectual support during the course of the project. I would also like to say a massive thank you to my supervisors, Dr. Christopher Dawson and Dr. John O'Neil, for your invaluable help, support and guidance. Thank you also to Dr. John Arrand for your guidance, particularly in the interpretation of the microarray data.

A big thank you to Sonia for all of the help and support in the lab, and a special thank you to Stephen and Tom, I couldn't have done without your support and advice, and I'll never forget all the laughs, and the mistakes!! Thanks also to Beckie for the help with the confocal microscopy, and to all past NPC group members for your support and encouragement; Mhairi, Lou, Khil, Jia, Haide, Rob, Olivia and Angela, it's been fantastic working with you all!

A massive thank you to Elisabeth, for sharing the joys of thesis writing with me, for always cheering me up and making me laugh, and for cider Tuesdays!! Thanks also to Imogen, Sam, Tom and Becky for making the office a fun place to be and for the epic Reflex visits! A huge thank you also to my lovely friends elsewhere in Cancer Studies for sharing all the ups and downs of PhD life, and for all the great memories!

Finally, an extra special thank you to my sister, Bex, for all your love and support, and my most important thank you to my parents; thank you for always being there and always believing in me, and for your unconditional love, support and encouragement. I am eternally grateful to you both, and I dedicate this thesis to you.

CONTENTS

Page

LIST OF FIGURES

Chapter 5

Page

LIST OF TABLES

Page

Chapter 1

Chapter 2

LIST OF ABBREVIATIONS

ActR	Activin receptor
AIDS	Acquired immunodeficiency disease
ALK	Activin receptor-like kinase
ATF2	Activating transcription factor 2
AP-1	Activator protein 1
BARTs	BamHIA Rightward Transcripts
BCR	B-cell receptor
bp	Base pairs
BL	Burkitt's lymphoma
BMP	Bone morphogenetic protein
BMPR	BMP receptor
BRE	BMP response element
Cav-1	Caveolin-1
CDK	Cyclin-dependent kinase
cDNA	Complementary DNA
CGH	Comparative genome hybridisation
ChIP	Chromatin immunoprecipitation
CHX	Cycloheximide
CMV	Cytomegalovirus
CR2	Complement receptor 2
CTAR	C-terminal activation region
CTL	Cytotoxic T-lymphocyte
Dab2	Disabled-2
DNA	Deoxyribonucleic acid
dnEBNA1	Dominant-negative EBNA1
DS	Dyad symmetry
EA	Early antigen
EBERs	Epstein-Barr virus encoded RNAs
EBNA	Epstein-Barr virus nuclear antigen
EBP2	EBNA1 binding protein 2
EBV	Epstein-Barr virus
EBVa-GC	EBV-associated gastric carcinoma
EEA1	Early endosomal antigen 1
EGFR	Epidermal growth factor receptor
EMSA	Electrophoretic mobility shift assay
EMT	Epithelial-mesenchymal transition
ENaC	Epithelial sodium channel
ERK	Extracellular signal-related kinase
FGF2	Fibroblast growth factor 2
FR	Family of repeats
GC	Gastric carcinoma
GDF	Growth and differentiation factor
GPCR	G-protein coupled receptor
GSK	Glycogen synthase kinase
HBV	Hepatitis B virus
HCV	Hepatitis C virus

HDAC	Histone deacetylase
HIV	Human immunodeficiency virus
HL	Hodgkin's lymphoma
HLA	Human leukocyte antigen
HNSCC	Head and neck squamous cell carcinoma
HPV	Human papilloma virus
HSV	Herpes simplex virus
HTLV-1	Human T-cell leukaemia virus
ICAM	Intracellular adhesion molecule
Id	Inhibitor of differentiation
IFN	Interferon
IHC	Immunohistochemistry
IKK	IkappaB kinase
IL	Interleukin
IM	Infectious mononucleosis
ISH	*In situ* hybridisation
ITG	Integrin
JAK	Janus activated kinase
JNK	c-Jun N-terminal kinase
kbp	Kilobase pairs
kDa	Kilodaltons
KSHV	Kaposi's sarcoma-associated herpesvirus
LANA	Latency-associated nuclear antigen
LCL	Lymphoblastoid cell line
LFA	Lymphocyte function-associated antigen
LMP	Latent membrane protein
MAPK	Mitogen-activated protein kinase
MEK	MAPK/ERK kinase
MFI	Mean fluorescence intensity
MH	Mad homology
MHC	Major histocompatibility complex
MLEC	Mink lung epithelial cell
miRNA	MicroRNA
mRNA	Messenger RNA
MMP	Matrix metalloproteinase
MTIIa	Metallothionein
NEDD4-2	Neural precursor cell-expressed developmentally down-regulated gene 4-2
NFκB	Nuclear factor kappa B
NLS	Nuclear localisation signal
NPC	Nasopharyngeal carcinoma
ORC	Origin recognition complex
ORF	Open reading frame
OriP	Origin of replication
OSCC	Oral squamous cell carcinoma
PAI-1	Plasminogen activator inhibitor 1
PCR	Polymerase chain reaction
PI3K	Phosphatidyl inositol 3-kinase

PPM1A	Protein phosphatase, Mg^{2+}/Mn^{2+} dependent, 1A
PPM1B	Protein phosphatase, Mg^{2+}/Mn^{2+} dependent, 1B
PRMT	Protein arginine methyltransferase
QPCR	Quantitative PCR
RASSF1A	Ras association domain family 1A
rEBV	Recombinant EBV
RNA	Ribonucleic acid
RNAi	RNA interference
RT-PCR	Reverse-transcriptase PCR
SARA	Smad anchor for receptor activation
SBE	Smad binding element
SCID	Severe combined immunodeficiency
SDS	Sodium dodecyl sulphate
SDS-PAGE	SDS-polyacrylamide gel electrophoresis
shRNA	Short hairpin RNA
STAT	Signal transduction and activator of transcription
SV40	Simian virus 40
TβR	TGFβ receptor
TGFβ	Transforming growth factor β
TIL	Tumour infiltrating lymphocytes
TLR	Toll-like receptor
TNF	Tumour necrosis factor
TRADD	TNF receptor associated death domain
TRAF	TNF receptor associated factor
TSA	Trichostatin A
TSG	Tumour suppressor gene
USP7	Ubiquitin specific protease 7
UTR	Untranslated region
VCA	Viral capsid antigen
wtEBNA	Wild-type EBNA1

CHAPTER 1

Introduction

1.1 The biology of cancer

Despite significant progress in the field of cancer research, cancer still remains a substantial health burden worldwide. Indeed an assessment of global cancer burden estimated that an overall 12.7 million new cancer cases and 7.6 million cancer deaths occurred in 2008 (Ferlay et al., 2010, Thun et al., 2010), which, by extrapolation, is projected to rise to almost 21.4 million new cases diagnosed annually and over 13.2 million cancer deaths in 2030.

An accumulating body of evidence defines cancer as a complex multistep process, predominantly reflecting genetic and epigenetic alterations that evolve to drive progressive cellular transformation. It has estimated that six major acquired capabilities collectively dictate the cancer phenotype; namely, self-sufficiency in growth signals, insensitivity to growth-inhibitory signals, evasion of apoptosis, limitless replicative potential, sustained angiogenesis, and tissue invasion and metastasis (Hanahan and Weinberg, 2000). Each constitutes a fundamental rate-limiting step during malignant development and their cooperative influence is required for complete malignant conversion.

1.2 Viruses and cancer

Globally, it is estimated that between 15-20% of all human cancers are aetiologically linked to viral infections (zur Hausen, 2001, Damania, 2006, Parkin, 2006, McLaughlin-Drubin and Munger, 2008, Kalland et al., 2009). The discovery of the first human tumour virus, Epstein-

Barr virus (EBV), in the 1960s laid the foundations for the identification of a number of viruses with oncogenic potential in humans (de Oliveira, 2007, Javier and Butel, 2008). The consistency of associations of a given virus with a specific cancer is found to range from approximately 15% to essentially 100% (Pagano et al., 2004, McLaughlin-Drubin and Munger, 2008). While several viruses have been unequivocally linked to the aetiology of certain human malignancies, for others only potential roles have been suggested, as is summarised in Table 1.1, adapted from (McLaughlin-Drubin and Munger, 2008)

Table 1.1: Human tumour viruses and viruses implicated in human cancers

Virus	Viral taxonomy	Genome	Human Cancers
HUMAN ONCOGENIC VIRUSES			
Human T-cell leukaemia virus (HTLV-1)	*Retroviridae*	dsRNA	Adult T-cell leukaemia
Hepatitis C virus (HCV)	*Flaviviridae*	dsRNA	Hepatocellular carcinoma
Human papillomavirus (HPV) (high-risk types)	*Papillomaviridae*	dsDNA	Cervical, head and neck, and other anogenital cancers
Hepatitis B virus (HBV)	*Hepadnaviridae*	Partially dsDNA	Hepatocellular carcinoma
Epstein-Barr virus (EBV)	*Herpesviridae*	dsDNA	Burkitt's lymphoma, nasopharyngeal carcinoma, HL, PTL, GC, NK/T-cell lymphoma
Kaposi's sarcoma herpesvirus (KSHV)	*Herpesviridae*	dsDNA	Kaposi's sarcoma, primary effusion lymphoma, Castleman's disease
VIRUSES IMPLICATED IN HUMAN CANCERS			
Simian virus 40 (SV40)	*Polyomaviridae*	dsDNA	Mesothelioma, osteosarcoma, non-Hodgkin lymphoma, brain?
JC virus (JCV)	*Polyomaviridae*	dsDNA	Brain?
BK virus (BKV)	*Polyomaviridae*	dsDNA	Prostate?
Human endogenous retroviruses (HERVs)	*Retroviridae*	dsRNA/DNA?	Germ cell tumours, breast, lymphoproliferative disease, ovarian, melanoma, prostate?
Human mammary tumour virus (HMTV)	*Retroviridae*	dsRNA/DNA?	Breast?
Xenotropic murine leukaemia virus-related virus (XMRV)	*Retroviridae*	ssRNA	Prostate?
Torque teno virus (TTV)	*Circoviridae*	ssDNA	Gastrointestinal, lung, breast, myeloma?

Although many oncogenic viruses are ubiquitous within the human population (zur Hausen, 2001), others display more localised distributions. As obligate intracellular parasites, oncogenic viruses have evolved strategies to exploit existing host cellular mechanisms to

establish infection and persist within the infected host. The frequency with which infected individuals progress to develop cancer is reasonably low (Butel, 2000, zur Hausen, 2001, Kalland et al., 2009), and there is usually a long latency period between primary infection and tumour development. Further criteria to establish such a link between viral infection and cancer include serological evidence of prior infection, and persistence of the virus in all tumour cells, epidemiological plausibility of the association, virus-induced target cell transformation *in vitro*, and virus-induced tumours in a suitable experimental host (zur Hausen, 2001, Pagano et al., 2004). It is now widely accepted that viruses act as tumour-promoting factors rather than the sole initiators of cancer development (Butel, 2000, Javier and Butel, 2008). In consequence, carcinogenesis is defined by the cooperative influence of multiple events, with viruses constituting one link in the chain.

1.3 Epstein-Barr Virus

In 1958, Denis Burkitt described the occurrence of multifocal jaw tumours afflicting children in equatorial Africa, that were subsequently named Burkitt's lymphomas (BL) (Burkitt, 1958). The climatic and geographical distribution, coincident with the prevalence of holoendemic malaria, led to the suggestion that an infectious agent transmitted by an arthropod vector might be the aetiological agent responsible for BL (Burkitt, 1962). Following this, Epstein, Achong and Barr succeeded in culturing lymphoma cells from a primary BL tumour biopsy, in which they identified actively replicating herpesvirus-like particles by electron microscopy (Epstein et al., 1964) The virus was subsequently shown to be antigenically and biologically distinct from previously characterised herpesviruses, and was thus named Epstein-Barr virus (EBV). Using serology-based techniques, Henle and co-workers then established a causal association between primary EBV infection and infectious

mononucleosis (Henle et al., 1968) and later, again using serology-based assays, identified a link between EBV and the epithelial malignancy, nasopharyngeal carcinoma (NPC) (zur Hausen et al., 1970). These founding observations led to the classification of EBV as the first candidate human tumour virus.

EBV has been classified as a lymphocryptovirus (γ-1 herpesvirus), and its ubiquitous nature has been demonstrated by seroepidemiological studies revealing infection of over 90% of the world population (Rickinson and Kieff, 2007). As a member of the *Gammaherpesvirinae* subfamily, it displays a narrow host range for efficient EBV infection, which is restricted to primary B lymphocytes and oral epithelial cells (Roizman and Baines, 1991, Kieff and Rickinson, 2007, Pellett and Roizman, 2007). Like other human herpesviruses, EBV has the ability to persist for the lifetime of the infected host (Roizman and Baines, 1991, Rickinson and Kieff, 2007). Indeed, in the early stages of research, EBV was proposed to possess a "passenger" role in infected cells (Epstein et al., 1964), replicating in synchrony with the host cells of infected carriers. In this way, EBV has demonstrated remarkable success in persistence in the human population and efficient spread to naïve individuals.

The γ-herpesviruses are distinguished from other herpesvirus families by their unique ability to transform resting B lymphocytes into continuously proliferating lymphoblastoid cell lines (LCLs) *in vitro* (Decker et al., 1996, Young and Rickinson, 2004). This observation has proven crucially important in confirming the oncogenic potential of EBV and its ability to induce neoplastic disease in the natural or experimental host (Damania, 2004, Kieff and Rickinson, 2007).

1.3.1 EBV genome

The EBV genome is a linear, double-stranded 172kbp DNA, depicted in Figure 1.1A, coding for around 90 ORFs (Kieff and Rickinson, 2007), which circularises on release from the EBV capsid into the host nucleus (Pellett and Roizman, 2007) via fusion of terminal repeat sequences to form a covalently closed episome, the preferred conformation for persistence (Adams and Lindahl, 1975, Kintner and Sugden, 1979, Raab-Traub and Flynn, 1986). The linear form of EBV DNA has variable numbers of these direct tandem 0.5kbp repeats at each terminus, as well as 3kbp internal repeat sequences which in combination serve to effectively divide the genome into unique long and short regions (Hayward et al., 1980). The prototype EBV strain B95-8 was the first human herpesvirus genome to be fully cloned and sequenced (Baer et al., 1984), and regions of the EBV genome were thus designated by their position on a *Bam*HI restriction endonuclease map (Murray and Young, 2001) (Figure 1.1B).

1.3.2 EBV evolution in the human host

Variation between natural EBV isolates has been identified, resulting in classification of EBV strains into two main sub-types, type 1 (EBV1) (prototype B95-8) and type 2 (EBV2) (prototype AG876), principally governed by the identity of the EBNA2 protein, but additionally by observed divergence in linked polymorphisms at EBNA3A, 3B and 3C gene loci (Young et al., 1987, Rowe et al., 1989, Sample et al., 1990, Chang et al., 2009). Type 1 isolates demonstrate a more competent *in vitro* B-cell transformation ability, thought to be primarily mediated by the antigenically distinct EBNA2 proteins (82-87kDa and 75kDa for types 1 and 2, respectively) (Rickinson et al., 1987, Cohen et al., 1989), and postulated to be attributed to the differing abilities of the EBNA2 proteins to induce LMP1, as well as differential induction of a small set of cellular genes (Lucchesi et al., 2008).

(FIGURE 1.1)

Virus isolation and seroepidemiological studies suggest that, while EBV1 is the more prevalent type detected in China and in Western countries, both types are relatively common in equatorial Africa and New Guinea (Rickinson et al., 1987, Young et al., 1987, Sixbey et al., 1989, Young et al., 2000). This more competitive survival of type 2 isolates could potentially be attributed to the depressed T-cell function and intense polyclonal B-cell stimulation that characterises patients in malaria-endemic areas (Sixbey et al., 1989). In this regard, increased rates of type 2 infection have been observed in immunodeficient hosts, and a positive correlation has been drawn with HIV seropositivity (Sixbey et al., 1989, van Baarle et al., 2000). Furthermore, studies have reported the high prevalence of co-infection of multiple distinct EBV strains in healthy viral carriers (Srivastava et al., 2000), as well as in a variety of EBV-associated diseases (Tierney et al., 2006, Chang et al., 2009, Santón et al., 2011), yet the number initially acquired during primary infection is undetermined.

1.4 EBV biology

1.4.1 EBV infection *in vitro* and *in vivo*

The lymphotropic nature of EBV is dictated by the restricted expression of the major EBV receptor, CD21/complement receptor 2 (CR2), which binds the viral envelope glycoprotein gp350 (Nemerow et al., 1987). Following this interaction, gp42, as an integral part of a trimolecular complex with gp85 and gp25 fusion proteins, acts as a ligand to bind human leukocyte antigen (HLA) class II molecules as co-receptors to initiate virus-cell fusion and permit viral entry (Borza and Hutt-Fletcher, 2002, Chesnokova et al., 2009).

EBV displays dual tropism, being capable of infecting epithelial cells in addition to B lymphocytes. While EBV is rarely detected in oropharyngeal epithelial cells in healthy

individuals (Borza and Hutt-Fletcher, 2002), the occurrence of epithelial cell infection *in vivo* is indisputable, as evidenced by its presence in the epithelial lesions of oral hairy leukoplakia, and in the EBV-associated epithelial tumour, NPC. However, the mechanism by which EBV gains access to epithelial cells remains somewhat elusive. To date, epithelial cells have proven largely resistant to infection with cell-free virus *in vitro*, likely due to the absence of CD21/CR2 on cultured epithelial cells. Previously, moderate success was achieved in epithelial cells by transient transfection of the CR2 receptor and co-culturing with the virus-producing Akata B-cell line (Li et al., 1992, Imai et al., 1998). However recent studies have demonstrated the more efficient delivery of virus to epithelial cells *in vitro* using EBV-coated resting B cells as transfer vehicles (Shannon-Lowe et al., 2006, Shannon-Lowe et al., 2009), indicating that epithelial cell infection *in vivo* may potentially occur as a result of being in close proximity with infected B cells.

1.4.2 EBV primary infection

Primary infection with EBV usually occurs during childhood and is generally asymptomatic; however, if infection is delayed until adolescence or later, as is more common in the Western world, it may provoke a self-limiting proliferative disease, infectious mononucleosis (IM) (Rickinson and Kieff, 2007). IM is initially characterised by B-cell activation, with a subset a virus-carrying cells found to express the latency III growth programme (Tierney et al., 1994, Niedobitek et al., 1997, Al Tabaa et al., 2011). However, a significant feature is the massive expansion of CD8+ T cell numbers in the blood (Rickinson and Kieff, 2007), thought to be an antigen-induced response that subsequently controls the unlimited growth potential of EBV-infected B lymphocytes (Klein et al., 1981, Robinson, 1982). Acute IM is therefore typified by significant lymphocytosis (Young and Rickinson, 2004). Regular high-titre virus shedding

into saliva is also consistently observed, believed to derive from differentiating plasma cells (Niedobitek et al., 1997).

1.4.3 EBV persistence

The frequency of EBV-infected B cells in the peripheral blood of healthy persistently infected carriers ranges from 1-50 per 10^6 B cells and remains relatively stable for each individual over long periods of time (Miyashita et al., 1995, Khan et al., 1996, Küppers, 2003). EBV establishment of persistent infection in B cells has been more clearly defined, owing to the ease of establishment of LCLs as a suitable *in vitro* model, and has been reviewed in (Thorley-Lawson and Gross, 2004).

Upon initial infection, the virus infects naïve B lymphocytes, which undergo transient activation and proliferation, so as to rapidly expand the pool of EBV-infected cells. This expansion is stimulated through induction of the EBV "growth programme", or latency III pattern of gene expression, where EBV-infected cells express the complete complement of latent viral proteins and RNAs (Masucci and Ernberg, 1994, Miyashita et al., 1997, Thorley-Lawson et al., 1996). Similarly, *in vitro*, LCLs mimic the growth-transformed cells known to arise during the initial stages of EBV infection *in vivo*, and constitutively express the full complement of latent genes.

After the initial replication phase, the primary objective of the virus is to gain access to a suitable niche in which to establish latency. According to the most current model, EBV is believed to persist within the resting memory B cell compartment in healthy individuals (Thorley-Lawson et al., 1996, Miyashita et al., 1997). The exact means by which this is

accomplished *in vivo* remains one of the major unanswered questions to date; however, it is believed to revolve around the ability of EBV to exploit the innate B-cell differentiation programme to first and foremost establish infection, then to advance the progression into the memory compartment, from which it can persist and replicate (reviewed in (Thorley-Lawson, 2001)).

The virus is able to selectively express its different latency programmes in accordance with B-cell differentiation status in order to transit through the B-cell system (Babcock et al., 2000). The initial activation of B cells by the growth programme is necessary to induce differentiation (Babcock et al., 2000); however, immunodominant proteins must then be silenced for successful evasion of EBV-specific cytotoxic T-lymphocytes (CTLs). Viral latent gene expression is therefore progressively down-regulated. This is believed to be specifically driven by the actual process of B-cell differentiation, as direct infection of germinal centre and tonsillar memory B cells also gives rise to the classical growth programme of gene expression (Babcock et al., 2000). Latently infected B cells detected within the germinal centre express the default latency programme (see section 1.4.4) as an intermediary step in transit towards the memory compartment (Roughan and Thorley-Lawson, 2009), switching off EBNA2 to allow differentiation to a germinal centre B-cell phenotype, and retaining expression of LMP1 and LMP2 to provide constitutive, ligand-independent surrogate CD40 and BCR signals, respectively, for B-cell proliferation and survival (Thorley-Lawson, 2001).

On reaching the memory compartment, the virus adopts the most stringently restricted gene expression programme, termed Latency 0, advantageous for latent persistence. EBV-infected peripheral memory B cells are largely silent in terms of latent gene expression (Babcock et al.,

2000), and are therefore not subject to elimination through immunosurveillance. A possible exception is the occasional detection of LMP2A, perhaps to protect against lytic reactivation, while periodic expression of EBNA1 in dividing cells is thought to be required as a homeostatic mechanism in periods of proliferation to replenish the infected cell pool and maintain a constant frequency (Khan et al., 1996). From this memory cell reservoir, cells are periodically subject to reactivation, allowing virus shedding into saliva for transmission to new hosts.

1.4.4 EBV latency programmes

In common with other members of the herpesvirus family, EBV displays a biphasic life cycle *in vivo* with both latent and lytic elements. As a general rule, it establishes long-term latency in the B-lymphocyte compartment, whilst it is capable of replicating in both B lymphocytes and epithelial cells (Kieff and Rickinson, 2007). However, the establishment of latent infection in epithelial cells has also been described in EBV-associated epithelial malignancies. Extensive analysis of EBV-associated malignancies and a number of EBV-infected cell lines, has led to the characterisation of different forms of EBV latency, each one defined by a distinct subset of viral gene expression.

Latency 0 is proposed to occur in peripheral resting memory B cells so as to permit viral persistence. As such, while the viral genome is retained, only EBER and BART RNAs are detected, with a characteristic absence of viral proteins, except perhaps LMP2A and occasionally EBNA1. The latency state described in Burkitt's lymphoma is termed latency I, limited to the EBER and BART RNAs, and selective expression of EBNA1 from the Qp promoter. Latency II, also referred to as the default programme, was initially identified in

nasopharyngeal carcinoma (Brooks et al., 1992), and has also been described in Hodgkin's disease and certain EBV-positive T cell lymphomas. It is characterised by expression of Qp-driven EBNA1, LMP1, LMP2, and the EBER and BART RNAs. The latency III, or growth programme, as exemplified *in vitro* by LCLs, can also be observed in post-transplant lymphoproliferative disorders. This includes expression of the full spectrum of EBNAs and LMPs, as well as the EBER and BART RNAs.

Due to the dynamic nature of latent gene expression throughout the life cycle of the virus, it is not uncommon to observe deviations from these classifications. For example, established BL tumour cell lines have been reported to drift to a latency III pattern upon serial passage *in vitro*, with concomitant development to a LCL-like cell surface phenotype (Rowe et al., 1992, Young et al., 2000). Furthermore, an atypical "Wp-restricted" form of latency has been described in a subset of BL tumours, in which most EBNAs are additionally expressed with the exception of EBNA2 due to gene deletion (Kelly et al., 2002).

1.4.5 Lytic cycle

Latently infected B lymphocytes in the peripheral blood of healthy carriers are susceptible to local periodic reactivation when recirculating through oropharyngeal sites. This produces new infectious virus progeny, which are shed into saliva, in order to facilitate efficient propagation via oral transmission to naïve individuals (Kieff and Rickinson, 2007). In the viral productive cycle, the EBV genome is amplified more than 100-fold (Tsurumi et al., 2005), and the epithelium is proposed to serve as an important site for virus amplification prior to shedding (Hadinoto et al., 2009).

Lytic cycle is orchestrated by the simultaneous expression of two immediate-early (α) genes, BZLF1 and BRLF1, which encode the transcription factors, Zta and Rta respectively (Feederle et al., 2000). These act as essential transactivators of viral DNA replication, which trigger a cascade of events involving the temporal expression of early (β) genes, with important roles in viral DNA replication and nucleotide metabolism, followed by late (γ) genes, which support viral DNA amplification and encode viral structural components, and whose expression is either augmented by, or totally dependent on, the onset of viral DNA synthesis (Pellett and Roizman, 2007).

The exact trigger for lytic replication is not fully understood; however, it is believed to be linked to a differentiation-dependent phenomenon. Indeed in B lymphocytes it can be initiated *in vivo* by the differentiation of memory cells into plasma cells (Laichalk and Thorley-Lawson, 2005), while lytic cycle activity *in vitro* in a human keratinocyte line, SCC12F, was found to be substantially increased upon induction of epithelial terminal differentiation (Karimi et al., 1995).

Full virus replication can be observed *in vivo* in oral hairy leukoplakia (OHL), a benign hyperproliferative lesion found principally on the lateral borders of the tongue, characterised by high-level EBV replication. It is associated with immunosuppression, and observed in AIDS patients, or occasionally in post-renal transplant patients (Friedman-Kien, 1986, Greenspan et al., 1984, Lopes et al., 2003). In accordance with observations *in vitro*, *in situ* hybridisation (ISH) for EBV DNA indicates replication is restricted to the upper, more differentiated epithelial layers of the tongue (Niedobitek et al., 1991) and a differentiation-associated pattern of BZLF1 expression is observed (Young et al., 1991).

1.5 EBV latent proteins

1.5.1 EBNA1

1.5.1.1 Structure of the EBNA1 protein

The prototypical B95-8 EBV nuclear antigen 1 (EBNA1) protein is a 641 amino acid nuclear phosphoprotein (Hearing and Levine, 1985) (Figure 1.2A). Its N-terminal region is inclusive of a glycine-alanine repeat sequence between residues 90 and 325, seen to be somewhat heterogeneous between different EBV isolates (Fischer et al., 1997). This glycine-alanine repeat domain is considered to be dispensable for the maintenance of a stable latent infection and, by default, the replication, transactivation and segregation functions of EBNA1 (Yates et al., 1985, Lee et al., 1999, Ceccarelli and Frappier, 2000). For a long time, EBNA1 was believed to utilise this domain to bestow reduced immunogenicity, as a unique means of evading recognition by CD8+ T lymphocytes through inhibition of endogenous processing and presentation through the MHC class I pathway (Levitskaya et al., 1997, Blake et al., 1997). More recently, its effects have been attributed to its capacity to retard its own mRNA translation (Yin et al., 2003, Tellam et al., 2008, Apcher et al., 2009, Apcher et al., 2010), as a means of reducing the frequency of production of EBNA1-derived defective ribosomal products (DriPs) (Lee et al., 2004), considered the major source of T-cell epitopes for CD8+ T-cell recognition (Voo et al., 2004).

Ambinder and colleagues identified a nuclear localisation signal (NLS), Leu-Lys-Arg-Pro-Arg-Ser-Pro-Ser-Ser, located between amino acids 379 and 386 (Ambinder et al., 1990), and of paramount importance in directing EBNA1 to the nucleus. Additionally, yeast two-hybrid screening identified an *in vitro* interaction of EBNA1 with the nuclear transporter, importin

(FIGURE 1.2)

α/Rch1 (Fischer et al., 1997, Kim et al., 1997, Ito et al., 2000), which is also likely to be important.

The EBNA1 protein lacks intrinsic enzymatic activity (Frappier and O'Donnell, 1991) and so exerts its key functions as a site-specific DNA binding protein, displaying an active dimeric conformation (Ambinder et al., 1991). In order to effectively accomplish this demand, the C-terminal region of the protein encompasses a DNA binding and dimerisation domain located within the C-terminal between amino acids 459 and 607, responsible for binding to target recognition sequences (Ceccarelli and Frappier, 2000). The ability of EBNA1 to bind to RNA through arg-gly-gly (RGG) motifs has also been characterised (Snudden et al., 1994, Lu et al., 2004), highlighting a potential involvement in the formation of ribonucleoprotein complexes *in vivo*.

1.5.1.2 Transcription of EBNA1

EBNA1 transcription in EBV-infected cells is driven from three different viral promoters, termed Cp/Wp, Qp and Fp, located in the *Bam*HI-C, *Bam*HI-Q, and *Bam*HI-F regions of the viral genome respectively (Kieff and Rickinson, 2007). Alternative promoter usage is important in the establishment of different latency programmes and lytic cycle in EBV-infected lymphocytes (Chen et al., 1999).

Upon initial infection of B cells, the constitutively active Wp promoter drives EBNA expression. This function is then assumed by the Cp promoter (Schlager et al., 1996), which is subsequently used as the promoter of choice to drive EBNA transcription as part of the latency III programme, as is typified in infectious mononucleosis and in LCLs (Schlager et

al., 1996, Chen et al., 1999). In this setting, EBNA1 is transcribed as part of a polycistronic unit coding for all six EBNAs (Schlager et al., 1996, Chen et al., 1999, Zetterberg et al., 1999), and is the product of differential splicing. The constitutively active Qp promoter is not subject to methylation control but instead is silenced by autoregulatory binding of EBNA1 to two low affinity EBNA1-binding sites immediately downstream of the transcription initiation site (Schaefer et al., 1997b, Tao et al., 1998, Davenport and Pagano, 1999, Yoshioka et al., 2008).

In contrast, in situations where the virus adopts either latency I or II patterns of gene expression, as exemplified in BL and C666-1 NPC cell lines, EBNA1 transcripts are initiated from the Qp promoter (Bakos et al., 2007). This switch to the EBNA1-specific Qp promoter in order for the more restricted exclusive expression of EBNA1 to prevail, is necessitated by host-mediated silencing of Cp (Chen et al., 1999), which in turn alleviates host-mediated repression of Qp. Qp-driven EBNA1 expression is also subject to further regulation via putative E2F binding sites (Nonkwelo et al., 1997, Ruf and Sample, 1999), as well as by the JAK/STAT pathway and cell cycle factors (Schaefer et al., 1997a, Chen et al., 1999, Chen et al., 2001, Davenport and Pagano, 1999). The Fp promoter, located around 200bp upstream of Qp, was found to be utilised to drive EBNA1 transcription upon entry into lytic cycle (Zetterberg et al., 1999).

1.5.1.3 Modulation of viral replication, episome segregation and transcription

EBNA1 is the most consistently expressed latent protein in all forms of viral latency on account of its absolute requirement in maintaining and efficiently replicating the EBV genome, and therefore intimate role in maintenance of latent EBV infection. In addition, its

ability to act as a transcriptional transactivator is key to the activation and regulation of viral Cp and LMP1 promoters (Sugden and Warren, 1989, Gahn and Sugden, 1995). EBNA1 is implicitly dependent upon its DNA-binding and dimerisation domain in order to fulfil its vital functions in the replication, segregation and transcriptional activation of the viral genome (Polvino-Bodnar and Schaffer, 1992). Further regions located upstream are responsible for subsequent full orchestration of these functions (Figure 1.2B).

Maintenance and replication of the viral episome is accomplished through the interaction of the *trans*-acting EBNA1 protein with *cis*-acting sequences within the viral origin of latent DNA replication, *OriP*, a 1.7kb region of the EBV episome containing two functional elements, the dyad symmetry (DS) and family-of-repeats (FR) (Reisman and Sugden, 1986, Ambinder et al., 1990, Ambinder et al., 1991, Bashaw and Yates, 2001). The approximately 120bp DS element of *OriP* has been identified as the main initiator of episomal EBV DNA replication (Yates et al., 2000), and contains 4 binding sites for EBNA1, shown to function in pairs. Replication initiation is greatly stimulated by the FR enhancer region (Frappier and O'Donnell, 1991) which contains 20 EBNA1 binding sites (Reisman et al., 1985), and possesses additional roles in mediating chromatin association and partitioning of EBV episomes (Reisman and Sugden, 1986, Bashaw and Yates, 2001, Deutsch et al., 2010).

EBNA1-mediated replication of *OriP*-containing plasmids occurs once per cell cycle, and is additionally facilitated by host chromosomal initiation factors, including ORC (Bashaw and Yates, 2001, Dhar et al., 2001), as well as interactions with the host mitochrondrial protein, p32 (Wang et al., 1997, Chen et al., 1998, Van Scoy et al., 2000), and histone chaperone

proteins such as nucleosome assembly protein 1 (NAP1) and template-activating factor (TAF-I) (Holowaty et al., 2003, Wang and Frappier, 2009).

Deletion of the gly-arg rich region between amino acids 325 and 376 has been shown to abrogate the ability to maintain *OriP* plasmids, and therefore a role in plasmid segregation has been assigned to this domain (Shire et al., 1999, Ceccarelli and Frappier, 2000, Wu et al., 2000, Kapoor and Frappier, 2003, Nayyar et al., 2009). The same deletion is seen to decrease association with metaphase chromosomes, thought to be mediated via an interaction with EBP2, and consistent with the requirement of chromosome tethering for efficient segregation (Marechal et al., 1999, Wu et al., 2000, Kapoor and Frappier, 2003, Nayyar et al., 2009).

Residues 325-376 are also deemed essential for transcriptional activation activity (Wu et al., 2002), while the vital contribution of amino acids 61-83 to transcriptional activation is, at least in part, thought to be mediated through its interaction with Brd4 (Lin et al., 2008). A further regulatory role in viral gene transactivation and episomal viral genome maintenance is contributed by amino acids 8-67, while the region between residues 395 and 450 has been shown to participate in an interaction with the cellular deubiquitinating enzyme, USP7 (Holowaty et al., 2003), as will be mentioned later.

Recent work has demonstrated that post-translational modifications may participate in the regulation of EBNA1 function. Phosphorylation sites of EBNA1 are thought to be involved in transcriptional activation and EBV plasmid maintenance (Duellman et al., 2009, Kang et al., 2011). Specifically, serine phosphorylation of the 325-376 region can enhance binding to EBP2 so increasing segregation efficiency, while arginine methylation of the same region by

arginine methyltransferases PRMT1 and PRMT5 is postulated to influence EBNA1 localisation (Shire et al., 2006). Furthermore, the specific patterns of serine phosphorylation within the NLS are speculated to impact upon the dynamic rate of nuclear transport (Kitamura et al., 2006).

Also, Deng and colleagues have found that EBNA1 is subjected to PAR modification *in vivo*. EBNA1 binds the poly(ADP-ribose) polymerase (PARP), tankyrase 1 and 2 proteins that function to maintain telomere length via interactions with telomere-repeat binding factor (TRF1) (Smith et al., 1998). Interestingly, tankyrase 1 and 2 negatively regulate *OriP* replication and maintenance. This modification may alter EBNA1's ability to interact with and recruit certain cellular proteins or, alternatively, decrease EBNA1 stability (Deng et al., 2002, Deng et al., 2005, Tempera et al., 2010).

1.5.1.4 The role of EBNA1 in the modulation of cellular transcription and tumourigenesis

While EBNA1 is principally regarded as a genome maintenance protein, an accumulating body of evidence now suggests that EBNA1 may contribute to cellular transformation and oncogenesis, largely through its ability to deregulate key cellular processes. However, the exact contribution of EBNA1 to the development of EBV-associated malignancies still remains controversial.

Early experiments targeting the expression of EBNA1 to the B-cell compartment in two lineages of transgenic mice reported increased frequencies of lymphoma formation, suggesting that EBNA1 may have oncogenic activity *in vivo* (Wilson et al., 1996). However these findings were later challenged by Kang and colleagues (Kang et al., 2005, Kang et al.,

2008), who dismissed a potential role for EBNA1 in lymphomagenesis. Further doubt was cast on the absolute requirement for EBNA1 in EBV-induced immortalisation, when growth-transformed LCLs were successfully established using an EBV strain deleted for EBNA1 (Humme et al., 2003). It is suggested that, while EBNA1 may increase the efficiency of B-cell transformation, its expression is not mandatory (Lee et al., 1999).

However, EBNA1 was found to enhance the tumourigenicity and metastatic capability of NPC cells in SCID mice (Sheu et al., 1996), and was observed to interact with the known suppressor of metastasis and cell migration, Nm23-H1, thereby overriding its repressive effects on cell migration (Murakami et al., 2005). It additionally confers a survival advantage to EBV-positive BL cells through inhibition of apoptosis (Kennedy et al., 2003, Sengupta et al., 2006), potentially through up-regulation of the inhibitor of apoptosis, survivin (Lu et al., 2011).

The observed interaction of EBNA1 with the deubiquitinating enzyme, USP7, is predicted to contribute to host cell immortalisation through sequestration of USP7 and destabilisation of p53 (Holowaty et al., 2003, Holowaty and Frappier, 2004), which may reduce sensitivity to DNA damage (Cheng et al., 2010). Further characterisation of this interaction has uncovered its involvement in the disruption of cellular promyelocytic leukaemia (PML) nuclear bodies, eliciting the degradation of their principal component (Sivachandran et al., 2008), which is additionally enhanced by a distinct interaction between EBNA1 and host CK2 kinase (Sivachandran et al., 2010), and potentially promotes the survival of cells harbouring DNA damage.

Furthermore, there is growing evidence to substantiate a role for EBNA1 in the modulation of cellular gene transcription in both B cells and epithelial cells, predicted to be related to EBNA1-mediated regulation of genes involved in chromatin remodelling complexes (Sompallae et al., 2010). Increased levels of the V(D)J recombinase-activating genes, RAG1 and RAG2, have been attributed to the presence of EBNA1 in EBV-positive BL cells (Srinivas and Sixbey, 1995), and may contribute to the observed genomic instability in BL tumours. Induction of the IL2 receptor α chain CD25 and the chemokine CCL20 have been attributed to the expression of EBNA1 in EBV-positive HL (Kube et al., 1999, Baumforth et al., 2008), which is also responsible for the down-regulation of the tumour suppressor, and TGFβ target gene, protein tyrosine phosphatase receptor kappa (PTPRK) following EBV infection of HL cells (Flavell et al., 2008).

Furthermore, evidence is gathering to support EBNA1 as a potent regulator of cellular gene transcription in carcinoma cell lines. In addition to priming cellular response to IFNγ through an induction of STAT1, EBNA1 has been shown to repress TGFβ-induced transcription via increased protein turnover of the Smad2 protein, modulate AP-1 transcription factor signalling through up-regulation of c-Jun and ATF2 subunits, and abrogate NFκB signalling through inhibition of IKKα/β phosphorylation (Wood et al., 2007, O'Neil et al., 2008, Valentine et al., 2010). Additionally, a recently discovered facet of EBNA1 behaviour is its ability to enhance EBER expression through increased cellular RNA polymerase III transcription and the induction of associated cellular transcription factors (Owen et al., 2010).

1.5.2 EBNA-2, -LP, -3A, -3B and -3C

Although frequently silenced in EBV-associated tumours, there is an unquestionable role for the transitory expression of these EBNAs in the initial establishment of latent infection in B lymphocytes. Indeed, recombinant EBV mutants lacking EBNA2, EBNA-LP, EBNA-3A or EBNA-3C are rendered transformation-incompetent *in vitro* (Tomkinson et al., 1993, Humme et al., 2003). However, EBNA3B is not considered essential (Tomkinson and Kieff, 1992).

EBNA2 and EBNA-LP are temporally the first EBV latent proteins to be detected following EBV infection (Kieff and Rickinson, 2007), and their importance is emphasised by the transformation-incompetent P3HR-1 EBV strain lacking all of the EBNA2 gene and the last two exons of the EBNA-LP gene (Bornkamm et al., 1980, Hammerschmidt and Sugden, 1989, Cohen et al., 1989, Rabson et al., 1982), and proven by reintroduction of deleted sequences, which restores the ability to immortalise B lymphocytes *in vitro* (Hammerschmidt and Sugden, 1989, Young et al., 2000).

EBNA2 is a transcriptional activator of both cellular and viral genes, inducing B-cell activation molecules such as the EBV receptor CD21 and the B-cell activation antigen CD23 (Cordier et al., 1990, Wang et al., 1990, Wang et al., 1987), as well as the proto-oncogene c-myc (Kaiser et al., 1999), and up-regulating the expression of LMP1 and LMP2 (Laux et al., 1994, Young et al., 2000), which is coactivated by EBNA-LP (Peng et al., 2005). Crucially, EBNA2 also transactivates the viral Cp promoter during the early stages of EBV infection (Woisetschläger et al., 1991, Sung et al., 1991, Chen et al., 1999, Young et al., 2000), and thereby governs the mutually exclusive usage of Wp and Cp promoters in B lymphocytes (Woisetschläger et al., 1989, Woisetschläger et al., 1990).

EBNA2 transactivation capabilities are not thought to be direct and appear to be mediated via interaction with the ubiquitous DNA binding protein, RBP-Jκ; in doing so, EBNA2 partially mimics aspects of Notch function (Henkel et al., 1994, Grossman et al., 1994, Young et al., 2000, Sakai et al., 1998, Zimber-Strobl and Strobl, 2001).

1.5.3 LMP1

Latent membrane protein 1 (LMP1) is a 63kDa integral membrane protein and is considered the major transforming protein encoded by EBV. LMP1 behaves as a classical oncogene in rodent fibroblast transformation assays (Wang et al., 1985) and has been shown to be absolutely essential for EBV-mediated transformation of primary B lymphocytes *in vitro* (Kaye et al., 1993). LMP1 expression in B cells is associated with the up-regulation of particular cell-surface proteins, notably CD21, CD23, CD39, CD40 and CD44 activation markers, and the cellular adhesion molecules LFA-1, ICAM-1 and LFA-3 (Wang et al., 1990), while LMP1-induced up-regulation of the anti-apoptotic proteins bcl2 and A20 may also have important implications for cell survival (Henderson et al., 1991, Rowe et al., 1994, Fries et al., 1996).

LMP1 functions as a constitutively active viral mimic of the TNF receptor (TNFR) family member, CD40, sustaining B-cell proliferation *in vitro* (Gires et al., 1997, Kilger et al., 1998, Uchida et al., 1999), primarily through recruitment of TRAFs and TRADD to its CTAR1 and CTAR2 signalling domains (Mosialos et al., 1995, Mainou et al., 2007, Floettmann and Rowe, 1997, Floettmann et al., 1998, Kilger et al., 1998). In this way, LMP1 is able to engage the NFκB, JNK and p38 MAPK cellular signalling pathways (Eliopoulos and Young, 1998,

Eliopoulos et al., 1999). Signal transduction by LMP1 has been more extensively reviewed in (Lam and Sugden, 2003, Kieser, 2007, Graham et al., 2010).

When expressed in epithelial cells, LMP1 induces profound phenotypic changes and inhibits terminal differentiation (Dawson et al., 1990), reviewed in (Tsao et al., 2002), through mechanisms that involve the generation of an "inflammatory wound" response (Morris et al., 2008). LMP1 activation of PI3-kinase (PI3K), which maps to CTAR1, is associated with actin filament remodelling and cell survival through the activation of Akt (Dawson et al., 2003), while activation of ERK-MAPK via the canonical Raf-MEK-ERK-MAPK pathway enhances cell motility and invasive properties (Lo et al., 2003, Dawson et al., 2008). Moreover, the ability of LMP1 to induce an epithelial-mesenchymal transition (EMT) in MDCK cells has been evidenced by characteristic morphological changes and an accompanying loss of E-cadherin (Kim et al., 2000)(Laverick et al. – manuscript in preparation).

1.5.4 LMP2A and LMP2B

The LMP2 gene gives rise to the expression of two distinct mRNA species, LMP2A and LMP2B, generated by transcription from two different promoters (Sample et al., 1989). The resulting proteins share structural similarity in 12 hydrophobic transmembrane domains and a 27 amino acid cytoplasmic C-terminal domain, and differ only in the first exon, which for LMP2A encodes a 119 amino acid N-terminal cytoplasmic domain, but is non-coding in LMP2B. There is evidence to suggest that LMP2B may act as a competitive regulator of LMP2A function (Rovedo and Longnecker, 2007), and both are generally considered dispensable for B-cell transformation *in vitro* (Speck et al., 1999), reviewed in (Longnecker, 2000).

LMP2A has been shown to block BCR signal transduction in EBV-infected B lymphocytes *in vitro* by sequestering key signalling proteins such as Syk and Lyn protein tyrosine kinases, and promoting their degradation, mediated by binding to the immunoreceptor tyrosine activation motif (ITAM) located in the cytoplasmic amino-terminal domain (Fruehling and Longnecker, 1997, Caldwell et al., 1998). Importantly, this impedes B-cell differentiation, thereby protecting against fortuitous lytic reactivation in latently infected cells (Miller et al., 1994, Miller et al., 1995). Phosphotyrosine (PY) motifs also present within the amino-terminal domain of LMP2A additionally serve as specific binding sites for Nedd4-like ubiquitin protein ligases, AIP4, WWP2/AIP2 and Nedd4 promoting the degradation of both LMP2A and Lyn to further modulate signalling (Ikeda et al., 2000).

Signalling of LMP2A in EBV latency and in malignant states has recently been reviewed (Pang et al., 2009). Specifically in carcinoma cells, LMP2A has demonstrated the ability to activate the PI3K-Akt pathway, to modulate both STAT and NFκB signalling activities, and to attenuate signalling from endosomal localised TLRs (Scholle et al., 2000, Stewart et al., 2004, Murphy, PhD thesis, 2010). In addition, both LMP2A and LMP2B were found to inhibit interferon (IFN)-mediated transcription, as a consequence of increased IFN receptor turnover (Shah et al., 2009).

Expression of LMP2A and LMP2B in squamous epithelial cells also confers an increased capacity for cell spreading and migration (Allen et al., 2005) which, at least for LMP2A, may be related to an up-regulation of the cellular protein ITGα6 (Pegtel et al., 2005). Similarly, LMP2A-expressing HaCaT cells demonstrated anchorage-independent growth and colony formation in soft agar, and induced the formation of aggressive, poorly differentiated and

metastatic tumours *in vivo* (Scholle et al., 2000). LMP2A has also recently been implicated in the induction of EMT in NPC cells (Kong et al., 2010).

1.5.5 EBERs

The small non-polyadenylated, untranslated RNAs, EBER1 and EBER2, 166 and 172 nucleotides long respectively, are encoded by the *Eco*RI-J fragment of EBV (B95-8) DNA, transcribed by host RNA polymerase III and are the most abundantly (up to 10^7 copies per cell) and consistently expressed EBV gene products in latently infected cells (Lerner et al., 1981, Rosa et al., 1981, Arrand and Rymo, 1982, Jat and Arrand, 1982, Howe and Steitz, 1986, Minarovits et al., 1992). They therefore serve as valuable diagnostic markers for EBV latent infection.

EBERs, although not essential for B-lymphocyte transformation, have been shown to enhance the transforming potential of EBV (Ruf et al., 2000, Yajima et al., 2005, Wu et al., 2007), through changes to cellular transcription machinery, specifically cellular RNA polymerase III-related factors (Felton-Edkins et al., 2006). Recognition of EBERs by retinoic acid-inducible gene I (RIG-I) results in the induction of type I IFNs and IFN-stimulated genes (ISGs) (Samanta et al., 2006). EBER1 additionally acts further downstream by interacting with the IFN-inducible, dsRNA-activated protein kinase PKR, so as to confer resistance to IFNα-induced apoptosis and also prevent its phosphorylation of the protein synthesis initiation factor, eIF2a, and its associated inhibition of protein synthesis (Young and Rickinson, 2004, Clarke et al., 1990, Clarke et al., 1991).

1.5.6 EBV-encoded miRNAs

EBV was the first human virus identified to encode microRNAs (miRNAs) (Pfeffer et al., 2004). Currently, a total of 25 EBV miRNA precursors and 48 mature miRNAs have thus far been identified. EBV encodes miRNAs from two primary transcripts: BHRF1 and the BamHI-A rightward transcripts (BARTs). The BHRF1 transcript encodes three miRNA precursors (ebv-miR-BHRF1-1, -2 and -3), which produce 4 mature miRNAs. Within the BART region, two clusters of miRNAs have been identified, producing 44 mature miRNAs from 22 miRNA precursors. BART Cluster 1 is located between BART exon I and IB, and gives rise to 8 miRNA precursors (ebv-miR-BART1, -BART3 to 6, and –BART15 to 17). BART Cluster 2 is located between BART exon II and III, and gives rise to 13 miRNA precursors (ebv-miR-BART7 to 14, and –BART18 to 22). The ebv miR-BART2-3p and 2-5p mature miRNA are located between exon IV and V (Zhu et al., 2009, Lung et al., 2009, Chen et al., 2005, Cai et al., 2006, Grundhoff et al., 2006, Pfeffer et al., 2004). The expression of BHRF1-encoded miRNAs is limited to B lymphocytes displaying type III latency (Pfeffer et al., 2004). As with the original BART transcripts, the BART miRNAs can be detected in all forms of EBV latency, but appear to be more abundantly expressed in EBV-associated epithelial cancers, NPC and EBVa-GC, compared to BL or LCLs. Whilst the function of BHRF1 and BART-encoded miRNAs are still being uncovered, several recent reports have shown that a number of BART miRNAs target EBV latent gene transcripts. At least three BART cluster 1 miRNAs (ebv-miR-BART1-5p, -BART16 and –BART17-5p) target the 3'UTR of the LMP1 gene, thereby regulating expression of LMP1 (Lo et al., 2007), whilst ebv-miR-BART22, which is abundantly detected in NPC specimens, targets the 3'UTR of LMP2A (Lung et al., 2009). BART miRNAs have also been shown to target cellular genes. Ebv-miR-BART5 targets and suppresses the expression of p53 up-regulated modulator of

apoptosis (PUMA) (Choy et al., 2008), whilst BART2-5p targets viral lytic BALF5 to maintain viral latency (Barth et al., 2008). EBV BART miRNAs expressed in NPC cells have been found to be involved in immune evasion. Nachmani and colleagues identified that ebv-miR-BART2-5p targets the 3'UTR of MHC class I-related chain B (MICB) gene, a cellular ligand for NKG2D (Nachmani et al., 2009), whilst importin 7 (IPO7) was also identified as a target of ebv-miR-BART3 (Dolken et al., 2010).

1.6 EBV-associated malignancies

EBV has been implicated as an etiologic agent in malignancies of both lymphoid and epithelial origin, reflecting the natural tropism of the virus *in vivo*. Such tumours are typified by the presence of multiple extrachromosomal copies of the viral genome in tumour cells (Young and Murray, 2003). B-cell malignancies can be traced and found to originate from different stages of the B-cell differentiation process. Indeed, the malignant cells detected in Hodgkin's disease (HD) are thought to arise from crippled germinal centre cells, supported by the observed constitutive expression of the default latency programme. Burkitt's lymphoma (BL) is predicted to derive from a cell exiting the germinal centre, but arrested at a point of continual proliferation owing to constitutive activation of the c-myc oncogene. If the immune system is compromised, such as following iatrogenic immunosuppression for transplant surgery, or in patients with AIDS, bystander B-cell blasts which would normally be destroyed by CTLs can give rise to post-transplant lymphoproliferative disorders (Lopes et al., 2003, Thorley-Lawson and Gross, 2004, Young and Rickinson, 2004). EBV has also been linked with a subset of nasal T-cell/NK cell lymphomas, which has recently been reviewed in (Fox et al., 2011).

EBV-associated epithelial malignancies include undifferentiated nasopharyngeal carcinoma and a subset of gastric carcinomas, both of which will be discussed in more detail, as well as undifferentiated squamous cell carcinomas of the salivary glands and uterine cervix. Potential relationships with hepatocellular carcinoma and breast cancer have also been described in recent years (Young and Murray, 2003, Hippocrate et al., 2011).

1.6.1 Nasopharyngeal carcinoma (NPC)

NPC is a distinctive type of head and neck cancer, arising from the squamous epithelial cells of the nasopharynx. The World Health Organisation (WHO) has acknowledged the histological classification of NPC into three distinct subgroups, differentiated, keratinising squamous cell carcinomas (type I), and non-keratinising carcinomas, the latter group being further divided into differentiated non-keratinising (type II) and undifferentiated carcinomas (type III) (Shanmugaratnam and Sobin, 1993).

Undifferentiated type III NPC is a highly metastatic disease (Spano et al., 2003), and is frequently described as a "lymphoepithelioma" due to a prominent lymphocyte infiltrate (Klein et al., 1974, Niedobitek et al., 1996, Raab-Traub, 2002, Lo et al., 2004). This form demonstrates the most consistent association with EBV infection (Nicholls et al., 1997), and comprises over 95% of NPC cases in high-incidence areas (Chang and Adami, 2006). NPC tumours generally display the default programme of gene expression with consistent expression of the EBER and BART RNAs, Qp-driven EBNA1, LMP2 and variable levels of LMP1 (Brooks et al., 1992, Busson et al., 1992). Also, elevated IgG and IgA reactivity to the EBV viral capsid antigen (VCA) and early antigen (EA) complex have been detected in NPC sera compared to healthy controls (Henle and Henle, 1976, Ho et al., 1976) and serve as

useful diagnostic markers for this disease. Furthermore, the detection of EBV in nasopharyngeal preinvasive lesions (Pathmanathan et al., 1995, Cheung et al., 2004) indicates the viral infection may be a relatively early event in NPC pathogenesis. In further support of this, tumour monoclonality can be deduced from the homogeneity of EBV with regard to the number of terminal repeats within individual tumours, suggesting tumours are the result of clonal proliferations of a single EBV-infected progenitor cell (Raab-Traub and Flynn, 1986, Raab-Traub, 2002).

The age-standardised incidence rate of NPC is generally under 1 per 100,000 persons per year in most parts of the world (Yu and Yuan, 2002, Lo et al., 2004, Parkin, 2006). However, a much higher incidence is reported among the Southern Chinese (~25-30 per 100,000 persons per year), particularly among the Cantonese who inhabit the central region of the Guangdong Province in Southern China (Yu and Yuan, 2002, Lo et al., 2004). Other populations with elevated rates include natives of Southeast Asia, the Arctic region, Maghrebi Arabic regions of North Africa and parts of the Middle East (Yu and Yuan, 2002, Chang et al., 2009). In addition, a unique peak incidence age plateau of ~40-50 years, and male: female ratio of 2-3:1 are consistently observed (Hildesheim and Levine, 1993, Spano et al., 2003, Parkin, 2006, Tao and Chan, 2007).

The remarkably distinct geographical and ethnic distribution suggests a strong association of NPC with both genetic and environmental factors. There is now a general consensus that the pathogenesis and development of NPC is a multistep process involving the accumulation of stochastically acquired features, that emerge in response to the interaction of multiple factors

(Lo et al., 2004, Young and Rickinson, 2004, Tao and Chan, 2007). A proposed schematic of events is illustrated in Figure 1.3.

Perhaps one of the most well-documented environmental risk factors is the consumption of salted fish traditional to the Cantonese diet, and other preserved foods containing volatile nitrosamine compounds (Yu and Yuan, 2002, Lo et al., 2004, Chang and Adami, 2006) (Yuan et al., 2000b, Ward et al., 2000, Ho et al., 1978, Yu et al., 1986, Zheng et al., 1994, Guo et al., 2009). Convincingly, an experimental salted fish diet was seen to induce malignant tumours in the nasal cavities of rats (Yu et al., 1989), and of particular interest, certain allelic polymorphisms of the cytochrome P450 2E1 enzyme (CYP2E1), responsible for the metabolic activation of nitrosamines, are more frequently detected in the high-risk Chinese population, and are associated with an increased risk of developing NPC (Hildesheim et al., 1995, Hildesheim et al., 1997).

Case-control studies in endemic regions have identified additional risk factors, including the consumption of Chinese medicinal herbs, and lack of vitamin C, as well as exposure to domestic wood cooking fires and occupational exposure to chemical fumes, smoke and dusts, particularly from wood and metals (Lo et al., 2004, Zheng et al., 1994, Guo et al., 2009, Armstrong et al., 2000, Hildesheim et al., 2001, Yuan et al., 2000b). The association of NPC with cigarette smoking or formaldehyde exposure is either weak or controversial (Lo et al., 2004), while alcohol consumption is unlikely associated with risk in high-incidence populations (Cheng et al., 1999).

(FIGURE 1.3)

The concept of a genetic predisposition is supported by studies documenting a family history of NPC, and by observations of significantly elevated risk of NPC in the first-degree relatives of probands with NPC, among the high-risk subgroup of the Cantonese population in the Guangdong province (Yuan et al., 2000a, Guo et al., 2009, Jia et al., 2004). A high NPC incidence is also retained among Southern Chinese who migrate to other nonendemic countries (Buell, 1974, Lo et al., 2004, Tao and Chan, 2007, Grulich et al., 1995) confirming this genetic importance. However, successive generations of Chinese immigrants appear to be at a progressively lower risk of developing NPC, emphasising the influence of environmental agents (King et al., 1985, Yu and Hussain, 2009).

Analyses of studies in the high-risk Southern Chinese also predict that specific HLA haplotypes may be associated with NPC susceptibility, by virtue of their comparative efficacies in triggering host immune responses (Lu et al., 1990, Lu et al., 2003, Lo et al., 2004, Chang and Adami, 2006). A positive correlation with the presence of NPC has been found for HLA alleles, A2, B14 and B46, while negative associations were identified for alleles A11, B13 and B22 (Goldsmith et al., 2002).

Cytogenetic or array-based CGH studies have uncovered multiple chromosomal abnormalities and identified consistent findings of gain of chromosomes 1q, 3q, 8, 12, 19 and loss of 1p, 3p, 9p, 9q, 11q, 13q, 14q and 16q (Lo and Huang, 2002, Tao and Chan, 2007). The highest frequencies of allelic loss are found on 3p (75%) and 9p (87%) (Lo and Huang, 2002), with most the commonly affected TSG regions at 3p21.3 (RASSF1A) and 9p21 (p16, p15, $p14^{ARF}$) (Lo et al., 1995, Lo et al., 2001, Tao and Chan, 2007). High incidence of chromosome 3p and 9p deletions are found in both low-grade and high-grade dysplastic lesions, and additionally

commonly observed in histologically normal nasopharyngeal epithelia from Southern Chinese, the high-risk population (Chan et al., 2000, Chan et al., 2002, Lo et al., 2004). In contrast, EBV is not detected in low-grade dysplastic lesions or normal nasopharyngeal epithelium, as determined by EBER1 ISH (Fan et al., 2006), suggesting the effect of these specific genetic changes precedes EBV infection during the initiation of NPC development.

1.6.2 EBV-associated gastric carcinoma (EBV-aGC)

The worldwide occurrence of EBV-associated gastric carcinoma (EBV-aGC) is estimated at more than 50,000 cases per year, with approximately 10% of all gastric cancers harbouring a latent EBV infection (Imai et al., 1994, Takada, 2000, Fukayama et al., 2008). While some cases have been found to bear resemblance to nasopharyngeal lymphoepithelioma (Shibata et al., 1991), EBV involvement has also been reported in a subset of typical gastric adenocarcinomas (Shibata and Weiss, 1992, Tokunaga et al., 1993).

In the EBV-positive subgroup, all malignant cells carry copies of the EBV genome, as demonstrated by EBER ISH (Takada, 2000), and, as in NPC, terminal repeat analysis detects a single genotype, indicating tumours are of monoclonal origin (Shibata et al., 1991, Imai et al., 1994). Elevated IgG antibody titres against VCA and EA are also observed (Takada, 2000), as is a similar gene expression pattern. However, while EBNA1, EBER1/2 and BART transcripts are routinely detected, LMP2A is only occasionally expressed, and in small amounts, whilst expression of LMP1 is absent (Takada, 2000, Fukayama, 2010).

In contrast to NPC, EBV-aGC demonstrates a worldwide incidence, irrespective of ethnic or geographical influences (Fukayama et al., 2008, Boysen et al., 2009). However, a key

molecular abnormality is the observation of global and non-random CpG island methylation of the promoter region of many cancer-related genes. In particular, repression of gene expression as a result of promoter methylation has been observed for the $p16^{INK4A}$, E-cadherin and p73 genes (Fukayama et al., 2008, Uozaki and Fukayama, 2008, Fukayama, 2010).

1.7 TGFβ superfamily signalling

As already stated (section 1.5.1.4), EBNA1 has been implicated in the deregulation of transforming growth factor (TGFβ) signalling. The TGFβ superfamily comprises over 40 members of functionally related proteins with conserved structures, and includes the TGFβs, activins/inhibins, nodal, bone morphogenetic proteins (BMPs), myostatin, GDFs and anti-Muellerian hormone (AMH) (ten Dijke and Hill, 2004, Massagué and Gomis, 2006). Extensive research has demonstrated pleiotropic functions both *in vitro* and *in vivo* (Miyazawa et al., 2002), particularly in early embryonic development, tissue homeostasis and specification of cell fate (Yue and Mulder, 2001, Herpin et al., 2004, Javelaud and Mauviel, 2004).

Its prototypical member, TGFβ was discovered through its ability to induce a transformed phenotype in rat kidney fibroblasts in cell culture (Roberts et al., 1980, Roberts et al., 1981, Roberts et al., 1983). It has since been exposed as a fundamental ubiquitous cellular signalling ligand and modulates a plethora of biological functions including cell proliferation, differentiation, migration, adhesion, apoptosis, extracellular matrix production, tissue repair, immune surveillance, epithelial-mesenchymal transition and early embryonic development (Yue and Mulder, 2001, Jakowlew, 2006, Massagué and Gomis, 2006, Javelaud and Mauviel, 2004). It is perhaps best characterised for its potent growth inhibitory effects, which have

been demonstrated in a wide variety of cell types, including epithelial, endothelial, fibroblast, neuronal, lymphoid, osteoblast, and hematopoietic cells (Yue and Mulder, 2001).

BMPs were originally identified by Marshall Urist in 1965, who demonstrated that demineralised bone extracts could induce *de novo* bone formation when implanted in ectopic sites in rats (Urist, 1965). BMPs were later isolated from bone extracts and further defined by virtue of their capabilities in inducing bone and cartilage formation *in vivo* (Wozney et al., 1988). Indeed, BMPs are perhaps still best characterised for their roles as osteogenic proteins in the regulation of osteoblast differentiation and subsequent bone formation (ten Dijke et al., 2003, Peng et al., 2003, Cao and Chen, 2005), but were later found to possess additional roles in diverse biological processes including cell differentiation, regulation of stem cell self-renewal and fate determination, cell growth, migration, neurogenesis, morphogenesis, apoptosis and early embryonic development (Hogan, 1996, Yue and Mulder, 2001, Miyazawa et al., 2002, Zhang and Li, 2005, Sieber et al., 2009).

Despite such a diverse array of physiological functions, the core pathway is, in itself comparatively simple, and is essentially conserved among TGFβ superfamily members (Figure 1.4). It is largely reliant upon a family of essential intracellular mediators called Smads, which constitute key points of integration for relaying ligand-induced signals from TGFβ family receptors at the cell surface directly into the nucleus (Attisano and Wrana, 2002). Type II and type I receptors are encoded by five and seven genes in the human genome, respectively (Schmierer and Hill, 2007).

(FIGURE 1.4)

Signalling is initiated by the binding of ligand to constitutively active type II serine/threonine kinase receptor homodimers, inducing their association with type I receptor homodimers to form an active tetrameric complex, in which type I receptors are subsequently phosphorylated at a unique glycine-serine rich regulatory GS domain (Wrana et al., 1992, Wrana et al., 1994, Franzén et al., 1995, Yamashita et al., 1994). BMPs exhibit slightly different binding properties in that they appear to bind optimally to heteromeric type I/type II receptor complexes (Liu et al., 1995, Piek et al., 1999, Josso and di Clemente, 1997).

Following phosphorylation, primed type I receptors then recruit Smad effector proteins. The discovery of Smads originates from genetic analyses of related signalling pathways in *Drosophila melanogaster*, *Caenorhabditis elegans*, and *Xenopus* (Sekelsky et al., 1995, Massagué and Hata, 1997, Savage et al., 1996, Graff et al., 1996), and a total of eight mammalian Smads have been identified (Zhang et al., 1996, Massagué et al., 2005). Receptor-regulated (R-Smads) Smads 1, 2, 3, 5 and 8, are directly recruited and phosphorylated by type I receptors, specifically on two conserved serine residues within an SXSS motif in their C-terminal domain (Macías-Silva et al., 1996, Kretzschmar et al., 1997), Smads 2 and 3 by activin/nodal and TGFβ type I receptors, and Smads 1, 5 and 8 by BMP type I receptors (Miyazawa et al., 2002, Massagué et al., 2005). This activation converts basally monomeric R-Smads into active heteromeric complexes, through increasing their affinity for the universal co-Smad, Smad4 (Kawabata et al., 1998, Qin et al., 2002). This partnering with Smad4 is essential for mediating the appropriate transcriptional responses (Lagna et al., 1996, Schmierer and Hill, 2007). The resulting active complexes accumulate in the nucleus where they interact with the appropriate DNA binding factors, as well as various transcriptional

coactivators or corepressors, to bind specific recognition sites on target gene promoters for effective positive or negative regulation of target gene transcription (Massagué, 2000).

Smad6 and Smad7 comprise a third class of Smad molecules, the inhibitory Smads (I-Smads) which form autoinhibitory feedback loops (Park, 2005), and are largely antagonistic, competitively inhibiting R-Smad association with type I receptors (Hayashi et al., 1997, Imamura et al., 1997, Nakao et al., 1997), as well as interfering with Smad complex formation (Hata et al., 1998, Massagué et al., 2005). They lack the C-terminal SXSS motif so are not themselves targets for receptor phosphorylation, and do not bind DNA, and thus have no direct effect on transcriptional responses.

R-Smad proteins share extensive sequence homology in conserved N-terminal and C-terminal regions, designated the Mad-homology domain 1 (MH1) and MH2 domains, respectively (Yue and Mulder, 2001). These form globular regions, flanking a divergent proline-rich linker segment containing multiple phosphorylation sites for several classes of protein kinases and a PY motif for recognition by ubiquitin ligases. Smads lack intrinsic catalytic activity and so exert their effects through protein-protein or protein-DNA interactions (Lutz and Knaus, 2002). The MH1 domain primarily mediates DNA binding activity, while MH2 regulates Smad homo- and hetero-oligomerisation and Smad-receptor interactions, as well as interacting with important transcription factors (Shi et al., 1998, Yue and Mulder, 2001, Massagué et al., 2005). In the inactive conformation, the MH1 and MH2 domains physically associate, and MH1 imposes an autoinhibitory effect over MH2 to prevent its transcriptional activity (Yue and Mulder, 2001, Miyazawa et al., 2002). This effect ensures Smads remain transcriptionally inert until relieved by phosphorylation-induced structural changes. The

linker region is poorly conserved, but contains several important consensus MAPK phosphorylation sites that effectively modulate its function (Yue and Mulder, 2001).

Smad-independent TGFβ signalling mechanisms have been additionally characterised, and often involve the integration of other signal transduction pathways, engaging a variety of protein kinases including ERK-MAPK, JNK and p38 MAPK, and also PI3K. Furthermore, PP2A phosphatases and Rho-like GTPases including RhoA, Rac and Cdc42 have also been identified as potential TGFβ targets. Such activity is reviewed in (Derynck and Zhang, 2003, Levy and Hill, 2005, Guo and Wang, 2009). Similar non-Smad pathways have also been described in BMP signalling (Miyazono et al., 2010)

1.7.1 TGFβ superfamily signalling in cancer

Dysregulation of TGFβ signalling has been reported as a common feature of cancer progression, and TGFβ is seen to exert both tumour suppressor and pro-oncogenic activities in accordance with tumour stage (Akhurst and Derynck, 2001, Heldin et al., 2009, Meulmeester and ten Dijke, 2011). Abrogation of the pathway is commonly accomplished by either selective blockade of TGFβ cytostatic responses and/or the acquisition of genetic alterations and epigenetic modifications in TGFβ pathway components (Levy and Hill, 2006, Seoane, 2006), often inactivating tumour-suppressing TGFβ functions, whilst conferring oncogenic traits. In this characteristic switch, TGFβ can promote many cellular responses associated with the "defined" hallmarks of cancer, including resistance to TGFβ-mediated cytostasis, inducing cell cycle progression and cancer cell survival, inhibiting immune surveillance, inducing EMT, tumour angiogenesis, and tissue invasion and metastasis, and promoting cancer cell immortality (Tian et al., 2011).

BMP signalling in cancer has been much less extensively characterised; however, evidence suggests that BMPs have similar actions to TGFβ, in that BMPs can both act as tumour suppressors and function to promote tumourigenesis. This has been reviewed recently in (Alarmo and Kallioniemi, 2010, Singh and Morris, 2010).

1.8 Aims and Objectives

The aim of this thesis was to develop existing observations pertaining to the specific role of EBNA1 in the modulation of the TGFβ signalling pathway, with the intent to elucidate defined mechanisms through which its effects are achieved. Initial work focussed on the reported inhibition of TGFβ-induced transcription, and involved investigating the potential of EBNA1 to influence specific regulators of Smad function. This was extended to determine whether EBNA1 could encourage the characteristic switch in TGFβ action during carcinogenesis, as a means by which to directly promote the progression of EBV-associated epithelial malignancies. This was studied by monitoring characteristic pro-oncogenic features of TGFβ behaviour, including differential Smad phosphorylation, TGFβ secretion and cell migration, in EBNA1-expressing carcinoma cell lines. This study further aimed to explore the novel hypothesis that the closely-related BMP signalling pathway, as yet uncharacterised in EBV-associated malignancies, may be specifically modulated by EBV infection, and more specifically by the expression of EBNA1, and may function in parallel with the observed effects in the TGFβ signalling pathway to precipitate the tumourigenic phenotype.

When studying the behaviour of EBV in an epithelial background, extensive investigation is largely challenged by difficulties in achieving stable infection. The development of a

lentiviral system for EBNA1 expression was designed to facilitate further research, providing a model system with enhanced efficiency of infection. The intention is that this may eventually be used to achieve infection of a wider variety of target cells, including primary epithelial cells, in the hope that the precise effects of EBNA1 in the pathogenesis of EBV-associated carcinomas may be more conclusively determined.

CHAPTER 2

Materials and Methods

2.1 Tissue Culture

2.1.1 Tissue culture media

RPMI 1640 (1X) liquid supplemented with 2mM L-Glutamine and adjusted to pH7.0 was purchased in sterile 500ml bottles from Sigma and stored at 4°C.

Dulbecco's Modified Eagle's Medium (DMEM) high glucose (1X) liquid supplemented with 2mM L-Glutamine and adjusted to pH7.0 was purchased in sterile 500ml bottles from Sigma and stored at 4°C.

Keratinocyte serum-free medium (SFM) (1X) liquid adjusted to pH7.0 was purchased in sterile 500ml bottles from Gibco® (Invitrogen) and stored at 4°C.

2.1.2 Other sterile solutions and supplements

Foetal Calf Serum (FCS): pre-screened for virus/mycoplasma contamination and purchased in sterile 500ml bottles from Gibco® (Invitrogen). FCS was aliquoted into 50ml sterile tubes and stored at -20°C.

Ciprofloxacin solution: purchased from Bayer. Filter sterilisation was performed before use at 2.5ml/500ml media.

Penicillin/Streptomycin: solution (10,000 units/ml penicillin-G and 10mg/ml streptomycin) was purchased from Sigma-Aldrich and filter sterilised before use at 5ml/500ml media.

Geneticin (G418): purchased in powder form from Sigma-Aldrich. 5g was dissolved in 100ml sterile distilled H_2O before filter sterilisation and storage in 5ml aliquots at 4°C.

TrypLE™ Express Stable Trypsin Replacement: supplied as 1X solution in a PBS-EDTA buffer in 100ml sterile bottles from Gibco® (Invitrogen) and stored at 4°C.

Phosphate-buffered saline (PBS): purchased from Oxoid Ltd and supplied in tablet form, containing 8g/L NaCl, 0.2g/L KCl, 1.15g/L Na_2HPO_4, 0.2g/L KH_2PO_4. 10 tablets were dissolved in 1L of distilled H_2O. 500ml aliquots were sterilised by autoclaving at 15psi, 120°C for 20 minutes.

Fibronectin: Purchased from Sigma-Aldrich, fibronectin solution from human plasma (0.1%) was supplied at a concentration of 1mg/ml and stored at 4°C.

2.1.3 Cell lines

Ad/AH: an immortalised human cell line derived from an adenocarcinoma of the nasopharynx.

HONE-1: a human EBV-negative tumour cell line established from an NPC biopsy that was originally EBV-positive but lost the viral genome during culture.

AGS: an immortalised tumourigenic human gastric-derived carcinoma cell line.

Ad/AH-, HONE-1- and AGS-EBNA1 and –Neo control lines: generated by transfection of an EBNA1 or neomycin control plasmid into the parental lines followed by drug selection and isolation of individual clones.

Ad/AH, HONE-1 and AGS-rEBV lines: stably infected with recombinant Akata strain of EBV, carrying a neomycin resistance cassette for drug selection.

All Ad/AH, HONE-1 and AGS lines were maintained in RPMI 1640 supplemented with 5% FCS and antibiotics. Ad/AH- and AGS-Neo, -EBNA1 and –rEBV lines were drug selected at 400μg/ml G418, while HONE-1 derivatives were selected at 200μg/ml G418.

Mv1Lu: a mink lung epithelial cell line.

MLEC-clone32: a mink lung epithelial cell line stably transfected with an 800bp fragment of the human plasminogen activator inhibitor (PAI-1) gene fused to the firefly luciferase reporter gene in a p19LUC-based vector containing the neomycin-resistance gene from pMAMneo. This cell line was a kind gift from the Rifkin Laboratory, Department of Cell Biology, New York University Medical Centre.

Mink cell lines were maintained in DMEM supplemented with 10% FCS and antibiotics, and MLEC-clone32 cells were additionally drug selected with 200μg/ml G418.

OKF6: a human immortalised normal oral epithelial line, maintained in Keratinocyte SFM supplemented with 25mg bovine pituitary extract (BPE) and antibiotics.

C666-1: a subclone of the parental line, C666, derived from an NPC xenograft of Southern Chinese origin.

X50-7: an LCL expressing the full array of EBV latent genes.

SL: an LCL immortalised with the B95-8 strain of EBV, generated within the University of Birmingham.

C666-1 cells and B-cell lines were maintained in RPMI 1640 supplemented with 10% FCS and antibiotics.

2.1.4 Maintenance of cell lines

All cell lines were maintained in 37°C incubators supplied with 5% CO_2.

Adherent cells were grown in 75cm^2 tissue culture flasks (Iwaki, Corning) until 90-95% confluent. Cells were washed with PBS and subsequently incubated with 3-4ml TrypLE™ Express for 5-10 minutes at 37°C to allow cell dissociation. Cells were recovered in an excess of complete growth medium to neutralise the trypsin reaction, and pelleted by centrifugation at 1500rpm for 5 minutes. Cells were resuspended in 10ml complete medium. 2ml was taken into a fresh flask to achieve a 1 in 5 dilution and 18ml fresh growth medium added. The appropriate concentration of drug was then applied if necessary. All tissue culture vessels used for C666-1 cells required pre-coating with 10μg/ml fibronectin solution for at least 1 hour at 37°C.

Non-adherent cells were maintained in 75cm^2 Iwaki tissue culture flasks in 10ml medium. Cells were passaged twice weekly by removal of 8ml cell suspension and replacement with complete growth medium (1 in 5 dilution).

For experiments, cell suspensions of both adherent and non-adherent cells were taken to perform haemocytometer counts and the required volumes added to the appropriate tissue culture vessels.

2.1.5 Cryopreservation

Cell suspensions were pelleted as described in section 2.1.4. Pellets were resuspended in 1ml freezing medium containing 50% complete medium, 40% FCS and 10% DMSO (Fisher Scientific). 1ml cell suspensions were added to cryovials (Nunc) and transferred to a Mr Frosty (Nalgene), before storage at -80°C overnight to enable gradual freezing, and

subsequent transfer to the vapour phase of a liquid nitrogen freezer (-140°C) for long-term storage.

Cryopreserved cells were recovered by rapid thawing in a 37°C water bath. Warmed growth medium was added drop-wise, followed by centrifugation at 1500rpm for 5 minutes. The supernatant was discarded and cells were resuspended in complete growth media and transferred to a tissue culture flask.

2.2 DNA transfection of mammalian cells

Transfection of plasmid DNA into eukaryotic cells was conducted using Lipofectamine™ LTX reagent (Invitrogen). The efficiency of transfection was enhanced by the addition of Plus™ reagent (Invitrogen) which pre-complexes DNA prior to the addition of the lipofectamine reagent. Briefly, for 6-well plates, cells were seeded at a density of 2-5x10^5 cells/well and allowed to adhere until approximately 70% confluent. Typically, 1-1.5µg DNA was diluted in 500µl serum-free Opti-MEM® (Invitrogen), before addition of Plus™ reagent at a 1:1 ratio of DNA (µg) to Plus reagent (µl) and incubation at room temperature for 5 minutes to allow DNA complex formation. Lipofectamine™ LTX was then added at a 3:1 ratio of LTX (µl) to Plus reagent (µl), and was followed by a further incubation at room temperature for 30 minutes, while 2ml OptiMEM® was added to cells to be transfected. Following incubation, DNA:lipid complexes were applied to the cells in a random drop-wise manner and mixed by gently rocking plates back and forth to ensure even distribution of complexes before incubation at 37°C. The following day cells were re-fed with the appropriate complete growth medium and subsequently harvested at the desired time points. DNA plasmids used for transfection are provided in Table 2.2.1.

Table 2.2.1: Plasmids used in DNA transfection

Plasmid	Control	Source
pcDNA3-WT-TβRI	pcDNA3	Kindly provided by Dr. J. Wrana, Samuel Lunenfeld Research Institute, Toronto
pcDNA3-TβRI (T204D)	pcDNA3	
pSG5-EBNA1	pSG5	Kindly provided by Dr. J. Sample, St. Jude Children's Research Hospital, Memphis
pLXIN-TβRII	pLXIN	Kindly provided by Dr. W. Grady, Fred Hutchinson Cancer Research Center, Seattle
pLXIN-TβRII D522N	pLXIN	
pSRG-shPPM1A881	pSRG	Kindly provided by Prof. X.-H. Feng, Baylor College of Medicine, Houston
shPPM1B-1	pSUPER.retro.puro	Synthesis described in section 2.12.2
shPPM1B-2	pSUPER.retro.puro	
pc3oriP-EBNA1 mutant plasmids	pc3oriP	Kindly provided by Dr. L. Frappier, University of Toronto, Toronto
pLenti6/R4R2/V5-DEST EBNA1 mutant plasmids	pLenti6/R4R2/V5-DEST	Generation of wild-type and dominant-negative EBNA1 constructs described in Chapter 5. Remaining mutants made by Miss S. Maia (University of Birmingham)

2.3 Tissue culture treatment of cells

2.3.1 Stimulation of cells with human recombinant cytokines

Cells were seeded at appropriate densities according to the tissue culture vessel and left to adhere overnight. Cells were then grown in 0.5% serum for 16 hours prior to stimulation to remove any traces of cytokines and soluble growth factors from the growth medium. Recombinant human cytokines (see Table 2.3.1) were then added at the appropriate concentrations in medium containing 0.5% serum, and incubated for varying lengths of time depending on the nature of the experiment, or left unstimulated as a control.

Table 2.3.1: Recombinant human cytokines

Cytokine	Concentration	Supplier
BMP2	50ng/ml	PeproTech
TGFβ1	5ng/ml	PeproTech

2.3.2 Treatment of cells with specific pharmacological inhibitors

Cells were seeded at appropriate densities according to the tissue culture vessel and left to adhere overnight. Cells were then grown in 0.5% serum for 16 hours prior to addition of

inhibitors. Pharmacological inhibitors, or the carrier solvent DMSO as a control (see Table 2.3.2), were then added at the indicated concentrations in medium containing 0.5% serum, and incubated for varying lengths of time depending on the nature of the experiment.

Table 2.3.2: Pharmacological inhibitors

Inhibitor	Concentration	Pathway targeted	Supplier
Cycloheximide	20µg/ml	Protein synthesis	Sigma
DMSO	-	Inert carrier solvent	Fisher
Flavopiridol	0.3µM	CDK	Sigma
Noggin	100ng/ml	BMP	PeproTech
SB203580	10µM	p38 MAPK	Tocris Bioscience
SB216753	10µM	GSK3	Tocris Bioscience
SB431542	10µM	TGFβ	Tocris Bioscience
SP600125	10µM	JNK	Sigma
UO126	10µM	MEK-ERK MAPK	Promega

2.4 Luciferase Reporter Assay

Reporter assays were conducted using the Dual-Luciferase Reporter Assay System (Promega), in which the luciferase activities of both firefly (*Photinus pyralis*) and Renilla (*Renilla reniformis*) can be sequentially measured from the same sample. While firefly luciferase is used to measure the activity of the experimental promoter of interest, Renilla activity provides an internal control for cell viability and transfection efficiency.

Cells were transfected according to the protocol described in section 2.2. Cells were co-transfected with a luciferase reporter plasmid (either empty control vector or test promoter under study) and Renilla plasmid, p-RL-TK, as well as additional effector DNA plasmids if required. For transfections in 6-well plates, 0.5µg test promoter and Renilla plasmids were normally used. Typically, cells were harvested 48 hours post-transfection by lysis in 500µl 1X Passive Lysis Buffer (Promega), then subjected to one cycle of freeze-thaw and repetitive pipetting to achieve complete lysis and homogenisation of samples. 20µl sample was added in

triplicate into a 96-well plate. To determine luciferase activity, 50µl LARII (Promega) was added to each sample, and firefly luciferase activity immediately quantified using a Victor plate reader (Wallac). Subsequent addition of 50µl Stop & Glo reagent to each sample simultaneously quenched firefly luciferase activity and initiated Renilla luciferase activity, which was immediately determined using the Victor plate reader.

Relative luciferase activity was determined by normalising the firefly luciferase activity against Renilla activity, and made relative to the appropriate firefly control plasmid to account for background activity. A list of reporter plasmids and their appropriate control plasmids are listed in Table 2.4.1.

Table 2.4.1: Plasmids used in luciferase assays

Reporter plasmid	Control plasmid	Source
p-RL-TK	N/A	Promega
p3TP-lux	pGL3-basic	Kindly provided by Dr. J. Massagué, Memorial Sloan-Kettering Cancer Centre, New York
$p(ARE)_3$-luc	pGL3-basic	Kindly provided by Dr. C. Hill, Cancer Research UK London Research Institute, London
Xfast1 in EF-Flag	N/A	Kindly provided by Dr. C. Hill, Cancer Research UK London Research Institute, London
pBRE-luc	pGL3-basic	Kindly provided by Dr. P. ten Dijke, Leiden University Medical Centre, Leiden
$p(CAGA)_{12}$-luc	pGL3-basic	Kindly provided by Dr. C. Hill, Cancer Research UK London Research Institute, London
pQp-luc	pGL2-basic	Kindly provided by the Rickinson group, University of Birmingham, Birmingham

2.5 Immunofluorescence (IF) staining

Cells were trypsinised and seeded at a density of $2x10^4$ onto sterile Teflon coated slides (Henley) in a sterile petri dish with 1ml PBS to prevent dessication. Slides were incubated for 24 hours at 37^{o}C before fixation for 10 minutes in either 4% PFA at room temperature followed by permeabilisation in 0.5% Triton X-100 for 5 minutes, or in ice-cold

methanol:acetone (1:1) at -20°C. Cells were then incubated with 50μl 20% heat-inactivated goat serum (HINGS) for 1 hour in a wet box at room temperature to minimise non-specific binding. Primary antibodies (see Table 2.5.1) diluted in 20% HINGS were applied to cells and incubated for 1 hour at room temperature. Following three washes in PBS, cells were incubated for 1 hour at room temperature in the dark with the appropriate Alexa Fluor® secondary antibody (see Table 2.5.2) also diluted in 20% HINGS. To control for background staining, cells were stained with secondary antibody alone. Slides were then washed three times for 5 minutes in PBS before mounting in DABCO anti-fading agent (90ml glycerol, 10ml PBS, 2.5g DABCO powder) and coverslips for viewing by fluorescence microscopy. Additional confocal microscopy was performed by Miss Rebecca Port (University of Birmingham).

Table 2.5.1: Primary antibodies used in IF staining

Antibody	Species	Dilution	Supplier
Cav-1	Rabbit	1:400	Cell Signalling Technology (#3267)
EBNA1 (R4)	Rabbit	1:1000	A kind gift from Dr. Lori Frappier
NEDD4-2	Rabbit	1:50	Cell Signalling Technology (#4013)
PPM1A	Rabbit	1:400	Cell Signalling Technology (#3549)
Smad2	Mouse	1:50	Santa Cruz (sc-101153)
Smad3	Mouse	1:50	Santa Cruz (sc-101154)

Table 2.5.2: Secondary antibodies used in IF staining

Antibody	Dilution	Supplier
Alexa Fluor® 488 goat anti-mouse	1:1000	Molecular Probes
Alexa Fluor® 594 goat anti-rabbit	1:1000	Molecular Probes

2.6 Immunoblotting

2.6.1 Preparation of protein extracts

On attainment of 80-90% confluency, cells were washed with cold PBS and lysed on ice in RIPA buffer (50mM Tris pH8.0, 150mM NaCl, 1% NP40, 0.5% sodium deoxycholate, 0.1%

SDS), to which complete protease inhibitor cocktail (Roche), and also PhosSTOP phosphatase inhibitor cocktail (Roche) if analysing phosphorylated proteins, were added immediately prior to use. Lysates were scraped into pre-chilled eppendorfs and sonicated to ensure full cell lysis. Samples were then centrifuged at 13,000rpm for 5 minutes at 4^{o}C to pellet any cellular debris and supernatants were transferred to fresh chilled eppendorfs. Sample protein concentrations were determined using a Bio-Rad Protein Assay kit (500-0112). Briefly, 5µl bovine serum albumin (BSA) protein standards in sterile distilled water (SDW) (0, 0.1, 0.2, 0.5, 1 and 2µg/µl) and 5µl samples diluted 1 in 4 in SDW were aliquoted in triplicate into a 96-well plate. 25µl reagent A, followed by 200µl reagent B were added to each well and the plate was incubated on a shaker for 5 minutes at room temperature. Absorbance values were read on a Bio-Rad Model 680 Microplate Reader at 595nm, and protein concentrations determined from a standard curve constructed using the BSA standards. 10-50µg protein lysate was used for immunblotting, dependent on the abundance of the protein of interest, and the quality of the specific primary antibody. Samples were diluted in 4X Laemmli loading buffer (250mM Tris-HCl pH 6.8, 8% w/v SDS, 40% glycerol, 0.05% w/v bromophenol blue, 10% β-mercaptoethanol), denatured at 95^{o}C for 5 minutes and returned to ice, prior to loading on to SDS-polyacrylamide gels.

2.6.2 SDS-polyacrylamide gel electrophoresis (SDS-PAGE)

SDS-PAGE was performed using the Mini-PROTEAN 3 Electrophoresis Kit (Bio-Rad). Percentage composition of polyacrylamide gels was adjusted in accordance with the molecular weight of the protein of interest so as to achieve optimum fractionation. Typically, polyacrylamide gels were prepared from the appropriate percentage of UltraPure ProtoGel acrylamide stock solution (30% w/v acrylamide and 0.8% v/v bis-acrylamide) (Geneflow),

25% v/v resolving buffer (1.5M Tris-HCl pH 8.8, 0.4% w/v SDS, 0.24% w/v TEMED) and SDW to the required volume. Polymerisation was initiated by the addition of 20% ammonium persulphate (APS) to a final concentration of 0.1%. Once the resolving gel was set, it was overlaid with a stacking gel consisting of 4% acrylamide, 50% v/v stacking buffer (0.75M Tris pH6.8, 0.2% w/v SDS, 0.12% v/v TEMED) and SDW to the required volume. 20% APS was added to a final concentration of 0.15% to catalyse polymerisation. Gel combs were inserted for the duration of the polymerisation. Gel combs were then removed, and gels were placed in an electrophoresis tank and submerged in running buffer (30g Tris, 144g glycine and 10g SDS in 10L distilled H_2O). Equal concentrations of protein samples were loaded alongside Spectra™ Multicolour Broad Range Protein Ladder, and electrophoresis was performed at 125V for 90-120 minutes.

2.6.3 Immunoblotting

Proteins separated by SDS-PAGE were transferred to a nitrocellulose membrane (Pall Life Sciences) using the Mini Trans-blot wet transfer system (Bio-Rad). The gel and membrane were sandwiched between two layers of 3MM filter paper (Whatman, UK) and sponges pre-soaked in transfer buffer (30g Tris, 144g glycine, 2L methanol and 8L distilled H_2O) and pressed to remove any air bubbles. Gel transfer was performed in transfer buffer on ice at 90V for 90 minutes. Following transfer, membranes were then incubated for 1 hour with gentle agitation in either 5% powdered non-fat milk in Tris-buffered saline (TBS)-Tween (20mM Tris, 150mM NaCl, 0.1% Tween-20) (for total protein-specific antibodies), or 5% BSA in TBS-Tween (for phospho-specific antibodies), to prevent non-specific binding. Membranes were then transferred into the relevant blocking buffer containing the appropriate antibody at the required concentration (see Table 2.6.1) and incubated with agitation overnight at 4^{o}C.

The following day, membranes were subjected to 3 x 5 minute washes in 1x TBS-Tween prior to incubation with the relevant horseradish peroxidase (HRP)-conjugated secondary antibody (see Table 2.6.2) in 5% milk blocking buffer for 1 hour at room temperature. Membranes were washed as earlier, then incubated with EZ-ECL reagents (Geneflow) (1:1 ratio of reagents A and B) for one minute to enable detection of protein-antibody complexes. Membranes were wrapped in saran wrap, and exposed to X-ray film (Thermo Scientific) for an appropriate period of time, which was subsequently developed in an automated film processor (X-Ograph Ltd).

For re-probing, immunoblots were incubated in stripping buffer (62.5mM Tris-Hcl pH6.8, 100mM β-mercaptoethanol, 2% (w/v) SDS) pre-heated to 55°C, for 30 minutes in a sealed container. The membrane was then washed five times in TBS-Tween, then blocked and probed as above.

Table 2.6.1: Primary antibodies used in immunoblotting

Antibody	Species	Dilution	Product size (kDa)	Supplier
β-actin	Mouse	1:10000	42	Abcam (ab8226)
βig-h3	Rabbit	1:500	68	Santa Cruz (sc-28660)
BMP2	Rabbit	1:1000	45	Abcam (ab14933)
EBNA1 (K67)	Rabbit	1:1000	~70	Kind gift from Jaap Middeldorp (Dept. Pathology, VU University Medical Centre, Amsterdam)
p44/42 MAPK (ERK1/2)	Rabbit	1:1000	42, 44	Cell Signalling (#9102)
p44/42 MAPK (ERK1/2) Thr202/Tyr204	Rabbit	1:1000	42, 44	Cell Signalling (#9101)
GSK3β	Rabbit	1:1000	46	Cell Signalling Technology (#9315)
pGSK3α/β Ser21/9	Rabbit	1:1000	46, 51	Cell Signalling Technology (#9331)
Id1	Rabbit	1:500	15	Santa Cruz (sc-488)
JNK	Rabbit	1:1000	46, 54	Cell Signalling Technology (#9258)
pJNK Thr183/Tyr185	Rabbit	1:1000	46, 54	Cell Signalling Technology (#9251)
NEDD4-2	Rabbit	1:1000	110, 135	Cell Signalling Technology (#4013)
p21	Rabbit	1:500	21	Santa Cruz (sc-397)
p38 MAPK	Rabbit	1:1000	43	Cell Signalling Technology (#9212)
p-p38 MAPK Thr180/Tyr182	Rabbit	1:1000	43	Cell Signalling Technology (#9215)
PAI-1	Mouse	1:500	47	BD Transduction (612024)
PPM1A	Rabbit	1:2000	43	Cell Signalling Technology (#3549)

PPM1B	Rabbit	1:2000	53	Abcam (ab70804)
pSmad1 (Ser463/465)/Smad5 (Ser463/465)/Smad8 (Ser426/428)	Rabbit	1:1000	60	Cell Signalling Technology (#9511)
Smad2	Rabbit	1:1000	60	Cell Signalling Technology (#3122)
pSmad2 Thr220	Rabbit	1:500	55-60	Santa Cruz (sc-135644
pSmad2 Ser245/250/255	Rabbit	1:1000	60	Cell Signalling Technology (#3104)
pSmad2 Ser 465/467	Rabbit	1:1000	60	Cell Signalling Technology (#3101)
Smad3	Rabbit	1:1000	52	Cell Signalling Technology (#9523)
pSmad3 Thr179	Rabbit	1:1000	48	Abcam (ab74062)
pSmad3 Ser204	Rabbit	1:1000	48	Abcam (ab63402)
pSmad3 Ser208	Rabbit	1:500	54	Santa Cruz (sc-130218)
pSmad3 Ser213	Rabbit	1:1000	48	Abcam (ab63403)
pSmad3 Ser423/425	Rabbit	1:1000	52	Cell Signalling Technology (#9520)
Smad6	Rabbit	1:1000	62	Zymed (51-0900)
Smad7	Mouse	1:1000	46	Abcam (ab55493)
TβRI	Rabbit	1:500	53	Santa Cruz (sc-398)
TβRII	Rabbit	1:500	70	Santa Cruz (sc-220)

Table 2.6.2: Secondary antibodies used in immunoblotting

Antibody	Dilution	Supplier
Goat anti-mouse HRP	1:1000	Dako
Goat anti-rabbit HRP	1:1000	Dako

2.7 Electrophoretic mobility shift assay (EMSA)

2.7.1 Nuclear and cytosolic protein extracts

Cells were seeded into 10cm dishes and left to adhere overnight. The following day, cells were incubated in 0.5% serum for 16 hours, before being stimulated, or left untreated in 0.5% serum for 1 hour. Nuclear and cytosolic protein extractions were performed using the NE-PER™ Nuclear and Cytoplasmic Extraction kit (Pierce) following the manufacturer's instructions. Briefly, cells were harvested by addition of 100µl CERI reagent and scraping into pre-chilled eppendorfs. 5.5µl CERII reagent was added before vortexing on the highest setting for 5 seconds, returning to ice for 1 minute and vortexing again for a further 5 seconds. The nuclear fraction was pelleted by centrifugation at 16,000g for 5 minutes, and the supernatant (cytoplasmic fraction) was transferred to a fresh pre-chilled eppendorf and stored at -80°C. The nuclei-containing pellet was resuspended in 50µl NER reagent and incubated on

ice for a total of 40 minutes, with vortexing for 15 seconds every 10 minutes. Nuclear membrane fragments were pelleted by subsequent centrifugation at 16,000g for 10 minutes, and the nuclear protein fraction was transferred to a fresh pre-chilled eppendorf and stored at -80°C until use. Protein concentrations were determined as described previously (Section 2.6.1).

2.7.2 Preparation of native polyacrylamide gels

Native polyacrylamide gels were prepared using 13.3ml 30% w/v acrylamide (Bio-Rad), 44ml 1X TBE (10.8g Tris, 4.5g boric acid, 0.74g EDTA in 1L SDW), 22.7ml SDW and 45µl TEMED. 450µl 20% APS was added to induce polymerisation and the gel mixture was added to novex cassettes (Invitrogen) followed by careful insertion of a gel comb to avoid air bubbles. Once cast, gels were wrapped in moist paper towels and saran wrap, and stored at 4°C until use.

2.7.3 Preparation of EMSA probes

Synthetic oligonucleotides 5´-end-labelled with IRDye® 700 infrared dye (MWG-Biotech) were diluted to 100pmol using PCR grade H_2O. 5µl sense and antisense oligonucleotides were mixed with 90µl restriction buffer B (Roche). Probes were annealed by incubating at 95°C in a heat block for 10 minutes, before the heat block was turned off and probes were left to cool to room temperature overnight. The following day, annealed probes were wrapped in foil and stored at -20°C. Unlabelled "cold competitor" oligonucleotides were used as a control reaction. These were diluted to 1000pmol and annealed as above. Oligonucleotide sequences are provided in Table 2.7.1.

Table 2.7.1: EMSA oligonucleotide sequences

Probe	Oligonucleotide sequence
SBE sense	TCGACAGGGTGTCTAGACGGCCACG
SBE antisense	CGTGGCCGTCTAGACACCCTGTCGA

2.7.4 EMSA binding reactions and visualisation

Optimal binding reaction conditions were first established, then binding reaction mastermixes were prepared as detailed in Table 2.7.2.

Table 2.7.2: EMSA binding reaction mastermix

Reagent	Volume (µl)
10X Binding Buffer (100mM Tris, 500mM KCl, 10mM DTT; pH 7.5)	2
25mM DTT/2.5% Tween-20	2
1µg/µl Poly (dI·dC)	1
1M KCl	1
IRDye® end labelled SBE oligo (50nM)	1
Protein extract (5µg/µl)	1
PCR grade H_2O	12

Samples were gently mixed and incubated for 20 minutes in the dark to allow formation of protein-DNA complexes, before addition of 2µl DNA loading buffer (0.025g bromophenol blue, 0.025g Xylene Cyanol FF and 6ml glycerol made up to 20ml with H_2O). Binding reactions were loaded onto pre-cast native polyacrylamide gels, which had been pre-electrophoresed in 0.5X TBE for 30 minutes at 70V to remove gel contaminants. Electrophoresis was then performed in the dark at 70V for 1-2 hours depending on dye front progression. Cold competitor reactions were assembled, containing 10µl annealed "cold" probe to give a 100-fold excess, with 5µg nuclear extract, adjusted to 19µl with PCR grade H_2O. Reactions were allowed to proceed for 1 hour, before addition of 1µl labelled probe and incubation for 20 minutess as above. Protein-DNA complexes were detected and

densitometric analysis performed using the Odyssey® Infrared Imaging System (LI-COR Biosciences).

2.8 Flow cytometry analysis

2.8.1 Flow cytometric analysis for cell surface expression

Cells were grown to 70-80% confluence in 10cm dishes and washed twice in EDTA before incubation at 37°C in fresh EDTA solution until cells had detached. Dissociation was conducted in the absence of trypsin in order to prevent cleavage of cell surface receptors. Cell suspensions were pelleted, counted and $5x10^5$ cells/well were seeded into a pre-chilled 96 V-well plate. Cells were then pelleted by centrifugation at 2,000rpm for 2 minutes at 4°C and supernatants discarded. Cells were then washed three times with 50µl ice-cold 1%FCS/PBS solution and re-pelleted by centrifugation as above. 50µl 1%FCS/PBS containing the appropriate dilution of primary antibody (see Table 2.8.1) was used to resuspend cells in each well, and incubated on ice for 1 hour on ice. The cells were then pelleted by centrifugation and washed three times in 50µl 1%FCS/PBS as described previously. 50µl of the relevant secondary antibody (see Table 2.8.2) at the appropriate dilution was added to each well and incubated for 1 hour on ice in the dark. Following incubation, cells were pelleted as above and resuspended in 150µl, which was then added to 500µl 1% PFA in a FACs tube, wrapped in foil and stored at 4°C until ready for analysis. Samples were run on a XL-MCL Beckman-Coulter FACs analyser, and subsequent data analysis performed using the WinMDI program.

Table 2.8.1: Primary antibodies used in flow cytometry

Antibody	Species	Dilution	Supplier
TβRI	Rabbit	1:50	Abcam (ab31013)
TβRII	Goat	1:10	R&D Systems (AF-241-NA)

Table 2.8.2: Secondary antibodies used in flow cytometry

Antibody	Dilution	Supplier
Alexa Fluor® 488 donkey anti-goat	1:1000	Molecular Probes
Alexa Fluor® 488 goat anti-rabbit	1:1000	Molecular Probes

2.8.2 Propidium iodide (PI) staining for cell cycle analysis

Cells were seeded into 10cm dishes and grown to approximately 60-70% confluence. Following trypsinisation and centrifugation to pellet cells, cells were resuspended in 1%FCS/PBS, counted, and adjusted to $1x10^6$ cells/ml 1%FCS/PBS. To fix the cells, 1ml ice-cold 95% ethanol was added drop-wise to 1ml cells with gentle vortexing, before an overnight incubation at 4°C. The following day, cells were pelleted by centrifugation, and the supernatants were carefully aspirated. Cells were washed in 1ml 1%FCS/PBS and resuspended in 500µl propidium iodide (PI) working solution. 10ml 50µg/ml PI working solution is composed of 1ml PI stock solution (0.5mg/ml in 0.038M sodium citrate, pH7.0), 100µl 1M Tris (pH7.5), 50µl 1M $MgCl_2$, 20µl RNase A and 8.9ml DEPC-treated H_2O, covered in foil and stored at 4°C. Following incubation in the dark for 30 minutes at 37°C, samples were immediately subjected to cell cycle analysis on a XL-MCL flow cytometer (Beckman-Coulter) and data analysed using the MultiCycle AV DNA analysis software (Phoenix Flow Systems).

2.9 PAI-1L (PAI-1/luciferase) assay

The PAI-1L (PAI-1/luciferase) assay for TGFβ was carried out according to a protocol provided by the Rifkin Laboratory, Department of Cell Biology, New York University Medical Centre. Prior to the assay, serum-free media, conditioned over 24-, 48- and 72-hour incubation periods, were collected from cells grown in 6cm dishes, and stored at -80°C until

use. For the assay, subconfluent MLEC-clone32 cells were trypsinised, pelleted and counted, and resuspended in complete growth media at $1.6x10^5$ cells/ml. Cells were seeded at 100µl/well into a 96-well plate and incubated at 37°C for 3 hours to allow attachment. Following incubation, medium was aspirated from the attached cells, and 100µl test samples added directly to cells, alongside dilutions of recombinant hTGFβ1 ranging from 1.5625 pg/ml to 500 pg/ml in DMEM (100µl/well). In order to assess total TGFβ, conditioned media test samples were heat-activated at 80°C for 5 minutes, and diluted to 25% before application to MLEC-clone32 cells. Samples were also incubated for 1 hour at room temperature with 10µg/ml mouse monoclonal TGFβ1/2/3 neutralising antibody, clone #1D11 (R&D Systems) prior to addition in order to confirm the specificity of the assay. Samples were then incubated for 16 hours at 37°C, before aspiration of culture media, and three washes in ice-cold PBS. Cells were then lysed in 1X Passive Lysis Buffer (Promega) and stored at -20°C, before analysis for luciferase activity.

2.10 Transwell migration assay

Subconfluent cultures of cells were incubated in 0.5% serum for 16 hours and recovered as single-cell suspensions in EDTA. Cells were then seeded in 0.5% serum growth media, containing the appropriate recombinant cytokine stimuli or small molecule inhibitors if required, at $5x10^4$ cells per well into the upper chamber of 24-well transwell inserts (8µm pore size; Corning), pre-coated with fibronectin (10µg/ml in PBS overnight at 4°C). Migration was measured over 16 hours by contacting the chambers with medium containing 0.5% serum at 37°C. This serum concentration was increased to 10% as a necessary chemoattractant for promoting migration of C666-1 cells. Following incubation, transwells were fixed in 30% ice-cold methanol for 5 minutes and air-dried prior to staining with 1%

crystal violet. Transwells were inverted and air-dried, and any non-migrating cells were removed using cotton swabs. Representative fields were photographed using an Axiovert 40CFL inverted microscope (Zeiss).

2.11 Molecular Biology Techniques

2.11.1 RNA extraction

RNA extractions were carried out using the EZ-RNA total RNA isolation kit (Geneflow) in accordance with the manufacturer's instructions, with reagent volumes adjusted appropriately according to the volume of the tissue culture vessel. Cells were grown to 70-90% confluence, before harvesting through lysis in denaturing solution (0.5ml/10cm^2 culture dish area), followed by cell scraping into 1.5ml eppendorfs. Homogenates were incubated for 5 minutes at room temperature to ensure cell lysis. Subsequently, an equal volume of extraction solution was added, and samples were mixed by vigorous shaking for 15 seconds, followed by a 10-minute incubation at room temperature. Samples were then centrifuged at 12,000g for 15 minutes at 4°C to separate the aqueous phase from the organic phase and interphase. The upper aqueous phase was transferred to a clean eppendorf and RNA precipitated by addition of 0.5ml isopropanol per 0.5ml denaturing solution and overnight incubation at -20°C.

Precipitated RNA was then pelleted by centrifugation at 12,000g for 8 minutes at 4°C, and the pellet washed in 75% ethanol. RNA was re-pelleted by centrifugation at 7,500g for 5 minutes at 4°C before careful aspiration of the ethanol. The pellet was air-dried before resuspension in PCR grade H_2O. RNA concentration was determined using a NanoDrop spectrophotometer (Thermo Scientific) and samples diluted to the appropriate working concentration and stored at -80°C.

2.11.2 cDNA synthesis

cDNA synthesis was performed using Superscript® III reverse transcriptase (Invitrogen). 1µg RNA, 1µl random primers (0.4µg/µl) (Promega) and 1µl dNTP mix (10mM) (Invitrogen) were adjusted to a total volume of 13µl with PCR grade H_2O, and heated at 65°C for 5 minutes to denature any dsRNA, then cooled on ice. 4µl 5X First-Strand buffer, 1µl DTT (0.1M), 1µl RNaseOUT™ Ribonuclease Inhibitor (40U/µl) (Invitrogen) and 1µl Superscript III (200U/µl) were added to each and mixed by pipetting. cDNA synthesis was performed in a thermal cycler under the following conditions: 25°C for 5 minutes, 50°C for 1 hour, 70°C for 15 minutes, with a final hold at 4°C. The cDNA was then diluted in 80µl PCR grade H_2O and stored at -20°C.

2.11.3 Reverse-transcriptase polymerase chain reaction (RT-PCR)

For RT-PCR, reaction components were assembled as outlined in Table 2.11.1, and typical PCR thermal cycler conditions are given in Table 2.11.2.

Table 2.11.1: Mastermix for RT-PCR

Reagent	Volume (µl)
DreamTaq™ Green PCR Master Mix (2x) (Fermentas)	25
5´ Forward primer (100pmol)	1
3´ Reverse primer (100pmol)	1
DEPC-treated H_2O	18
cDNA	5

Table 2.11.2: RT-PCR thermal cycler conditions

Temperature	Time (minutes)	Number of cycles
94°C	5	1
94°C	0.5	25-35
x°C	0.5	
72°C	2	
72°C	5	1
4°C	HOLD	

Oligonucleotide primers for RT-PCR were synthesised by Sigma-Aldrich. Primer sequences, specific annealing temperatures and predicted product size are shown in Table 2.11.3.

Table 2.11.3: RT-PCR primer sequences and annealing temperatures

Gene	Sequence	Annealing temperature (°C)	Product size (bp)
ActRI	Forward: GCTGCCCACTAAAGGAAAAT Reverse: GCGAGCCACTGTTCTTTGTA	56	300
ActRIIB	Forward: TCCCTCACGGATTACCTCA Reverse: CCTCCTCAAAAGGCAGCA	56	440
Big-h3	Forward: GGAAGGAGTCTACACAGTCTTT Reverse: CCTCTGGGAAGCCCTGGAAAA	51	399
BMP2	Forward: CCTGAAACAGAGACCCACC Reverse: GCATTCTGATTCACCAACCT	56	417
BMP4	Forward: GCCAGCATGTCAGGATTA Reverse: GGGCACACAACAGGCTTT	55	380
BMP6	Forward: CGACAAGCAGCCCTTCAT Reverse: GCACGGTTTGGGGACATA	59	373
BMP7	Forward: GGTCCACTTCCGCAGCAT Reverse: GGCACACTCCCCCTCACA	61	238
BMPRIA	Forward: GTGGGTCTGGACTACCTT Reverse: GGGCACATCAACTTCATT	52	539
BMPRIB	Forward: CCACCCTAGACGCTAAAT Reverse: GCTCTCGTCCAACACTTCT	52	278
BMPRII	Forward: CCTGATGTTCTGCCTACT Reverse: GCTCTTCTGGGCTTTGAT	52	602
Cav-1	Forward: GGAACAGGGCAACATCTACAA Reverse: CACGGCTGATGCACTGAAT	55	383
Dab2	Forward: GGTCAACAACAAGCCCTT Reverse: CTGGCAAAGGCACTCAAA	55	301
EBNA1	Forward: GGGTGGTTTGGAAAGCAT Reverse: TGGAAACCAGGGAGGCAAAT	58	447
GAPDH	Forward: GCCTCCTGCACCACCAACTG Reverse: CGACGCCTGCTTCACCACCTTCT	52	351
Id1	Forward: CCTCAACGGCGAGATCAG Reverse: GAGACCCACAGAGCACGTAA	58	148
Id2	Forward: CGTGAGGTCCGTTAGGAAAA Reverse: GGTGATGCAGGCTGACAATA	51	504
Id3	Forward: GCTTGCTGGACGACATGAA Reverse: CGTTGGAGATGACAAGTT	55	222
NEDD4-2	Forward: CCGGTTACTGCAGTTTGT Reverse: CCACCCCTTCAAATCCTT	55	236
PAI-1	Forward: GTGGTCTGTGTCACCGTATC Reverse: GTAGTTGAATCCGAGCTGCC	55	440
PPM1A	Forward: CTGGGATGTTATGGGAAAT Reverse: CGGCTTCAATAACATTCCTCTT	55	359
PPM1B	Forward: GGCAGCGTGATGATACAA Reverse: CCCGTGATTCCAAGTGCTTAT	55	406
SARA	Forward: GGCTATCAGTATTCACAA Reverse: CCTCTGTCCATCTGATTA	50	403
Smad1	Forward: CTCTCCCACCAGCTCAGA Reverse: CACTAAGGCATTCGGCAT	57	452

Smad5	Forward: CGCCTCCTCCTGCCTATA Reverse: GCTGCTGGGAATCTTACA	54	470
Smad7	Forward: CAGATTCCCAACTTCTTCTG Reverse: GTTGAAGATGACCTCCAGCC	53	533
Smad8	Forward: CGCCTACTATGAACTGAA Reverse: GGAAGCCGTGTTGATAGT	52	278
Smurf2	Forward: GGCTCTGCAGAAAGGATT Reverse: GGGCTTTCGGCAGGTTGT	53	344
TβRI	Forward: ATGGGCTTAGTATTCTGGGAAA Reverse: GGCATACCAACATTCTCTCATA	57	221
TβRII	Forward: GCAGTGGGAGAAGTAAAAGAT Reverse: GGGAGCCGTCTTCAGGAAT	56	301
TGFβ1	Forward: GTTGAGCCGTGGAGGGGAAA Reverse: CTGCGTGTCCAGGCTCCAAAT	58	386
TGFβ2	Forward: AAATGGATACACGAACCCAA Reverse: GCTGCATTTGCAAGACTTTAC	55	250
TGFβ3	Forward: AAGTGGGTCCATGAACCTAA Reverse: GCTACATTTACAAGACTTCAC	55	250

2.11.4 Agarose gel electrophoresis

PCR products were fractionated on 1% agarose gels. Agarose powder was weighed and dissolved in the appropriate volume of 1X TBE by boiling in a glass conical flask. The agarose solution was cooled to approximately 50°C before addition of SYBR® Safe DNA gel stain (Invitrogen) (0.5µl per 100ml). The solution was subsequently poured into a sealed casting tray with gel combs inserted and left to set. Once set, the gel was placed into a horizontal electrophoresis tank (Eurogentec). Gel combs were removed and the gel was fully submerged in 1X TBE. 20µl PCR product was loaded into each well alongside either GeneRuler™ 100bp Plus or GeneRuler™ 1kb Plus DNA ladders (Fermentas). Gel electrophoresis was typically performed at 130V for 1 hour, and PCR products were visualised using a UV transilluminator.

2.11.5 Real-time quantitative PCR (QPCR)

QPCR for cellular genes was performed on cDNA generated as described in section 2.11.2 using commercially available TaqMan® Gene Expression Assays purchased from Applied

Biosystems (see Table 2.11.4), in reactions assembled as in Table 2.11.5. Probes in cellular target primer and probe sets were FAM™ dye-labelled, while that of the internal baseline control, huGAPDH primer/probe set (Applied Biosystems) used for data normalisation was VIC™ dye-TAMRA™ dye-labelled.

Table 2.11.4: TaqMan® Gene Expression Assays used in QPCR

Gene	TaqMan® Gene Expression Assay
BMP2	Hs00154192_m1
PPM1A	Hs00221372_m1
TβRI	Hs00610318_m1
TβRII	Hs00559660_m1
TGFβ1	Hs00998133_m1
TGFβ2	Hs00234244_m1
TGFβ3	Hs01086000_m1

Table 2.11.5: Mastermix for QPCR

Reagent	Volume (µl)
cDNA	5
TaqMan® Gene Expression Assay	1
huGAPDH primer and probe	0.5
2X Sensimix™ (dU) (Quantace)	10
PCR grade H_2O	3.5

Reactions were performed in technical triplicate and analysed on an ABI 7500 Fast Real-time PCR machine. Analysis was performed using the $2^{-\Delta\Delta Ct}$ method (Livak and Schmittgen, 2001). In brief, cycle threshold (Ct) values were obtained by determining the point at which amplification occurred above background in the linear range of amplification for each reaction. The test primer data was then normalised against the multiplexed endogenous reference GAPDH data to obtain the ΔCt values and the average determined for each triplicate to obtain the mean ΔCt. These values were then made relative to a calibrator (often the neomycin control cell line counterpart) to derive ΔΔCt values, from which the fold changes relative to the control were calculated using the formula $2^{-\Delta\Delta Ct}$.

2.12 Molecular cloning

2.12.1 Solutions

L-Broth (LB): 10g L-broth base (Gibco®) dissolved in 500ml SDW and sterilised by autoclaving.

LB-agar plates: 7.5g agar dissolved in 500ml LB before autoclaving. Agar was melted prior to use and cooled to approximately 55°C before adding antibiotic. Plates were poured and, once set, inverted and stored at 4°C.

Ampicillin: 100mg/ml stock was prepared in SDW, sterilised through a 0.45µm filter and stored in 5ml aliquots at -20°C.

Spectinomycin: 100mg/ml stock was prepared in SDW, sterilised through a 0.45µm filter and stored in 5ml aliquots at -20°C.

2.12.2 shRNA preparation

Oligonucleotides for generation of shRNAs were purchased from Invitrogen, and were designed to encompass the unique 19-nucleotide target sequence in both sense and antisense orientation, separated by a 9-nucleotide spacer sequence, and inclusive of *Bgl*II and *Hind*III ends to assist ligation into the pSUPER.retro.puro vector (OligoEngine). PPM1B target sequences were obtained from (Sun et al., 2009), and the complete oligonucleotide sequences are given in Table 2.12.1.

Table 2.12.1: PPM1B shRNA oligonucleotide sequences

shRNA name	Oligonucleotide sequence
shPPM1B-1 sense	5′-gatccccAATGCAGGAAAGCCATACTGAttcaagaggTCAGTATGGCTTTCCTGCATTttttta-3′
shPPM1B-1 antisense	5′-agcttaaaaaAATGCAGGAAAGCCATACTGAcctcttgaaTCAGTATGGCTTTCCTGCATTggg-3′
shPPM1B-2 sense	5′-gatcccAACTTCTGGAGGAGATGCTGAttcaagaggTCAGCATCTCCTCCAGAAGTTttttta-3′
shPPM1B-2 antisense	5′-agcttaaaaaAACTTCTGGAGGAGATGCTGAcctcttgaaTCAGCATCTCCTCCAGAAGTTggg-3′

Oligonucleotides were reconstituted in TE buffer (10mM Tris-HCl pH 8.0, 1mM EDTA) to give a 100μM stock, and annealed in annealing buffer (100mM NaCl, 50mM HEPES pH7.4) by heating to 100°C for 5 minutes, before cooling gradually to room temperature, and subsequent storage overnight at 4°C. The pSUPER.retro.puro vector was linearised by sequential restriction-endonuclease cutting with *Hind*III and *Bgl*II as described in section 2.12.4, and annealed shRNA oligonucleotides were ligated into the digested pSUPER.retro.puro using T4 DNA ligase (see section 2.12.5). This was then subjected to a further *Bgl*II restriction-endonuclease reaction for 30 minutes at 37°C prior to bacterial transformation to reduce the level of background.

2.12.3 PCR amplification

PCR amplification of desired sequences for use in the TOPO® cloning procedure (Invitrogen) was performed on 0.01ng DNA per reaction, using primers listed in Table 2.12.2, and carried out according to conditions given in Table 2.12.3.

Table 2.12.2: Dominant-negative EBNA1 cloning oligonucleotide sequences

Primer	Oligonucleotide sequence
dnEBNA1 fwd	5′-ATGAAGAGGCCCAGGAGTCCCA-3′
dnEBNA1 rev	5′-CTCCTGCCCTTCCTCACCCTCA-3′

Table 2.12.3: Thermal cycler conditions for PCR cloning

Temperature	Time (minutes)	Number of cycles
94°C	5	1
94°C	0.5	35
58°C	0.5	
72°C	2	
72°C	5	1
4°C	HOLD	

2.12.4 Restriction endonuclease digestion

For a typical restriction endonuclease digestion, 1µg purified DNA was digested in a total volume of 20µl with the appropriate restriction enzymes and buffers (Roche Diagnostics, New England Biolabs, Promega). Briefly, a reaction was composed of 2µl 10X BSA stock (10mg/ml), 2µl 10X restriction enzyme buffer, 1µl each restriction enzyme and nuclease-free water up to a final volume of 20µl. The reaction mixture was incubated for 1.5 hours in a 37°C water bath and if required, reactions were stopped by heating the sample at 65°C for 20 minutes. Digested DNA was analysed by agarose gel electrophoresis.

2.12.5 Ligation of DNA insert into vectors

For shRNA cloning, ligation reactions were performed using T4 DNA ligase (Promega). Vector and insert were added, typically in a ratio of 1:3, to a total volume of 20µl, including 2µl 10X T4 ligase buffer, 1µl T4 ligase and sterile water. The reaction was incubated at 16°C overnight to allow ligation to occur.

For TOPO® cloning, sequences were ligated in the presence of a salt solution (1.2M NaCl, 0.06M $MgCl_2$) into the linearised pCR®8/GW/TOPO® entry vector supplied in the pCR®8/GW/TOPO® TA Cloning® kit (Invitrogen), for 5 minutes at room temperature, then cooled to 4°C.

2.12.6 Bacterial transformation of competent cells

2µl ligation reaction was used to transform either One Shot® TOP10 *E.coli* cells (Invitrogen), ONE SHOT® Stabl3™ strain of *E.coli* (Invitrogen) or Gold Efficiency α-select chemically competent cells (Bioline). The ligation reaction was gently mixed with the cells, incubated on

ice for 30 minutes, heat-shocked for 30 seconds at 42°C, and then immediately returned to ice for 5 minutes. 250µl S.O.C. medium (Invitrogen) was added to cells prior to incubation in an orbital shaker at 37°C for 1 hour. The transformed cell mixture was then spread onto pre-warmed LB-agar plates containing 100µg/ml ampicillin or 100µg/ml spectinomycin as required. Plates were inverted and incubated at 37°C overnight before examination of plates for drug-resistant bacterial colony growth the following day.

2.12.7 Isolation of DNA from bacterial cultures

2.12.7.1 Mini-preps

Colonies on bacterial transformation plates were picked with a sterile pipette tip and incubated in 3ml LB supplemented with the required antibiotic for 16 hours at 37°C in an orbital shaker. To extract plasmid DNA, 1.5ml overnight bacterial culture was processed using the Qiagen QIAprep Spin Miniprep Kit (Qiagen) according to the manufacturer's protocol. Briefly, cells were pelleted by centrifugation at 13000rpm for 10 minutes, supernatants discarded, and resuspended in 250µl Buffer P1. Cells were then lysed by addition of 250µl Buffer P2 and mixed by inversion, then neutralised by addition of 350µl Buffer N3 and again mixed by inversion. Samples were centrifuged at 13000rpm for 10 minutes, and supernatants were transferred to supplied QIAprep spin DNA binding columns. Following centrifugation at 13000rpm at 4°C for 1 minute, samples were washed with 750µl Buffer PE and centrifuged again. Complete removal of wash buffer from the DNA binding column was ensured by a second centrifugation upon emptying the waste. The inner sleeve of the column was transferred into a clean labelled 1.5ml eppendorf and 50µl Buffer EB added to the centre of the binding column for elution of DNA. After incubation for 2 minutes at room temperature, the column was centrifuged as before, and a further 20µl Buffer EB added

and re-centrifuged. DNA concentrations were measured using a NanoDrop spectrophotometer and samples stored at -20°C.

2.12.7.2 Maxi-preps

Validated cultures were used to inoculate 400ml LB supplemented with the required antibiotic, and were incubated at 37°C for 16 hours in an orbital incubator. Using the Invitrogen PureLink HiPure Plasmid Filter Maxiprep kit, DNA was extracted and purified according to the manufacturer's instructions. Bacterial cells were first pelleted using a Sorvall bucket centrifuge at 4000g for 10 minutes, and supernatants carefully decanted off and discarded. 15ml Buffer R3 was added to resuspend the pellet, which was subjected to repetitive pipetting and vortexing until homogenous. Cells were then lysed by addition of 15ml L7 Lysis Buffer, gently mixed by inversion, and incubated at room temperature for 5 minutes. 15ml Precipitation Buffer N3 was added to each sample and mixed by inversion, to both neutralise the lysis buffer and precipitate cellular debris and solutions. DNA binding columns were equilibrated by addition of 30ml Equilibration Buffer EQ1 to each column, allowed to drain by gravity flow. Samples were carefully transferred into the equilibrated columns and allowed to drain by gravity. Residual bacterial lysate was washed with 10ml Wash Buffer (W8) and, once drained, the inner filtration cartridge was removed and the columns washed with 50ml W8 wash buffer. DNA was then eluted by addition of 15ml E4 elution buffer to the column. 10.5ml 100% isopropanol was added to each collection tube before centrifugation at 15000g for 30 minutes at 4°C. Supernatants were discarded, pellets washed in 5ml 70% ethanol and samples centrifuged at 15000g for 5 minutes at 4°C. All residual ethanol was carefully removed and the pellet air-dried prior to resuspension in 500µl DEPC-treated water, and transfer to clean 1.5ml eppendorfs. The concentration of each

plasmid was determined using a NanoDrop spectrophotometer and samples were diluted to a stock concentration of 1µg/µ1 before storage at -20°C.

2.12.8 DNA sequencing

The authenticity of cloned plasmids was verified by DNA sequencing using the BigDye® Terminator v3.1 Cycle Sequencing Kit (Applied Biosystems). Briefly, this involved amplifying the gene sequence of interest with primers specific to the entry plasmid (either GW1 or GW2 for cloning into TOPO® vectors, and H1 sequencing primer for shRNA constructs contained in pSUPER.retro.puro – see Table 2.12.4). The PCR reaction mix was set up according to Table 2.12.5 and run using the thermocycler program outlined in Table 2.12.6.

Table 2.12.4: Primers used for sequencing

Primer	Sequence	Source
GW1	5´-GTTGCAACAAATTGATGAGCAATGC-3´	Invitrogen
GW2	5´-GTTGCAACAAATTGATGAGCAATTA-3´	Invitrogen
H1	5´-TCGCTATGTGTTCTGGGAAA-3´	Addgene

Table 2.12.5: Sequencing reaction PCR mastermix

Reagent	Volume (µl)
DNA (100ng/µl)	1
Ready Reaction Premix	2
Big Dye sequencing buffer	2
Primer (3.2pmol)	1
DEPC-treated H_2O	14

Table 2.12.6: Sequencing PCR thermal cycler conditions

Temperature	Time	Number of cycles
96°C	1min	1
96°C	10s	25
50°C (55°C for shRNAs)	5s	
60°C	4min	
4°C	HOLD	

PCR products were subsequently purified by addition of 2µl 125mM EDTA, 2µl 3M sodium acetate and 50µl 100% ethanol to each reaction, and mixed by inversion. Reactions were incubated for 15 minutes at room temperature, followed by centrifugation at 2000g for 45 minutes at 4°C. Supernatant was carefully aspirated and 70µl 70% ethanol added to each pellet before further centrifugation at 1650g for 15 minutes at 4°C. Supernatant was aspirated and pellets were air-dried at 37°C for 30 minutes. Pellets were resuspended in HiDi formamide buffer (Applied Biosystems) and samples were stored at 4°C until use.

Samples were loaded into a 96-well plate and run using a standard sequencing protocol on a 3130xl Genetic Analyser (Applied Biosystems). Collected data was subsequently analysed using Chromas Version 1.45, and the NCBI website sequence alignment tool (http://www.ncbi.nlm.nih.gov/blast/bl2seq/wblast2.cgi) utilised to verify homology to the desired sequence.

2.12.9 Multisite Gateway® LR Recombination

pENTR™5′-TOPO® and pCR®8/GW/TOPO® entry vectors carrying the desired sequences were added in combination with the lentiviral destination vector, pLenti6/R4R2/V5-DEST (Invitrogen), in a LR clonase II®-driven homologous recombination reaction, incubated at room temperature for 16 hours, followed by addition of 1µl 2µg/µl Proteinase K solution (Invitrogen), and incubation for 10 minutes at 37°C.

2.13 Statistics

Statistical significance of data was established using the Student's t-test, following determination of equal or unequal variance of samples using an f-test.

CHAPTER 3

Modulation of the TGFβ signalling pathway by the EBV-encoded EBNA1 protein

3.1 Introduction

The initial suggestion that EBNA1 may act as a modulator of cellular gene transcription provided the catalyst for an accumulating body of evidence in support of this hypothesis. These findings are particularly pertinent as they demonstrate that the transactivation capabilities of EBNA1 can now be extended beyond its well-established role in the transactivation of viral genes, and intimate that, in the context of an EBV infection, EBNA1 may specifically modify host cellular signalling pathways, perhaps simply in order to assist its genome maintenance function but, more intriguingly, to foster malignant progression. To date, reports have documented the ability of EBNA1 to induce the expression of CD25, RAG1, RAG2 and CCL20 genes in B cells (Kube et al., 1999, Srinivas and Sixbey, 1995, Baumforth et al., 2008), whilst deregulating the STAT1, AP-1, TGFβ and NFκB signalling pathways in epithelial cells (Wood et al., 2007, O'Neil et al., 2008, Valentine et al., 2010).

In this laboratory, EBNA1-related research has centred around microarray-based gene expression analyses carried out on Ad/AH carcinoma cells stably expressing EBNA1 (Wood et al., 2007, Valentine et al., 2010), which identify key signalling pathways as potential targets of EBNA1. Here, the focus of the work has been to expand upon existing observations relating to the effect of EBNA1 expression on the TGFβ signalling pathway, with particular

emphasis on the effect on phosphorylation status of Smad mediator proteins as an essential means of controlling signalling output.

The ability of EBNA1 to modulate the TGFβ signalling pathway was considered particularly deserving of further exploration due to the well-established roles of TGFβ in many critical cellular processes, including cell proliferation and apoptosis, differentiation, migration and extracellular matrix production (Massagué and Gomis, 2006, Jakowlew, 2006). Disruption of TGFβ signalling and, by default, these fundamental cellular mechanisms, invariably yields oncogenic results. It is therefore not surprising that aberrant TGFβ signalling is a common event in many cancers (Akhurst and Derynck, 2001, Jakowlew, 2006, Massagué, 2008) and, significantly, dysregulation of the TGFβ pathway has already been documented in NPC (Harn et al., 2002, Sriuranpong et al., 2004). In normal epithelial cells, TGFβ performs homeostatic, largely growth inhibitory and pro-apoptotic functions, responses which are characteristically lost during tumourigenesis in favour of its tumour promoting roles in enhancing cell motility, invasion and metastasis (Massagué, 2008). Abrogation of the TGFβ pathway has already been attributed to EBV infection and, more specifically, the presence of EBNA1, in carcinoma cells (Wood et al., 2007), and it is therefore feasible that the observed alterations will directly impact upon NPC pathogenesis.

Normally, negative regulation of the Smad signal is used to precisely control Smad signal termination (Itoh and ten Dijke, 2007). However, if this balance becomes deregulated, this can adversely affect TGFβ signalling and encourage tumour progression. Previous work has revealed the ability of EBNA1 to repress the transcription of the well-recognised TGFβ-responsive target genes, PAI-1 and βig-h3, and this effect has been specifically correlated

with diminished levels of Smad2-activating phosphorylation in response to TGFβ stimulation, coupled with enhanced Smad2 protein turnover in both EBV-infected B cells and carcinoma cell lines (Wood et al., 2007, Flavell et al., 2008).

While many mutations of Smad proteins, particularly Smad2 and Smad4, have been characterised (Riggins et al., 1997, Massagué et al., 2000, Xu and Attisano, 2000, Miyaki et al., 1999, Qiu et al., 2007, Bornstein et al., 2007, Losi et al., 2007, Levy and Hill, 2006), there are no reports to date of their occurrence in NPC, indicating that the Smad proteins may be adversely regulated rather than mutated in this cancer. Subsequent investigations therefore focussed on negative regulation or attenuation of TGFβ signalling in the context of EBV-infected epithelial cells. Termination of the Smad signal is achieved either irreversibly through ubiquitination and degradation of the R-Smads (Lo and Massagué, 1999), or by dephosphorylation in the nucleus which permits the R-Smads to translocate back into the cytoplasm to participate in further signalling (Wrighton et al., 2009). Several proteins have been implicated in these processes, including PPM1A, MTMR4, TMEPAI, NEDD4-2, Smurf2, WWP1/Tiul1, CHIP, CKIγ2 and Pin1 (Lin et al., 2006, Yu et al., 2010a, Watanabe et al., 2010, Gao et al., 2009, Lin et al., 2000b, Zhang et al., 2001, Seo et al., 2004, Xin et al., 2005, Guo et al., 2008, Nakano et al., 2009). In order to select potential candidate proteins for further investigation, the existing Affymetrix gene expression array data was scrutinised for deregulated expression of the above genes. With the fold change threshold set at ≥1.5, both PPM1A and NEDD4-2 were identified as being significantly up-regulated in the Ad/AH EBNA1 cells, with respective fold changes of 2.18 and 1.73 in comparison to control cells. The expression of these two genes was therefore examined in EBNA1-expressing carcinoma cell lines.

Inhibition of TGFβ signalling in cancer is often acquired progressively as the tumour advances and generally confers resistance to TGFβ-mediated cytostatic effects (Roberts and Wakefield, 2003). Several potential mechanisms have been proposed for this effect, including down-regulation or loss of TGFβ receptor expression, and increased production of TGFβ ligands, both of which have been associated with a higher risk of developing invasive and metastatic traits, and inversely correlated with clinical stage (Kang, 2006, Diamond et al., 2008, Peng et al., 2006). Each of these features will be addressed in this chapter.

TGFβ receptors, in particular TβRII, are frequently lost or down-regulated in several cancers, including oesophageal squamous cell carcinoma, renal cell carcinoma, gastric cancer, lung cancer, prostate cancer and breast cancer (Fukai et al., 2003, Peng et al., 2006, Miyajima et al., 2003, Tateishi et al., 2000, Osada et al., 2001, Yamashita et al., 2008b, Park et al., 2002), although mutations have been the most extensively studied in colorectal cancer (Grady et al., 1999, Biswas et al., 2008). This loss of TβRII is thought to accelerate TGFβ-associated malignant changes, as is evidenced by the introduction of a dominant negative TβRII construct into the transgenic adenocarcinoma of mouse prostate (TRAMP) *in vivo* model (Pu et al., 2009). Multiple mechanisms have been proposed including gene silencing through methylation, histone hypoacetylation, reduced or altered binding activities of distinct transcription factors at TβRII gene promoter regions, and post-transcriptional down-regulation of the TβRII protein (Chen et al., 2007, Osada et al., 2001, Yamashita et al., 2008b, Park et al., 2002, Kim et al., 1997, Lee et al., 2007, Fukasawa et al., 2010). Some TβRI mutations have been characterised (Kim and Ahn, 1996, Chen et al., 1998), but are found to be comparatively rare, possibly as the TβRI gene is structurally less susceptible to mutation (Kim et al., 2000).

Tumour cells, particularly of late-stage carcinomas, often secrete higher, non-physiological levels of TGFβ, compared to their normal cell counterparts (Yu et al., 2010b). This over-expression has been reported for many cancer types, including NPC (Xiao et al., 2010), and is strongest in the most advanced stages of malignancies (Miyajima et al., 2003). The effect of this is two-fold; it exhibits autocrine effects, mostly concerning remodelling of the extracellular matrix and augmentation of invasion and metastasis, and also acts in a paracrine manner to modify the neighbouring stroma, evade immunosurveillance, and overall create a microenvironment more conducive to tumour growth (Leivonen and Kähäri, 2007, Teicher, 2007).

It is common to find mutations in the TβRII gene in cells resistant to TGFβ growth inhibition, as shown in human gastric cancer cell lines among many others (Park et al., 1994, Inman and Allday, 2000, Osada et al., 2001, Fukuda et al., 2006). Similarly, the production of TGFβ is often increased once cells are no longer susceptible to its anti-proliferative effects (Gold et al., 2000, Di Bartolo et al., 2008). It follows that the anti-proliferative response can be inversely correlated with malignant potential. The expression levels of both TGFβ receptors and TGFβ ligands, and their putative consequences on cell cycle distribution were therefore studied to determine whether EBNA1 promotes these mechanisms to inhibit TGFβ signalling.

Although the canonical Smad pathway is the most-characterised and commonly enlisted method of relaying TGFβ signals, there is growing evidence to substantiate a role for Smad-independent responses in some aspects of TGFβ signalling (Moustakas and Heldin, 2005). In this scenario, TGFβ is able to establish connections with various other signalling pathways, including the MAPKs, ERK-MAPK, JNK and p38, PI3K/Akt, PP2A and RhoA/Rac/Cdc42

(Funaba et al., 2002, Javelaud and Mauviel, 2005, Massagué and Gomis, 2006, Derynck and Zhang, 2003, Seoane, 2006, Matsuzaki et al., 2009, Nagata et al., 2009). These pathways can function to further fine-tune Smad-dependent responses, but may also occur independently of Smads. For example, TGFβ is able to activate both JNK and p38 by targeting TβRI-associated TRAF6 in a process independent of receptor kinase activity, and resulting in activation of TAK1-mediated pathways leading to apoptosis (Yamashita et al., 2008a, Sorrentino et al., 2008). Non-Smad signalling pathways are reviewed in more detailed in (Zhang, 2009).

Many of these interconnecting signalling pathways have also been implicated in the differential phosphorylation of the R-Smad proteins. Recent evidence suggests that, in addition to the canonical phosphorylation of the Smad proteins within their C-terminal SXSS motif by TβRI, Smads can also be phosphorylated at residues within their divergent serine/threonine linker region (Moustakas et al., 2001) by a variety of kinases, including ERK-MAPK, JNK, p38 MAPK, CDK4 and GSK3 (Matsuzaki and Okazaki, 2006, Matsuzaki et al., 2009, Wang et al., 2009) thus giving rise to different Smad phospho-isoforms, the C-terminally phosphorylated pSmad2/3C and the linker phosphorylated pSmad2/3L. While pSmad2/3C primarily transmits the classical tumour suppressive TGFβ signal (Nagata et al., 2009), linker Smads have been associated with late-stage, more invasive cancers (Matsuzaki and Okazaki, 2006, Matsuzaki et al., 2009). In cancer, oncogenic Ras mutations can play a predominant role in this effect. Hyperactive Ras has been reported to activate both ERK and JNK pathways (Kretzschmar et al., 1999, Sekimoto et al., 2007), and this can override canonical TGFβ signalling by promoting Smad2/3 linker phosphorylation. Work presented here tested the hypothesis that EBNA1 may be able to enlist other signalling pathways so as to modulate Smad activity.

To conclude, work was extended to the more relevant NPC model cell line, C666-1, fortuitously found to consistently carry EBV genomes in long-term culture and to resemble an EBV latency II pattern of gene expression (Cheung et al., 1999). Innate defective TGFβ signalling within this cell line is thought to be a consequence of an absence in expression of TβRII (Wood et al., 2007). TGFβ signalling was also investigated in the highly TGFβ-sensitive Mv1Lu mink lung epithelial cell line, with the aim of highlighting any common mechanisms employed by EBNA1 in dysregulation of the pathway.

3.2 EBNA1 modulates the canonical TGFβ signalling pathway

3.2.1 The level of EBNA1 expression in Ad/AH EBNA1 cl8 cells is more physiologically relevant than that in Ad/AH EBNA1 cl3 cells

Initial experiments were designed to confirm the previously observed effects of EBNA1 on TGFβ signalling (Wood et al., 2007). However, in the aforementioned study, the clone used, Ad/AH EBNA1 clone 3, was found to express higher levels of EBNA1 than those observed in stable, latently infected Ad/AH cells, or in the EBV-positive NPC cell line, C666-1. With this in mind, it was decided to perform Affymetrix gene expression profiling on an additional clone, Ad/AH EBNA1 clone 8, which expressed physiological levels of EBNA1 (Owen et al., 2010, Valentine et al., 2010). The EBNA1 expression levels of these cells, when compared to a variety of EBV-infected epithelial and B cell lines was examined by immunoblotting analysis (Figure 3.1A). It is evident that the level of EBNA1 expressed in the EBNA1 clone 8 cells more closely resembles expression levels not only of Ad/AH cells latently infected with wild-type recombinant EBV (rEBV), but also levels in C666-1 cells and EBV-transformed LCLs.

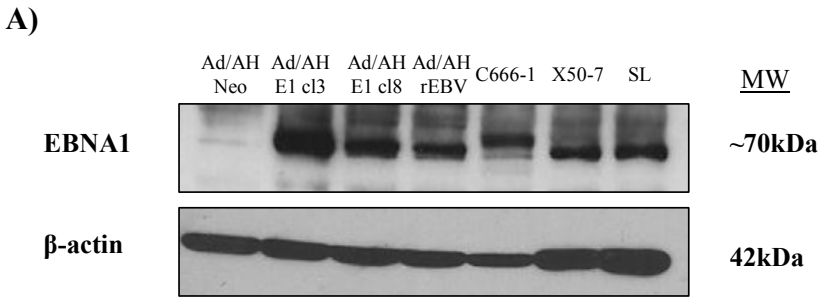

Figure 3.1: EBNA1 is expressed at physiological levels in Ad/AH EBNA1 clone 8 cells and has similar effects to clone 3 cells on TGFβ signalling

A) Immunoblotting for levels of EBNA1 protein in Ad/AH Neo, Ad/AH EBNA1 clone 3, Ad/AH EBNA1 clone 8, Ad/AH rEBV, the EBV-positive C666-1 and the lymphoblastoid cell lines X50-7 and SL (immortalised with the B95-8 strain of EBV). β-actin was included as a loading control The larger size of C666-1 EBNA1 is presumably due to a larger gly-ala repeat in this strain of EBV.

B) Immunoblotting for protein levels of total and serine 465/467 phosphorylated form of Smad2, and total and serine 423/425 phosphorylated form of Smad3, in serum-starved Ad/AH Neo, Ad/AH EBNA1 clone 3, Ad/AH EBNA1 clone 8 and Ad/AH rEBV cells, under basal conditions or following stimulation with 5ng/ml recombinant hTGFβ1 for 24 hours. β-actin was included to confirm equal protein loading

C) Immunoblotting for total Smad2 protein levels over a 12-hour time-course following cycloheximide treatment of Ad/AH Neo, Ad/AH EBNA1 clone 8 and Ad/AH rEBV cells, with β-actin included to confirm equal protein loading.

B)

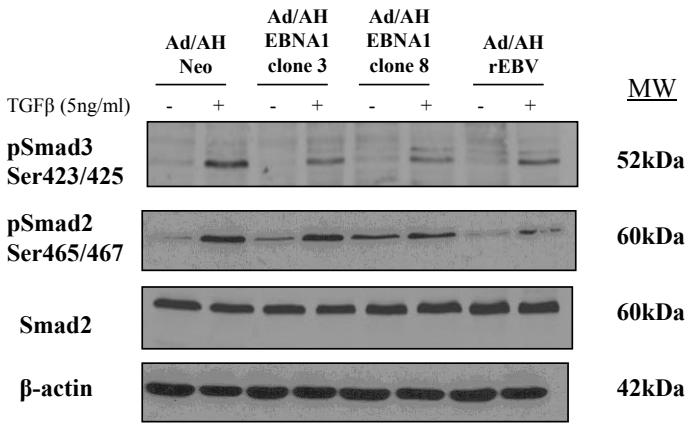
Ad/AH Neo
Ad/AH EBNA1 clone 3
Ad/AH EBNA1 clone 8
Ad/AH rEBV
MW
TGFβ (5ng/ml)
- + - + - + - +
pSmad3 Ser423/425
52kDa
pSmad2 Ser465/467
60kDa
Smad2
60kDa
β-actin
42kDa

C)

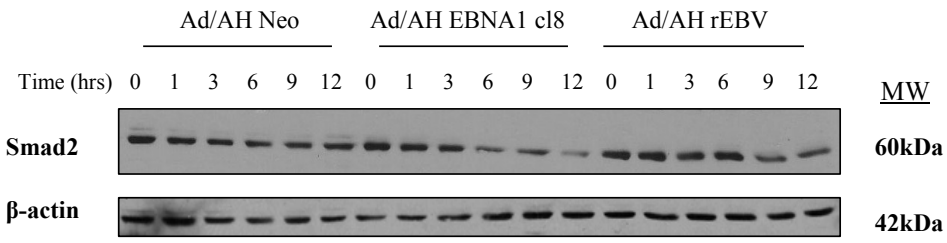
Ad/AH Neo
Ad/AH EBNA1 cl8
Ad/AH rEBV
Time (hrs) 0 1 3 6 9 12 0 1 3 6 9 12 0 1 3 6 9 12
MW
Smad2
60kDa
β-actin
42kDa

3.2.2 EBNA1 inhibits Smad2 and Smad3 SSXS motif phosphorylation in response to TGFβ and enhances Smad2 degradation

A decline in levels of phosphorylated, and therefore active, Smad2 (pSmad2) was reported to be a key feature of the abrogated TGFβ response (Wood et al., 2007). Indeed it seems important in several cancers, including head and neck squamous cell carcinoma (HNSCC) and oesophageal squamous cell carcinoma (OSCC), where a lack of pSmad2 was positively correlated with tumour progression, whereas the loss of total Smad2 appeared much less common (Muro-Cacho et al., 2001, Fukuchi et al., 2006).

To confirm this observation and determine whether Ad/AH EBNA1 clone 8 cells displayed the same trend, levels of the phosphorylated forms of both TGFβ-specific R-Smads were measured by immunoblotting. As is evident from Figure 3.1B, the reduction in the TGFβ-induced phosphorylated forms of Smad2 (pSmad2 Ser465/467) was confirmed in both EBNA1-expressing clones and in the rEBV-infected cell line. Expression of the phosphorylated form of Smad3 (pSmad3 Ser423/425) was also found to be reduced in both EBNA1-expressing and rEBV-infected cell lines, further expanding the initial finding.

Additionally, a time-course of treatment with the protein synthesis inhibitor cycloheximide was carried out in Neo control, EBNA1 clone 8 and rEBV-infected Ad/AH cells to examine the half-life of the Smad2 protein. Subsequent examination of the Smad2 protein levels by immunoblotting (shown in Figure 3.1C), confirmed increased turnover of Smad2 in Ad/AH EBNA1 clone 8 cells compared to Ad/AH Neo controls.

3.2.3 Smad2- and Smad3-specific TGFβ reporter activity is attenuated in the presence of EBNA1

As final confirmation and justification for the use of Ad/AH EBNA1 clone 8 cells as opposed to the EBNA1-overexpressing clone 3, TGFβ/Smad luciferase reporter activity was also measured. Ad/AH cells stably expressing either EBNA1 or a control neomycin resistance cassette, and cells latently infected with rEBV were transiently transfected with either one of two synthetic TGFβ-responsive luciferase reporters, $p(CAGA)_{12}$-Luc and $p(ARE)_3$-Luc, or the p3TP-lux reporter containing fragments of the PAI-1 promoter. Cells used to measure $p(ARE)_3$-Luc reporter activity were additionally transfected with the Xfast1 transcription factor, which is essential for mediating Smad2 DNA binding (Chen et al., 1996, Chen et al., 1997). Relative luciferase activity is depicted graphically in Figure 3.2 and represents the mean of three independent experiments. The results show marked reductions of greater than 50% in activity of the TGFβ/Smad-responsive luciferase reporters in Ad/AH EBNA1 and rEBV-infected cells compared to Neo controls for each of the three reporter constructs studied. The capacity of these EBNA1-expressing and rEBV-infected cells to respond to TGFβ was also noticeably reduced, as reflected by much smaller differences between basal and TGFβ1-stimulated levels of reporter activity in these cells in comparison with Neo control cells, supporting a defect specifically in the Smad activation mechanism.

The ability of Ad/AH EBNA1 clone 8 cells to respond in a similar manner to Ad/AH EBNA1 clone 3 cells, whilst expressing more physiological levels of the EBNA1 protein, affirmed the choice to hereafter use only the clone 8 cells, which will from now on be referred to as Ad/AH EBNA1.

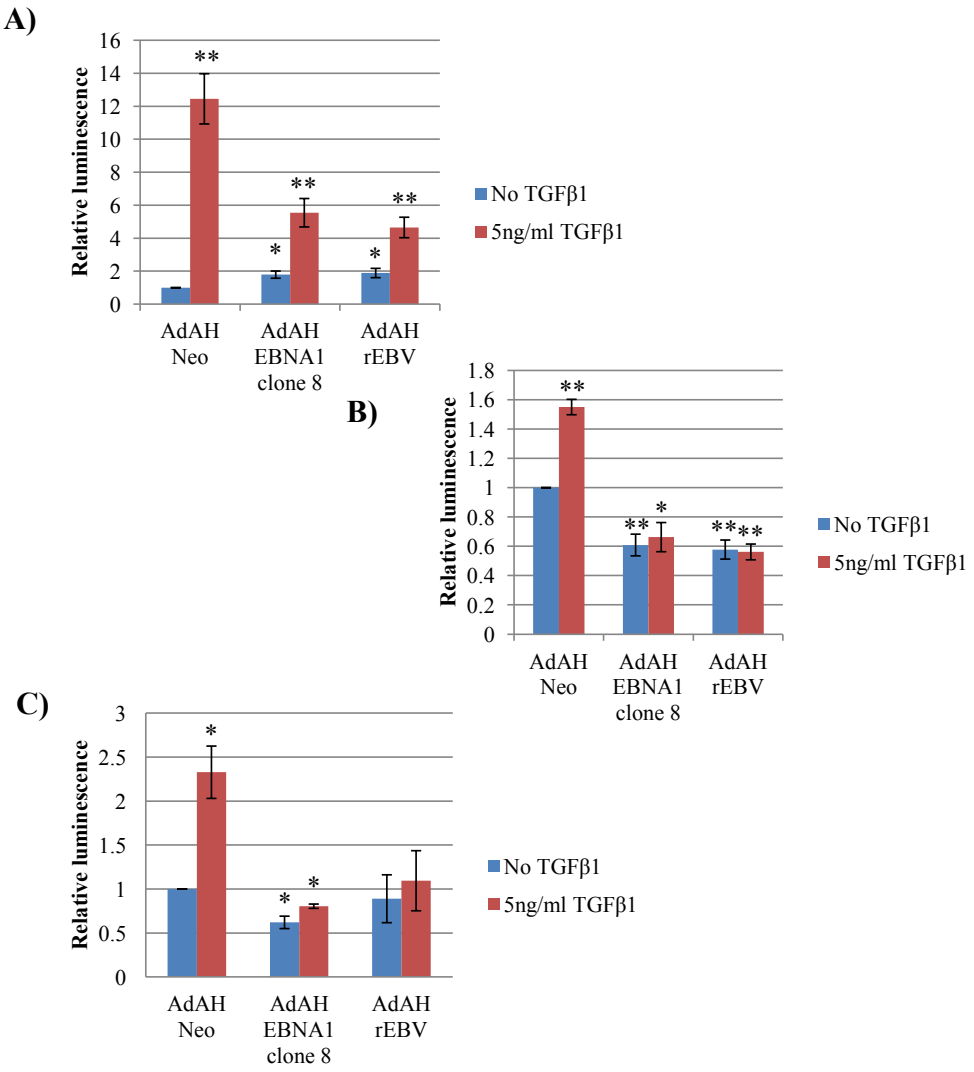

Figure 3.2: The effect of EBNA1 and EBV on TGFβ-induced promoter activity in stable Ad/AH cell lines

Dual luciferase reporter assays showing $p(CAGA)_{12}$-Luc, $p(ARE)_3$-Luc or p3TP-lux luciferase reporter activity in Ad/AH Neo, Ad/AH EBNA1 clone 8 and Ad/AH rEBV cells stimulated with 5ng/ml recombinant hTGFβ1 for 24 hours, or left unstimulated as a control. Histograms are shown to depict the relative luminescence after normalising to Renilla luciferase values and expressing as a ratio of activity relative to the control vector pGL3-basic. Data from three independent experiments is presented as the mean fold differences in activity ± SE, relative to that observed in unstimulated Ad/AH Neo control cells which is given an arbitrary value of 1 (** denotes a P-value <0.01 and * denotes a P-value <0.05).

3.2.4 EBNA1 decreases TGFβ/Smad DNA binding basally and in response to TGFβ

Having confirmed the ability of EBNA1 to attenuate TGFβ/Smad-responsive reporter activity and attenuate Smad activation, the binding of Smad transcriptional mediators to their target DNA sequences was explored. While Smad2 is intrinsically unable to directly bind DNA (Dennler et al., 1999), Smad3 and Smad4 recognise and bind through their MH1 domains (Shi et al., 1998) to an 8bp palindromic sequence (5′-GTCTAGAC-3′) termed the Smad binding element (SBE) (Zawel et al., 1998). To assess whether the observed decrease in TGFβ/Smad-luciferase reporter activity was a direct result of reduced binding at TGFβ-responsive promoter regions, electrophoretic mobility shift assays were performed using a probe specific to the SBE motif, as described in section 2.7.3. Briefly, nuclear extracts were isolated from Neo control, EBNA1-expressing and rEBV-infected Ad/AH cells, and C666-1 cells following stimulation for 1hr with 5ng/ml TGFβ1 to activate the Smad transcriptional response. Nuclear extracts were then incubated with an IRDye®-700 labelled probe specific to the SBE motif and resulting protein:DNA complexes resolved by gel electrophoresis. Binding was measured after scanning of the EMSA gel using an Odyssey® infrared imaging system and quantified by measuring relative fluorescence intensities. Densitometric analysis, represented graphically, along with a representative scanned EMSA gel, are shown in Figure 3.3A. Comparing the binding intensities of nuclear extracts at SBE sequences, it is apparent that protein binding to the SBE probe was significantly increased in response to TGFβ1 stimulation in Neo control cells, whereas binding in both EBNA1 and rEBV-infected Ad/AH cells was substantially reduced, showing only a modest increase in response to TGFβ stimulation. Although not found to be significant, the data suggests reductions of approximately 50% in SBE binding in these cells. Similarly, and significantly, protein binding in nuclear extracts taken from C666-1 cells was reduced down to almost negligible levels and appeared unchanged by the addition of

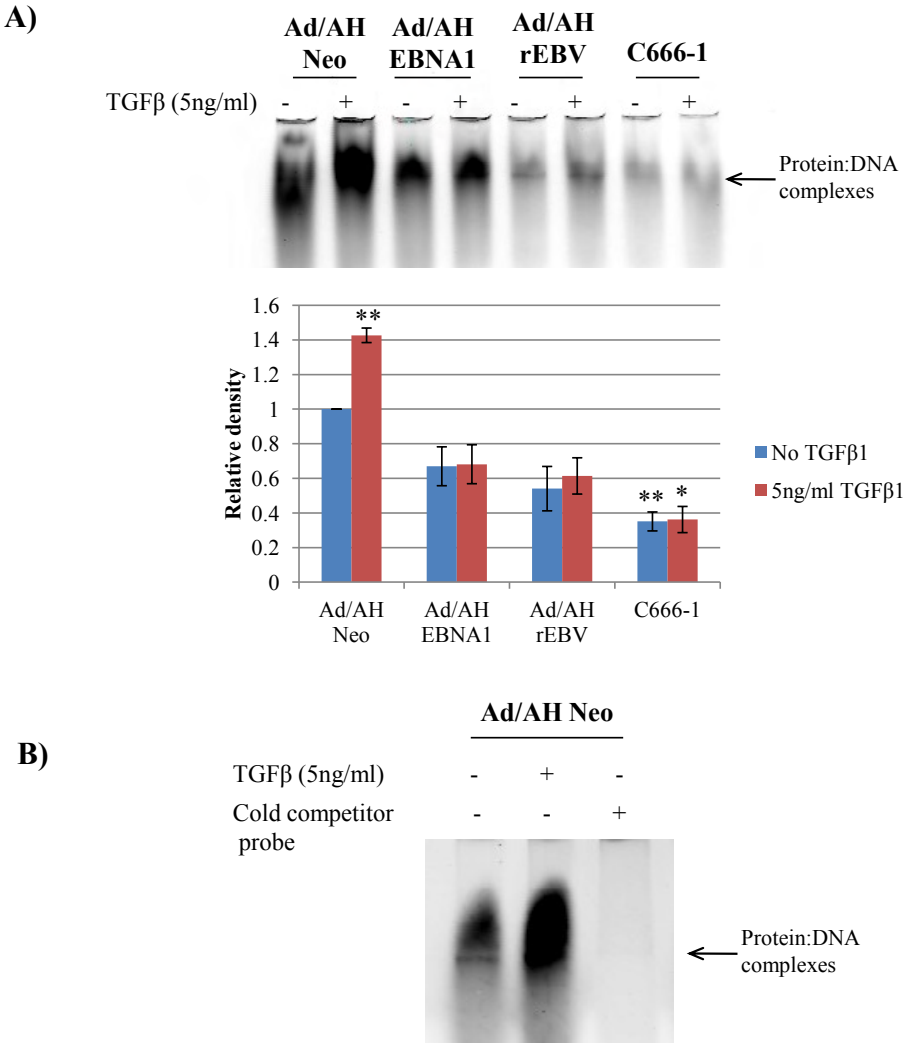

Figure 3.3: The effect of EBNA1 on binding at SBE sites in Ad/AH and C666-1 cells

A) EMSA analysis of SBE sequence binding in serum-starved Neo control, EBNA1-expressing and rEBV-infected Ad/AH cells, and C666-1 cells, under basal conditions and in response to stimulation with 5ng/ml recombinant hTGFβ1 for 1 hour. Densitometry was performed on three independent experiments, and a histogram created depicting mean differences in binding affinities SE, between cell types with and without stimulation (** denotes a P-value <0.01 and * denotes a P-value <0.05). A representative image of the infrared scanning is shown.

B) EMSA analysis was repeated in the Ad/AH Neo control cells including an additional incubation step with a 100-fold excess of non-labelled SBE probe which functions as a cold competitor prior to incubation with the IRDye-700® end-labelled version.

exogenous TGFβ1. This supports a hypothesis that an abrogation of Smad binding at TGFβ target gene promoters may largely contribute to the observed attenuation in TGFβ activity in these cells. To confirm the high degree of specificity of the EMSA assay, extracts from the control cells were additionally incubated with a 100-fold excess of unlabelled probe prior to incubation with the IRDye-700® labelled version. A representative experiment, Figure 3.3B, shows complete abrogation of probe binding.

3.2.5 Screening of Ad/AH EBNA1 Affymetrix Array data for Smad negative regulators

With a view to ascertaining how EBNA1 might adversely influence TGFβ signalling, a list of acknowledged putative negative regulators of the TGFβ signalling pathway was used to interrogate gene expression microarray data of Ad/AH cells stably expressing EBNA1. Of these, PPM1A and NEDD4-2 were identified as potential candidates.

3.2.5.1 EBNA1 increases the expression of the Smad-specific phosphatase PPM1A in carcinoma cell lines and NPC biopsies

PPM1A (protein phosphatase, Mg^{2+}/Mn^{2+} dependent, 1A) has recently been identified as a Smad-specific phosphatase, and is able to specifically dephosphorylate active Smad2 and Smad3 (pSmad2/3), inducing subsequent nuclear export, and hence acting to terminate the TGFβ-induced signal (Lin et al., 2006). RNA and protein samples were extracted from panels of Ad/AH and HONE-1 cells expressing either the neomycin resistance cassette, EBNA1, or stably infected with rEBV. RT-PCR, QPCR and immunoblotting techniques were employed to analyse the levels of PPM1A RNA and protein. As shown in Figure 3.4, compared to Neo control cells, the levels of PPM1A mRNA and protein were increased in both Ad/AH and HONE-1 cells expressing EBNA1 or stably infected with rEBV. QPCR analysis, represented

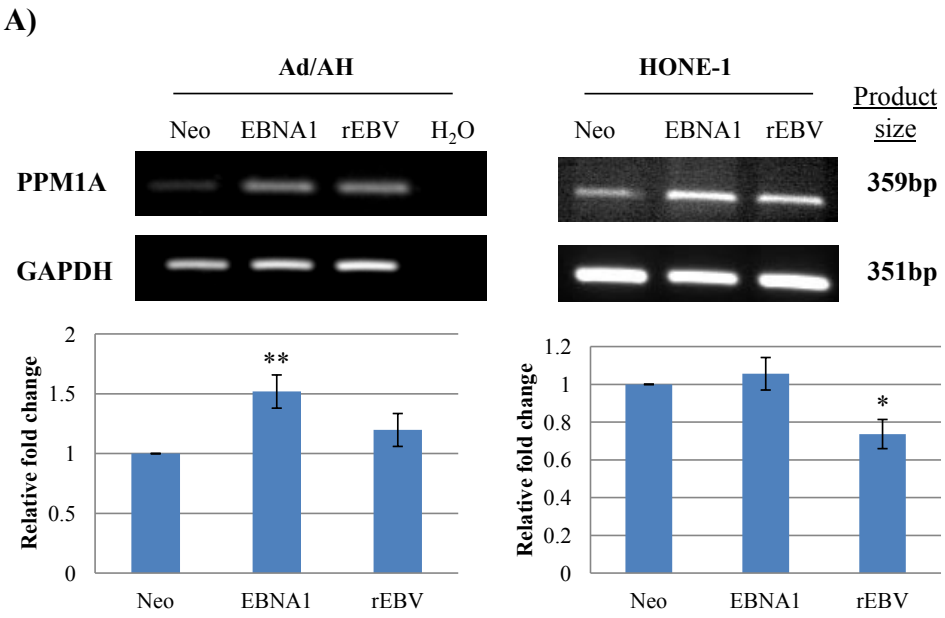

Figure 3.4: PPM1A expression in Ad/AH and HONE-1 carcinoma cell lines

A) RT-PCR analysis of PPM1A mRNA levels in Ad/AH and HONE-1 cells expressing either a control neomycin resistance cassette or EBNA1, or stably infected with rEBV. The housekeeping gene GAPDH was included as a positive control to confirm equal RNA input into the PCR reactions, while negative water controls confirmed the absence of contamination. QPCR analysis for PPM1A mRNA is also shown, in which GAPDH was included as an internal baseline control. Histograms are shown displaying the mean fold change differences SE (n=4) relative to Neo control cells (** denotes a P-value <0.01 and * denotes a P-value <0.05).

B) QPCR analysis was repeated in serum-starved Neo control, EBNA1-expressing and rEBV-infected Ad/AH cells either stimulated with 5ng/ml recombinant hTGFβ1 for 24 hours or left unstimulated as a control. Again, the histogram shows the mean fold change differences SE (n=4) relative to unstimulated Neo control cells (** denotes a P-value <0.01 and * denotes a P-value <0.05).

C) Immunoblotting for levels of PPM1A protein in Ad/AH and HONE-1 cells expressing either a neomycin resistance cassette, or EBNA1, or stably infected with rEBV, with β-actin included to confirm equal protein loading.

B)

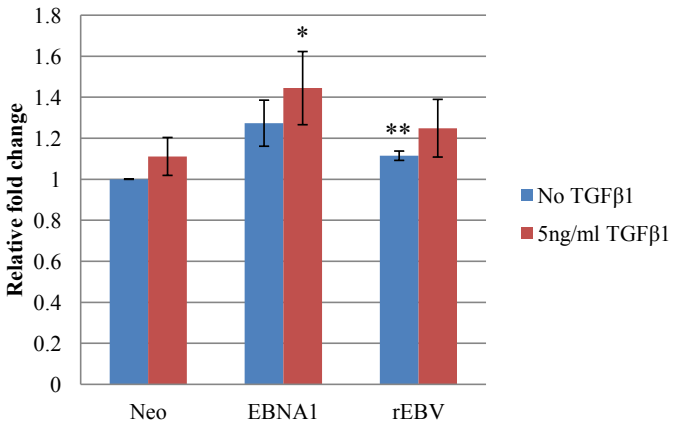
1.8
1.6
1.4
1.2
1
0.8
0.6
0.4
0.2
0
Relative fold change
*
**
Neo
EBNA1
rEBV
No TGFβ1
5ng/ml TGFβ1

C)

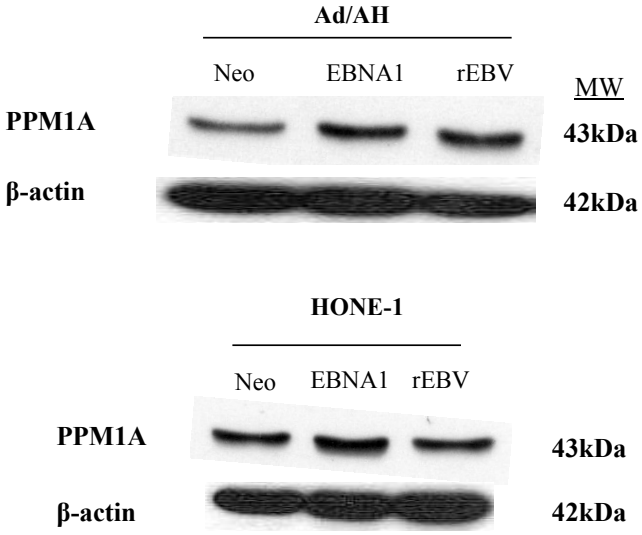
Ad/AH
Neo
EBNA1
rEBV
MW
PPM1A
43kDa
β-actin
42kDa
HONE-1
Neo
EBNA1
rEBV
PPM1A
43kDa
β-actin
42kDa

in Figure 3.4A, indicates that, basally, EBNA1 induced a significant approximate 1.5-fold increase in PPM1A expression whilst a 1.2-fold increase was observed in rEBV-infected Ad/AH cells. As shown in Figure 3.4B, TGFβ stimulation did not markedly alter the expression of PPM1A, findings that are in broad agreement with the observations of others (Lin et al., 2006), showing that PPM1A is itself not a TGFβ-regulated gene. In HONE-1 cells, despite an apparent upregulation of PPM1A mRNA by RT-PCR in EBNA1-expressing cells (Figure 3.4A), QPCR failed to detect a significant change. However, immunoblotting indicated that the protein level was increased in these cells (Figure 3.4C), which may reflect an increase in PPM1A protein stability or altered turnover. However, this finding could not be replicated in the EBV-infected HONE-1 cells.

Immunofluorescence staining of Neo control, EBNA1 and rEBV-infected Ad/AH cells was performed to examine the expression of PPM1A, Smad2 and Smad3 at the single cell level, using a rabbit polyclonal antibody to PPM1A, and mouse monoclonal antibodies to Smad2 and Smad3, followed by subsequent detection with Alexa-Fluor® 546-conjugated goat anti-rabbit and Alexa-Fluor® 488-conjugated goat anti-mouse Ig. Representative confocal images, in Figure 3.5, show increased levels of nuclear PPM1A in EBNA1-expressing cells compared to their Neo control counterparts and, in addition, show an overall increase in colocalisation of PPM1A with both Smad2 (Figure 3.5A) and Smad3 (Figure 3.5B). Surprisingly however, this phenomenon was not replicated in the rEBV-infected cells.

Further examination of the expression levels in the *in vivo* context allows increased significance to be attributed to these findings in the context of NPC pathogenesis. The GCOS graph derived from normalised PPM1A expression levels in four normal and 15 NPC tumour

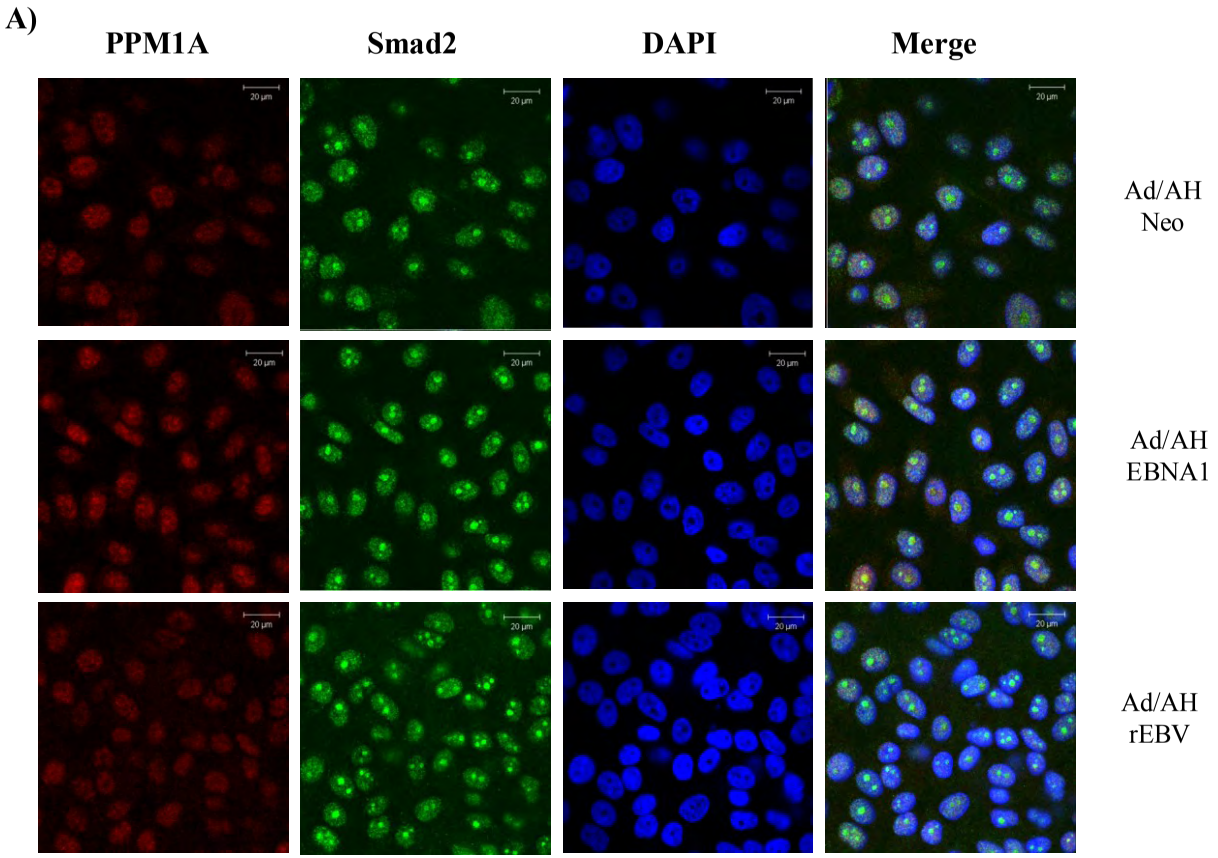

Figure 3.5: Immunofluorescence staining of PPM1A and R-Smads in Ad/AH cells
Immunofluorescence staining for expression of PPM1A and either A) Smad2 or B) Smad3 protein in Ad/AH cells expressing either a control neomycin resistance cassette or EBNA1, or infected with rEBV. DAPI staining is included to stain cellular nuclei. Representative confocal images are shown. Bar = 20μm.

B)

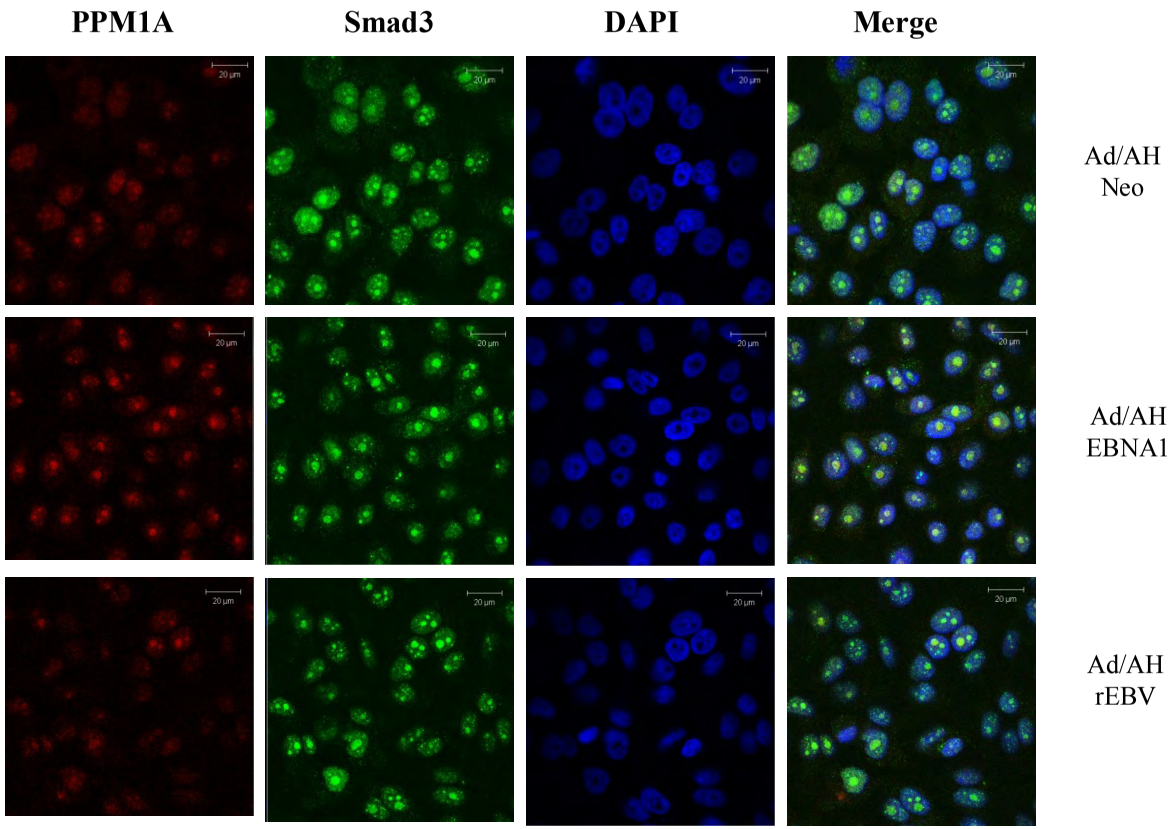

samples plus the C666-1 EBV-positive NPC cell line can be seen in Figure 3.6, and demonstrates an increase in PPM1A mRNA expression in 6/16 (38%) NPC tumours compared to normal epithelia (data kindly provided by Dr. J. Arrand, University of Birmingham).

3.2.5.2 Validation of PPM1A shRNA vectors

To further explore the possibility that EBNA1 may increase the expression of PPM1A as a mechanism to downregulate TGFβ signalling, it was hypothesised that shRNA-mediated knockdown of PPM1A in EBNA1-expressing cells might restore TGFβ responsiveness. A shRNA construct specific for PPM1A (pSRG-shPPM1A881) was kindly provided by Professor Xin-Hua Feng, Baylor College of Medicine, and was tested to confirm its ability to reduce PPM1A expression *in vitro*. Initially, the optimal conditions for shRNA knockdown were determined by transient transfection of increasing concentrations of the pSRG-shPPM1A881 vector into Ad/AH cells. The level of PPM1A mRNA and protein was then examined 24 and 48 hours later by RT-PCR (Figure 3.7A), and 24, 48 and 72 hours post-transfection by immunoblotting (Figure 3.7B). Compared to cells transfected with the empty vector, pSRG, a marked decrease in PPM1A mRNA and protein expression was observed in cells transfected with the shPPM1A881 plasmid; the most pronounced results were observed after 48 hours at the mRNA level, whereas a reduction in protein was more pronounced after 72 hours. QPCR of cDNA samples derived from RNA extracted 48 hours post-transfection into Ad/AH stable cell lines confirmed that PPM1A knockdown could also be achieved in the presence of stable EBNA1 expression. As can be seen from Figure 3.7C, PPM1A mRNA levels were significantly reduced by greater than half by the introduction of the PPM1A shRNA into Ad/AH Neo, EBNA1 and rEBV-infected cells.

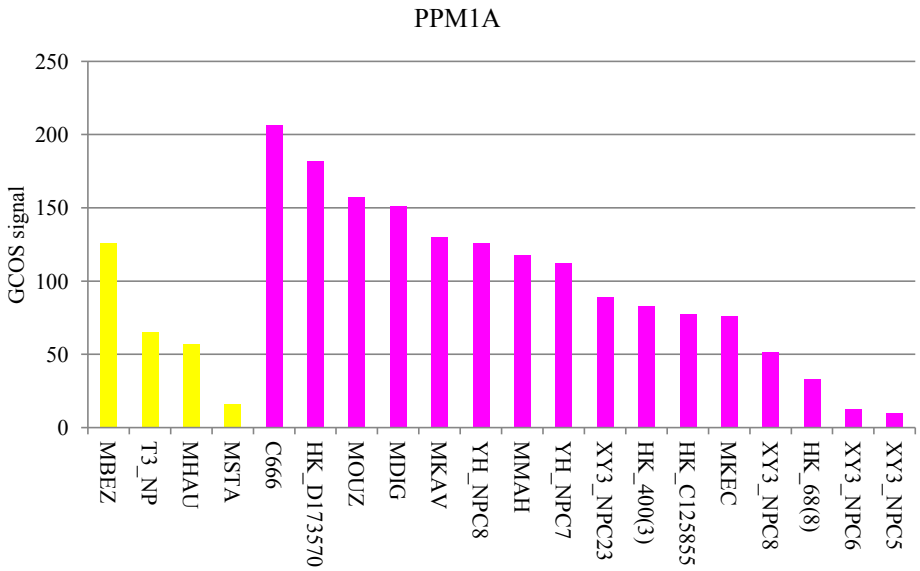

Figure 3.6: PPM1A expression in EBV-positive NPC tumour cells
Existing expression array data analysed using GCOS (Affymetrix) was probed for PPM1A expression levels. Normalised expression array intensities for 4 normal samples (yellow) and 15 NPC tumours plus the C666-1 EBV-positive NPC cell line (pink) are shown.

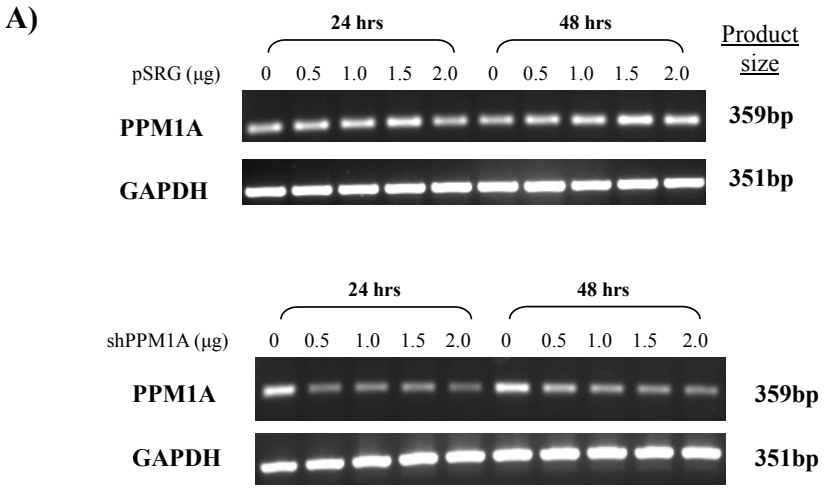

Figure 3.7: Validation of PPM1A shRNA construct

A) RT-PCR analysis for PPM1A mRNA levels in Ad/AH cells transiently transfected with increasing concentrations of either the shPPM1A881 construct or pSUPER.retro (pSRG) control vector, measured 24 and 48 hours post-transfection. GAPDH was included as a positive control.

B) Immunoblotting for levels of PPM1A protein in Ad/AH cells transiently transfected with increasing concentrations of either the shPPM1A881 construct or pSUPER.retro (pSRG) control vector, measured 24, 48 and 72 hours post-transfection. Blots were re-probed for β-actin to confirm equal protein loading.

C) QPCR analysis for PPM1A mRNA levels in Ad/AH cells expressing either the control neomycin resistance cassette or EBNA1, or infected with rEBV, transiently transfected with either the shPPM1A881 or control pSRG vector, and stimulated with 5ng/ml recombinant hTGFβ1 for 24 hours, or left unstimulated as a control. GAPDH was included as an internal baseline control. A histogram is shown displaying the mean fold change differences SE (n=3) relative to Neo control cells transfected with control vector (** denotes a P-value <0.01 and * denotes a P-value <0.05).

B)

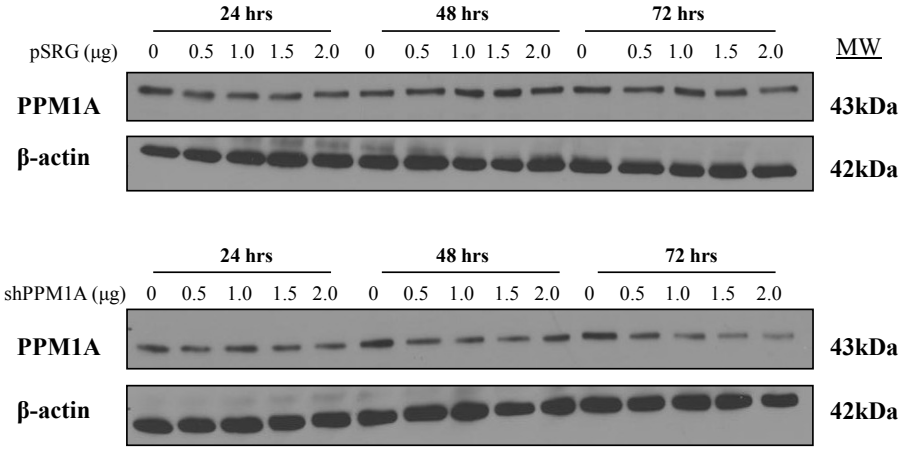
24 hrs
48 hrs
72 hrs
pSRG (μg) 0 0.5 1.0 1.5 2.0 0 0.5 1.0 1.5 2.0 0 0.5 1.0 1.5 2.0
MW
PPM1A
43kDa
β-actin
42kDa
24 hrs
48 hrs
72 hrs
shPPM1A (μg) 0 0.5 1.0 1.5 2.0 0 0.5 1.0 1.5 2.0 0 0.5 1.0 1.5 2.0
PPM1A
43kDa
β-actin
42kDa

C)

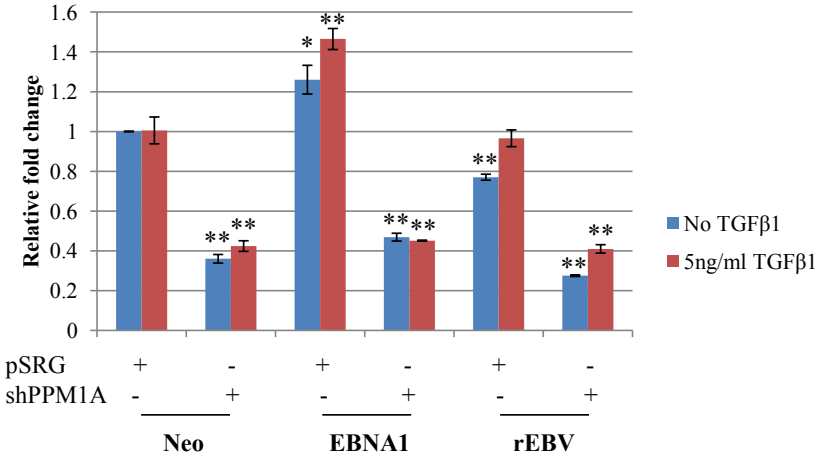
Relative fold change
1.6
1.4
1.2
1
0.8
0.6
0.4
0.2
0
No TGFβ1
5ng/ml TGFβ1
pSRG + - + - + -
shPPM1A - + - + - +
Neo
EBNA1
rEBV

3.2.5.3 RNAi-mediated knockdown of PPM1A in EBNA1-expressing cells does not significantly restore TGFβ activity

Once the conditions required for successful knockdown of PPM1A had been established, the biological consequences of this were investigated. Neo control, EBNA1 and rEBV-infected Ad/AH cells were transiently transfected with either the shPPM1A881 or pSRG control vector, and the $p(CAGA)_{12}$-Luc and Renilla luciferase reporter constructs. 48 hours post-transfection, cells were either left untreated, or stimulated with 5ng/ml TGFβ for 24 hours. Cells were then assayed for luciferase reporter activity at a time, 72 hours, when maximal silencing of PPM1A had been achieved. Figure 3.8 represents the mean of three independent experiments, and shows that PPM1A knockdown only marginally increased the levels of $p(CAGA)_{12}$-Luc activity in EBNA1-expressing and rEBV-infected cells, and did not significantly restore TGFβ reporter activity.

3.2.5.4 EBNA1 increases the expression of PPM1B

The closely related phosphatase PPM1B (protein phosphatase, Mg^{2+}/Mn^{2+} dependent, 1B) has also been identified as exhibiting Smad specificity but is thought to play a less prominent role owing to its comparatively more cytoplasmic localisation (Lin et al., 2006). However, both PPM1A and PPM1B have been reported to negatively affect the phosphorylation of IKKβ in canonical TNFα-induced NFκB signalling (Sun et al., 2009), and so it was hypothesised that the two phosphatases may function in a similar fashion to effectively modulate Smad phosphorylation status. Expression of PPM1B transcripts in the Ad/AH cell panel was investigated using RT-PCR, and demonstrated an increase in PPM1B expression in both EBNA1-expressing and rEBV-infected Ad/AH cells (Figure 3.9A). In the HONE-1 cell line, an increase in mRNA level in EBNA1-expressing cells was also observed, yet no increase in

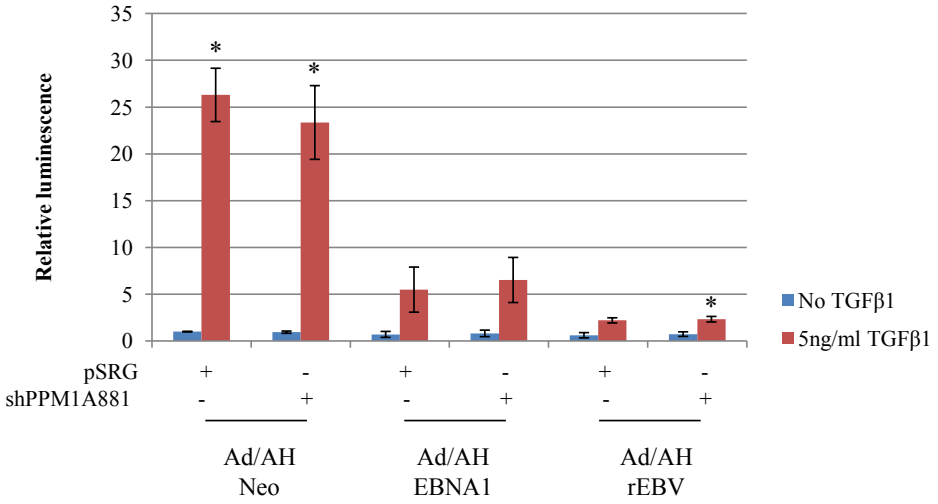

Figure 3.8: The effect of shRNA-mediated knockdown of PPM1A on TGFβ promoter activity in Ad/AH cells
Dual luciferase reporter assay showing p(CAGA)$_{12}$-Luc activity in Ad/AH Neo, Ad/AH EBNA1 and Ad/AH rEBV cells transiently transfected with either the shPPM1A881 or pSUPER.retro (pSRG) control vectors, measured under basal conditions and in response to stimulation with 5ng/ml recombinant hTGFβ1 for 24 hours. A histogram is shown to depict the relative luminescence after normalising to Renilla luciferase values and expressing as a ratio of activity relative to the control vector pGL3-basic. Data from three independent experiments is presented as the mean fold differences in activity ± SE, relative to that observed in unstimulated Ad/AH Neo control cells transfected with control vector, which is given an arbitrary value of 1 (* denotes a P-value <0.05).

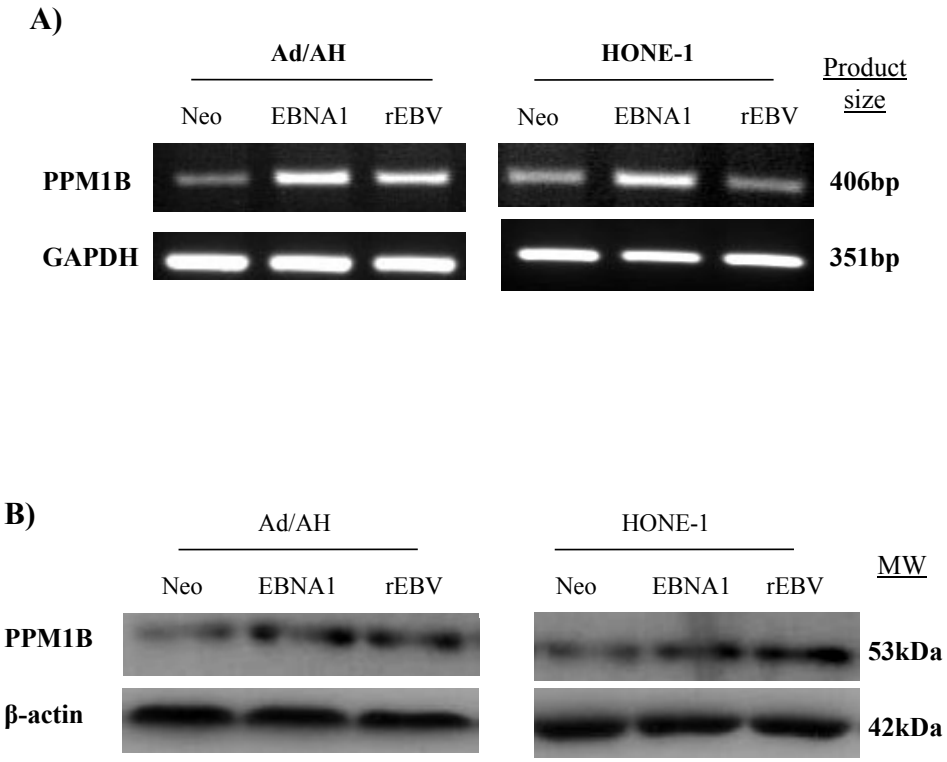

Figure 3.9: PPM1B expression in Ad/AH and HONE-1 carcinoma cell lines

A) RT-PCR analysis for PPM1B mRNA levels in Ad/AH and HONE-1 cells expressing either a control neomycin resistance cassette or EBNA1, or stably infected with rEBV. GAPDH was included as a positive control to confirm equal RNA input into the PCR reactions, while negative water controls confirmed the absence of contamination.

B) Immunoblotting for levels of PPM1B protein in Ad/AH and HONE-1 cells expressing either a neomycin resistance cassette, or EBNA1, or stably infected with rEBV, with β-actin included to confirm equal protein loading.

mRNA expression was observed in rEBV-infected HONE-1 cells. However, protein levels appeared to be increased in EBNA1-expressing and rEBV-infected cells in both cell panels (Figure 3.9B). Subsequent data mining of the NPC gene expression data revealed a significant upregulation of PPM1B transcripts in approximately 13/16 (81%) NPC tumours compared to normal epithelia (Figure 3.10).

3.2.5.5 Validation of PPM1B shRNA oligonucleotides

To further investigate the actions of this particular phosphatase, shRNA vectors specific for PPM1B were generated. shRNA-encoding oligonucleotide sequences were previously defined by Sun *et al.* (Sun et al., 2009), and were designed accordingly. Following ligation into the linearised pSUPER.retro.puro vector and transformation of chemically competent cells, clones for each vector were selected and double restriction digests were performed using *Eco*RI and *Hind*III enzymes to confirm the correct insertion of the shPPM1B sequences. As shown in Figure 3.11, reactions A, C and D for shPPM1B-1, and B and C for shPPM1B-2 contained the 281bp fragment indicative of positive clones. DNA sequencing was then used to confirm precise and error-free cloning. Representative traces of the sequencing outputs are shown in Figure 3.12.

To validate the functionality of the two PPM1B shRNAs, the vectors were transiently transfected into Ad/AH cells, and immunoblotting performed at 24-hour, 48-hour and 72-hours post-transfection. Representative immunoblots are shown in Figure 3.13. While, as expected, the control pSUPER.retro.puro vector did not affect PPM1B expression levels, there were no marked differences in the levels of PPM1B protein expression in response to increasing concentrations of either shRNA at any of the given timepoints, except for a

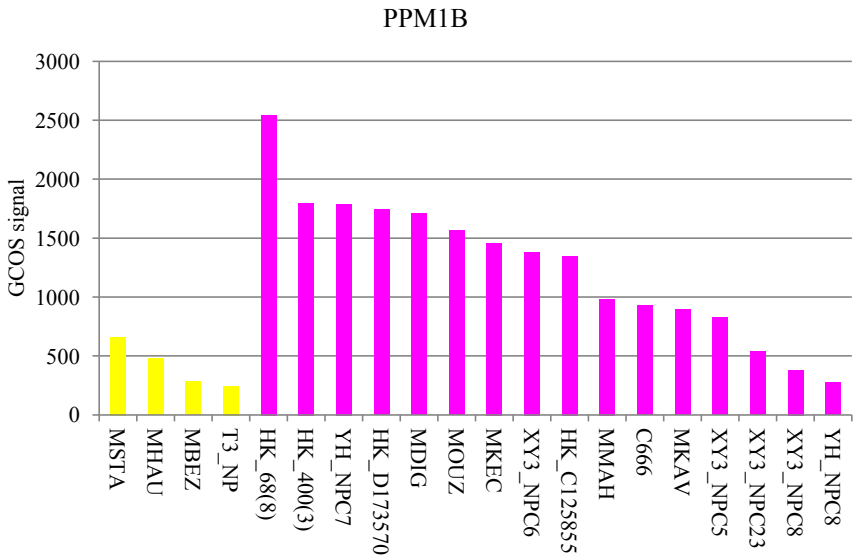

Figure 3.10: PPM1B expression in EBV-positive NPC tumour cells
Existing expression array data analysed using GCOS (Affymetrix) was probed for PPM1B expression levels. Normalised expression array intensities for 4 normal samples (yellow) and 15 NPC tumours plus the C666-1 EBV-positive NPC cell line (pink) are shown.

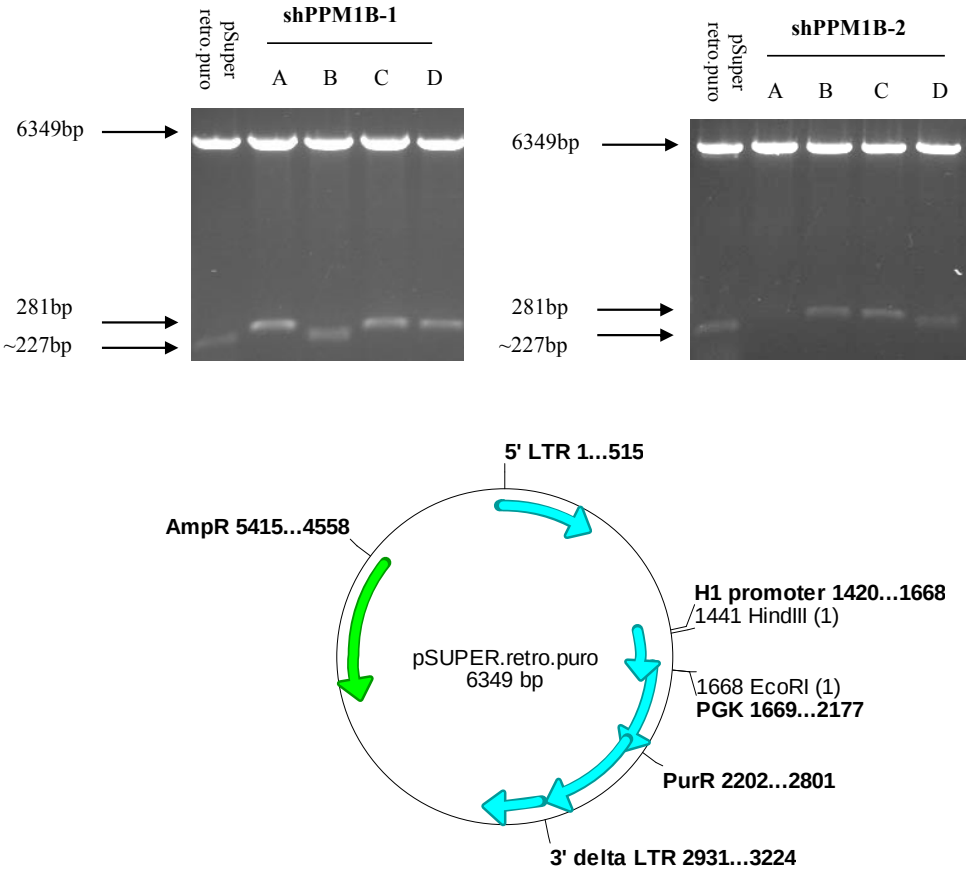

Figure 3.11: Restriction digestion to confirm the presence of the correct shPPM1B insert within recombinant pSUPER.retro vectors
Diagnostic *Eco*RI and *Hind*III restriction digestions were performed on plasmid DNA extracted from selected clones to validate the insertion of the annealed shPPM1B oligonucleotides into the pSUPER.retro plasmid. The empty pSUPER.retro vector was included as a control for efficient enzyme cutting. Reactions were analysed by gel electrophoresis. The 6349bp fragment represents the pSUPER.retro vector. The 281bp fragment identifies positive clones carrying the oligonucleotide insert, while the ~227bp fragment is indicative of negative clones. Two different oligonucleotide pairs were tested (shPPM1B-1 and shPPM1B-2). A plasmid map of pSUPER.retro.puro, highlighting its key features and generated using ApE Plasmid Editor software, is shown, adapted from the map found at: http://www.oligoengine.com/products/psuper/documentation/maps/pSUPER_retro_puro_map.pdf

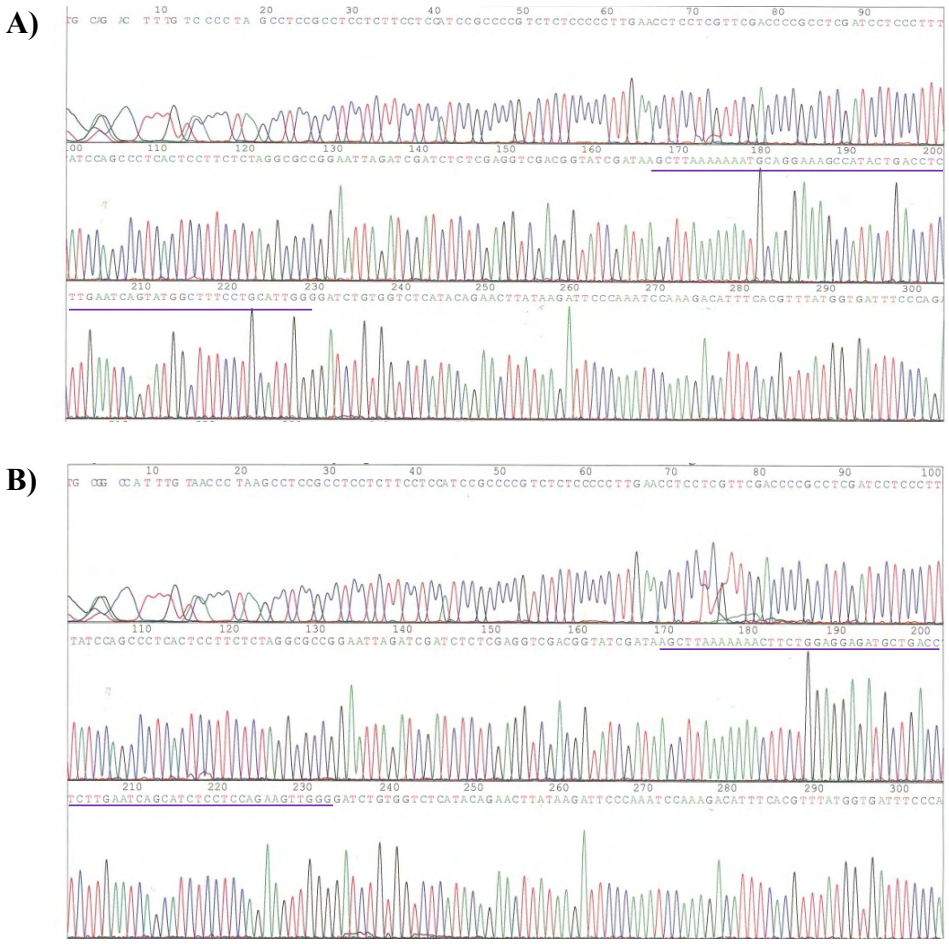

Figure 3.12: Sequencing reactions to confirm the presence of the correct shPPM1B insert within recombinant pSUPER.retro vectors

The ABI Prism 310 protocol was used to sequence the predicted positives generated from the cloning of shPPM1B oligonucleotide sequences into the pSUPER.retro vector. The output of the sequencing reaction was visualised using the Chromas program and schematic representations for shPPM1B-1 (A) and shPPM1B-2 (B) are shown. Each peak represents a discrete signal from each base of the analysed sequence (red = thymine, green = adenine, blue = cytosine and black = guanine). The shRNA sequences are underlined in purple.

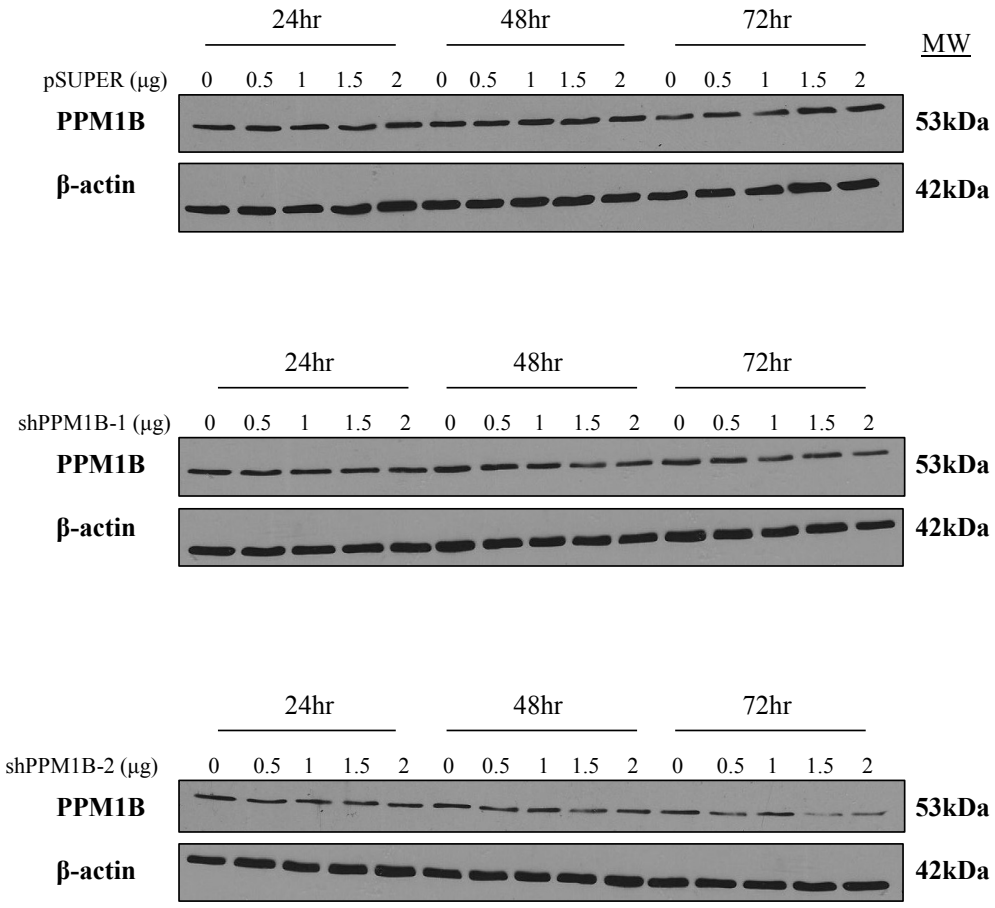

Figure 3.13: Validation of PPM1B shRNA constructs
Immunoblotting for levels of PPM1B protein on lysates collected from Ad/AH cells 24, 48 and 72 hours after transient transfection with increasing concentrations of either of the two shPPM1B constructs (shPPM1B-1 or shPPM1B-2) or the pSUPER.retro control vector. Blots were re-probed for β-actin to confirm equal protein loading.

marginal knockdown after 72hours with 1.5 and 2μg of shPPM1B-2. The time-course was therefore extended to 120 hours, where the 2μg shRNA concentration dramatically reduced PPM1B expression for both constructs (Figure 3.14). Efficient knockdown was also accomplished with 2μg shPPM1B-2 after 96 hours. As the effect was more dramatic using shPPM1B-2, this construct was selected for use in subsequent experiments.

3.2.5.6 Dual knockdown of PPM1A and PPM1B is not sufficient to restore TGFβ activity

It was predicted that, in the absence of one phosphatase, the other may be able to compensate, and therefore the effect of a dual knockdown was studied. shPPM1A881 and shPPM1B-2 constructs were transfected, both individually, and in combination, into Neo control, EBNA1 and rEBV-infected Ad/AH cells, and the resultant effects on TGFβ signalling determined using TGFβ/Smad luciferase reporter assays. So as to ensure knockdown of both genes, maximal amounts of each were used for transfection and, after 72 hours, the assay was stimulated for 24 hours with 5ng/ml TGFβ1, and then harvested a total of 96 hours post-transfection. Luciferase activity was measured and normalised data are represented in Figure 3.15. Neither transfection of shPPM1A881 nor shPPM1B 2 alone had a pronounced effect on the levels of TGFβ-induced $p(CAGA)_{12}$-Luc and $p(ARE)_3$-Luc reporter activity in EBNA1-expressing and rEBV-infected Ad/AH cells. However, in combination, shRNA-knockdown of both PPM1A and PPM1B partially restored levels to those observed in the Neo control cells. These observations however were not borne out in the rEBV-infected Ad/AH cells, reflecting also the pattern in PPM1A immunofluorescence staining, suggesting that this mechanism may not be of significant importance in the context of a latent EBV infection.

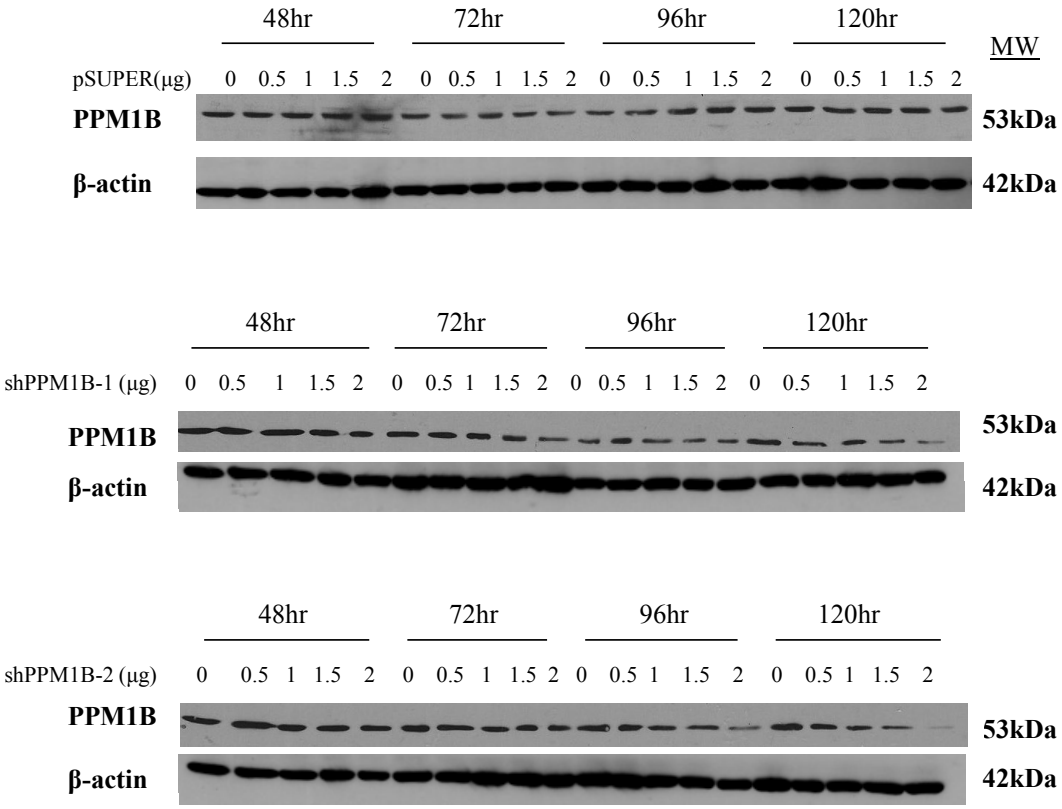

Figure 3.14: Extended time-course of PPM1B knockdown
Immunoblotting for levels of PPM1B protein in Ad/AH cells transiently transfected with increasing concentrations of either of the two shPPM1B constructs (shPPM1B-1 or shPPM1B-2) or the pSUPER.retro control vector, on lysates harvested 48, 72, 96 and 120 hours post-transfection. Blots were re-probed for β-actin to confirm equal protein loading.

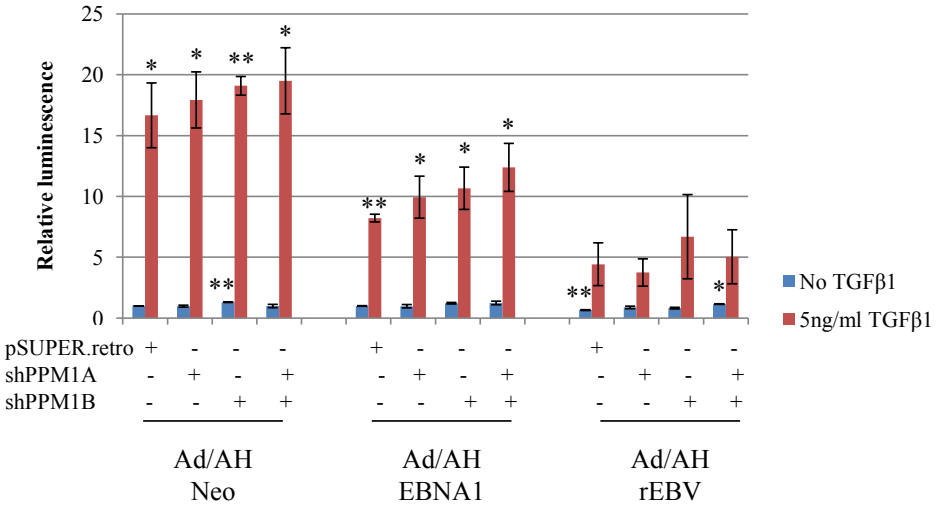

Figure 3.15: The effect of dual shRNA-mediated knockdown of PPM1A and PPM1B on TGFβ promoter activity

Dual luciferase reporter assay showing levels of $p(CAGA)_{12}$-Luc activity in Ad/AH Neo, Ad/AH EBNA1 and Ad/AH rEBV cells transiently transfected with either the control pSUPER.retro, shPPM1A881 or shPPM1B-2 vectors, measured under basal conditions and in response to stimulation with 5ng/ml recombinant hTGFβ1 for 24 hours. Histograms are shown to depict the relative luminescence after normalising to Renilla luciferase values and expressing as a ratio of activity relative to the control vector pGL3-basic. Data from three independent experiments is presented as the mean fold differences in activity $\pm$ SE, relative to that observed in unstimulated Ad/AH Neo control cells transfected with control vector, which is given an arbitrary value of 1 (** denotes a P-value <0.01 and * denotes a P-value <0.05).

3.2.5.7 EBNA1 increases the expression of the E3 ubiquitin ligase NEDD4-2 in carcinoma cell lines and tumour biopsies

Although dephosphorylation is thought to contribute towards dissociation of active Smad complexes in the nucleus, inactivation of the phosphorylated R-Smads is thought to require ubiquitination, which targets them for proteasomal degradation (Lo and Massagué, 1999, Heldin and ten Dijke, 1999, Zhang and Laiho, 2003). Abnormally high expression of a Smad ubiquitin ligase would negatively impact upon Smad stability and thereby contribute to TGFβ pathway inactivation (Lönn et al., 2009), and indeed the observed attenuation of TGFβ signalling in the presence of EBNA1 has previously been attributed to an increase in Smad2 protein turnover (Wood et al., 2007, Flavell et al., 2008). Interrogation of the Affymetrix gene expression array data also identified an up-regulation of the ubiquitin ligase, NEDD4-2 (neural precursor cell-expressed developmentally down-regulated gene 4-2, also known as NEDD4L), in EBNA1-expressing Ad/AH cells. NEDD4-2 is a member of the NEDD4 HECT-type E3 ubiquitin ligase family (Yang and Kumar, 2010) and its expression is found to be up-regulated in several human carcinoma cell lines including lung, colon, gastric, breast, ovary and melanoma lines (Kuratomi et al., 2005). Research into the NEDD4-2 protein was initially focussed on its regulation of the epithelial sodium channel (ENaC) (Kamynina et al., 2001). However, since then, NEDD4-2 over-expression in invasive gallbladder cancers has been reported to promote invasion through an up-regulation of MMP1 and MMP13 (Takeuchi et al., 2011) and, of most interest, TGFβ-induced NEDD4-2 binding to R-Smads to induce their ubiquitin-dependent degradation has been demonstrated (Kuratomi et al., 2005).

The purported increase in NEDD4-2 expression in EBNA1-expressing Ad/AH cells, was validated by RT-PCR and immunoblotting analysis, and was extended to both rEBV-infected

Ad/AH cells, and their counterparts in the HONE-1 cell panel (Figure 3.16). Additionally, immunofluorescence staining was performed on the Ad/AH cell panel using a polyclonal rabbit antibody to NEDD4-2. Representative confocal images in Figure 3.16C show increased cytoplasmic NEDD4-2 staining was observed in the EBNA1 and rEBV-infected Ad/AH cells. In further support of this, the GCOS analysis of NPC tumour microarray data shown in Figure 3.17 demonstrates that NEDD4-2 expression is increased in approximately 14/16 (88%) NPC tumours compared to normal epithelia.

3.2.6 EBNA1 modulates the expression levels of TGFβ receptors, TβRI and TβRII, in a range of epithelial cell lines

TGFβ signal transduction is highly dependent on the formation of a hetero-oligomeric receptor complex of both TβRI and TβRII (Yamashita et al., 1994, Chen et al., 1995, Vivien et al., 1995). Aberration of TGFβ signalling in carcinoma cells, in particular the development of resistance to its anti-proliferative and pro-apoptotic effects, frequently derives from a defect at the receptor level. Whereas a previous study suggested no significant changes in the mRNA and protein levels of TβRI and TβRII in EBNA1-expressing Ad/AH cells (Wood et al., 2007), RT-PCR analyses conducted in this study demonstrate increases at the transcriptional level in the expression of both TβRI and TβRII in Ad/AH, HONE-1 and AGS cell panels, findings that were confirmed by QPCR in Ad/AH and AGS cell lines, but not for TβRI in the HONE-1 cell line (Figure 3.18).

Although an increase in expression of TβRI and TβRII in EBNA1-expressing cells was observed, it was hypothesised that a reduction in cell surface expression levels may reduce the availability of receptors for active participation in TGFβ signalling at any particular time,

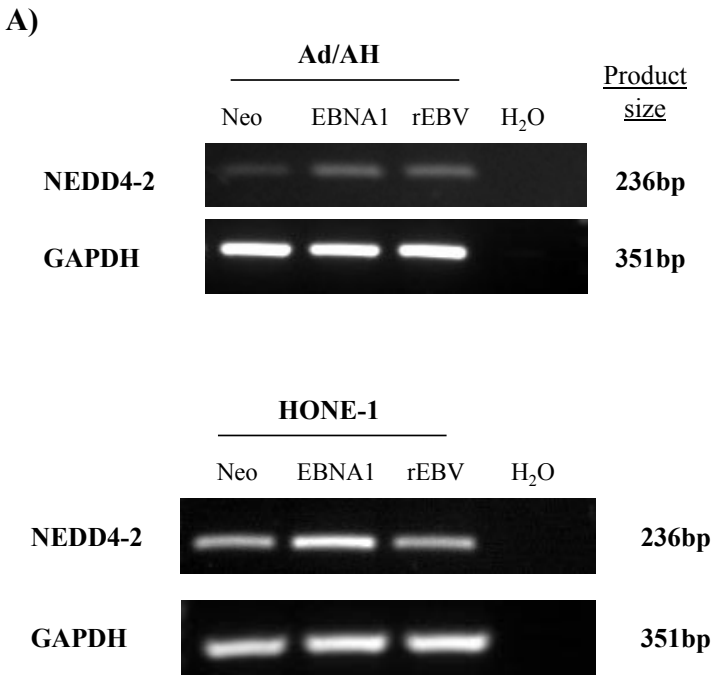

Figure 3.16: NEDD4-2 expression in Ad/AH and HONE-1 carcinoma cell lines

A) RT-PCR analysis for NEDD4-2 mRNA expression in Ad/AH and HONE-1 cells expressing either a control neomycin resistance cassette or EBNA1, or stably infected with rEBV. The housekeeping gene GAPDH was included as a positive control to confirm equal RNA input into the PCR reactions, while negative water controls confirmed the absence of contamination.

B) Immunoblotting for NEDD4-2 protein levels in Ad/AH and HONE-1 cells expressing either a neomycin resistance cassette, or EBNA1, or stably infected with rEBV, with β-actin included to confirm equal protein loading.

C) Immunofluorescence staining for expression of NEDD4-2 protein in Ad/AH cells expressing either a control neomycin resistance cassette or EBNA1, or infected with rEBV. DAPI staining was included to stain cellular nuclei. Representative confocal images are shown. Bar = 20μm.

B)

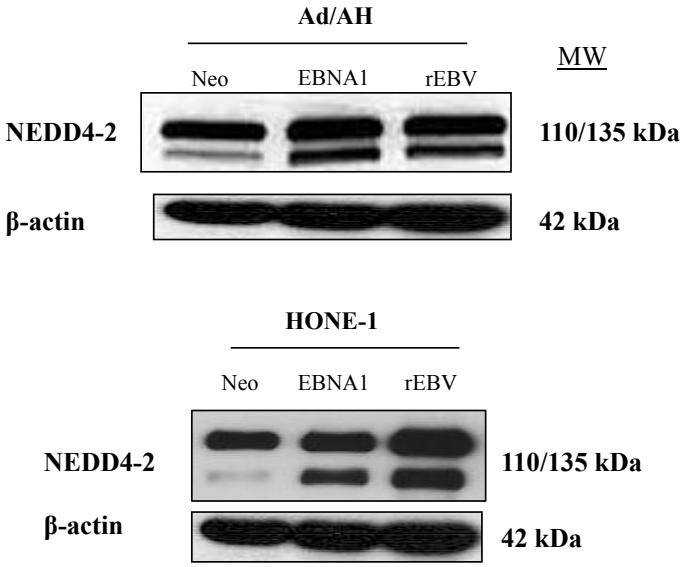
Ad/AH
MW
Neo
EBNA1
rEBV
NEDD4-2
110/135 kDa
β-actin
42 kDa
HONE-1
Neo
EBNA1
rEBV
NEDD4-2
110/135 kDa
β-actin
42 kDa

C)

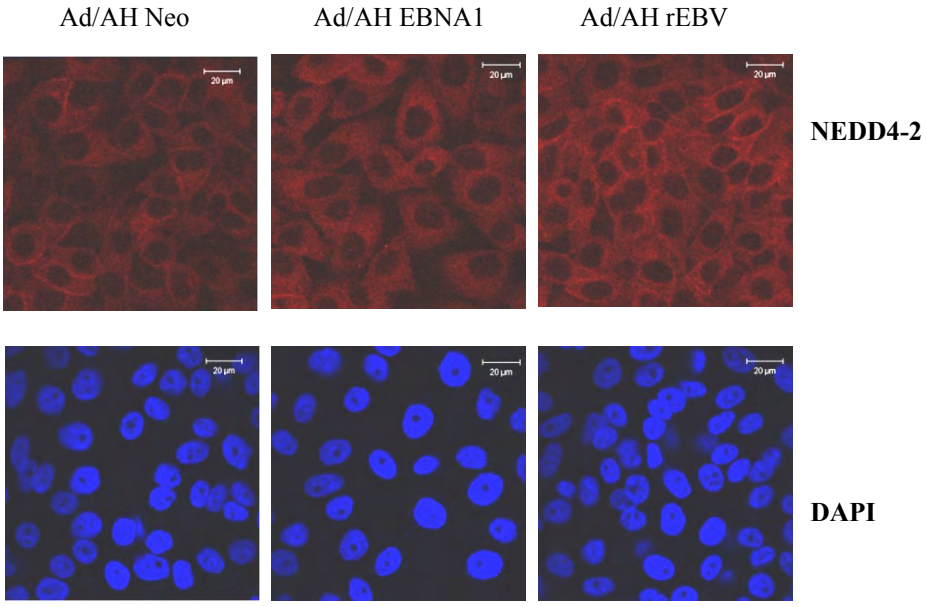
Ad/AH Neo
Ad/AH EBNA1
Ad/AH rEBV
NEDD4-2
DAPI

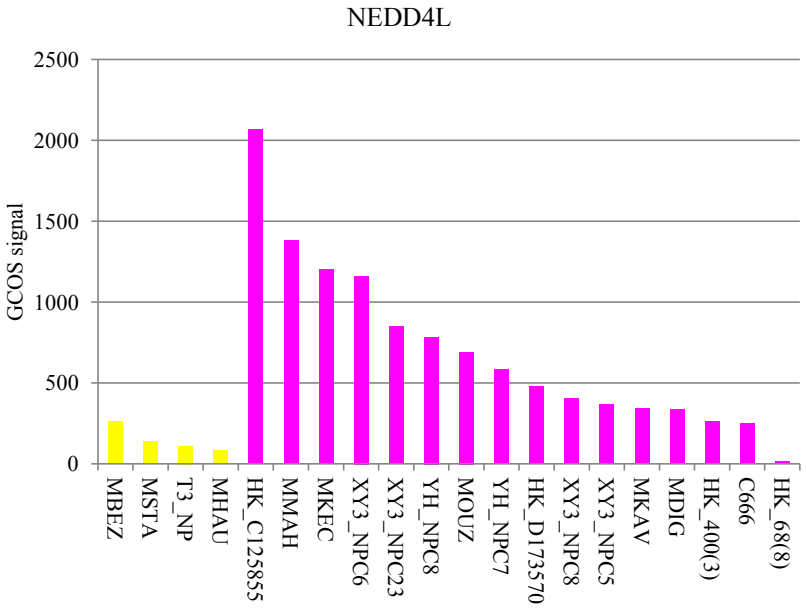

Figure 3.17: NEDD4-2 expression in EBV-positive NPC tumour cells
Existing expression array data analysed using GCOS (Affymetrix) was probed for NEDD4-2 expression levels. Normalised expression array intensities for 4 normal samples (yellow) and 15 NPC tumours plus the C666-1 EBV-positive NPC cell line (pink) are shown.

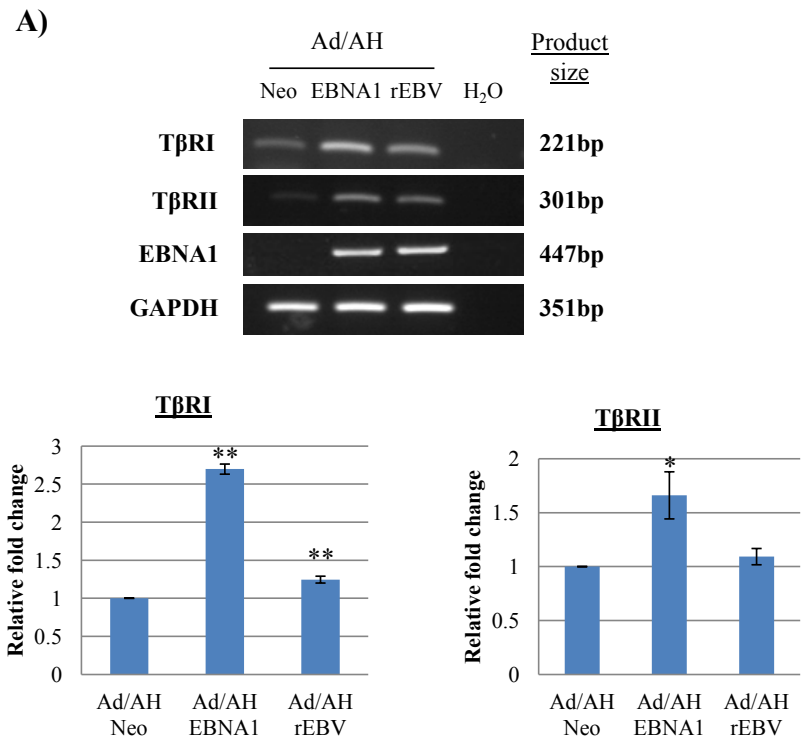

Figure 3.18: TGFβ receptor expression in Ad/AH, HONE-1 and AGS carcinoma cell lines

RT-PCR and QPCR analysis for levels of TβRI and TβRII mRNA in Ad/AH (A), HONE-1 (B) and AGS (C) cells expressing either a control neomycin resistance cassette or EBNA1, or stably infected with rEBV. For RT-PCR, GAPDH was included as a positive control to confirm equal RNA input into the PCR reactions, while negative water controls confirmed the absence of contamination. For QPCR, GAPDH was included as an internal baseline control. Histograms are shown displaying the mean fold change differences SE (n=3) (** denotes a P-value <0.01 and * denotes a P-value <0.05).

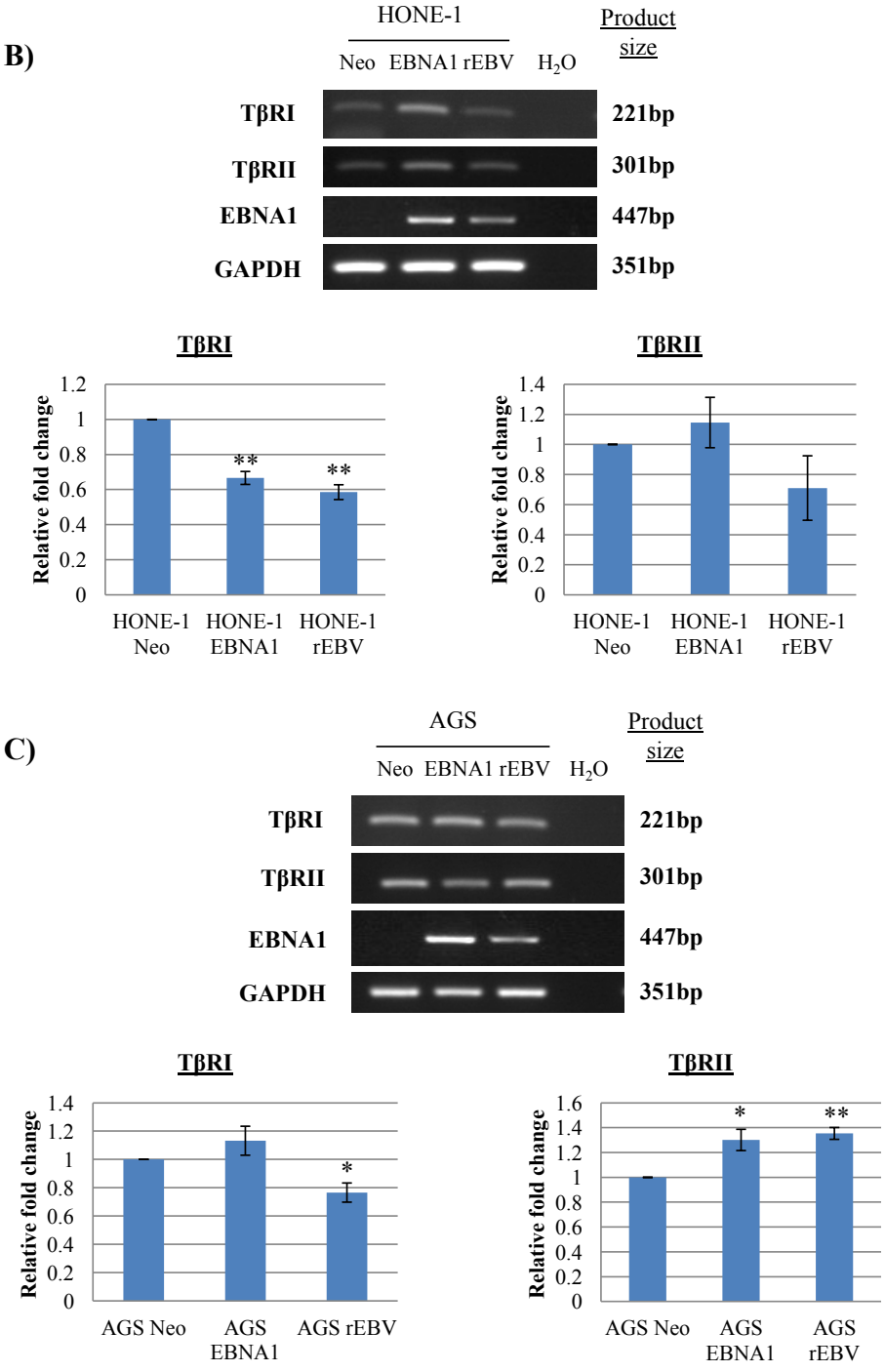
B)
HONE-1
Product size
Neo EBNA1 rEBV H2O
TβRI
TβRII
EBNA1
GAPDH
221bp
301bp
447bp
351bp
TβRI
TβRII
Relative fold change
HONE-1 Neo
HONE-1 EBNA1
HONE-1 rEBV
C)
AGS
Product size
Neo EBNA1 rEBV H2O
TβRI
TβRII
EBNA1
GAPDH
221bp
301bp
447bp
351bp
TβRI
TβRII
Relative fold change
AGS Neo
AGS EBNA1
AGS rEBV

which is a direct determinant of signalling capability. Flow cytometric analysis was therefore performed to compare the levels of cell surface TGFβ receptor expression between Neo control, EBNA1-expressing and rEBV-infected Ad/AH cells following incubation with either a rabbit polyclonal antibody to TβRI or a goat polyclonal antibody to TβRII. Data was analysed using the WinMDI program and graphical representations of the analyses are shown in Figure 3.19. Results indicated that levels of cell surface TGFβ receptors appeared to be reduced in EBNA1-expressing and rEBV-infected Ad/AH cells. While the relative mean fluorescence intensity (MFI) values indicate that this effect was only marginal for the surface expression of TβRI, a reduction of approximately fifty percent was observed for TβRII in EBNA1-expressing and rEBV-infected Ad/AH cells compared to Neo control cells.

3.2.6.1 Degradation of the TGFβ type I receptor, TβRI, is increased in the presence of EBNA1

Expression and activity of receptors is largely regulated by a variety of receptor-interacting proteins and distinct endocytic processes (Runyan et al., 2006, Chen, 2009). Traditionally considered a mechanism for terminating receptor signalling, endocytosis has since been recognised to have important consequences in signalling modulation (Penheiter et al., 2002, Penheiter et al., 2010). Endocytosis of TGFβ receptors is not only important in mediating rapid receptor degradative turnover, but also crucial in ensuring efficient recycling of receptors to the cell surface (Di Guglielmo et al., 2003, Chen, 2009). While internalisation of receptors into EEA1-positive endosomes is found to enhance TGFβ signal transduction through receptor recycling, partitioning via the lipid-raft-caveolar pathway promotes termination of the signal by controlling degradation (Hayes et al., 2002, Di Guglielmo et al., 2003). It was hypothesised that the observed reduction in expression at the cell surface may

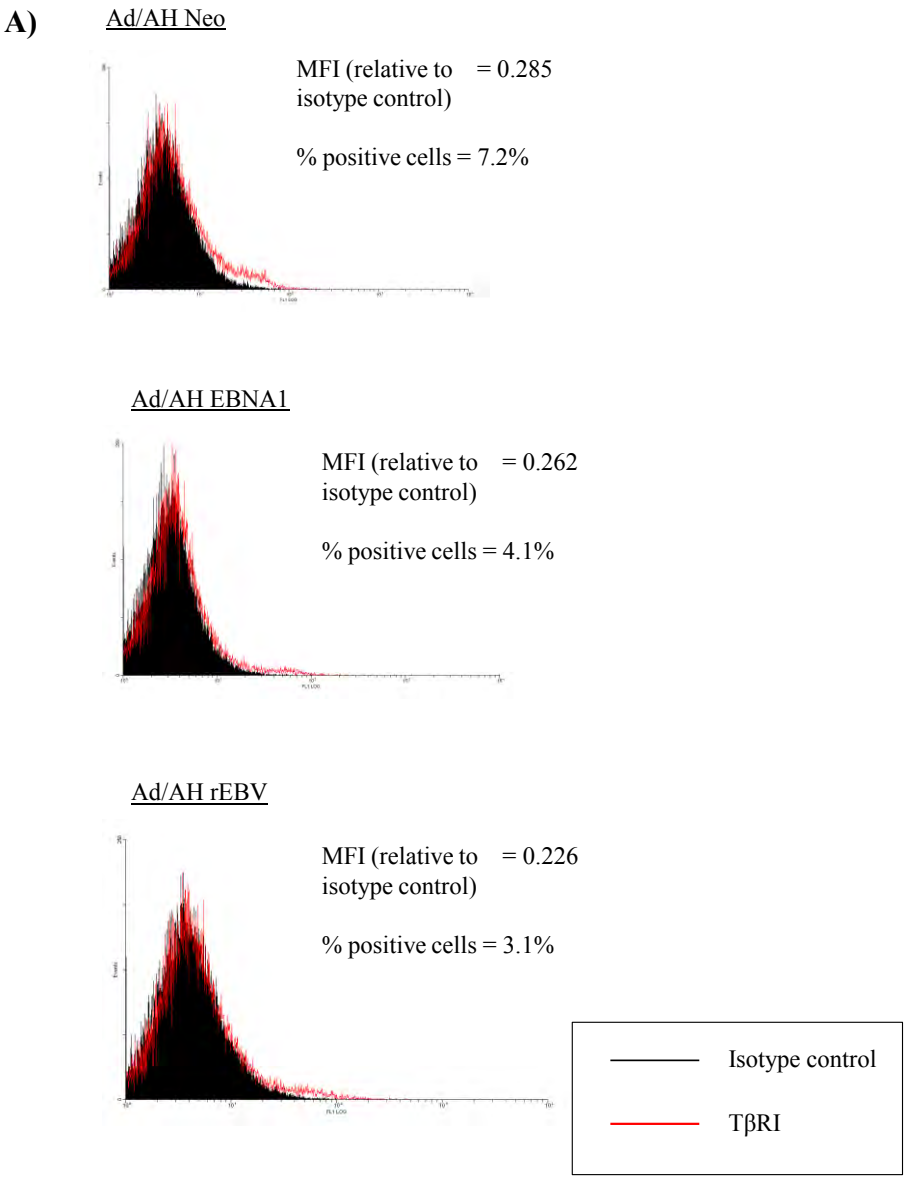

Figure 3.19: Flow cytometric analysis of TGFβ receptor expression in Ad/AH cells
Flow cytometric analysis of surface TβRI (A) and TβRII (B) expression in Ad/AH cells expressing either a neomycin resistance cassette or EBNA1, or stably infected with rEBV. Cells were incubated with antibodies specific to either TβRI or TβRII, or an anti-IgG antibody as an isotype control. Graphical representations of the analyses are displayed.

B)

Ad/AH Neo

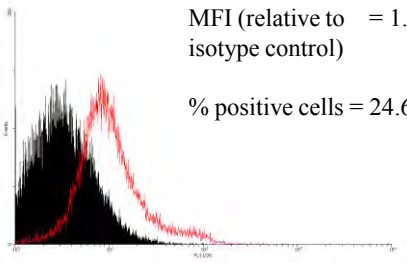

MFI (relative to isotype control) = 1.293

% positive cells = 24.6%

Ad/AH EBNA1

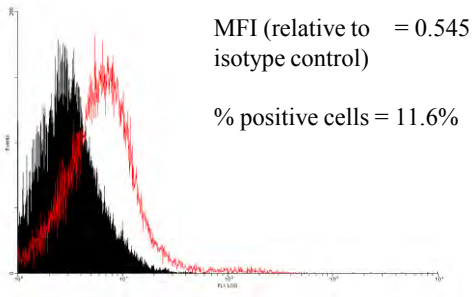

MFI (relative to isotype control) = 0.545

% positive cells = 11.6%

Ad/AH rEBV

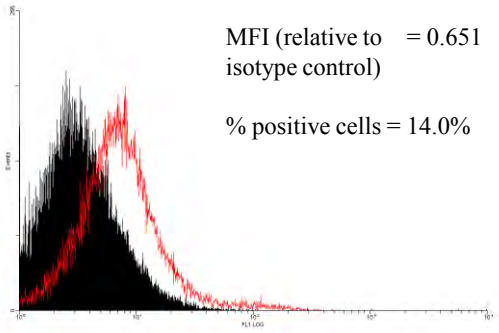

MFI (relative to isotype control) = 0.651

% positive cells = 14.0%

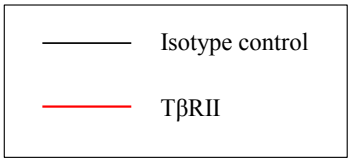

be a result of an accelerated rate of receptor turnover. While TβRII is essential for the binding of the TGFβ ligand, it is TβRI that is directly responsible for Smad activation. Therefore the turnover rate of TβRI was examined following treatment of Neo control, EBNA1-expressing and rEBV-infected Ad/AH cells with the protein synthesis inhibitor, cycloheximide (CHX). The Ad/AH cell panel were seeded into 6-well plates and treated with 20μg/ml CHX; protein lysates were collected at 0, 1, 3, 6, 9 and 12 hours after CHX addition. Subsequent immunoblotting of the lysates for TβRI revealed a more rapid turnover of TβRI protein in both EBNA1-expressing and rEBV-infected Ad/AH cells compared to the Neo controls. Control treatment with DMSO as expected revealed no changes in expression level throughout the time-course. Densitometry was performed and data plotted on a scatterplot, shown in Figure 3.20, from which the half-life of TβRI was seen to be reduced from 6 hours in control cells to 4 and 3.5 hours in EBNA1 and rEBV-infected cells, respectively.

3.2.6.2 EBNA1 modulates the expression of factors associated with TGFβ receptor endocytosis

In an attempt to further characterise these observations, various components of the endocytic pathway machinery were investigated. Dab2 which, at the time of its identification in 1994, was labelled a tumour suppressor gene (Mok et al., 1994), has since been found to be frequently down-regulated in human cancers, including human squamous cell carcinoma (Hannigan et al., 2010). Recently, epigenetic inactivation of the Dab2 gene promoter has also been reported in NPC (Tong et al., 2010). A role for Dab2 has been established in TGFβ receptor trafficking, specifically as a key adaptor protein in the clathrin-dependent recycling of receptors via endosomes (Morris and Cooper, 2001, Mishra et al., 2002, Gong et al., 2008, Penheiter et al., 2010). These EEA1-positive endosomes are also enriched for the Smad

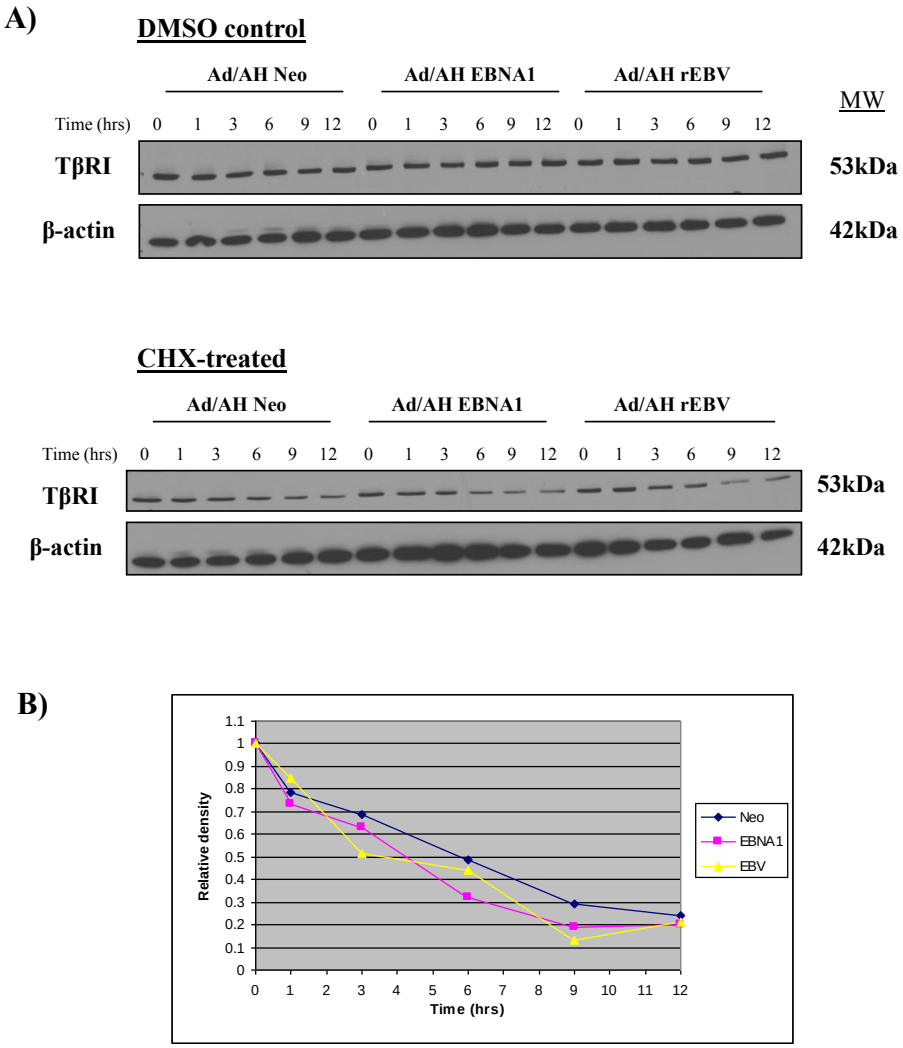

Figure 3.20: The effect of EBNA1 on the half-life of TβRI in Ad/AH cells

A) Immunoblotting for protein levels of TβRI in Ad/AH Neo, Ad/AH EBNA1 and Ad/AH rEBV cells following treatment with cycloheximide (CHX), or DMSO as a control, over a 12-hour time-course. Blots were re-probed with a monoclonal antibody against β-actin to confirm equal protein loading.

B) Densitometric scanning was performed on the TβRI immunoblot representing CHX-treated samples and the corresponding β-actin. Following normalisation of densitometry values for TβRI against β-actin, an X and Y scatterplot was generated illustrating the half-life of TβRI in Ad/AH EBNA1 and rEBV-infected cells compared with Ad/AH Neo control cells.

anchor for receptor activation (SARA) protein (Itoh et al., 2002, Di Guglielmo et al., 2003, Runyan et al., 2005), which enhances TGFβ signalling by positioning R-Smads in close proximity with receptors (Tsukazaki et al., 1998).

Representative RT-PCR analysis of Dab2 and SARA mRNA levels in the Ad/AH, HONE-1 and AGS cell panels is shown in Figure 3.21. While the expression of Dab2 appeared to be elevated in EBNA1-expressing and rEBV-infected Ad/AH cell lines, relative to Neo control cells, its expression was decreased in HONE-1 and AGS cells expressing EBNA1 or infected with rEBV; no major differences in the transcription of SARA were observed between EBNA1-expressing and rEBV-infected cell lines.

Caveolin-1 (Cav-1), a principal structural marker of lipids rafts (Razani et al., 2001), has been reported to impact both positively and negatively on aspects of tumour progression (reviewed in (Williams and Lisanti, 2005, Goetz et al., 2008)), but is reportedly over-expressed in NPC tumour samples (Du et al., 2009). These caveolin-positive lipid rafts also contain complexes of Smad7 and Smurf2, which facilitate receptor turnover (Kavsak et al., 2000, Di Guglielmo et al., 2003). The relative expression of all three genes was examined by RT-PCR; a representative analysis is shown in Figure 3.22. This analysis revealed increased levels of Cav-1, Smad7 and Smurf2 mRNA in EBNA1-expressing and rEBV-infected cells in all three cell backgrounds. To validate these findings, immunofluorescence staining for Cav-1 protein was performed on Neo control, EBNA1-expressing and rEBV-infected Ad/AH cells (Figure 3.23). The relevance of these findings, as related to NPC pathogenesis, was examined by mining the Affymetrix gene expression profiles of 15 authentic NPC tumours and the EBV-positive C666-1 cell line compared to 4 normal samples. GCOS analysis of microarray data,

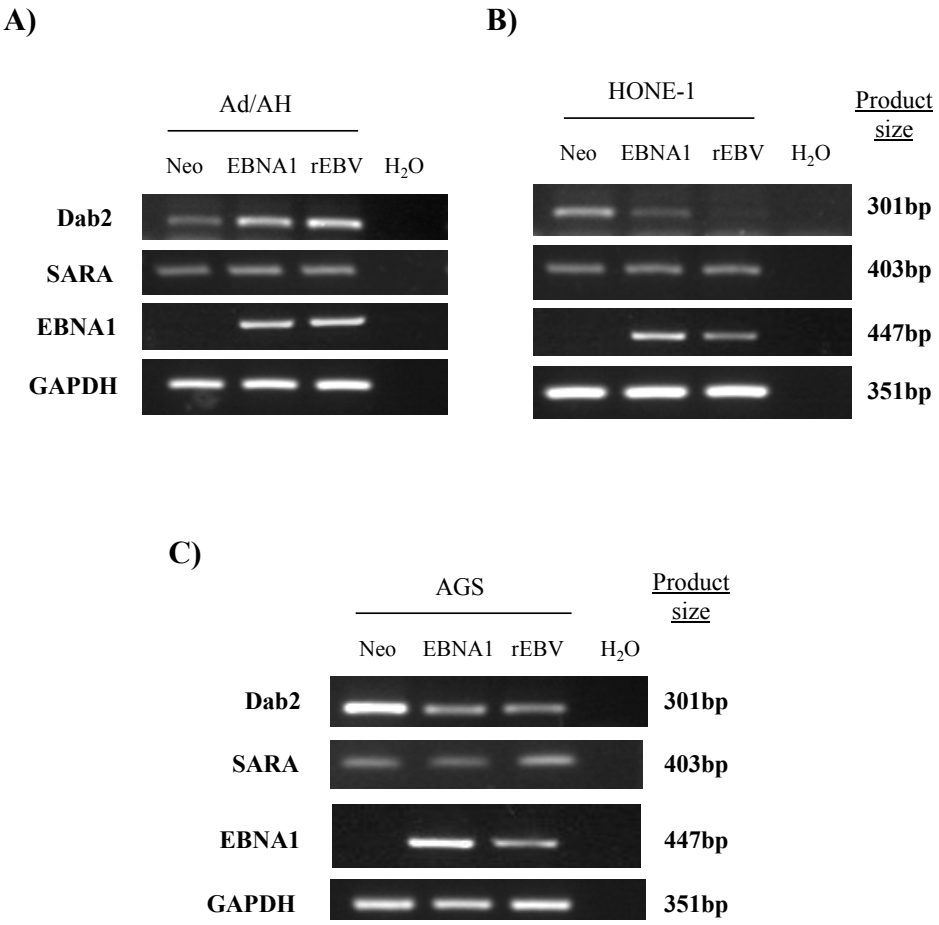

Figure 3.21: Dab2 and SARA expression in Ad/AH, HONE-1 and AGS carcinoma cell lines
RT-PCR analysis for mRNA levels of Dab2 and SARA in Ad/AH (A), HONE-1 (B) and AGS (C) cells expressing either a control neomycin resistance cassette or EBNA1, or stably infected with rEBV. GAPDH was included as a positive control to confirm equal RNA input into the PCR reactions, while negative water controls confirmed the absence of contamination.

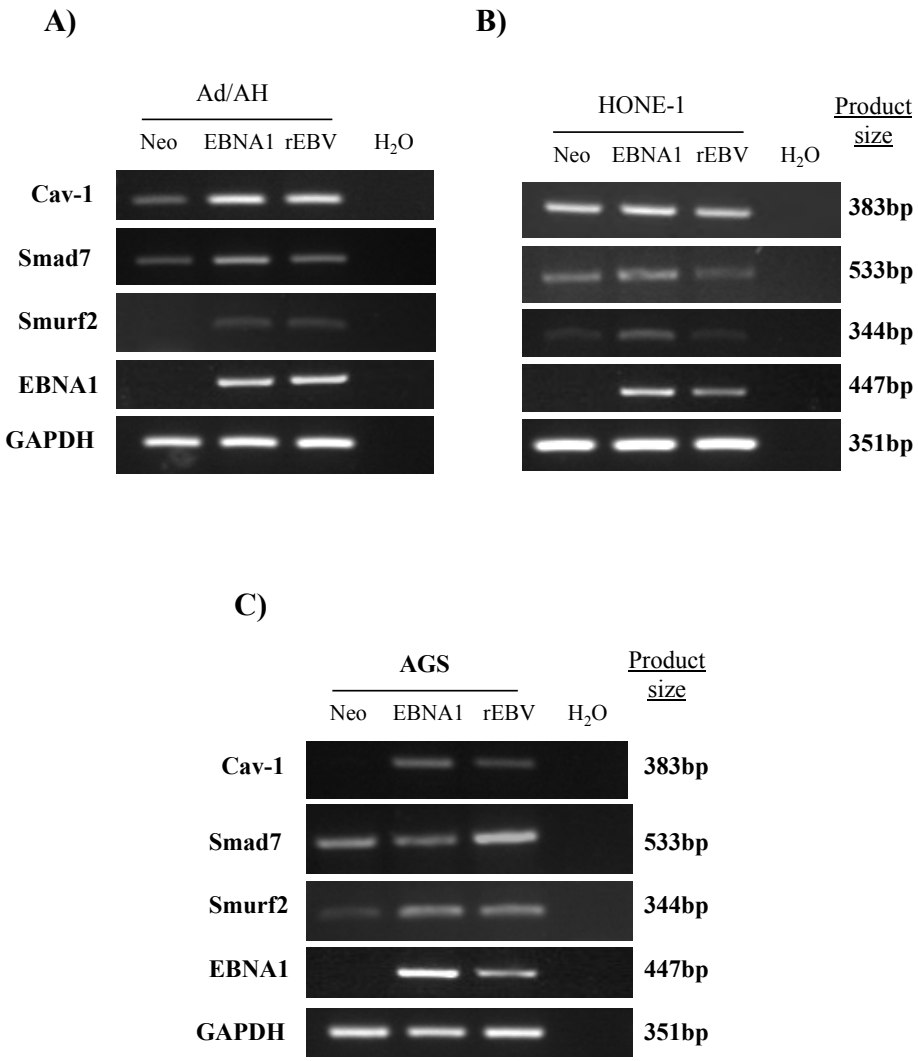

Figure 3.22: Cav-1, Smad7 and Smurf2 expression in Ad/AH, HONE-1 and AGS carcinoma cell lines
RT-PCR analysis for mRNA levels of Cav-1, Smad7 and Smurf2 in Ad/AH (A), HONE-1 (B) and AGS (C) cells expressing either a control neomycin resistance cassette or EBNA1, or stably infected with rEBV, with GAPDH was included as a positive control to confirm equal RNA input into the PCR reactions, while negative water controls confirmed the absence of contamination.

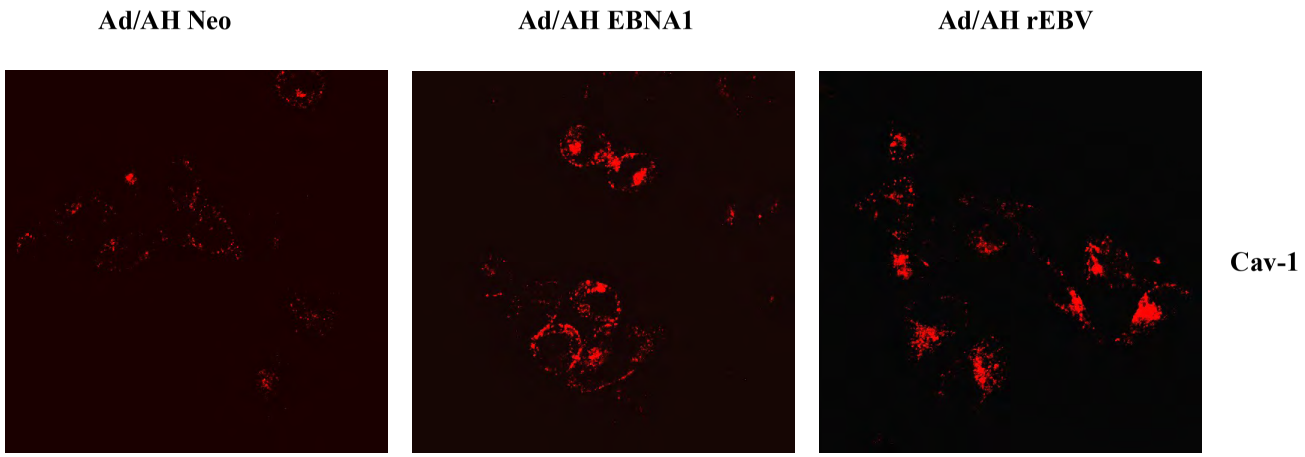

Figure 3.23: Immunofluorescence staining of Cav-1 in Ad/AH cells
Immunofluorescence staining for Cav-1 protein expression in Ad/AH cells expressing either a control neomycin resistance cassette or EBNA1, or infected with rEBV. Representative images are shown.

showing relative normalised array intensities, revealed that the expression of Cav-1, Smad7 and Smurf2 was up-regulated in approximately 9/16 (56%), 11/16 (69%) and 7/16 (44%) of NPC tumours (Figure 3.24).

3.2.7 Expression levels of the TGFβ isoforms are augmented in the presence of EBNA1

An important determinant of a cell's response to TGFβ ligand stimulation is the concentration and species of ligand produced by the cells themselves. Such "autocrine" production of TGFβ ligands can dictate cellular responsiveness to additional ligand stimulation (Clarke et al., 2009). To explore the possibility that EBNA1 and rEBV-infected cells were producing elevated levels of TGFβ family ligands, the relative expression levels of the canonical TGFβ ligands, TGFβ1, 2 and 3, were examined by RT-PCR, and subsequently by QPCR (Figure 3.25) in the Ad/AH, HONE-1 and AGS panels of cell lines. RT-PCR indicated increased expression of TGFβ1, 2 and 3 in EBNA1-expressing Ad/AH cells, yet only of TGFβ2 in rEBV-infected Ad/AH cells. However, TGFβ1 levels were relatively unchanged in both EBNA1-expressing and rEBV-infected HONE-1 and AGS cells, yet expression of TGFβ2 appeared to be significantly increased and TGFβ3 decreased in both EBNA1-expressing HONE-1 and AGS cells. These effects were further investigated by QPCR analysis which confirmed an increase in TGFβ1 in Ad/AH EBNA1 cells and showed a modest increase in EBNA1-expressing and rEBV-infected AGS cells. TGFβ2 meanwhile was increased in all three cell lines in both EBNA1-expressing and rEBV-infected cells, and TGFβ3, while increased in Ad/AH EBNA1, was decreased in AGS EBNA1 and HONE-1 EBNA1 and rEBV-infected cells.

A)

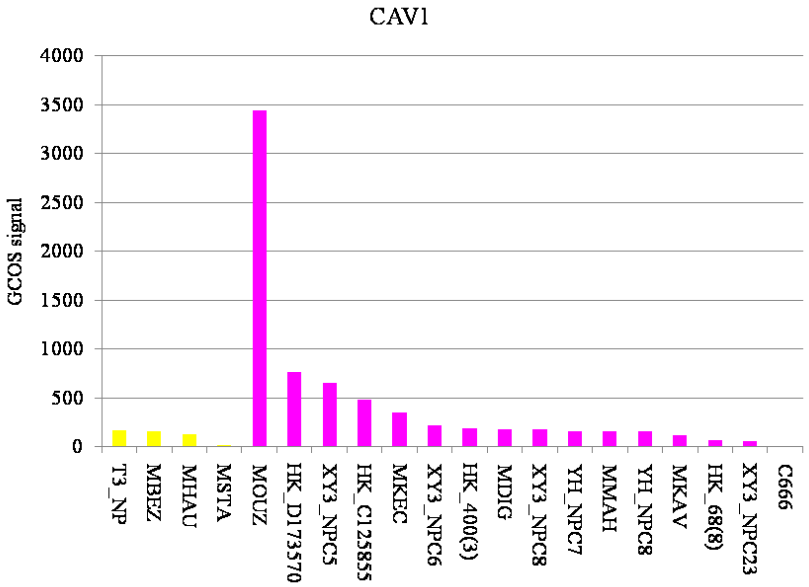

Figure 3.24: Cav-1, Smad7 and Smurf2 expression in EBV-positive NPC tumour cells

Existing expression array data analysed using GCOS (Affymetrix) was probed for Cav-1, Smad7 and Smurf2 expression levels. Normalised expression array intensities for 4 normal samples (yellow) and 15 NPC tumours plus the C666-1 EBV-positive NPC cell line (pink) are shown.

B)

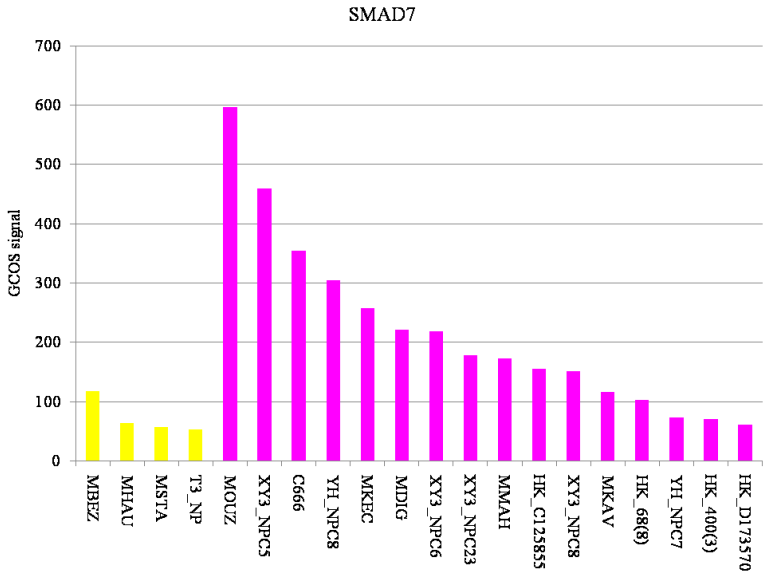
SMAD7
GCOS signal
700
600
500
400
300
200
100
0
MBEZ
MHAU
MSTA
T3_NP
MOUZ
XY3_NPC5
C666
YH_NPC8
MKEC
MDIG
XY3_NPC6
XY3_NPC23
MMAH
HK_C125855
XY3_NPC8
MKAV
HK_68(8)
YH_NPC7
HK_400(3)
HK_D173570

C)

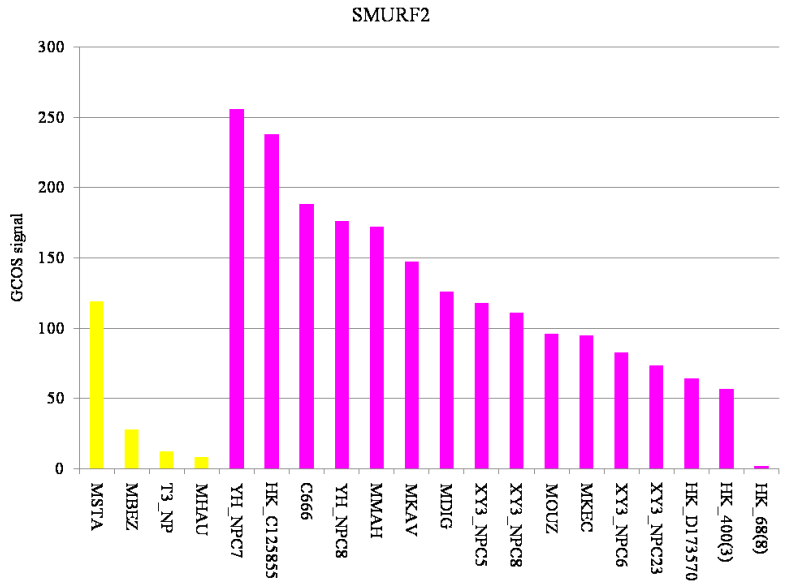
SMURF2
GCOS signal
300
250
200
150
100
50
0
MSTA
MBEZ
T3_NP
MHAU
YH_NPC7
HK_C125855
C666
YH_NPC8
MMAH
MKAV
MDIG
XY3_NPC5
XY3_NPC8
MOUZ
MKEC
XY3_NPC6
XY3_NPC23
HK_D173570
HK_400(3)
HK_68(8)

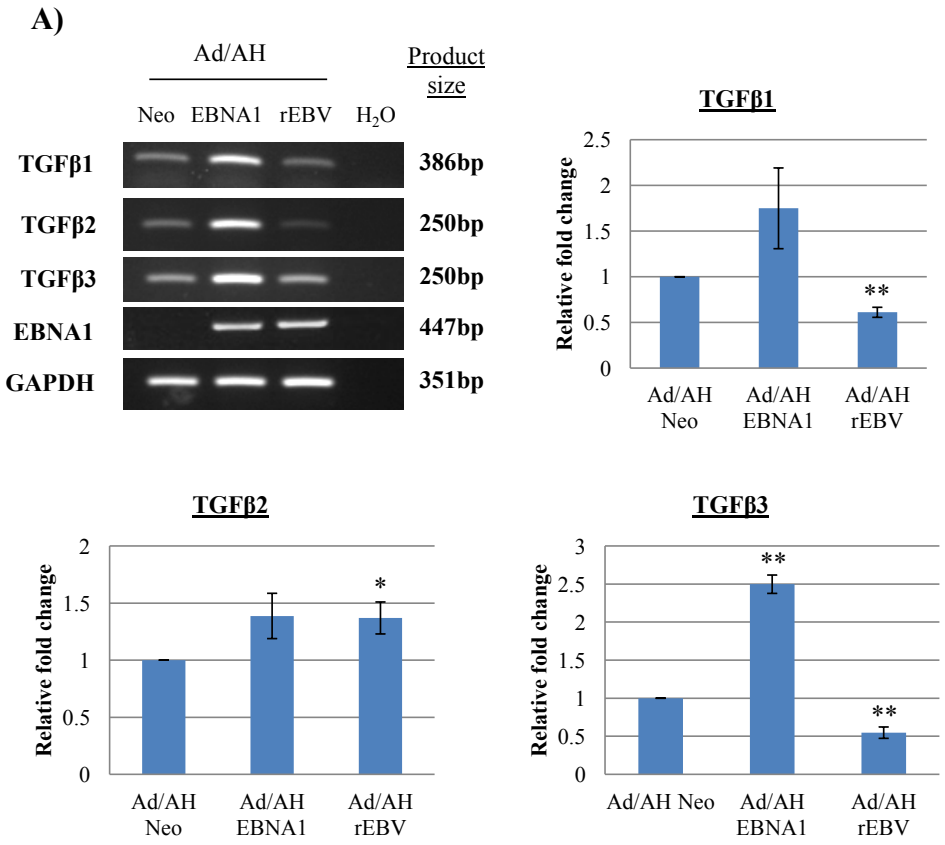

Figure 3.25: TGFβ isoform expression in Ad/AH, HONE-1 and AGS carcinoma cell lines

RT-PCR and QPCR analysis for TGFβ1, TGFβ2 and TGFβ3 mRNA expression in Ad/AH (A), HONE-1 (B) and AGS (C) cells expressing either a control neomycin resistance cassette or EBNA1, or stably infected with rEBV. For RT-PCR, GAPDH was included as a positive control to confirm equal RNA input into the PCR reactions, while negative water controls confirmed the absence of contamination. For QPCR, GAPDH was included as an internal baseline control. Histograms are shown displaying the mean fold change differences SE (n=3) relative to Neo control cells (** denotes a P-value <0.01 and * denotes a P-value <0.05).

B)

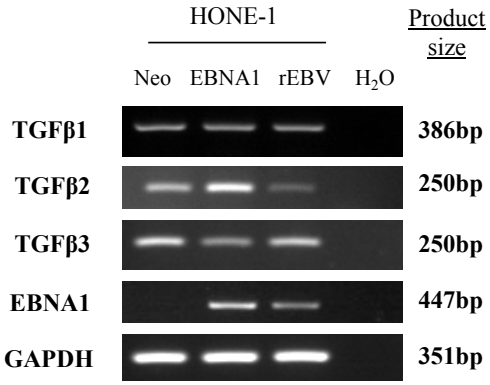
HONE-1
Product size
Neo
EBNA1
rEBV
H_2O
TGFβ1
386bp
TGFβ2
250bp
TGFβ3
250bp
EBNA1
447bp
GAPDH
351bp

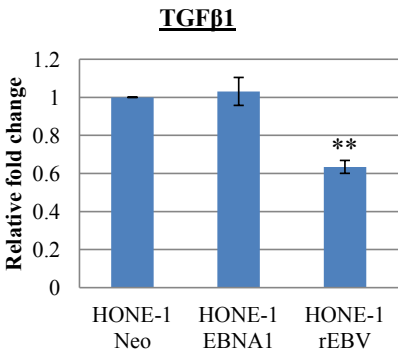
TGFβ1
Relative fold change
1.2
1
0.8
0.6
0.4
0.2
0
**
HONE-1 Neo
HONE-1 EBNA1
HONE-1 rEBV

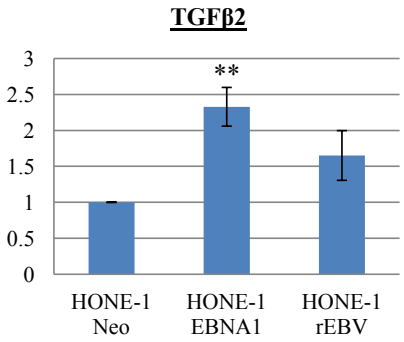
TGFβ2
3
2.5
2
1.5
1
0.5
0
**
HONE-1 Neo
HONE-1 EBNA1
HONE-1 rEBV

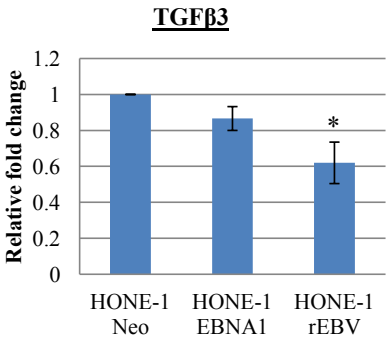
TGFβ3
Relative fold change
1.2
1
0.8
0.6
0.4
0.2
0
*
HONE-1 Neo
HONE-1 EBNA1
HONE-1 rEBV

C)

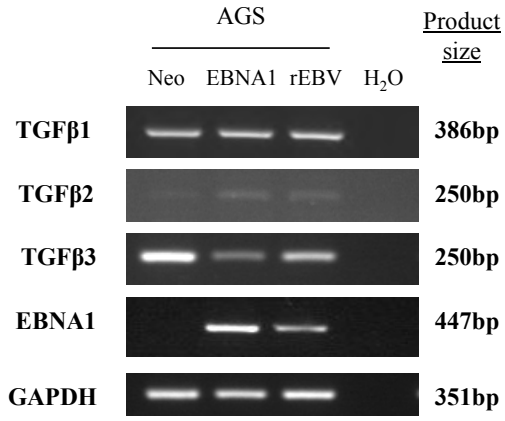
AGS
Product size
Neo
EBNA1
rEBV
H_2O
TGFβ1
386bp
TGFβ2
250bp
TGFβ3
250bp
EBNA1
447bp
GAPDH
351bp

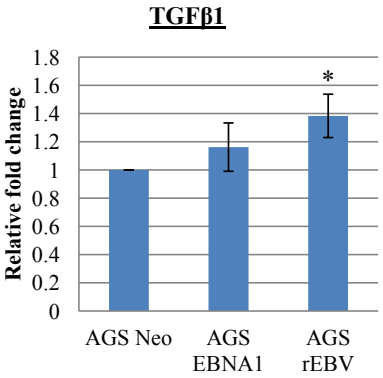
TGFβ1
Relative fold change
1.8
1.6
1.4
1.2
1
0.8
0.6
0.4
0.2
0
*
AGS Neo
AGS EBNA1
AGS rEBV

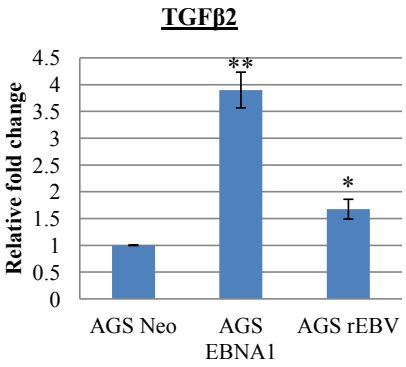
TGFβ2
Relative fold change
4.5
4
3.5
3
2.5
2
1.5
1
0.5
0
**
*
AGS Neo
AGS EBNA1
AGS rEBV

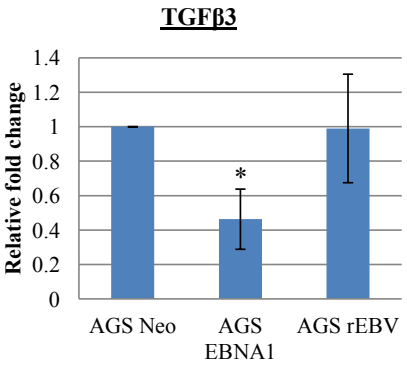
TGFβ3
Relative fold change
1.4
1.2
1
0.8
0.6
0.4
0.2
0
*
AGS Neo
AGS EBNA1
AGS rEBV

3.2.7.1 The secretion of TGFβ is increased in EBNA1-expressing cells

TGFβ is initially synthesised and secreted as a biologically inert prohormone precursor, designated the small latent complex (SLC), consisting of a C-terminal fragment, which constitutes the mature growth factor, and the N-terminal propeptide, termed the latency-associated peptide (LAP) (Annes et al., 2003, Javelaud and Mauviel, 2004). This is often additionally covalently associated with latent TGFβ-binding protein (LTBP) forming the large latent complex (LLC), probably as a means of localising the inactive complex to the extracellular matrix. The majority of cell types secrete TGFβ as part of the LLC (Wipff and Hinz, 2008), and its activation from this complex, often involving proteolytic cleavage, is a critical rate-limiting step in determining its signalling potential (Khalil, 1999, Javelaud and Mauviel, 2004). The exact mechanism for activation of TGFβ *in vivo* is not fully understood, yet putative roles have been reported for plasmin, cathepsins B and D, calpain, thrombospondin-1, furin, matrix metalloproteinases, integrins and BMP1-like proteinases (Khalil, 1999, Jenkins, 2008, Munger et al., 1999, Wipff and Hinz, 2008, Ge and Greenspan, 2006).

Whilst the level and nature of intracellular TGFβ signalling can be extensively studied using an array of molecular and biochemical assays and techniques, it has proven more difficult to accurately quantify the levels of active TGFβ generated by particular cells (Mazzieri et al., 2000). However, an integral PAI-1 luciferase assay using the mink lung cell line, MLEC-clone32 can be used as a relatively sensitive assay technique. These cells are stably transfected with an 800bp fragment of the PAI-1 gene fused to the firefly luciferase reporter gene, the activity of which is directly translated into an appreciation of the levels of TGFβ actively secreted by cells. Activation of latent TGFβ can be artificially induced *in vitro* by

extreme pH, high heat, chaotropic agents and substances like SDS and urea (Khalil, 1999) and, advantageously, the assay can encompass treatments to activate the latent fraction in order to provide an overall estimate of the total TGFβ released (Mazzieri et al., 2000).

In brief, conditioned supernatants collected from serum-starved Neo control, EBNA1-expressing and rEBV-infected Ad/AH cells at 24-, 48-, and 72-hour time-points were incubated overnight with MLEC-clone32 cells, which were subsequently analysed for luciferase reporter activity. Results are represented graphically in Figure 3.28. An increase in the levels of active secreted TGFβ in EBNA1-expressing and rEBV-infected cells was observed in the untreated sample set (Figure 3.26A), while samples activated by heat treatment also demonstrated an increase in the total TGFβ levels in these cells (Figure 3.26B). Additionally, pre-treatment of samples with 10μg/ml pan-anti-TGFβ neutralising antibody (clone 1D11) to neutralise TGFβ bioactivity served to confirm the specificity of the assay by effectively reducing TGFβ levels back down to diminutive levels. The ratio of active: latent TGFβ measured in the conditioned media samples was calculated and data is shown, using the 48-hour timepoint as an example, represented graphically as pie charts in Figure 3.26C. Although the effects are relatively small, the proportion of active TGFβ was increased in both EBNA1-expressing and rEBV-infected Ad/AH cells in comparison with Neo control cells.

3.2.8 EBNA1 does not influence cell cycle distribution in response to TGFβ in Ad/AH carcinoma cells

Several viral oncoproteins have shown the ability to override growth-suppressive signals, deregulating cell-cycle control so as to promote host cell proliferation (Jansen-Dürr, 1996), and cellular transformation driven by the adenovirus E1A oncogene has been specifically

A)

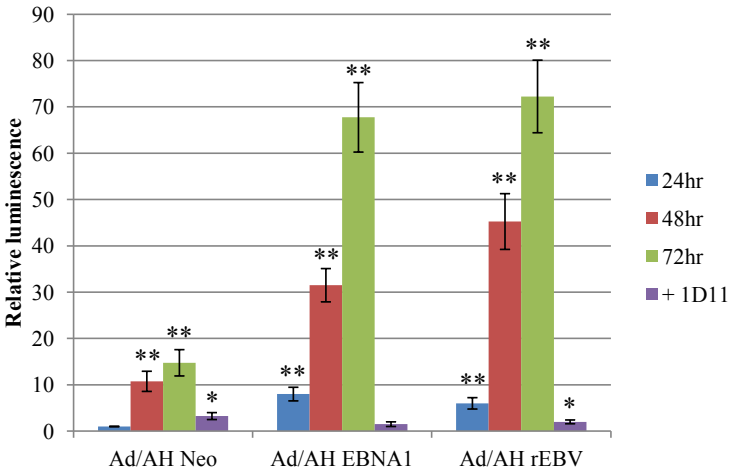

Figure 3.26: Measurement of TGFβ secretion in Ad/AH cells using the PAI-1L assay

A) Conditioned media samples were collected after 24, 48 and 72 hours from serum-starved Ad/AH Neo, Ad/AH EBNA1 and Ad/AH rEBV cells, and were applied to MLEC-clone32 cells. Luciferase activity was determined following incubation overnight. The histogram shown displays the relative luminescence after subtracting 0.5% serum medium control background values. Incubation of samples with anti-TGFβ antibody (clone 1D11) prior to addition to the reporter cells confirmed assay specificity. Data from three independent experiments is presented as the mean fold differences in activity ± SE, relative to that observed in the 24-hour Ad/AH Neo control cell sample which is given an arbitrary value of 1 (** denotes a P-value <0.01 and * denotes a P-value <0.05).

B) The PAI-1L assay was performed as above using heat-inactivated conditioned media samples. Results are depicted as a histogram showing the relative luminescence after subtracting heat-treated 0.5% serum medium control background values. Data from three independent experiments is presented as the mean fold differences in activity ± SE, relative to that observed in the 24-hour Ad/AH Neo control cell sample which is given an arbitrary value of 1 (** denotes a P-value <0.01 and * denotes a P-value <0.05).

C) Pie charts show the levels of active secreted TGFβ (untreated) expressed as a proportion of the total TGFβ (heat-activated) levels measured in conditioned media samples taken after 48 hours incubation from Ad/AH Neo, EBNA1 and rEBV-infected cells.

B)

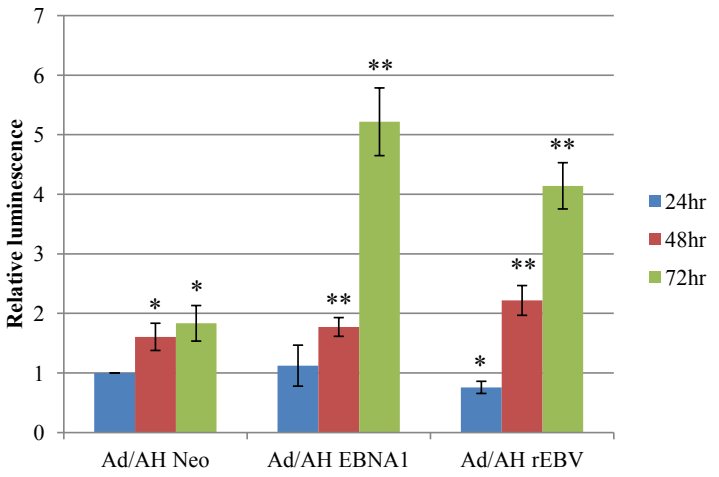

C)

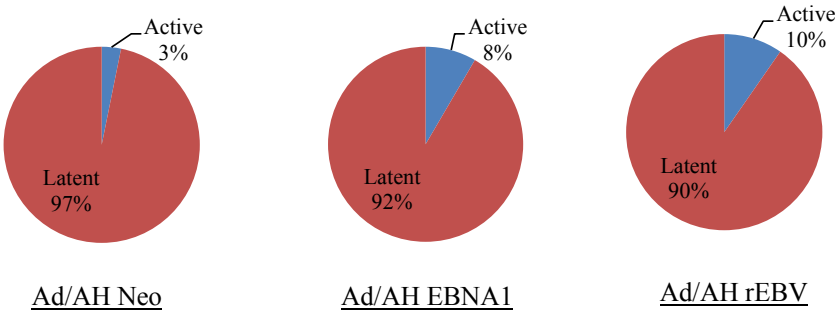

Ad/AH Neo Ad/AH EBNA1 Ad/AH rEBV

associated with development of cellular resistance to growth inhibitory effects of TGFβ (Kim et al., 1997). Due to its confirmed ability to inhibit TGFβ signalling, and particularly the alteration of cell surface receptor expression and increased TGFβ secretion, it was reasoned that EBNA1 may specifically aid the acquisition of resistance to TGFβ-mediated G1 growth arrest, as a direct means of promoting tumour cell proliferation. This was investigated by examining cell cycle distribution. To this end, cells were treated with TGFβ1 (5ng/ml) for 24 hours and fixed in 95% ethanol, before staining with propidium iodide and analysis by flow cytometry. Cell cycle profiles were subsequently generated using MultiCycle, and representative traces from three independent experiments are shown in Figure 3.27. In all instances, Neo control, EBNA1-expressing and rEBV-infected Ad/AH cells failed to respond to TGFβ by undergoing cell cycle arrest in the G1 phase. No significant changes in cell cycle distribution were observed in any of the cell lines, regardless of the presence of EBNA1 or rEBV.

3.3 EBNA1 augments a number of the tumour-promoting functions of TGFβ

3.3.1 EBNA1 expression increases Smad2 and Smad3 phosphorylation at specific linker region residues

While the anti-proliferative response appears unaffected by EBNA1, it was reasoned that EBNA1 may instead function to promote the pro-tumourigenic functions of TGFβ. Reports have suggested that increased phosphorylation at Smad linker regions can encourage this switch. Relative expression levels of various Smad2 and Smad3 phospho-isoforms were examined by immunoblotting of protein lysates from Ad/AH, HONE-1 and AGS cell panels, and representative immunoblots are shown in Figure 3.28. An increase in expression of pSmad2 Ser245/250/255 and Thr220, and pSmad3 Ser204, Ser208, Ser213 and Thr179 was

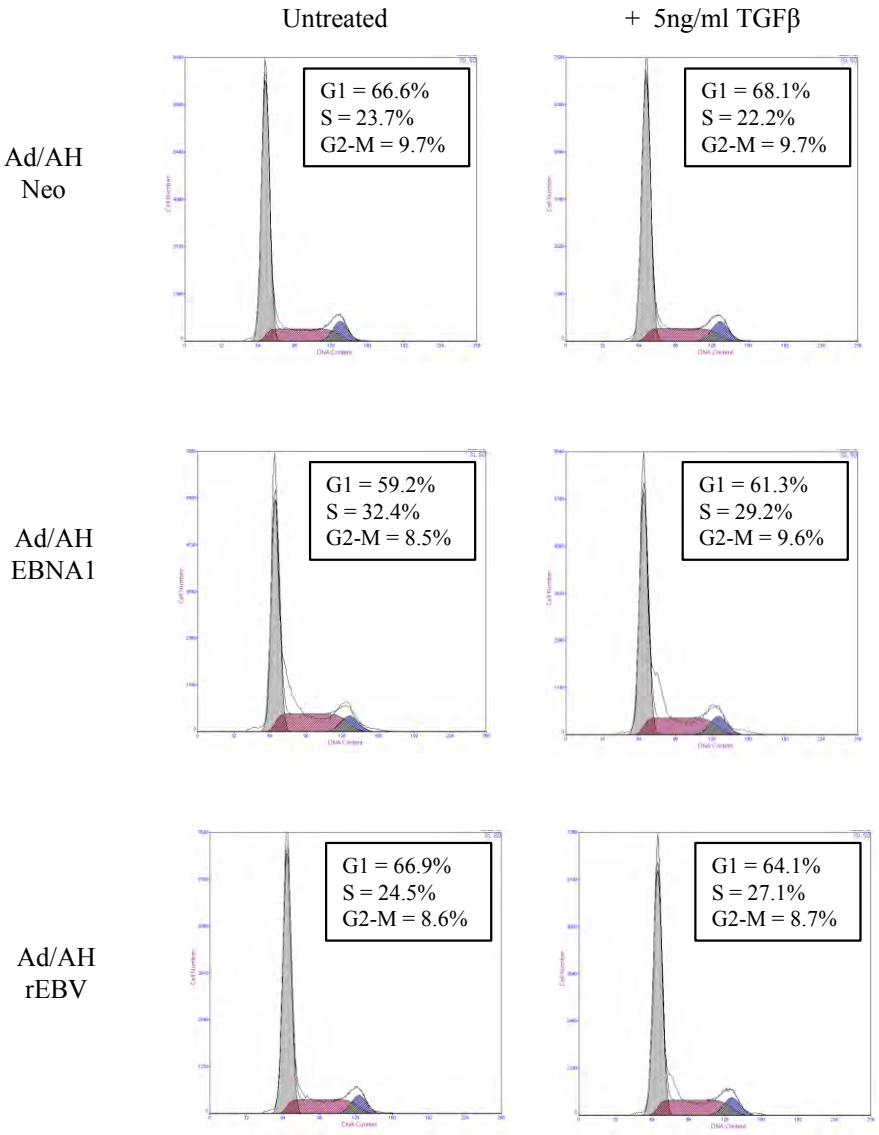

Figure 3.27: Cell cycle analysis by propidium iodide staining of Ad/AH cells
Analysis of cell cycle in serum-starved Ad/AH cells expressing either a control neomycin resistance cassette or EBNA1, or infected with rEBV, treated with 5ng/ml recombinant hTGFβ1 for 24 hours or left unstimulated as a control. DNA content was measured by propidium iodide staining and subsequent flow cytometric analysis. Resulting histogram files were analysed for cell cycle distribution using MultiCycle. Representative traces from one of three independent experiments are shown, with percentages of cells in G1, S and G2-M phases indicated.

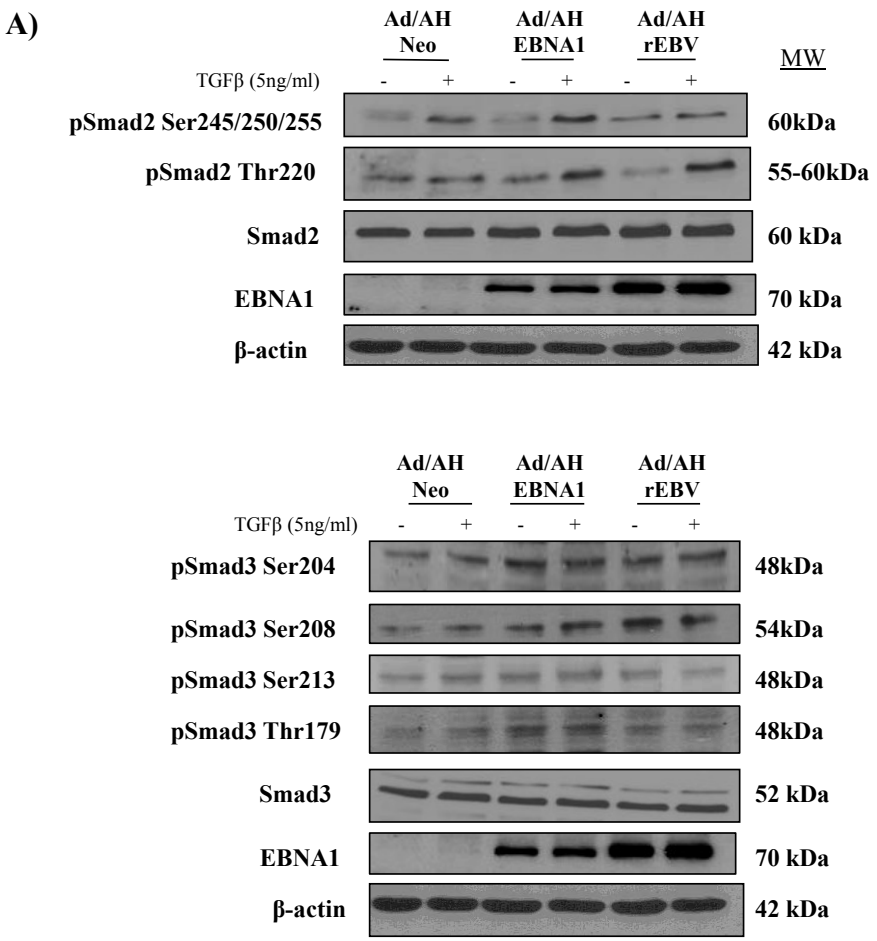

Figure 3.28: Expression of linker phosphorylated Smad2 and Smad3 in Ad/AH, HONE-1 and AGS cells

Immunoblotting for protein levels of the serine 245/250/255 and threonine 220 phosphorylated forms of Smad2, and the serine 204, serine 208, serine 213 and threonine 179 phosphorylated forms of Smad3 in serum-starved Ad/AH (A), HONE-1 (B) and AGS (C) cells expressing either a control neomycin resistance cassette or EBNA1, or stably infected with rEBV, under basal conditions and following stimulation with 5ng/ml recombinant hTGFβ1 for 24 hours. Immunoblotting for levels of total Smad2 and Smad3, and also EBNA1 protein expression in cell lysates is also shown, with β-actin included to confirm equal protein loading.

B)

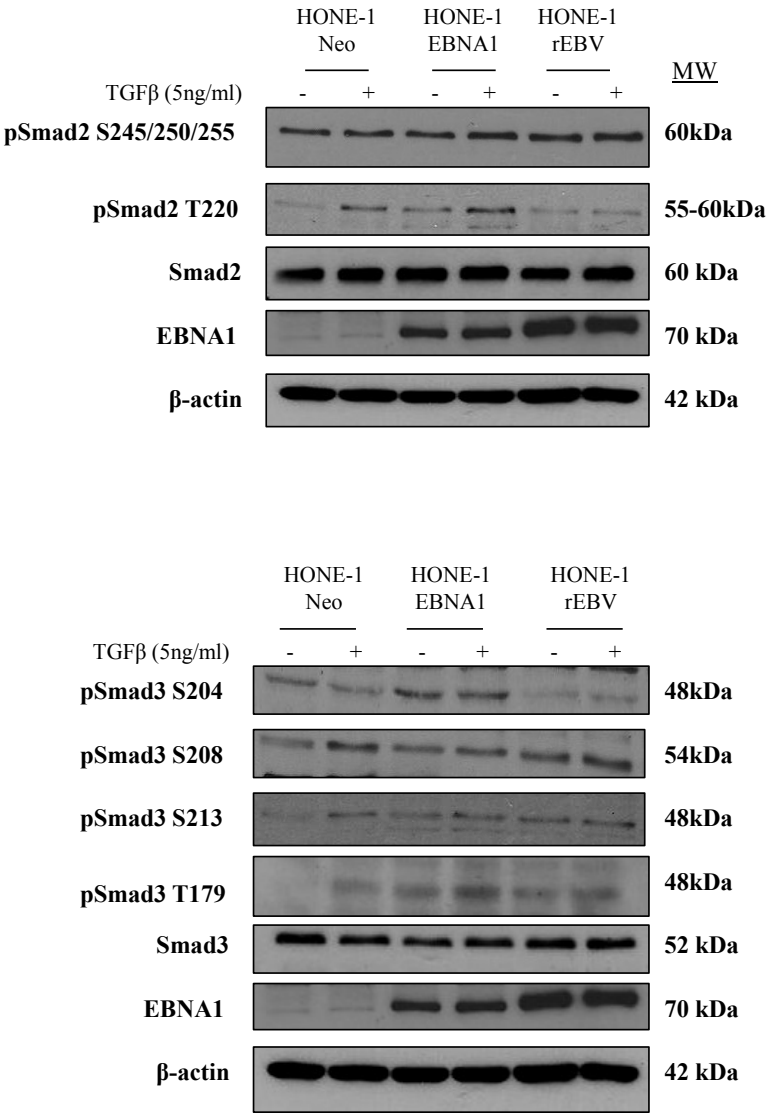
HONE-1 Neo
HONE-1 EBNA1
HONE-1 rEBV
MW
TGFβ (5ng/ml)
- + - + - +
pSmad2 S245/250/255
60kDa
pSmad2 T220
55-60kDa
Smad2
60 kDa
EBNA1
70 kDa
β-actin
42 kDa
HONE-1 Neo
HONE-1 EBNA1
HONE-1 rEBV
TGFβ (5ng/ml)
- + - + - +
pSmad3 S204
48kDa
pSmad3 S208
54kDa
pSmad3 S213
48kDa
pSmad3 T179
48kDa
Smad3
52 kDa
EBNA1
70 kDa
β-actin
42 kDa

C)

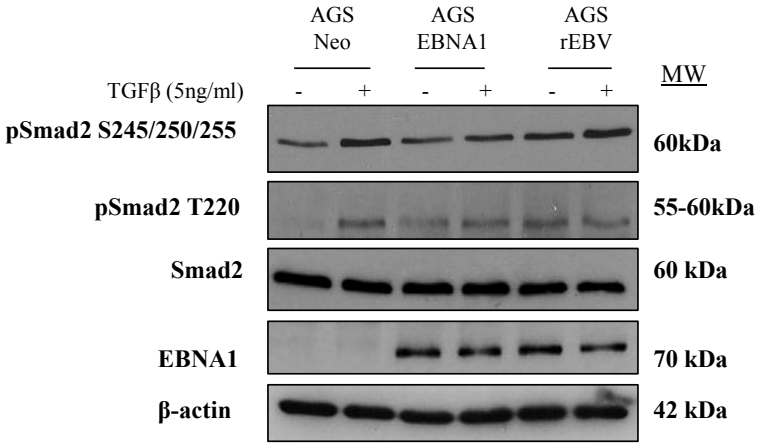
AGS Neo
AGS EBNA1
AGS rEBV
TGFβ (5ng/ml)
- + - + - +
MW
pSmad2 S245/250/255
60kDa
pSmad2 T220
55-60kDa
Smad2
60 kDa
EBNA1
70 kDa
β-actin
42 kDa

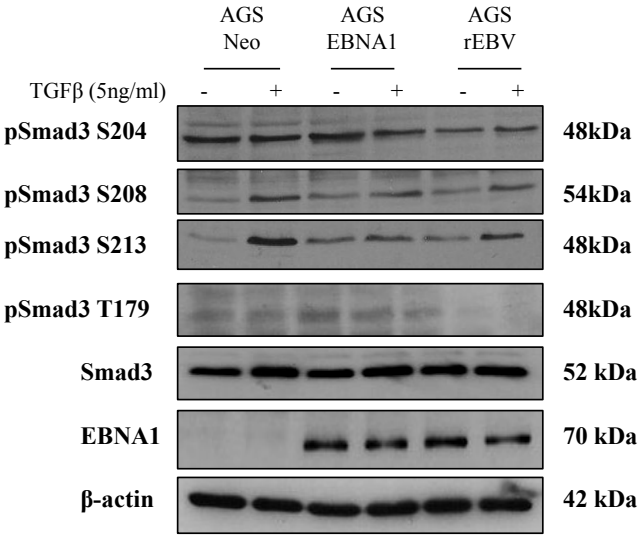
AGS Neo
AGS EBNA1
AGS rEBV
TGFβ (5ng/ml)
- + - + - +
pSmad3 S204
48kDa
pSmad3 S208
54kDa
pSmad3 S213
48kDa
pSmad3 T179
48kDa
Smad3
52 kDa
EBNA1
70 kDa
β-actin
42 kDa

observed in Ad/AH EBNA1 cells, and was generally repeated in the rEBV cells, with the exception of pSmad2 Ser245/250/255 and pSmad3 Ser213. In the HONE-1 cell panel, increasing levels of pSmad2 Ser245/250/255 and Thr220, and pSmad3 Ser204 and Thr179 were observed in the EBNA1-expressing cells, while in AGS EBNA1 cells, only pSmad3 Ser204 and Thr179 expression were increased.

3.3.2 EBNA1 may activate non-Smad signalling pathways to increase Smad linker phosphorylation

A recent interpretation of the role of Smad linker region phosphorylation is that it can be used to regulate the potential for transcriptional activity of the oligomeric Smad complex (Burch et al., 2010). The result is variable, in some cases inhibiting transcriptional activity, whereas in others enhancing TGFβ-induced transcription (Wrighton et al., 2006, Alarcón et al., 2009, Gao et al., 2009). This discrepancy ultimately seems dependent on both the availability and location of the specific kinases involved. Linker phosphorylation by cytosolic MAPKs, for example, phosphorylation by p38 MAPK and ROCK (at Smad3 Ser204, Ser208 and Ser213), and JNK (at Smad3 Ser208 and Ser213) generally results in enhancement of gene transcription (Engel et al., 1999, Mori et al., 2004, Kamaraju and Roberts, 2005), particularly of the Smad-dependent expression of extracellular matrix protein-related genes and matrix metalloproteinases (Burch et al., 2010, Matsuzaki et al., 2009). Similarly, TGFβ-induced JNK1 phosphorylation at MAPK sites in linker region of Smad3 results in the induction of EMT-related genes in lung epithelial cells (van der Velden et al., 2011). In contrast, if linker phosphorylation is delayed until the protein has translocated to the nucleus following prerequisite C-terminal phosphorylation, the effect is largely antagonistic, inhibiting transcriptional activity, conferring resistance to growth inhibitory effects, and often priming

for degradation (Burch et al., 2010). CDK family members, as well as nuclear MAPKs, play a significant role here, as Smad3 Thr179 and Ser213 are reportedly phosphorylated by CDK2/4, and CDK phosphorylation of Smad3 at Ser208 acts as a priming site for the activity of GSK3, which phosphorylates Smad3 at Ser204, decreasing Smad3 transcriptional activity (Millet et al., 2009, Wang et al., 2009). Moreover, CDK4-dependent Smad2/3 linker phosphorylation can override the TGFβ growth response through an up-regulation of c-myc (Matsuzaki et al., 2009), and phosphorylation in the nucleus by CDK8 and CDK9 is reported to render Smads subject to proteasome-mediated turnover (Alarcón et al., 2009).

To further characterise this observed linker phosphorylation, the expression levels of associated kinases and their active forms were measured by immunoblotting analysis. Neo control, EBNA1-expressing and rEBV-infected Ad/AH cells were grown in 0.5% serum for 16 hours before treatment with 5ng/ml TGFβ1 for 24 hours. Extracted protein samples were resolved by SDS-PAGE and membranes were probed using antibodies against JNK, pJNK, ERK, pERK, p38, p-p38, GSK3β and pGSK3α/β, with β-actin as a loading control. From Figure 3.29, it is apparent that the total levels of most kinases were largely unchanged, as was the case for most of the phosphorylated forms, with the exception of pERK and pJNK, whose expression was increased in the EBNA1-expressing and rEBV-infected Ad/AH cells.

To extend these observations, Neo control, EBNA1-expressing and rEBV-infected Ad/AH cells were again cultured in 0.5% serum for 16 hours before treatment with a panel of inhibitors for 1 hour prior to stimulation with 5ng/ml TGFβ1 for 24 hours. Protein extracts were resolved by SDS-PAGE and subjected to immunoblotting with antibodies to the linker Smad phospho-isoforms. Representative immunoblots are shown in Figure 3.30. SB431542, a

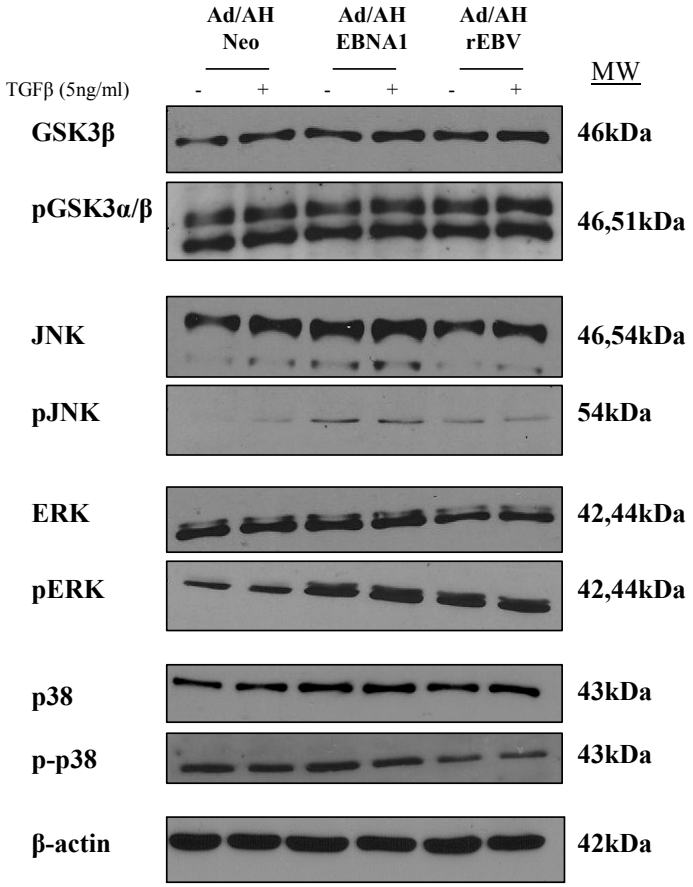

Figure 3.29: Expression of Smad linker region kinases in Ad/AH cells
Immunoblotting for protein levels of total GSK3β, serine 21/9 phosphorylated GSK3α/β, total JNK, threonine 183/tyrosine 185 phosphorylated JNK, total ERK 1/2 (p42/44 MAPK), phosphorylated p42/44, total p38 and threonine 180/tyrosine 182 phosphorylated p38 in serum-starved Ad/AH cells expressing either a control neomycin resistance cassette or EBNA1, or stably infected with rEBV, under basal conditions or following stimulation with 5ng/ml recombinant hTGFβ1 for 24 hours. Blots were re-probed for β-actin to confirm equal protein loading.

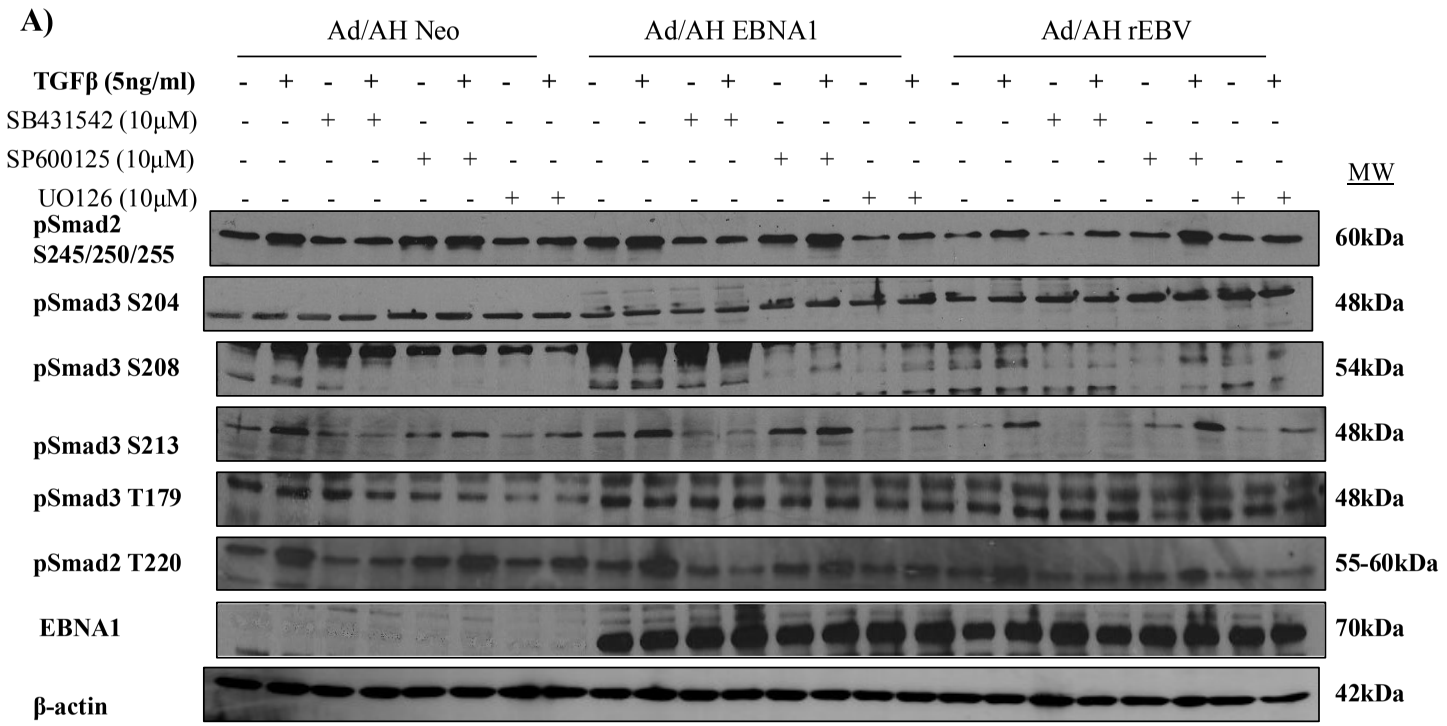

Figure 3.30: Expression of linker phosphorylated Smad2 and Smad3 in Ad/AH cells following kinase inhibitor treatments
Immunoblotting for protein levels of the serine 245/250/255 and threonine 220 phosphorylated forms of Smad2, and the serine 204, serine 208, serine 213 and threonine 179 phosphorylated forms of Smad3, in serum-starved Ad/AH cells expressing either a control neomycin resistance cassette or EBNA1, or stably infected with rEBV. Cells were treated with a panel of specific kinase inhibitors as indicated for 1 hour before stimulation with 5ng/ml recombinant hTGFβ1 for a further 24 hours, or left unstimulated as controls. Blots were re-probed for β-actin to confirm equal protein loading.

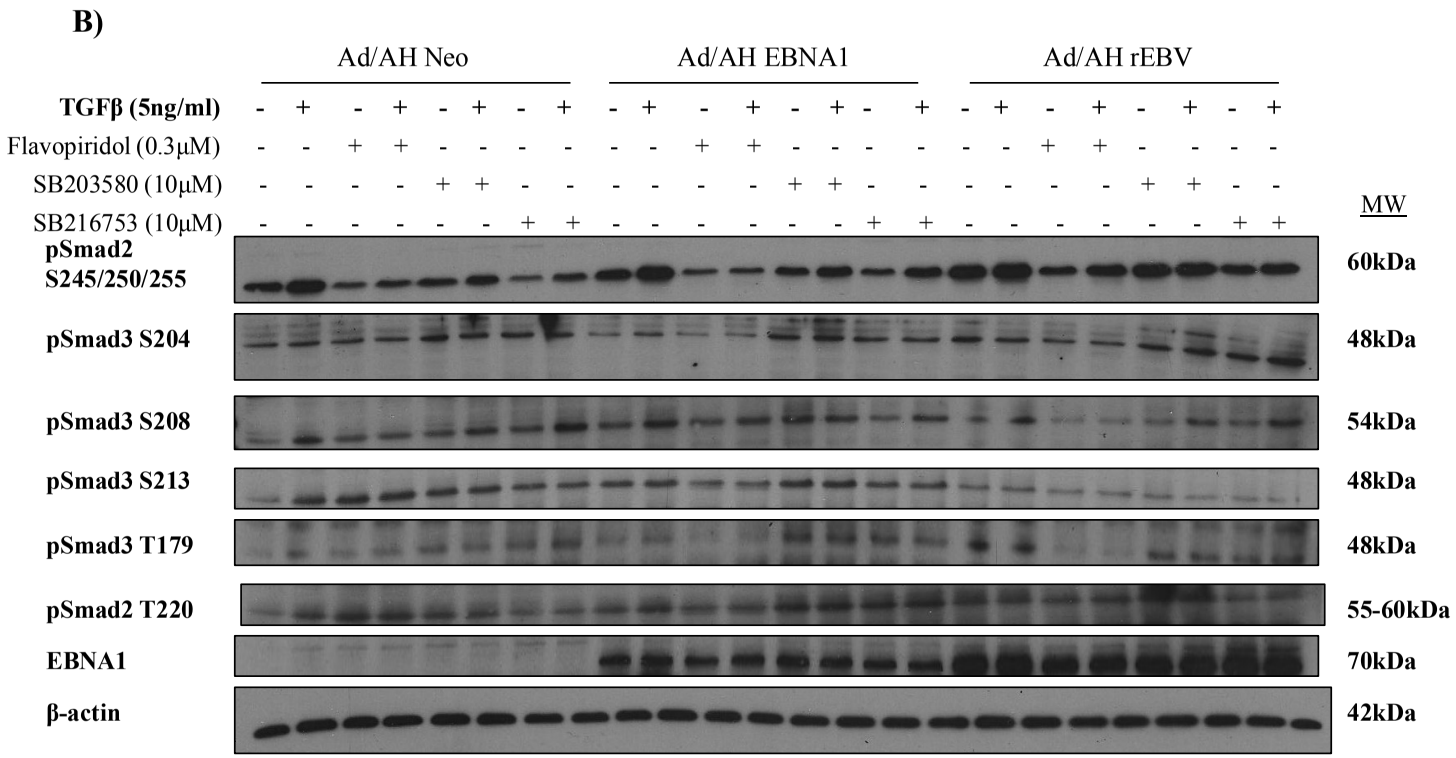
B)
Ad/AH Neo
Ad/AH EBNA1
Ad/AH rEBV
TGFβ (5ng/ml)
Flavopiridol (0.3μM)
SB203580 (10μM)
SB216753 (10μM)
MW
pSmad2 S245/250/255
60kDa
pSmad3 S204
48kDa
pSmad3 S208
54kDa
pSmad3 S213
48kDa
pSmad3 T179
48kDa
pSmad2 T220
55-60kDa
EBNA1
70kDa
β-actin
42kDa

potent TβRI kinase inhibitor, was used to distinguish those responses that may rely on an initial C-terminal phosphorylation for nuclear targeting, and was seen to reduce phosphorylation at pSmad2 Ser245/250/255 and Thr220, and pSmad3 Ser208 and Ser213 residues. The JNK inhibitor, SP600125 reduced expression of the Ser208-phosphorylated Smad3, while U0126, a MEK-ERK/MAPK inhibitor, reduced phosphorylation at pSmad2 Ser245/250/255 and pSmad3 Ser208 residues. The greatest effects were seen with the CDK inhibitor, flavopiridol, which reduced phosphorylation of Smad2 at Ser245/250/255 and Thr220, and of Smad3 at Ser204, Ser213 and T179. This is consistent with the reported role for CDKs in the phosphorylation of these residues. The p38 MAPK inhibitor, SB203580, and GSK3 inhibitor, SB216753, in contrast appeared to have little effect in this context.

3.3.3 EBNA1 increases the migration of carcinoma cells

An increase in linker phosphorylation and also TGFβ over-expression have been specifically correlated with an increase in the invasive capacity of tumour cells (Matsuzaki and Okazaki, 2006, Tobin et al., 2002). In agreement with this, transwell migration assays confirmed that EBNA1-expressing cells, like their rEBV-infected counterparts, displayed increased rates of migration on fibronectin compared to Neo control cells (Figure 3.31). However, whereas treatment with the TβRI inhibitor, SB431542 enhanced the migration of Ad/AH Neo control cells, SB431542 treatment reduced the rates of migration in EBNA1-expressing and rEBV-infected cells, findings which suggest that dysregulated TGFβ signalling contributes to the increased motile responses in these cells. This feature was not confined to Ad/AH cells, as SB431542 treatment also potentiated the migration of HONE-1 and AGS Neo clones, yet reduced the migration of EBNA1-expressing and rEBV-infected AGS cell lines (Figure 3.31B&C).

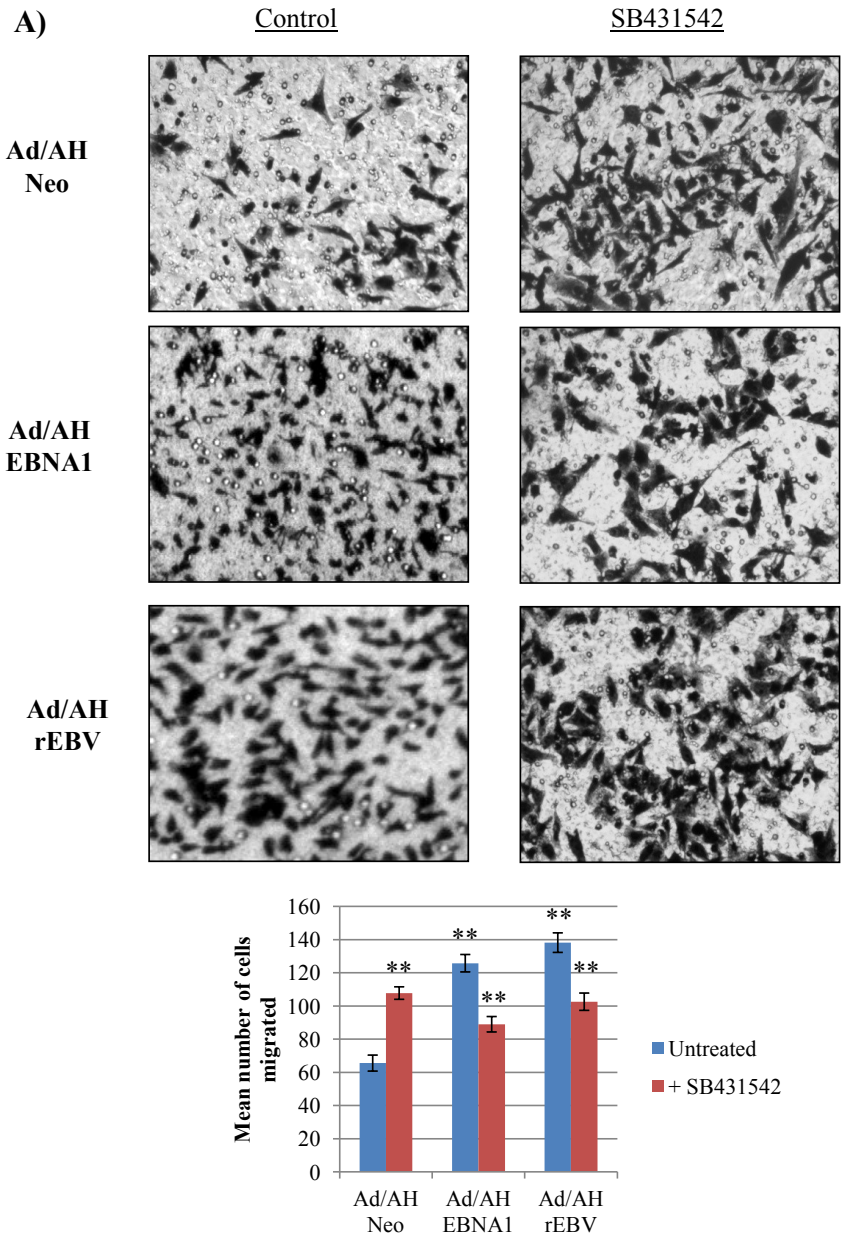

Figure 3.31: The effect of inhibition of TGFβ signalling on the migration of Ad/AH, HONE-1 and AGS carcinoma cell lines

Serum-starved Ad/AH (A), HONE-1 (B) and AGS (C) cells expressing either a control neomycin resistance cassette or EBNA1, or stably infected with rEBV were seeded into the upper wells of transwell migration chambers in serum-free medium with and without 10μM SB431542, and allowed to migrate for 24 hours. The number of migrated cells in five representative fields were counted and histograms were created showing the mean number of cells migrated (SD) (** denotes a P-value <0.01).

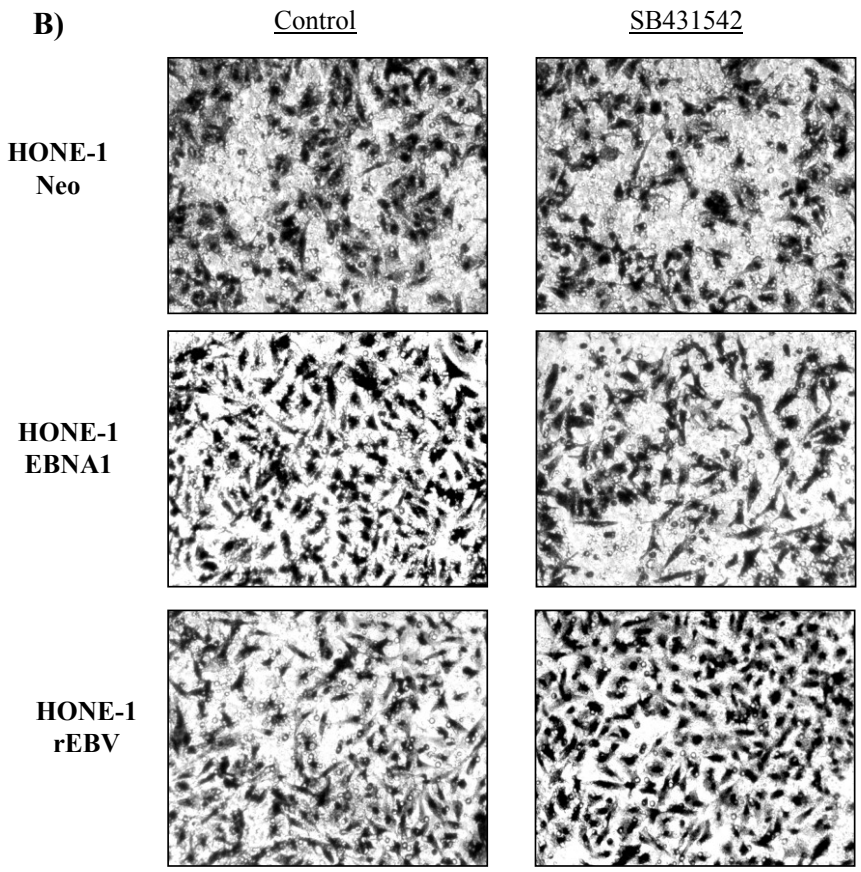
B)
Control
SB431542
HONE-1
Neo
HONE-1
EBNA1
HONE-1
rEBV

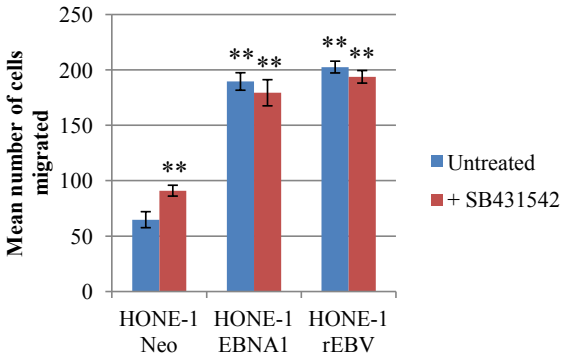
Mean number of cells migrated
250
200
150
100
50
0
**
**
**
**
**
HONE-1 Neo
HONE-1 EBNA1
HONE-1 rEBV
Untreated
+ SB431542

C)

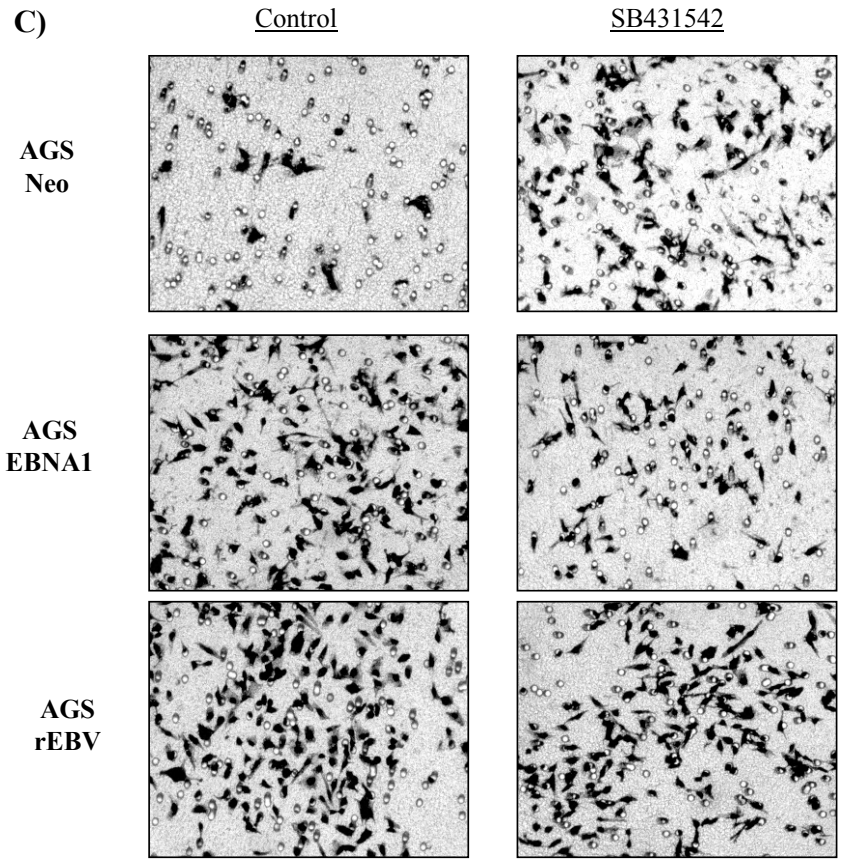
Control
SB431542
AGS Neo
AGS EBNA1
AGS rEBV

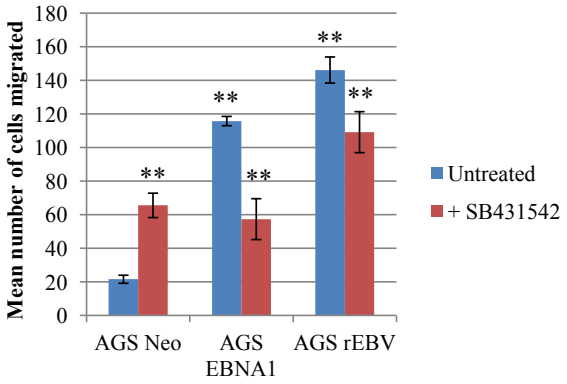
Mean number of cells migrated
180
160
140
120
100
80
60
40
20
0
**
**
**
**
**
AGS Neo
AGS EBNA1
AGS rEBV
Untreated
+ SB431542

Unexpectedly, SB431542 treatment failed to impact on the migration of EBNA1-expressing and rEBV-infected HONE-1 cell lines (Figure3.31A, B & C).

3.4 Modelling TGFβ signalling in C666-1 cells

3.4.1 A constitutively active TβRI mutant restores TGFβ activity in C666-1 cells

In comparison to normal samples, the EBV-positive C666-1 cell line was found to approximate an authentic NPC tumour in terms of its gene expression pattern by microarray analyses, and can be considered a good *in vitro* model for NPC (Hu, PhD thesis, 2010). In attempting to model TGFβ signalling in this cell line, it was essential that inherent defects in the pathway, attributed to an absence in expression of TβRII (Wood et al., 2007), were taken into account. Signalling is strictly dependent on receptor complex formation, as TβRII is essential for phosphorylation of TβRI, which is unable to recognise free TGFβ ligand of its own accord, and requires this activation for further signal propagation (Wrana et al., 1994, Zwaagstra et al., 2008). It was hypothesised that the introduction of a constitutively active TβRI variant (T204D) may bypass the TβRII defect in C666-1 cells, thereby testing the functional integrity of the remainder of the pathway. To this end, increasing concentrations of TβRI (T204D) were transiently transfected into C666-1 cells and their effects studied by TGFβ/Smad-luciferase reporter assay (Figure 3.32). The introduction of the constitutively active TβRI was sufficient to significantly induce the otherwise absent activity of the TGFβ-responsive $p(CAGA)_{12}$-luciferase reporter, while titration of a wild-type version of TβRI had little or no effect.

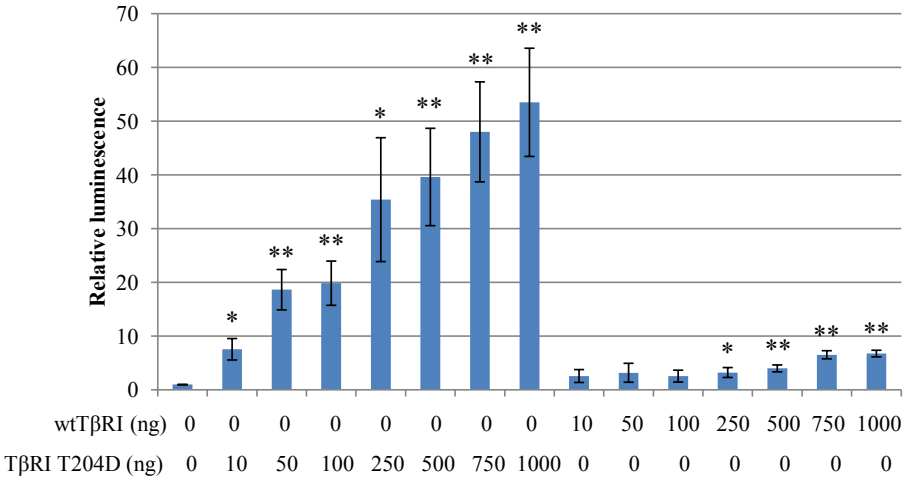

Figure 3.32: Bypassing of the TβRII defect in C666-1 cells using a constitutively active TβRI

Dual luciferase reporter assay showing p(CAGA)$_{12}$-Luc activity in C666-1 cells following transient transfection with either a wild-type TβRI, a constitutively active TβRI T204D, or the control pcDNA3 vector. A histogram is shown to depict the relative luminescence after normalising to Renilla luciferase values and expressing as a ratio of activity relative to the control vector pGL3-basic. Data from four independent experiments is presented as the mean fold differences in activity $\pm$ SE, relative to that observed in C666-1 cells transfected with the pcDNA3 vector only which is given an arbitrary value of 1 (** denotes a P-value <0.01 and * denotes a P-value <0.05).

3.4.2 Re-establishment of TβRII expression in C666-1 cells restores TGFβ activity and R-Smad C-terminal phosphorylation

In a previous study, Biswas and colleagues reported that expression of the TβRII gene could be restored in colon cancer cells where microsatellite instability induces mutational inactivation (Biswas et al., 2008). These plasmids were obtained in an attempt to restore TβRII expression and TGFβ responsiveness in C666-1 cells. As is shown in Figure 3.33, transient transfection of increasing concentrations of the pLXIN-TβRII plasmid significantly restored both $p(CAGA)_{12}$-Luc and $p(ARE)_3$-Luc reporter activities in a dose-dependent manner, while the kinase inactive D522N mutant was intrinsically unable to induce reporter activity. Additionally, the effect of TGFβ stimulation on the reporter response was progressively enhanced with increasing concentrations of pLXIN-TβRII.

This notable absence of TβRII expression in the C666-1 cell line would predictably render C666-1 cells incapable of R-Smad activation, as was characterised by the negligible levels of Smad2 C-terminal phosphorylation shown by immunoblotting, which could only be stimulated once this defect had been repaired (Figure 3.34); however, the ability of TGFβ to further augment phosphorylation levels still appeared defective, while linker phosphorylation appeared unimpeded by the defect.

3.4.3 TGFβ target gene expression is restored by the introduction of a functional TβRII

C666-1 cells transiently transfected with either the wild-type pLXIN-TβRII or kinase defective pLXIN-TβRII variant were cultured in 0.5% serum for 16 hours, prior to stimulation with 5ng/ml TGFβ1 for a further 24 hours. As indicated by both RT-PCR and immunoblotting

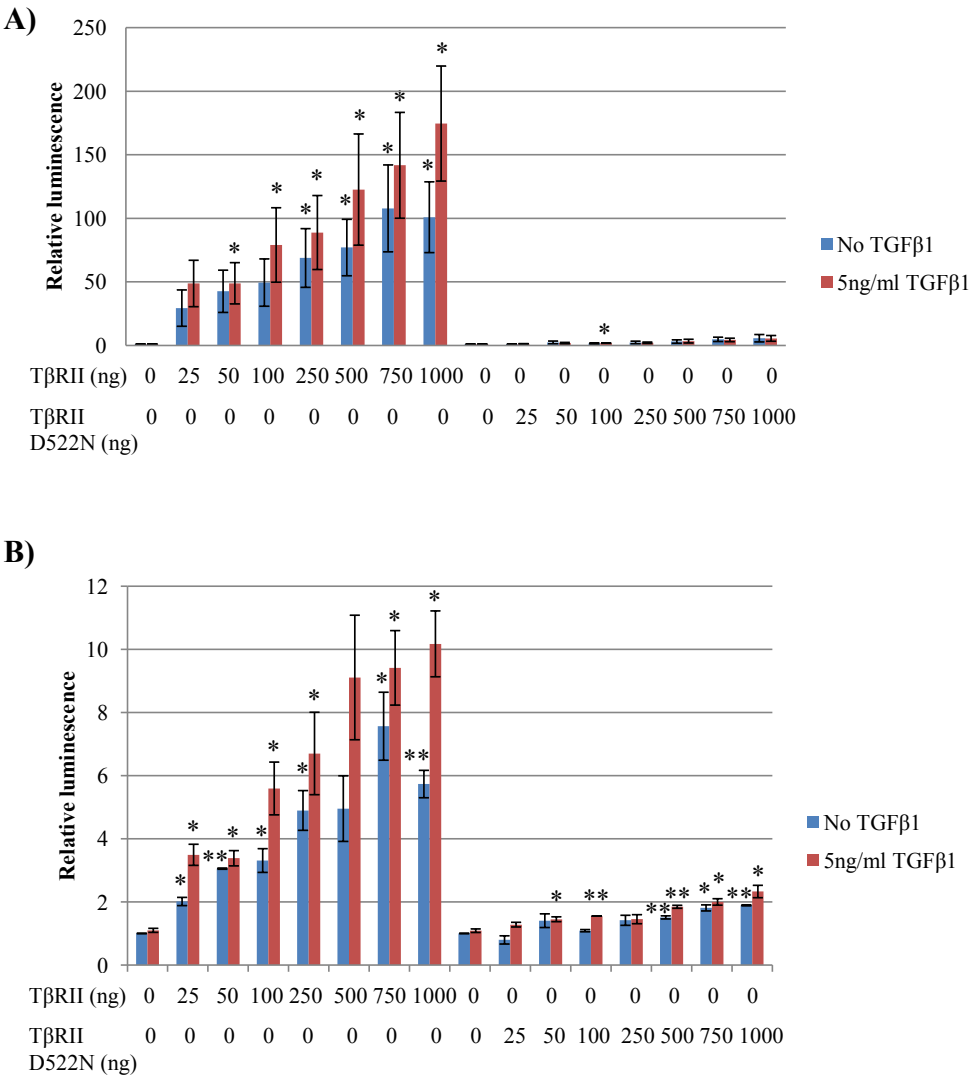

Figure 3.33: The effect of repairing the TβRII defect on TGFβ reporter activity in C666-1 cells
Dual luciferase reporter assays showing levels of $p(CAGA)_{12}$-Luc (A) or $p(ARE)_3$-Luc (B) luciferase reporter activity in C666-1 cells transiently transfected with either the wild-type pLXIN-TβRII, kinase inactive pLXIN-TβRII D522N or control vector, determined under basal conditions and following stimulation with 5ng/ml recombinant hTGFβ1 for 24 hours. Histograms are shown to depict the relative luminescence after normalising to Renilla luciferase values and expressing as a ratio of activity relative to the control vector pGL3-basic. Data from three independent experiments is presented as the mean fold differences in activity $\pm$ SE, relative to that observed in unstimulated C666-1 cells transfected with the pLXIN control vector only which is given an arbitrary value of 1 (** denotes a P-value <0.01 and * denotes a P-value <0.05).

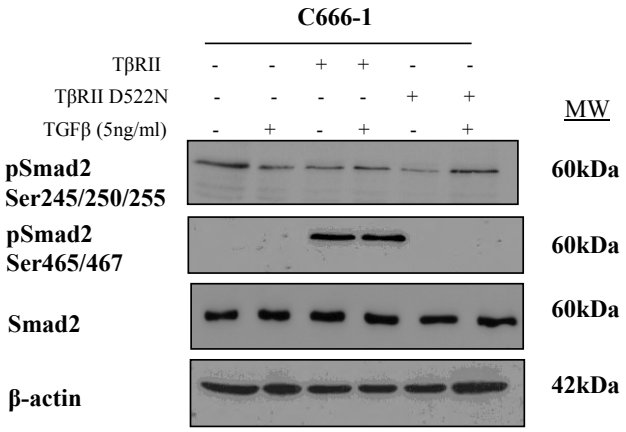

Figure 3.34: Expression of Smad2 phospho-isoforms following TβRII defect repair in C666-1 cells
Immunoblotting for protein levels of total, linker region serine 245/250/255 and C-terminal serine 465/467 phosphorylated forms of Smad2 in serum-starved C666-1 cells following transient transfection with either the wild-type pLXIN-TβRII or constitutively active pLXIN-TβRII D522N plasmids, under basal conditions and following stimulation with 5ng/ml recombinant hTGFβ1 for 24 hours. Blots were reprobed for β-actin to confirm equal protein loading.

analysis (Figure 3.35), restoration of TβRII expression resulted in downstream effects on TGFβ-responsive genes. βig-h3 and PAI-1 are established TGFβ-responsive genes (Skonier et al., 1992, Skonier et al., 1994, Thapa et al., 2007, Dennler et al., 1998) and, as previously demonstrated, are negatively regulated in the presence of EBNA1 (Wood et al., 2007). In the presence of pLXIN-TβRII, expression of PAI-1 was basally detectable and dramatically induced by TGFβ, but remained absent with pLXIN-TβRII D522N, while the transcription of βig-h3 was significantly enhanced when the pathway was repaired.

3.4.4 Repair of the TβRII defect in C666-1 cells is not sufficient to restore the TGFβ-mediated growth arrest response

After establishing that TGFβ1-mediated target gene responses could be restored, the possibility of resultant effects on C666-1 cell cycle progression following TβRII repair was investigated. C666-1 cells were transfected with either pLXIN-TβRII or pLXIN-TβRII D522N plasmids and, after incubation in 0.5% serum for 16 hours, stimulated with 5ng/ml TGFβ1. 24, 48, 72 and 96 hours after stimulation, cells were recovered as single-cell suspensions and stained with propidium iodide. Subsequently, cells were subjected to flow cytometric analysis to examine the impact of TβRII expression on TGFβ-mediated cell cycle inhibition. Examples of the subsequent analyses of resulting histograms using MultiCycle are shown in Figure 3.36. This analysis revealed no significant differences in cell cycle distribution between samples transfected with either wild-type or kinase inactive receptors, in untreated cells, or cells treated with TGFβ. These findings indicate that whilst re-expression of TβRII is sufficient to instigate Smad phosphorylation and subsequent downstream target activation, C666-1 cells may have defective responses linking TGFβ/Smad activity to pathways involved in growth inhibition.

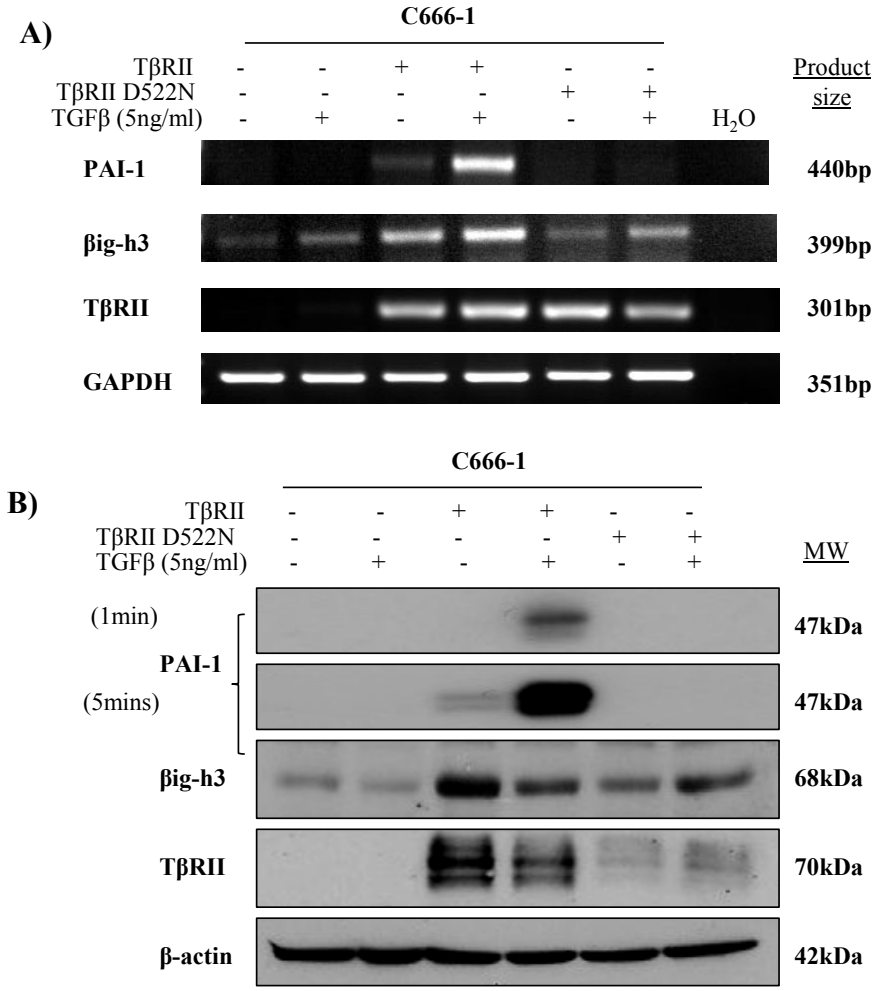

Figure 3.35: Expression of TGFβ target genes following TβRII defect repair in C666-1 cells

A) RT-PCR analysis for mRNA levels of TβRII, and the TGFβ target genes, PAI-1 and βig-h3, in serum-starved C666-1 cells transiently transfected with either the wild-type pLXIN-TβRII or constitutively active pLXIN-TβRII D522N plasmids, under basal conditions or following stimulation with 5ng/ml recombinant hTGFβ1 for 24 hours. The housekeeping gene GAPDH was included as a positive control to confirm equal RNA input into the PCR reactions, while negative water controls confirmed the absence of contamination.

B) Immunoblotting for PAI-1, βig-h3 and TβRII protein expression levels in serum-starved C666-1 cells transiently transfected with either the wild-type pLXIN-TβRII or constitutively active pLXIN-TβRII D522N plasmids, under basal conditions of following stimulation with 5ng/ml recombinant hTGFβ1 for 24 hours. Blots were reprobed for β-actin to confirm equal protein loading. A second immunoblot for PAI-1, exposed for the longer time of 5 minutes, is also shown.

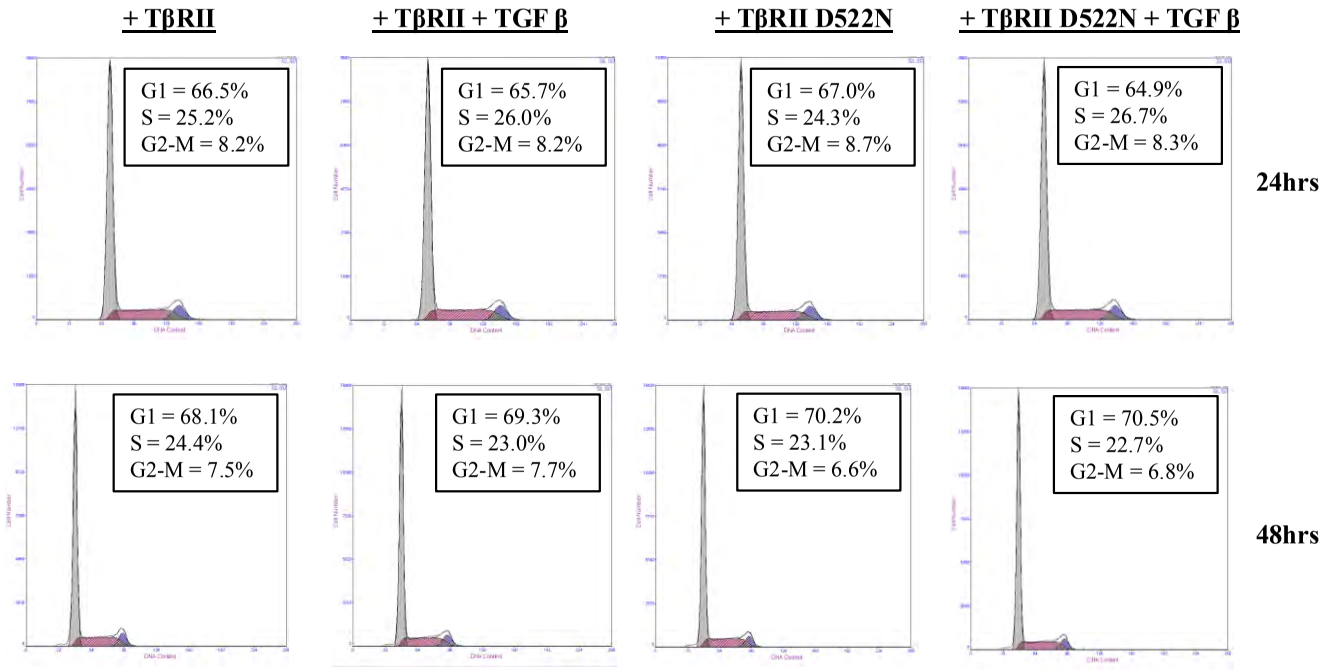

Figure 3.36: Cell cycle analysis by propidium iodide staining of C666-1 cells following TβRII defect repair
Analysis of cell cycle in serum-starved C666-1 cells after transient transfection with either the wild-type pLXIN-TβRII or constitutively active pLXIN-TβRII D522N plasmids, and treated with 5ng/ml recombinant hTGFβ1 or left unstimulated as a control. DNA content was measured at 24, 48, 72 and 96 hours by propidium iodide staining and subsequent flow cytometric analysis. Resulting histogram files were analysed for cell cycle distribution using MultiCycle. Representative traces from one of three independent experiments are shown, with percentages of cells in G1, S and G2-M phases indicated.

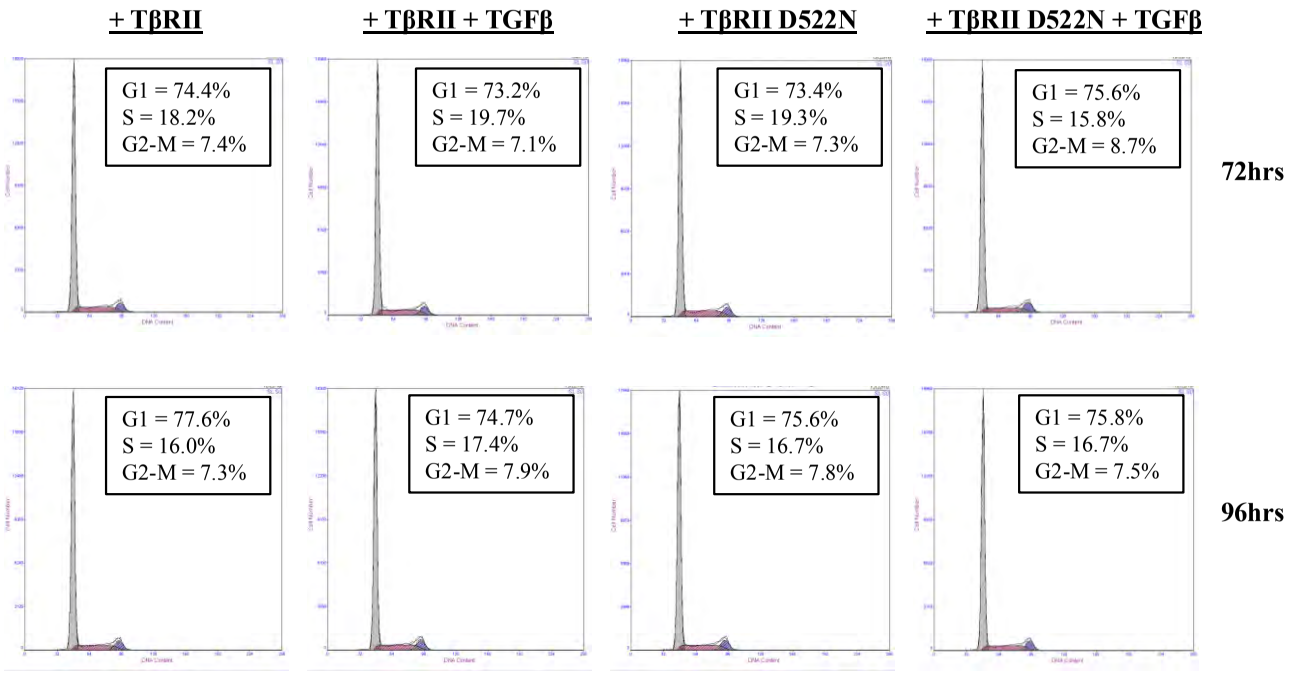
+ TβRII
+ TβRII + TGFβ
+ TβRII D522N
+ TβRII D522N + TGFβ
G1 = 74.4%
S = 18.2%
G2-M = 7.4%
G1 = 73.2%
S = 19.7%
G2-M = 7.1%
G1 = 73.4%
S = 19.3%
G2-M = 7.3%
G1 = 75.6%
S = 15.8%
G2-M = 8.7%
72hrs
G1 = 77.6%
S = 16.0%
G2-M = 7.3%
G1 = 74.7%
S = 17.4%
G2-M = 7.9%
G1 = 75.6%
S = 16.7%
G2-M = 7.8%
G1 = 75.8%
S = 16.7%
G2-M = 7.5%
96hrs

3.4.5 Linker phosphorylated Smads are expressed in C666-1 cells

While the absence of C-terminally phosphorylated Smads in C666-1 cells has been previously reported, and confirmed here, the expression of linker phosphorylated forms had not yet been characterised. Owing to the substantial involvement of non-Smad kinases in their generation, it was reasoned that phosphorylation at these linker residues may be induced in C666-1 cells. Immunoblotting analysis was performed on total cell lysates obtained from serum-starved cultures of C666-1 cells, either untreated or treated with TGFβ1 to examine the extent of Smad2/3 linker phosphorylation. A representative experiment, depicted in Figure 3.37, shows that the linker phosphorylated forms of both Smad2 and Smad3 were clearly visible in C666-1 cells. Interestingly however, the extent of linker region phosphorylation appeared to be largely unaffected in response to TGFβ stimulation.

3.4.6 TβRII expression increases Qp-luciferase reporter activity in C666-1 cells

To determine whether restoring TβRII expression had any effect on EBNA1 protein function, the effect of TβRII repair on both EBNA1 expression and on native Qp promoter activity was examined. C666-1 cells were transiently transfected with either wild-type pLXIN-TβRII or kinase inactive pLXIN-TβRII D522N plasmids and, 48 hours later, the levels of endogenous Qp-driven EBNA1 mRNA examined by RT-PCR. This analysis revealed that, following complete TβRII repair, TGFβ1 stimulation served to reduce EBNA1 expression. In Figure 3.38, a titration of the wild-type pLXIN-TβRII plasmid with the Qp-luciferase promoter construct demonstrated the ability of increasing amounts of the receptor to significantly enhance basal Qp-luciferase reporter activity, which was further increased by TGFβ stimulation. In contrast, the kinase inactive receptor variant had little or no effect on Qp-luciferase reporter activity.

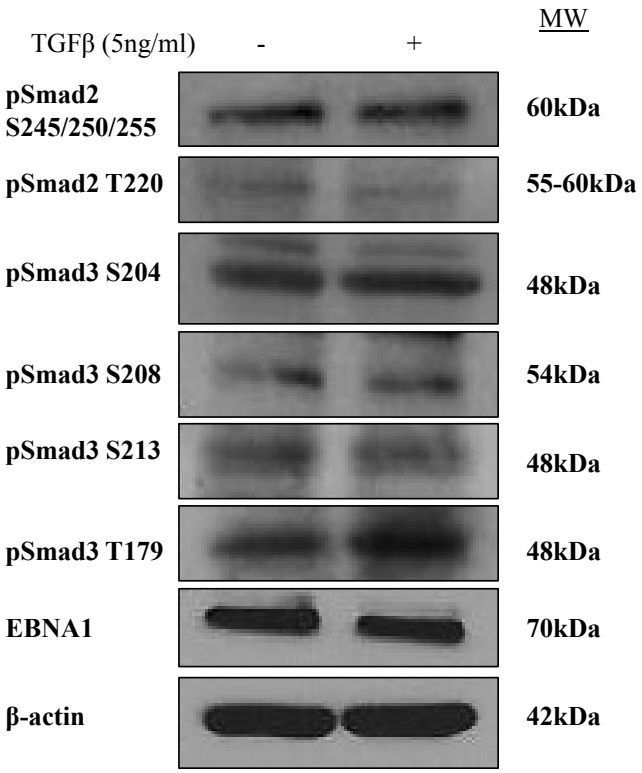

Figure 3.37: Expression of linker phosphorylated Smad2 and Smad3 in C666-1 cells
Immunoblotting for protein levels of the serine 245/250/255 and threonine 220 phosphorylated forms of Smad2, and the serine 204, serine 208, serine 213 and threonine 179 phosphorylated forms of Smad3 in serum-starved C666-1 cells stimulated with 5ng/ml recombinant hTGFβ1 for 24 hours, or left unstimulated as controls. Immunoblotting for EBNA1 is also shown, with β-actin included to confirm equal protein loading.

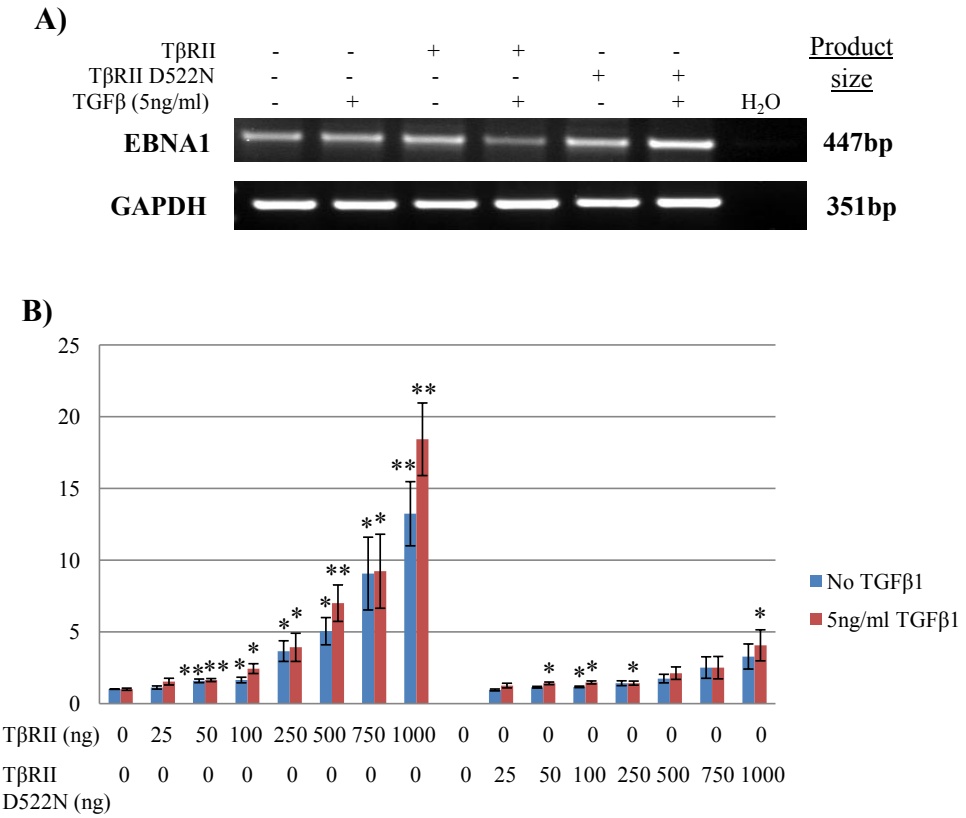

Figure 3.38: The effect of TβRII defect repair on EBNA1 expression and Qp promoter reporter activity in C666-1 cells

A) RT-PCR analysis for levels of EBNA1 mRNA expression in serum-starved C666-1 cells transiently transfected with either the wild-type pLXIN-TβRII or constitutively active pLXIN-TβRII D522N plasmids, both basally and following stimulation with 5ng/ml recombinant hTGFβ1 for 24 hours. GAPDH was included as a positive control to confirm equal RNA input into the PCR reactions, while negative water controls confirmed the absence of contamination.

B) Dual luciferase reporter assay for pQp-Luc activity in C666-1 cells transiently transfected with either the wild-type pLXIN-TβRII, kinase inactive pLXIN-TβRII D522N or control vector, determined under basal conditions and following stimulation with 5ng/ml recombinant hTGFβ1 for 24 hours. A histogram is shown to depict the relative luminescence after normalising to Renilla luciferase values and expressing as a ratio of activity relative to the control vector pGL2-basic. Data from three independent experiments is presented as the mean fold differences in activity ± SE, relative to that observed in unstimulated C666-1 cells transfected with the pLXIN control vector only which is given an arbitrary value of 1 (** denotes a P-value <0.01 and * denotes a P-value <0.05).

3.5 EBNA1 does not inhibit TGFβ signalling in Mv1Lu cells

It was hypothesised that the propensity of EBNA1 to attenuate TGFβ signalling may reflect the oncogenic status of the cell, the levels of endogenous TGFβ ligand expression, and the integrity of the TGFβ signalling pathway. To this end, experiments were extended to examine the effects of EBNA1 on TGFβ signalling in cells containing an intact and fully functional TGFβ signalling pathway. Experiments were subsequently performed in the untransformed mink lung epithelial cell line, Mv1Lu, an established "indicator" cell line that has been used extensively to study TGFβ signalling. The Mv1Lu cell line proves most useful in studies of TGFβ signalling as it carries an intact TGFβ pathway, and demonstrates a well-characterised growth arrest response when stimulated with TGFβ.

3.5.1 EBNA1 does not affect TGFβ luciferase reporter activity in Mv1Lu cells

Initially, EBNA1 protein expression in Mv1Lu cells transiently transfected with increasing concentrations of pSG5-EBNA1 was confirmed by immunoblotting (Figure 3.39A). Subsequent dual luciferase reporter assays were used to demonstrate that transient transfection of pSG5-EBNA1 into Mv1Lu cells resulted in negligible differences in the level of activity of the TGFβ-responsive luciferase reporters, $p(CAGA)_{12}$-Luc and $p(ARE)_3$-Luc (Figure 3.39B&C). As expected, cells demonstrated a robust increase in activity in response to TGFβ stimulation, which did not appear to be abrogated by the presence of EBNA1.

3.5.2 EBNA1 does not affect TGFβ1-mediated growth arrest in Mv1Lu cells

Mv1Lu cells are sensitive to TGFβ stimulation, arresting in the G1 phase of the cell cycle. The growth arrest response after 24 hours was examined in these cells using propidium iodide staining followed by flow cytometric analysis. Cell cycle profiles were subsequently

A)

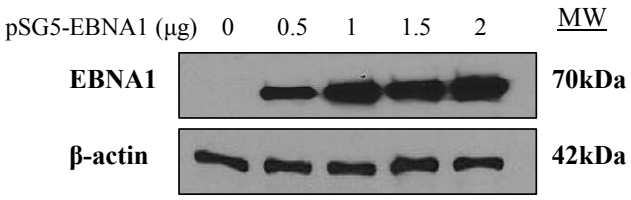

Figure 3.39: The effect of EBNA1 on TGFβ-induced reporter activity in the Mv1Lu cell line

A) Immunoblotting for EBNA1 protein expression in Mv1Lu cells transiently transfected with increasing concentrations of pSG5-EBNA1 to confirm transfection efficiency. β-actin was included to confirm equal protein loading.

Dual luciferase reporter assays showing $p(CAGA)_{12}$-Luc (B) and $p(ARE)_3$-Luc (C) luciferase reporter activity in Mv1Lu cells transiently transfected with increasing amounts of a pSG5-EBNA1 plasmid, and either stimulated with 5ng/ml recombinant hTGFβ1 for 24 hours or left unstimulated as a control. Histograms are shown to depict the relative luminescence after normalising to Renilla luciferase values and expressing as a ratio of activity relative to the control vector pGL3-basic. Data from three independent experiments is presented as the mean fold differences in activity $\pm$ SE, relative to that observed in unstimulated Mv1Lu cells expressing the empty pSG5 control vector only which is given an arbitrary value of 1.

B)

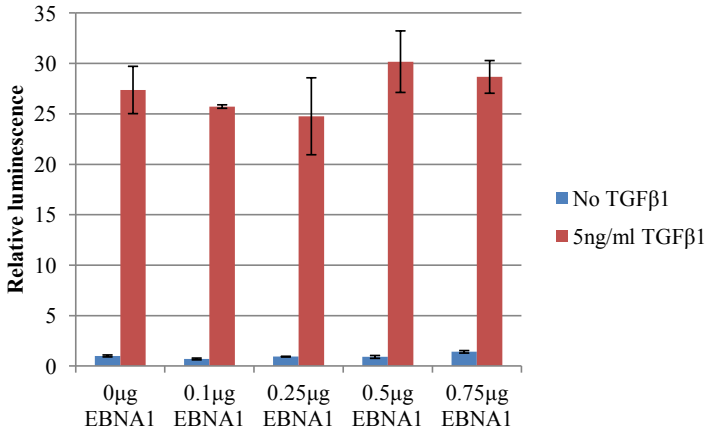
Relative luminescence
35
30
25
20
15
10
5
0
0µg EBNA1
0.1µg EBNA1
0.25µg EBNA1
0.5µg EBNA1
0.75µg EBNA1
No TGFβ1
5ng/ml TGFβ1

C)

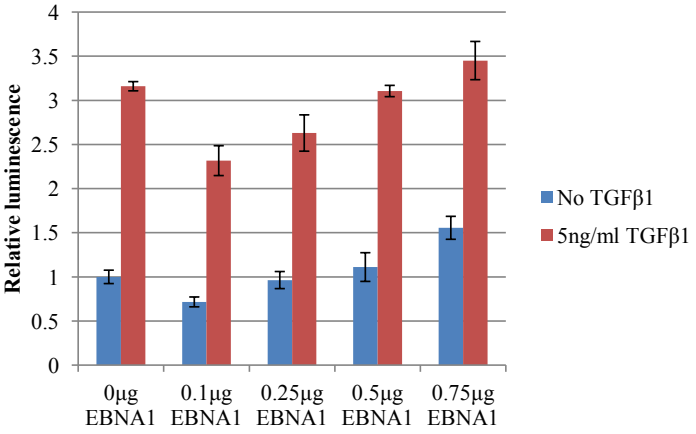
Relative luminescence
4
3.5
3
2.5
2
1.5
1
0.5
0
0µg EBNA1
0.1µg EBNA1
0.25µg EBNA1
0.5µg EBNA1
0.75µg EBNA1
No TGFβ1
5ng/ml TGFβ1

generated using MultiCycle, and representative traces are shown in Figure 3.40. In accordance with previous reports, TGFβ stimulation increased the number of cells in the G1 phase of the cell cycle, with appropriate reductions detected in both S and G2-M phases, 24 hours post-stimulation. The effect of TGFβ on cell cycle arrest appeared consistent, and was not altered with increasing concentrations of pSG5-EBNA1.

3.6 Discussion and Future Work

Data presented in this chapter confirm and extend the original observations of Wood *et al.* (Wood et al., 2007), demonstrating an ability of EBNA1 to modulate TGFβ signalling in established carcinoma cell lines. The inhibitory effect of EBNA1 on canonical TGFβ signalling is manifest at multiple levels as a decline in Smad2/3 C-terminal phosphorylation, increased Smad2 protein degradation, diminished activity of TGFβ-responsive reporters, reduced binding at SBE sites, and reduced expression of classical TGFβ target genes, overall indicative of an attenuation of Smad activity. The ability of exogenous Smad2 to overcome the inhibitory effect of EBNA1 on p3TP-lux reporter activity in EBNA1-expressing cells (Wood et al., 2007) implied that the main defect was mainly Smad-related, and the repression of both the Smad2-responsive $p(ARE)_3$-Luc reporter and Smad3-responsive $p(CAGA)_{12}$-Luc reporter, as well as reduction in the C-terminal phosphorylation of both Smad2 and Smad3 suggests this is a general effect, not specific to a particular R-Smad.

The reduction in reporter activity and also binding to SBE sites may be a direct result of the observed reduction in the pool of activated R-Smads available for participation in DNA binding. They may also reflect EBNA1-mediated differences in the availability of transcriptional cofactors between the cell lines. This may be particularly relevant to Smad2-

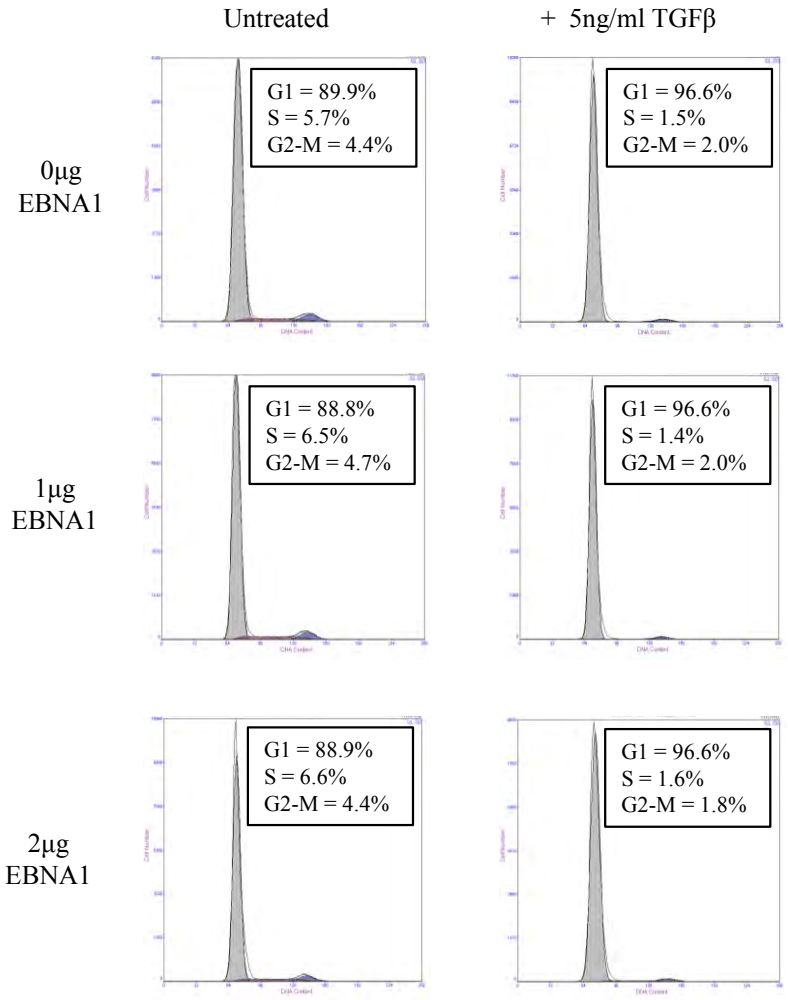

Figure 3.40: Cell cycle analysis by propidium iodide staining of Mv1Lu cells
Analysis of cell cycle in serum-starved Mv1Lu cells after transient transfection with increasing concentrations of pSG5-EBNA1 or the empty pSG5 control vector, and treated with 5ng/ml recombinant hTGFβ1 for 24 hours or left unstimulated as a control. DNA content was measured by propidium iodide staining and subsequent flow cytometric analysis. Resulting histogram files were analysed for cell cycle distribution using MultiCycle. Representative traces from one of three independent experiments are shown, and the percentages of cells in G1, S and G2-M phases are indicated.

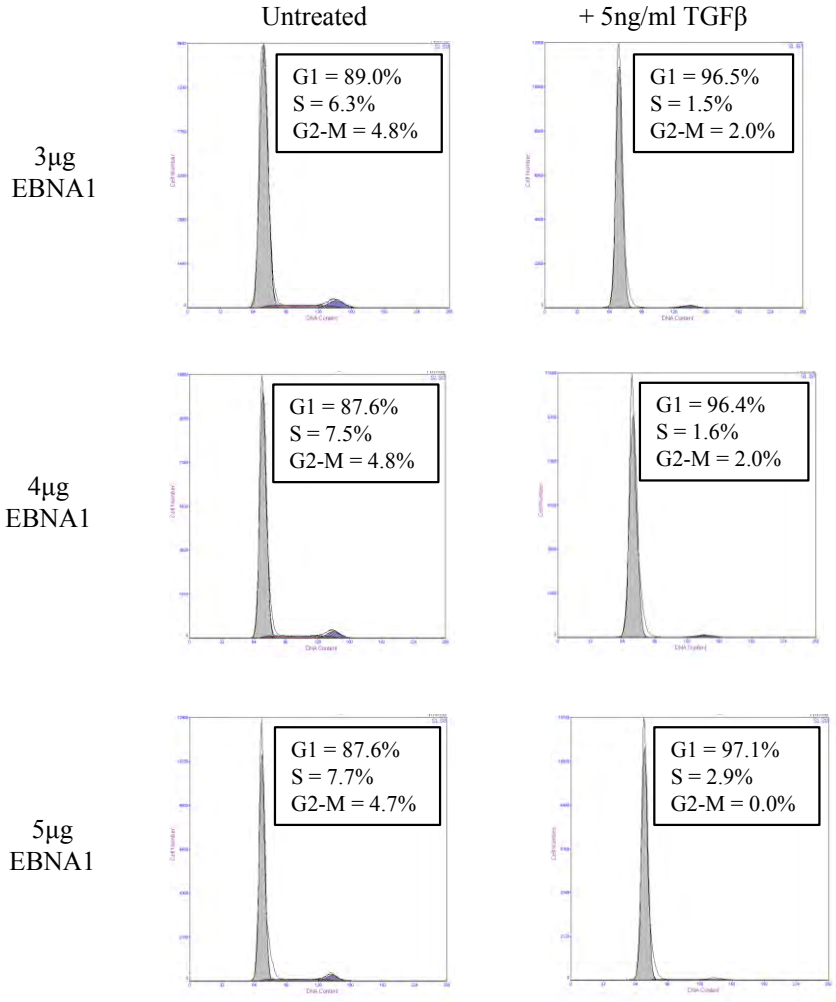
Untreated
+ 5ng/ml TGFβ
3μg EBNA1
4μg EBNA1
5μg EBNA1
G1 = 89.0%
S = 6.3%
G2-M = 4.8%
G1 = 96.5%
S = 1.5%
G2-M = 2.0%
G1 = 87.6%
S = 7.5%
G2-M = 4.8%
G1 = 96.4%
S = 1.6%
G2-M = 2.0%
G1 = 87.6%
S = 7.7%
G2-M = 4.7%
G1 = 97.1%
S = 2.9%
G2-M = 0.0%

mediated responses, as Smad2 cannot directly bind DNA (Dennler et al., 1999), and so is heavily reliant upon such factors. To further investigate this hypothesis, it would be interesting to utilise chromatin immunoprecipitation (ChIP) techniques at these sites to identify the protein compositions of bound transcription factor complexes.

PPM1A expression is increased in both EBNA1-expressing and rEBV-infected Ad/AH cells and, moreover, shows enhanced nuclear colocalisation with Smad2 and Smad3 in these cells. PPM1A may directly reduce R-Smad levels through increased dephosphorylation and nuclear export. It has been reported that inducible expression of PPM1A renders cells resistant to the anti-proliferative effects of TGFβ (Lin et al., 2006), and so the increased levels of PPM1A expression induced by EBNA1 were predicted to impart protection against the growth inhibitory effects of TGFβ in EBNA1-expressing and EBV-infected carcinoma cells. Also, its selectivity in targeting only C-terminally phosphorylated Smads, and leaving linker residues and TGFβ-dependent activation of Smad-independent pathways unaltered (Lin et al., 2006) added to the appeal that PPM1A induction was a key effector in regulating Smad2/3 phosphorylation and transcriptional activity in EBNA1-expressing and rEBV-infected cells. Similarly, PPM1B displays very similar functional properties, and it was hoped that an exciting parallel could be drawn with the ability of the two together to inhibit NFκB activity through increased IKKβ dephosphorylation (Sun et al., 2009). Although knockdown of the two phosphatases together did increase TGFβ/Smad reporter activity in EBNA1-expressing cells suggesting the inhibition was in part relieved, the pattern could not be repeated in rEBV-infected cells, hinting that another EBV-encoded protein may counteract the observed effects of EBNA1.

NEDD4-2 instead poses a promising candidate due to its ability to promote the degradation of both R-Smads and TβRI (Kuratomi et al., 2005). A recent report by Gao *et al.* describes how phosphorylation of specific threonine residues within the Smad linker region, Thr220 in Smad2 and Thr179 in Smad3, marks Smads for proteasome-mediated degradation, by priming an association with Nedd4-2 (Gao et al., 2009), and in agreement with this theory, the expression of these specific Smad2 and Smad3 phospho-isoforms were elevated in the presence of EBNA1. This mechanism could therefore account for the reported increase in Smad degradation (Wood et al., 2007) and, in limiting Smad half-life, may be important to constrain TGFβ signalling. The defect may therefore be the result of a reduced interaction between Smads and their receptors as either or both are targeted for increased degradation. shRNA-mediated knockdown of NEDD4-2 in EBNA1-expressing cells will be a useful tool to test this hypothesis.

It is unlikely, due to its strict requirement in the cell nucleus, that EBNA1 may function to inhibit Smad activity through interacting directly with TβRI, as exemplified by HCV NS5A (Choi and Hwang, 2006). Other viral proteins, such as adenovirus E1A oncoprotein, the human papilloma virus (HPV) type 16 E7 oncoprotein, HPV type 5 oncoprotein E6 and KSHV viral IFN regulatory factor 1 (vIRF1) (Nishihara et al., 1999, Lee et al., 2002, Mendoza et al., 2006, Seo et al., 2005) are able to interact directly with the Smad proteins themselves to thereby abrogate TGFβ signalling; EBNA1 however, while capable of altering the half-life of Smad2, and despite demonstrating an ability to interact with host proteins, as is exemplified by its sequestration of the cellular deubiquitinating enzyme, USP7 (Holowaty et al., 2003), shows no notable physical interaction with the Smad2 protein (Flavell et al., 2008). It does however remain a possibility that EBNA1 is able to bind modifiers of Smad activity,

such as PPM1A or NEDD4-2, in order to influence their activity, which should be verified using immunoprecipitation experiments.

Receptor expression levels can serve as a predictor of TGFβ-mediated biological responses (Rojas et al., 2009). TβRII expression is frequently down-regulated in human cancers and may be a direct target of EBV, as it is reportedly down-regulated in some BL cell lines (Inman and Allday, 2000). Furthermore, TβRII gene mutation is though to result from microsatellite instability on chromosome 11 in a proportion of NPC samples (Harn et al., 2002). This loss of TβRII holds great potential as the mechanism by which resistance to anti-proliferative TGFβ-mediated stimuli can be acquired, and is likely the key mechanism employed by C666-1 cells.

In KSHV-infected primary effusion lymphoma (PEL) cell lines, the inhibition of TGFβ signalling attributed to the epigenetic down-regulation of TβRII is instigated by KSHV-encoded LANA (Di Bartolo et al., 2008). Considering the high degree of functional similarity between EBNA1 and LANA (Renne et al., 2001), it seemed reasonable to assume that EBNA1 may have a similar effect. The lack of TβRII expression in the C666-1 cell line supports an EBV-induced cause (Harn et al., 2002, Wood et al., 2007). In dissecting TGFβ signalling in C666-1 cells, a constitutively active TβRI was found to alleviate the inherent repression on TGFβ activity, signalling independently of both ligand binding and activation by the type II receptor, while a wild-type version proved unable to overcome the defect.

Successful reconstitution of TβRII gene expression in deficient human colon cancer cell lines has been shown to effectively restore TGFβ-mediated growth inhibition in these cells (Biswas

et al., 2008). However, while subsequent transfection of TβRII plasmids into C666-1 cells was sufficient to restore TGFβ signalling activity and associated target gene expression in these cells, it was unable to restore TGFβ-mediated growth inhibition, suggesting that growth inhibitory pathways that feed into cell cycle control are corrupted in these cells. Indeed, transient transfection of a dominant-negative EBNA1 construct into C666-1 cells does not restore TβRII expression (data not shown), and attempts to permanently repair the defect and generate clones with stable expression of TβRII proved unsuccessful, as the cells appear to select against long-term maintenance of TβRII. Treatment of Akata BL cells with 5′-azacytidine reinstates the expression of the TβRII message, subsequently restoring Smad phosphorylation and TGFβ-mediated responses (Chen et al., 2007), while transcription of TβRII in these cells can also be induced by treatment with the HDAC inhibitor, trichostatin A (TSA), which not only restores cell growth inhibition and apoptotic responses, but also the propensity to reactivate EBV into lytic cycle (Fukuda et al., 2006). With this in mind, it would be useful to treat C666-1 cells with TSA and 5′-azacytidine to hopefully underpin the mechanism for TβRII loss in C666-1 cells, and subsequently examine the effects of reverting the defect both on C666-1 cellular phenotype and behaviour, but also on the behaviour of EBV.

In contrast to the C666-1 cell line, all other cell lines studied expressed detectable levels of TβRII, and the expression of both receptors was, for the most part, increased in the presence of EBNA1. Moreover, the expression of LMP1 in SCC12F cells was found to induce the expression of both TβRI and TβRII (Dr. Mhairi Morris, unpublished observations), and RP analysis of NPC tumour microarray data has previously revealed an up-regulation of TβRI and TβRII genes in NPC biopsies, further confirmed by IHC staining of NPC tumour sections

(Hu *et al.*, manuscript in preparation). Interestingly, TβRII expression was found to be abrogated in cells having undergone epithelial-to-mesenchymal transition (EMT), a major feature of invasive cancer subject to TGFβ control (Heldin et al., 2009), hinting that loss of TβRII could in fact be a later event, involved in the promotion of an EMT-like phenotype to assist in cancer cell invasion and migration. Data in support of this comes from the finding that MDCK cells undergoing EMT in response to LMP1, lose TβRII expression (Laverick *et al.*, manuscript in preparation).

Despite the overall increases in TGFβ receptor expression, a reduction in the levels of expression at the cell surface were observed in EBNA1-expressing and rEBV-infected Ad/AH cells, which also demonstrated a decreased TβRI half-life through a mechanism presumed to involve increased receptor turnover. The targeting of cell surface receptors is a common means of interfering with downstream signal transduction cascades to promote carcinogenesis, and the intracellular route undertaken by the TGFβ receptors directly governs signalling outcomes (Di Guglielmo et al., 2003, Sadowski et al., 2009). Increased proteasome-mediated degradation and ubiquitination of TβRII has been associated with the down-regulation of TGFβ signalling in renal cell carcinoma (Fukasawa et al., 2010), and the ability of viral proteins to enhance receptor turnover is not a new concept. The EBV-encoded LMP2A and LMP2B proteins have been reported to accelerate the turnover rate of the interferon receptors, IFNAR1 and IFNGR1, thereby decreasing cellular responsiveness to IFNα and IFNγ (Shah et al., 2009). In EBNA1-expressing cells, the observed effects would reduce the relative levels of TβRI available for participation in active receptor complex formation, thereby reducing the ability of TβRI to engage Smad phosphorylation. It would

therefore be useful to further extend this work using immunoprecipitation to determine the abundance of active complexes induced in response to TGFβ.

A further reduction in TβRI degradation is observed in the rEBV-infected Ad/AH cells, suggesting additional contributions from other EBV-encoded latent genes. This is complemented by a further increased level of cytoplasmic NEDD4-2 expression in these cells. Intriguingly, NEDD4-2-dependent ubiquitination of ENaC is increased by an interaction between ENaC and Cav-1 (Lee et al., 2009). It is possible Cav-1 and NEDD4-2 may similarly synergise in this setting to target TβRI, as Cav-1 has also been shown to interact with TβRI (Razani et al., 2001). The ability of virally-encoded proteins to localise to lipid rafts is not uncommon. Herpes simplex virus (HSV) uses lipid rafts to mediate viral entry, and the association of HSV-2-encoded UL11 protein with lipid rafts is thought to play a specific role in virion maturation (Koshizuka et al., 2007). While EBNA1 itself is unlikely to be associated with lipid raft structures, it would be interesting to determine whether perhaps either LMP1 or LMP2A, due to their intrinsic tendency to hijack lipid rafts (Kaykas et al., 2001, Coffin III et al., 2003, Dykstra et al., 2001), may further potentiate this effect. It would also be interesting to re-examine both TGFβ receptor cell surface expression and degradation in the presence of a TGFβ stimulus, although it is reported that TGFβ has no detectable effect on the cell surface distribution of receptor complexes (Zwaagstra et al., 2008).

In further characterising receptor degradation, these findings now propose a role for EBNA1 in increasing the transcription of the lipid raft-residing proteins Cav-1, Smad7 and Smurf2, promoting entrance of receptors into the lipid raft pathway, enhancing their degradation and thus inhibiting ligand-induced signalling initiated by the TGFβ receptor complex. Preliminary

evidence suggests that EBNA1 may increase the abundance of Cav-1 in both EBNA1-expressing and rEBV-infected Ad/AH cells, showing increased peripheral staining at the plasma membrane in EBNA1-expressing cells. In support of this theory, recently published data reports on the over-expression of Cav-1 in NPC tumour samples (Du et al., 2009) and correlates this with increased MMP secretion and metastasis. Interestingly, in rEBV-infected cells, Cav-1 appears to adopt a more perinuclear localisation, the significance of which remains to be elucidated, yet supporting the concept that this effect may be further modified by other EBV-encoded proteins. Smad7 not only negatively regulates TGFβ signalling through active competition with R-Smads for binding to TβRI (Hayashi et al., 1997), but can also recruit the HECT-type E3 ubiquitin ligases WWP1/Tiul1 and NEDD4-2 so as to promote both TβRI and R-Smad degradation (Seo et al., 2004). TβRI can also be effectively targeted by Smad7, in combination with Smurf2, which has additionally been inversely correlated with the expression of pSmad2 in oesophageal squamous cell carcinoma (Fukuchi et al., 2002). It is therefore unsurprising that the expression of both Smad7 and Smurf2 is up-regulated in EBNA1-expressing carcinoma cell lines, in which Smads and TβRI are increasingly degraded. To continue this work, a sucrose gradient fractionation protocol can be used to determine the relative abundance of receptors in lipid-raft fractions and conclusively establish whether the increase in Cav-1 transcription is directly reflected in an augmentation of lipid raft activity.

Receptor recycling has been shown to occur constitutively, regardless of receptor activation state (Doré Jr. et al., 2001, Di Guglielmo et al., 2003, Mitchell et al., 2004, Penheiter et al., 2010). Consequently, as an integral but downstream component of this constitutive recycling process, a loss of Dab2 would not be manifest as a decline in receptor internalisation rate

(Penheiter et al., 2010). It would however impact upon later events in the pathway, due to its specific involvement in the transition from the EEA1-positive to Rab-11 positive compartment (Mitchell et al., 2004, Penheiter et al., 2010), disrupting the association of receptors with Rab11 and thereby arresting receptors in EEA1-positive endosomes, which would likely contribute to a substantial reduction in Smad2 phosphorylation (Penheiter et al., 2010). Reduction in pSmad2/3C may therefore be a result of the combination of increased Cav-1 and decreased Dab2 expression levels, both of which are reported to suppress TGFβ-mediated Smad2 phosphorylation (Razani et al., 2001, Penheiter et al., 2010).

PCR analysis has demonstrated that EBNA1-expressing cells show elevated expression of all three TGFβ ligands. This has similarly been observed in LMP1-expressing cells undergoing an EMT (Dr. Louise Laverick, unpublished observations), while Do *et al.* have also highlighted the potential of all three isoforms to induce EMT *in vitro* (Do et al., 2008). A study in hepatocytes suggests that this increase in TGFβ production afforded by an EMT-like conversion can confer apoptotic resistance and thereby promote cell survival (del Castillo et al., 2006). It at first seems counterintuitive that the expression levels of the TGFβ isoforms are raised, yet the response, at least to TGFβ1, is defective. A possibility is that the TGFβ1 response may be specifically ablated, while that to the other isoforms prevails. Indeed, it has been suggested that the individual TGFβ isoforms can in fact play differential roles in epidermal carcinogenesis (Gold et al., 2000). Whilst TGFβ1 was deemed important in the maintenance of a more differentiated keratinocyte phenotype, TGFβ2 prevailed in enhancing the invasion and migration of undifferentiated tumour cells, and TGFβ3 in promoting stroma formation and angiogenesis. Although there is slight variation over the effect of EBNA1 on TGFβ isoform expression, elevation of TGFβ2 is consistent across cell lines. Thus selective

TGFβ1 inactivation may allow TGFβ2-mediated effects to predominate. Taking this into consideration it would be useful to examine TGFβ signalling activity in response to the addition of exogenous TGFβ2 and TGFβ3.

Evidence to support a role for EBV infection in the secretion of TGFβ is conflicting. Elevated measurements of serum TGFβ1 levels have been recorded in NPC patients (Xu et al., 1999), and later, in a second study, extended to cases of BL and chronic active EBV infection (CEI) (Xu et al., 2000). However, Lin *et al.* failed to detect a change in TGFβ1 expression level in EBV-infected NPC cells, despite measuring increases in mRNA expression of EGFR, TGFα, IL-1β, IL-6 and GM-CSF (Lin et al., 2000a), while cytokine profiling identified only elevated expression of IL-1α and IL-1β in primary tumours and NPC metastases compared to control tissues (Huang et al., 1999). Nonetheless, data presented here suggests TGFβ secretion is increased in EBNA1-expressing cells. This may simply be a consequence of defective signalling as, particularly in the presence of TβRII defects, the ability of cells to actively deplete extracellular TGFβ is impaired (Clarke et al., 2009). It may however be strategically increased so as to mediate the characteristic tumour-promoting effects of autocrine and paracrine TGFβ signalling. Indeed chronic exposure of mammary epithelial NMuMG cells to TGFβ was sufficient to convert the typical anti-proliferative and pro-apoptotic response to one of EMT promotion (Gal et al., 2008).

One of the most striking and consistent histopathological features of undifferentiated NPC is the abundance of tumour-infiltrating lymphocytes (TIL) (Gourzones et al., 2011), and the production of cytokines (including TGFβ) by malignant cells has profound effects on the activity of this infiltrate. In this way, the interaction between tumour cells, TIL and the

surrounding microenvironment can largely influence tumour growth and metastasis (Agathanggelou et al., 1995, Dennler et al., 2008). EBNA1 has already been reported to enhance the secretion of cytokines, interleukin-8 (IL-8) and vascular endothelial growth factor (VEGF) (O'Neil et al., 2008), potentially as a mechanism to enhance angiogenesis in NPC (Yoshizaki et al., 2001) and, just as the EBNA1-mediated increase in expression of the CCL20 chemokine in HL tumours and cell lines serves as a chemoattractant for $FoxP3^{+}CD4^{+}$ T cells (T_{regs}) (Baumforth et al., 2008), EBNA1 may increase secretion of TGFβ to serve a similar purpose. Analysis of the characteristic lymphoid infiltrate of NPC tumours detected a proportion of T_{reg} cells (Lau et al., 2007), and TGFβ has been specifically implicated in the induction of FoxP3 expression and therefore their regulatory phenotype (Fantini et al., 2004, Teicher, 2007). Indeed this phenomenon has been observed as a consequence of increased TGFβ production in gastric cancer cells (Yuan et al., 2011). The enhancement of T_{reg} cell prevalence in the peripheral circulation of NPC patients has been associated with suppressive activity against $CD4^{+}$ and $CD8^{+}$ effector T-cell function (Lau et al., 2007, Yip et al., 2009), a strategy employed by tumour cells to subvert the immune response, which may therefore be important for viral persistence. The ability of the increased TGFβ secreted from EBNA1-expressing cells to facilitate the recruitment of T_{reg} cells could be further investigated by measuring the migration of isolated tonsillar T cells in response to conditioned media samples collected from the cells.

The efficiency of latent TGFβ activation is also an important consideration. Data presented here indicates that the active component forms a greater proportion of the total secreted TGFβ in EBNA1-expressing and rEBV-infected Ad/AH cells. In support of this, Xu *et al.* reported that the active TGFβ forms a greater proportion of the total in NPC patient samples when

compared to control sera (Xu et al., 1999). This indicates that TGFβ secretion is not only increased, but, in addition, is more rapidly subject to activation in the presence of EBV, perhaps potentially to enhance T_{reg} recruitment. Whether EBNA1 itself may be capable of directly activating latent TGFβ, as observed *in vitro* for the neuraminidase glycoprotein of influenza A and B viruses (Schultz-Cherry and Hinshaw, 1996), remains to be determined.

A loss of TβRII and increased TGFβ1 expression are often linked, and also positively correlated, in relation to disease progression (Inman and Allday, 2000, Osada et al., 2001, Fukai et al., 2003, Fukuda et al., 2006). However, in most of the carcinoma cell lines studied here, the increase in receptor expression, in combination with the measured increase in TGFβ ligand secretion, supports the notion that the TGFβ signalling pathway is constitutively activated in epithelial cells latently infected with EBV. It is feasible that the increase in receptor expression may be effectively counteracted by the increase in receptor degradation, or instead chronic receptor stimulation may result in the sequestration of receptors away from the active signal cascade to juxtanuclear compartments, as described by Idkowiak-Baldys *et al.* for sustained phorbol ester-stimulation of GPCRs (Idkowiak-Baldys et al., 2009), as part of a mechanism to attenuate the constitutive TGFβ signalling response.

The precise mechanism by which TGFβ signalling is compromised in the presence of EBNA1 remains to be elucidated. The ability of EBNA1 to directly bind to cellular promoters has been reported, and potential binding sites have been identified in the promoters of numerous cellular genes (Dresang et al., 2009, Canaan et al., 2009), but not specifically demonstrated for any TGFβ-associated genes. Using both conventional and variant (HaloCHIP) chromatin immunoprecipitation procedures, EBNA1 was shown to associate at ATF-2 and c-Jun

promoters (O'Neil et al., 2008, Owen et al., 2010), potentially directing the transcriptional induction of these genes, which has been associated with an increase in AP-1 activity. Its presence also at the promoter of the c-myc gene (Owen et al., 2010) may also cause up-regulation of c-myc expression and thereby enhance resistance to TGFβ-mediated growth inhibition. In contrast, EBNA1's inhibition of IKKβ phosphorylation in the canonical NFκB pathway, while potentially associated with its gene transactivation capabilities, is unlikely to be caused by EBNA1 binding to IKKβ (Valentine et al., 2010). Future work would use ChIP analysis to test the possibility that EBNA1 may be present at the promoters of the genes it is seen to transcriptionally induce in this study, i.e. PPM1A, NEDD4-2 and Cav-1, as well as a variety of TGFβ-related genes. Further to this, while gene expression profiling of NPC tumours has been used to support findings of gene up-regulation, it would be pertinent to conduct immunohistochemical staining of NPC tumour sections in order to suitably validate this.

The results suggest that many of the carcinoma cell lines used in this study already harbour some degree of insensitivity to TGFβ-mediated effects, which was then further exacerbated by the presence of EBNA1 alone or by stable latent infection with rEBV. As shown here, Ad/AH cells were refractory to TGFβ-mediated growth arrest, yet TGFβ/Smad-luciferase reporter activity, Smad phosphorylation status and target gene expression were all modulated in EBNA1-expressing cells. It remains a possibility that these cell lines may in fact exhibit reduced expression levels of TβRII when compared to untransformed cell lines, and that this is raised slightly in the presence of EBNA1, yet still fails to reach a significant threshold in order to restore signalling.

An increasing number of genetic and epigenetic changes have been associated with the development of NPC (Tao and Chan, 2007) and, while the detection of the EBV genome in high-grade preinvasive lesions suggests that EBV infection is a relatively early event, certain of these chromosomal abnormalities, in particular chromosome 3p and 9p aberrations, are thought to precede EBV infection (Pathmanathan et al., 1995, Lo and Huang, 2002, Lo et al., 2004). Loss of heterozygosity and promoter hypermethylation within these regions has been associated with the silencing of several genes including the tumour suppressor, Ras association domain family 1A (RASSF1A) and the CDK inhibitors, $p15^{INK4B}$ and $p16^{INK4A}$ (Lo and Huang, 2002). This may account for the reported cell cycle dysregulation identified from microarray analysis of NPC biopsies (Zhang et al., 2009); however, the temporal occurrence of these defects in relation to EBV infection in the course of NPC pathogenesis was not determined in this study.

Premalignant genetic changes associated with transformation may be responsible for the pre-existing lack of TGFβ sensitivity in the carcinoma cell lines, and it is tantalising to speculate that this may predispose the epithelial cells to EBV infection, and create a suitable environment for the persistent maintenance of EBNA1 expression and, accordingly, stable latent infection. The TGFβ pathway is intricately linked to squamous epithelial differentiation and it has for some time now been suggested that the stable maintenance of EBV in epithelial cells requires an undifferentiated environment (Knox et al., 1996, Jones et al., 2003). It is therefore possible that changes affecting the differentiation status of the target cell may dictate the ability of the cell to respond to TGFβ, perhaps even playing a significant role in the switch of TGFβ between tumour-suppressive and tumour-promoting roles (Ikushima and Miyazono, 2010), and may also govern the ability of EBNA1 to modulate TGFβ signalling within.

Interestingly, the differentiation of EBV-infected B cells into plasma cells is associated with the initiation of lytic cycle *in vivo* (Laichalk and Thorley-Lawson, 2005), while in epithelial cells, stable EBV infection was only achievable in those cells that had lost the competence to differentiate and also failed to enter virus lytic cycle (Knox et al., 1996). EBV lytic cycle is reportedly induced by TGFβ in EBV-positive B cells (di Renzo et al., 1994, Fahmi et al., 2000), and therefore both features are indicative of a loss of typical responses to TGFβ.

Repairing the main TGFβ defect in C666-1 cells alleviates the assumed EBNA1-mediated repression of Qp, and activity is subsequently increased by TGFβ stimulation, while TGFβ normally exerts a repressive effect on Qp-promoter activity, certainly in EBV-infected BL cells (Liang et al., 2000). This indicates that reversing acquired defects may be incompatible with stable EBNA1 expression and genome maintenance, and indeed the level of EBNA1 transcription appears reduced following this effect. Dysregulated TGFβ signalling may therefore play a significant role in the successful maintenance of EBV in the C666-1 cell line. Once these defects have been more extensively characterised, it will be interesting to specifically disable TGFβ signalling in differentiated cell lines currently unpermissive to EBV infection, to examine the phenotypic consequences and determine whether stable infection can now be tolerated.

It has been reported that the EBV-mediated loss of sensitivity to the anti-proliferative effects of TGFβ is not synonymous with a complete abolition of TGFβ signalling (Horndasch et al., 2002). Indeed it would be somewhat detrimental to the tumour to totally eradicate TGFβ signalling due to its ubiquitous role in a multitude of cellular processes and also for its requirement in pro-tumourigenic functions. In the work conducted by Horndasch and

colleagues, the EBV-immortalised B cells studied demonstrated resistance to the anti-proliferative and pro-apoptotic effects of TGFβ, but no significant changes in cell surface TβRII expression. Heldin *et al.* reported similar findings in a comparison of non-neoplastic and neoplastic thyroid follicle cells, and were unsuccessful in assigning a definitive mechanism for the observed insensitivity to growth inhibition by TGFβ1 in the HTh7 cell line (Heldin et al., 1999). Defective TGFβ signalling in cancer can be broadly categorised into two groups (Massagué, 2008); complete loss of the core pathway through inactivation of central components, as exemplified by the loss of TβRII in the C666-1 cell line, or selective loss of the tumour suppressor arm only, which appears to be the case in the majority of other carcinoma cell lines studied. In the latter case, remaining TGFβ responses can be co-opted by cells for their own tumourigenic advantage.

The exact mechanism by which cancer cells acquire resistance to TGFβ-mediated anti-proliferative effects but are still able to benefit from some TGFβ responses has long been a puzzle, yet features identified in this work, for example down-regulation of Dab2 and over-expression of Cav-1 seem to support this switch in TGFβ activity. Indeed whilst cell lines expressing high levels of Dab2 responded appropriately to TGFβ-induced growth inhibition, this response was not maintained in low-expressing lines, which instead demonstrated a modest increase in motility rate, as well as promotion of anchorage-independent growth. (Hannigan et al., 2010). Similarly, Cav-1 expression in NIH3T3 fibroblast cells is seen to down-regulate TβRII gene transcription with ensuing diminished TGFβ-induced responses (Lee et al., 2007), while in melanoma cell lines it was found to enhance proliferation, and to promote anchorage independence, migration and invasion (Felicetti et al., 2009). Both effects

have also been ascribed to the development of EMT (Martin et al., 2010, Bailey and Liu, 2008).

In addition, Kim *et al*. published a study showing the ability of Cav-1 to increase both basal and TGFβ1-induced type I procollagen expression, despite the fact that Cav-1 overexpression is proven to inhibit TGFβ/Smad signalling (Kim et al., 2008) This was attributed to a Smad-independent mechanism involving Cav-1-induced activation of the PI3K/Akt pathways. There has also already been some suggestion that Smad-dependent TGFβ signalling in hepatocytes is accomplished via association with a clathrin-associated AP-2 complex, whilst non-Smad signalling via Akt activation is mediated by dynamin and caveolin-1 (Meyer et al., 2011). Moreover, TGFβ-induced MAPK activation is thought to be dependent on TGFβ receptor heterocomplex localisation in lipid rafts (Zuo and Chen, 2009). A proposed hypothesis is that the increased Cav-1 in conjunction with loss of Dab2 expression may preferentially divert receptors down the lipid raft route, from which they would receive instruction to activate non-Smad signalling pathways so as to promote invasion, metastasis and EMT-like conversions, while also being subjected to increased pressure from Smad7 and Smurf2 for receptor degradation.

Although both Smad7 and Smurf2 are themselves TGFβ target genes (Nagarajan et al., 1999, Ohashi et al., 2005), their expression is not exclusively reliant on canonical TGFβ/Smad signalling. Evidence suggests that Smad7 expression can be stimulated by IFNγ, acting through Jak1 and STAT1, and that this in turn induces the accumulation of Smad7-Smurf2 complexes in the cytoplasm, where they can effectively target both TGFβ receptors and Smads (Ulloa et al., 1999, Kavsak et al., 2000). This observation is of particular interest in

light of previously published data highlighting the ability of EBNA1 to enhance STAT1 expression and activation in response to IFNγ (Wood et al., 2007). Additionally, although Smurf2 is transcriptionally induced by TGFβ, this stimulation of expression is thought to occur via a Smad-independent pathway, as inhibition of PI3K/Akt pathway suppressed TGFβ-mediated Smurf2 induction (Ohashi et al., 2005).

Data presented here supports a model in which the negative influence of EBNA1 may in fact be confined to the Smad-dependent signalling arm, targeted specifically to exploiting existing defects in carcinoma cell lines, counteracting the adverse effects of canonical signalling, and so favouring cell survival. At the same time, EBNA1 may help to divert the focus of the response and channel TGFβ to preferentially activate non-Smad signalling pathways, which enhance tumour-promoting functions and may even further negatively regulate classical Smad signalling (Moustakas and Heldin, 2005). Other studies have shown that EBV-encoded LMP1 inhibits TGFβ signalling via constitutive ERK1/2 phosphorylation and NFκB activation (Fukuda et al., 2002, Prokova et al., 2002, Mori et al., 2003), whereas LMP2A appears to require activation of the PI3K/Akt pathway to achieve similar effects (Fukuda and Longnecker, 2004). Interconnection with other signalling pathways therefore appears to be a key mechanism employed by EBV-encoded proteins for TGFβ signal regulation, and thus the ability of EBNA1 to engage with Smad-independent pathways is likely to be of paramount importance in augmenting the TGFβ-associated tumour promoting effects.

This effect appears to be in part mediated by differential expression of Smad phospho-isoforms. Indeed a switch towards preferential expression of linker phosphorylated Smads is thought to parallel the conversion of TGFβ from tumour suppressor to tumour promoter. In

examining the relative expression levels of phospho-isoforms during sporadic human colorectal carcinogenesis, Yamagata and co-workers (Yamagata et al., 2005) describe a model, which has recently also been extended to hepatocellular carcinoma (Murata et al., 2009), in which tumour cells are able to gain advantage through the selective inhibition of the TβRI-dependent pSmad3C pathway, deemed responsible for anti-proliferative tumour suppressor functions of TGFβ, with concomitant enhancement of the JNK-dependent pSmad3L, which promotes cell growth and induces a more invasive tumour phenotype (Matsuzaki et al., 2009, Matsuzaki and Okazaki, 2006, Sekimoto et al., 2007). This linker phosphorylation may even be directly important in acquiring resistance to TGFβ. Indeed a linker phosphorylation-resistant Smad3 mutant (EPSM) was able to restore sensitivity of Ras-transformed epithelial cells to growth inhibition (Kretzschmar et al., 1999), and induced expression of $p15^{INK4B}$ and $p21^{WAF1/Cip1}$ in melanoma cells (Cohen-Solal et al., 2011).

In all studies to date, the C666-1 cell line has demonstrated a profound lack of TGFβ responsiveness in terms of both R-Smad activation and complex formation, and TGFβ/Smad reporter activity, for which a lack of TβRII expression is held accountable (Wood et al., 2007). However, it is shown here that linker phosphorylated Smads are still expressed by C666-1 cells, yet cannot be induced by TGFβ due to the absence of the ligand-binding TβRII. They may therefore emphasise the importance of Smad-independent signalling in carcinoma cell lines and be essential in mediating TGFβ-related effects in C666-1 cells.

This domain specific phosphorylation of Smad2 and Smad3 may also prove to be a key determinant in enabling EBNA1 to confer a selective advantage to tumour cells, inducing a preferential shift towards the expression of linker phosphorylated Smad2 and Smad3 in order

to specifically up-regulate those genes which favour tumour cell invasion and promote oncogenic effects. Future studies would assess the contribution of various signalling pathways to Smad linker phosphorylation in EBNA1-expressing and EBV-infected cells, and the effects of these linker-phosphorylated forms on cell motility and invasion by selectively targeting Smad2/3 with shRNAs.

Although Ad/AH, HONE-1 and AGS cell lines all show an increase in expression of at least some linker-phosphorylated isoforms, the pattern of Smad linker phosphorylation is not rigidly repeated across the panels, emphasising the cell-specific nature of TGFβ signalling in the three cell lines. Indeed the overall response may depend on the total combination of linker Ser/Thr sites phosphorylated, which will most likely be cell type- and context-dependent (Wrighton et al., 2006). A reduction in C-terminally phosphorylated pSmad2 has previously been confirmed by immunohistochemical staining of NPC tumour biopsies (Dr. Victoria Wood, unpublished observations). In this respect it would be useful to also examine the expression and localisation of linker phosphorylated Smads in a similar manner. Additional sites, as yet unstudied, within the Smad3 linker domain, glutamine 222 and proline 229, have been characterised as contributing towards Smad oligomerisation and DNA binding (Vasilaki et al., 2009), and so would also warrant investigation once commercial antibodies become available.

In examining potential kinase involvement in the enhancement of Smad linker phosphorylation, the main kinase inhibitors seen to reduce phosphorylation were flavopiridol, U0126 and SP600125, which inhibit CDK, MEK-ERK/MAPK and JNK activities respectively. This suggests that the observed effects in EBNA1-expressing cells may be

mediated by enlisting CDKs, ERK-MAPK and JNK. Increased expression of the active forms of ERK-MAPK and JNK is observed in EBNA1-expressing cells in support of this, and, of all of the pathways investigated, ERK-MAPK, as well as PI3K signalling pathways were judged most significant in mediating LMP1-induced EMT (Laverick *et al.*, manuscript in preparation).

Furthermore, when studying Smad linker phosphorylation in the panel of three epithelial lines used in this study, some of the phosphorylated isoforms, particularly of Smad3, are no longer induced in response to exogenous stimulation with TGFβ. In cancer cells, linker phosphorylation is often constitutive, and has been recently demonstrated in melanoma cells (Cohen-Solal et al., 2011). Potential mechanisms for this include hyperactivation of associated MAPK pathways, or a down-regulation of linker phosphatases, or acquired resistance to their action (Sekimoto et al., 2007, Cohen-Solal et al., 2011). This is worthy of further investigation to determine whether EBNA1 potentiates this aberrant activation.

Overall, data presented here implies that EBNA1 specifically modulates TGFβ signalling in carcinoma cells so as to facilitate pro-tumourigenic roles. It increases the transcription of several key proteins involved in the negative regulation of both TGFβ receptors and Smad proteins which may in part account for the previously reported attenuation of responses (Wood et al., 2007), while potentially manipulating Smad-independent signalling pathways and thereby modulating the nature of Smad phosphorylation, to ensure tumour-promoting effects predominate. Further analysis is required in order to pinpoint the exact mechanism for these observations and to further understand the contribution of these effects to NPC pathogenesis.

CHAPTER 4

Modulation of BMP signalling by the EBV-encoded EBNA1 protein

4.1 Introduction

The TGFβ signalling pathway has been extensively investigated with regard to its role in cancer, yet the involvement of the closely-related BMP signalling pathway in tumour progression has only recently drawn attention. BMP signalling, as detailed in section 1.7, represents a branch of the TGFβ superfamily most extensively characterised for its roles in embryonic development, osteoblast differentiation and subsequent bone formation (Katagiri et al., 1994, Ducy and Karsenty, 2000, Cao and Chen, 2005, Sieber et al., 2009). Studies are now emerging to suggest a specific function for BMPs in tumour development and progression (Alarmo and Kallioniemi, 2010, Singh and Morris, 2010). Although the precise roles that BMPs play in this setting are still largely uncertain, an accumulating body of evidence suggests that the BMP signalling pathway is modulated in certain types of cancer, and that it can contribute to the invasive and metastatic properties of tumour cells.

Over-expression of BMP2 has been documented in a variety of carcinoma-derived cell lines (Hatakeyama et al., 1997), and has been identified as being dysregulated in primary pancreatic cancer, oral squamous cell carcinoma, and in non-small-cell lung cancers (Kleeff et al., 1999, Jin et al., 2001, Soares et al., 2010, Langenfeld et al., 2005). Additionally, BMP6 is found to be over-expressed in metastatic prostate adenocarcinoma (Bentley et al., 1992), whilst over-expression of BMP7 has been documented in primary breast tumours (Alarmo et al., 2006), and both BMP4 and BMP7 are reportedly up-regulated in melanoma (Rothhammer

et al., 2005). Furthermore, activation of the BMP signalling pathway, typically interpreted as increased levels of phosphorylated Smad1/5/8, has been reported in primary colon carcinoma (Lorente-Trigos et al., 2010), non-small-cell lung cancer (Langenfeld et al., 2006), renal cell carcinoma (Markić et al., 2010), and in oestrogen-receptor positive and metastatic breast cancers (Helms et al., 2005, Katsuno et al., 2008).

To date, the status and integrity of the BMP signalling pathway has not been investigated in NPC. However, recent gene expression profiling of microdissected NPC tumours has identified up-regulation of the TGFβ superfamily ligands, BMP2 and activin A in NPC tumours (Hu, PhD thesis, 2010). This study has also revealed gene expression profiles which indicate significant dysregulation of TGFβ/Activin/BMP signalling in authentic NPC tumours and in the EBV-positive NPC cell line C666-1. This at first appears counterintuitive, given the established TβRII defect and the consequential ablation of canonical TGFβ signalling in C666-1 cells, as well as the attenuation of TGFβ signalling in EBNA1-expressing and rEBV-infected carcinoma cell lines, as reported in Chapter 3. It was therefore hypothesised that alternative but related members of the TGFβ superfamily and their associated effects may contribute to this observed gene expression signature.

A high degree of concordance is found between TGFβ and activin transcriptional responses. This is not surprising, given that both TGFβ and activin ligands share the same receptor binding properties and utilise the same set of R-Smads, Smad2 and Smad3, in combination with the co-Smad, Smad4 for signal transduction (Ryu and Kern, 2003, Schnepp and Hua, 2003). A previous study therefore sought to determine the status of activin signalling in the C666-1 cell line (Hu, PhD thesis, 2010). This study confirmed an intact activin signalling

pathway which, in the face of an abrogated TGFβ signalling pathway, enabled the induction of Smad2 phosphorylation and expression of TGFβ-responsive genes, PAI-1 and $p21^{WAF1/Cip1}$, in response to activin A stimulation. However, the absence of significant activin A ligand expression in C666-1 cells cast doubt on the relative importance of the pathway to signalling within these cells.

A more detailed analysis of the gene expression profiles of NPC tumours and the C666-1 cell line identified over-expression of the BMP family member BMP2, findings which suggest that the BMP signalling pathway may play a more prominent role or cooperate with TGFβ in NPC pathogenesis. The essential structure of the BMP pathway is similar to that described for TGFβ and activin, in that BMPs also signal via heterotetrameric receptor complexes at the cell surface and intracellular Smad complexes containing the common Smad mediator, Smad4. However, BMP signals are propagated through a different set of R-Smads, Smad 1/5/8 (Miyazono, 1998, Piek et al., 1999, Miyazono et al., 2001), and the methods of receptor oligomerisation are thought to be more flexible in nature (Groppe et al., 2008, Nickel et al., 2009). Contrary to the mode of receptor binding employed by TGFβ and activin ligands, BMPs possess a comparatively low affinity for their type II receptors, with a higher affinity instead to their type I receptors (Rosenzweig et al., 1995, Nickel et al., 2009); binding is further substantially increased in the presence of heteromeric type I/type II receptor complexes (Rosenzweig et al., 1995, Piek et al., 1999).

Despite this, a degree of functional similarity is apparent between BMPs and TGFβ, particularly in their corresponding abilities to function in a context-dependent fashion as both tumour suppressors and tumour promoters (Singh and Morris, 2010). Furthermore, some

BMPs are also predicted to exhibit a comparable switch in behaviour to that of TGFβ in cancer progression. In colon cancer, cells isolated from a primary colon cancer biopsy underwent growth inhibition in response to BMP2, but developed resistance with sustained exposure, and instead acquired the ability to undergo BMP2-mediated EMT, and displayed enhanced cellular motility and invasion (Kang et al., 2009).

In addition to the increase in BMP2 ligand expression, gene profiling has identified a general up-regulation of several BMP signalling pathway components in NPC tumours; namely, ActRI, BMPRIA, BMPRII, Smad1, Smad4 and Smad5 (Hu, 2010). This study therefore sought to explore the possible contribution of BMP2 to TGFβ family signalling in C666-1 cells, and extended these observations to other carcinoma cell lines to determine whether EBV or, more specifically, EBNA1 might be involved in regulating BMP signalling.

4.2 The status of the BMP signalling pathway in NPC tumours and C666-1 cells

4.2.1 Gene expression profiling of the BMP signalling pathway in NPC tumour biopsies

To obtain an overall impression of the status of the BMP signalling pathway in NPC tumours, normalised array intensities obtained from gene expression array analysis were subjected to further hierarchical clustering using dChip software so as to generate a heat map displaying differentially regulated genes associated with the BMP signalling pathway. Here, array intensities from authentic NPC tumours and the EBV-positive C666-1 cell line were compared to normal epithelium. As shown in Figure 4.1, a large number of BMP signalling pathway components were found to be up-regulated, suggesting an overall activation of the BMP signalling pathway in NPC tumours and the C666-1 cell line. Two tumour samples

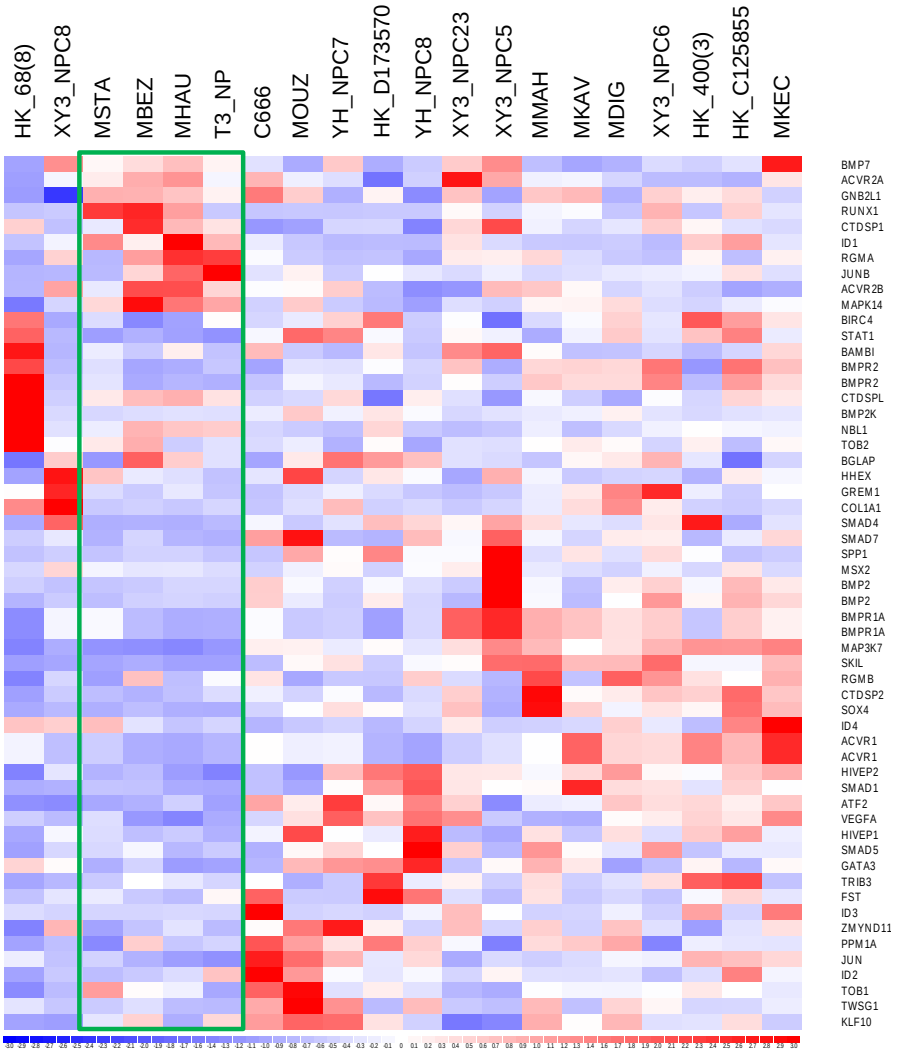

Figure 4.1: Gene expression profiling of BMP pathway-associated genes in NPC tumours

Extensive literature searches revealed a set of genes associated with the BMP signalling pathway. The resulting gene list was utilised to identify significantly differentially regulated genes, using expression array data generated in a separate study from 16 tumours and 4 normal controls, which were visualised using dChip software for hierarchical clustering analysis. The expression level of each gene in an individual sample is colour coded: blue for downregulation, red for upregulation and white for unchanged. Normal samples are highlighted by the green box.

(HK_68(8) and XY3_NPC8) however do not appear to cluster with the rest, indicating that, although BMP pathway activation is a common feature of a large proportion of NPC tumours, it is not universally observed.

4.2.2 The expression of BMP pathway components in C666-1 cells

In an earlier study where TGFβ and activin signalling responses were examined in C666-1 cells, the telomerase-immortalised oral keratinocyte line OKF6 was used as a suitable control (Hu, PhD thesis, 2010), given its sensitivity to TGFβ1-mediated cell growth suppression (Peng et al., 2006). It was therefore also used in this study so as to provide a direct comparison with previously published data.

The elevated expression of BMP2 in the EBV-positive cell line C666-1 had already been validated by QPCR (Hu, PhD thesis, 2010). To expand upon this observation, RT-PCR analysis was enlisted to profile key components of the BMP pathway in the EBV-positive C666-1 versus the OKF6 cell line, so as to identify genes whose expression may be specifically altered by the presence of EBV. These findings are depicted in Figure 4.2. Several BMP ligands were examined and, in addition to confirming the increase of BMP2 expression, this analysis also identified a substantial up-regulation of BMP7 at the mRNA level. Conversely, the expression of both BMP4 and BMP6 appeared to be transcriptionally down-regulated in C666-1 cells.

BMP ligands are reported to bind a variety of type I and type II receptors and, of those receptors studied, an up-regulation of ActRIIB was identified, with little change in the

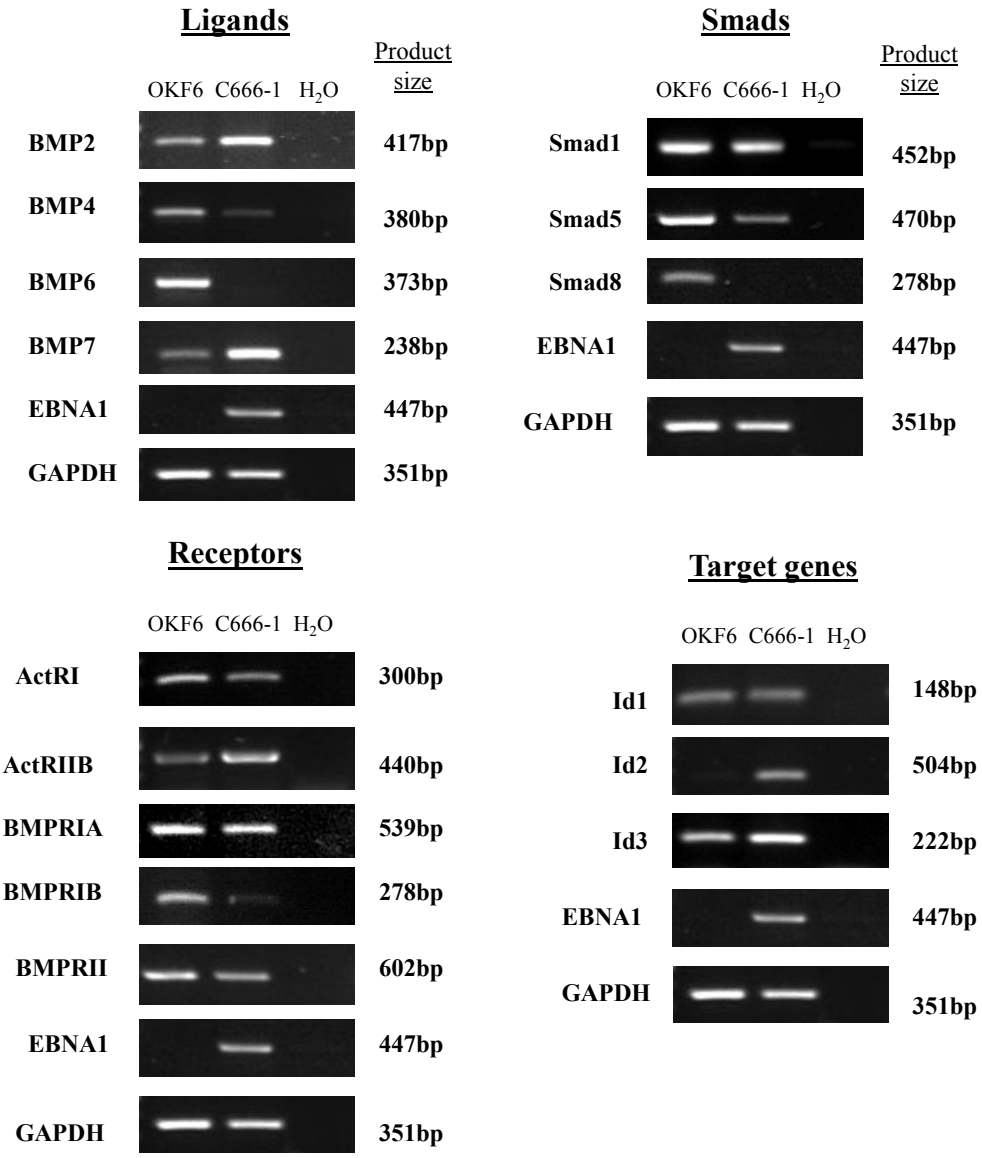

Figure 4.2: Expression of BMP pathway components in OKF6 and C666-1 cells
RT-PCR analysis for mRNA expression levels of BMP ligands (BMP2, 4, 6 and 7), BMP receptors (ActRI, ActRIIB, BMPRIA, BMPRIB and BMPRII), BMP-specific Smads (Smad1, Smad5 and Smad8) and classical BMP target genes (Id1, Id2 and Id3) in OKF6 and C666-1 cells. EBNA1 was included as a control for EBV expression in the C666-1 cells and GAPDH was included as a positive control to confirm equal RNA input into the PCR reactions, while negative water controls confirmed the absence of contamination.

expression of BMPRIA, but down-regulation of ActRI, BMPRIB and BMPRII. These receptors recruit and specifically activate the BMP-specific R-Smads, Smad1, Smad5 and Smad8 to propagate the BMP signal. The expression of Smad1 was relatively unchanged between OKF6 and C666-1 cells, while Smad5 expression was decreased and Smad8 could not be detected in C666-1 cells.

In several studies, BMP treatment has identified the Id genes, Id1, Id2 and Id3 as direct BMP target genes (Hollnagel et al., 1999, Korchynskyi and ten Dijke, 2002, Kang et al., 2003a, Kowanetz et al., 2004). Examination of their relative expression levels in OKF6 and C666-1 cells revealed little difference between the two cell lines in terms of Id1 expression, but increased expression of both Id2 and Id3 in C666-1 cells compared to OKF6 cells.

4.2.3 BMP pathway activation in C666-1 cells

A representation of the degree of BMP pathway activation can be gained by examining the relative levels of phosphorylated Smad1/5/8. This was measured in OKF6 and C666-1 cells by immunoblotting of total cell lysates after treatment with BMP2, or subsequent inhibition with the BMP inhibitor, Noggin. A representative immunoblot, shown in Figure 4.3, demonstrates that the basal levels of phosphorylated Smad1/5/8 were substantially higher in C666-1 cells compared to OKF6 cells. Stimulation with BMP2 resulted in an appropriate induction of Smad1/5/8 phosphorylation in OKF6 cells, but did not further potentiate the constitutively raised levels observed in C666-1 cells, perhaps indicating that the BMP signalling pathway was saturated in this cell line. The BMP antagonist, Noggin, was effective in reducing the levels of Smad1/5/8 phosphorylation, which were partially restored by the addition of BMP2 in C666-1 cells, but not in OKF6 cells.

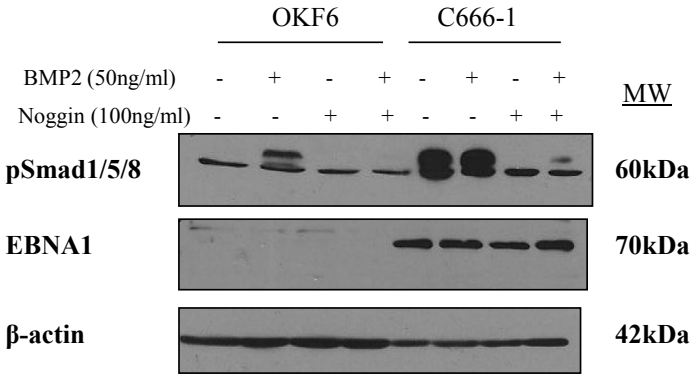

Figure 4.3: Smad1/5/8 phosphorylation in OKF6 and C666-1 cells
Immunoblotting for protein expression levels of the phosphorylated form of Smad1/5/8 in serum-starved OKF6 and C666-1 cells treated with 100ng/ml recombinant hNoggin, for 1 hour, followed by 50ng/ml recombinant hBMP2 for a further 24 hours, or left unstimulated as controls. β-actin was included to confirm equal protein loading.

4.2.4 BMP reporter activity in C666-1 cells

The integrity of the BMP signalling pathway was further investigated using a BMP-specific reporter construct, BRE-Luc, which contains a BMP-response element (BRE) from the mouse Id1 promoter. The BRE-luciferase reporter construct is specifically activated by BMP, but not by either TGFβ or activin (Korchynskyi and ten Dijke, 2002). OKF6 and C666-1 cells were transiently transfected with the BRE-luc reporter, and were subsequently either stimulated with increasing concentrations of BMP2, or incubated with various concentrations of the BMP antagonist, Noggin, for 24 hours. Relative luciferase activity was determined, and is depicted graphically in Figure 4.4. Stimulation with BMP2 was sufficient to induce a dose-dependent increase in the levels of BRE-Luc reporter activity in OKF6 cells, while a titration of BMP2 had little influence on the measured levels of BRE-Luc reporter activity in C666-1 cells, possibly reflecting saturation of the BRE by the particularly high endogenous levels of activated pSmad1/5/8. In both cell lines, Noggin was effective in inhibiting the level of BRE-Luc activity by greater than fifty percent over the concentration range used.

4.2.5 The effect of exogenous Noggin on BMP responses

Once it had been established that the levels of BMP signalling were constitutively elevated in C666-1 cells, the study sought to investigate whether disruption of the pathway would noticeably impact upon BMP gene expression. BMP2 has been implicated in the induction of $p21^{WAF1/Cip1}$ and Id1 expression (Wen et al., 2004, Ogata et al., 1993, Clement et al., 2000, Langenfeld et al., 2006). As shown in Figure 4.5, addition of the BMP antagonist, Noggin, had little detectable effect on the expression level of Id1 protein in OKF6 cells, which was basally much higher than that detected in C666-1 cells. In contrast however, Id1 expression in C666-1 cells was completely abolished in response to BMP inhibition with Noggin. The

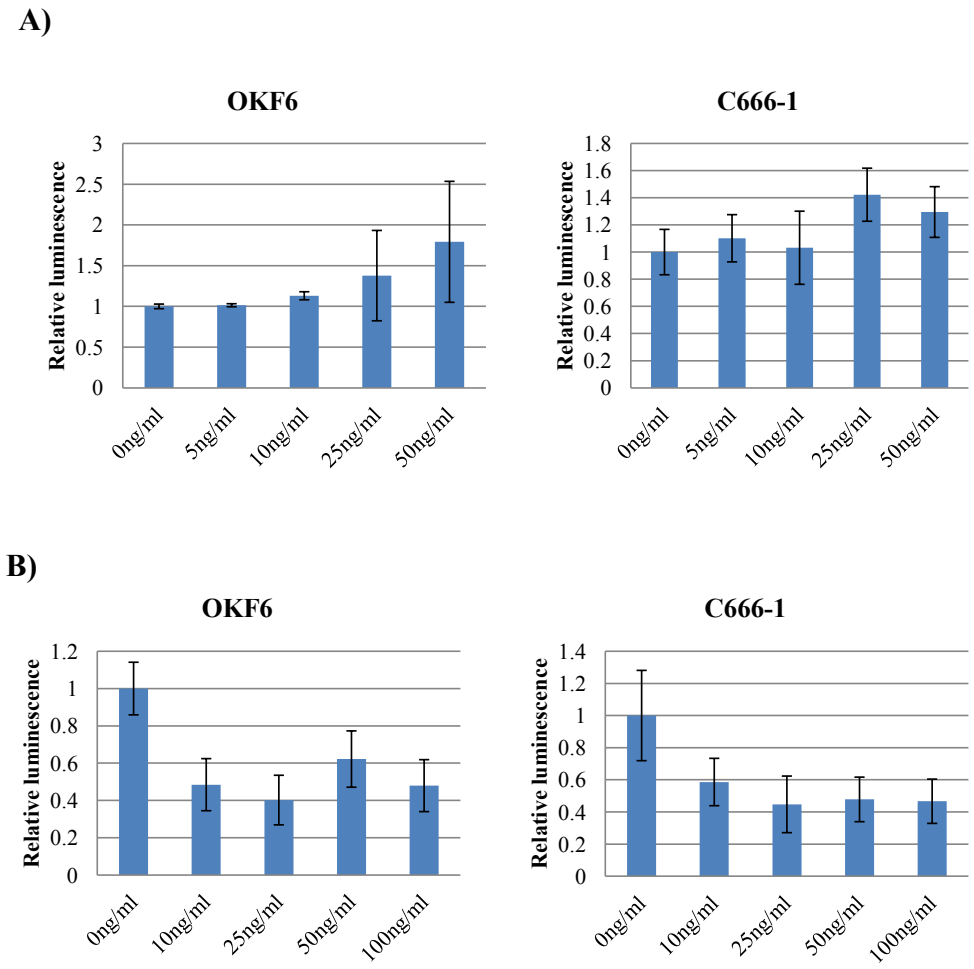

Figure 4.4: The effect of BMP2 and Noggin on BRE-luc reporter activity in OKF6 and C666-1 cells

Dual luciferase reporter assays showing BRE-Luc activity in OKF6 and C666-1 cells stimulated with increasing concentrations of either recombinant hBMP2 (A) or recombinant hNoggin (B) for 24 hours or left unstimulated as a control. Histograms are shown to depict the relative luminescence after normalising to Renilla luciferase values and expressing as a ratio of activity relative to the control vector pGL3-basic. Data from three independent experiments is presented as the mean fold differences in activity $\pm$ SE, relative to that observed in unstimulated cells which is given an arbitrary value of 1.

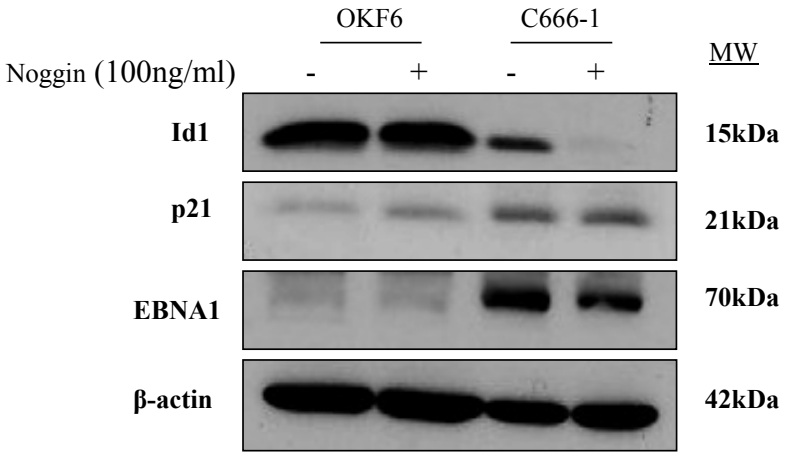

Figure 4.5: The effect of BMP pathway inhibition on the expression of BMP target genes, Id1 and p21, in OKF6 and C666-1 cells
Immunoblotting for protein levels of Id1 and p21 in serum-starved OKF6 and C666-1 cells treated with 100ng/ml recombinant hNoggin for 24 hours, or left unstimulated as controls. Immunoblotting for EBNA1 is included to confirm EBV status and blots were re-probed for β-actin to confirm equal protein loading.

expression of $p21^{WAF1/Cip1}$ however was relatively unaffected by interfering with BMP signalling in both cell lines studied.

4.2.6 The effect of BMP pathway stimulation and inhibition over a 24-hour time period

To extend this investigation, time-courses of BMP2 and Noggin treatment were undertaken over a 24-hour period. OKF6 and C666-1 cells were treated with either 50ng/ml BMP2 or 100ng/ml Noggin, and protein samples were collected at 0, 1, 2, 4, 6, 8 and 24 hour time-points, before subsequent analysis by immunoblotting for a variety of both BMP- and TGFβ-associated Smad proteins and BMP/TGFβ targets. Representative immunoblots are shown in Figure 4.6 and 4.7. Phosphorylation of Smad 1/5/8 were induced by exogenous BMP2 stimulation in OKF6 cells and maintained for the most part before declining slightly after 24 hours. The levels of pSmad1/5/8 in C666-1 cells were significantly elevated prior to stimulation and remained consistently high over the 24-hour time-course.

As a result of the defective TGFβ signalling pathway in C666-1 cells, phosphorylation of the TGFβ-associated R-Smads, Smad2 and Smad3, was not induced to detectable levels by TGFβ stimulation. To determine whether BMP2 might be able to cross-activate the TGFβ pathway, and thereby negate the TβRII receptor defect, the phosphorylation of Smad2 was also analysed in response to BMP2 stimulation. It was found however that Smad2 phosphorylation was largely unaffected by BMP2 stimulation in OKF6 cells, and remained absent in C666-1 cells. In accordance, the classical TGFβ target gene, PAI-1, showed little change in expression in response to BMP2 stimulation in OKF6 cells and remained undetected in C666-1 cells. Id1 and $p21^{WAF1/Cip1}$, while well-established as targets of TGFβ (Kang et al., 2003a, Datto et al., 1995, Levy and Hill, 2005), and key players in the TGFβ-induced cytostatic

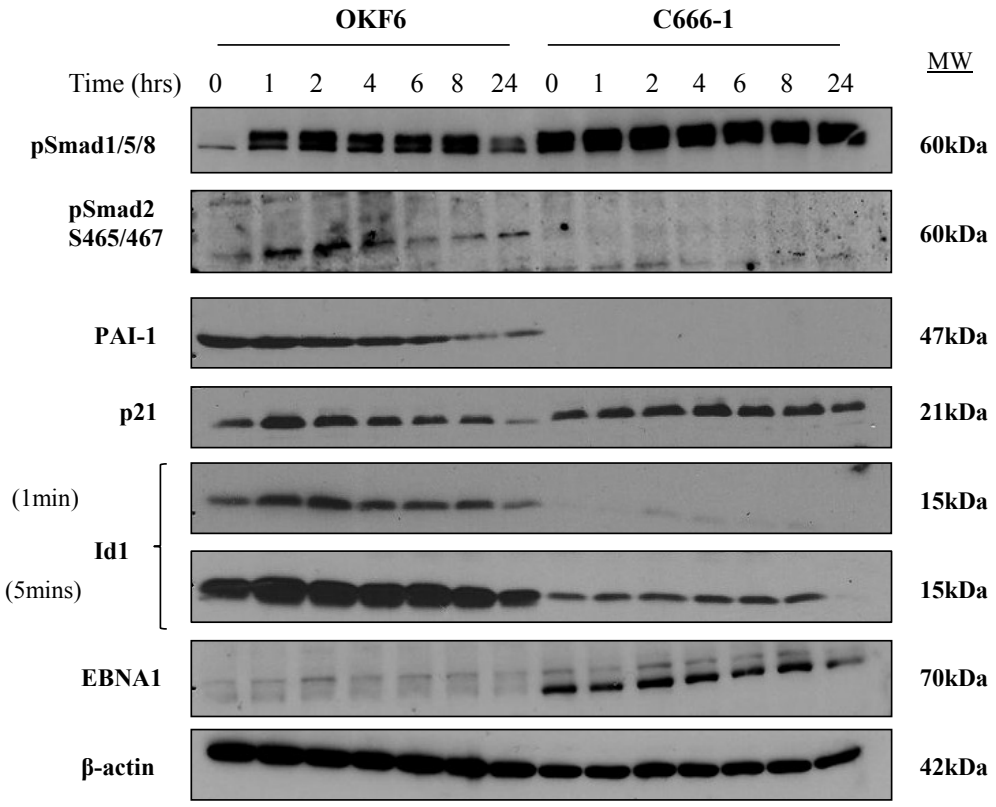

Figure 4.6: Expression of BMP- and TGFβ-associated proteins over a time-course of BMP2 treatment

Immunoblotting for protein levels of the phosphorylated form of Smad1/5/8, the serine 465/467 phosphorylated forms of Smad2, PAI-1, p21 and Id1 in serum-starved OKF6 and C666-1 cells treated with 50ng/ml recombinant hBMP2 and harvested at 0, 1, 2, 4, 6, 8 and 24 hours post-treatment. Blots were re-probed for β-actin to confirm equal protein loading. A second immunoblot for Id1, exposed for the longer time of 5 minutes, is also shown.

response (Siegel and Massagué, 2003, Massagué and Gomis, 2006), can also respond to BMP signalling. In OKF6 cells, $p21^{WAF1/Cip1}$ expression was induced by BMP2, peaking one hour after stimulation, and gradually decreasing over the remainder of the time-course. Expression was only marginally induced in C666-1 cells, with the greatest response observed at around 4 hours and, by 24 hours had returned to basal levels. Id1 followed a similar pattern in OKF6 cells, with the highest level of induction 1 to 2 hours after stimulation, before gradually returning to basal levels. Id1 expression was only detected in C666-1 cells once the exposure time of the blot was increased, and was relatively unchanged in response to BMP2 exposure.

In studying the effect of Noggin treatment on cells (Figure 4.7), the levels of basal Smad1/5/8 phosphorylation were much lower in OKF6 cells, and were rapidly, and almost completely inhibited after only one hour of Noggin treatment. In C666-1 cells, the levels of phosphorylated Smad1/5/8 were also efficiently reduced by the addition of Noggin, although this effect required more time. Noggin treatment effectively reduced the expression of the $p21^{WAF1/Cip1}$ and Id1 target genes in OKF6 cells, but not until later time-points. Unexpectedly, in C666-1 cells, the addition of Noggin produced an increase in $p21^{WAF1/Cip1}$ expression at the 4, 6 and 8-hour time-points. Increased exposure of the Id1 immunoblot revealed an effective abrogation of Id1 expression with increased exposure to Noggin.

4.2.7 The effect of Noggin treatment on expression of the inhibitory I-Smads

The inhibitory Smads (I-Smads), Smad6 and Smad7, are reported target genes of both TGFβ and BMP signalling (Afrakhte et al., 1998, Takase et al., 1998, von Gersdorff et al., 2000, Ishida et al., 2000, Pogoda and Meyer, 2002, Benchabane and Wrana, 2003), and demonstrate an ability to form negative feedback loops which directly impact upon the signalling

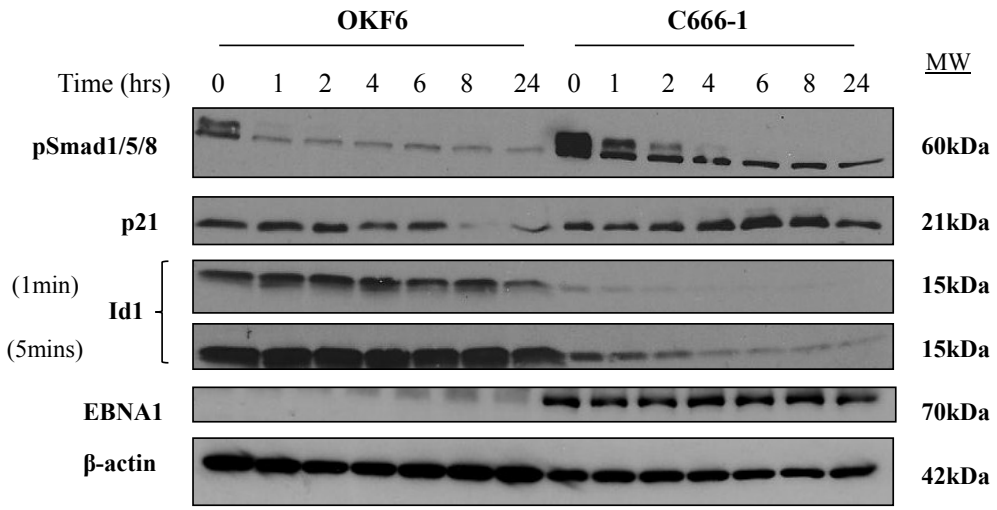

Figure 4.7: Expression of BMP- and TGFβ-associated proteins over a time-course of Noggin treatment

Immunoblotting for protein levels of the phosphorylated form of Smad1/5/8, p21 and Id1 in serum-starved OKF6 and C666-1 cells treated with 100ng/ml recombinant hNoggin and harvested at 0, 1, 2, 4, 6, 8 and 24 hours post-treatment. Blots were re-probed for β-actin to confirm equal protein loading. A second immunoblot for Id1, exposed for the longer time of 5 minutes, is also shown.

pathways. In this way, they function to directly antagonise both TGFβ and BMP signalling (Hayashi et al., 1997, Imamura et al., 1997, Nakao et al., 1997, Hata et al., 1998, Nakayama et al., 1998, Souchelnytskyi et al., 1998, Ishisaki et al., 1999, Denissova et al., 2000, Miyazono et al., 2005). A time-course of Noggin treatment, shown in Figure 4.8, indicated that the BMP signalling pathway was not particularly influential in determining the levels of Smad6 and Smad7 expression in either OKF6 or C666-1 cells. However, the study did reveal that, while expression of Smad6 was much higher in the OKF6 cells compared to C666-1 cells, the opposite result was seen for Smad7 expression.

4.2.8 The effect of BMP pathway stimulation and inhibition on cell cycle progression

BMP2 has demonstrated an ability to induce cell cycle arrest in several human B cell lines (Ishisaki et al., 1999, Yamato et al., 2000) and to inhibit the growth of androgen-sensitive LNCaP prostate cancer cells, MCF-7 and MDA-MB-231 human breast cancer cells and human MKN74 gastric cancer cells (Ide et al., 1997, Ghosh-Choudhury et al., 2000a, Ghosh-Choudhury et al., 2000b, Wen et al., 2004), Similarly, both BMP2 and BMP7 have been reported to induce growth suppression in human colon cancer cells (Beck et al., 2006), while the growth inhibitory effect of BMP7 has additionally been reported on anaplastic thyroid carcinoma cells and androgen-insensitive PC-3 and DU-145 prostate cancer cells (Franzén and Heldin, 2001, Miyazaki et al., 2004).

Given the ability of BMP2 signalling to govern the expression of genes contributing to a growth arrest response, the effect of both stimulating and inhibiting the BMP pathway on cell cycle progression was investigated. OKF6 and C666-1 cells were grown in 0.5% serum for 16 hours prior to stimulation with either 50ng/ml BMP2 or 100ng/ml Noggin, or left

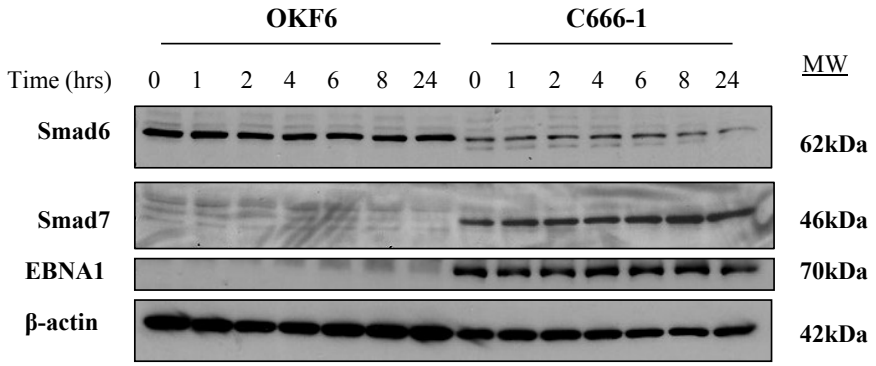

Figure 4.8: Expression of inhibitory Smads over a time-course of Noggin treatment

Immunoblotting for levels of Smad6 and Smad7 protein expression in serum-starved OKF6 and C666-1 cells treated with 100ng/ml recombinant hNoggin and harvested at 0, 1, 2, 4, 6, 8 and 24 hours post-treatment. Blots were re-probed for β-actin to confirm equal protein loading.

unstimulated as a control. After 24, 48, 72 and 96 hours, cells were harvested and stained with propidium iodide, then analysed by flow cytometry. Data was subsequently analysed using MultiCycle, and representative histograms are shown in Figure 4.9. The analysis revealed no significant differences in cell cycle distribution between cell lines in the absence of stimulation. Addition of either BMP2 or Noggin did not markedly shift the distribution pattern, suggesting that BMP signalling within these cell lines does not influence cell cycle progression.

4.3 The status of the BMP signalling pathway in EBNA1-expressing carcinoma cell lines

4.3.1 BMP2 levels in Ad/AH, HONE-1 and AGS carcinoma cell lines

Having identified increased levels of BMP2 expression and constitutive activation of the BMP signalling pathway in the C666-1 cell line, it was important to determine whether a similar phenomenon was observed in the Ad/AH, HONE-1 and AGS carcinoma cell lines and, specifically, whether a role for EBNA1 could be demonstrated in this effect. Therefore, it was initially considered vital to examine the basal expression levels of BMP2 in these cell lines.

To this end, RNA was extracted from Ad/AH, HONE-1 and AGS cells expressing either a neomycin resistance cassette or EBNA1, or infected with rEBV. Following cDNA synthesis, RT-PCR was performed using oligonucleotides specific to BMP2. It is apparent from Figure 4.10A that BMP2 transcription was increased in EBNA1-expressing cells across all three cell lines. This increase was supported in rEBV-infected Ad/AH and AGS cells, but could not be shown for rEBV-infected HONE-1 cells. These same differences were confirmed and

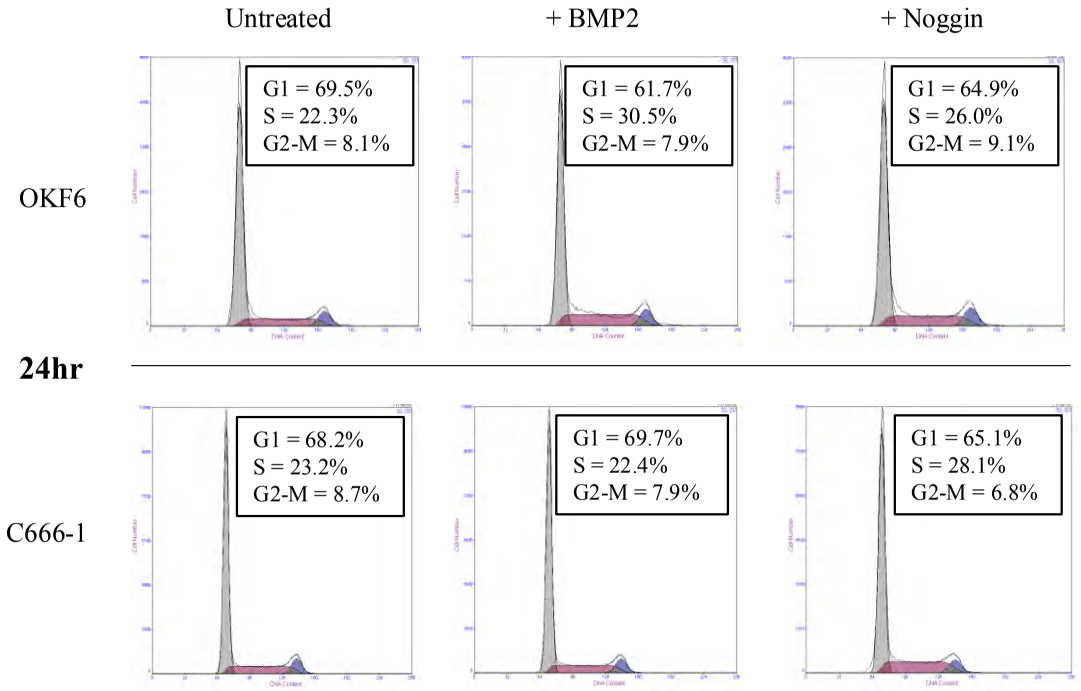

Figure 4.9: Cell cycle analysis by propidium iodide staining of OKF6 and C666-1 cells
Analysis of cell cycle in serum-starved OKF6 and C666-1 cells after treatment with either 50ng/ml recombinant hBMP2 or 100ng/ml recombinant hNoggin, or left unstimulated as a control. DNA content was measured at 24, 48, 72 and 96 hours by propidium iodide staining and subsequent flow cytometric analysis. Resulting histogram files were analysed for cell cycle distribution using MultiCycle. Representative traces from one of three independent experiments are shown, and the percentages of cells in G1, S and G2-M phases are indicated.

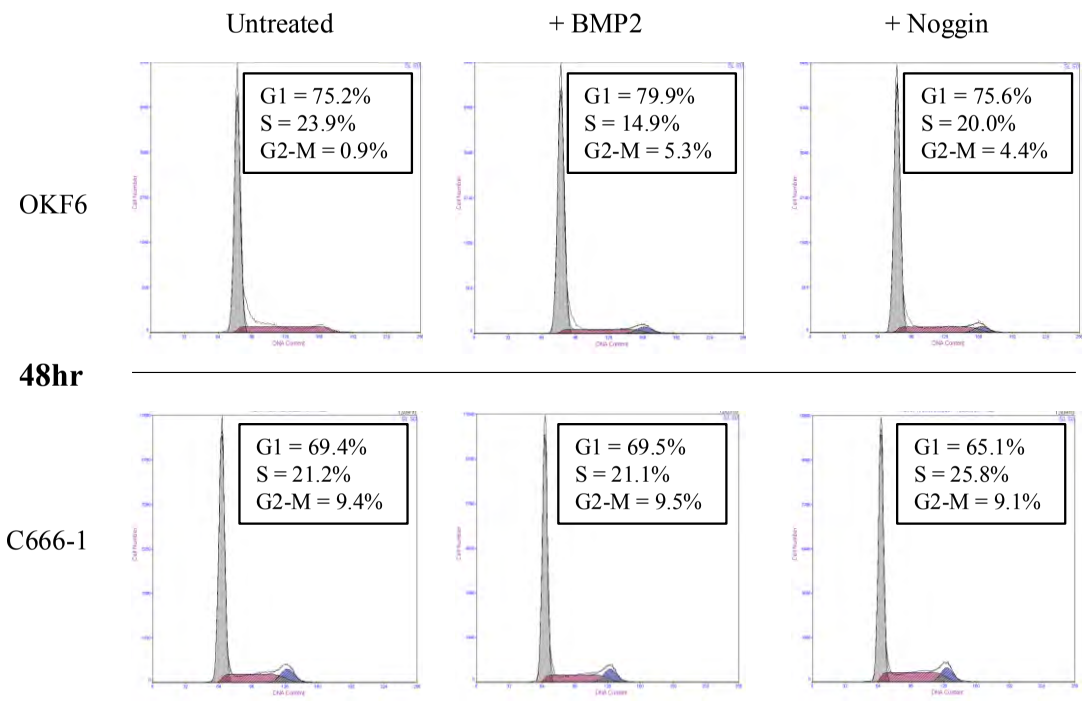
Untreated
+ BMP2
+ Noggin
OKF6
G1 = 75.2%
S = 23.9%
G2-M = 0.9%
G1 = 79.9%
S = 14.9%
G2-M = 5.3%
G1 = 75.6%
S = 20.0%
G2-M = 4.4%
48hr
C666-1
G1 = 69.4%
S = 21.2%
G2-M = 9.4%
G1 = 69.5%
S = 21.1%
G2-M = 9.5%
G1 = 65.1%
S = 25.8%
G2-M = 9.1%

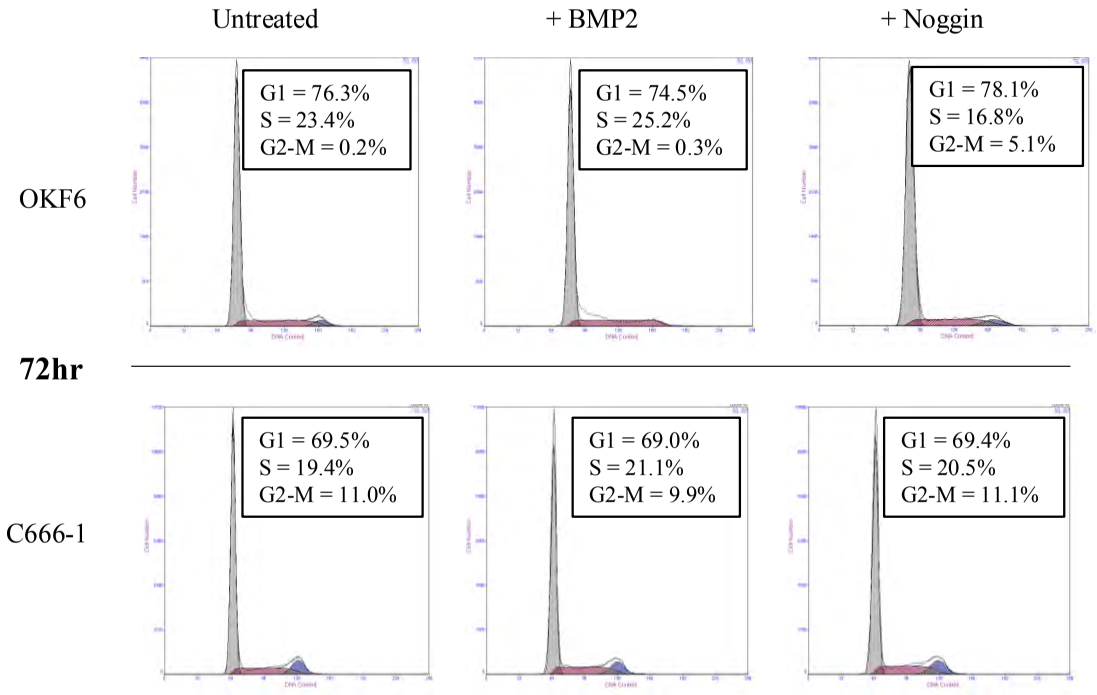
Untreated
+ BMP2
+ Noggin
OKF6
G1 = 76.3%
S = 23.4%
G2-M = 0.2%
G1 = 74.5%
S = 25.2%
G2-M = 0.3%
G1 = 78.1%
S = 16.8%
G2-M = 5.1%
72hr
C666-1
G1 = 69.5%
S = 19.4%
G2-M = 11.0%
G1 = 69.0%
S = 21.1%
G2-M = 9.9%
G1 = 69.4%
S = 20.5%
G2-M = 11.1%

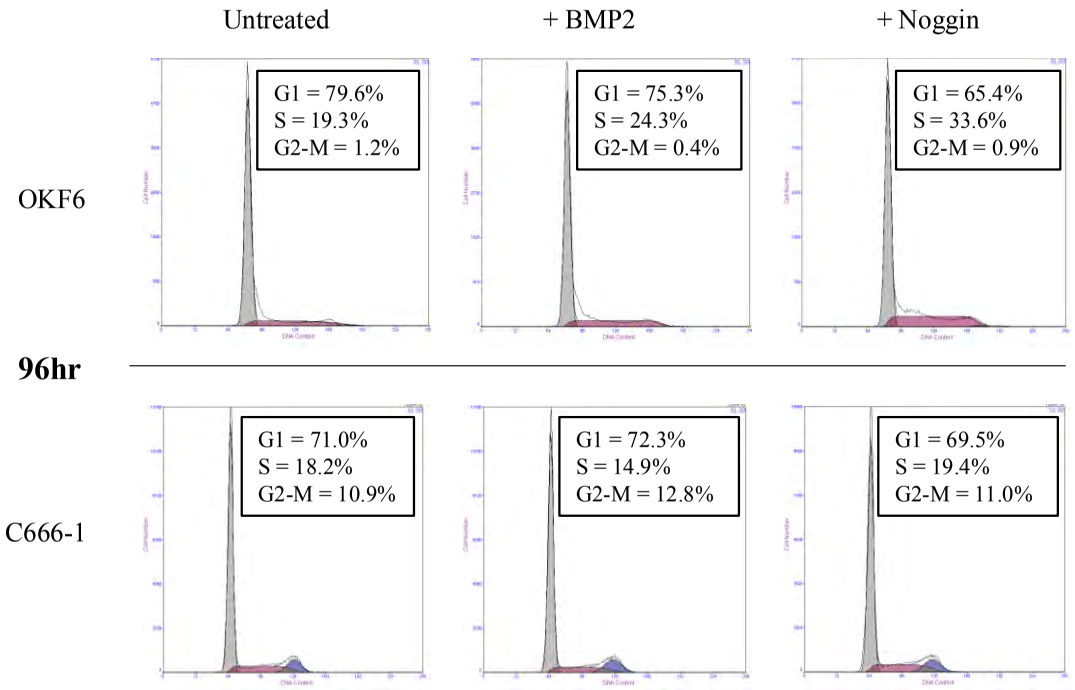
Untreated
+ BMP2
+ Noggin
OKF6
G1 = 79.6%
S = 19.3%
G2-M = 1.2%
G1 = 75.3%
S = 24.3%
G2-M = 0.4%
G1 = 65.4%
S = 33.6%
G2-M = 0.9%
96hr
C666-1
G1 = 71.0%
S = 18.2%
G2-M = 10.9%
G1 = 72.3%
S = 14.9%
G2-M = 12.8%
G1 = 69.5%
S = 19.4%
G2-M = 11.0%

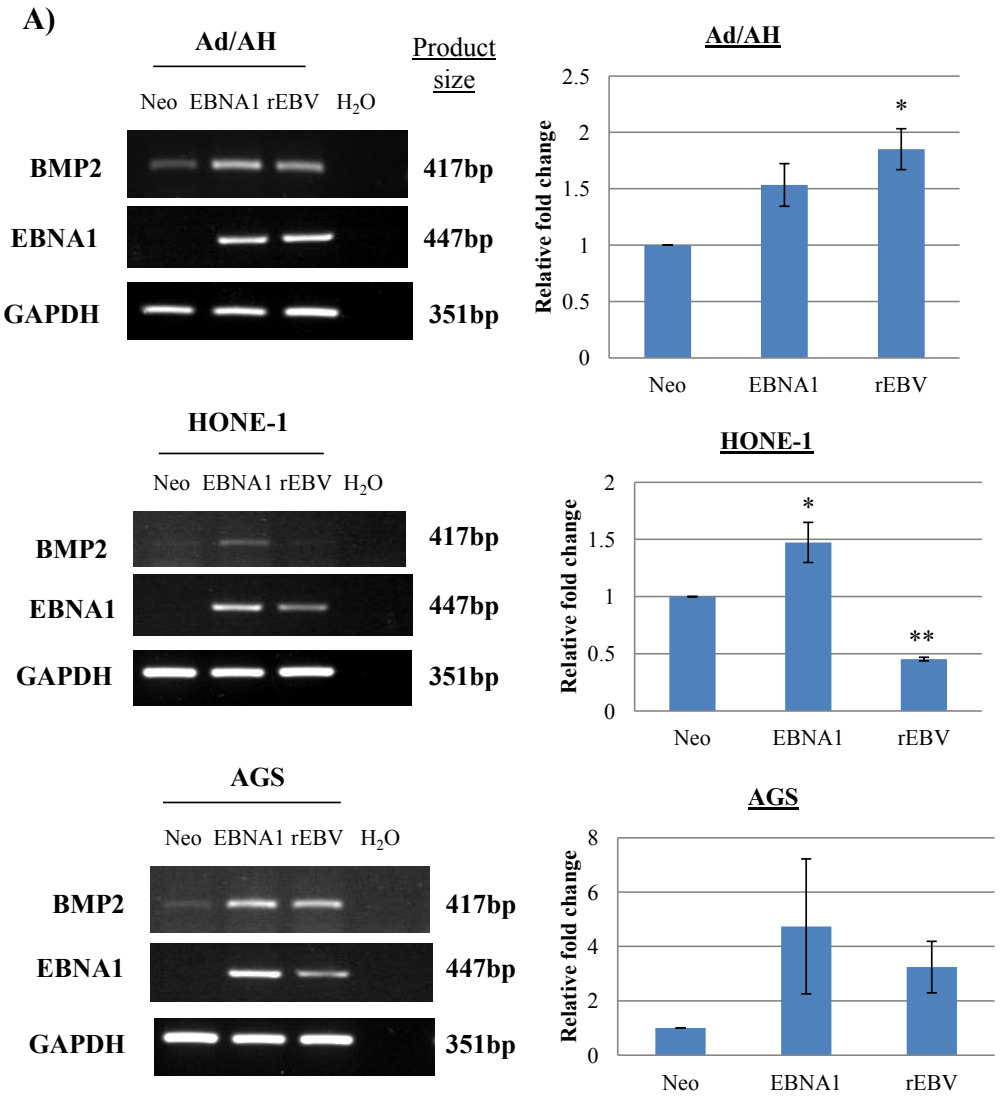

Figure 4.10: The expression of BMP2 in Ad/AH, HONE-1 and AGS carcinoma cell lines

A) RT-PCR analysis of levels of BMP2 mRNA expression in Ad/AH, HONE-1 and AGS cells expressing either a control neomycin resistance cassette or EBNA1, or stably infected with rEBV. GAPDH was included as a positive control to confirm equal RNA input into the PCR reactions, while negative water controls confirmed the absence of contamination. QPCR analysis for BMP2 mRNA levels is also shown, in which GAPDH was included as an internal baseline control. Histograms are shown displaying the mean fold change differences SE (n=3) relative to Neo control cells (** denotes a P-value <0.01 and * denotes a P-value <0.05).

B) Immunoblotting for BMP2 protein levels in Ad/AH, HONE-1 and AGS cells expressing either a neomycin resistance cassette, or EBNA1, or stably infected with rEBV, with β-actin included to confirm equal protein loading.

B)

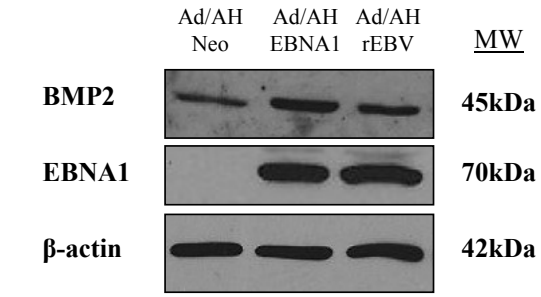
Ad/AH Neo
Ad/AH EBNA1
Ad/AH rEBV
MW
BMP2
45kDa
EBNA1
70kDa
β-actin
42kDa

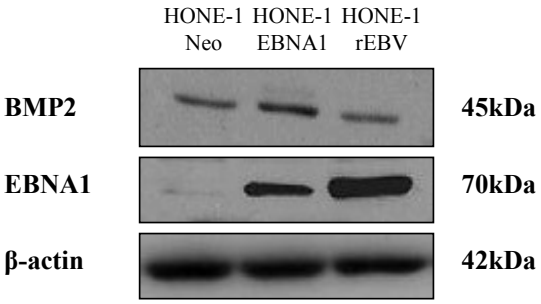
HONE-1 Neo
HONE-1 EBNA1
HONE-1 rEBV
BMP2
45kDa
EBNA1
70kDa
β-actin
42kDa

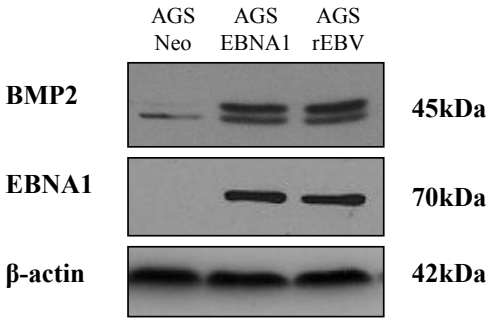
AGS Neo
AGS EBNA1
AGS rEBV
BMP2
45kDa
EBNA1
70kDa
β-actin
42kDa

quantified by QPCR, which served to demonstrate an approximate 1.5-fold increase in expression attributable to the presence of EBNA1 in Ad/AH and HONE-1 cell lines, with more pronounced increases in the AGS-EBNA1 cell line, in relation to their respective Neo control counterparts.

Protein lysates were subsequently generated and immunoblotting performed to determine the relative levels of BMP2 protein. Figure 4.10B shows that the levels of BMP2 protein were increased in EBNA1-expressing and rEBV-infected cell lines, where corresponding increases in BMP2 transcripts were observed.

4.3.2 Gene expression profiling of the BMP signalling pathway in Ad/AH cell lines

To ascertain whether EBNA1 had any effect on BMP signalling, an overall view of differentially regulated BMP pathway-associated genes was obtained through hierarchical clustering analysis of existing Affymetrix gene expression array data obtained from Ad/AH cells stably expressing EBNA1 versus the parental Ad/AH cell line (Valentine et al., 2010). The resultant heat map of differentially regulated genes generated using dChip software is shown in Figure 4.11. A large number of up-regulated genes (red) implies a specific role for EBNA1 in the activation of the BMP signalling pathway.

4.3.3 Profiling of BMP pathway components in Ad/AH, HONE-1 and AGS cell lines

RT-PCR analyses of BMP ligands, receptors, Smads and target genes were conducted in Ad/AH, HONE-1 and AGS cells expressing either a neomycin resistance cassette, EBNA1, or stably infected with rEBV. As can be deduced from Figure 4.12, the majority of pathway components are expressed in all cell lines with the exception of the AGS cell panel which,

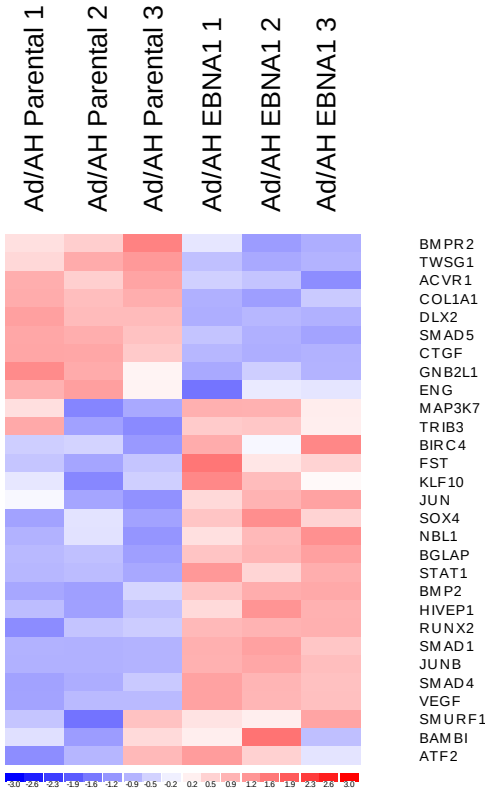

Figure 4.11: Gene expression profiling of BMP pathway-associated genes in Ad/AH cell lines

Extensive literature searches revealed a set of genes associated with the BMP signalling pathway. The resultant gene list was utilised to identify significantly differentially regulated genes, using expression array data generated in a separate study from Ad/AH cells stably expressing EBNA1 and parental Ad/AH cells, which were visualised using dChip software for hierarchical clustering analysis. The expression level of each gene in an individual sample is colour coded: blue for down-regulation, red for up-regulation and white for unchanged.

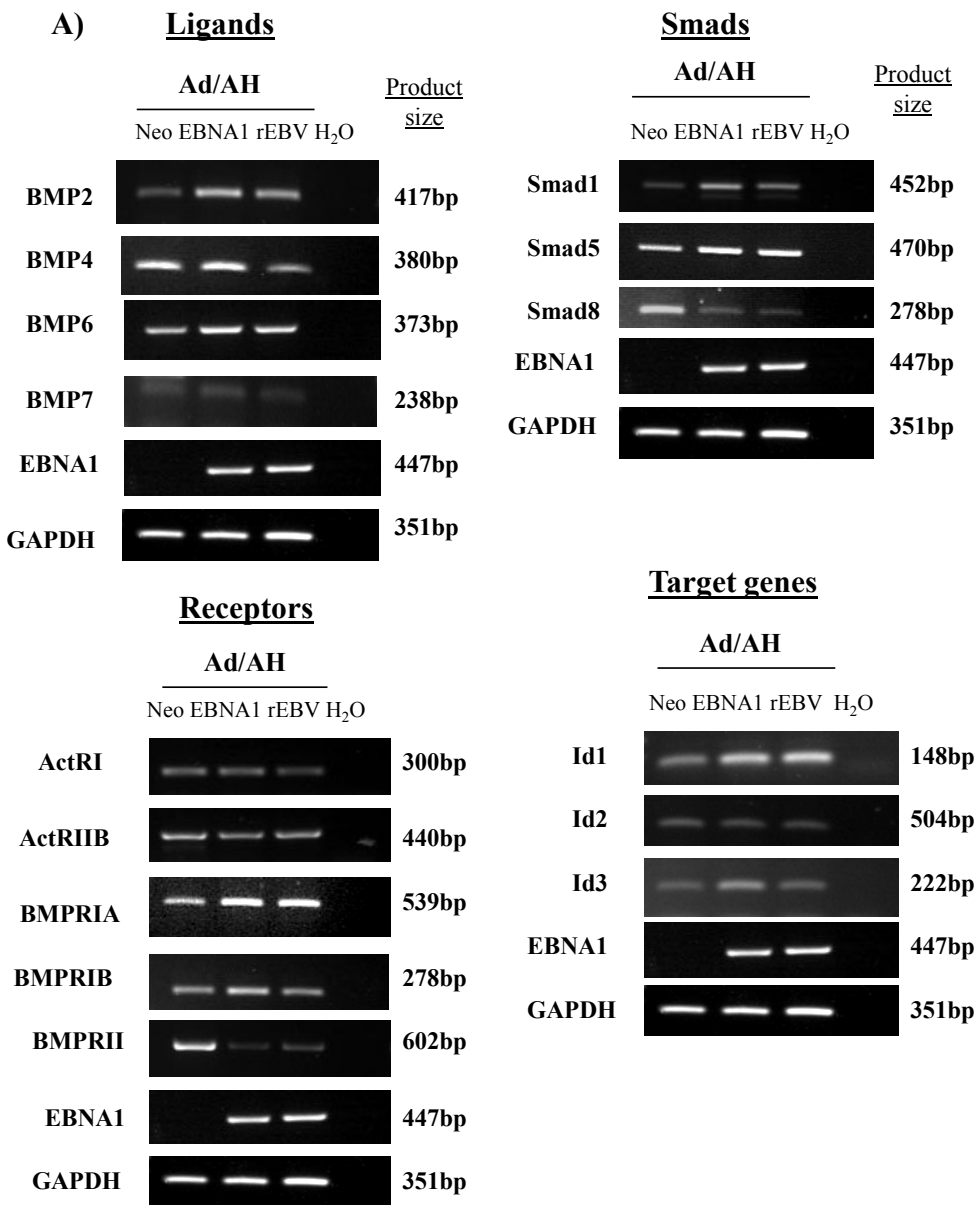

Figure 4.12: Expression of BMP pathway components in Ad/AH, HONE-1 and AGS carcinoma cell lines

RT-PCR analysis for mRNA expression levels of BMP ligands (BMP2, 4, 6 and 7), BMP receptors (ActR1, ActRIIB, BMPRIA, BMPRIB and BMPRII), BMP-specific Smads (Smad1, Smad5 and Smad8) and classical BMP target genes (Id1, Id2 and Id3) in Ad/AH (A), HONE-1 (B) and AGS (C) cells expressing either a control neomycin resistance cassette or EBNA1, or stably infected with rEBV. RT-PCR reactions were also performed to confirm EBNA1 status and the housekeeping gene GAPDH was included as a positive control to confirm equal RNA input into the PCR reactions, while negative water controls confirmed the absence of contamination.

B)

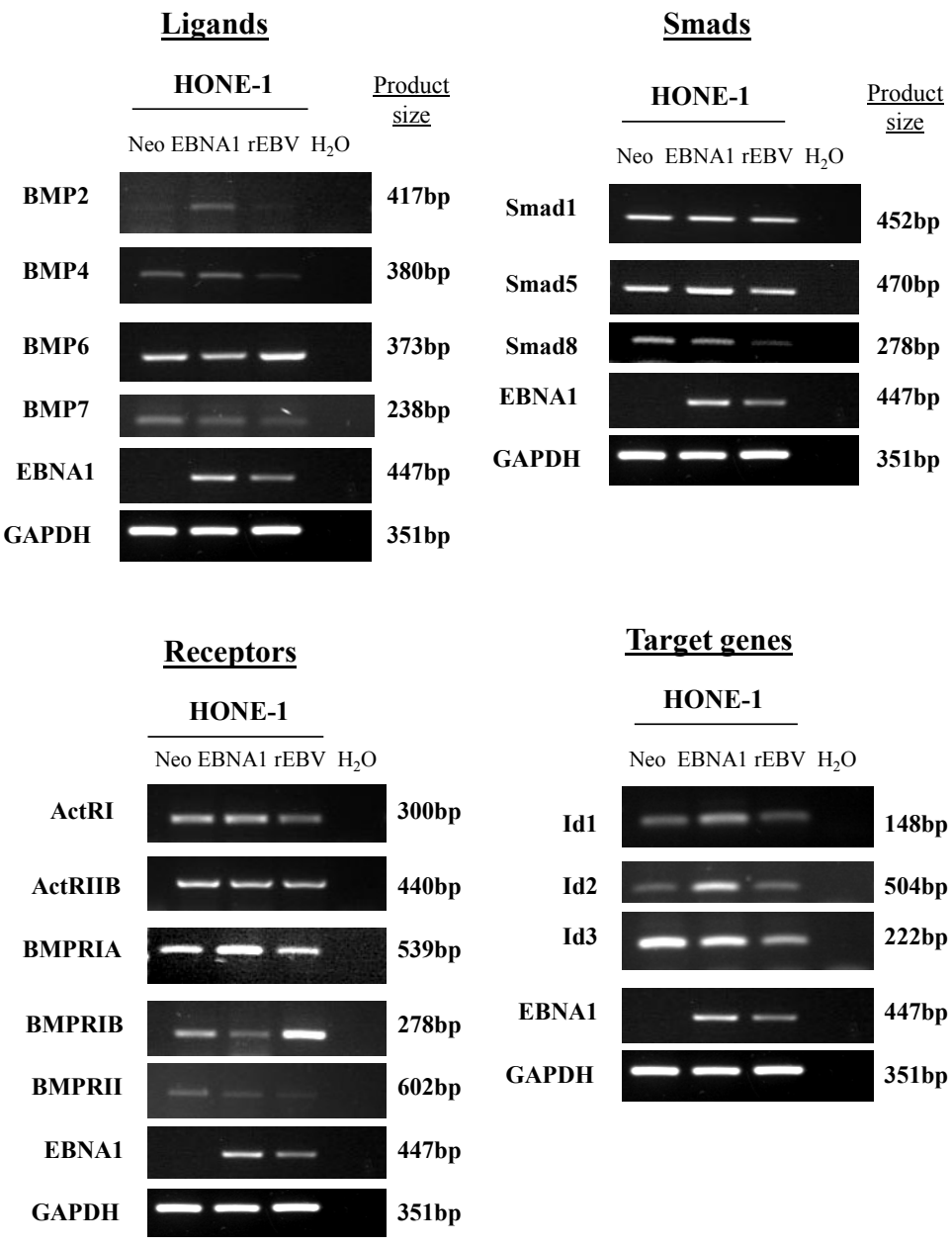
Ligands
HONE-1
Product size
Neo EBNA1 rEBV H2O
BMP2
417bp
BMP4
380bp
BMP6
373bp
BMP7
238bp
EBNA1
447bp
GAPDH
351bp
Smads
HONE-1
Product size
Neo EBNA1 rEBV H2O
Smad1
452bp
Smad5
470bp
Smad8
278bp
EBNA1
447bp
GAPDH
351bp
Receptors
HONE-1
Neo EBNA1 rEBV H2O
ActRI
300bp
ActRIIB
440bp
BMPRIA
539bp
BMPRIB
278bp
BMPRII
602bp
EBNA1
447bp
GAPDH
351bp
Target genes
HONE-1
Neo EBNA1 rEBV H2O
Id1
148bp
Id2
504bp
Id3
222bp
EBNA1
447bp
GAPDH
351bp

C)

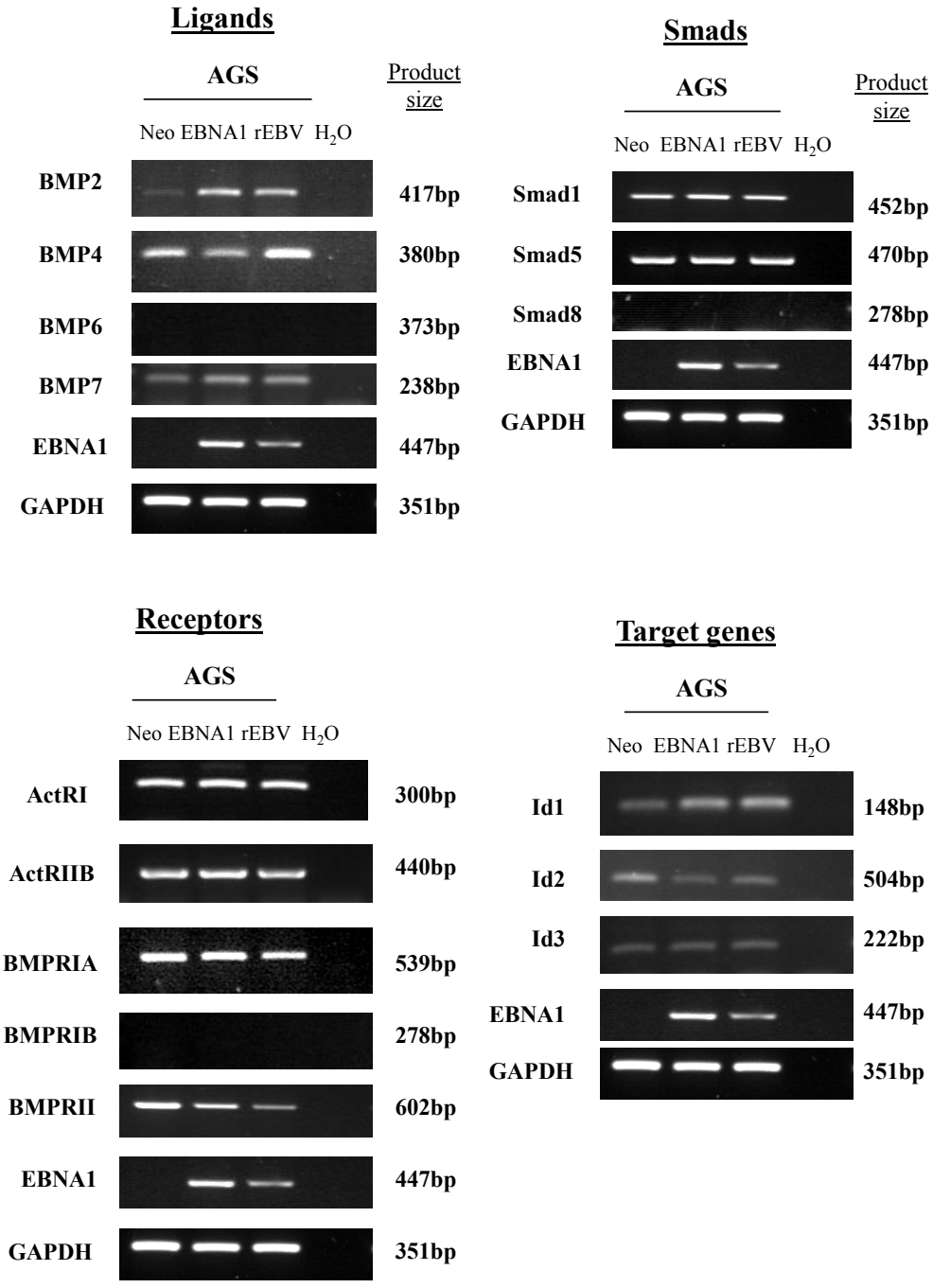
Ligands
AGS
Product size
Neo EBNA1 rEBV H2O
BMP2
417bp
BMP4
380bp
BMP6
373bp
BMP7
238bp
EBNA1
447bp
GAPDH
351bp
Smads
AGS
Product size
Neo EBNA1 rEBV H2O
Smad1
452bp
Smad5
470bp
Smad8
278bp
EBNA1
447bp
GAPDH
351bp
Receptors
AGS
Neo EBNA1 rEBV H2O
ActRI
300bp
ActRIIB
440bp
BMPRIA
539bp
BMPRIB
278bp
BMPRII
602bp
EBNA1
447bp
GAPDH
351bp
Target genes
AGS
Neo EBNA1 rEBV H2O
Id1
148bp
Id2
504bp
Id3
222bp
EBNA1
447bp
GAPDH
351bp

regardless of the presence of EBNA1, lacked detectable expression of BMP6, BMPRIB and Smad8 transcripts. A closer agreement of expression patterns was discovered for Ad/AH and HONE-1 cell panels, with a reduction in BMP4 expression and increase in BMP6 expression in rEBV-infected lines, and also an increase in BMP6 expression in the EBNA1-expressing Ad/AH cells. In addition, increased BMPRIA expression was observed in EBNA1-expressing Ad/AH and HONE-1 cells, and also rEBV-infected Ad/AH cells, while a down-regulation of Smad8 was found in both EBNA1-expressing and rEBV-infected Ad/AH and HONE-1 cells. Of particular note, BMPRII was consistently down-regulated in the presence of EBNA1 and rEBV across all three cell lines.

In examining the Id genes as examples of classical BMP target genes, it was found that expression of Id1 was consistently up-regulated in the EBNA1-expressing clones of all three cell lines, as well as the rEBV-infected Ad/AH and AGS cells. Increased expression of Id2 however was observed in HONE-1 EBNA1-expressing and rEBV-infected cells only, while Id3, although up-regulated in Ad/AH EBNA1-expressing and rEBV-infected cells, appeared to be down-regulated across the HONE-1 panel and showed little change in expression across the AGS panel.

4.3.4 BMP pathway activation in Ad/AH, HONE-1 and AGS cells

The expression levels of phosphorylated Smad1/5/8 in Ad/AH, HONE-1 and AGS Neo control, EBNA1 and rEBV-infected cells were then determined by immunoblotting. As can be seen in Figure 4.13, the basal levels of phosphorylated Smad1/5/8 were elevated in the EBNA1-expressing cells across all three cell lines, and this was particularly well supported in the rEBV-infected Ad/AH cell line. Again, unlike their Neo control counterparts, and as

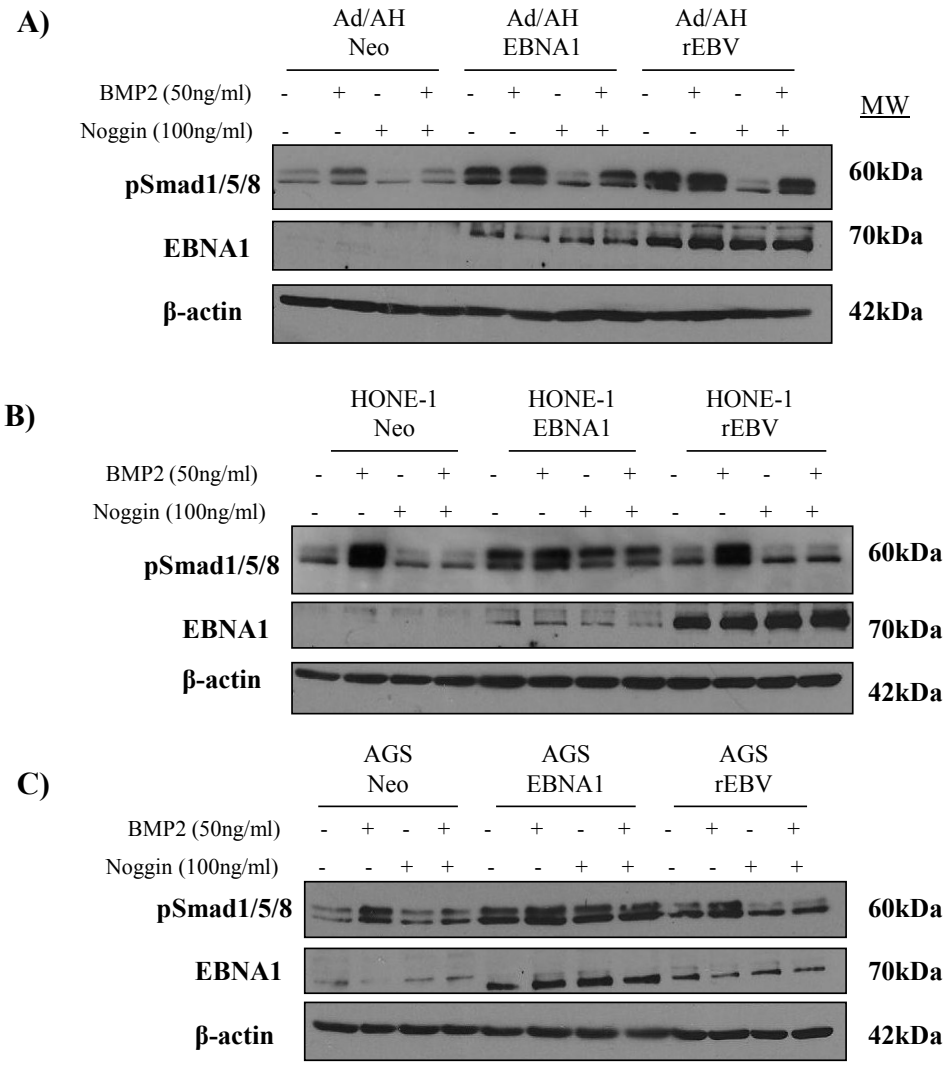

Figure 4.13: Smad1/5/8 phosphorylation in Ad/AH, HONE-1 and AGS carcinoma cell lines

Immunoblotting for protein expression levels of the phosphorylated form of Smad1/5/8 in serum-starved Ad/AH (A), HONE-1 (B) and AGS (C) cells expressing either a control neomycin resistance cassette or EBNA1, or stably infected with rEBV, and treated with 100ng/ml recombinant hNoggin for 1 hour, then subsequently with 50ng/ml recombinant hBMP2 for a further 24 hours. Blots were re-probed for β-actin to confirm equal protein loading.

demonstrated in C666-1 cells, the response of EBNA1-expressing cells was not further induced by BMP2 stimulation, again possibly because the response may already be saturated. For the majority of cell lines, treatment with Noggin effectively suppressed the levels of Smad1/5/8 phosphorylation which, in the Ad/AH EBNA1-expressing and rEBV-infected cell lines, were regained following exogenous BMP2 stimulation. However, Noggin treatment had little effect on the levels of Smad1/5/8 phosphorylation in the HONE-1 and AGS EBNA1-expressing cells.

4.3.5 BMP reporter activity in Ad/AH, HONE-1 and AGS cells

BMP signalling activity in the Ad/AH, HONE-1 and AGS cell panels was further investigated by transient transfection of the BRE-Luc reporter construct. Cells were subsequently stimulated with 50ng/ml BMP2 or treated with 100ng/ml Noggin for 24 hours, and their relative luciferase activity was determined. Results are represented graphically in Figure 4.14.

In the Ad/AH cell panel, the basal levels of BRE-Luc reporter activity were elevated in both EBNA1-expressing and rEBV-infected cells compared to Neo control cells. This was further significantly induced to greater than two-fold in response to BMP2 stimulation, and was reduced below basal levels in the presence of Noggin. In contrast, in HONE-1 cells, there appeared to be a general decrease in the levels of BMP2-induced reporter activity in EBNA1-expressing and rEBV-infected cells. Furthermore, a significant decrease in BRE-Luc reporter activity was observed both basally and under stimulation in AGS EBNA1-expressing and rEBV-infected cells compared to their Neo control counterparts.

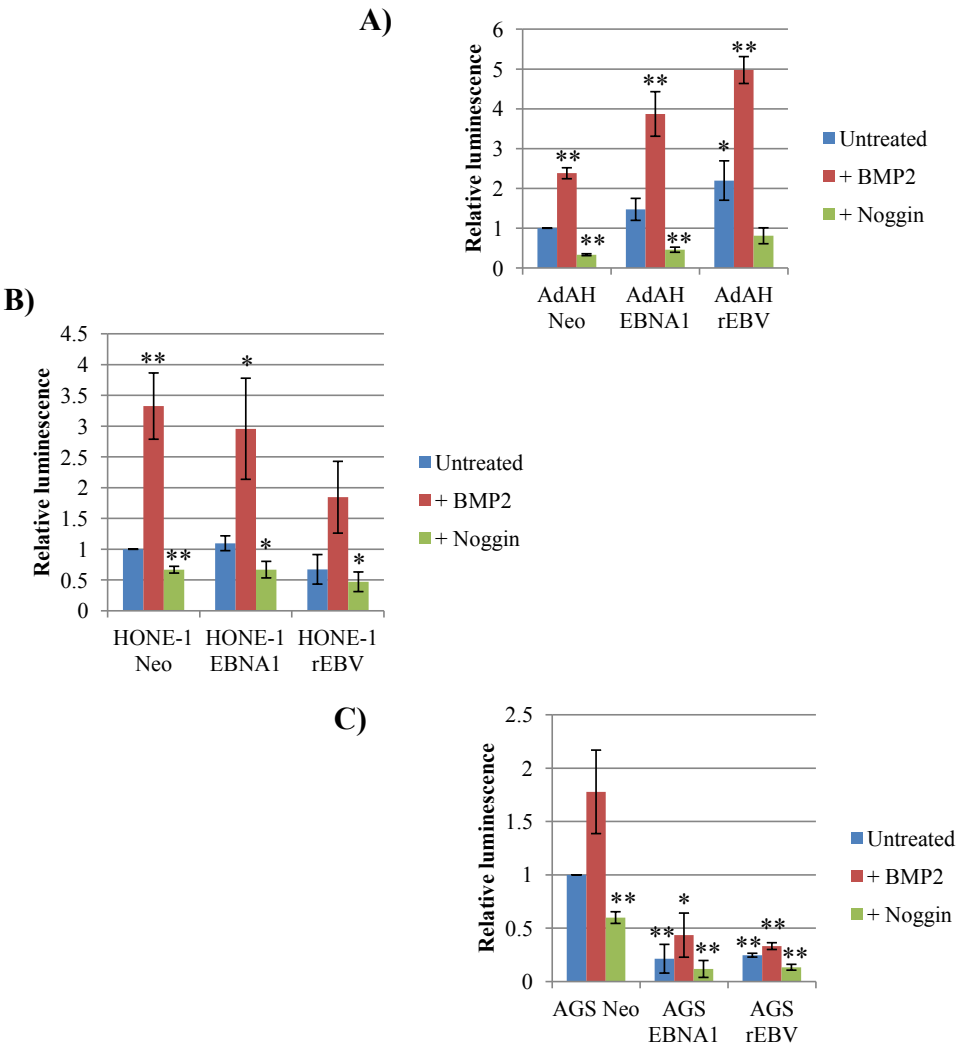

Figure 4.14: The effect of BMP2 and Noggin on BRE-luc reporter activity in Ad/AH, HONE-1 and AGS cells

Dual luciferase reporter assays showing BRE-Luc activity in Ad/AH (A), HONE-1 (B) and AGS (C) cells expressing either a control neomycin resistance cassette or EBNA1, or stably infected with rEBV, treated with either 50ng/ml recombinant hBMP2 or 100ng/ml recombinant hNoggin for 24 hours or left untreated as a control. Histograms are shown to depict the relative luminescence after normalising to Renilla luciferase values and expressing as a ratio of activity relative to the control vector pGL3-basic. Data from five independent experiments is presented as the mean fold differences in activity $\pm$ SE, relative to that observed in unstimulated Neo control cells which is given an arbitrary value of 1 (** denotes a P-value <0.01 and * denotes a P-value <0.05).

4.4 Potential functional consequences of BMP signalling pathway activation

4.4.1 The effect of BMP pathway inhibition on cell migration

BMP2 has been specifically associated with the migratory and invasive capacity of liver cancer SMMC7221 cells (Wu et al., 2011), while BMP2, and slightly less potently, BMP4 and BMP7, have been shown to stimulate the migration and invasion of prostate cancer cells *in vitro* (Feeley et al., 2005, Feeley et al., 2006a). In the latter study, the BMP antagonist, Noggin, was used effectively to inhibit cellular migration of both BMP2- and BMP4-stimulated cells.

The effect of BMP pathway inhibition on the migration of Ad/AH, HONE-1 and AGS cell panels was similarly measured by transwell migration assay. Representative fields from one of five experiments are shown in Figure 4.15. As previously shown in section 3.3.3, compared to Neo control cells, both EBNA1-expressing cells and their rEBV-infected counterparts displayed increased rates of migration on fibronectin over a 24-hour period. In the AGS and HONE-1 panels, treatment of Neo control cells with Noggin increased migration, whereas cell migration was partially inhibited by Noggin treatment in EBNA1-expressing cells. This pattern did not however appear to be repeated in the rEBV-infected cell lines. In the Ad/AH cells however, Noggin was effective in causing partial inhibition of the migration of both EBNA1-expressing and rEBV-infected cells, with a comparative negligible effect in the Neo control cells (Figure 4.15B).

To investigate this further, C666-1 cell migration was also studied under conditions where TGFβ and BMP signalling were inhibited. Representative fields from one of five experiments are shown in Figure 4.16. Whereas SB431542 had little or no effect on the migration of

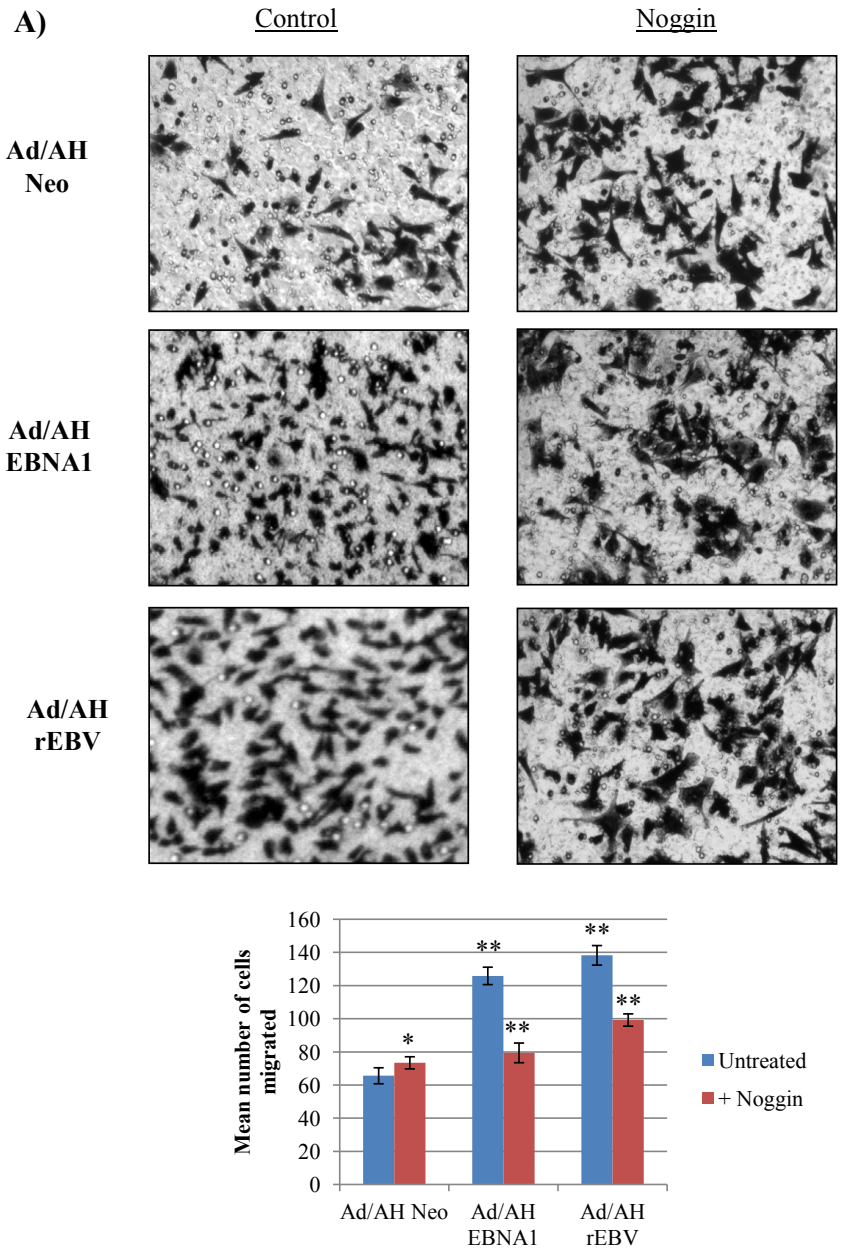

Figure 4.15: The effect of inhibition of BMP signalling on the migration of Ad/AH, HONE-1 and AGS carcinoma cell lines

Serum-starved Ad/AH (A), HONE-1 (B) and AGS (C) cells expressing either a control neomycin resistance cassette or EBNA1, or stably infected with rEBV were seeded into the upper wells of transwell migration chambers in serum-free medium with and without 100ng/ml Noggin, and allowed to migrate for 24 hours. The number of migrated cells in five representative fields were counted and histograms were created showing the mean number of cells migrated (SD) (** denotes a P-value <0.01 and * denotes a P-value<0.05).

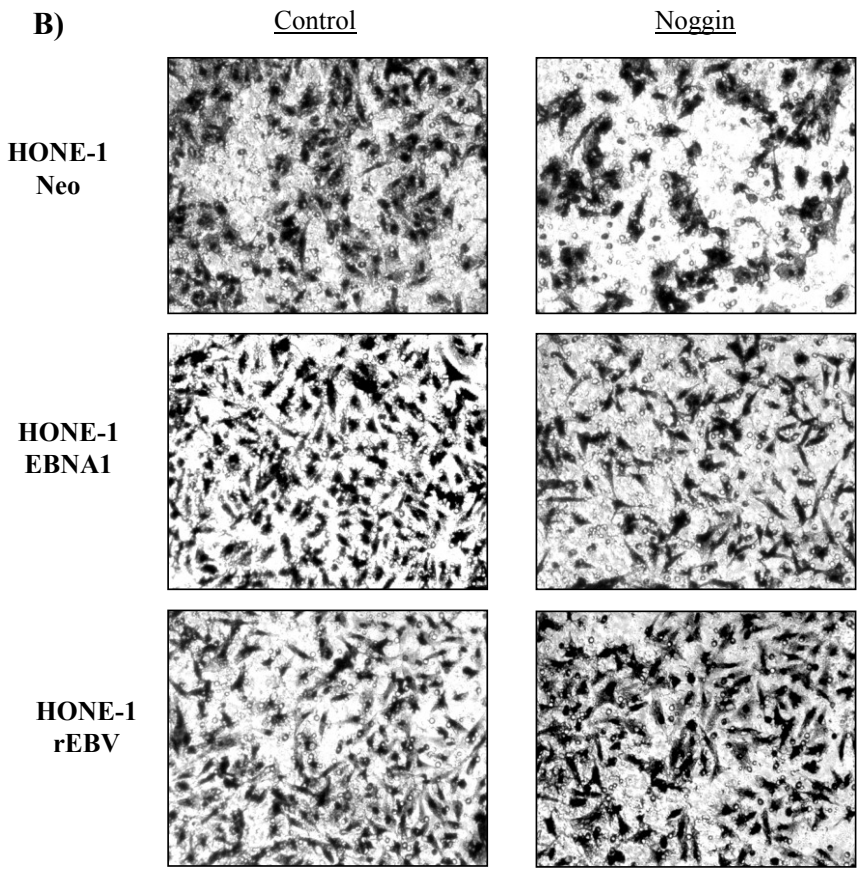
B)
Control
Noggin
HONE-1
Neo
HONE-1
EBNA1
HONE-1
rEBV

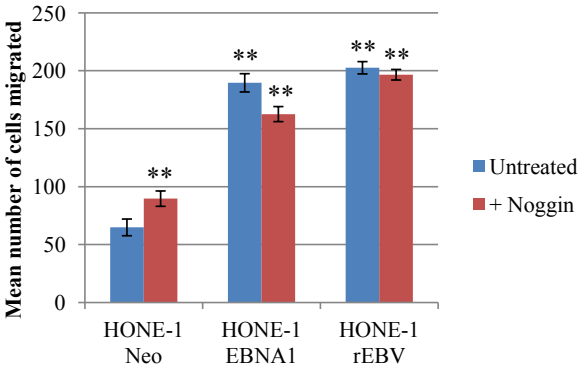
Mean number of cells migrated
250
200
150
100
50
0
**
**
**
**
**
HONE-1
Neo
HONE-1
EBNA1
HONE-1
rEBV
Untreated
+ Noggin

C)

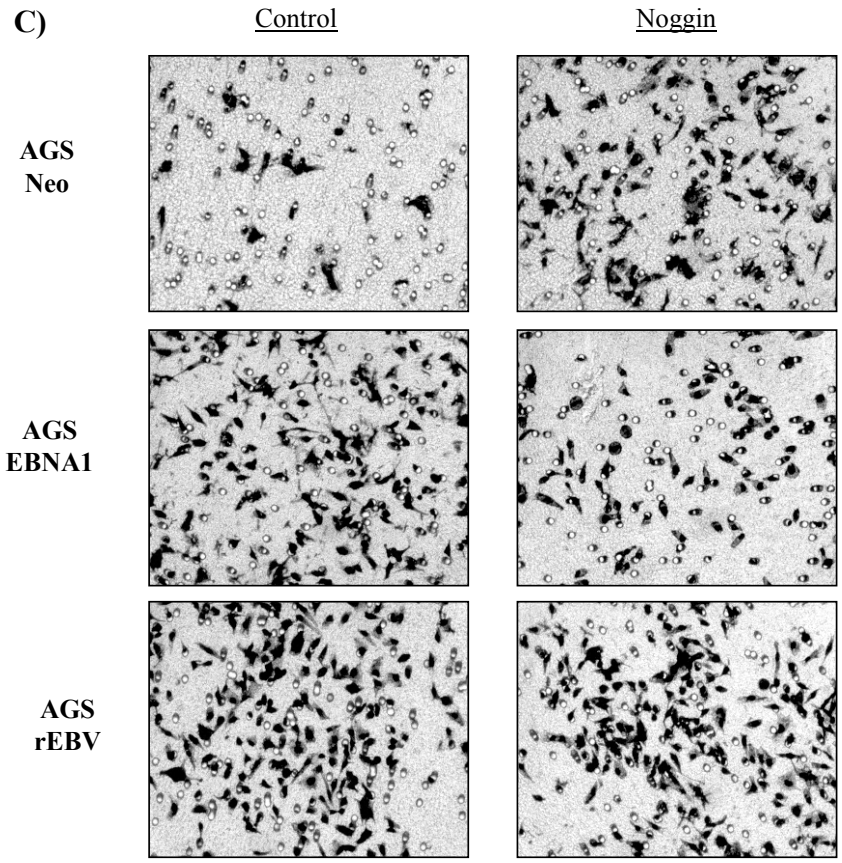
Control
Noggin
AGS Neo
AGS EBNA1
AGS rEBV

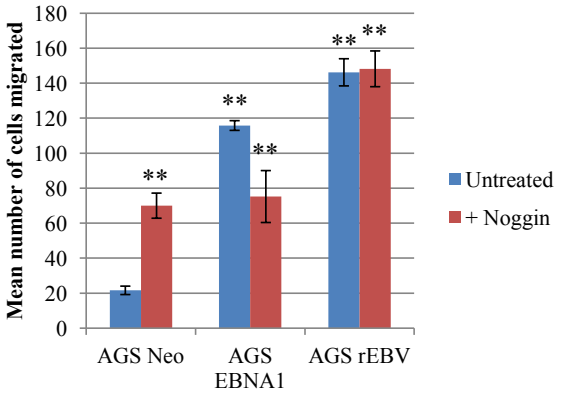
Mean number of cells migrated
180
160
140
120
100
80
60
40
20
0
**
**
**
**
**
AGS Neo
AGS EBNA1
AGS rEBV
Untreated
+ Noggin

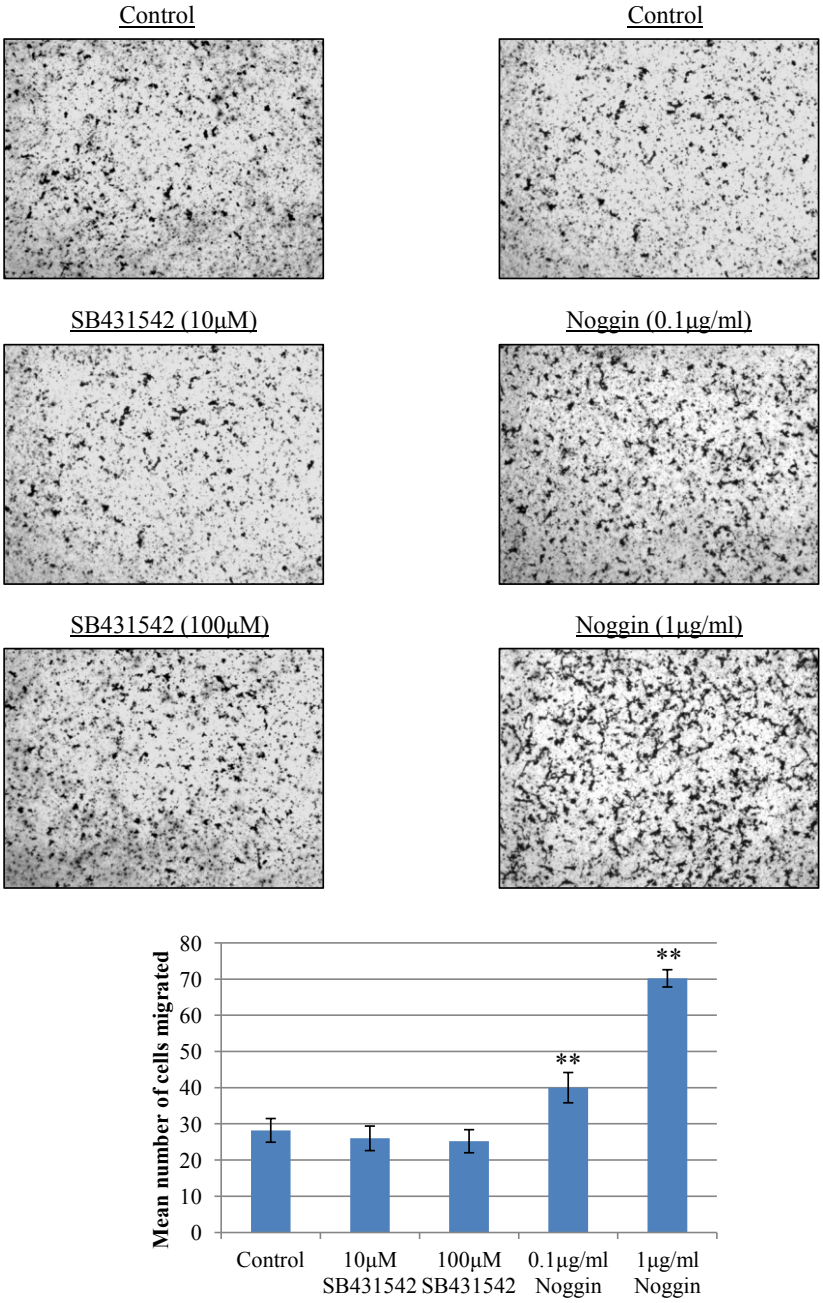

Figure 4.16: The effect of inhibition of TGFβ and BMP signalling on the migration of C666-1 cells
Serum-starved C666-1 cells were seeded into the upper wells of transwell migration chambers in serum-free medium with and without either 10μM or 100μM SB431542, or 100ng/ml or 1μg/ml Noggin, and allowed to migrate for 24 hours toward 10% FCS. The number of migrated cells in five representative fields were counted and histograms were created showing the mean number of cells migrated (SD) (** denotes a P-value <0.01).

C666-1 cells, treatment with Noggin slightly enhanced cell migration, which was significantly potentiated by a ten-fold increase in Noggin concentration.

4.4.2 Potential crosstalk between TGFβ and BMP signalling pathways

Much debate exists over the possibility and potential mechanism by which alternative TGFβ family ligands may be capable of promiscuous activation of related signalling pathways through differential receptor utilisation and subsequent activation of the appropriate Smad effectors. The premise for such a hypothesis among TGFβ superfamily members was illustrated at an early stage by the proven ability of BMPs to signal through receptors classically regarded as activin receptors (Yamashita et al., 1995, Macías-Silva et al., 1998, Nagaso et al., 1999).

Firstly the possibility that BMP2 may also exert some influence over TGFβ signalling was investigated. The expression of the serine 465/467 phosphorylated form of the TGFβ pathway-specific R-Smad, Smad2, was examined in the Ad/AH, HONE-1 and AGS cell panels, and also the OKF6 and C666-1 cells, by immunoblotting in the presence and absence of 50ng/ml BMP2. As shown in Figure 4.17, stimulation of cells with BMP2 for 24 hours had negligible effects on levels of serine 465/467 phosphorylated forms of Smad2 in all cell lines studied.

TGFβ, on the otherhand, has already been shown to cross-activate BMP-Smads, Smad1 and Smad5 in C2C12 cells, HaCaT human keratinocytes, mammary epithelial and breast cancer cells (Wrighton et al., 2009, Daly et al., 2008, Liu et al., 1998, Liu et al., 2009). In some instances, this is predicted to be mediated via mixed type I receptor complexes comprising

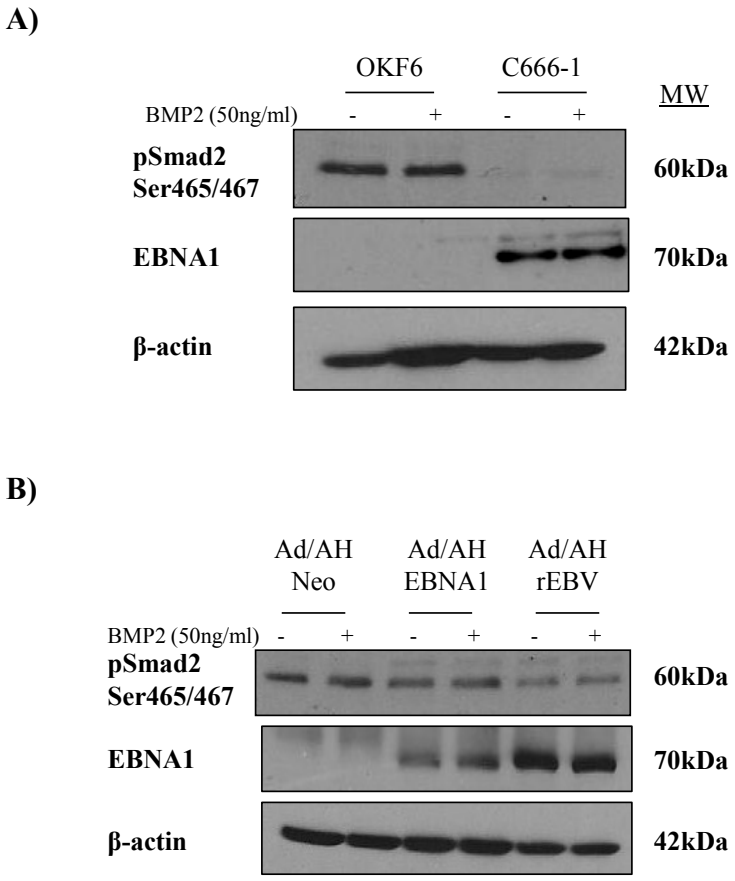

Figure 4.17: The effect of BMP2 on the phosphorylation of Smad2
Immunoblotting for protein expression levels of the serine 465/467 phosphorylated form of Smad2 in serum-starved OKF6 and C666-1 cells (A), and Ad/AH (B), HONE-1 (C) and AGS (D) cells expressing either a control neomycin resistance cassette or EBNA1, or stably infected with rEBV, stimulated with 50ng/ml recombinant hBMP2 for 24 hours. Immunoblotting for EBNA1 expression was included for confirmation of cell line status and blots were re-probed for β-actin to confirm equal protein loading.

C)

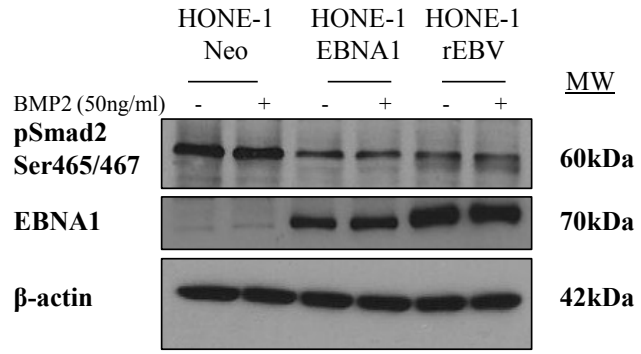
HONE-1 Neo
HONE-1 EBNA1
HONE-1 rEBV
MW
BMP2 (50ng/ml) - + - + - +
pSmad2 Ser465/467
EBNA1
β-actin
60kDa
70kDa
42kDa

D)

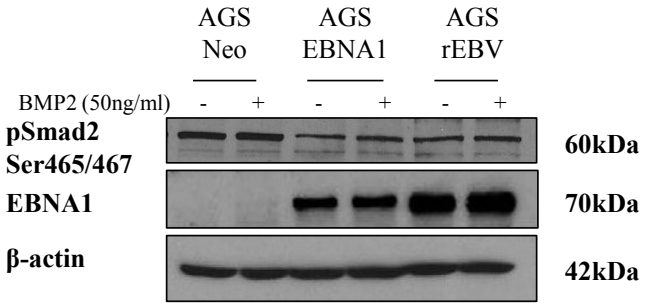
AGS Neo
AGS EBNA1
AGS rEBV
BMP2 (50ng/ml) - + - + - +
pSmad2 Ser465/467
EBNA1
β-actin
60kDa
70kDa
42kDa

TβRI, ActRIA and/or BMPRIA (Daly et al., 2008), while in others it is thought to occur completely independently of BMP type I receptors (Wrighton et al., 2009).

It was therefore questioned whether TGFβ could instead signal via the BMP pathway in carcinoma cells. In C666-1 cells, it was hypothesised that, in the absence of a functional TGFβ pathway, due to loss of TβRII expression, C666-1 cells might possess the ability to divert TGFβ signalling into a more focussed BMP response. Representative immunoblots shown in Figure 4.18 demonstrate that treatment of Ad/AH, HONE-1 and AGS cells with TGFβ promoted an increase in the levels of phosphorylated Smad1/5/8. As shown previously, the basal levels of pSmad1/5/8 were higher in EBNA1-expressing and rEBV-infected cell lines, including C666-1, and this was further augmented by TGFβ treatment. A noticeable TGFβ-induced increase could not be detected in the C666-1 cells, presumably due to the lack of responsiveness of C666-1 cells to TGFβ.

These observations were extended in the C666-1 cell line to examine the effects of Noggin pre-treatment so that a potential induction of Smad1/5/8 phosphorylation might be more easily observed. As shown in Figure 4.19, treatment with Noggin significantly depleted pSmad1/5/8 levels, which could be partially restored by stimulation with TGFβ in OKF6 cells only, but not in C666-1 cells. Similarly, a time-course of treatment with a neutralising antibody to TGFβ (clone 1D11) was carried out, and its effects on the activation of the BMP-specific Smads were studied by immunoblotting. As shown in Figure 4.20, neutralisation of TGFβ bioactivity did not markedly impact upon levels of Smad1/5/8 phosphorylation, indicating that TGFβ is not a significant contributor to the high levels of activated Smad1/5/8 in C666-1 cells.

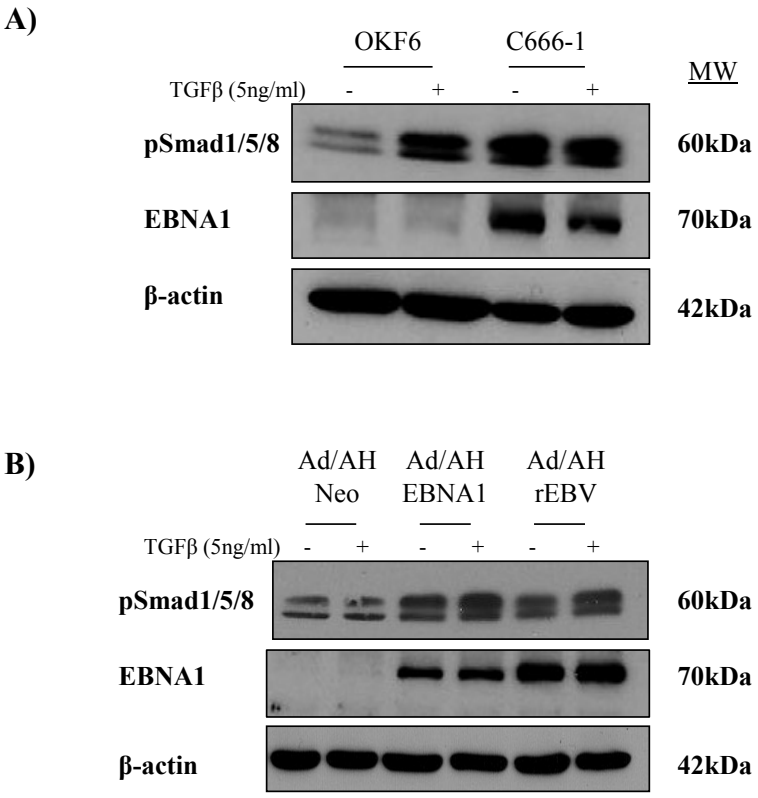

Figure 4.18: The effect of TGFβ on the phosphorylation of Smad1/5/8
Immunoblotting for protein levels of the phosphorylated form of Smad1/5/8 in serum-starved OKF6 and C666-1 cells (A), and Ad/AH (B), HONE-1 (C) and AGS (D) cells expressing either a control neomycin resistance cassette or EBNA1, or stably infected with rEBV, stimulated with 5ng/ml recombinant hTGFβ1 for 24 hours. Immunblotting for EBNA1 was included for confirmation of cell line status and blots were re-probed for β-actin to confirm equal protein loading.

C)

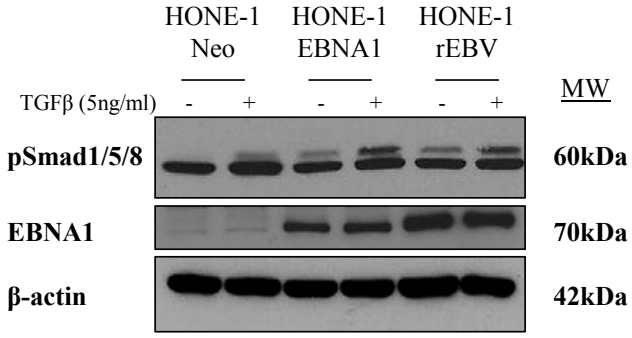
HONE-1 Neo
HONE-1 EBNA1
HONE-1 rEBV
TGFβ (5ng/ml)
- + - + - +
MW
pSmad1/5/8
60kDa
EBNA1
70kDa
β-actin
42kDa

D)

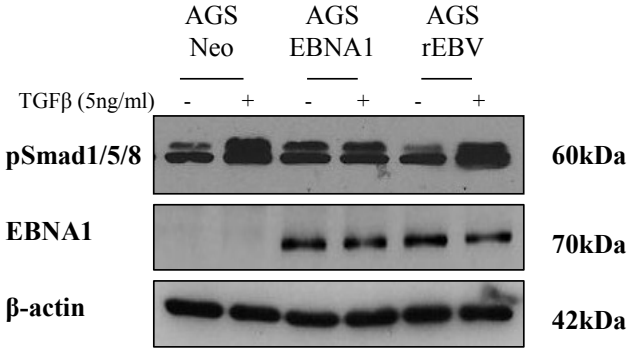
AGS Neo
AGS EBNA1
AGS rEBV
TGFβ (5ng/ml)
- + - + - +
pSmad1/5/8
60kDa
EBNA1
70kDa
β-actin
42kDa

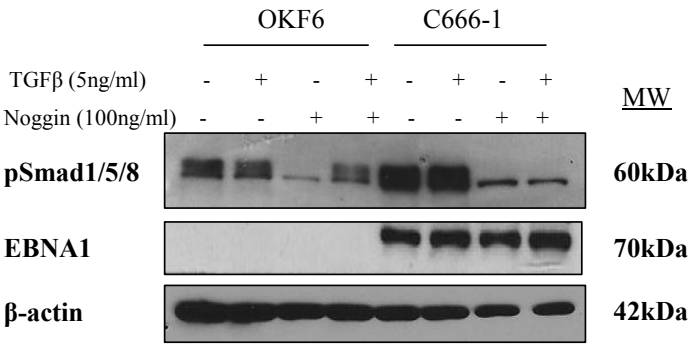

Figure 4.19: The effect of TGFβ stimulation on Smad1/5/8 phosphorylation following BMP pathway inhibition in C666-1 cells
Immunoblotting for protein levels of the phosphorylated form of Smad1/5/8 in serum-starved OKF6 and C666-1 cells treated with 100ng/ml recombinant hNoggin for 1 hour, before stimulation with 5ng/ml recombinant hTGFβ1 for a further 24 hours. EBNA1 expression status was confirmed and blots were re-probed for β-actin to confirm equal protein loading.

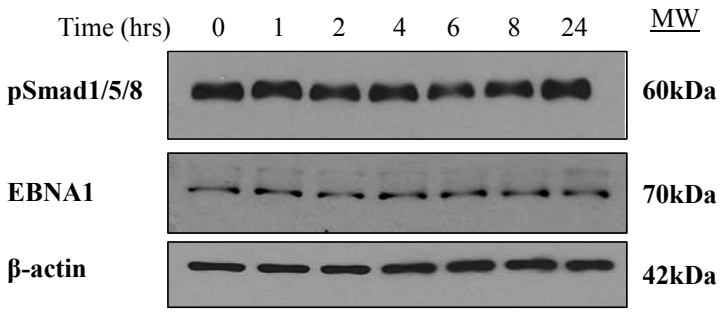

Figure 4.20: The effect of TGFβ pathway inhibition on Smad1/5/8 phosphorylation in C666-1 cells
Immunoblotting for protein levels of the phosphorylated form of Smad1/5/8 in C666-1 cells treated with 10μg/ml monoclonal anti-TGFβ antibody (clone 1D11), and harvested at 0, 1, 2, 4, 6, 8 and 24 hour post-treatment. β-actin was included to confirm equal protein loading.

4.4.3 Bone metastasis

Given the prominent role of BMPs in bone formation, it is feasible that the enhanced BMP signalling pathway activity may specifically contribute to bone metastasis in NPC. Bone metastasis has been reported as a complication of the more advanced stages of NPC, where it is generally associated with poor prognosis (Micheau et al., 1987). Although bone metastases in NPC have not been extensively characterised, bone is a common site of metastasis in prostate, lung and breast cancers (Mundy, 2002), where its occurrence has gained considerably more attention. Indeed BMPs have been specifically linked to accelerated bone metastasis formation in all three cancer types (Feeley et al., 2005, Dai et al., 2008, Feeley et al., 2006b, Alarmo et al., 2008, Katsuno et al., 2008).

A study by Kang and co-workers identified a specific set of genes found to be significantly differentially regulated in human breast cancer cell lines that demonstrate a defined propensity for metastasis to bone (Kang et al., 2003b). This gene set was deemed important in cooperatively promoting bone metastasis. To determine whether similar gene expression signatures could be induced by EBNA1, and also existed in NPC tumours, the same gene list was used to identify genes that were commonly differentially regulated, using gene expression data obtained from separate studies (Hu, PhD thesis, 2010, Valentine et al., 2010). Although it is important to appreciate that these genes are specific to breast cancer and therefore precise matches are not expected due to dissimilar cell origin, they were useful in providing a general guideline and suggesting potential genes with common involvement in bone metastasis.

Data was subjected to hierarchical clustering analysis using dChip software and findings were visualised as heat maps. As illustrated in Figure 4.21, several genes identified as being

A)

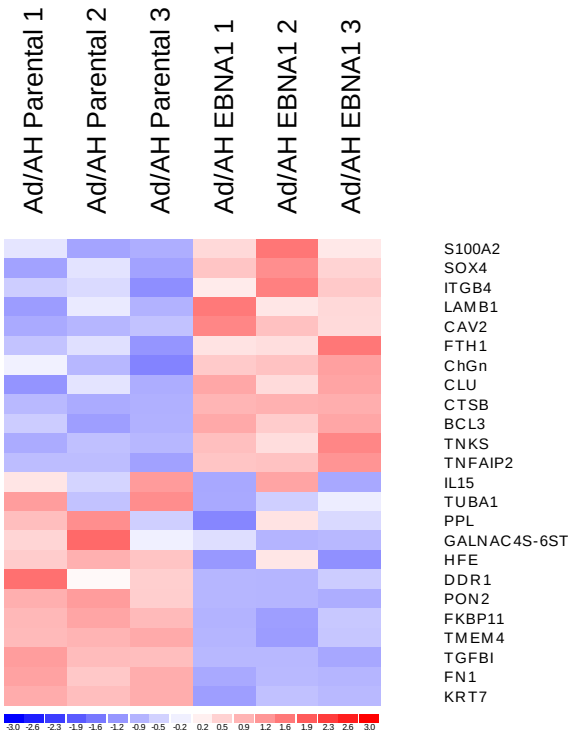

Figure 4.21: Gene expression profiling of bone metastasis-associated genes in Ad/AH cell lines

Gene expression signatures specifically associated with bone metastasis in breast cancer (Kang et al., 2003) were utilised to identify commonly differentially regulated genes found to be either under-expressed (A) or over-expressed (B) in Ad/AH cells stably expressing EBNA1 compared to parental Ad/AH cells. Expression array data generated in a separate study was subjected to further hierarchical clustering analysis, the results of which were visualised as a heat map using dChip software. The expression level of each gene in an individual sample is colour coded: blue for down-regulation, red for up-regulation and white for unchanged.

B)

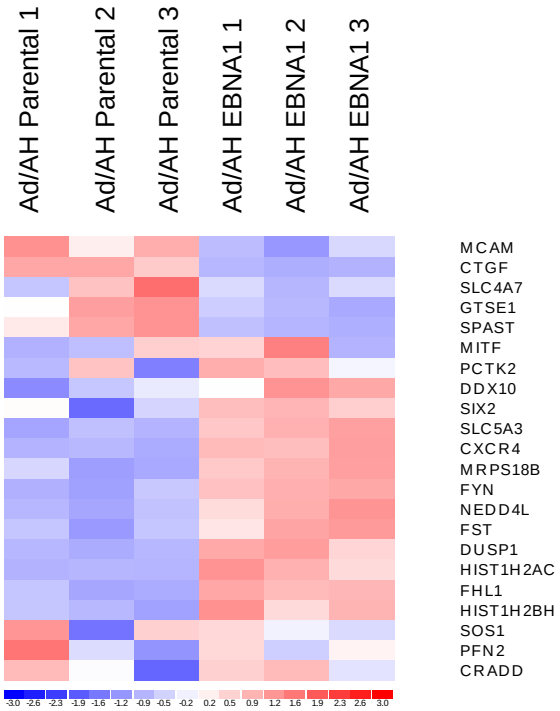
Ad/AH Parental 1
Ad/AH Parental 2
Ad/AH Parental 3
Ad/AH EBNA1 1
Ad/AH EBNA1 2
Ad/AH EBNA1 3
MCAM
CTGF
SLC4A7
GTSE1
SPAST
MITF
PCTK2
DDX10
SIX2
SLC5A3
CXCR4
MRPS18B
FYN
NEDD4L
FST
DUSP1
HIST1H2AC
FHL1
HIST1H2BH
SOS1
PFN2
CRADD
-3.0 -2.6 -2.3 -1.9 -1.6 -1.2 -0.9 -0.5 -0.2 0.2 0.5 0.9 1.2 1.6 1.9 2.3 2.6 3.0

under-expressed in the breast cancer bone metastasis signature were also down-regulated in EBNA1-expressing Ad/AH cells compared to control cells, and a number of over-expressed genes associated with bone metastasis were similarly up-regulated. In contrast, less concordance was observed between the breast cancer bone metastasis gene set and gene expression signatures of the NPC tumours (Figure 4.22), although normal samples did behave similarly, and NPC tumours clustered together, although into two separate subgroups for the over-expressed genes.

4.5 Discussion and Future Work

Findings presented in this chapter identify a novel function for the EBV-encoded EBNA1 protein, namely its ability to stimulate expression of the TGFβ family member, BMP2. The generality of this effect was substantiated, as expression of EBNA1 in a variety of epithelial cell lines was sufficient to stimulate the expression of both BMP2 mRNA and protein, suggesting that these effects are probably linked to transcriptional up-regulation of BMP2. These findings serve to complement existing data describing elevated levels of BMP2 in authentic NPC tumours and the EBV-positive NPC cell line, C666-1 (Hu, PhD thesis, 2010). Profiling of the BMP signalling pathway in these carcinoma cell lines confirmed the integrity of the signalling pathway, indicating the capability of cells to respond to BMP signals, while measurement of Smad1/5/8 phosphorylation and detectable activation of the BRE-Luc reporter confirmed the functional integrity of the BMP signalling response. The elevated levels of phosphorylated Smad1/5/8 in the presence of EBNA1 and also EBV infection in all cell lines studied support a role for EBV, and more specifically for EBNA1, in modulating the BMP signalling pathway, through autocrine induction of BMP ligands.

A)

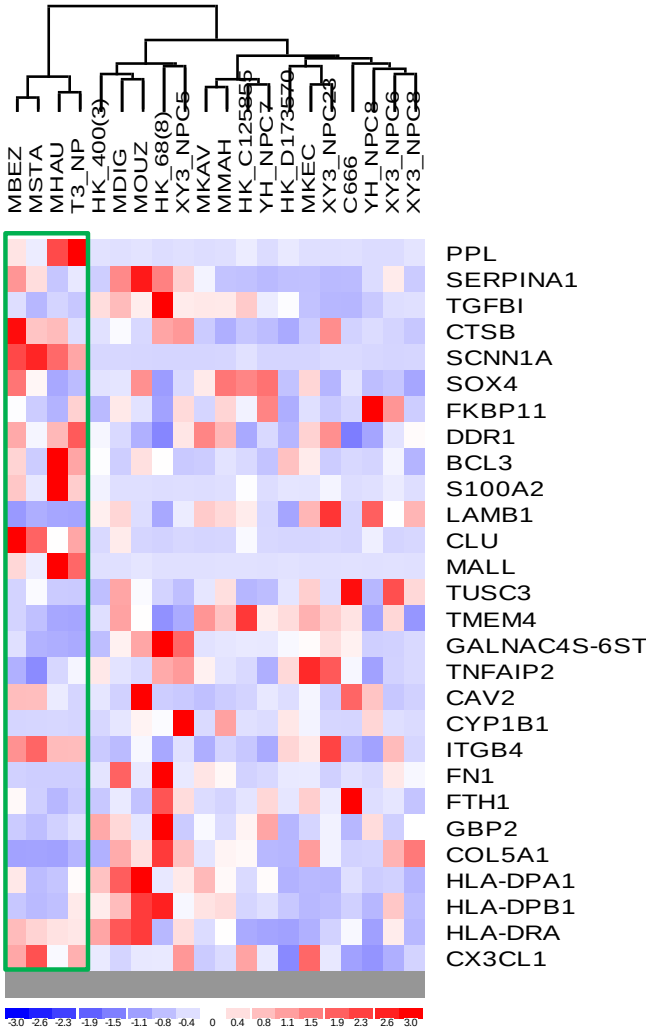

Figure 4.22: Gene expression profiling of bone metastasis-associated genes in NPC tumours

Gene expression signatures specifically associated with bone metastasis in breast cancer (Kang et al., 2003) were utilised to identify commonly differentially regulated genes found to be either under-expressed (A) or over-expressed (B) in 4 normal samples and 15 NPC tumours plus the C666-1 EBV-positive NPC cell line. Expression array data generated in a separate study was subjected to further hierarchical clustering analysis, the results of which were visualised as a heat map using dChip software. The expression level of each gene in an individual sample is colour coded: blue for down-regulation, red for up-regulation and white for unchanged. Normal samples are highlighted by green boxes.

B)

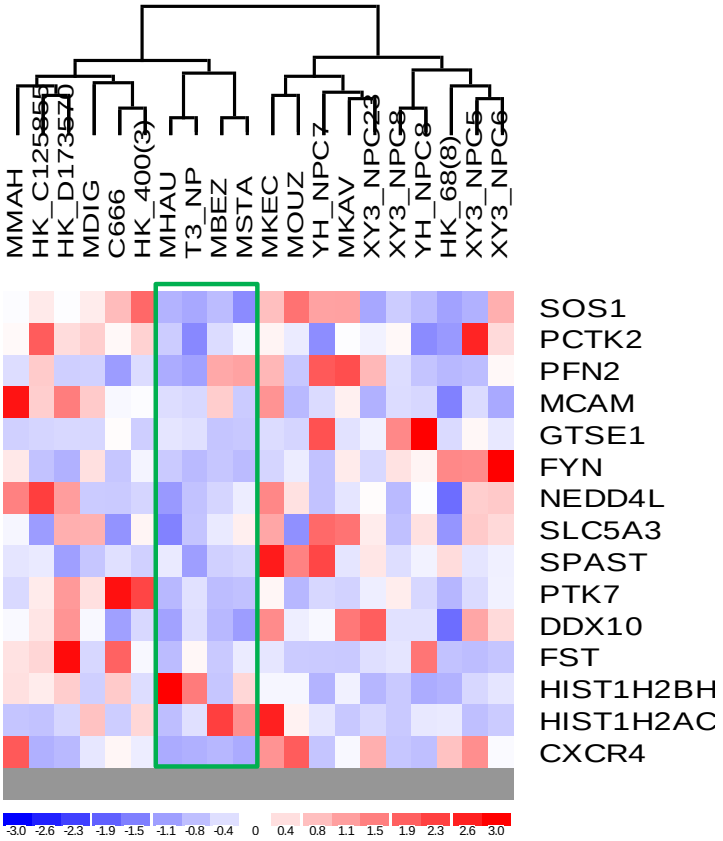
MMAH
HK_C125(5)
HK_D173(7)
MDIG
C666
HK_400(3)
MHAU
T3_NP
MBEZ
MSTA
MKEC
MOUZ
YH_NPC7
MKAV
XY3_NPC2
XY3_NPC4
YH_NPC8
HK_68(8)
XY3_NPC5
XY3_NPC6
SOS1
PCTK2
PFN2
MCAM
GTSE1
FYN
NEDD4L
SLC5A3
SPAST
PTK7
DDX10
FST
HIST1H2BH
HIST1H2AC
CXCR4
-3.0 -2.6 -2.3 -1.9 -1.5 -1.1 -0.8 -0.4 0 0.4 0.8 1.1 1.5 1.9 2.3 2.6 3.0

The initial RT-PCR analyses revealed a number of changes in the transcription of genes associated with the BMP signalling pathway. The relevance of these observations is presently unclear, and it is important to note that further validation at the protein level is required before firm conclusions can be drawn. The RT-PCR analysis did suggest that the expression of different BMP receptors was frequently modified by the expression of EBNA1 or infection with EBV, although the observed patterns were not always consistent.

It is generally accepted that BMP ligand specificity of a receptor complex is mainly dictated by the type I receptor (Alarmo and Kallioniemi, 2010). In the cell lines studied, expression of BMPRIA was found to be increased in Ad/AH and HONE-1 cells expressing EBNA1, an effect which, in the context of squamous cell carcinoma, has been attributed a specific role in the malignant transformation of the oral epithelium (Jin et al., 2001, Soares et al., 2010). Additionally, prominent expression of BMPRIB in malignant glioma, breast cancer and renal cell carcinoma has been correlated with tumour grade (Yamada et al., 1996, Helms et al., 2005, Markić et al., 2010), though in the results presented here, a failure to detect BMPRIB in all AGS-derived cell lines, as well as an observed down-regulation of BMPRIB in C666-1 cells are not in support of this observation. In contrast however, EZH2-dependent epigenetic silencing of BMPRIB has been detected in a subset of glioblastoma tumour-initiating cells, where it is proposed to impair BMP-mediated astroglial differentiation and instead favour tumourigenicity (Lee et al., 2008). Interestingly, up-regulation of EZH2 has already been observed in a number of NPC tumour samples (Hu *et al.*, manuscript in preparation), while increased levels of expression of EZH2 have also been noted in EBV-positive NPC and GC cell lines (R. Port, unpublished observations); However, its potential contribution to

epigenetic effects has yet to be determined, as does the significance of EBNA1 to this observation.

The expression profile of BMPRIB is reportedly more restricted across cell types in contrast to the wider expression of BMPRIA (Kawabata et al., 1998, Miyazono et al., 2010), which may account for its absence in the AGS cell lines. In addition, several studies suggest BMPRIA and BMPRIB mediate discrete functions. Indeed, they are found to regulate distinct processes during chick limb development (Zou et al., 1997), transmit divergent signals in specifying the commitment and differentiation of osteoblasts and adipocytes from bone-derived mesenchymal progenitor cells (Chen et al., 1998) and, furthermore, differentially modulate prostate cancer growth in response to BMP, with BMPRIA conveying growth stimulation and BMPRIB eliciting growth suppressive effects (Ide et al., 1997). If a similar phenomenon were to be observed in the carcinoma cell lines used in this study, the increase in BMPRIA expression and/or down-regulation of BMPRIB would be in keeping with the promotion of tumour cell growth.

One particularly striking result was the observed down-regulation of BMPRII in all cell lines studied. Loss-of-function mutations in BMPRII have been implicated in the development of primary pulmonary hypertension (Yu et al., 2005), while the loss of BMPRII expression appears to be a frequent event in cancer progression, as has been observed, particularly in metastatic variants, in renal cell carcinoma, prostate cancer and bladder cancer (Kim et al., 2003, Markić et al., 2010, Kim et al., 2004a, Kim et al., 2004b). In support of this, expression of a dominant-negative BMPRII potentiated tumour cell proliferation and lung metastases in a mouse model of mammary carcinoma formation (Owens et al., 2011). In contrast however, a

requirement for BMPRII has been demonstrated for the enhanced proliferation of breast cancer cells in response to BMP2 (Pouliot et al., 2003) suggesting that its loss is only beneficial to certain tumour cell types. The evidence gathered here however suggests that rEBV-infected epithelial cells may fall into this category.

Although the precise mechanism for this loss of BMPRII is undetermined at this stage, it is known to occur at the transcriptional level in EBNA1-expressing cell lines. Treatment with the demethylating agent 5-aza-2′-deoxycytidine was able to restore BMPRII expression in the human bladder cancer cell line TSU-Pr1, hinting at the involvement of epigenetic mechanisms in BMPRII silencing (Kim et al., 2004); this has yet to be determined in these carcinoma lines. In the context of viral infection and BMP signalling, KSHV infection, and in particular the expression of the K5 E3 ubiquitin ligase gene, has been associated with a reduction of cell surface BMPRII in the development of pulmonary arterial hypertension (PAH), through a mechanism involving increased ubiquitination and lysosomal degradation of the BMPRII receptor (Durrington et al., 2010). Fortuitously, an increase in receptor degradation is unlikely to impact on Smad1/5/8 phosphorylation, which occurs at the cell surface and precedes endosomal sorting and degradation (Hartung et al., 2006). It may therefore also be informative to study potential ubiquitin ligases that may target BMPRII.

Poorly differentiated prostate cancers are commonly found to exhibit a loss of expression of at least one BMP receptor (Kim et al., 2000), potentially as a mechanism of evading the growth-inhibitory effect of naturally high levels of BMPs in the bone microenvironment. This strategy may provide tumour cells with a mechanism for ablating certain growth-inhibitory signalling responses whilst retaining other more favourable effects. Moreover, a loss of

expression of the BMPRII receptor would unlikely have such a profound impact as, for example, a loss of TβRII on TGFβ signalling, as BMPs can also signal through the activin receptors ActRIIA and ActRIIB. Indeed, deletion of *Bmpr2* in pulmonary artery smooth muscle cells in an *ex vivo* system did not abolish BMP signalling (Yu et al., 2005), with cells instead transmitting signals via ActRIIA. This observation is particularly pertinent to C666-1 cells which, although lacking BMPRII, show up-regulation of ActRIIB which may adequately compensate in the transmission of BMP signals. Type II receptors do however differ in their ability to interact with type I receptors and the resulting receptor complexes formed therefore vary in signalling capacity. The exact nature of the effects of this shift in receptor usage is therefore worthy of further investigation.

Furthermore, the loss of BMPRII in the cell lines studied did not seem to adversely affect Smad1/5/8 activation, suggesting that BMP signalling is not completely attenuated. This adds credence to the hypothesis that the high levels of pSmad1/5/8 observed in EBNA1-expressing cells may occur as a result of signalling through alternative receptor combinations, which may shift the nature of the BMP signalling response. In the pulmonary artery smooth muscle cell model, siRNA-mediated knockdown of *Bmpr2* abrogated, but did not completely abolish BMP2 and BMP4 signalling, and concomitantly augmented signalling by BMP6 and BMP7 (Yu et al., 2005). This is likely a result of the varying affinities exhibited by different BMP ligands for the various receptor combinations. BMP2 was found to bind more efficiently to BMPRII in combination with ActRI or BMPRIB compared to BMPRIA, while BMP7 binding to BMPRII was more potent with ActRI rather than BMPRIA or BMPRIB (Liu et al., 1995). Similarly, BMP7 can bind ActRI, BMPRIA and BMPRIB in the presence of the type II activin receptors, ActRII and ActRIIB (ten Dijke et al., 1994, Yamashita et al., 1995), while

BMP4, while efficiently binds BMPRIA and BMPRIB, does not share the demonstrated ability of BMP7 to signal through the activin receptor, ActRIA. Intriguingly, in the induction of osteoblast differentiation in C2C12 cells, BMP4 activates Smads 1, 5 and 8, whereas BMP6 and BMP7 target only Smad1 and 5 (Aoki et al., 2001), probably as a result of preferential binding to different type I receptors, and likely generate distinctive signalling outputs. The observed response is in fact likely to be determined by the overall complement of BMP ligands and receptor complexes present in different cell types. There also exists the additional possibility in some cell lines that the increase in Smad1/5/8 phosphorylation may be mediated instead by TGFβ, as will be discussed later.

Smad8 is reported to be epigenetically silenced in multiple types of cancer including breast and colon cancers (Cheng et al., 2004). It was therefore unsurprising that it was not expressed at detectable levels in either C666-1 or AGS cells. The significance of this remains to be elucidated, however the additional down-regulation of Smad8 in EBNA1-expressing and rEBV-infected Ad/AH and HONE-1 cells suggest that it may be commonly targeted. An interesting study by Pardali and colleagues concluded that, of all five R-Smads, Smad8 displayed the best efficiency in both promoter activation and endogenous gene induction of $p21^{WAF1/Cip1}$ (Pardali et al., 2005). Down-regulation of Smad8 may potentially be part of a selective mechanism to protect against the induction of growth arrest.

The observed increase of the BMP target Id1 in EBNA1-expressing Ad/AH, HONE-1 and AGS cells is encouraging given the increased expression of Id1 in NPC tumour samples (Wang et al., 2002). The reported ability of the EBNA1 homologue of KSHV, LANA, to contribute to Id1 expression in Kaposi's sarcoma tumour cells suggests that LANA may also

engage the BMP signalling pathway (Tang et al., 2003). However, the low levels of protein expression in C666-1 cells in comparison with the OKF6 cells indicate that Id1 is not consistently up-regulated in response to stable latent infection with EBV.

In monitoring the levels of Smad1/5/8 phosphorylation, it was discovered that, in some cell lines where the levels were particularly high, stimulation with BMP2 failed to elevate this further. This implies that the cells have, at this stage, attained a level of resistance to the effects of BMP2, which is not uncommon in the acquisition of tumourigenic features. The high levels of Smad1/5/8 phosphorylation may therefore be attributable to the actions of other BMPs. Alternatively, this may be indicative of the attainment of a saturation threshold within these cells, or a constitutive activation, possibly attributable at least in part to the observed increases in BMP2 ligand expression.

In EBNA1-expressing and rEBV-infected Ad/AH cells, inhibition of Smad1/5/8 phosphorylation by Noggin treatment could be effectively reversed to initial levels by the subsequent exogenous addition of BMP2, indicating that BMP2 is the predominant contributor to the phosphorylated Smad1/5/8 in these cells. However, in the rEBV-infected HONE-1 and AGS cell lines stimulation with BMP2 was not sufficient to restore levels, and could only achieve a partial restoration in C666-1 cells. In these cell lines it is possible that other BMP subtypes may play a more influential role. Indeed, a study comparing osteoinductive and non-osteoinductive strains of osteosarcoma cells concluded that the potential for osteoinductivity was likely conferred by the specific complement of BMP subtypes present, their threshold levels and interactions with each other (Raval et al., 1996). RT-PCR detected increases in the expression of BMP7 in C666-1 cells, and also of BMP6 in

some EBNA1-expressing and rEBV-infected lines, which are likely to produce differential effects. In addition, certain BMPs have demonstrated the ability to form heterodimers, generally reported to exhibit more potent activity in comparison with homodimers, both in terms of biological activity and also in the secretion rate of active BMPs (Sampath et al., 1990, Aono et al., 1995, Hazama et al., 1995, Nishimatsu and Thomsen, 1998, Piek et al., 1999, Valera et al., 2010). A more comprehensive profiling of BMP ligand expression and their potential for heterodimerisation in the presence of EBNA1 is required to gain further insights into possible cooperative effects.

If, as discussed earlier, constitutive activation of the BMP signalling pathway does occur within the cell lines, further stimulation with BMP2 may fail to elicit noticeable effects on target gene expression. Indeed, in C666-1 cells, expression of the BMP target gene, Id1, was unaltered over the course of the treatment with BMP2 over a 24-hour period. However, a loss of expression over time in response to Noggin treatment reinforces the idea that BMP signalling contributes to Id1 expression in this cell line.

Conversely, it appears that the expression levels of the I-Smads, Smad6 and Smad7 are unlikely governed by BMP signalling. However, it is most interesting to observe the higher levels of Smad6 in OKF6 cells, but of Smad7 in C666-1 cells, given that Smad7 is generally more potent than Smad6 in repressing TGFβ and activin signalling (Hanyu et al., 2001, Itoh et al., 1998), while Smad6 preferentially inhibits the BMP pathway (Itoh et al., 1998, Miyazono et al., 2005). This may be indicative of a relative suppression of BMP signalling in OKF6 cells and further compounded inhibition of TGFβ signalling in C666-1 cells.

Despite the ability of BMP signalling to modulate genes such as $p21^{WAF1/Cip1}$ and Id genes in the OKF6 and C666-1 cell lines, no demonstrable effects were observed on cell cycle distribution in either cell line. However, this is in agreement with the inability of BMP2 to stimulate proliferation of OSCC cells (Gao et al., 2010), and also studies in which it was concluded that the BMP2-dependent stimulation of Id expression was not sufficient to direct cells into proliferation or apoptosis (Clement et al., 2000), while high level induction of $p21^{WAF1/Cip1}$ expression in various epithelial cells could only very weakly suppress epithelial cell proliferation due to concomitant induction of Id2 (Pardali et al., 2005). It is highly possible that the effects of BMPs in the epithelial cell lines may parallel those observed with TGFβ, uncoupling and acquiring resistance to potentially tumour suppressive effects while allowing pro-tumourigenic response to predominate.

An example of one such response is the enhanced cellular migration in the presence of EBNA1 and EBV, as assessed by transwell migration assay. The results also suggest that increased BMP signalling within EBNA1-expressing and rEBV-infected carcinoma cell lines contributed at least to a partial extent to this increase in cell migration, as it was susceptible to reduction by treatment with Noggin. The opposite effect however was seen in C666-1 cells. An interesting study by Hsu and co-workers describes a correlation between melanoma tumour progression and the over-expression of BMP7 (Hsu et al., 2008). Forced expression of Noggin in melanoma cells was found to protect cells from BMP7-induced growth inhibitory effects, conferring the cells with a growth advantage. It is possible that, in a similar fashion, the addition of increasing concentrations of Noggin to C666-1 cells further promotes the acquisition of resistance to the potentially growth suppressive effects of BMP7 in favour of enhanced proliferation and migration. These observations are particularly relevant in light of

the observed increase in BMP7 mRNA expression detected in C666-1 cells. It will therefore be useful to specifically examine the effects of BMP7 stimulation on the cell cycle profile of C666-1 cells, as well as on their migration ability in transwell migration assays. Interestingly, the Ad/AH, HONE-1 and AGS EBNA1-expressing and rEBV-infected cells, whose migration is inhibited by Noggin, do not demonstrate this same increase in BMP7 expression. It will however be necessary to examine the migration of these other carcinoma cells lines using higher concentrations of Noggin.

The BMP antagonist, Noggin, is a cysteine-knot containing protein, which acts effectively as a BMP ligand trap, sequestering the BMP ligand in an inactive complex, thereby inhibiting its engagement with the cell-surface receptors (Groppe et al., 2002). However, Noggin was not always efficient in inhibiting Smad1/5/8 phosphorylation in certain cell lines. There are several possible explanations for this; a higher concentration of Noggin may be required to effectively quench BMP activity in cell lines in which levels of pSmad1/5/8 are particularly high. Alternatively, the observed Smad1/5/8 phosphorylation may be mediated by BMPs not targeted by Noggin. As determined by *in vitro* experiments, Noggin binds BMP2 and BMP4 with very high affinity, BMP7 with lower affinity, and has variable effects also on BMP5, BMP13 and BMP14 (Zimmerman et al., 1996, Krause et al., 2011). It may be informative to instead use the newer small-molecule inhibitors, dorsomorphin and its optimised derivative, LDN-193189, which instead target the kinase domain of type I receptors and therefore have a more global effect (Yu et al., 2008, Cuny et al., 2008, Boergermann et al., 2010). Additionally, the ineptitude of Noggin in reducing Smad1/5/8 phosphorylation in certain scenarios could also be explained if a significant contribution to the measured levels of pSmad1/5/8 was instead a result of TGFβ-induced phosphorylation.

Of particular interest was the finding that, while Noggin proved ineffectual in decreasing pSmad1/5/8 levels in HONE-1 and AGS EBNA1-expressing cells, it retained the ability to diminish BRE-Luc reporter activity in the same cell lines. In marked contrast to the increase in levels of Smad1/5/8 phosphorylation in these cells compared to their Neo control counterparts, the luciferase reporter activity was instead reduced. A possible explanation for this is that the pSmad1/5/8 signal is composed predominantly of the TGFβ-induced form, which has a demonstrated ability to increase the activity of the TGFβ-responsive promoter p3TP-lux (Liu et al., 1998, Wrighton et al., 2009), but fails to induce transcriptional activity from the BRE-Luc reporter (Liu et al., 2009, Wrighton et al., 2009). Moreover, Daly *et al.* suggest TGFβ stimulation can actually induce formation of mixed R-Smad complexes, again unable to activate BMP-responsive elements (Daly et al., 2008). Further to this, the formation of such complexes is thought to require higher concentrations of TGFβ (Daly et al., 2008, Wrighton et al., 2009), which has fortuitously been reported in Chapter 3. These points considered, it would be useful in future studies to examine the effects of TGFβ receptor inhibitors on Smad1/5/8 phosphorylation in the carcinoma cell lines, in addition to conducting a more detailed analysis of the Smad complexes found within the cells.

The ability of TGFβ to induce Smad1/5 phosphorylation is an interesting concept. In endothelial cells, while activation of canonical TGFβ signalling via TβRI had an inhibitory effect on cellular proliferation and migration, TGFβ-mediated Smad1/5 phosphorylation via the ALK1 receptor stimulates endothelial cell proliferation and migration (Goumans et al., 2002, Wrighton et al., 2009). In fact, ALK1 has been shown to function as a direct lateral antagonist of TGFβ/TβRI signalling (Goumans et al., 2003). Whether a similar setting is recapitulated in epithelial cells is not yet known, although it would likely be mediated by a

different type I receptor, as ALK1 is generally considered to be an endothelial-specific TGFβ type I receptor (Piek et al., 1999).

Nevertheless, this ability to stimulate Smad1/5 phosphorylation may provide an additional method, supplementary to the BMP-mediated effects, through which the tumour-promoting facets of TGFβ behaviour are enhanced in the absence of a functional Smad2/3 pathway. It may therefore be directly relevant to the extensively reported switch in TGFβ behaviour during tumour progression. Intriguingly, the homozygous missense TGFBR2 mutation, R537P, which rendered HNSCC A253 cells refractory to TGFβ-mediated growth arrest, was found to result in the constitutive activation of Smad1/5 of the BMP pathway, and a highly motile and invasive cell type (Bharathy et al., 2008). Despite a loss of Smad2/3 activation, high intrinsic TβRII kinase activity was observed. The mutation of TβRII may therefore favour interaction with an alternative type I receptor with consequent selective hyperactivation of the Smad1/5 pathway. With this in mind, it would be interesting to screen for the occurrence of such mutations in NPC tumours, but also to determine the levels of TβRII kinase activity as well as the preferred binding partners of the receptor in the panels of carcinoma cells.

TGFβ-induced Smad1/5 phosphorylation in all reported cases requires TβRII (Daly et al., 2008, Wrighton et al., 2009). Therefore, although still totally feasible in the Ad/AH, HONE-1 and AGS carcinoma cell lines, it is unlikely to be a significant mechanism in C666-1 cells. Indeed the pan-TGFβ neutralising antibody, clone 1D11, had little effect on pSmad1/5/8 levels in C666-1 cells over the time-course of treatment. On a similar note, it would be interesting to examine the subsequent effects of restoring responsiveness to TGFβ signalling

by transient transfection of a TβRII expression plasmid, as has been described earlier in Chapter 3, on the BMP signalling pathway.

BMPs are among a number of factors believed to be secreted by metastatic tumour cells and to act locally in the bone microenvironment to stimulate proliferation and differentiation of osteoblasts (Bentley et al., 1992, Mundy, 2002). Furthermore, increased serum BMP2 levels have been reported in gastric cancer and non-small-cell lung cancer (Park et al., 2008, Park et al., 2010, Choi et al., 2011), where they demonstrate a strong positive correlation with both tumour grade and metastatic burden. Despite the consistent observations of increased endogenous BMP2 expression in the presence of either EBNA1 expression or EBV infection, an associated increase in BMP2 secretion could not be demonstrated by ELISA (data not shown). It may however be useful to verify this using an analogous model to the mink lung epithelial cell assay for TGFβ secretion described in Chapter 3. Such assays have already been generated by stable transfection of a variety of cell lines with the BRE-Luc reporter (Logeart-Avramoglou et al., 2006, Zilberberg et al., 2007), and are generally considered more sensitive.

The patterns of gene expression observed in breast cancer cell lines displaying a predilection for metastasis to bone did not match particularly well with the NPC tumour biopsy samples. However, this could partly be a result of sample selection, as tumours within this particular set were derived from primary tumour biopsies and not metastatic disease. Additionally, as the authors of the original paper discuss, those genes that demonstrate a general association with metastasis, irrespective of the target site, were not included, and therefore the expression of these metastasis-related genes in NPC tumours was not determined. It is possible that BMP

pathway-associated genes may fall within this category. Despite this, it is encouraging that EBNA1 is seen to induce a similar increase or decrease in expression of genes considered over-expressed or under-expressed respectively in the bone metastasis signature.

Bone has been identified as a preferential site for NPC metastasis and, in a study dating back to 1987, it was suggested that the undifferentiated form of NPC had the highest incidence of bone metastases compared to other subtypes (Micheau et al., 1987). Furthermore, the epithelial cell line, NPC-BM1, established from the bone marrow biopsy of a female Taiwanese patient with NPC was histopathogically characterised as non-keratinising, poorly differentiated subtype (Liao et al., 1998). Given the significant association of EBV with the undifferentiated NPC subtype, these studies support a hypothesis for the role of EBV in potentiating metastasis to bone. In order to pursue this further, it would be prudent to characterise the NPC-BM1 cell line specifically in terms of the BMP pathway. This could be extended to examine the metastatic ability of NPC-BM1 cells *in vivo* under BMP pathway inhibition. However it would be necessary to obtain pairs of autologous metastatic and primary tumours in order to conclusively investigate this observation.

Secretome analysis of NPC-BM1 cells and NPC tissue transcriptome analysis detected cystatin A release from NPC cells *in vitro* and statistically elevated levels of cathepsin B and MnSOD, each with prospective roles in tumour metastasis (Chang et al., 2010). Probing of microarray data generated from EBNA1-expressing Ad/AH cells for cystatin A, cathepsin B and MnSOD predicted up-regulation of each of the genes by fold-changes of 2.61, 1.82 and 2.19, respectively.

BMP2 is able to induce classical osteoblast differentiation markers, ALP, osteocalcin and Osf2/Cbfa1 gene transcription and positively regulates bone formation *in vivo* (Spinella-Jaegle et al., 2001, Vaes et al., 2002, Lee et al., 2000). Runx2, the product of the Osf2/Cbfa1 gene, is a transcription factor with a well-characterised role in the induction of osteoblast marker genes (Yang et al., 2003), and whose aberrant expression has been noted in both prostate and breast cancer cells, which frequently metastasise to bone (Baniwal et al., 2010, Leong et al., 2010). Significantly, osteocalcin (BGLAP) was found to be up-regulated 2.5-fold on the Ad/AH EBNA1 microarray, while Osf2/Cbfa1 was up-regulated approximately 3-fold. These findings, although requiring further validation, create fascinating avenues for further investigation. The potential that EBNA1 may be able to induce genes associated with osteoblast differentiation and/or bone metastases either directly, or indirectly through an enhancement of BMP2 signalling, may allude to a specific role for EBNA1 in promoting the formation of bone metastases. Further investigation could involve the use of existing cell models, such as the breast cancer cell line, MDA-MB-231, with a proven ability to metastasise to bone, to determine whether either the additional expression of EBNA1 or infection with EBV could accelerate metastatic development. Ultimately, an *in vivo* model is required in which to accurately measure the osteoinductive activity of both C666-1 and EBNA1-expressing carcinoma cells.

While at present the interaction of viral proteins with the BMP signalling pathway has not been widely researched in cancer, one study has reported the ability of the hepatitis B virus-encoded oncoprotein pX to activate BMP2-induced transcription *in vivo*, providing a potential contributory factor to hepatitis B virus-induced liver fibrosis (Lee et al., 2001). These data therefore represent the novel discovery that a virally-encoded protein may specifically

activate BMP signalling as a means by which to foster cellular migration to distant sites so as to establish a metastatic focus. This hypothesis is further enhanced by the intriguing possibility that this phenomenon may be specifically enhanced by the tumour-promoting aspect of TGFβ signalling.

CHAPTER 5

Generation and validation of a panel of EBNA1 constructs in a lentiviral expression system.

5.1 Introduction

The role of the EBV-encoded EBNA1 protein in the modulation of cellular gene transcription in epithelial cell lines has been further extended in Chapters 3 and 4, yet the accountable mechanism could not be definitively determined. While its critical functions in the maintenance, replication and transcription of the EBV genome have been ascribed to specific domains of the EBNA1 protein (Wu et al., 2002), as described in more detail in section 1.5.1.3, research implicating particular regions of the protein in cellular gene transactivation is very limited. Therefore, in order to pursue this further, a panel of EBNA1 domain mutants was generated in the hope of elucidating a suitable mechanism. A contemporary lentiviral cloning strategy was employed in order to provide more stable, long-term expression beyond that offered by existing retroviral-based systems. The deletion mutants were obtained by PCR amplification of a series of EBNA1-derived sequences contained within pc3*oriP* vectors (Wu et al., 2002). In addition to deletions of specific individual domains, the sequences each encompass a deletion of the gly-ala repeat region, located between residues 90-325, mainly to ensure suitability for PCR-directed cloning, as this region is highly repetitive and GC rich. This region is generally considered dispensable for the major replication, segregation and viral gene transactivation functions of EBNA1 (Yates et al., 1985, Ceccarelli and Frappier, 2000), so in theory exclusion of this region should not dramatically impact upon the behaviour of the derived mutants. The initial panel of mutants was created by Miss Sonia

Maia (University of Birmingham, UK) in the Multisite Gateway® Lentiviral Expression System (Invitrogen), under the control of the human metallothionein (hMTIIa) promoter, which is positively regulated by the addition of zinc to the growth medium. This panel was used to generate stable cell lines, which are validated herein. To further this work, and to corroborate the suggestion that a gly-ala-deleted EBNA1 can substitute as a pseudo wild-type, a complete wild-type version was generated for comparison. Dominant-negative derivatives of the EBNA1 protein were also created and validated, before subsequent cloning into the same lentiviral expression system.

The Multisite Gateway® Lentiviral Expression System uses replication-incompetent HIV-derived lentiviral vectors within a 2nd generation packaging system to generate stable cell lines by viral transduction and subsequent drug selection. An overall schematic of the cloning procedure is depicted in Figure 5.1, and is described in more detail in the following sections. While previously used retroviruses were capable only of infecting replicating cells (Miller et al., 1990, Lewis and Emerman, 1994), these lentiviruses additionally possess the ability to infect and thereby facilitate highly efficient *in vitro* delivery of target genes to non-dividing, terminally differentiated cells (Naldini et al., 1996, Buchschacher and Wong-Staal, 2000). This method therefore carries the attractive potential for use in the transduction of primary keratinocytes, and a prospective use in examining the contribution of EBNA1 in the earliest stages of cell transformation, with subsequent monitoring of its action and requirement throughout the transformation process.

Figure 5.1: Schematic representation of the cloning procedure for generation of EBNA1 lentiviral constructs

The desired EBNA1 gene fragments were generated either by restriction endonuclease digestion or PCR amplification and subsequently ligated into the pCR®8/GW/TOPO® vector at the site indicated. pCR®8/GW/TOPO® vectors were combined in a homologous recombination reaction with a second entry vector containing the promoter of choice, pENTR™5′-TOPO®-hMTIIa, so as to insert the hMTIIa promoter and EBNA1 sequences into the destination vector, pLenti6/R4R2/V5-DEST. The resulting lentiviral vectors were validated by diagnostic restriction digests and by transient transfection to determine correct expression. These were then used to produce lentivirus, ready for viral transduction of the cell line of interest. Plasmid maps were obtained from the Invitrogen website.

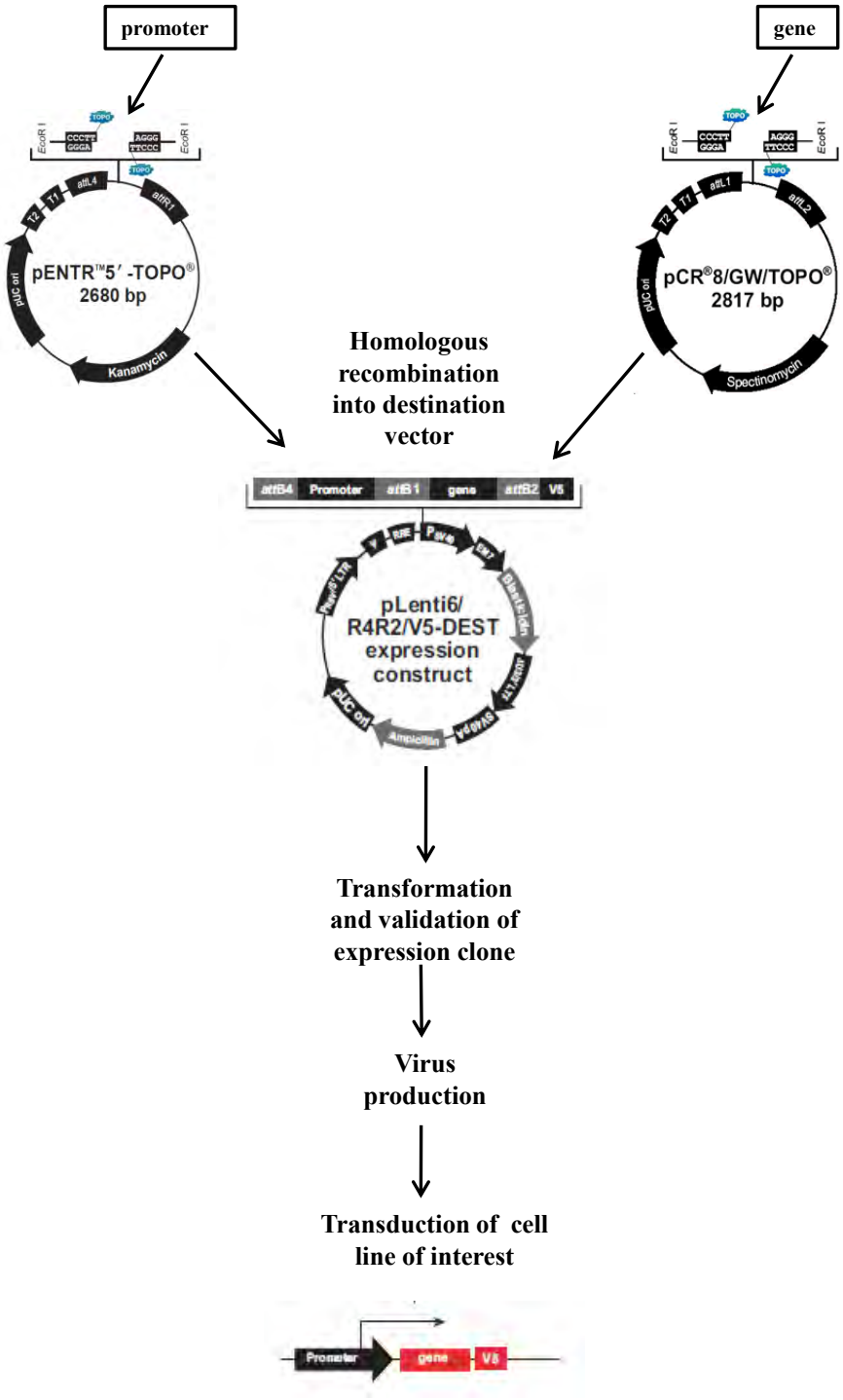
promoter
gene
pENTR™5′ -TOPO®
2680 bp
Kanamycin
pCR®8/GW/TOPO®
2817 bp
Spectinomycin
Homologous
recombination
into destination
vector
attB4
Promoter
attB1
gene
attB2
V5
pLenti6/
R4R2/V5-DEST
expression
construct
Transformation
and validation of
expression clone
Virus
production
Transduction of cell
line of interest
Promoter
gene
V5

5.2 Validation of EBNA1 mutant lentiviral constructs

5.2.1 Transient transfection of EBNA1 mutant lentiviruses

Ad/AH cells were transiently transfected with either pc3*oriP* or pLenti6/R4R2/V5-DEST EBNA1 mutant plasmids. 24 hours post-transfection, cells transfected with lentiviral vectors were additionally stimulated with 50μM $ZnSO_4$ for 16 hours, or left unstimulated as a control. Protein samples were harvested and lysates subjected to immunoblotting analysis using K67, a rabbit polyclonal antibody specific for EBNA1. Lysates from Ad/AH Neo control, EBNA1 and rEBV-infected cells were also included for EBNA1 protein molecular weight comparison. Figure 5.2 shows that EBNA1 protein was successfully expressed from each of the vectors, with appropriate differences in molecular weight corresponding with the size of the deletion.

5.2.2 Validation of stable EBNA1 mutant Ad/AH cell lines

Ad/AH cells stably expressing each of the panel of EBNA1 mutant lentiviruses were seeded into 10cm dishes at a density of $1x10^6$ and were incubated for 48 hours before stimulation with 50μM $ZnSO_4$ for 16 hours. RNA samples were extracted and subsequent RT-PCR analysis, shown in Figure 5.3A, indicates that EBNA1 transcripts were absent in the cells carrying a control lentiviral vector expressing the hMTIIa promoter only, but were expressed in all of the mutant EBNA1 cell lines. EBNA1-expressing cell lines also all demonstrated responsiveness to zinc induction at this level, with greater levels of EBNA1 expression seen following the addition of $ZnSO_4$.

Cells were additionally seeded at a density of $2x10^4$ onto 12-well Teflon-coated slides, and subsequently grown for 24 hours, before stimulation with 50μM $ZnSO_4$ for 16 hours. Immunofluorescence staining was performed using R4, a rabbit polyclonal antibody specific

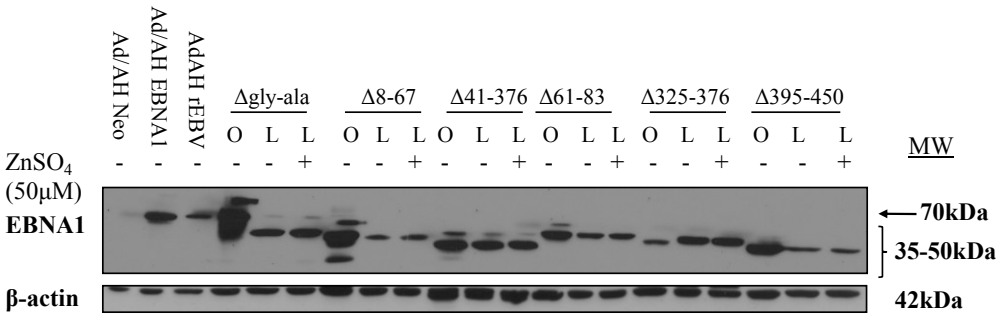

Figure 5.2: Validation of EBNA1 expression from pc3oriP and pLenti6/R4R2/V5-DEST constructs

Immunoblotting for EBNA1 protein expression in Ad/AH cells transiently transfected with either pc3*oriP* (O) or pLenti6/R4R2/V5-DEST (L) vectors containing the panel of EBNA1 mutant sequences. After 24 hours, cells transfected with the lentiviral vectors were stimulated with 50μM $ZnSO_4$ for 16 hours or left unstimulated as a control. β-actin was included to confirm equal protein loading. Lysates taken from Ad/AH Neo control, EBNA1 and rEBV-infected cells were included for comparison of the relative molecular weights of mutant proteins to wild-type EBNA1.

(

A)

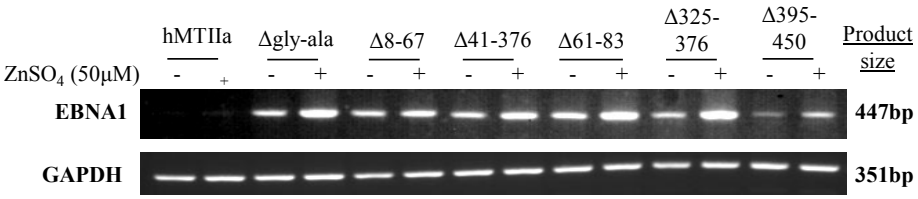

Figure 5.3: Validation of EBNA1 expression in stable Ad/AH cell lines

A) RT-PCR analysis of EBNA1 mRNA expression in Ad/AH cells stably expressing pLenti6/R4R2/V5-DEST lentiviral constructs containing EBNA1 mutant sequences under the control of an hMTIIa promoter, and either stimulated with 50μM $ZnSO_4$ for 16 hours, or left unstimulated. GAPDH was included as a positive control.

B) Immunofluorescence staining for EBNA1 protein expression was performed in the same cell lines, either stimulated with 50μM $ZnSO_4$ for 16 hours, or left unstimulated. Representative images are shown.

B)

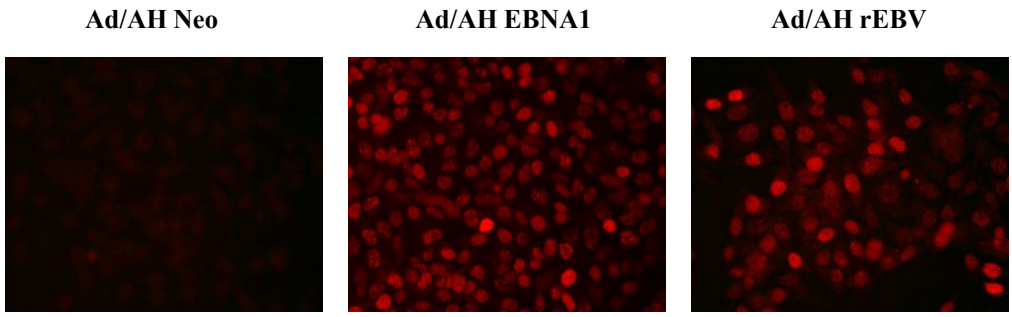
Ad/AH Neo
Ad/AH EBNA1
Ad/AH rEBV

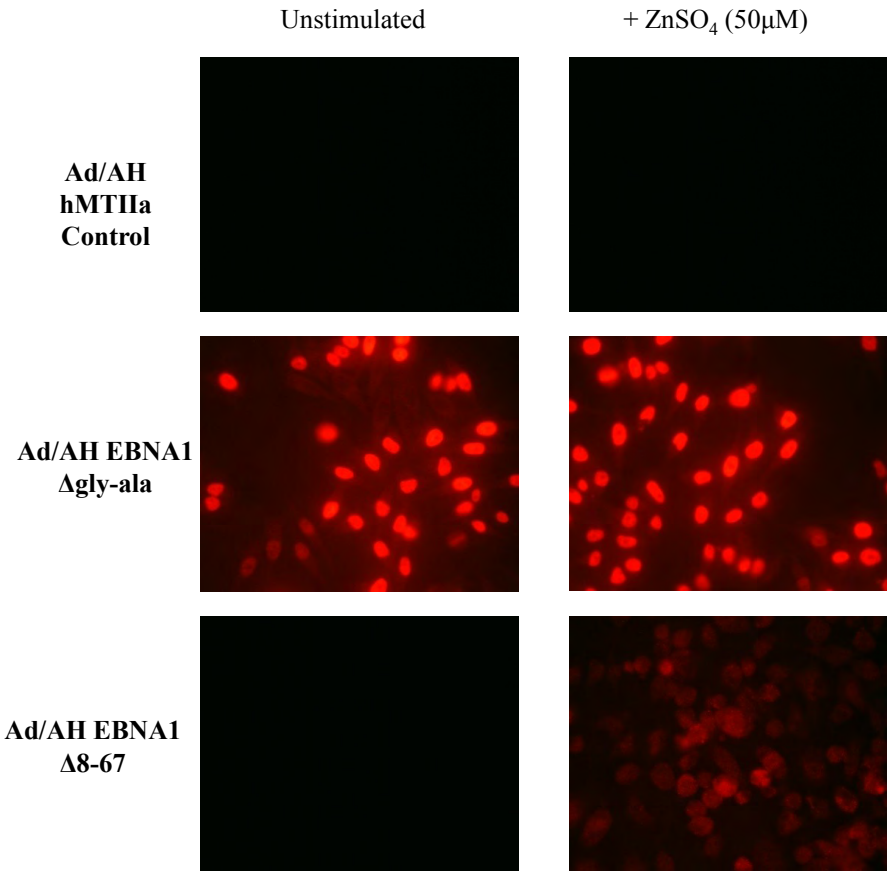
Unstimulated
+ ZnSO4 (50µM)
Ad/AH hMTIIa Control
Ad/AH EBNA1 Δgly-ala
Ad/AH EBNA1 Δ8-67

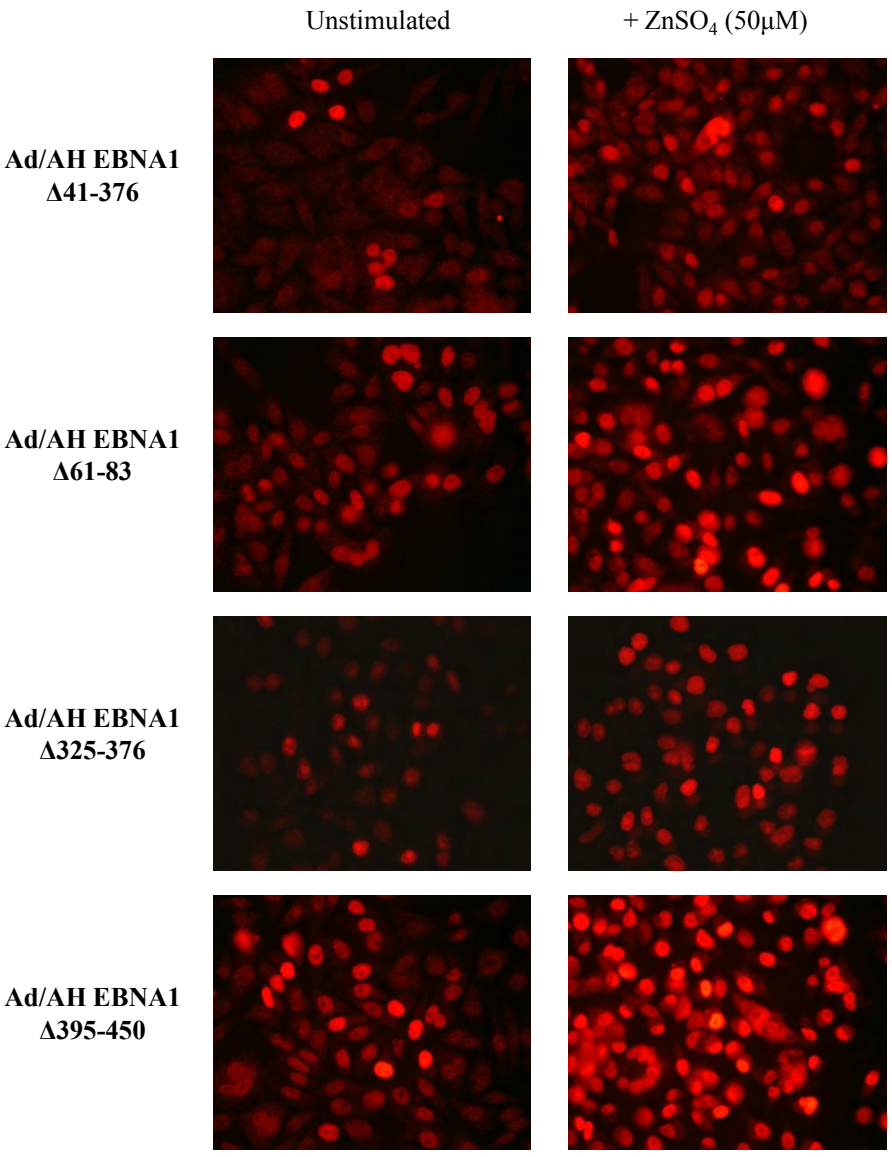
Unstimulated
+ ZnSO4 (50μM)
Ad/AH EBNA1 Δ41-376
Ad/AH EBNA1 Δ61-83
Ad/AH EBNA1 Δ325-376
Ad/AH EBNA1 Δ395-450

for EBNA1, and protein expression was examined by fluorescence microscopy. Representative images shown in Figure 5.3B indicate that EBNA1 protein was successfully expressed and was susceptible to further induction by zinc stimulation in the majority of cell lines, with the exception of a noticeable loss of signal in the Ad/AH EBNA1 Δ8-67 mutant cell line, suggesting this deletion may markedly affect protein stability, as expression was detected at the mRNA level (Figure 5.3A), and at the protein level following transient transfection (Figure 5.2). The lack of staining in Ad/AH Neo and hMTIIa controls confirmed antibody specificity.

5.3 Generation of recombinant pCR®8/GW/TOPO® transfer plasmid containing wild-type EBNA1

5.3.1 Isolation of the wild-type EBNA1 sequence by restriction endonuclease digestion

The complete wild-type EBNA1 sequence is inclusive of the gly-ala repeat region between residues 90-325, and is therefore, as already stated, not a favourable template for PCR-based cloning strategies. DNA encoding wild-type EBNA1 was therefore excised by *Eco*RI and *Bgl*II restriction endonuclease digestion from a pSG5-EBNA1 vector containing the *Sau*3A-*Pvu*II subfragment of the EBV *Bam*HI-K fragment (Sample et al., 1992). The EBNA1 fragment was then isolated using the QIAEX II Agarose Gel Extraction kit (Qiagen), and subjected to a *Bsa*HI restriction digestion to remove a polyadenylation site in the sequence, and so prevent premature transcription termination. Successful isolation of the desired EBNA1 fragments was verified by agarose gel electrophoresis of the restriction fragments, as shown in Figure 5.4. To create a template suitable for use within the TOPO® Cloning procedure, the restriction fragment was end-filled using T4 DNA polymerase and terminal 3′ deoxyadenosine nucleotides added with *Taq* DNA polymerase.

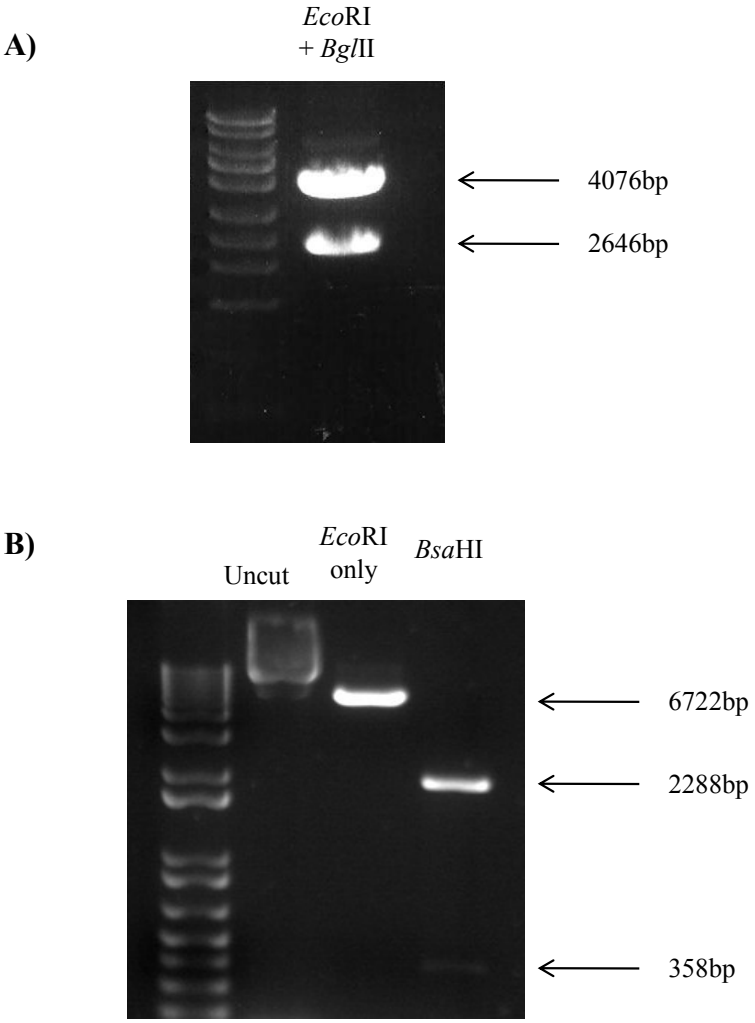

Figure 5.4: Excision of wild-type EBNA1 fragment by restriction endonuclease digestion

A) Restriction digestion of pSG5-EBNA1 using *Eco*RI and *Bgl*II restriction endonucleases to excise the *Sau*3A-*Pvu*II subfragment of the EBV *Bam*HI-K fragment (2646bp) from the pSG5 vector (4076bp).

B) Restriction digestion of the *Sau*3A-*Pvu*II subfragment using *Bsa*HI restriction endonuclease to excise the required wild-type EBNA1 fragment (2288bp) and remove sequence containing a polyadenylation site (358bp). Restriction digestion of pSG5-EBNA1 (6722bp) using *Eco*RI and uncut pSG5-EBNA1 plasmid are shown for size comparison.

5.3.2 PCR of dominant-negative EBNA1 sequences

A dominant-negative EBNA1 construct was derived in a similar manner to the existing panel of mutants from the pc3*oriP*-EBNA1 Δgly-ala plasmid using oligonucleotide primers (see Table 2.12.2) targeting sequences within the EBNA1 cDNA such that all sequence upstream of the nuclear localisation signal, situated between amino acids 379 and 386 (Ambinder et al., 1991), would be deleted, effectively removing domains responsible for the transcriptional activation, segregation and replication functions of EBNA1. In this way, the DNA binding and dimerisation motifs, located between C-terminal residues 459 and 607 (Ceccarelli and Frappier, 2000), are retained, so fulfilling the defined criteria of efficient dominant-negative EBNA1 inhibitors, as outlined by Kirchmaier and Sugden (Kirchmaier and Sugden, 1997). Additionally, the same set of primers was used in a reaction with the pc3*oriP*-EBNA1 Δ395-450 construct to create a second dominant-negative construct carrying the additional domain deletion, due to the reported interaction of this region with the human deubiquitinating enzyme, USP7 (Holowaty et al., 2003). As predictions outlined in Chapter 3 suggest that the mechanism through which EBNA1 is able to modulate TGFβ signalling may in part be related to its ability to influence ubiquitination, it was considered necessary to also eliminate this region.

PCR amplification was performed on 0.01ng DNA in a reaction using the Expand High Fidelity PCR System (Roche). The optimum annealing temperature was determined prior to the final cloning PCR by PCR amplification over a temperature gradient. Gel-loading buffer was added to the PCR reactions, before analysis by agarose gel electrophoresis. As can be confirmed in Figure 5.5, fragments of the correct sizes were successfully amplified in the PCR reactions.

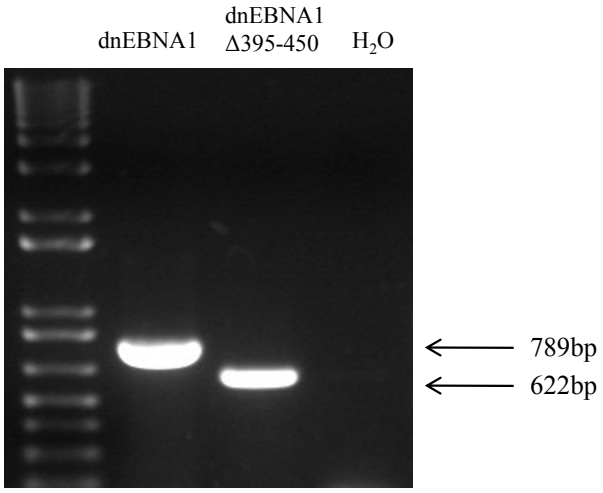

Figure 5.5: PCR amplification of dominant negative EBNA1 gene fragments
Amplification of the dominant negative EBNA1 gene fragments (dnEBNA1 = 789bp, dnEBNA1 Δ395-450 = 622bp) was performed by PCR on 0.01ng pc3*oriP*-EBNA1 Δgly/ala and pc3*oriP*-EBNA1 Δ395-450 templates, using High fidelity DNA polymerase.

5.3.3 Generation of pCR®8/GW/TOPO® entry vectors

The excised wild-type EBNA1 coding sequence and *Taq* polymerase-amplified dominant-negative EBNA1 PCR products were ligated into the linearised pCR®8/GW/TOPO® vector, as detailed in section 2.12.5. pCR®8/GW/TOPO® vectors containing the EBNA1 sequences were then used to transform One Shot® TOP10 *E.coli* cells under spectinomycin selection. 10pg of pUC19 DNA was transformed in a similar manner, but under ampicillin selection, as a positive control for transformation efficiency, while a non-transformed bacterial culture was used as a negative control.

Between ten and twenty colonies were picked for analysis and grown overnight in 3ml LB nutrient broth containing 100µg/ml spectinomycin in an orbital shaker at 37°C, and DNA isolated from overnight bacterial cell cultures using the Qiagen QIAprep Spin Miniprep Kit (Qiagen), as detailed in section 2.12.7.1. DNA concentrations were measured using a Nano-drop spectrophotometer and samples were stored at -20°C.

5.3.3.1 Diagnostic restriction endonuclease digests

In order to ensure that the pCR®8/GW/TOPO® vectors contained the desired EBNA1 fragments in the correct orientation, a series of diagnostic restriction digests were performed. *Eco*RI was used for both the wild-type and dominant-negative sequence-containing constructs to identify which samples contained the inserted fragment of the correct size. A double restriction digest reaction with *Nco*I and *Eco*RV revealed the fragment orientation of wild-type sequences, while *Sac*II and *Xba*I were used to determine the orientation of dominant-negative sequences.

Gel images of the resolved products of wild-type EBNA1 restriction digests are shown in Figure 5.6. The *Eco*RI cut of a positive clone should effectively separate the desired 2.29kb wild-type EBNA1 fragment from the pCR®8/GW/TOPO® vector (2.82kb). It is apparent from Figure 5.6A that, of the twenty clones analysed, only samples 2, 5, 12, 14 and 18 were digested correctly, indicating that, although some colonies grew and plasmid DNA could be successfully extracted, the ligation reaction had not been successful. Those samples selected from the initial *Eco*RI digest were then subjected to a second restriction digest using *Nco*I and *Eco*RV. While a single cut with *Nco*I confirmed the linearization of the vector, retrieval of 3.15kb and 1.95kb fragments indicated the correct orientation of the EBNA1 sequence, as can be seen for samples 12 and 18 in Figure 5.6B.

Similarly, for the dominant-negative EBNA1 sequences, successful insertion of the PCR-amplified products is exemplified by the detection of 789bp and 622bp fragments in addition to the pCR®8/GW/TOPO® vector, for dominant-negative and the 395-450 deleted dominant-negative EBNA1 respectively. Ten colonies were analysed for each and, as can be ascertained from Figure 5.7A, all samples appeared to contain the correct EBNA1 sequence, with the exceptions of sample 8 for the standard dominant-negative, and sample 5 for the dominant-negative with 395-450 deletion.

Subsequent *Sac*II and *Xba*I double restriction digests are shown in Figure 5.7B. Again, digestion with *Sac*II confirmed linearization of the vector, while the double digest identified samples 2, 4 and 7 for dominant-negative EBNA1 and samples 4, 5, 6 and 10 for dominant-negative EBNA1 Δ395-450, as containing the correct fragments in the right orientation.

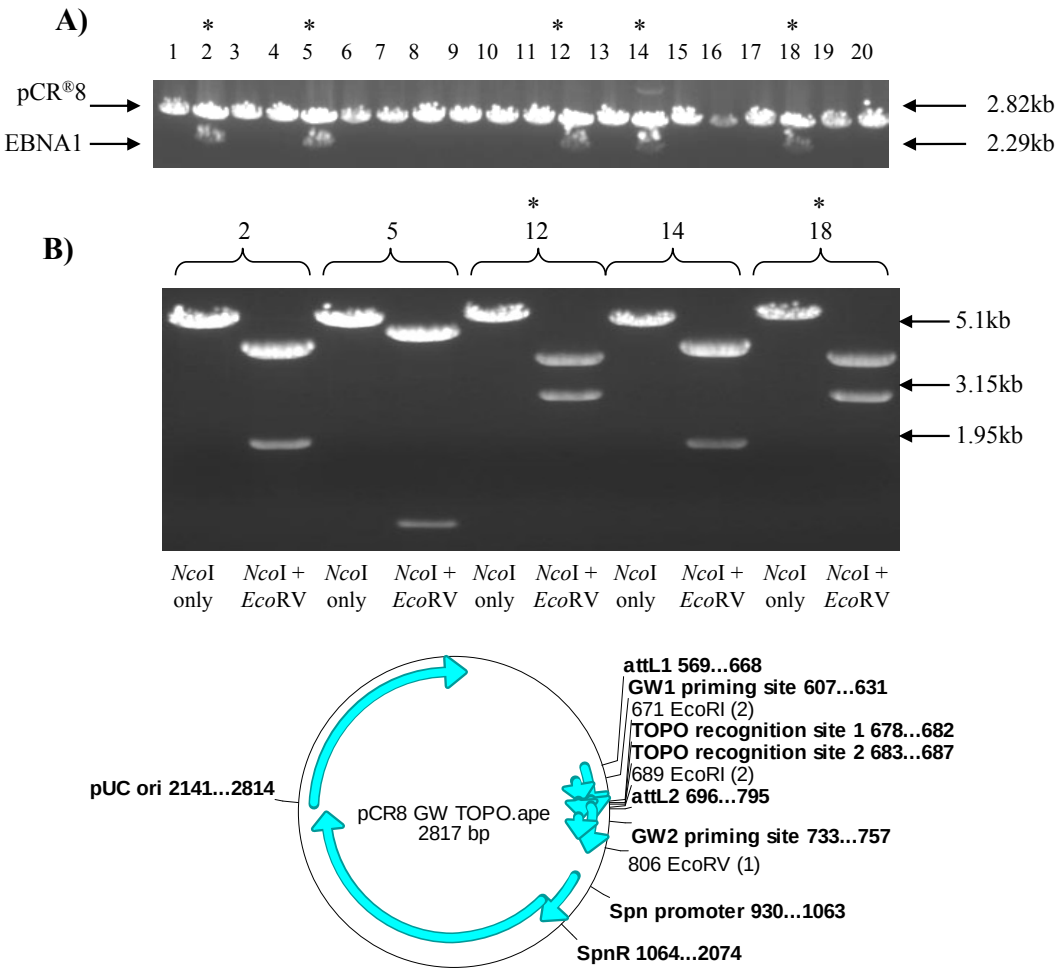

Figure 5.6: Diagnostic restriction digests of pCR®8/GW/TOPO® vector containing wild-type EBNA1

A series of diagnostic digestions were performed to validate insertion of the wild-type EBNA1 (wtEBNA1) gene fragment into the pCR®8/GW/TOPO® vector.

A) *Eco*RI restriction digests were performed on the pCR®8/GW/TOPO®-wtEBNA1 plasmid to confirm the insertion of the gene fragment of interest. The asterisk (*) marks those samples containing a fragment of the correct size.

B) *Nco*I and *Eco*RV double restriction endonuclease digests were performed on the pCR®8/GW/TOPO®-wtEBNA1 vector to validate the correct orientation of the inserted wild-type EBNA1 gene fragment. The asterisk (*) marks those samples containing the EBNA1 sequence in the correct orientation.

A plasmid map of pCR®8/GW/TOPO® , highlighting its key features and generated using ApE Plasmid Editor software, is shown, adapted from the map found at:
http://tools.invitrogen.com/content/sfs/vectors/pcr8gwtopo_map.pdf

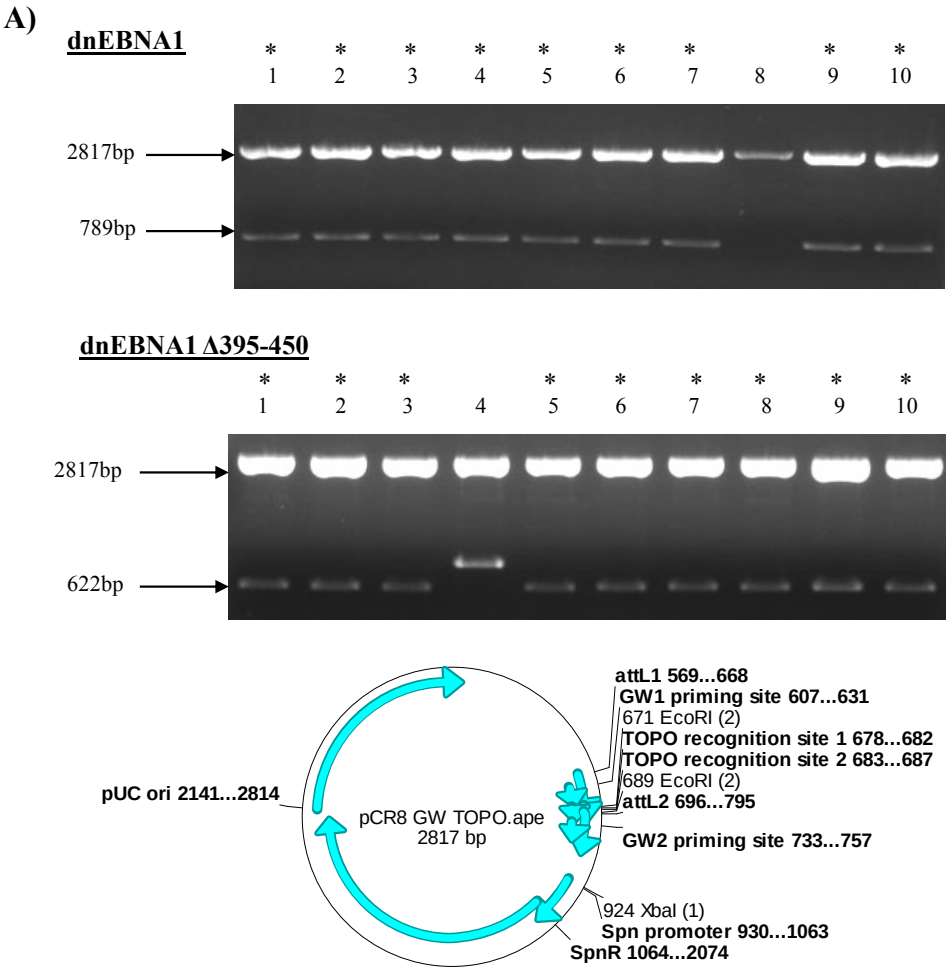

Figure 5.7: Diagnostic restriction digests of pCR®8/GW/TOPO® vector containing dominant negative EBNA1 sequences

A series of diagnostic digestions were performed to validate insertion of the dominant-negative EBNA1 (dnEBNA1) gene fragments into the pCR®8/GW/TOPO® vector (2817bp).

A) *Eco*RI restriction digests were performed on the pCR®8/GW/TOPO®-dnEBNA1 and dnEBNA1 Δ395-450 plasmids to confirm the insertion of the gene fragments of interest. The asterisk (*) marks those samples containing a fragment of the correct size.

B) *Sac*II and *Xba*I double restriction endonuclease digests were performed on the pCR®8/GW/TOPO®-dnEBNA1 and dnEBNA1 Δ395-450 vectors to validate the correct orientation of the inserted dominant negative EBNA1 gene fragments. The asterisk (*) marks those samples containing the EBNA1 sequences in the correct orientation.

A plasmid map of pCR®8/GW/TOPO® , highlighting its key features and generated using ApE Plasmid Editor software, is shown, adapted from the map found at: http://tools.invitrogen.com/content/sfs/vectors/pcr8gwtopo_map.pdf

B)

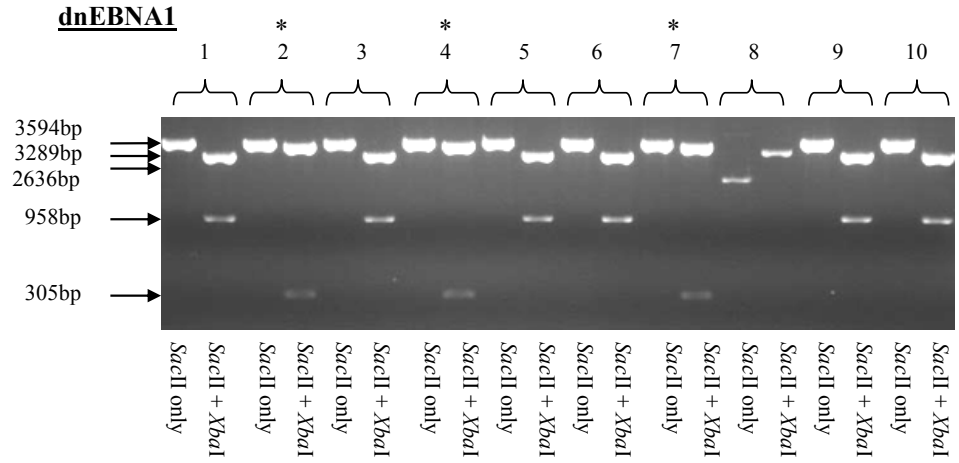
dnEBNA1
1
2
3
4
5
6
7
8
9
10
3594bp
3289bp
2636bp
958bp
305bp
SacII only
SacII + XbaI

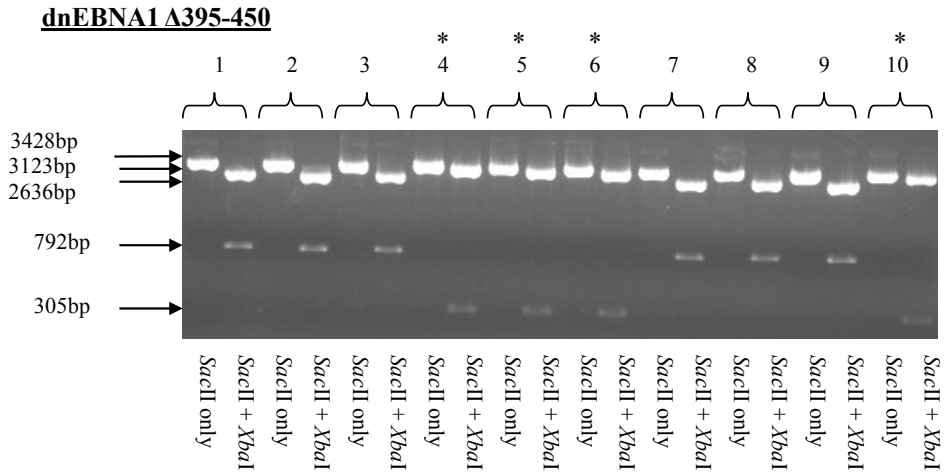
dnEBNA1 Δ395-450
1
2
3
4
5
6
7
8
9
10
3428bp
3123bp
2636bp
792bp
305bp
SacII only
SacII + XbaI

5.3.3.2 DNA Sequencing

Potentially positive transformants were selected from the restriction digest screening process and their sequences determined to ensure precise cloning. Chosen samples were sequenced using the ABI Prism 310 (Applied Biosystems) sequencing protocol (see section 2.12.8). Results were then analysed using Chromas software and the sequences were checked against a consensus EBV genome sequence using the online alignment tool BLAST (bl2seq) (NCBI). Segments of the sequencing traces and their respective proportional identities with the EBV genome sequence are shown in Figure 5.8.

5.4 Multisite Gateway® LR Recombination

The recombinant lentiviral expression vectors containing the EBNA1 mutant sequences were designed so that EBNA1 expression could be driven under the influence of the zinc-inducible human metallothionein (hMTIIa) promoter. The same configuration was therefore required for the wild-type and dominant-negative EBNA1 constructs. The hMTIIa promoter had been previously cloned into the pENTR™5′-TOPO® vector by Miss Sonia Maia using the pENTR™5′-TOPO® TA cloning kit (Invitrogen). This entry clone was added in combination with a second entry vector, pCR®8/GW/TOPO®-EBNA1, in a homologous recombination reaction with pLenti6/R4R2/V5-DEST, as detailed in section 2.12.9.1, which juxtaposed the hMTIIa promoter and desired EBNA1 sequences within the same lentiviral vector.

Reactions were used to transform the ONE SHOT® Stabl3™ strain of *E.coli* competent cells under ampicillin selection, and resulting bacterial colonies were selected to derive overnight cultures, which were mini-prepped as outlined in section 2.12.7.1. Remaining cultures were stored at 4°C for Maxi-Prep of cultures found to contain successfully recombined plasmids.

A)

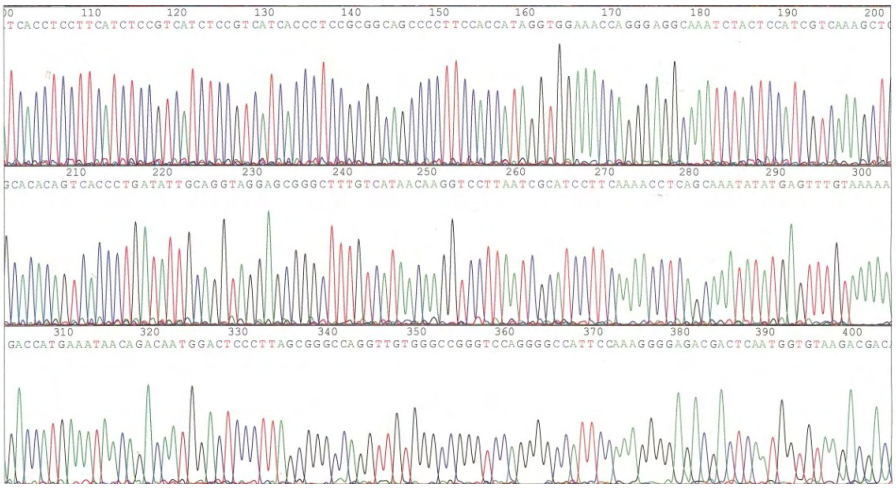

```
>ref|NC_007605.1| Human herpesvirus 4 type 1, complete genome
Length=171823

 Score = 1284 bits (695),  Expect = 0.0
 Identities = 715/723 (99%), Gaps = 8/723 (1%)
 Strand=Plus/Minus

Query  50     CGTCTCCTAACAAGTTACATCACTCCTGCCCTTCCTCACCCTCATCTCCATCACCTCCTT  109
              ||||||||||||||||||||||||||||||||||||||||||||||||||||||||||||
Sbjct  97606  CGTCTCCTAACAAGTTACATCACTCCTGCCCTTCCTCACCCTCATCTCCATCACCTCCTT  97547

Query  110    CATCTCCGTCATCTCCGTCATCACCCTCCGCGGCAGCCCCTTCCACCATAGGTGGAAACC  169
              ||||||||||||||||||||||||||||||||||||||||||||||||||||||||||||
Sbjct  97546  CATCTCCGTCATCTCCGTCATCACCCTCCGCGGCAGCCCCTTCCACCATAGGTGGAAACC  97487

Query  170    AGGGAGGCAAATCTACTCCATCGTCAAAGCTGCACACAGTCACCCTGATATTGCAGGTAG  229
              ||||||||||||||||||||||||||||||||||||||||||||||||||||||||||||
Sbjct  97486  AGGGAGGCAAATCTACTCCATCGTCAAAGCTGCACACAGTCACCCTGATATTGCAGGTAG  97427

Query  230    GAGCGGGCTTTGTCATAACAAGGTCCTTAATCGCATCCTTCAAAACCTCAGCAAATATAT  289
              ||||||||||||||||||||||||||||||||||||||||||||||||||||||||||||
Sbjct  97426  GAGCGGGCTTTGTCATAACAAGGTCCTTAATCGCATCCTTCAAAACCTCAGCAAATATAT  97367

Query  290    GAGTTTGTAAAAAGACCATGAAATAACAGACAATGGACTCCCTTAGCGGGCCAGGTTGTG  349
              ||||||||||||||||||||||||||||||||||||||||||||||||||||||||||||
Sbjct  97366  GAGTTTGTAAAAAGACCATGAAATAACAGACAATGGACTCCCTTAGCGGGCCAGGTTGTG  97307
```

Figure 5.8: Sequencing reaction outputs
Sequencing outputs were visualised using Chromas and segments of example traces for wild-type EBNA1 (A), dominant-negative EBNA1 (B) and dominant-negative EBNA1 Δ395-450 (C) are shown. Each peak represents a discrete signal from each base of the analysed sequence (red = thymine, green = adenine, blue = cytosine and black = guanine). Gene sequences were exported from Chromas in FASTA format and aligned against the EBV genome sequence using BLAST. A sample of the BLAST output is shown for each. Small errors in sequence were analysed and resolved by equating mismatches in the alignment with overlapping peaks on the Chromas traces.

B)

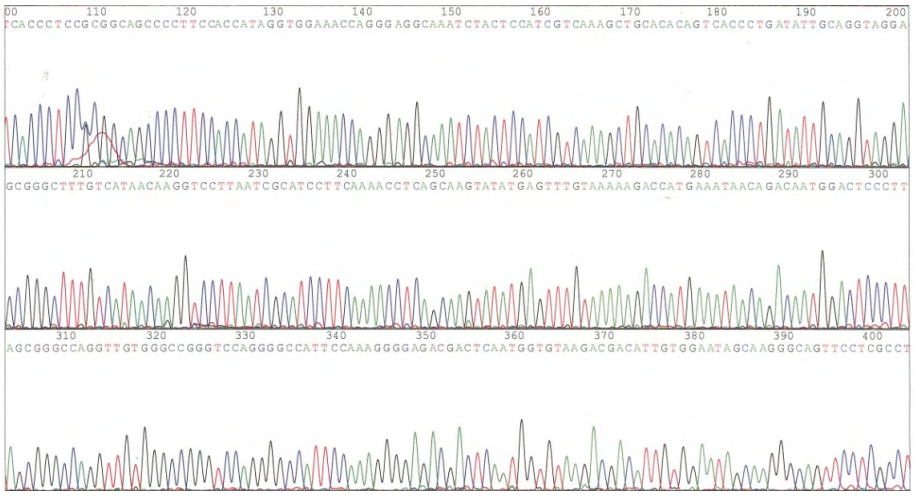

>ref|NC_007605.1| Human herpesvirus 4 type 1, complete genome
Length=171823

Score = 1382 bits (748), Expect = 0.0
Identities = 779/792 (98%), Gaps = 9/792 (1%)
Strand=Plus/Minus

```
Query  42     CTCCTGCCCTTCCTCACCCTCATCT-CAACACCTCCTTCATCTCCGTCATCTCCGTCATC  100
              ||||||||||||||||||||||||| || ||||||||||||||||||||||||||||||
Sbjct  97584  CTCCTGCCCTTCCTCACCCTCATCTCCATCACCTCCTTCATCTCCGTCATCTCCGTCATC  97525

Query  101    ACCCTCCGCGGCAGCCCCTTCCACCATAGGTGGAAACCAGGGAGGCAAATCTACTCCATC  160
              ||||||||||||||||||||||||||||||||||||||||||||||||||||||||||||
Sbjct  97524  ACCCTCCGCGGCAGCCCCTTCCACCATAGGTGGAAACCAGGGAGGCAAATCTACTCCATC  97465

Query  161    GTCAAAGCTGCACACAGTCACCCTGATATTGCAGGTAGGAGCGGGCTTTGTCATAACAAG  220
              ||||||||||||||||||||||||||||||||||||||||||||||||||||||||||||
Sbjct  97464  GTCAAAGCTGCACACAGTCACCCTGATATTGCAGGTAGGAGCGGGCTTTGTCATAACAAG  97405

Query  221    GTCCTTAATCGCATCCTTCAAAACCTCAGCAAGTATATGAGTTTGTAAAAAGACCATGAA  280
              |||||||||||||||||||||||||||||| ||||||||||||||||||||||||||||
Sbjct  97404  GTCCTTAATCGCATCCTTCAAAACCTCAGCAAATATATGAGTTTGTAAAAAGACCATGAA  97345

Query  281    ATAACAGACAATGGACTCCCTTAGCGGGCCAGGTTGTGGGCCGGGTCCAGGGGCCATTCC  340
              ||||||||||||||||||||||||||||||||||||||||||||||||||||||||||||
Sbjct  97344  ATAACAGACAATGGACTCCCTTAGCGGGCCAGGTTGTGGGCCGGGTCCAGGGGCCATTCC  97285
```

C)

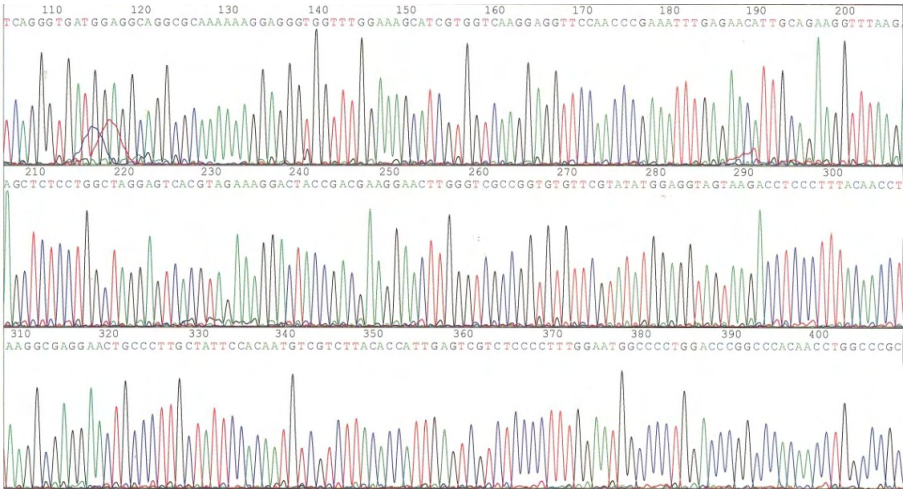

>**ref|NC_007605.1|** Human herpesvirus 4 type 1, complete genome
Length=171823

Score = 1053 bits (570), Expect = 0.0
Identities = 573/574 (99%), Gaps = 1/574 (0%)
Strand=Plus/Plus

```
Query  99     CGGGGTCAGGGTGATGGAGGCAGGCGCAAAAAAGGAGGGTGGTTTGGAAAGCATCGTGGT  158
              ||||||||||||||||||||||||||||||||||||||||||||||||||||||||||||
Sbjct  97012  CGGGGTCAGGGTGATGGAGGCAGGCGCAAAAAAGGAGGGTGGTTTGGAAAGCATCGTGGT  97071

Query  159    CAAGGAGGTTCCAACCCGAAATTTGAGAACATTGCAGAAGGTTTAAGAGCTCTCCTGGCT  218
              ||||||||||||||||||||||||||||||||||||||||||||||||||||||||||||
Sbjct  97072  CAAGGAGGTTCCAACCCGAAATTTGAGAACATTGCAGAAGGTTTAAGAGCTCTCCTGGCT  97131

Query  219    AGGAGTCACGTAGAAAGGACTACCGACGAAGGAACTTGGGTCGCCGGTGTGTTCGTATAT  278
              ||||||||||||||||||||||||||||||||||||||||||||||||||||||||||||
Sbjct  97132  AGGAGTCACGTAGAAAGGACTACCGACGAAGGAACTTGGGTCGCCGGTGTGTTCGTATAT  97191

Query  279    GGAGGTAGTAAGACCTCCCTTTACAACCTAAGGCGAGGAACTGCCCTTGCTATTCCACAA  338
              ||||||||||||||||||||||||||||||||||||||||||||||||||||||||||||
Sbjct  97192  GGAGGTAGTAAGACCTCCCTTTACAACCTAAGGCGAGGAACTGCCCTTGCTATTCCACAA  97251

Query  339    TGTCGTCTTACACCATTGAGTCGTCTCCCCTTTGGAATGGCCCCTGGACCCGGCCCACAA  398
              ||||||||||||||||||||||||||||||||||||||||||||||||||||||||||||
Sbjct  97252  TGTCGTCTTACACCATTGAGTCGTCTCCCCTTTGGAATGGCCCCTGGACCCGGCCCACAA  97311

Query  399    CCTGGCCCGCTAAGGGAGTCCATTGTCTGTTATTTCATGGTCTTTTTACAAACTCATATA  458
              ||||||||||||||||||||||||||||||||||||||||||||||||||||||||||||
Sbjct  97312  CCTGGCCCGCTAAGGGAGTCCATTGTCTGTTATTTCATGGTCTTTTTACAAACTCATATA  97371
```

5.4.1 Diagnostic restriction digests

The recombinant pLenti6/R4R2/V5-DEST vectors containing the wild-type and dominant-negative EBNA1 sequences were validated by separate *Eco*RI and *Eco*RV restriction digests, designed to isolate, for *Eco*RI, the pLenti6/R4R2/V5-DEST vector, EBNA1 sequence and hMTIIa promoter separately, and for *Eco*RV, the pLenti6/R4R2/V5-DEST vector with the promoter and EBNA1 sequence as a single fragment. Restriction digest reaction products were resolved by agarose gel electrophoresis and gel images are shown in Figures 5.9 and 5.10. For the wild-type EBNA1 (Figure 5.9), it is evident following restriction digestion that all ten colonies contained lentiviral vectors into which both desired sequences had been successfully recombined.

For the standard dominant-negative EBNA1, *Eco*RI digests, shown in Figure 5.10A, indicate the convincing presence of hMTIIa and EBNA1 sequence in samples 1, 4, 5, 6, 8 and 10, with low levels of detection in the remaining samples. This pattern is appropriately reflected in the result with *Eco*RV (Figure 5.10B). The restriction digests of pLenti6/R4R2/V5-DEST-dnEBNA1 Δ395-450 again indicate the presence of the desired sequences in all samples, although with only low levels of detection in samples 2, 6 and 7 (Figures 5.10C and 5.10D).

5.4.2 Maxi-prep of plasmid DNA

Cultures corresponding to samples that yielded correctly sized fragments after digestion were used to inoculate 500ml LB nutrient broth containing 100μg/ml ampicillin. Bacterial cultures were left to grow overnight in an orbital shaker at 37°C. Using Invitrogen PureLink HiPure Plasmid Filter Maxiprep kit, DNA was extracted and purified according to the manufacturer's instructions, and as detailed in section 2.12.7.2. The DNA concentration of each plasmid was

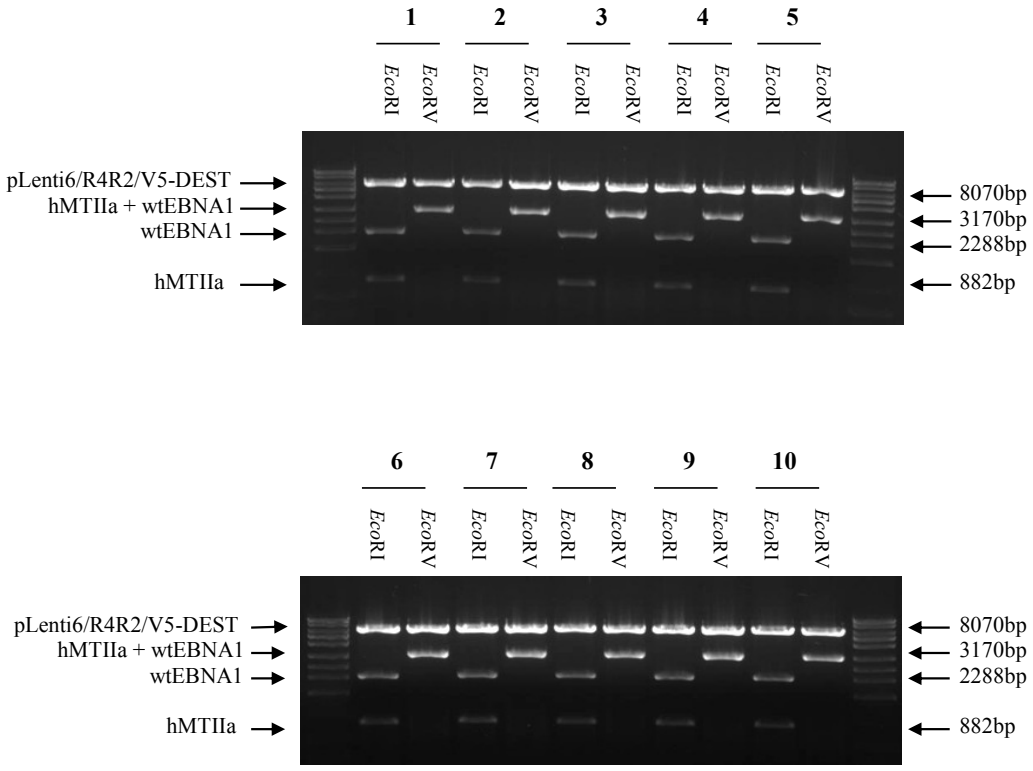

Figure 5.9: Diagnostic restriction digests of pLenti6/R4R2/V5-DEST vector containing the hMTIIa promoter and wild-type EBNA1
*Eco*RI and *Eco*RV restriction endonuclease digestion to validate the insertion of the hMTIIa promoter and wild-type EBNA1 (wtEBNA1) gene fragment into the pLenti6/R4R2/V5-DEST vector.
(A plasmid map of pLenti6/R4R2/V5-DEST can be found at:
http://toolszh.invitrogen.com/contents/sfs/vectors/plenti6_r4r2_v5dest_map.pdf)

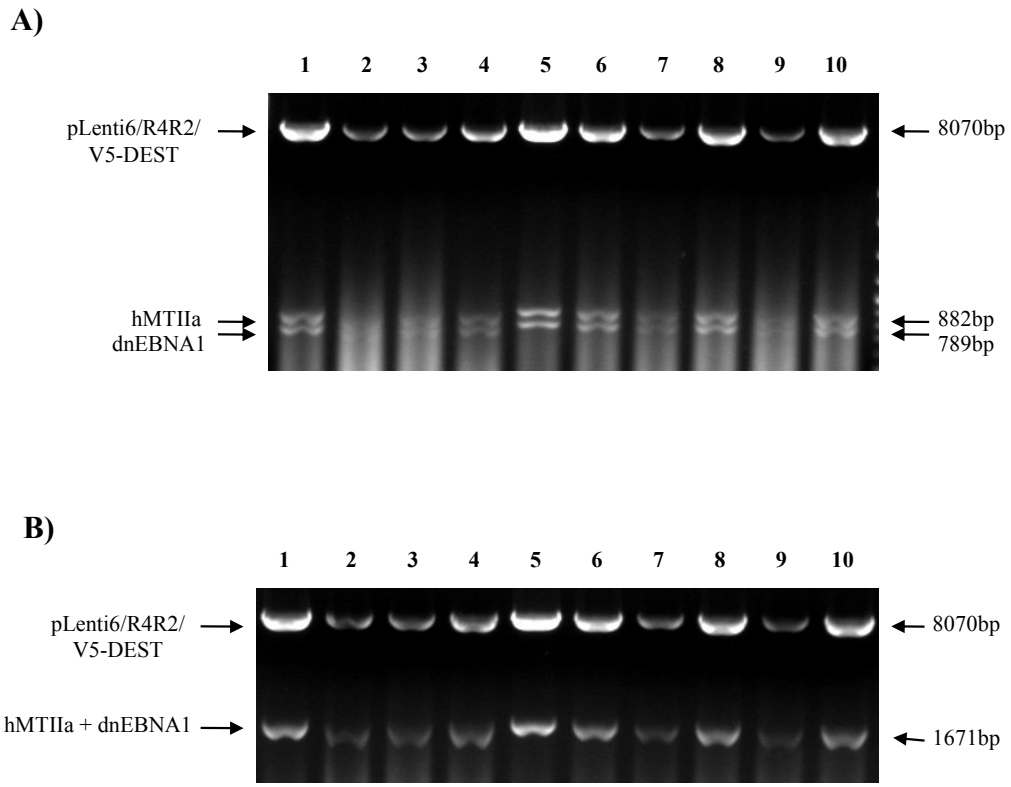

Figure 5.10: Diagnostic restriction digests of pLenti6/R4R2/V5-DEST vector containing the hMTIIa promoter and dominant negative EBNA1 sequences

A series of diagnostic digestions were performed to validate insertion of the hMTIIa promoter and dominant negative EBNA1 (dnEBNA1) gene fragments into the pLenti6/R4R2/V5-DEST vector.

A) *Eco*RI restriction digestion was performed to individually isolate the hMTIIa promoter and standard dnEBNA1 gene fragment from the pLenti6/R4R2/V5-DEST vector.
B) *Eco*RV restriction digests were performed to determine whether the juxtaposed hMTIIa promoter and dnEBNA1 gene fragments could be isolated from the pLenti6/R4R2/V5-DEST vector.
C) As above, *Eco*RI restriction digests were performed on clones obtained from transformation with pLenti6/R4R2/V5-DEST-dnEBNA1 Δ395-450.
D) As above, *Eco*RV restriction digests were performed on clones obtained from transformation with pLenti6/R4R2/V5-DEST-dnEBNA1 Δ395-450.

(A plasmid map of pLenti6/R4R2/V5-DEST can be found at: http://toolszh.invitrogen.com/contents/sfs/vectors/plenti6_r4r2_v5dest_map.pdf)

C)

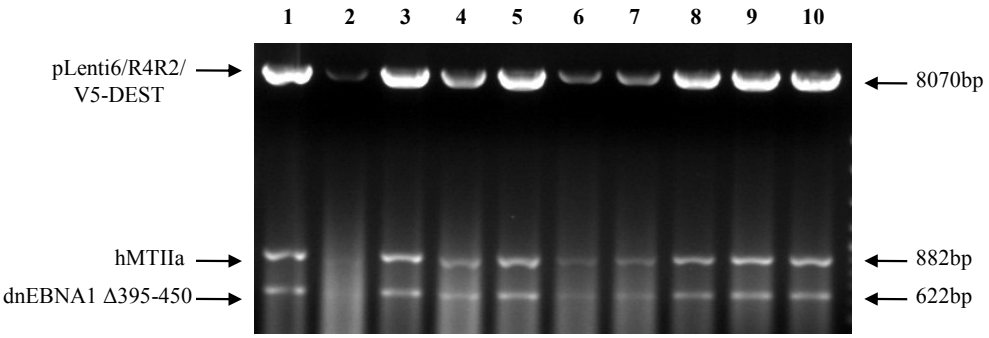
1 2 3 4 5 6 7 8 9 10
pLenti6/R4R2/
V5-DEST
8070bp
hMTIIa
882bp
dnEBNA1 Δ395-450
622bp

D)

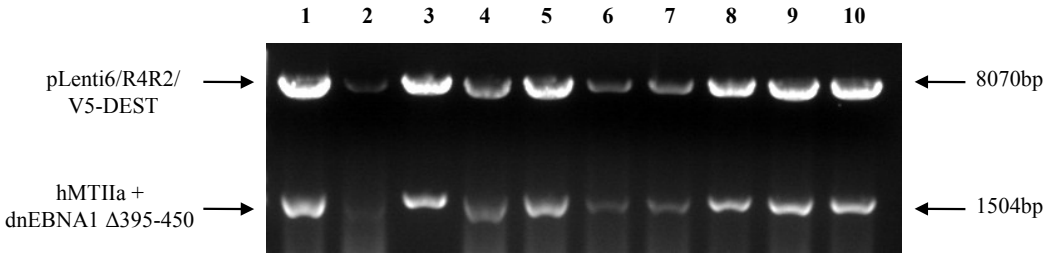
1 2 3 4 5 6 7 8 9 10
pLenti6/R4R2/
V5-DEST
8070bp
hMTIIa +
dnEBNA1 Δ395-450
1504bp

measured using a Nano-drop spectrophotometer, and samples were aliquoted and stored at -20°C for further use.

5.5 Validation of recombinant lentiviral vectors

5.5.1 Transient transfection of lentiviral constructs into Ad/AH cells

Ad/AH cells were transiently transfected with 2µg pLenti6/R4R2/V5-DEST-wtEBNA1 and incubated for 24 hours post-transfection, before stimulating with 50µM $ZnSO_4$ for a further 16 hours, or leaving unstimulated as a control. Both RNA and protein were harvested and subsequently used in RT-PCR and immunoblotting procedures to detect expression of the EBNA1 mRNA and protein respectively. Extracts from Ad/AH Neo control and Ad/AH EBNA1 cells were included as references for EBNA1 size and molecular weight, and representative images are shown in Figure 5.11. It is evident that EBNA1 transcripts can be successfully derived from the pLenti6/R4R2/V5-DEST vector (Figure 5.11A), and that the resulting protein is of the correct molecular weight for the wild-type protein (Figure 5.11B).

In order to determine the relative expression levels of EBNA1 from the lentiviral construct in comparison to an existing equivalent construct, both pSG5- and pLenti6/R4R2/V5-DEST-wtEBNA1 plasmids were transfected in increasing concentrations into Ad/AH cells. Protein lysates were analysed by immunoblotting for EBNA1 using the K67 rabbit polyclonal antibody, and a representative immunoblot is shown in Figure 5.12. For both EBNA1 vectors, the level of EBNA1 protein detected rose in accordance with the increase in transfected protein. However, it is very apparent that the levels of EBNA1 expression were much lower for the pLenti6/R4R2/V5-DEST vector, compared to the pSG5 vector, at each corresponding concentration.

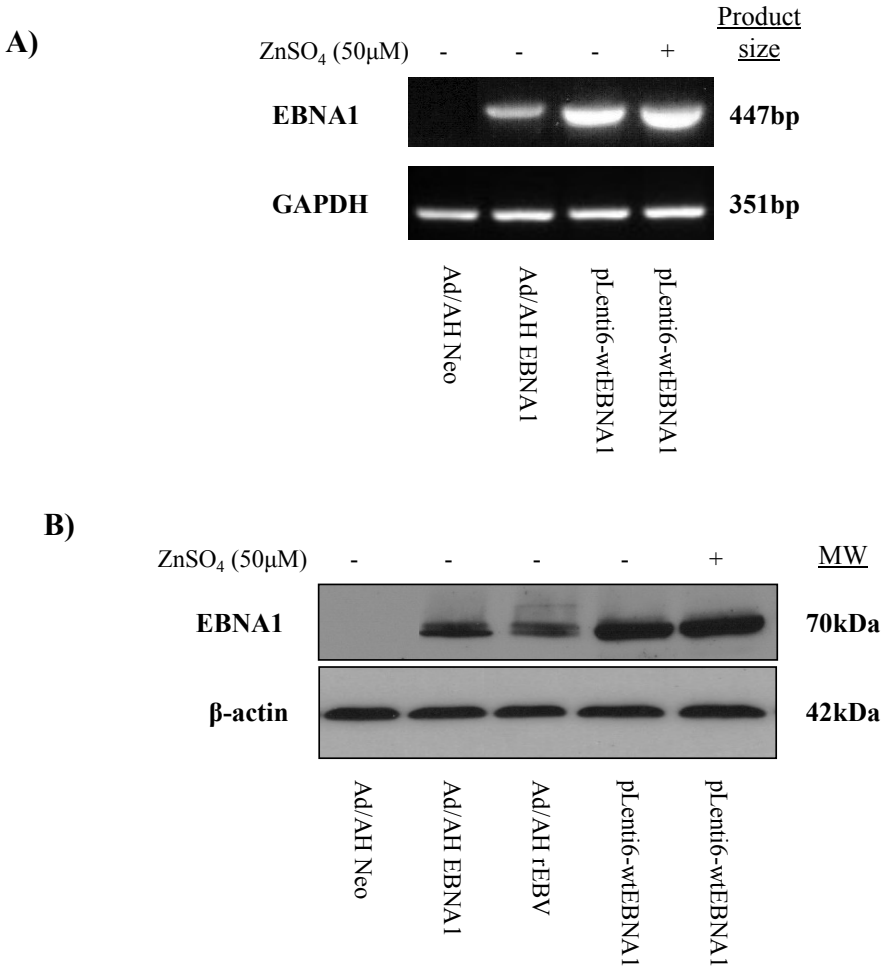

Figure 5.11: Validation of EBNA1 expression from pLenti6/R4R2/V5-DEST-hMTIIa-wtEBNA1 upon transient transfection into Ad/AH cells

A) RT-PCR analysis for EBNA1 mRNA expression in Ad/AH cells transiently transfected with the recombinant wtEBNA1 lentiviral plasmid and either stimulated with 50μM $ZnSO_4$ for 16 hours, or left unstimulated. GAPDH was included as a positive control to confirm equal RNA input into the PCR reactions, while samples generated from Ad/AH Neo control and Ad/AH EBNA1 lysates served as controls for EBNA1 expression.

B) Immunoblotting for EBNA1 protein expression in Ad/AH cells transiently transfected with the recombinant wtEBNA1 lentiviral plasmid and either stimulated with 50μM $ZnSO_4$ for 16 hours, or left unstimulated. Protein lysates obtained from Ad/AH Neo control, EBNA1 and rEBV-infected cells were included as controls for EBNA1 expression, while β-actin served as a loading control.

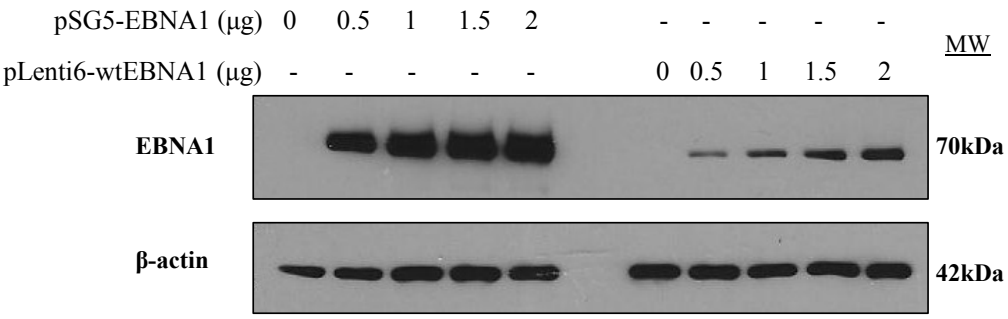

Figure 5.12: Determination of relative levels of EBNA1 expression following transient titration of pSG5-EBNA1 and pLenti6/R4R2/V5-DEST-hMTIIa-wtEBNA1 plasmids into Ad/AH cells
Immunoblotting for EBNA1 protein expression in Ad/AH cells transiently transfected with increasing concentrations of either a pSG5-EBNA1 plasmid or the recombinant wtEBNA1 lentiviral plasmid (pLenti6-wtEBNA1), with β-actin included as a loading control.

Dominant-negative EBNA1 lentiviral constructs were then validated in a similar manner, subsequent to verification of the wild-type version, and so are shown alongside the wild-type lentivirus for comparison. As demonstrated in Figure 5.13A, EBNA1 transcripts were successfully detected from both vectors carrying dominant-negative sequences, and these were efficiently translated into EBNA1 protein of appropriately reduced molecular weight according to their respective deletions, as shown in Figure 5.13B. The level of expression of the Δ395-450 version did however appear to be significantly reduced.

5.6 Generation of stable cell lines

5.6.1 Lentivirus production

The human kidney epithelial packaging cell line 293FT was used to produce whole virus from the recombinant lentiviral plasmids. Cells were seeded into 10cm dishes at a density of $1x10^6$ and grown to 80-90% confluency, before transient co-transfection with 4μg pLenti6/R4R2/V5-DEST expression vector, and 4μg of each of the packaging plasmids, pMD2.G and psPAX2 (Addgene). Transfected cells were incubated overnight, then refed with DMEM supplemented with 10% heat-inactivated FCS. Cells were then grown for approximately 48 hours, after which viral supernatants were harvested and filtered through 0.45μm filters. Virus-containing supernatants were then aliquoted into 1ml fractions and stored at -80°C.

5.6.2 Lentiviral transduction of Ad/AH target cells

Ad/AH cells were seeded into 6-well plates at density of $2.5x10^5$ cells per well and grown at 37°C until approximately 60% confluent. 1ml supernatants containing wild-type, dominant-negative and dominant-negative Δ395-450 EBNA1 lentiviruses, as well as a GFP control

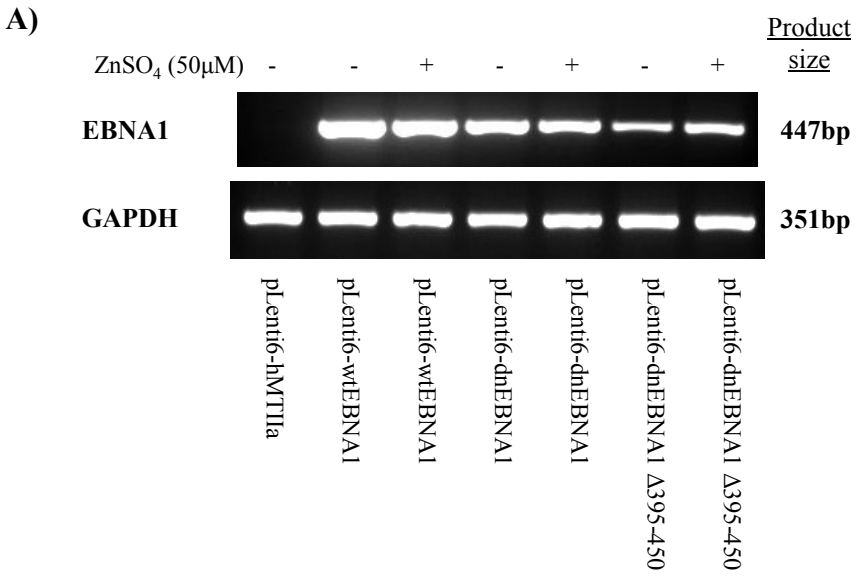

Figure 5.13: Validation of EBNA1 expression from pLenti6/R4R2/V5-DEST-hMTIIa-dnEBNA1 and pLenti6/R4R2/V5-DEST-hMTIIa-dnEBNA1 Δ395-450 upon transient transfection into Ad/AH cells

A) RT-PCR analysis for EBNA1 mRNA expression in Ad/AH cells transiently transfected with either the recombinant dnEBNA1 lentiviral plasmids or the hMTIIa promoter control vector, and either stimulated with 50μM $ZnSO_4$ for 16 hours, or left unstimulated. GAPDH was included as a positive control to confirm equal RNA input into the PCR reactions, while samples generated from Ad/AH Neo control and Ad/AH EBNA1 lysates served as controls for EBNA1 expression.

B) Immunoblotting for EBNA1 protein expression in Ad/AH cells transiently transfected with either the recombinant dnEBNA1 lentiviral plasmids or the hMTIIa promoter control vector, and either stimulated with 50μM $ZnSO_4$ for 16 hours, or left unstimulated. Protein lysates obtained from Ad/AH Neo control, EBNA1 and rEBV-infected cells are included as controls for EBNA1 expression, while β-actin served as a loading control.

B)

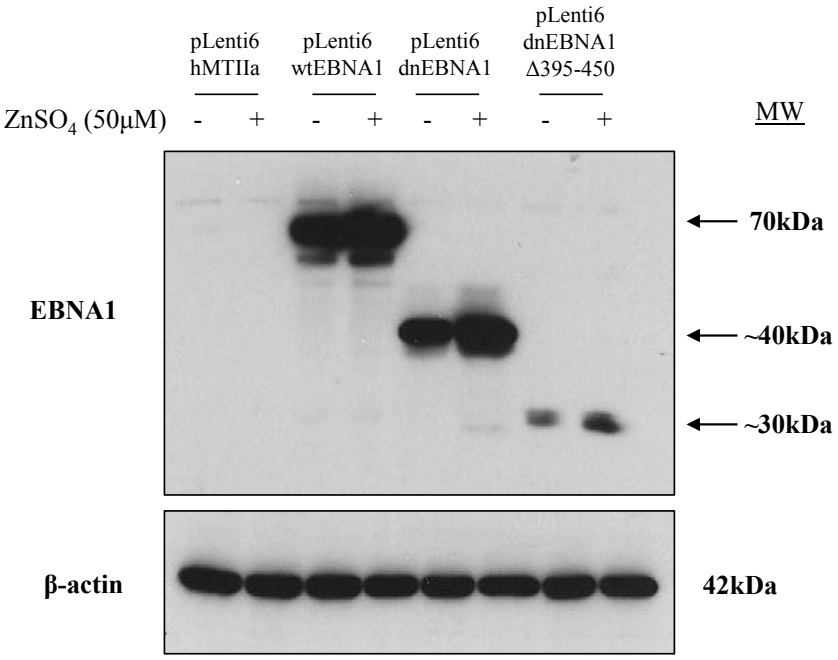
pLenti6 hMTIIa
pLenti6 wtEBNA1
pLenti6 dnEBNA1
pLenti6 dnEBNA1 Δ395-450
ZnSO4 (50μM) - + - + - + - +
MW
EBNA1
70kDa
~40kDa
~30kDa
β-actin
42kDa

virus, were mixed with Polybrene® (Millipore) at a final concentration of 6μg/ml, then applied to cells in each well. Cells were incubated overnight at 37°C and then refed the following day with fresh normal growth medium. After 72 hours, successful lentiviral transduction was assessed by GFP visualisation in those cells transduced with control virus. A blasticidin resistance cassette within the pLenti6/R4R2/V5-DEST plasmid was exploited for drug selection of positively transduced cells.

5.6.3 Immunofluorescent staining of stable lentivirally transduced Ad/AH cells

Ad/AH cells stably expressing the wild-type and dominant-negative lentiviruses were seeded at a density of $2x10^4$ onto each well of a 12-well Teflon-coated slide and grown for 24 hours before stimulating with 50μM $ZnSO_4$ for a further 16 hours. Immunofluorescence staining was then performed using R4, a rabbit polyclonal antibody specific for EBNA1. Representative fluorescence microscopy images are shown in Figure 5.14. It is evident that the lentiviral constructs exhibited a degree of inherent leakiness, resulting in levels of EBNA1 expression roughly comparable with levels observed in Ad/AH EBNA1 cells, which can then be further induced by the addition of zinc.

5.7 Deletion of different EBNA1 protein domains differentially affects TGFβ/Smad luciferase reporter activity

In order to validate the functionality of the expression plasmids, the panel of pLenti6/R4R2/V5-DEST EBNA1 mutants, along with the wild-type EBNA1 vector, were transiently transfected into Ad/AH cells in addition to the TGFβ-responsive $p(CAGA)_{12}$-Luc reporter, demonstrated in Chapter 3 to be inhibited by functional EBNA1 expression. The relative luciferase activity is depicted graphically in Figure 5.15. Transfection of wild-type

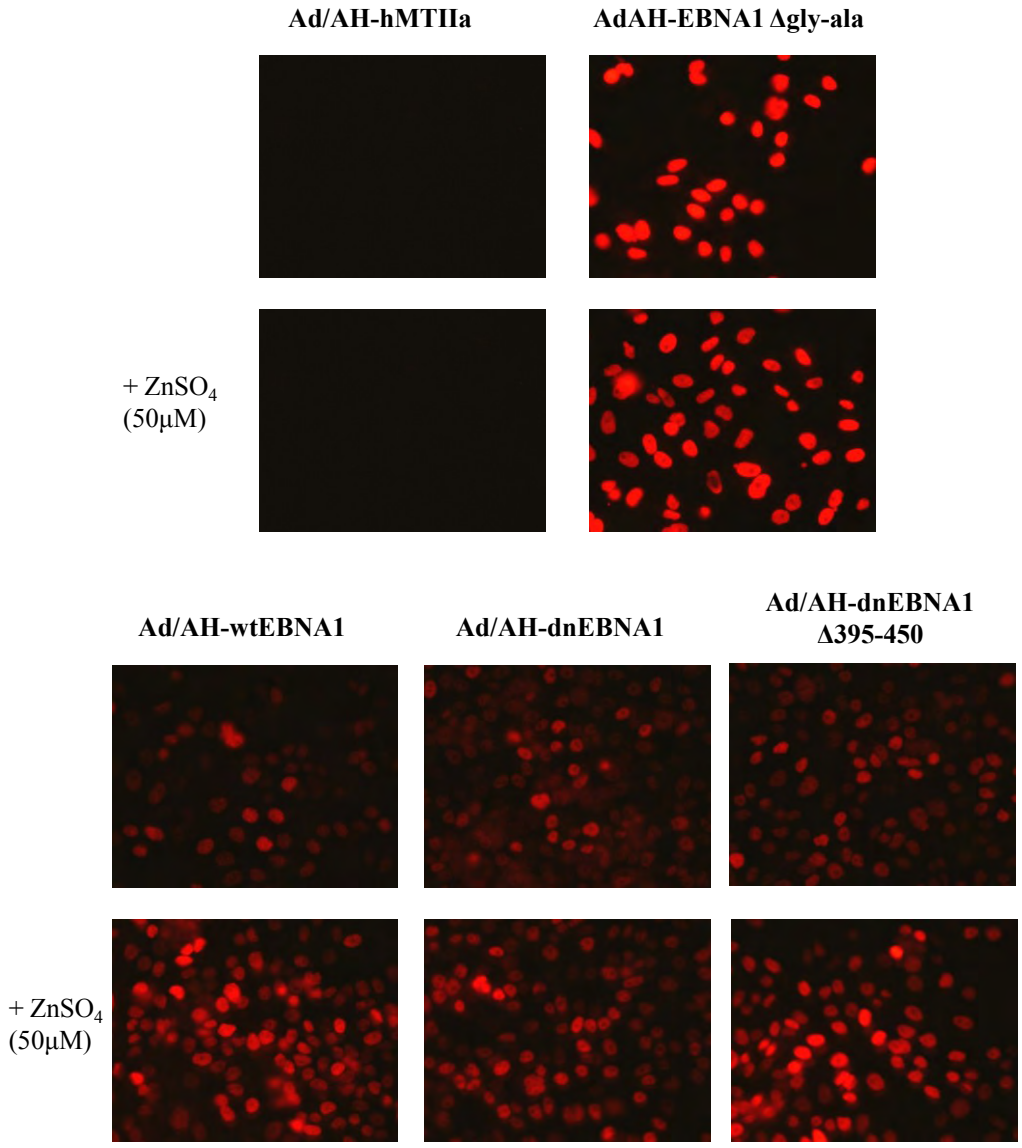

Figure 5.14: Validation of recombinant EBNA1 protein expression in stable Ad/AH cell lines by immunofluorescence staining
Immunofluorescence staining for EBNA1 protein expression in Ad/AH cells stably expressing the pLenti6/R4R2/V5-DEST plasmid carrying the wtEBNA1, dnEBNA1 and dnEBNA1 Δ395-450 sequences. Representative images are shown.

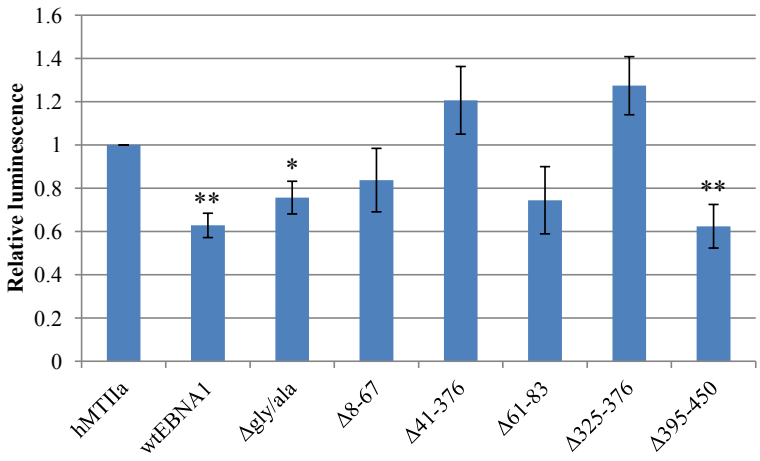

Figure 5.15: The effect of transient expression of EBNA1 mutant proteins on TGFβ reporter activity

Dual luciferase reporter assay showing p(CAGA)$_{12}$-Luc activity in Ad/AH cells transiently transfected with one of the panel of pLenti6/R4R2/V5-DEST-EBNA1 mutants or the wild-type EBNA1. A histogram is shown to depict the relative luminescence after normalising to Renilla luciferase values and expressing as a ratio of activity relative to the control vector pGL3-basic. Data from four independent experiments is presented as the mean fold differences in activity $\pm$ SE, relative to that observed in the Ad/AH pLenti6/R4R2/V5-DEST-hMTIIa control cells which is given an arbitrary value of 1 (** denotes a P-value <0.01 and * denotes a P-value <0.05).

EBNA1 effectively and significantly recapitulated the expected decrease in luciferase reporter activity in relation to the control vector carrying the hMTIIa promoter only. While deletion of the gly-ala repeat region, and also additional deletions of the 8-67, 61-83 and 395-450 regions did not dramatically impact upon the levels demonstrated with the wild-type construct, deletions of residues 41-376 and also 325-376 were sufficient to restore levels of TGFβ reporter activity and even to elevate them slightly above control levels.

5.8 Discussion and Future Work

Wild-type, dominant-negative and domain mutant EBNA1 sequences have been successfully cloned into a readily-inducible lentiviral expression system. Viral transduction and subsequent blasticidin drug selection has enabled the generation of stable cell lines in the Ad/AH epithelial cell background. The advantage of maintaining these cell lines as polyclonal populations, in comparison to the existing EBNA1-expressing cell lines derived from a single clone, is that they eliminate the risk that observations may be skewed by clonal variation.

While continuation of this work was limited by time constraints, validation of the stable cell lines suggests that, at this stage, direct comparisons between the lines may not be possible due to differences in EBNA1 protein expression levels. Expression of both EBNA1 mRNA and protein was confirmed and shown to be successfully responsive to zinc induction for the majority of mutants, with the exception of the mutant deleted for the 8-67 region. While the EBNA1 transcript could be detected at the mRNA level, expression of the EBNA1 protein was detected only with transient transfection of the vector, indicating that this particular deletion may interfere with the long-term maintenance of the protein within the cells. Others have reported similar findings using the same protein sequence contained within a pc3*oriP*

vector (Wu et al., 2002) and also a version fused to HaloTag protein for use in ChIP experiments (Owen, PhD thesis, 2010). It is therefore possible that deletion of the 8-67 region, in combination with the gly-ala repeat deletion, may create a particularly unstable conformation.

Generation of the wild-type EBNA1 sequence allowed comparison with the gly-ala-deleted mutant. Indeed preliminary evidence suggests that the two constructs mediate a similar reduction in TGFβ reporter activity; however more extensive functional investigation is required. The dominant-negative EBNA1 proteins will be useful in proving that any observed effects achieved with the remaining EBNA1 lentiviruses were solely attributable to the actions of EBNA1, rather than a simple stress response to the applied protein dose. In future studies they would also provide useful tools to compete out EBNA1 activity in EBV-infected cells and so determine whether continued EBNA1 function is required to maintain the phenotype of EBV-infected cells. Furthermore, it has been reported that adenovirus-mediated transduction of a dominant-negative EBNA1 protein was able to negatively influence viral episome maintenance within EBV-infected cells, independent of cell lineage and viral latency, and therefore potentially impede tumour cell growth (Nasimuzzaman et al., 2005), highlighting a prospective method of eliminating EBV from infected cells. Ultimately, such a protein capable of outcompeting regular EBNA1 function could be of great significance from a therapeutic angle.

As determined by immunoblotting, the Δ395-450 dominant-negative variant appears to exhibit a much reduced level of EBNA1 expression when compared to both wild-type and standard dominant-negative versions. In previous reports, deletion of the 395-450 region had

no noticeable effect on the turnover and cell-surface MHC class I presentation of EBNA1 (Holowaty et al., 2003), but the effect of its deletion in combination with the gross mutation of upstream sequence was not studied. In the stable cell line generated using this particular recombinant lentiviral vector however, the level of EBNA1 expression detected by immunofluorescence is comparable with the other derivatives, suggesting the issue lies with the immunoblot procedure and the associated difficulties in simultaneously detecting proteins of disparate molecular weights.

In agreement with an earlier observation, the lentiviral vectors do appear to drive a lower level of transgene expression when compared with previously used retroviral versions (Vigna and Naldini, 2000). The hMTIIa promoter has been shown to exhibit an inherent leakiness, permitting low levels of EBNA1 expression in the absence of zinc stimulation. This is a particularly favourable trait as these levels are much closer to physiological levels than the inevitable overexpression of EBNA1 when driven from CMV (as in the pc3*oriP* vectors) or SV40 promoters (as shown with pSG5-EBNA1).

In the context of this thesis, the panel of EBNA1 mutants will be an invaluable toolset in determining the regions of the EBNA1 protein involved in its modulation of TGFβ superfamily signalling. From this it is hoped that a specific mechanism can be delineated. Already, these lentiviral constructs have been utilised transiently to demonstrate that deletion of EBNA1 domains required for transactivation of EBV-encoded genes abrogates EBNA1's ability to inhibit NFκB activity (Valentine et al., 2010). Preliminary luciferase reporter assay data obtained here is in agreement with this, with deletion of the 325-376 region, implicated in both the segregation and viral gene transactivation functions (Shire et al., 1999, Ceccarelli

and Frappier, 2000, Wu et al., 2000, Wu et al., 2002) increasing the inhibited TGFβ reporter activity above control levels and the gross mutant, Δ41-376, with the additional deletion of the 61-83 region, also with a reported role in transcriptional activation (Wu et al., 2002), showing a similar effect.

Due to the broader tropism of the lentiviral vector, the panel can now be tested in its ability to target a much wider range of target cells, particularly those differentiation-competent lines currently considered unpermissive to stable EBNA1 expression (Jones et al., 2003), in the hope of ultimately achieving infection of primary nasopharyngeal epithelial cells. Subsequent detailed phenotypic analysis would additionally facilitate examination of the role of EBNA1 in the early stages of tumourigenesis, which is at present not possible using current cell models based on cell lines that are initially immortalised prior to viral transduction.

CHAPTER 6

General Discussion and Future Work

As the only EBV-encoded protein consistently expressed in all forms of viral latency and, by definition, all EBV-associated malignancies, the function of EBNA1 in EBV-infected cells has been intensely scrutinised. Aside from its essential roles in genome maintenance and segregation, there is now an increasing appreciation that EBNA1 possesses supplementary roles in the dysregulation of key cellular signalling pathways, largely associated with its ability to modulate cellular gene transcription and interact with important host cell proteins. Inadvertent activation of these pathways may, under certain circumstances, contribute to the pathogenesis of EBV-associated tumours. Within this thesis, existing observations have been extended to further define the effects of EBNA1 in the modulation of TGFβ signalling, while an EBNA1-mediated activation of the closely-related BMP pathway has been discovered.

TGFβ classically evokes an anti-proliferative response in epithelial cells, via a Smad2/3-mediated pathway that ultimately regulates the transcription of key cell cycle regulatory proteins. Data presented in Chapter 3 suggests that in cells stably expressing EBNA1, or stably infected with a recombinant EBV, canonical TGFβ signalling is dysregulated, either through a complete abrogation of pathway signalling through defects in TβRII, as observed in C666-1 cells, or alternatively, via specific modulation of Smad transcriptional activity, through alterations in Smad phosphorylation status.

Interestingly, profiling of TGFβ signalling pathway components in the carcinoma cell lines conducted in an earlier study, revealed that the TGFβ signalling pathway is largely intact in these cells lines (Wood et al., 2007). Indeed, in Chapter 3 it is confirmed that C-terminal Smad phosphorylation is still induced in response to TGFβ in these lines, albeit to a lesser extent than in control cells. Furthermore, in C666-1 cells, the restoration of TβRII expression dramatically induced TGFβ/Smad reporter activity and stimulated Smad2/3 phosphorylation, findings which indicate that the essential components of this signalling pathway are intact in these cells. However, as exemplified in the Ad/AH cell line, both EBNA1-expressing and rEBV-infected cells, and their control counterparts, were refractory to TGFβ-mediated growth arrest, suggesting this defect cannot be directly attributed to the expression of EBNA1 or EBV infection. Although the defects involved are currently unknown, they may reflect changes in key tumour suppressor genes that function downstream in the TGFβ signalling pathway and may likely occur through mutation or epigenetic inactivation. Possible candidates include RASSF1A and the CDK inhibitors, $p16^{INK4A}$ and $p15^{INK4B}$, whose dysregulation have been reported in NPC tumours, and whose inactivation are predicted to occur prior to EBV infection and subsequent progression to NPC (Lo and Huang, 2002). Interestingly, high frequencies of methylation of both $p16^{INK4A}$ and RASSF1A have also been documented in EBV-positive GC (Kang et al., 2002), findings which suggest that inactivation of these tumour suppressor proteins may be an essential component in EBV-driven tumourigenesis. The lack of a TGFβ-mediated growth arrest response may therefore be due to a lack or disruption of expression of key components required for its completion. Indeed, the inability of TβRII to restore a growth arrest response in C666-1 cells adds credence to the importance of such epigenetic changes.

This is supported further by the recent identification of MDS1-EVI1, mapping to 3q26, as a susceptibility locus for NPC development (Bei et al., 2010), and the reported amplification of Evi1 in NPC cell lines (Guo et al., 2002). The ability of Evi1 to antagonise the growth inhibitory effects of TGFβ by suppressing Smad3 transcriptional activity (Kurokawa et al., 1998) may have important consequences in the modification of TGFβ signalling and may constitute a key determinant in NPC pathogenesis.

The profound inhibition of TGFβ reporter activity and reduction in TGFβ-mediated phosphorylation of Smad2 and Smad3 by EBNA1, seems counterintuitive in terms of the virus's propensity to replicate in epithelial tissue, and the well-documented ability of TGFβ1 to trigger lytic reactivation in EBV-infected B cells (di Renzo et al., 1994, Fahmi et al., 2000). While viral replication in epithelial cells is an integral part of the natural life cycle of EBV, EBV-associated epithelial tumours are instead characterised by the maintenance of a latent EBV infection. These findings suggest that expression of EBNA1 may, under normal circumstances, positively regulate viral replication through autocrine induction of TGFβ1, while inappropriate infection of pre-malignant cells carrying TGFβ signalling defects may complement pre-existing changes in the TGFβ signalling network to facilitate stable latent infection.

The mechanism of TGFβ1-mediated EBV reactivation appears to enlist the concerted actions of both canonical, implicating Smad3 and multiple SBE sites (Liang et al., 2002, Oussaief et al., 2009, Iempridee et al., 2011) and non-canonical TGFβ signalling elements, implicating ERK/MAPK, PI3K/Akt and NFκB pathways (Fahmi et al., 2000, Oussaief et al., 2009, Oussaief et al., 2011), resulting in the activation of BZLF1 transcription and a corresponding

increase in the production of Zta (ZEBRA). Reports of BZLF1 RNA transcripts and Zta protein expression, and also antibodies to Zta in many NPC tumour lesions (Cochet et al., 1993, Martel-Renoir et al., 1995) suggest canonical TGFβ signalling must still function in NPC tumour cells, and imply the likely occurrence of sporadic abortive lytic cycle in NPC cells. In this regard, studies in a SCID mouse model suggest that lytic infection may play a key role in EBV-associated disease progression (Hong et al., 2005), dependent on the expression of immediate early and early lytic viral genes, but not full viral lytic replication.

The absence of TβRII expression in C666-1 cells would presumably render them incapable of inducing BZLF1 and subsequent lytic cycle. A similar phenomenon is observed in Akata BL cells which lack sensitivity to TGFβ1-mediated EBV reactivation until TβRII expression is induced by treatment with the HDAC inhibitor TSA (Fukuda et al., 2006). However, in a recent report, activation of the BMP signalling pathway, as is observed in C666-1 cells, has been shown to facilitate EBV reactivation in latency I BL cells (Yin et al., 2010). However, in newly infected primary B cells, BMP-mediated viral reactivation is effectively inhibited through the sustained induction of the cellular microRNA, miR-155 (Lu et al., 2008), and indeed up-regulation of miR-155 has also been documented in NPC cell lines and tumour samples (Chen et al., 2009, Du et al., 2011). In this context it may therefore serve to prevent BMP-mediated EBV reactivation and maintain viral latency. It is therefore not surprising that the BZLF1 protein product could not be detected by Western blotting of C666-1 cell lysates, and only rare cells were stained by IHC (Cheung et al., 1999). The C666-1 cell line may therefore be representative of only a rare subset of tumours in which EBV residence is stringently latent. It may therefore be important to determine whether miR-155 is similarly induced in C666-1 cells and other EBV-infected epithelial cell lines, while further attempts

should be made to establish a C666-1 derivative cell line stably expressing TβRII to enable more detailed analysis.

During epithelial cell infection *in vitro*, the virus preferentially targets differentiated primary epithelial cells (Feederle et al., 2007), presumably as these are more compliant with viral reactivation and propagation. Viral access into undifferentiated cells is therefore considered a rare event, probably restricted to rare pathological conditions where expression of an as yet unidentified epithelial EBV receptor is expressed under conditions of chronic inflammation or wound healing (Tsang et al., 2010). The abortion of complete viral productive cycle in NPC implies that this process is in someway defective in tumour cells, and is likely dictated by the permissivity of the host cell. Given their largely undifferentiated phenotype, it is feasible that the ability of NPC tumour cells to respond to pro-differentiation stimuli may be specifically abrogated, either by epigenetic changes and/or insensitivity to TGFβ. Viral replication may rely on cellular factors specifically associated with the differentiated phenotype which, by definition, would not be expressed in undifferentiated cells. Indeed studies have shown that "initiated" progenitor cells within keratinocyte populations have acquired resistance to the terminal differentiation signals of both TGFβ and the phorbol ester, TPA and, as a result, display a selective growth advantage in the formation of squamous cell carcinomas (Parkinson et al., 1983, Parkinson et al., 1984, Parkinson, 1985, Parkinson and Balmain, 1990). Furthermore, less differentiated immature hepatocytes have been found to demonstrate resistance to TGFβ1-induced apoptosis (Sánchez et al., 1999), again conferring a survival advantage to these undifferentiated cells. The absence of such factors may also be responsible for disparate effects of EBNA1 in carcinoma cell lines compared to the differentiation-competent OKF6 and Mv1Lu cells. An important experiment required to extend this work

would be to inactivate components of the canonical TGFβ signalling pathway in non-permissive, i.e. TGFβ-responsive, cell lines, and assess their susceptibility to EBV infection. The identification of a mechanism that may alleviate defects in carcinoma cells thereby permitting complete productive cycle and resultant cell death may facilitate the development of treatments for EBV-positive epithelial malignancies, such as NPC and EBV-aGC.

An additional feature of lytic cycle reactivation is the ability of Zta to increase TGFβ1 mRNA levels as well as the amount of secreted active TGFβ1 (Cayrol and Flemington, 1995). The increased production of TGFβ1 by EBNA1-expressing and EBV-infected epithelial cells may therefore represent an attempt of the virus to stimulate EBV reactivation via autocrine methods, and so may be a side-effect of increased Zta expression in the absence of complete productive lytic cycle. This may have an early role in facilitating horizontal transmission of the virus in epithelium and increasing the total number of latently infected cells, which may inadvertently favour disease development. Indeed Tsang *et al.* (Tsang et al., 2010) reported exogenous TGFβ1 can promote EBV infection of pre-malignant nasopharyngeal epithelial cells. The additional possibility however still remains, as discussed in Chapter 3, that the observed increase in TGFβ1 expression and secretion may constitute a strategy by EBV, through EBNA1, to diminish immune surveillance through effects on infiltrating T cells. Such a strategy may also inadvertently enhance pro-tumourigenic effects in EBV-infected epithelial cells that have acquired defects in the TGFβ signalling pathway.

With this is mind, the observed repression of TGFβ-mediated signalling seems unlikely to be a direct inhibitory effect on Smad activity, as is observed for other viral proteins, including adenovirus E1A, HBV pX, HTLV-1 Tax, HPV-5 E6 and HPV-16 E7, HCV core and non-

structural protein 3 (NS3) and KSHV vIRF1 (Nishihara et al., 1999, Lee et al., 2001, Lee et al., 2002a, Mendoza et al., 2006, Lee et al., 2002b, Cheng et al., 2004, Seo et al., 2005). This is corroborated by the observed inability of EBNA1 to interact with Smad2 protein *in vitro* (Flavell et al., 2008). The reduction in binding at SBE transcriptional sites in the presence of EBNA1 highlights a need to examine the relative compositions of active Smad complexes, as EBNA1 may instead alter the transcription and subsequent availability of cofactors or, as reported for adenovirus E1A in its interaction with the transcriptional co-activators p300/CBP (Nishihara et al., 1999), may directly interfere with their recruitment to target gene promoter sites as a means of modulating the response.

The observed decrease in TGFβ activity may therefore constitute an indirect consequence of increased negative regulation rather than a direct inhibitory effect, and indeed, this is supported by evidence presented in Chapter 3. The initial hypothesis implicating the increased expression of closely-related PPM1A and PPM1B phosphatases proved inconclusive, as their knockdown by shRNA methods could only partially restore Smad phosphorylation levels in EBNA1-expressing cells, and these effects could not be repeated in rEBV-infected cells. More convincing evidence however was provided in studies of the ubiquitin ligase, NEDD4-2, in increasing Smad protein turnover, particularly in light of the observation that the Smad linker residues specifically targeted by NEDD4-2 are increasingly phosphorylated in the presence of EBNA1. Moreover, the reported increases in Smad7 suggest greater antagonism of R-Smad function in these cells. Furthermore, the high level of Smad7 expression in C666-1 compared to OKF6 cells suggests EBV infection may indeed be responsible for this method of TGFβ signalling inhibition.

Although EBNA1 may uncouple the Smad-dependent arm of the TGFβ signalling pathway, it does not appear to inhibit non-canonical signalling. It can now be speculated that the pro-tumourigenic aspects of TGFβ are further potentiated by the cross-talk with other signalling pathways, which are activated by EBNA1. In particular, ERK-MAPK and JNK pathways have been identified as potentially significant candidates. These signalling pathways are particularly important in the differential phosphorylation of Smad2 and Smad3 proteins in their linker regions, which specifically promote these effects, but can also serve to impede classical transcriptional responses mediated by C-terminally phosphorylated Smads. These linker-phosphorylated Smads may be directly involved in the observed increases in cell migration of EBNA1-expressing cells. It will therefore be important to assess the relative abundance of these linker phosphorylated Smad isoforms in NPC tumour biopsies to substantiate this hypothesis, and to further dissect the respective contributions of connecting signalling pathways. In addition, transgenic mice with targeted expression of EBNA1 to either the epidermis or gastric compartments are currently being generated which may be used to determine whether these effects are replicated *in vivo*, and to assess their relevance to the pathogenesis of NPC and EBV-positive GC.

In contrast, as measured by pSmad1/5/8 phosphorylation, the BMP signalling pathway appears to be constitutively activated in EBNA1-expressing and rEBV-infected cells, which may be a direct result of the ability of EBNA1 to enhance BMP2 expression at the transcriptional level; however, elucidation of the ability of EBNA1 to associate with the promoters of BMP-related genes would be required to verify this. Several reports have implicated retinoids, Sp1 transcription factors and the protein kinase C pathway in the transcriptional regulation of BMP2 gene expression (Heller et al., 1999, Abrams et al., 2004,

Xu and Rogers, 2007, Helvering et al., 2000), but perhaps of most interest is the reported up-regulation of BMP2 by FGF2, and the mediation of this effect by Runx2 (Choi et al., 2005). The Ad/AH microarray data suggests that both FGF2 and Runx2 are up-regulated in EBNA1-expressing cells, by fold changes of 1.69- and 2.97-fold, respectively, and so may contribute significantly to the observed up-regulation of BMP2.

The characteristic induction of Id proteins suggests an overall inhibitory influence of BMPs on cell differentiation. Although unfavourable in terms of promoting viral reactivation, this effect may be important in supporting the undifferentiated phenotype of the host cell. Evidence presented here further suggests this increased BMP activity may serve to increase the migratory capacity of EBNA1-expressing cells and, additionally, may play a role in promoting metastasis, particularly to bone. Again, the transgenic mouse models will be useful in providing an *in vivo* setting in which to enable clarification of these points.

The mechanism by which this preferential activation of BMP signalling is achieved is at yet undetermined, and certainly warrants further investigation. The BMP signalling pathway is undoubtedly, as has also been shown for the TGFβ signalling pathway, further complicated by cross-talk with further interconnecting signalling pathways. The potential contribution of such cross-talk in the modification of the overall signalling response remains to be investigated. Indeed, a more comprehensive investigation of the dynamics of BMP signalling in the presence of EBNA1 is essential to provide further mechanistic insight.

Another possibility is that the larger number of both ligands and receptors that participate in the BMP signalling pathway activity, and therefore greater variety of signalling combination

possibilities may effectively mask any abrogations. Although down-regulation of certain receptors is reported in the presence of EBNA1, the expression of other receptors of the same type is maintained, so may functionally compensate. Furthermore, the relative expression levels of the different isoforms of both TGFβ and BMP ligands present in the cells will inevitably influence the nature of the overall response. While total ablation of either pathway in an attempt to reduce tumourigenic activity would not be practical, given their ubiquitous roles in cellular homeostasis, if the predominant effect were to be attributed to a single isoform, selective inhibition using neutralising antibodies and/or shRNA techniques may be of clinical importance.

The extent of cooperation between the pathways in eliciting the observed effects in epithelial cells is not precisely clear. In this study, BMP2 was unable to induce Smad2 phosphorylation in any of the carcinoma cell lines examined, while studies in C666-1 cells further suggested that TGFβ-mediated Smad transcriptional responses cannot be mediated by BMP2. However, the observed ability of TGFβ to induce pSmad1/5/8 phosphorylation in the presence of EBNA1 may be of great significance in modulating the tumourigenic effects of TGFβ, and identifies a need to more extensively monitor the function of each pathway when the other is specifically inhibited.

In osteoblasts, BMP2 treatment has been shown to decrease TGFβ ligand binding to TβRII, yet without affecting steady state mRNA or total protein TβRII levels, and with resultant dampening of TGFβ-mediated effects (Centrella et al., 1995, Chang et al., 2002). This is achieved through a reduction of cell surface TβRII, with relocation to more intracellular and perinuclear regions. It is interesting to speculate that the observed reduction in cell surface

expression of TGFβ receptors in EBNA1-expressing cells may in fact be a result of the higher expression levels of BMP2. This reinforces the importance of monitoring the cellular localisation of TGFβ receptors in EBNA1-expressing cells, as well as their ligand binding activity, if this work were to be further developed.

Finally, the generation of wild-type and mutant versions of EBNA1 in self-inactivating lentivirus vectors will provide valuable tools for the extension of this work. With the potential to achieve successful infection of primary nasopharyngeal epithelial cells they may prove important in determining where the changes identified herein occur in relation to EBV infection and the specific roles they play in dictating the maintenance of a latent infection. It is hoped that it may be established whether BMP signalling and the changes to the TGFβ signalling pathway play a role in malignant transformation or whether their effects are confined to the later stages of cancer.

In summary, data presented within this thesis has extended our knowledge on the function of EBNA1 in the modulation of cellular signalling pathways, specifically in directing TGFβ superfamily signalling in inactivating their tumour suppressive influences and potentiating oncogenic effects, while the development of lentiviral technologies has provided an effective model for subsequent investigation of these observations. In due course, the elucidation of specific mechanisms employed by EBNA1 in manipulating these key cellular signalling pathways may enable the development of specific treatments to counteract its effects in EBV-associated malignancies such as NPC and EBV-positive GC.

REFERENCES

ABRAMS, K. L., XU, J., NATIVELLE-SERPENTINI, C., DABIRSHAHSAHEBI, S. & ROGERS, M. B. 2004. An evolutionary and molecular analysis of *Bmp2* expression. *J. Biol. Chem.,* 279**,** 15916-15928.

ADAMS, A. & LINDAHL, T. 1975. Epstein-Barr virus genomes with properties of circular DNA molecules in carrier cells. *Proc. Natl. Acad. Sci USA,* 72**,** 1477-1481.

AGATHANGGELOU, A., NIEDOBITEK, G., CHEN, R., NICHOLLS, J., YIN, W. & YOUNG, L. S. 1995. Expression of immune regulatory molecules in Epstein-Barr virus-associated nasopharyngeal carcinomas with prominent lymphoid stroma. *Am. J. Pathol.,* 147**,** 1152-1160.

AKHURST, R. J. & DERYNCK, R. 2001. TGF-β signalling in cancer - a double-edged sword. *Trends Cell Biol.,* 11**,** S44-S51.

AL TABAA, Y., TUAILLON, E., JEZIORSKI, E., OUEDRAOGO, D. E., BOLLORÉ, K., RUBBO, P.-A., FOULONGNE, V., RODIÈRE, M. & VENDRELL, J.-P. 2011. B-cell activation and Epstein-Barr viral abortive lytic cycle are two key features in acute infectious mononucleosis. *J. Clin. Virol.,* 52**,** 33-37.

ALARCÓN, C., ZAROMYTIDOU, A.-I., XI, Q., GAO, S., YU, J., FUJISAWA, S., BARLAS, A., MILLER, A. N., MANOVA-TODOROVA, K., MACIAS, M. J., SAPKOTA, G., PAN, D. & MASSAGUÉ, J. 2009. Nuclear CDKs drive Smad transcriptional activation and turnover in BMP and TGF-β pathways. *Cell,* 139**,** 757-769.

ALARMO, E.-L. & KALLIONIEMI, A. 2010. Bone morphogenetic proteins in breast cancer: dual role in tumourigenesis? *Endocrine-Related Cancer,* 17**,** R123-R139.

ALARMO, E.-L., KORHONEN, T., KUUKASJÄRVI, T., HUHTALA, H., HOLLI, K. & KALLIONIEMI, A. 2006. Bone morphogenetic protein 7 expression associates with bone metastasis in breast carcinomas. *Annals of Oncology,* 19**,** 308-314.

ALARMO, E.-L., KORHONEN, T., KUUKASJÄRVI, T., HUHTALA, H., HOLLI, K. & KALLIONIEMI, A. 2008. Bone morphogenetic protein 7 expression associated with bone metastasis in breast carcinomas. *Ann. Oncol.,* 19**,** 308-314.

ALLEN, M. D., YOUNG, L. S. & DAWSON, C. W. 2005. The Epstein-Barr virus-encoded LMP2A and LMP2B proteins promote epithelial cell spreading and motility. *J. Virol.,* 79**,** 1789-1802.

AMBINDER, R. F., MULLEN, M., CHANG, Y.-N., HAYWARD, G. S. & HAYWARD, S. D. 1991. Functional domains of Epstein-Barr virus nuclear antigen EBNA-1. *J. Virol.,* 65**,** 1466-1478.

AMBINDER, R. F., SHAH, W. A., RAWLINS, D. R., HAYWARD, G. S. & HAYWARD, S. D. 1990. Definition of the sequence requirements for the binding of the EBNA-1 protein to its palindromic target sites in Epstein-Barr virus DNA. *J. Virol.,* 64**,** 2369-2379.

ANNES, J. P., MUNGER, J. S. & RIFKIN, D. B. 2003. Making sense of latent TGFβ activation. *J. Cell Sci.,* 116**,** 217-224.

AOKI, H., FUJII, M., IMAMURA, T., YAGI, K., TAKEHARA, K., KATO, M. & MIYAZONO, K. 2001. Synergistic effects of different bone morphogenetic protein type I receptors on alkaline phosphatase induction. *J. Cell Sci.,* 114**,** 1483-1489.

AONO, A., HAZAMA, M., NOTOYA, K., TAKETOMI, S., YAMASAKI, H., TSUKUDA, R., SASAKI, S. & FUJISAWA, Y. 1995. Potent ectopic bone-inducing activity of bone morphogenetic protein-4/7 heterodimer. *Biochem. Biophys. Res. Comm.,* 210**,** 670-677.

APCHER, S., DASKALOGIANNI, C., MANOURY, B. & FÅHRAEUS, R. 2010. Epstein Barr virus-encoded EBNA1 interference with MHC class I antigen presentation reveals a close correlation between mRNA translation initiation and antigen presentation. *PLoS Pathogens,* 6**,** e1001151.

APCHER, S., KOMAROVA, A., DASKALOGIANNI, C., YIN, Y., MALBERT-COLAS, L. & FÅHRAEUS, R. 2009. mRNA translation regulation by the Gly-Ala repeat of Epstein-Barr virus nuclear antigen 1. *J. Virol.,* 83**,** 1289-1298.

ARMSTRONG, R. W., IMREY, P. B., LYE, M. S., ARMSTRONG, M. J., YU, M. C. & SANI, S. 2000. Nasopharyngeal carcinoma in Malaysian Chinese: occupational exposures to particles, formaldehyde and heat. *Int. J. Epidemiol.,* 29**,** 991-998.

ARRAND, J. R. & RYMO, L. 1982. Characterisation of the major Epstein-Barr virus-specific RNA in Burkitt lymphoma-derived cells. *J. Virol.,* 41**,** 376-389.

ATTISANO, L. & WRANA, J. L. 2002. Signal transduction by the TGF-β superfamily. *Science,* 296**,** 1646-1647.
BABCOCK, G. J., HOCHBERG, D. & THORLEY-LAWSON, D. A. 2000. The expression pattern of Epstein-Barr virus latent genes in vivo is dependent upon the differentiation stage of the infected B cell. *Immunity,* 13**,** 497-506.
BAER, R., BANKLER, A. T., BIGGIN, M. D., DEININGER, P. L., FARRELL, P. J., GIBSON, T. J., HATFULL, G., HUDSON, G. S., SATCHWELL, S. C., SÉGUIN, C., TUFFNELL, P. S. & BARRELL, B. G. 1984. DNA sequence and expression of the B95-8 Epstein-Barr virus genome. *Nature,* 310**,** 207-211.
BAILEY, K. M. & LIU, J. 2008. Caveolin-1 up-regulation during epithelial to mesenchymal transition is mediated by focal adhesion kinase. *J. Biol. Chem.,* 283**,** 13714-13724.
BAKOS, A., BANATI, F., KOROKNAI, A., TAKACS, M., SALAMON, D., MINAROVITS-KORMUTA, S., SCHWARZMANN, F., WOLF, H., NILLER, H. H. & MINAROVITS, J. 2007. High-resolution analysis of CpG methylation and in vivo protein-DNA interactions at the alternative Epstein-Barr virus latency promoters Qp and Cp in the nasopharyngeal carcinoma cell line C666-1. *Virus Genes,* 35**,** 195-202.
BANIWAL, S. K., KHALID, O., GABET, Y., SHAH, R. R., PURCELL, D. J., MAV, D., KOHN-GABET, A. E., SHI, Y., COETZEE, G. A. & FRENKEL, B. 2010. Runx2 transcriptome of prostate cancer cells: insights into invasiveness and bone metastasis. *Molecular Cancer,* 9**,** 258.
BARTH, S., PFUHL, T., MAMIANI, A., EHSES, C., ROEMER, K., KREMMER, E., JAKER, C., HOCK, J., MEISTER, G. & GRASSER, F. A. 2008. Epstein-Barr virus-encoded microRNA miR-BART2 down-regulates the viral DNA polymerase BALF5. *Nucleic Acid Research,* 36**,** 666-675.
BASHAW, J. M. & YATES, J. L. 2001. Replication from oriP of Epstein-Barr virus requires exact spacing of two bound dimers of EBNA1 which bend DNA. *J. Virol.,* 75**,** 10603-10611.
BAUMFORTH, K. R. N., BIRGERSDOTTER, A., REYNOLDS, G. M., WEI, W. & KAPATI, G. 2008. Expression of the Epstein-Barr virus-encoded Epstein-Barr virus nuclear antigen 1 in Hodgkin's lymphoma cells mediates up-regulation of CCL20 and the migration of regulatory T cells. *Am. J. Pathol.,* 173**,** 195-204.
BECK, S. E., JUNG, B. H., FIORINO, A., GOMEZ, J., DEL ROSARIO, E., CABRERA, B. L., HUANG, S. C., CHOW, J. Y. C. & CARETHERS, J. M. 2006. Bone morphogenetic protein signalling and growth suppression in colon cancer. *Am. J. Physiol. Gastrointest. Liver Physiol.,* 291**,** 135-145.
BEI, J.-X., LI, Y., JIA, W.-H., FENG, B.-J., ZHOU, G., CHEN, L.-Z., FENG, Q.-S., LOW, H.-Q., ZHANG, H. X., HE, F., TAI, E. S., KANG, T., LIU, E. T., LIU, J. & ZENG, Y.-X. 2010. A genome-wide association study of nasopharyngeal carcinoma identifies three new susceptibility loci. *Nat. Genet.,* 42**,** 599-603.
BENTLEY, H., HAMDY, F. C., HART, K. A., SEID, J. M., WILLIAMS, J. L., JOHNSTONE, D. & RUSSELL, R. G. 1992. Expression of bone morphogenetic proteins in human prostatic adenocarcinoma and benign prostatic hyperplasia. *Br. J. Cancer,* 66**,** 1159-1163.
BHARATHY, S., XIE, W., YINGLING, J. M. & REISS, M. 2008. Cancer-associated transforming growth factor β type II receptor gene mutant causes activation of bone morphogenic protein-Smads and invasive phenotype. *Cancer Res.,* 68**,** 1656-1666.
BISWAS, S., TROBRIDGE, P., ROMERO-GALLO, J., BILLHEIMER, D., MYEROFF, L. L., WILSON, J. K. V., MARKOWITZ, S. D. & GRADY, W. M. 2008. Mutational inactivation of TGFBR2 in microsatellite unstable colon cancer arises from the cooperation of genomic instability and the clonal outgrowth of transforming growth factor β resistant cells. *Genes Chromosomes Cancer,* 47**,** 95-106.
BLAKE, N., LEE, S., REDCHENKO, I., THOMAS, W., STEVEN, N., LEESE, A., STEIGERWALD-MULLEN, P., KURILLA, M. G., FRAPPIER, L. & RICKINSON, A. 1997. Human CD8+ T cell responses to EBV EBNA1: HLA class I presentation of the (Gly-Ala)-containing protein requires exogenous processing. *Immunity,* 7**,** 791-802.
BOERGERMANN, J. H., KOPF, J., YU, P. B. & KNAUS, P. 2010. Dorsomorphin and LDN-193189 inhibit BMP-mediated Smad, p38 and Akt signalling in C2C12 cells. *Int. J. Biochem. Cell Biol.,* 42**,** 1802-1807.

BORNKAMM, G. W., DELIUS, H., ZIMBER, U., HUDEWENTZ, J. & EPSTEIN, M. A. 1980. Comparison of Epstein-Barr virus strains of different origin by analysis of the viral DNAs. *J. Virol.,* 35**,** 603-618.
BORNSTEIN, S., HOOT, K., HAN, G.-W., LU, S.-L. & WANG, X.-J. 2007. Distinct roles of individual Smads in skin carcinogenesis. *Mol. Carcinog.,* 46**,** 660-664.
BORZA, C. M. & HUTT-FLETCHER, L. M. 2002. Alternative replication in B cells and epithelial cells switches tropism of Epstein-Barr virus. *Nat. Med.,* 8**,** 594-599.
BOYSEN, T., MOHAMMADI, M., MELBYE, M., HAMILTON-DUTOIT, S., VAINER, B., HANSEN, A. V., WOHLFAHRT, J. & FRIBORG, J. 2009. EBV-associated gastric carcinoma in high- and low-incidence areas for nasopharyngeal carcinoma. *Br. J. Cancer,* 101**,** 530-533.
BROOKS, L., YAO, Q. Y., RICKINSON, A. B. & YOUNG, L. S. 1992. Epstein-Barr virus latent gene transcription in nasopharyngeal carcinoma cells: coexpression of EBNA1, LMP1 and LMP2 transcripts. *J. Virol.,* 66**,** 2689-2697.
BUCHSCHACHER, G. L. & WONG-STAAL, F. 2000. Development of lentiviral vectors for gene therapy for human diseases. *Blood,* 95**,** 2499-2504.
BUELL, P. 1974. The effect of migration on the risk of nasopharyngeal cancer among Chinese. *Cancer Res.,* 34**,** 1189-1191.
BURCH, M. L., ZHENG, W. & LITTLE, P. J. 2010. Smad linker region phosphorylation in the regulation of extracellular matrix synthesis. *Cell. Mol. Life Sci.,* 68**,** 97-107.
BURKITT, D. 1958. A sarcoma involving the jaws in African children. *British Journal of Surgery,* 46**,** 218-223.
BURKITT, D. 1962. A children's cancer dependent on climatic factors. *Nature,* 194**,** 232-234.
BUSSON, P., MCCOY, R., SADLER, R., GILLIGAN, K., TURSZ, T. & RAAB-TRAUB, N. 1992. Consistent transcription of the Epstein-Barr virus LMP2 gene in nasopharyngeal carcinoma. *J. Virol.,* 66**,** 3257-3262.
BUTEL, J. S. 2000. Viral carcinogenesis: revelation of molecular mechanisms and etiology of human disease. *Carcinogenesis,* 21**,** 405-426.
CAI, X., SCHAFER, A., LU, S., BILELLO, J. P., DESROSIERS, R. C., EDWARDS, R., RAAB-TRAUB, N. & CULLEN, B. R. 2006. Epstein-Barr virus microRNAs are evolutionarily conserved and differentially expressed. *PLoS Pathogens,* 2**,** e23.
CALDWELL, R. G., WILSON, J. B., ANDERSON, S. J. & LONGNECKER, R. 1998. Epstein-Barr virus LMP2A drives B cell development and survival in the absence of normal B cell receptor signals. *Immunity,* 9**,** 405-411.
CANAAN, A., HAVIV, I., URBAN, A. E., SCHULZ, V. P., HARTMAN, S., ZHANG, Z., PALEJEV, D., DEISSEROTH, A. B., LACY, J., SNYDER, M., GERSTEIN, M. & WEISSMAN, S. M. 2009. EBNA1 regulates cellular gene expression by binding cellular promoters. *Proc. Natl. Acad. Sci USA,* 106**,** 22421-22426.
CAO, X. & CHEN, D. 2005. The BMP signalling and in vivo bone formation. *Gene,* 357**,** 1-8.
CAYROL, C. & FLEMINGTON, E. K. 1995. Identification of cellular target genes of the Epstein-Barr virus transactivator Zta: activation of transforming growth factor βigh3 (TGF-βigh3) and TGF-β1. *J. Virol.,* 69**,** 4206-4212.
CECCARELLI, D. F. J. & FRAPPIER, L. 2000. Functional analyses of the EBNA1 origin DNA binding protein of Epstein-Barr virus. *J. Virol.,* 74**,** 4939-4948.
CENTRELLA, M., CASINGHINO, S., KIM, J., PHAM, T., ROSEN, V., WOZNEY, J. & MCCARTHY, T. L. 1995. Independent changes in type I and type II receptors for transforming growth factor β induced by bone morphogenetic protein 2 parallel expression of the osteoblast phenotype. *Mol. Cell. Biol.,* 15**,** 3273-3281.
CHAN, A. S.-C., TO, K. F., LO, K. W., DING, M., LI, X., JOHNSON, P. & HUANG, D. P. 2002. Frequent chromosome 9p losses in histologically normal nasopharyngeal epithelia from Southern Chinese. *Int. J. Cancer,* 102**,** 300-303.
CHAN, A. S.-C., TO, K. F., LO, K. W., MAK, K. F., PAK, W., CHIU, B., TSE, G. M. K., DING, M., LI, X., LEE, J. C. K. & HUANG, D. P. 2000. High frequency of chromosome 3p deletion in histologically normal nasopharyngeal epithelia from Southern Chinese. *Cancer Res.,* 60**,** 5365-5370.

CHANG, C. M., YU, K. J., MBULAITEYE, S. M., HILDESHEIM, A. & BHATIA, K. 2009. The extent of genetic diversity of Epstein-Barr virus and its geographic and disease patterns: a need for reappraisal. *Virus Research,* 143**,** 209-221.

CHANG, E. T. & ADAMI, H.-O. 2006. The enigmatic epidemiology of nasopharyngeal carcinoma. *Cancer Epidemiol. Biomarkers Prev.,* 15**,** 1765-1777.

CHANG, K.-P., WU, C.-C., CHEN, H.-C., CHEN, S.-J., PENG, P.-H., TSANG, N.-M., LEE, L.-Y., LIU, S.-C., LIANG, Y., LEE, Y.-S., HAO, S.-P., CHANG, Y.-S. & YU, J.-S. 2010. Identification of candidate nasopharyngeal carcinoma serum biomarkers by cancer cell secretome and tissue transcriptome analysis: potential usage of cystatin A for predicting nodal stage and poor prognosis. *Proteomics,* 10**,** 2644-2660.

CHANG, W., PARRA, M., JI, C., LIU, Y., EICKELBERG, O., MCCARTHY, T. L. & CENTRELLA, M. 2002. Transcriptional and post-transcriptional regulation of transforming growth factor β type II receptor expression in osteoblasts. *Gene,* 299**,** 65-77.

CHEN, D., JI, X., HARRIS, M. A., FENG, J. Q., KARSENTY, G., CELESTE, A. J., ROSEN, V., MUNDY, G. R. & HARRIS, S. E. 1998a. Differential roles for bone morphogenetic protein (BMP) receptor type IB and IA in differentiation and specification of mesenchymal precursor cells to osteoblast and adipocyte lineages. *J. Cell Biol.,* 142**,** 295-305.

CHEN, G., GHOSH, P., OSAWA, H., SASAKI, C. Y., REZANKA, L., YANG, J., O'FARRELL, T. J. & LONGO, D. L. 2007. Resistance to TGF-β1 correlates with aberrant expression of TGF-β receptor II in human B-cell lymphoma cell lines. *Blood,* 109**,** 5301-5307.

CHEN, H.-C., CHEN, G.-H., CHEN, Y.-H., LIAO, W.-L., LIU, C.-Y., CHANG, K.-P., CHANG, Y.-S. & CHEN, S.-J. 2009. MicroRNA deregulation and pathway alterations in nasopharyngeal carcinoma. *Br. J. Cancer,* 100**,** 1002-1011.

CHEN, H., HUANG, J., WU, F. Y., LIAO, G., HUTT-FLETCHER, L. & HAYWARD, S. D. 2005. Regulation of expression of the Epstein-Barr virus BamHI-A rightward transcripts. *J. Virol.,* 79**,** 1724-1733.

CHEN, H., LEE, J. M., WANG, Y., HUANG, D. P., AMBINDER, R. F. & HAYWARD, S. D. 1999. The Epstein-Barr virus latency BamHI-Q promoter is positively regulated by STATs and Zta interference with JAK/STAT activation leads to loss of BamHI-Q promoter activity. *Proc. Natl. Acad. Sci USA,* 96**,** 9339-9344.

CHEN, H., LEE, J. M., ZONG, Y., BOROWITZ, M., NG, M. H., AMBINDER, R. F. & HAYWARD, S. D. 2001. Linkage between STAT regulation and Epstein-Barr virus gene expression in tumours. *J. Virol.,* 75**,** 2929-2937.

CHEN, M.-R., YANG, J.-F., WU, C.-W., MIDDELDORP, J. M. & CHEN, J.-Y. 1998b. Physical association between the EBV protein EBNA-1 and p32/TAP/hyaluronectin. *J. Biomed. Sci.,* 5**,** 173-179.

CHEN, R.-H., MOSES, H. L., MARUOKA, E. M., DERYNCK, R. & KAWABATA, M. 1995. Phosphorylation-dependent interaction of the cytoplasmic domains of the type I and type II transforming growth factor-β receptors. *J. Biol. Chem.,* 270**,** 12235-12241.

CHEN, T., CARTER, D., GARRIGUE-ANTAR, L. & REISS, M. 1998c. Transforming growth factor β type I receptor kinase mutant associated with metastatic breast cancer. *Cancer Res.,* 58**,** 4805-4810.

CHEN, X., RUBOCK, M. J. & WHITMAN, M. 1996. A transcriptional partner for MAD proteins in TGF-β signalling. *Nature,* 383**,** 691-696.

CHEN, X., WEISBERG, E., FRIDMACHER, V., WATANABE, M., NACO, G. & WHITMAN, M. 1997. Smad4 and FAST-1 in the assembly of activin-responsive factor. *Nature,* 389**,** 85-89.

CHEN, Y.-G. 2009. Endocytic regulation of TGF-β signalling. *Cell Res.,* 19**,** 58-70.

CHENG, K.-H., PONTE, J. F. & THIAGALINGAM, S. 2004a. Elucidation of epigenetic inactivation of SMAD8 in cancer using targeted expressed gene display. *Cancer Res.,* 64**,** 1639-1646.

CHENG, P.-L., CHANG, M.-H., CHAO, C.-H. & LEE, Y.-H. W. 2004b. Hepatitis C viral proteins interact with Smad3 and differentially regulate TGF-β/Smad3-mediated transcriptional activation. *Oncogene,* 23**,** 7821-7838.

CHENG, T.-C., HSIEH, S.-S., HSU, W.-L., CHEN, Y.-F., HO, H.-H. & SHEU, L.-F. 2010. Expression of Epstein-Barr nuclear antigen 1 in gastric carcinoma cells is associated with enhanced tumourigenicity and reduced cisplatin sensitivity. *Int. J. Oncol.,* 36**,** 151-160.

CHENG, Y.-J., HILDESHEIM, A., HSU, M.-M., CHEN, I.-H., BRINTON, L. A., LEVINE, P. H., CHEN, C.-J. & YANG, C.-S. 1999. Cigarette smoking, alcohol consumption and risk of nasopharyngeal carcinoma in Taiwan. *Cancer Causes and Control,* 10**,** 201-207.

CHESNOKOVA, L. S., NISHIMURA, S. L. & HUTT-FLETCHER, L. M. 2009. Fusion of epithelial cells by Epstein-Barr virus proteins is triggered by binding of viral glycoproteins gHgL to integrins αvβ6 or αvβ8. *Proc. Natl. Acad. Sci USA,* 106**,** 20464-20469.

CHEUNG, F. M. F., PANG, S. W., YAU, T. K., CHOW, S. K. & LO, K. W. 2004. Nasopharyngeal intraepithelial lesion: latent Epstein-Barr virus infection with malignant potential. *Histopathology,* 45**,** 171-179.

CHEUNG, S. T., HUANG, D. P., HUI, A. B., LO, K. W., KO, C. W., TSANG, Y. S., WONG, N., WHITNEY, B. M. & LEE, J. C. 1999. Nasopharyngeal carcinoma cell line (C666-1) consistently harbouring Epstein-Barr virus. *Int. J. Cancer,* 83**,** 121-126.

CHOI, K.-Y., KIM, H.-J., LEE, M.-H., KWON, T.-G., NAH, H.-D., FURUICHI, T., KOMORI, T., NAM, S.-H., KIM, Y.-J., KIM, H.-J. & RYOO, H.-M. 2005. Runx2 regulates FGF2-induced Bmp2 expression during cranial bone development. *Developmental Dynamics,* 233**,** 115-121.

CHOI, S.-H. & HWANG, S. B. 2006. Modulation of the transforming growth factor-β signal transduction pathway by hepatitis C virus nonstructural 5A protein. *J. Biol. Chem.,* 281**,** 7468-7478.

CHOI, Y. J., KIM, S. T., PARK, K. H., OH, S. C., SEO, J. H., SHIN, S. W., KIM, J. S. & KIM, Y. H. 2011. The serum bone morphogenetic protein-2 level in non-small-cell lung cancer patients. *Med. Oncol.*

CHOY, E. Y., SIU, K. L., KOK, K. H., LUNG, R. W., TSANG, C. M., TO, K. F., KWONG, D. L., TSAO, S. W. & JIN, D. Y. 2008. An Epstein-Barr virus-encoded microRNA targets PUMA to promote host cell survival. *J. Exp. Med.,* 205**,** 2551-2560.

CLARKE, D. C., BROWN, M. L., ERICKSON, R. A., SHI, Y. & LIU, X. 2009. Transforming growth factor β depletion is the primary determinant of Smad signalling kinetics. *Mol. Cell. Biol.,* 29**,** 2443-2455.

CLARKE, P. A., SCHWEMMLE, M., SCHICKINGER, J., HILSE, K. & CLEMENS, M. J. 1991. Binding of Epstein-Barr virus small RNA EBER-1 to the double-stranded RNA-activated protein kinase DAI. *Nucleic Acid Research,* 19**,** 243-248.

CLARKE, P. A., SHARP, N. A. & CLEMENS, M. J. 1990. Translational control by the Epstein-Barr virus small RNA EBER-1: reversal of the double-stranded RNA-induced inhibition of protein synthesis in reticulocyte lysates. *Eur. J. Biochem.,* 193**,** 635-641.

CLEMENT, J. H., MARR, N., MEISSNER, A., SCHWALBE, M., SEBALD, W., KLICHE, K.-O., HÖFFKEN, K. & WÖLFL, S. 2000. Bone morphogenetic protein 2 (BMP-2) induces sequential changes of Id gene expression in the breast cancer cell line MCF-7. *J. Cancer Res. Clin. Oncol.,* 126**,** 271-279.

COCHET, C., MARTEL-RENOIR, D., GRUNEWALD, V., BOSQ, J., COCHET, G., SCHWAAB, G., BERNAUDIN, J.-F. & JOAB, I. 1993. Expression of the Epstein-Barr virus immediate early gene, BZLF1, in nasopharyngeal carcinoma tumour cells. *Virology,* 197**,** 358-365.

COFFIN III, W. F., GEIGER, T. R. & MARTIN, J. M. 2003. Transmembrane domains 1 and 2 of the latent membrane protein 1 of Epstein-Barr virus contain a lipid raft targeting signal and play a critical role in cytostasis. *J. Virol.,* 77**,** 3749-3758.

COHEN-SOLAL, K. A., MERRIGAN, K. T., CHAN, J. L. K., GOYDOS, J. S., CHEN, W., FORAN, D. J., LIU, F., LASFAR, A. & REISS, M. 2011. Constitutive Smad linker phosphorylation in melanoma: A mechanism of resistance to transforming growth factor-β-mediated growth inhibition. *Pigment Cell & Melanoma Research,* 24**,** 512-524.

COHEN, J. I., WANG, F., MANNICK, J. & KIEFF, E. 1989. Epstein-Barr virus nuclear protein 2 is a key determinant of lymphocyte transformation. *Proc. Natl. Acad. Sci USA,* 86**,** 9558-9562.

CORDIER, M., CALENDER, A., BILLAUD, M., ZIMBER, U., ROUSSELET, G., PAVLISH, O., BANCHEREAU, J., TURSZ, T., BORNKAMM, G. & LENOIR, G. M. 1990. Stable transfection of Epstein-Barr virus (EBV) nuclear antigen 2 in lymphoma cells containing the EBV P3HR1 genome induces expression of B-cell activation molecules CD21 and CD23. *J. Virol.,* 64**,** 1002-1013.

CUNY, G. D., YU, P. B., LAHA, J. K., XING, X., LIU, J.-F., LAI, C. S., DENG, D. Y., SACHIDANANDAN, C., BLOCH, K. D. & PETERSON, R. T. 2008. Structure-activity

relationship study of bone morphogenetic protein (BMP) signalling inhibitors. *Bioorganic & Medicinal Chemistry Letters,* 18**,** 4388-4392.
DAI, J., HALL, C. L., ESCARA-WILKE, J., MIZOKAMI, A., KELLER, J. M. & KELLER, E. T. 2008. Prostate cancer induces bone metastasis through Wnt-induced bone morphogenetic protein-dependent and independent mechanisms. *Cancer Res.,* 68**,** 5785-5794.
DALY, A. C., RANDALL, R. A. & HILL, C. S. 2008. Transforming growth factor β-induced Smad1/5 phosphorylation in epithelial cells is mediated by novel receptor complexes and is essential for anchorage-independent growth. *Mol. Cell. Biol.,* 28**,** 6889-6902.
DAMANIA, B. 2004. Oncogenic γ-herpesviruses: comparison of viral proteins involved in tumourigenesis. *Nat. Rev. Microbiol.,* 2**,** 656-668.
DAMANIA, B. 2006. DNA tumour viruses and human cancer. *Trends Microbiol.,* 15**,** 38-44.
DATTO, M. B., LI, Y., PANUS, J. F., HOWE, D. J., XIONG, Y. & WANG, X. F. 1995. Transforming growth factor beta induces the cyclin-dependent kinase inhibitor p21 through a p53-independent mechanism. *Proc. Natl. Acad. Sci USA,* 92**,** 5545-5549.
DAVENPORT, M. G. & PAGANO, J. S. 1999. Expression of EBNA1 mRNA is regulated by cell cycle during Epstein-Barr virus type I latency. *J. Virol.,* 73**,** 3154-3161.
DAWSON, C. W., LAVERICK, L., MORRIS, M. A., TRAMOUTANIS, G. & YOUNG, L. S. 2008. Epstein-Barr virus-encoded LMP1 regulates epithelial cell motility and invasion via the ERK-MAPK pathway. *J. Virol.,* 82**,** 3654-3664.
DAWSON, C. W., RICKINSON, A. B. & YOUNG, L. S. 1990. Epstein-Barr virus latent membrane protein inhibits human epithelial cell differentiation. *Nature,* 344**,** 777-780.
DAWSON, C. W., TRAMOUTANIS, G., ELIOPOULOS, A. G. & YOUNG, L. S. 2003. Epstein-Barr virus latent membrane protein 1 (LMP1) activates the phosphatidylinositol 3-kinase/Akt pathway to promote cell survival and induce actin filament remodelling. *J. Biol. Chem.,* 278**,** 3694-3704.
DE OLIVEIRA, D. E. 2007. DNA viruses in human cancer: an integrated overview on fundamental mechanisms of viral carcinogenesis. *Cancer Letters,* 247**,** 182-196.
DECKER, L. L., KLAMAN, L. D. & THORLEY-LAWSON, D. A. 1996. Detection of the latent form of Epstein-Barr virus DNA in the peripheral blood of healthy individuals. *J. Virol.,* 70**,** 3286-3289.
DEL CASTILLO, G., MURILLO, M. M., ÁLVAREZ-BARRIENTOS, A., BERTRAN, E., FERNÁNDEZ, M., SÁNCHEZ, A. & FABREGAT, I. 2006. Autocrine production of TGF-β confers resistance to apoptosis after an epithelial-mesenchymal transition process in hepatocytes: Role of EGF receptor ligands. *Exp. Cell Res.,* 312**,** 2860-2871.
DENG, Z., ATANASIU, C., ZHAO, K., MARMORSTEIN, R., SBODIO, J. I., CHI, N. W. & LIEBERMAN, P. M. 2005. Inhibition of Epstein-Barr virus OriP function by tankyrase, a telomere-associated poly-ADP ribose polymerase that binds and modifies EBNA1. *J. Virol.,* 79**,** 4640-4650.
DENG, Z., LEZINA, L., CHEN, C. J., SHTIVELBAND, S., SO, W. & LIEBERMAN, P. M. 2002. Telomeric proteins regulate episomal maintenance of Epstein-Barr virus origin of plasmid replication. *Mol. Cell,* 9**,** 493-503.
DENISSOVA, N. G., POUPONNOT, C., LONG, J., HE, D. & LIU, F. 2000. Transforming growth factor β-inducible independent binding of SMAD to the Smad7 promoter. *Proc. Natl. Acad. Sci USA,* 97**,** 6397-6402.
DENNLER, S., HUET, S. & GAUTHIER, J.-M. 1999. A short amino-acid sequence in MH1 domain is responsible for functional differences between Smad2 and Smad3. *Oncogene,* 18**,** 1643-1648.
DENNLER, S., ITOH, S., VIVIEN, D., TEN DIJKE, P., HUET, S. & GAUTHIER, J.-M. 1998. Direct binding of Smad3 and Smad4 to critical TGFβ-inducible elements in the promoter of human plasminogen activator inhibitor-type 1 gene. *EMBO J.,* 17**,** 3091-3100.
DENNLER, S., MAUVIEL, A. & VERRECCHIA, F. 2008. TGF-β and stromal influences over local tumour invasion. *In:* JAKOWLEW, S. B. (ed.) *Cancer Drug Discovery and Development: Transforming Growth Factor-β in Cancer Therapy.* Totowa, NJ: Humana Press Inc.
DERYNCK, R. & ZHANG, Y. E. 2003. Smad-dependent and Smad-independent pathways in TGF-β family signalling. *Nature,* 425**,** 577-584.
DEUTSCH, M. J., OTT, E., PAPIOR, P. & SCHEPERS, A. 2010. The latent origin of replication of Epstein-Barr virus directs viral genomes to active regions of the nucleus. *J. Virol.,* 84**,** 2533-2546.

DHAR, S. K., YOSHIDA, K., MACHIDA, Y., KHAIRA, P., CHAUDHURI, B., WOHLSCHLEGEL, J. A., LEFFAK, M., YATES, J. & DUTTA, A. 2001. Replication from oriP of Epstein-Barr virus requires human ORC and is inhibited by geminin. *Cell,* 106**,** 287-296.

DI BARTOLO, D. L., CANNON, M., LIU, Y.-F., RENNE, R., CHADBURN, A., BOSHOFF, C. & CESARMAN, E. 2008. KSHV LANA inhibits TGF-β signalling through epigenetic silencing of the TGF-β type II receptor. *Blood,* 111**,** 4731-4740.

DI GUGLIELMO, G. M., LE ROY, C., GOODFELLOW, A. F. & WRANA, J. L. 2003. Distinct endocytic pathways regulate TGF-β receptor signalling and turnover. *Nat. Cell Biol.,* 5**,** 410-421.

DI RENZO, L., ALTTOK, A., KLEIN, G. & KLEIN, E. 1994. Endogenous TGF-β contributes to the induction of the EBV lytic cycle in two burkitt lymphoma cell lines. *Int. J. Cancer,* 57**,** 914-919.

DIAMOND, M. E., SUN, L., OTTAVIANO, A. J., JOSEPH, M. J. & MUNSHI, H. G. 2008. Differential growth factor regulation of N-cadherin expression and motility in normal and malignant oral epithelium. *J. Cell Sci.,* 121**,** 2197-2207.

DO, T.-V., KUBBA, L. A., DU, H., STURGIS, C. D. & WOODRUFF, T. K. 2008. Transforming growth factor-β1, transforming growth factor-β2, and transforming growth factor-β3 enhance ovarian cancer metastatic potential by inducing a Smad3-dependent epithelial-mesenchymal transition. *Mol. Cancer Res.,* 6**,** 695-705.

DOLKEN, L., MALTERER, G., ERHARD, F., KOTHE, S., FRIEDEL, C. C., SUFFERT, G., MARCINOWSKI, L., MOTSCH, N., BARTH, S., BEITZINGER, M., LIEBER, D., BAILER, S. M., HOFFMAN, R., RUZSICS, Z., KREMMER, E., PFEFFER, S., ZIMMER, R., KOSZINOWSKI, U. H., GRASSER, F., MEISTER, G. & HAAS, J. 2010. Systematic analysis of viral and cellular microRNA targets in cells latently infected with human gamma-herpesviruses by RISC immunoprecipitation assay. *Cell Host. Microbe,* 7**,** 324-334.

DORÉ JR., J. J. E., YAO, D., EDENS, M., GARAMSZEGI, N., SHOLL, E. L. & LEOF, E. B. 2001. Mechanisms of transforming growth factor-β receptor endocytosis and intracellular sorting differ between fibroblasts and epithelial cells. *Mol. Biol. Cell,* 12**,** 675-684.

DRESANG, L. R., VEREIDE, D. T. & SUGDEN, B. 2009. Identifying sites bound by Epstein-Barr virus nuclear antigen 1 (EBNA1) in the human genome: defining a position-weighted matrix to predict sites bound by EBNA1 in viral genomes. *J. Virol.,* 83**,** 2930-2940.

DU, Z.-M., HU, L.-F., WANG, H.-Y., YAN, L.-X., ZENG, Y.-X., SHAO, J.-Y. & ERNBERG, I. 2011. Upregulation of miR-155 in nasopharyngeal carcinoma is partly driven by LMP1 and LMP2A and downregulates a negative prognostic marker JMJD1A. *PLoS ONE,* 6**,** e19137.

DU, Z.-M., HUM, C.-F., SHAO, Q., HUANG, M.-Y., KOU, C.-W., ZHU, X.-F., ZENG, Y.-X. & SHAO, J.-Y. 2009. Upregulation of caveolin-1 and CD147 expression in nasopharyngeal carcinoma enhanced tumour cell migration and correlated with poor prognosis of the patients. *Int. J. Cancer,* 125**,** 1832-1841.

DUCY, P. & KARSENTY, G. 2000. The family of bone morphogenetic proteins. *Kidney International,* 57**,** 2207-2214.

DUDAS, M., KIM, J., LI, W.-Y., NAGY, A., LARSSON, J., KARLSSON, S., CHAI, Y. & KAARTINEN, V. 2006. Epithelial and ectomesenchymal role of the type I TGFβ receptor ALK5 during facial morphogenesis and palatal fusion. *Develop. Biol.,* 296**,** 298-314.

DUELLMAN, S. J., THOMPSON, K. L., COON, J. J. & BURGESS, R. R. 2009. Phosphorylation sites of Epstein-Barr virus EBNA1 regulate its function. *J. Gen. Virol.,* 90**,** 2251-2259.

DUMONT, N., BAKIN, A. V. & ARTEAGA, C. L. 2003. Autocrine transforming growth factor-β signalling mediates Smad-independent motility in human cancer cells. *J. Biol. Chem.,* 278**,** 3275-3285.

DURRINGTON, H. J., UPTON, P. D., HOER, S., BONAME, J., DUNMORE, B. J., YANG, J., CRILLEY, T. K., BUTLER, L. M., BLACKBOURN, D. J., NASH, G. B., LEHNER, P. J. & MORRELL, N. W. 2010. Identification of a lysosomal pathway regulating degradation of the bone morphogenetic protein receptor type II. *J. Biol. Chem.,* 285**,** 37641-37649.

DYKSTRA, M. L., LONGNECKER, R. & PIERCE, S. K. 2001. Epstein-Barr virus coopts lipid rafts to block the signalling and antigen transport functions of the BCR. *Immunity,* 14**,** 57-67.

ELIOPOULOS, A. G., GALLAGHER, N. J., BLAKE, S. M. S., DAWSON, C. W. & YOUNG, L. S. 1999. Activation of the p38 mitogen-activated protein kinase pathway by Epstein-Barr virus-encoded

latent membrane protein 1 coregulates interleukin-6 and interleukin-8 production. *J. Biol. Chem.,* 274**,** 16085-16096.
ELIOPOULOS, A. G. & YOUNG, L. S. 1998. Activation of the cJun N-terminal kinase (JNK) pathway by the Epstein-Barr virus-encoded latent membrane protein 1 (LMP1). *Oncogene,* 16**,** 1731-1742.
ENGEL, M. E., MCDONNELL, M. A., LAW, B. K. & MOSES, H. L. 1999. Interdependent SMAD and JNK signalling in transforming growth factor-β-mediated transcription. *J. Biol. Chem.,* 274**,** 37413-37420.
EPSTEIN, M. A., ACHONG, B. G. & BARR, Y. M. 1964. Virus particles in cultured lymphoblasts from Burkitt's lymphoma. *Lancet,* 15**,** 702-703.
FAHMI, H., COCHET, C., HMAMA, Z., OPOLON, P. & JOAB, I. 2000. Transforming growth factor beta1 stimulates expression of the Epstein-Barr virus BZLF1 immediate-early gene product ZEBRA by an indirect mechanism which requires the MAPK kinase pathway. *J. Virol.,* 74**,** 5810-5818.
FAN, S.-Q., MA, J., ZHOU, J., XIONG, W., XIAO, B.-Y., ZHANG, W.-L., TAN, C., LI, X.-L., SHEN, S.-R., ZHOU, M., ZHANG, Q.-H., OU, Y.-J., ZHUA, H.-D., SONGQUING, F., ZHOU, Y.-H. & LI, G.-Y. 2006. Differential expression of Epstein-Barr virus-encoded RNA and several tumour-related genes in various types of nasopharyngeal epithelial lesions and nasopharyngeal carcinoma using tissue microarray analysis. *Hum. Pathol.,* 37**,** 593-605.
FANTINI, M. C., BECKER, C., MONTELEONE, G., PALLONE, F., GALLE, P. R. & NEURATH, M. F. 2004. Cutting edge: TGF-β induces a regulatory phenotype in CD4+CD25- T cells through Foxp3 induction and down-regulation of Smad7. *J. Immunol.,* 172**,** 5149-5153.
FEEDERLE, R., KOST, M., BAUMANN, M., JANZ, A., DROUET, E., HAMMERSCHMIDT, W. & DELECLUSE, H.-J. 2000. The Epstein-Barr virus lytic program is controlled by the co-operative functions of two transactivators. *EMBO J.,* 19**,** 3080-3089.
FEEDERLE, R., NEUHIERL, B., BANNERT, H., GELETNEKY, K., SHANNON-LOWE, C. & DELECLUSE, H.-J. 2007. Epstein-Barr virus B95.8 produced in 293 cells shows marked tropism for differentiated primary epithelial cells and reveals interindividual variation in susceptibility to viral infection. *Int. J. Cancer,* 121**,** 588-594.
FEELEY, B. T., GAMRADT, S. C., HSU, W. K., LIU, N., KRENEK, L., ROBBINS, P., HUARD, J. & LIEBERMAN, J. R. 2005. Influence of BMPs on formation of osteoblastic lesions in metastatic prostate cancer. *J. Bone Miner. Res.,* 20**,** 2189-2199.
FEELEY, B. T., KRENEK, L., LIU, N., HSU, W. K., GAMRADT, S. C., SCHWARZ, E. M., HUARD, J. & LIEBERMAN, J. R. 2006a. Overexpression of noggin inhibits BMP-mediated growth of osteolytic prostate cancer lesions. *Bone,* 38**,** 154-166.
FEELEY, B. T., LIU, N. Q., CONDUAH, A. H., KRENEK, L., ROTH, K., DOUGALL, W. C., HUARD, J., DUBINETT, S. & LIEBERMAN, J. R. 2006b. Mixed metastatic lung cancer lesions in bone are inhibited by noggin overexpression and Rank:Fc administration. *J. Bone Miner. Res.,* 21**,** 1571-1580.
FELICETTI, F., PAROLINI, I., BOTTERO, L., FECCHI, K., ERRICO, M. C., RAGGI, C., BIFFONI, M., SPADARO, F., LISANTI, M. P., SARGIACOMO, M. & CARÈ, A. 2009. Caveolin-1 tumour-promoting role in human melanoma. *Int. J. Cancer,* 125**,** 1514-1522.
FELTON-EDKINS, Z. A., KONDRASHOV, A., KARALI, D., FAIRLEY, J. A., DAWSON, C. W., ARRAND, J. R., YOUNG, L. S. & WHITE, R. J. 2006. Epstein-Barr virus induces cellular transcription factors to allow active expression of EBER genes by RNA polymerase III. *J. Biol. Chem.,* 281**,** 33871-33880.
FERLAY, J., SHIN, H. R., BRAY, F. F., D, MATHERS, C. & PARKIN, D. M. 2010. Estimates of worldwide burden of cancer in 2008: GLOBOCAN 2008. *Int. J. Cancer,* 127**,** 2893-2917.
FISCHER, N., KREMMER, E., LAUTSCHAM, G., MUELLER-LANTZSCH, N. & GRÄSSER, F. A. 1997. Epstein-Barr virus nuclear antigen 1 forms a complex with the nuclear transporter karyopherin α2. *J. Biol. Chem.,* 272**,** 3999-4005.
FLAVELL, J. R., BAUMFORTH, K. R. N., WOOD, V. H. J., DAVIES, G. L., WEI, W., REYNOLDS, G. M., MORGAN, S., BOYCE, A., KELLY, G. L., YOUNG, L. S. & MURRAY, P. G. 2008. Down-regulation of the TGF-beta target gene, PTPRK, by the Epstein-Barr virus encoded EBNA1 contributes to the growth and survival of Hodgkin lymphoma cells. *Blood,* 111**,** 292-301.

FLOETTMANN, J. E., ELIOPOULOS, A. G., JONES, M., YOUNG, L. S. & ROWE, M. 1998. Epstein-Barr virus latent membrane protein-1 (LMP1) signalling is distinct from CD40 and involves physical cooperation of its two C-terminus functional regions. *Oncogene,* 17**,** 2382-2392.

FLOETTMANN, J. E. & ROWE, M. 1997. Epstein-Barr virus latent membrane protein-1 (LMP1) C-terminus activation region 2 (CTAR2) maps to the far C-terminus and requires oligomerisation for NF-κB activation. *Oncogene,* 15**,** 1851-1858.

FOX, C., SHANNON-LOWE, C. & ROWE, M. 2011. Deciphering the role of Epstein-Barr virus in the pathogenesis of T and NK cell lymphoproliferations. *Herpesviridae*.

FRANZÉN, A. & HELDIN, N.-E. 2001. BMP-7-induced cell cycle arrest of anaplastic thyroid carcinoma cells via $p21^{CIP1}$ and $p27^{KIP1}$. *Biochem. Biophys. Res. Comm.,* 285**,** 773-781.

FRANZÉN, P., HELDIN, C.-H. & MIYAZONO, K. 1995. The GS domain of the transforming growth factor-β type I receptor is important in signal transduction. *Biochem. Biophys. Res. Comm.,* 2**,** 682-689.

FRAPPIER, L. & O'DONNELL, M. 1991. Overproduction, purification, and characterisation of EBNA1, the origin binding protein of Epstein-Barr virus. *J. Biol. Chem.,* 266**,** 7819-7826.

FRIEDMAN-KIEN, A. E. 1986. Viral origin of hairy leukoplakia. *Lancet,* 328**,** 694-695.

FRIES, K. L., MILLER, W. E. & RAAB-TRAUB, N. 1996. Epstein-Barr virus latent membrane protein 1 blocks p53-mediated apoptosis through the induction of the A20 gene. *J. Virol.,* 70**,** 8653-8659.

FRUEHLING, S. & LONGNECKER, R. 1997. The immunoreceptor tyrosine-based activation motif of Epstein-Barr virus LMP2A is essential for blocking BCR-mediated signal transduction. *Virology,* 235**,** 241-251.

FUKAI, Y., FUKUCHI, M., MASUDA, N., OSAWA, H., KATO, H., NAKAJIMA, T. & KUWANO, H. 2003. Reduced expression of transforming growth factor-β receptors is an unfavorable prognostic factor in human esophageal squamous cell carcinoma. *Int. J. Cancer,* 104**,** 161-166.

FUKASAWA, H., YAMAMOTO, T., FUJIGAKI, Y., MISAKI, T., OHASHI, N., TAKAYAMA, T., SUZUKI, S., MUGIYA, S., ODA, T., UCHIDA, C., KITAGAWA, K., HATTORI, T., HAYASHI, H., OZONO, S., KITAGAWA, M. & HISHIDA, A. 2010. Reduction of transforming growth factor-β type II receptor is caused by the enhanced ubiquitin-dependent degradation in human renal cell carcinoma. *Int. J. Cancer,* 127**,** 1517-1525.

FUKAYAMA, M. 2010. Epstein-Barr virus and gastric carcinoma. *Pathology International,* 60**,** 337-350.

FUKAYAMA, M., HINO, R. & UOZAKI, H. 2008. Epstein-Barr virus and gastric carcinoma: virus-host interactions leading to carcinoma. *Cancer Sci.,* 99**,** 1726-1733.

FUKUCHI, M., FUKAI, Y., MASUDA, N., MIYAZAKI, T., NAKAJIMA, M., SOHDA, M., MANDA, R., TSUKADA, K., KATO, H. & KUWANO, H. 2002. High-level expression of the Smad ubiquitin ligase Smurf2 correlates with poor prognosis in patients with esophageal squamous cell carcinoma. *Cancer Res.,* 62**,** 7162-7165.

FUKUCHI, M., NAKAJIMA, M., MIYAZAKI, T., MASUDA, N., OSAWA, H., MANDA, R., TSUKUDA, K., KATO, H. & KUWANO, H. 2006. Lack of activated Smad2 in transforming growth factor-beta signalling is an unfavourable prognostic factor in patients with esophageal squamous cell carcinoma. *J. Surg. Oncol.,* 94**,** 51-56.

FUKUDA, M., KUROSAKI, H. & SAIRENJI, T. 2006. Loss of functional transforming growth factor (TGF)-β type II receptor results in insensitivity to TGF-β1-mediated apoptosis and Epstein-Barr virus reactivation. *J. Med. Virol.,* 78**,** 1456-1464.

FUKUDA, M., KUROSAKI, W., YANAGIHARA, K., KURATSANE, H. & SAIRENJI, T. 2002. A mechanism in Epstein-Barr virus oncogenesis: inhibition of transforming growth factor-β1-mediated induction of MAPK/p21 by LMP1. *Virology,* 302**,** 310-320.

FUKUDA, M. & LONGNECKER, R. 2004. Latent membrane protein 2A inhibits transforming growth factor-β1-induced apoptosis through the phosphatidylinositol 3-kinase/Akt pathway. *J. Virol.,* 78**,** 1697-1705.

FUNABA, M., ZIMMERMAN, C. M. & MATHEWS, L. S. 2002. Modulation of Smad2-mediated signalling by extracellular signal-related kinase. *J. Biol. Chem.,* 277**,** 41361-41368.

GAHN, T. A. & SUGDEN, B. 1995. An EBNA-1-dependent enhancer acts from a distance of 10 kilobase pairs to increase expression of the Epstein-Barr virus LMP gene. *J. Virol.,* 69**,** 2633-2636.

GAL, A., SJÖBLOM, T., FEDOROVA, L., IMREH, S., BEUG, H. & MOUSTAKAS, A. 2008. Sustained TGFβ exposure suppresses Smad and non-Smad signalling in mammary epithelial cells, leading to EMT and inhibition of growth arrest and apoptosis. *Oncogene,* 27**,** 1218-1230.
GAO, Q., TONG, W., LURIA, J. S., WANG, Z., NUSSENBAUM, B. & KREBSBACH, P. H. 2010. Effects of bone morphogenetic protein-2 on proliferation and angiogenesis in oral squamous cell carcinoma. *Int. J. Oral Maxillofac. Surg.,* 39**,** 266-271.
GAO, S., ALARCÓN, C., SAPKOTA, G., RAHMAN, S., CHEN, P.-Y., GOERNER, N., MACIAS, M. J., ERDJUMENT-BROMAGE, H., TEMPST, P. & MASSAGUÉ, J. 2009. Ubiquitin ligase Nedd4L targets activated Smad2/3 to limit TGF-β signalling. *Mol. Cell,* 36**,** 457-468.
GE, G. & GREENSPAN, D. S. 2006. BMP1 controls TGFβ1 activation via cleavage of latent TGFβ-binding protein. *J. Cell Biol.,* 175**,** 111-120.
GHOSH-CHOUDHURY, N., GHOSH-CHOUDHURY, G., CELESTE, A., GHOSH, P. M., MOYER, M., ABBOUD, S. L. & KREISBERG, J. 2000a. Bone morphogenetic protein-2 induces cyclin kinase inhibitor p21 and hypophosphorylation of retinoblastoma protein in estradiol-treated MCF-7 human breast cancer cells. *Biochim. Biophys. Acta,* 1497**,** 186-196.
GHOSH-CHOUDHURY, N., WOODRUFF, K., QI, W., CELESTE, A., ABBOUD, S. L. & GHOSH-CHOUDHURY, G. 2000b. Bone morphogenetic protein-2 blocks MDA MB 231 human breast cancer cell proliferation by inhibiting cyclin-dependent kinase-mediated retinoblastoma protein phosphorylation. *Biochem. Biophys. Res. Comm.,* 272**,** 705-711.
GIRES, O., ZIMBER-STROBL, U., GONNELLA, R., UEFFING, M., MARSCHALL, G., ZEIDLER, R., PICH, D. & HAMMERSCHMIDT, W. 1997. Latent membrane protein 1 of Epstein-Barr virus mimics a constitutively active receptor molecule. *EMBO J.,* 16**,** 6131-6140.
GOETZ, J. G., LAJOIE, P., WISEMAN, S. M. & NABI, I. R. 2008. Caveolin-1 in tumour progression: the good, the bad and the ugly. *Cancer Metastasis Rev.,* 27**,** 715-735.
GOLD, L. I., JUSSILA, T., FUSENIG, N. E. & STENBÄACK, F. 2000. TGF-β isoforms are differentially expressed in increasing malignant grades of HaCaT keratinocytes, suggesting separate roles in skin carcinogenesis. *J. Pathol.,* 190**,** 579-588.
GOLDSMITH, D. B., WEST, T. M. & MORTON, R. 2002. HLA associations with nasopharyngeal carcinoma in Southern Chinese: a meta-analysis. *Clin. Otolaryngol.,* 27**,** 61-67.
GONG, Q., HUNTSMAN, C. & MA, D. 2008. Clathrin-independent internalization and recycling. *J. Cell. Mol. Med.,* 12**,** 126-144.
GOUMANS, M.-J., VALDIMARSDOTTIR, G., ITOH, S., LEBRIN, F., LARSSON, J., MUMMERY, C., KARLSSON, S. & TEN DIJKE, P. 2003. Activin receptor-like kinase (ALK)1 is an antagonistic mediator of lateral TGFβ/ALK5 signalling. *Mol. Cell,* 12**,** 817-828.
GOUMANS, M.-J., VALDIMARSDOTTIR, G., ITOH, S., ROSENDAHL, A., SIDERAS, P. & TEN DIJKE, P. 2002. Balancing the activation state of the endothelium via two distinct TGF-β type I receptors. *EMBO J.,* 21**,** 1743-1753.
GOURZONES, C., KLIBI, J., FRIBOULET, L., JLIDI, R. & BUSSON, P. 2011. Cellular interactions in nasopharyngeal carcinomas. *In:* BUSSON, P. (ed.) *Nasopharyngeal Carcinomas.* Landes Bioscience and Springer Science+Business Media.
GRADY, W. M., MYEROFF, L. L., SWINLER, S. E., RAJPUT, A., THIAGALINGAM, S., LUTTERBAUGH, J. D., NEUMANN, A., BRATTAIN, M. G., CHANG, J., KIM, S.-J., KINZLER, K. W., VOGELSTEIN, B., WILLSON, J. K. V. & MARKOWITZ, S. 1999. Mutational inactivation of transforming growth factor β receptor type II in microsatellite stable colon cancers. *Cancer Res.,* 59**,** 320-324.
GRAFF, J. M., BANSAL, A. & MELTON, D. A. 1996. Xenopus Mad proteins transduce distinct subsets of signals for the TGFβ superfamily. *Cell,* 85**,** 479-487.
GRAHAM, J. P., ARCIPOWSKI, K. M. & BISHOP, G. A. 2010. Differential B-lymphocyte regulation by CD40 and its viral mimic, latent membrane protein 1. *Immunol. Rev.,* 237**,** 226-248.
GREENSPAN, D., CONANT, M., SILVERMAN JR., S., GREENSPAN, J. S., PETERSEN, V. & DE SOUZA, Y. 1984. Oral "hairy" leucoplakia in male homosexuals: evidence of association with both papillomavirus and a herpes-group virus. *Lancet,* 324**,** 831-834.
GROPPE, J., GREENWALD, J., WIATER, E., RODRIGUEZ-LEON, J., ECONOMIDES, A. N., KWIATKOWSKI, W., AFFOLTER, M., VALE, W. W., BELMONTE, J. C. I. & CHOE, S. 2002.

Structural basis of BMP signalling inhibition by the cysteine knot protein Noggin. *Nature,* 420**,** 636-642.
GROPPE, J., HINCK, C. S., SAMAVARCHI-TEHRANI, P., ZUBIETA, C., SCHUERMANN, J. P., TAYLOR, A. B., SCHWARZ, P. M., WRANA, J. L. & HINCK, A. P. 2008. Cooperative assembly of TGF-β superfamily signalling complexes is mediated by two disparate mechanisms and distinct modes of receptor binding. *Mol. Cell,* 29**,** 157-168.
GROSSMAN, S. R., JOHANNSEN, E., TONG, X., YALAMANCHILI, R. & KIEFF, E. 1994. The Epstein-Barr virus nuclear antigen 2 transactivator is directed to response elements by the Jκ recombination signal binding protein. *Proc. Natl. Acad. Sci USA,* 91**,** 7568-7572.
GRULICH, A. E., MCCREDIE, M. & COATES, M. 1995. Cancer incidence in Asian migrants to New South Wales, Australia. *Br. J. Cancer,* 71**,** 400-408.
GRUNDHOFF, A., SULLIVAN, C. S. & GANEM, D. 2006. A combined computational and microarray-based approach identifies novel microRNAs encoded by human gamma-herpesviruses. *RNA,* 12**,** 733-750.
GUO, X., JOHNSON, R. C., DENG, H., LIAO, J., GUAN, L., NELSON, G. W., TANG, M., ZHENG, Y., DE THÉ, G., O'BRIEN, S. J., WINKLER, C. A. & ZENG, Y. 2009. Evaluation of nonviral risk factors for nasopharyngeal carcinoma in a high-risk population of Southern China. *Int. J. Cancer,* 124**,** 2942-2947.
GUO, X., LUI, W.-O., QIAN, C.-N., CHEN, J.-D., GRAY, S. G., RHODES, D., HAAB, B., STANBRIDGE, E., WANG, H., HONG, M.-H., MIN, H.-Q., LARSSON, C. & TEH, B. T. 2002. Identifying cancer-related genes in nasopharyngeal carcinoma cell lines using DNA and mRNA expression profiling analyses. *Int. J. Oncol.,* 21**,** 1197-1204.
GUO, X., WADDELL, D. S., WANG, W., WANG, Z., LIBERATI, N. T., YONG, S., LIU, X. & WANG, X.-F. 2008. Ligand-dependent ubiquitination of Smad3 is regulated by casein kinase 1 gamma 2, an inhibitor of TGF-β signalling. *Oncogene,* 27**,** 7235-7247.
GUO, X. & WANG, X.-F. 2009. Signalling cross-talk between TGF-β/BMP and other pathways. *Cell Res.,* 19**,** 71-88.
HADINOTO, V., SHAPIRO, M., SUN, C. C. & THORLEY-LAWSON, D. A. 2009. The dynamics of EBV shedding implicate a central role for epithelial cells in amplifying viral output. *PLoS Pathogens,* 5**,** e1000496.
HAMMERSCHMIDT, W. & SUGDEN, B. 1989. Genetic analysis of immortalising functions of Epstein-Barr virus in human B lymphocytes. *Nature,* 340**,** 393-397.
HANAHAN, D. & WEINBERG, R. A. 2000. The hallmarks of cancer. *Cell,* 100**,** 57-70.
HANNIGAN, A., SMITH, P., KALNA, G., LO NIGRO, C., ORANGE, C., O'BRIEN, D. I., SHAH, R., SYED, N., SPENDER, L. C., HERRERA, B., THURLOW, J. K., LATTANZIO, L., MONTEVERDE, M., MAURER, M. E., BUFFA, F. M., MANN, J., CHU, D. C. K., WEST, C. M. L., PATRIDGE, M., OIEN, K. A., COOPER, J. A., FRAME, M. C., HARRIS, A. L., HILLER, L., NICHOLSON, L. J., GASCO, M., CROOK, T. & INMAN, G. J. 2010. Epigenetic downregulation of human disabled homolog 2 switches TGF-β from a tumour suppressor to a tumour promoter. *J. Clin. Invest.,* 120**,** 2842-2857.
HANYU, A., ISHIDOU, Y., EBISAWA, T., SHIMANUKI, T., IMAMURA, T. & MIYAZONO, K. 2001. The N domain of Smad7 is essential for specific inhibition of transforming growth factor-β signalling. *J. Cell Biol.,* 155**,** 1017-1028.
HARN, H.-J., FAN, H.-C., CHEN, C.-J., TSAI, N.-M., YEN, C.-Y. & HUANG, S.-C. 2002. Microsatellite alteration at chromosome 11 in primary human nasopharygeal carcinoma in Taiwan. *Oral Oncology,* 38**,** 23-29.
HARTUNG, A., BITTON-WORMS, K., MOULER RECHTMAN, M., WENZEL, V., BOERGERMANN, J. H., HASSEL, S., HENIS, Y. I. & KNAUS, P. 2006. Different routes of bone morphogenic protein (BMP) receptor endocytosis influence BMP signalling. *Mol. Cell. Biol.,* 26**,** 7791-7805.
HATA, A., LAGNA, G., MASSAGUÉ, J. & HEMMATI-BRIVANLOU, A. 1998. Smad6 inhibits BMP/Smad1 signalling by specifically competing with the Smad4 tumour suppressor. *Genes Dev.,* 12**,** 186-197.
HATAKEYAMA, S., GAO, Y.-H., OHARA-NEMOTO, Y., KATAOKA, H. & SATOH, M. 1997. Expression of bone morphogenetic proteins of human neoplastic epithelial cells. *Biochemistry and Molecular Biology International,* 42**,** 497-505.

HAYASHI, H., ABDOLLAH, S., QIU, Y., CAI, J., XU, Y.-Y., GRINNELL, B. W., RICHARDSON, M. A., TOPPER, J. N., GIMBRONE, M. A., WRANA, J. L. & FALB, D. 1997. The MAD-related protein Smad7 associates with the TGFβ receptor and functions as an antagonist of TGFβ signalling. *Cell,* 89**,** 1165-1173.

HAYES, S., CHAWLA, A. & CORVERA, S. 2002. TGFβ receptor internalization into EEA1-enriched early endosomes: role in signalling to Smad2. *J. Cell Biol.,* 158**,** 1239-1249.

HAYWARD, S. D., NOGEE, L. & HAYWARD, G. S. 1980. Organisation of repeated regions within the Epstein-Barr virus DNA molecule. *J. Virol.,* 33**,** 507-521.

HAZAMA, M., AONO, A., UENO, N. & FUJISAWA, Y. 1995. Efficient expression of a heterodimer of bone morphogenetic protein subunits using a baculovirus expression system. *Biochem. Biophys. Res. Comm.,* 209**,** 859-866.

HEARING, J. C. & LEVINE, A. J. 1985. The Epstein-Barr virus nuclear antigen (BamHI K antigen) is a single-stranded DNA binding phosphoprotein. *Virology,* 145**,** 105-116.

HELDIN, C.-H. & TEN DIJKE, P. 1999. SMAD destruction turns off signalling. *Nat. Cell Biol.,* 1**,** E195-E197.

HELDIN, C. H., LANDSTRÖM, M. & MOUSTAKAS, A. 2009. Mechanisms of TGF-β signalling to growth arrest, apoptosis, and epithelial-mesenchymal transition. *Curr. Opin. Cell Biol.,* 21**,** 1-11.

HELDIN, N.-E., BERGSTRÖM, D., HERMANSSON, A., BERGENSTRÅHLE, A., NAKAO, A., WESTERMARK, B. & TEN DIJKE, P. 1999. Lack of responsiveness to TGF-β1 in a thyroid carcinoma cell line with functional type I and type II TGF-β receptors and Smad proteins, suggests a novel mechanism for TGF-β insensitivity in carcinoma cells. *Mol. Cell. Endocrinol.,* 153**,** 79-90.

HELLER, L. C., LI, Y., ABRAMS, K. L. & ROGERS, M. B. 1999. Transcriptional regulation of the *Bmp2* gene. *J. Biol. Chem.,* 274**,** 1394-1400.

HELMS, M. W., PACKEISEN, J., AUGUST, C., SCHITTEK, B., BOECKER, W., BRANDT, B. H. & BUERGER, H. 2005. First evidence supporting a potential role for the BMP/SMAD pathway in the progression of oestrogen receptor-positive breast cancer. *J. Pathol.,* 206**,** 366-376.

HELVERING, L. M., SHARP, R. L., OU, X. & GEISER, A. G. 2000. Regulation of the promoters for the human bone morphogenetic protein 2 and 4 genes. *Gene,* 256**,** 123-138.

HENDERSON, S., ROWE, M., GREGORY, C., CROOM-CARTER, D., WANG, F., LONGNECKER, R., KIEFF, E. & RICKINSON, A. 1991. Induction of bcl-2 expression by Epstein-Barr virus latent membrane protein 1 protects infected B cells from programmed cell death. *Cell,* 65**,** 1107-1115.

HENKEL, T., LING, P. D., HAYWARD, S. D. & PETERSON, M. G. 1994. Mediation of Epstein-Barr virus EBNA2 transactivation by recombination signal-binding protein Jκ. *Science,* 265**,** 92-95.

HENLE, G. & HENLE, W. 1976. Epstein-Barr virus-specific IgA serum antibodies as an outstanding feature of nasopharyngeal carcinoma. *Int. J. Cancer,* 17**,** 1-7.

HENLE, G., HENLE, W. & DIEHL, V. 1968. Relation of Burkitt's tumour-associated herpes-type virus to infectious mononucleosis. *Proc. Natl. Acad. Sci USA,* 59**,** 94-101.

HERPIN, A., LELONG, C. & FAVREL, P. 2004. Transforming growth factor-β-related proteins: an ancestral and widespread superfamily of cytokines in metazoans. *Developmental & Comparative Immunology,* 28**,** 461-485.

HILDESHEIM, A., ANDERSON, L. M., CHEN, C.-J., CHENG, Y.-J., BRINTON, L. A., DALY, A. K., REED, C. D., CHEN, I.-H., CAPORASO, N. E., HSU, M.-M., CHEN, J.-Y., IDLE, J. R., HOOVER, R. N., YANG, C.-S. & CHHABRA, S. K. 1997. CYP2E1 genetic polymorphisms and risk of nasopharyngeal carcinoma in Taiwan. *J. Natl. Cancer Inst.,* 89**,** 1207-1212.

HILDESHEIM, A., CHEN, C.-J., CAPORASO, N. E., CHENG, Y.-J., HOOVER, R. N., HSU, M.-M., LEVINE, P. H., CHEN, I.-H., CHEN, J.-Y., YANG, C.-S., DALY, A. K. & IDLE, J. R. 1995. Cytochrome P4502E1 genetic polymorphisms and risk of nasopharyngeal carcinoma: results from a case-control study conducted in Taiwan. *Cancer Epidemiol. Biomarkers Prev.,* 4**,** 607-610.

HILDESHEIM, A., DOSEMECI, M., CHAN, C.-C., CHEN, C.-J., CHENG, Y.-J., HSU, M.-M., CHEN, I.-H., MITTL, B. F., SUN, B., LEVINE, P. H., CHEN, J.-Y., BRINTON, L. A. & YANG, C.-S. 2001. Occupational exposure to wood, formaldehyde, and solvents and risk of nasopharyngeal carcinoma. *Cancer Epidemiol. Biomarkers Prev.,* 10**,** 1145-1153.

HILDESHEIM, A. & LEVINE, P. H. 1993. Etiology of nasopharyngeal carcinoma: a review. *Epidemiologic Reviews,* 15**,** 466-485.

HIPPOCRATE, A., OUSSAIEF, L. & JOAB, I. 2011. Possible role of EBV in breast cancer and other unusually EBV-associated cancers. *Cancer Letters,* 305**,** 144-149.
HO, H. C., NG, M. H., KWAN, H. C. & CHAU, J. C. W. 1976. Epstein-Barr virus-specific IgA and IgG serum antibodies in nasopharyngeal carcinoma. *Br. J. Cancer,* 34**,** 655-660.
HO, J. H. C., HUANG, D. P. & FONG, Y. Y. 1978. Salted fish and nasopharyngeal carcinoma in Southern Chinese. *Lancet,* 2**,** 626.
HOGAN, B. L. M. 1996. Bone morphogenetic proteins: multifunctional regulators of vertebrate development. *Genes Dev.,* 10**,** 1580-1594.
HOLLNAGEL, A., OEHLMANN, V., HEYMER, J., RÜTHER, U. & NORDHEIM, A. 1999. *Id* genes are direct targets of bone morphogenetic protein induction in embryonic stem cells. *J. Biol. Chem.,* 274**,** 19838-19845.
HOLOWATY, M. N. & FRAPPIER, L. 2004. HAUSP/USP7 as an Epstein-Barr virus target. *Biochem. Soc. Trans.,* 32**,** 731-732.
HOLOWATY, M. N., ZEGHOUF, M., WU, H., TELLAM, J., ATHANASOPOULOS, V., GREENBLATT, J. & FRAPPIER, L. 2003. Protein profiling with Epstein-Barr nuclear antigen 1 reveals an interaction with the herpesvirus-associated ubiquitin-specific protease HAUSP/USP7. *J. Biol. Chem.,* 278**,** 29987-29994.
HONG, G. K., GULLEY, M. L., FENG, W.-H., DELECLUSE, H.-J., HOLLEY-GUTHRIE, E. & KENNEY, S. C. 2005. Epstein-Barr virus lytic infection contributes to lymphoproliferative disease in a SCID mouse model. *J. Virol.,* 79**,** 13993-14003.
HORNDASCH, M., RASCHKE, E. E., BOMMER, G., SCHUHMACHER, M., DUMONT, E., KUKLIK-ROOS, C., EICK, D. & KEMPKES, B. 2002. Epstein-Barr virus antagonizes the antiproliferative activity of transforming growth factor-β but does not abolish its signalling. *Int. J. Cancer,* 101**,** 442-447.
HOWE, J. G. & STEITZ, J. A. 1986. Localisation of Epstein-Barr virus-encoded small RNAs by in situ hybridisation. *Proc. Natl. Acad. Sci USA,* 83**,** 9006-9010.
HSU, M.-Y., ROVINSKY, S. A., LAI, C.-Y., QASEM, S., LIU, X., HOW, J., ENGELHARDT, J. F. & MURPHY, G. F. 2008. Aggressive melanoma cells escape from BMP7-mediated autocrine growth inhibition through coordinated Noggin upregulation. *Lab. Invest.,* 88**,** 842-855.
HU, C. 2010. *Genetic and gene expression analysis of nasopharyngeal carcinoma (NPC).* Ph.D. thesis, University of Birmingham.
HUANG, Y.-T., SHEEN, T.-S., CHEN, C.-L., LU, J., CHANG, Y., CHEN, J.-Y. & TSAI, C.-H. 1999. Profile of cytokine expression in nasopharygeal carcinomas: a distinct expression of interleukin 1 in tumour and $CD4^+$ T cells. *Cancer Res.,* 59**,** 1599-1605.
HUMME, S., REISBACH, G., FEEDERLE, R., DELECLUSE, H.-J., BOUSSET, K., HAMMERSCHMIDT, W. & SCHEPERS, A. 2003. The EBV nuclear antigen 1 (EBNA1) enhances B cell immortalisation several thousandfold. *Proc. Natl. Acad. Sci USA,* 100**,** 10989-10994.
IDE, H., YOSHIDA, T., MATSUMOTO, N., AOKI, K., OSADA, Y., SUGIMURA, T. & TERADA, M. 1997. Growth regulation of human prostate cancer cells by bone morphogenetic protein-2. *Cancer Res.,* 57**,** 5022-5027.
IDKOWIAK-BALDYS, J., BALDYS, A., RAYMOND, J. R. & HANNUN, Y. A. 2009. Sustained receptor stimulation leads to sequestration of recycling endosomes in a classical protein kinase C- and phospholipase D-dependent manner. *J. Biol. Chem.,* 284**,** 22322-22331.
IEMPRIDEE, T., DAS, S., XU, I. & MERTZ, J. E. 2011. Transforming growth factor β-induced reactivation of Epstein-Barr virus involves multiple Smad-binding elements cooperatively activating expression of the latent-lytic switch BZLF1 gene. *J. Virol.,* 85**,** 7836-7848.
IKEDA, M., IKEDA, A., LONGAN, L. C. & LONGNECKER, R. 2000. The Epstein-Barr virus latent membrane protein 2A PY motif recruits WW domain-containing ubiquitin-protein ligases. *Virology,* 268**,** 178-191.
IKUSHIMA, H. & MIYAZONO, K. 2010. Cellular context-dependent "colours" of transforming growth factor-β signalling. *Cancer Sci.,* 101**,** 306-312.
IMAI, S., KOIZUMI, S., SUGIURA, M., TOKUNAGA, M., UEMURA, Y., YAMAMOTO, N., TANAKA, S., SATO, E. & OSATO, T. 1994. Gastric carcinoma: monoclonal epithelial malignant

cells expressing Epstein-Barr virus latent infection protein. *Proc. Natl. Acad. Sci USA,* 91**,** 9131-9135.
IMAI, S., NISHIKAWA, J. & TAKADA, K. 1998. Cell-to-cell contact as an efficient mode of Epstein-Barr virus infection of diverse human epithelial cells. *J. Virol.,* 72**,** 4371-4378.
IMAMURA, T., TAKASE, M., NISHIHARA, A., OEDA, E., HANAI, J.-I., KAWABATA, M. & MIYAZONO, K. 1997. Smad6 inhibits signalling by the TGF-β superfamily. *Nature,* 389**,** 622-626.
INMAN, G. J. & ALLDAY, M. J. 2000. Resistance to TGF-β1 correlates with a reduction of TGF-β type II receptor expression in Burkitt's lymphoma and Epstein-Barr virus-transformed B lymphoblastoid cell lines. *J. Gen. Virol.,* 81**,** 1567-1578.
ISHISAKI, A., YAMATO, K., HASHIMOTO, S., NAKAO, A., TAMAKI, K., NONAKA, K., TEN DIJKE, P., SUGINO, H. & NISHIHARA, T. 1999. Differential inhibition of Smad6 and Smad7 on bone morphogenetic protein- and activin-mediated growth arrest and apoptosis in B cells. *J. Biol. Chem.,* 274**,** 13637-13642.
ITO, S., IKEDA, M., KATO, N., MATSUMOTO, A., ISHIKAWA, Y., KUMAKUBO, S. & YANAGI, K. 2000. Epstein-Barr virus nuclear antigen-1 binds to nuclear transporter karyopherin α1/NPI-1 in addition to karyopherin α2/Rch1. *Virology,* 266**,** 110-119.
ITOH, F., DIVECHA, N., BROCKS, L., OOMEN, L., JANSSEN, H., CALAFAT, J., ITOH, S. & TEN DIJKE, P. 2002. The FYVE domain in Smad anchor for receptor activation (SARA) is sufficient for localization of SARA in early endosomes and regulates TGF-β/Smad signalling. *Genes to Cells,* 7**,** 321-331.
ITOH, S., LANDSTRÖM, M., HERMANSSON, A., ITOH, F., HELDIN, C.-H., HELDIN, N.-E. & TEN DIJKE, P. 1998. Transforming growth factor β1 induces nuclear export of inhibitory Smad7. *J. Biol. Chem.,* 273**,** 29195-29201.
ITOH, S. & TEN DIJKE, P. 2007. Negative regulation of TGF-β receptor/Smad signal transduction. *Curr. Opin. Cell Biol.,* 19**,** 176-184.
JAKOWLEW, S. B. 2006. Transforming growth factor-β in cancer and metastasis. *Cancer Metastasis Rev.,* 25**,** 435-457.
JANSEN-DÜRR, P. 1996. How viral oncogenes make the cell cycle. *TIG,* 12**,** 270-275.
JAT, P. & ARRAND, J. R. 1982. In vitro transcription of two Epstein-Barr virus specified small RNA molecules. *Nucleic Acid Research,* 10**,** 3407-3425.
JAVELAUD, D. & MAUVIEL, A. 2004. Mammalian transforming growth factor-βs: Smad signalling and physio-pathological roles. *Int. J. Biochem. Cell Biol.,* 36**,** 1161-1165.
JAVELAUD, D. & MAUVIEL, A. 2005. Crosstalk mechanisms between the mitogen-activated protein kinase pathways and Smad signalling downstream of TGF-β: implications for carcinogenesis. *Oncogene,* 24**,** 5742-5750.
JAVIER, R. T. & BUTEL, J. S. 2008. The history of tumour virology. *Cancer Res.,* 68**,** 7693-7706.
JENKINS, G. 2008. The role of proteases in transforming growth factor-β activation. *Int. J. Biochem. Cell Biol.,* 40**,** 1068-1078.
JIA, W.-H., FENG, B.-J., XU, Z.-L., ZHANG, X.-S., HUANG, P., HUANG, L.-X., YU, X.-J., FENG, Q.-S., YAO, M.-H., SHUGART, Y. Y. & ZENG, Y.-X. 2004. Familial risk and clustering of nasopharyngeal carcinoma in Guangdong, China. *Cancer,* 101**,** 363-369.
JIN, Y., TIPOE, G. L., LIONG, E. C., LAU, T. Y. H., FUNG, P. C. W. & LEUNG, K. M. 2001. Overexpression of BMP-2/4, -5 and BMPR-IA associated with malignancy of oral epithelium. *Oral Oncology,* 37**,** 225-233.
JONES, R. J., SMITH, L. J., DAWSON, C. W., HAIGH, T. A., BLAKE, N. W. & YOUNG, L. S. 2003. Epstein-Barr virus nuclear antigen 1 (EBNA1) induced cytotoxicity in epithelial cells is associated with EBNA1 degradation and processing. *Virology,* 313**,** 663-676.
JOSSO, N. & DI CLEMENTE, N. 1997. Serine/threonine kinase receptors and ligands. *Curr. Opin. Gen. Dev.,* 7**,** 371-377.
KAISER, C., LAUX, G., EICK, D., JOCHNER, N., BORNKAMM, G. W. & KEMPKES, B. 1999. The proto-oncogene c-myc is a direct target gene of Epstein-Barr virus nuclear antigen 2. *J. Virol.,* 73**,** 4481-4484.
KALLAND, K.-H., KE, X.-S. & ØYAN, A. M. 2009. Tumour virology - history, status and future challenges. *APMIS,* 117**,** 382-399.

KAMARAJU, A. K. & ROBERTS, A. B. 2005. Role of Rho/ROCK and p38 MAP kinase pathways in transforming growth factor-β-mediated Smad-dependent growth inhibition of human breast carcinoma cells *in vitro*. *J. Biol. Chem.,* 280**,** 1024-1036.
KAMYNINA, E., DEBONNEVILLE, C., BENS, M., VANDEWALLE, A. & STAUB, O. 2001. A novel mouse Nedd4 protein suppresses the activity of the epithelial Na+ channel. *FASEB J.,* 15**,** 204-214.
KANG, G. H., LEE, S., KIM, W. H., LEE, H. W., KIM, J. C., RHYU, M.-G. & RO, J. Y. 2002. Epstein-Barr virus-positive gastric carcinoma demonstrates frequent aberrant methylation of multiple genes and constitutes CpG island methylator phenotype-positive gastric carcinoma. *Am. J. Pathol.,* 160**,** 787-794.
KANG, M.-S., LEE, E. K., SONI, V., LEWIS, T. A., KOEHLER, A. N., SRINIVASAN, V. & KIEFF, E. 2011. Roscovitine inhibits EBNA1 serine 393 phosphorylation, nuclear localisation, transcription, and episome maintenance. *J. Virol.,* 85**,** 2859-2868.
KANG, M.-S., LU, H., YASUI, T., SHARPE, A., WARREN, H., CAHIR-MCFARLAND, E., BRONSON, R., HUNG, S. C. & KIEFF, E. 2005. Epstein-Barr virus nuclear antigen 1 does not induce lymphoma in transgenic FVB mice. *Proc. Natl. Acad. Sci USA,* 102**,** 820-825.
KANG, M.-S., SONI, V., BRONSON, R. & KIEFF, E. 2008. Epstein-Barr virus nuclear antigen 1 does not cause lymphoma in C57BL/6J mice. *J. Virol.,* 82**,** 4180-4183.
KANG, M. H., KANG, H. N., KIM, J. L., KIM, J. S., OH, S. C. & YOO, Y. A. 2009. Inhibition of PI3 kinase/Akt pathway is required for BMP2-induced EMT and invasion. *Oncology Reports,* 22**,** 525-534.
KANG, Y. 2006. Pro-metastasis function of TGFβ mediated by the Smad pathway. *J. Cell Biochem.,* 98**,** 1380-1390.
KANG, Y., CHEN, C.-R. & MASSAGUÉ, J. 2003a. A self-enabling TGFβ response coupled to stress signalling: Smad engages stress response factor ATF3 for Id1 repression in epithelial cells. *Mol. Cell,* 11**,** 915-926.
KANG, Y., SIEGEL, P. M., SHU, W., DROBNJAK, M., KAKONEN, S. M., CORDÓN-CARDO, C., GUISE, T., A & MASSAGUÉ, J. 2003b. A multigenic program mediating breast cancer metastasis to bone. *Cancer Cell,* 3**,** 537-549.
KAPOOR, P. & FRAPPIER, L. 2003. EBNA1 partitions Epstein-Barr virus plasmids in yeast cells by attaching to human EBNA1-binding protein 2 on mitotic chromosomes. *J. Virol.,* 77**,** 6946-6956.
KARIMI, L., CRAWFORD, D. H., SPECK, S. & NICHOLSON, L. J. 1995. Identification of an epithelial cell differentiation responsive region within the BZLF1 promoter of the Epstein-Barr virus. *J. Gen. Virol.,* 76**,** 759-765.
KATAGIRI, T., YAMAGUCHI, A., KOMAKI, M., ABE, E., TAKAHASHI, N., IKEDA, T., ROSEN, V., WOZNEY, J. M., FUJISAWA-SEHARA, A. & SUDA, T. 1994. Bone morphogenetic protein-2 converts the differentiation pathway of C2C12 myoblasts into the osteoblast lineage. *J. Cell Biol.,* 127**,** 1755-1766.
KATSUNO, Y., HANYU, A., KANDA, H., ISHIKAWA, Y., AKIYAMA, F., IWASE, T., OGATA, E., EHATA, S., MIYAZONO, K. & IMAMURA, T. 2008. Bone morphogenetic protein signalling enhances invasion and bone metastasis of breast cancer cells through Smad pathway. *Oncogene,* 27**,** 6322-6333.
KAVSAK, P., RASMUSSEN, R. K., CAUSING, C. G., BONNI, S., ZHU, H., THOMSEN, G. H. & WRANA, J. L. 2000. Smad7 binds to Smurf2 to form an E3 ubiquitin ligase that targets the TGFβ receptor for degradation. *Mol. Cell,* 6**,** 1365-1375.
KAWABATA, M., IMAMURA, T. & MIYAZONO, K. 1998a. Signal transduction by bone morphogenetic proteins. *Cytokine Growth Factor Rev.,* 9**,** 49-61.
KAWABATA, M., INOUE, H., HANYU, A., IMAMURA, T. & MIYAZONO, K. 1998b. Smad proteins exist as monomers in vivo and undergo homo- and hetero-oligomerisation upon activation by serine/threonine kinase receptors. *EMBO J.,* 17**,** 4056-4065.
KAYE, K. M., IZUMI, K. M. & KIEFF, E. 1993. Epstein-Barr virus latent membrane protein 1 is essential for B-lymphocyte growth transformation. *Proc. Natl. Acad. Sci USA,* 90**,** 9150-9154.
KAYKAS, A., WORRINGER, K. & SUGDEN, B. 2001. CD40 and LMP-1 both signal from lipid rafts but LMP-1 assembles a distinct, more efficient signalling complex. *EMBO J.,* 20**,** 2641-2654.
KELLY, G., BELL, A. & RICKINSON, A. 2002. Epstein-Barr virus-associated Burkitt lymphomagenesis selects for downregulation of the nuclear antigen EBNA2. *Nat. Med.,* 8**,** 1098-1104.

KENNEDY, G., KOMANO, J. & SUGDEN, B. 2003. Epstein-Barr virus provides a survival factor to Burkitt's lymphoma. *Proc. Natl. Acad. Sci USA,* 100**,** 14269-14274.
KHALIL, N. 1999. TGF-β: from latent to active. *Microbes and Infection,* 1**,** 1255-1263.
KHAN, G., MIYASHITA, E. M., YANG, B., BABCOCK, G. J. & THORLEY-LAWSON, D. A. 1996. Is EBV persistence in vivo a model for B cell homeostasis? *Immunity,* 5**,** 173-179.
KIEFF, E. D. & RICKINSON, A. B. 2007. Epstein-Barr virus and its replication. *In:* KNIPE, D. M. & HOWLEY, P. M. (eds.) *Fields Virology.* 5th ed.: Lippincott Williams & Wilkins.
KIESER, A. 2007. Signal transduction by the Epstein-Barr virus oncogene latent membrane protein 1 (LMP1). *Signal Transduction,* 7**,** 20-33.
KILGER, E., KIESER, A., BAUMANN, M. & HAMMERSCHMIDT, W. 1998. Epstein-Barr virus-mediated B-cell proliferation is dependent upon latent membrane protein 1, which stimulates an activated CD40 receptor. *EMBO J.,* 17**,** 1700-1709.
KIM, A. L., MAHER, M., HAYMAN, J. B., OZER, J., ZERBY, D., YATES, J. L. & LIEBERMAN, P. M. 1997a. An imperfect correlation between DNA replication activity of Epstein-Barr virus nuclear antigen 1 (EBNA1) and binding to the nuclear import receptor, Rch1/importin α. *Virology,* 239**,** 340-351.
KIM, D. H., CHANG, J. H., LEE, K. H., LEE, H.-Y. & KIM, S.-J. 1997b. Mechanism of E1A-induced transforming growth factor-β (TGF-β) resistance in mouse keratinocytes involves repression of TGF-β type II receptor transcription. *J. Biol. Chem.,* 272**,** 688-694.
KIM, I. Y. & AHN, H. J. Z., D J 1996. Genetic change in transforming growth factor β (TGF-β) receptor type I gene correlates with insensitivity to TGF-β1 in human prostate cancer cells. *Cancer Res.,* 56**,** 44-48.
KIM, I. Y., LEE, D.-H., AHN, H.-J., TOKUNAGA, H., SONG, W., DEVEREAUX, L. M., JIN, D., SAMPATH, T. K. & MORTON, R. A. 2000a. Expression of bone morphogenetic protein receptors type-IA, -IB and -II correlates with tumour grade in human prostate cancer tissues. *Cancer Res.,* 60**,** 2840-2844.
KIM, I. Y., LEE, D.-H., LEE, D. K., KIM, W. J., KIM, M. M., MORTON, R. A., LERNER, S. P. & KIM, S. J. 2004. Restoration of bone morphogenetic protein receptor type II expression leads to a decreased rate of tumour growth in bladder transitional cell carcinoma cell line TSU-Pr1. *Cancer Res.,* 64**,** 7355-7360.
KIM, K. R., YOSHIZAKI, T., MIYAMORI, H., HASEGAWA, K., HORIKAWA, T., FURUKAWA, M., HARADA, S., SEIKI, M. & SATO, H. 2000b. Transformation of Madin-Darby canine kidney (MDCK) epithelial cells by Epstein-Barr virus latent membrane protein 1 (LMP1) induces expression of Ets1 and invasive growth. *Oncogene,* 19**,** 1764-1771.
KIM, S.-J., IM, Y.-H., MARKOWITZ, S. D. & BANG, Y.-J. 2000c. Molecular mechanisms of inactivation of TGF-β receptors during carcinogenesis. *Cytokine Growth Factor Rev.,* 11**,** 159-168.
KIM, S., LEE, Y., SEO, J. E., CHO, K. H. & CHUNG, J. H. 2008. Caveolin-1 increases basal and TGF-β1-induced expression of type I procollagen through PI-3 kinase/Akt/mTOR pathway in human dermal fibroblasts. *Cell Signal.,* 20**,** 1313-1319.
KING, H., LI, J.-Y., LOCKE, F. B., POLLACK, E. S. & TU, J.-T. 1985. Patterns of site-specific displacement in cancer mortality among migrants: the Chinese in the United States. *Am. J. Public Health,* 75**,** 237-242.
KINTNER, C. R. & SUGDEN, B. 1979. The structure of the termini of the DNA of Epstein-Barr virus. *Cell,* 17**,** 661-671.
KIRCHMAIER, A. L. & SUGDEN, B. 1997. Dominant-negative inhibitors of EBNA-1 of Epstein-Barr virus. *J. Virol.,* 71**,** 1766-1775.
KITAMURA, R., SEKIMOTO, T., ITO, S., HARADA, S., YAMAGATA, H., MASAI, H., YONEDA, Y. & YANAGI, K. 2006. Nuclear import of Epstein-Barr virus nuclear antigen 1 mediated by NPI-1 (importin α5) is up- and down-regulated by phosphorylation of the nuclear localisation signal for which Lys379 and Arg380 are essential. *J. Virol.,* 80**,** 1979-1991.
KLEEFF, J., MARUYAMA, H., ISHIWATA, T., SAWHNEY, H., FREISS, H., BÜCHLER, M. W. & KORC, M. 1999. Bone morphogenetic protein 2 exerts diverse effects on cell growth in vitro and is expressed in human pancreatic cancer in vivo. *Gastroenterology,* 116**,** 1202-1216.

KLEIN, E., ERNBERG, I., MASUCCI, M. G., SZIGETI, R., WU, Y. T., MASUCCI, G. & SREDMYR, E. 1981. T-cell response to B-cells and Epstein-Barr virus antigens in infectious mononucleosis. *Cancer Res.,* 41**,** 4210-4215.

KLEIN, G., GIOVANELLA, B. C., LINDAHL, T., FIALKOW, P. J., SINGH, S. & STEHLIN, J. S. 1974. Direct evidence for the presence of Epstein-Barr virus DNA and nuclear antigen in malignant epithelial cells from patients with poorly differentiated carcinoma of the nasopharynx. *Proc. Natl. Acad. Sci USA,* 71**,** 4737-4741.

KNOX, P. M., LI, Q.-X., RICKINSON, A. B. & YOUNG, L. S. 1996. *In vitro* production of stable Epstein-Barr virus-positive epithelial cell clones which resemble the virus:cell interaction observed in nasopharyngeal carcinoma. *Virology,* 215**,** 40-50.

KONG, Q. L., HU, L. J., CAO, J. Y., HUANG, Y. J., XU, L. H., LIANG, Y., XIONG, D., GUAN, S., GUO, B. H., MAI, H. Q., CHEN, Q. Y., ZHANG, X., LI, M. Z., SHAO, J. Y., QIAN, C. N., XIA, Y. F., SONG, L. B., X, Z. Y. & ZENG, M. S. 2010. Epstein-Barr virus-encoded LMP2A induces an epithelial-mesenchymal transition and increases the number of side population stem-like cancer cells in nasopharyngeal carcinoma. *PLoS Pathogens,* 6**,** e1000940.

KORCHYNSKYI, O. & TEN DIJKE, P. 2002. Identification and functional characterization of distinct critically important bone morphogenetic protein-specific response elements in the Id1 promoter. *J. Biol. Chem.,* 277**,** 4883-4891.

KOSHIZUKA, T., KAWAGUCHI, Y., NOZAWA, N., MORI, I. & NISHIYAMA, Y. 2007. Herpes simplex virus protein UL11 but not UL51 is associated with lipid rafts. *Virus Genes,* 35**,** 571-575.

KOWANETZ, M., VALCOURT, U., BERGSTRÖM, R., HELDIN, C.-H. & MOUSTAKAS, A. 2004. Id2 and Id3 define the potency of cell proliferation and differentiation responses to transforming growth factor β and bone morphogenetic protein. *Mol. Cell. Biol.,* 24**,** 4241-4254.

KRAUSE, C., GUZMAN, A. & KNAUS, P. 2011. Noggin. *Int. J. Biochem. Cell Biol.,* 43**,** 478-481.

KRETZSCHMAR, M., DOODY, J., TIMOKHINA, I. & MASSAGUÉ, J. 1999. A mechanism of repression of TGFβ/Smad signalling by oncogenic Ras. *Genes Dev.,* 13**,** 804-816.

KRETZSCHMAR, M., LIU, F., HATO, A., DOODY, J. & MASSAGUÉ, J. 1997. The TGF-β family mediator Smad1 is phosphorylated directly and activated functionally by the BMP receptor kinase. *Genes Dev.,* 11**,** 984-995.

KUBE, D., VOCKERODT, M. & WEBER, O. 1999. Expression of Epstein-Barr virus nuclear antigen 1 is associated with enhanced expression of CD25 in the Hodgkin cell line L428. *J. Virol.,* 73**,** 1630-1636.

KÜPPERS, R. 2003. B cells under influence: transformation of B cells by Epstein-Barr virus. *Nat. Rev. Immunol.,* 3**,** 801-812.

KURATOMI, G., KOMURO, A., GOTO, K., SHINOZAKI, M., MIYAZAWA, K., MIYAZONO, K. & IMAMURA, T. 2005. NEDD4-2 (neural precursor cell expressed, developmentally down-regulated 4-2) negatively regulates TGF-β (transforming growth factor-β) signalling by inducing ubiquitin-mediated degradation of Smad2 and TGF-β type I receptor. *Biochem. J.,* 386**,** 461-470.

KUROKAWA, M., MITANI, K., IRIE, K., MATSUYAMA, T., TAKAHASHI, T., CHIBA, S., YAZAKI, Y., MATSUMOTO, K. & HIRAI, H. 1998. The oncoprotein Evi-1 represses TGF-β signalling by inhibiting Smad3. *Nature,* 394**,** 92-96.

LAGNA, G., HATA, A., HEMMATI-BRIVANLOU, A. & MASSAGUÉ, J. 1996. Partnership between DPC4 and SMAD proteins in TGF-β signalling pathways. *Nature,* 383**,** 832-836.

LAICHALK, L. L. & THORLEY-LAWSON, D. A. 2005. Terminal differentiation into plasma cells initiates the replicative cycle of Epstein-Barr virus in vivo. *J. Virol.,* 79**,** 1296-1307.

LAM, N. & SUGDEN, B. 2003. CD40 and its viral mimic, LMP1: similar means to different ends. *Cellular Signalling,* 15**,** 9-16.

LANGENFELD, E. M., BOJNOWSKI, J., PERONE, J. & LANGENFELD, J. 2005. Expression of bone morphogenetic proteins in human lung carcinomas. *Ann. Thorac. Surg.,* 80**,** 1028-1032.

LANGENFELD, E. M., KONG, Y. & LANGENFELD, J. 2006. Bone morphogenetic protein 2 stimulation of tumour growth involves the activation of Smad-1/5. *Oncogene,* 25**,** 685-692.

LAU, K.-M., CHENG, S. H., LO, K. W., LEE, S. A. K. W., WOO, J. K. S., VAN HASSELT, C. A., LEE, S. P., RICKINSON, A. B. & NG, M. H. L. 2007. Increase in circulating Foxp3+CD4+CD25^{high} regulatory T cells in nasopharyngeal carcinoma patients. *British Journal of Cancer,* 96**,** 617-622.

LAUX, G., DUGRILLON, F., ECKERT, C., ADAM, B., ZIMBER-STROBL, U. & BORNKAMM, G. W. 1994. Identification and characterisation of an Epstein-Barr virus nuclear antigen 2-responsive cis element in the bidirectional promoter region of latent membrane protein and terminal protein 2 genes. *J. Virol.,* 68**,** 6947-6958.

LEE, D. K., KIM, B.-C., BRADY, J. N., JEANG, K.-T. & KIM, S.-J. 2002a. Human T-cell lymphotropic virus type I Tax inhibits transforming growth factor-β signalling by blocking the association of Smad proteins with Smad-binding element. *J. Biol. Chem.,* 277**,** 33766-33775.

LEE, D. K., KIM, B.-C., KIM, I. Y., CHO, E.-A., SATTERWHITE, D. J. & KIM, S.-J. 2002b. The human papilloma virus E7 oncoprotein inhibits transforming growth factor-β signalling by blocking binding of the Smad complex to its target sequence. *J. Biol. Chem.,* 277**,** 38557-38564.

LEE, D. K., PARK, S. H., YI, Y., CHOI, S.-G., LEE, C., PARKS, W. T., CHO, H. S., DE CAESTECKER, M. P., SHAUL, Y., ROBERTS, A. B. & KIM, S. J. 2001. The hepatitis B virus encoded oncoprotein pX amplifies TGFβ family signalling through direct interaction with Smad4: potential mechanism of hepatitis B virus-induced liver fibrosis. *Genes Dev.,* 15**,** 455-466.

LEE, E. K., LEE, Y. S., HAN, I.-O. & PARK, S. H. 2007. Expression of caveolin-1 reduced cellular responses to TGF-β1 through down-regulating the expression of TGF-β type II receptor gene in NIH3T3 fibroblast cells. *Biochem. Biophys. Res. Comm.,* 359**,** 385-390.

LEE, I.-H., CAMPBELL, C. R., SONG, S.-H., DAY, M. L., KUMAR, S., COOK, D. I. & DINUDOM, A. 2009. The activity of the epithelial sodium channels is regulated by caveolin-1 via a Nedd4-2-dependent mechanism. *J. Biol. Chem.,* 284**,** 12663-12669.

LEE, J., SON, M. J., WOOLARD, K., DONIN, N. M., LI, A., CHENG, C. H., KOTLIAROVA, S., KOTLIAROV, Y., WALLING, J., AHN, S., KIM, M., TOTONCHY, M., CUSACK, T., ENE, C. W., MA, H., SU, Q., ZENKLUSEN, J. C., ZHANG, W., MARIC, D. & FINE, H. A. 2008. Epigenetic-mediated dysfunction of the bone morphogenetic protein pathway inhibits differentiation of glioblastoma-initiating cells. *Cancer Cell,* 13**,** 69-80.

LEE, K.-S., KIM, H.-J., LI, Q.-L., CHI, X.-Z., UETA, C., KOMORI, T., WOZNEY, J. M., KIM, E.-G., CHOI, J.-Y., RYOO, H.-M. & BAE, S.-C. 2000. Runx2 is a common target of transforming growth factor β1 and bone morphogenetic protein 2, and cooperation between Runx2 and Smad5 induces osteoblast-specific gene expression in the pluripotent mesenchymal precursor cell line C2C12. *Mol. Cell. Biol.,* 20**,** 8783-8792.

LEE, M.-A., DIAMOND, M. E. & YATES, J. L. 1999. Genetic evidence that EBNA-1 is needed for efficient, stable latent infection by Epstein-Barr virus. *J. Virol.,* 73**,** 2974-2982.

LEE, S. P., BROOKS, J. M., AL-JARRAH, H., THOMAS, W. A., HAIGH, T. A., TAYLOR, G. S., HUMME, S., SCHEPERS, A., HAMMERSCHMIDT, W., YATES, J. L., RICKINSON, A. B. & BLAKE, N. W. 2004. CD8 T cell recognition of endogenously expressed Epstein-Barr virus nuclear antigen 1. *J. Exp. Med.,* 199**,** 1409-1420.

LEIVONEN, S.-K. & KÄHÄRI, V.-M. 2007. Transforming growth factor-β signalling in cancer invasion and metastasis. *Int. J. Cancer,* 121**,** 2119-2124.

LEONG, D. T., LIM, J., GOH, X., PRATAP, J., PEREIRA, B. P., KWOK, H. S., NATHAN, S. S., DOBSON, J. R., LIAN, J. B., ITO, Y., VOORHOEVE, P. M., STEIN, G. S., SALTO-TELLEZ, M., COOL, S. M. & VAN WIJNEN, A. J. 2010. Cancer-related ectopic expression of the bone-related transcription factor RUNX2 in non-osseous metastatic tumour cells is linked to cell proliferation and motility. *Breast Cancer Res.,* 12**,** R89.

LERNER, M. R., ANDREWS, N. C., MILLER, G. & STEITZ, J. A. 1981. The small RNAs encoded by Epstein-Barr virus and complexed with protein are precipitated by antibodies from patients with systemic lupus erythematosus. *Proc. Natl. Acad. Sci USA,* 78**,** 805-809.

LEVITSKAYA, J., SHARIPO, A., LEONCHIKS, A., CIECHANOVER, A. & MASUCCI, M. G. 1997. Inhibition of ubiquitin/proteasome-dependent protein degradation by the Gly-Ala repeat domain of the Epstein-Barr virus nuclear antigen 1. *Proc. Natl. Acad. Sci USA,* 94**,** 12616-12621.

LEVY, L. & HILL, C. S. 2005. Smad4 dependency defines two classes of transforming growth factor β (TGF-β) target genes and distinguishes TGF-β-induced epithelial-mesenchymal transition from its antiproliferative and migratory responses. *Mol. Cell. Biol.,* 25**,** 8108-8125.

LEVY, L. & HILL, C. S. 2006. Alterations in components of the TGF-β superfamily signalling pathways in human cancer. *Cytokine Growth Factor Rev.,* 17**,** 41-58.

LEWIS, P. F. & EMERMAN, M. 1994. Passage through mitosis is required for oncoretroviruses but not for the human immunodeficiency virus. *J. Virol.,* 68**,** 510-516.
LI, Q. X., YOUNG, L. S., NIEDOBITEK, G., DAWSON, C. W., BIRKENBACH, M., WANG, F. & RICKINSON, A. B. 1992. Epstein-Barr virus infection and replication in a human epithelial cell system. *Nature,* 356**,** 347-350.
LIANG, C.-L., CHEN, J.-L., HSU, Y.-P. P., OU, J. T. & CHANG, Y.-S. 2002. Epstein-Barr virus BZLF1 gene is activated by transforming growth factor-β through cooperativity of Smads and c-Jun/c-Fos proteins. *J. Biol. Chem.,* 277**,** 23345-23357.
LIANG, C.-L., TSAI, C.-N., CHUNG, P.-J., CHEN, J.-L., SUN, C.-M., CHEN, R.-H., HONG, J.-H. & CHANG, Y.-S. 2000. Transcription of Epstein-Barr virus-encoded nuclear antigen 1 promoter Qp is repressed by transforming growth factor-β via Smad4 binding element in human BL cells. *Virology,* 277**,** 184-192.
LIAO, S.-K., PERNG, Y.-P., SHEN, Y.-C., CHUNG, P.-J., CHANG, Y.-S. & WANG, C.-H. 1998. Chromosomal abnormalities of a new nasopharyngeal carcinoma cell line (NPC-BM1) derived from a bone marrow metastatic lesion. *Cancer Genetics and Cytogenetics,* 103**,** 52-58.
LIN, A., WANG, S., NGUYEN, T., SHIRE, K. & FRAPPIER, L. 2008. The EBNA1 protein of Epstein-Barr virus functionally interacts with Brd4. *J. Virol.,* 82**,** 12009-12019.
LIN, C.-T., KAO, H.-J., LIN, J.-L., CHAN, W.-Y., WU, H.-C. & LIANG, S.-T. 2000a. Response of nasopharyngeal carcinoma cells to Epstein-Barr virus infection in vitro. *Lab. Invest.,* 80**,** 1149-1160.
LIN, X., DUAN, X., LIANG, Y.-Y., SU, Y., WRIGHTON, K. H., LONG, J., HU, M., DAVIS, C. M., WANG, J., BRUNICARDI, F. C., SHI, Y., CHEN, Y.-G., MENG, A. & FENG, X.-H. 2006. PPM1A functions as a Smad phosphatase to terminate TGFβ signalling. *Cell,* 125**,** 915-928.
LIN, X., LIANG, M. & FENG, X.-H. 2000b. Smurf2 is a ubiquitin E3 ligase mediating proteasome-dependent degradation of Smad2 in transforming growth factor-β signalling. *J. Biol. Chem.,* 275**,** 36818-36822.
LIU, F., VENTURA, F., DOODY, J. & MASSAGUÉ, J. 1995. Human type II receptor for bone morphogenic proteins (BMPs): extension of the two-kinase receptor model to the BMPs. *Mol. Cell. Biol.,* 15**,** 3479-3486.
LIU, I. M., SCHILLING, S. H., KNOUSE, K. A., CHOY, L., DERYNCK, R. & WANG, X.-F. 2009. TGFβ-stimulated Smad1/5 phosphorylation requires the ALK5 L45 loop and mediates the pro-migratory TGFβ switch. *EMBO J.,* 28**,** 88-98.
LIU, X., YUE, J., FREY, R. S., ZHU, Q. & MULDER, K. M. 1998. Transforming growth factor β signalling through Smad1 in human breast cancer cells. *Cancer Res.,* 58**,** 4752-4757.
LIVAK, K. J. & SCHMITTGEN, T. D. 2001. Analysis of relative gene expression data using real-time quantitative PCR and the $2^{-\Delta\Delta Ct}$ method. *Methods,* 25**,** 402-408.
LO, A. K., TO, K. F., LO, K. W., LUNG, R. W., HUI, J. W., LIAO, G. & HAYWARD, S. D. 2007. Modulation of LMP1 protein expression by EBV-encoded microRNAs. *Proc. Natl. Acad. Sci USA,* 104**,** 16164-16169.
LO, A. K. F., LIU, Y., WANG, X. H., HUANG, D. P., YUEN, P. W., WONG, Y. C. & TSAO, G. S. W. 2003. Alterations of biologic properties and gene expression in nasopharyngeal epithelial cells by the Epstein-Barr virus-encoded latent membrane protein 1. *Lab. Invest.,* 83**,** 697-709.
LO, K.-W. & HUANG, D. P. 2002. Genetic and epigenetic changes in nasopharyngeal carcinoma. *Semin. Cancer Biol.,* 12**,** 451-462.
LO, K.-W., HUANG, D. P. & LAU, K.-M. 1995. p16 gene alterations in nasopharyngeal carcinoma. *Cancer Res.,* 55**,** 2039-2043.
LO, K.-W., KWONG, J., HUI, A. B.-Y., CHAN, S. Y.-Y., TO, K.-F., CHAN, A. S.-C., CHOW, L. S.-N., TEO, P. M. L., JOHNSON, P. J. & HUANG, D. P. 2001. High frequency of promoter hypermethylation of *RASSF1A* in nasopharyngeal carcinoma. *Cancer Res.,* 61**,** 3877-3881.
LO, K. W., TO, K. F. & HUANG, D. P. 2004. Focus on nasopharyngeal carcinoma. *Cancer Cell,* 5**,** 423-428.
LO, R. S. & MASSAGUÉ, J. 1999. Ubiquitin-dependent degradation of TGF-β-activated Smad2. *Nat. Cell Biol.,* 1**,** 472-478.
LOGEART-AVRAMOGLOU, D., BOURGUIGNON, M., OUDINA, K., TEN DIJKE, P. & PETITE, H. 2006. An assay for the determination of biologically active bone morphogenetic proteins using

cells transfected with an inhibitor of differentiation promoter-luciferase construct. *Analytical Biochemistry,* 349**,** 78-86.
LONGNECKER, R. 2000. Epstein-Barr virus latency: LMP2, a regulator or means for Epstein-Barr virus persistence? *Adv. Cancer Res.,* 79**,** 175-200.
LÖNN, P., MORÉN, A., RAJA, E., DAHL, M. & MOUSTAKAS, A. 2009. Regulating the stability of TGFβ receptors and Smads. *Cell Res.,* 19**,** 21-35.
LOPES, V., YOUNG, L. S. & MURRAY, P. G. 2003. Epstein-Barr virus-associated cancers: aetiology and treatment. *Herpes,* 10**,** 78-82.
LORENTE-TRIGOS, A., VARNAT, F., MELOTTI, A. & RUIZ I ALTABA, A. 2010. BMP signalling promotes the growth of primary human colon carcinomas in vivo. *J. Mol. Cell Biol.,* 2**,** 318-332.
LOSI, L., BOUZOURENE, H. & BENHATTAR, J. 2007. Loss of Smad4 expression predicts liver metastasis in human colorectal cancer. *Oncology Reports,* 17**,** 1095-1099.
LU, C.-C., CHEN, J.-C., JIN, Y.-T., YANG, H.-B., CHAN, S.-H. & TSAI, S.-T. 2003. Genetic susceptibility to nasopharyngeal carcinoma within the HLA-A locus in Taiwanese. *Int. J. Cancer,* 103**,** 745-751.
LU, C.-C., WU, C.-W., CHANG, S. C., CHEN, T.-Y., HU, C.-R., YEH, M.-Y., CHEN, J.-Y. & CHEN, M.-R. 2004. Epstein-Barr virus nuclear antigen 1 is a DNA-binding protein with strong RNA-binding activity. *J. Gen. Virol.,* 85**,** 2755-2765.
LU, F., WEIDMER, A., LIU, C.-G., VOLINIA, S., CROCE, C. M. & LIEBERMAN, P. M. 2008. Epstein-Barr virus-induced miR-155 attenuates NF-κB signalling and stabilises latent virus persistence. *J. Virol.,* 82**,** 10436-10443.
LU, J., MURAKAMI, M., VERMA, S. C., CAI, Q., HALDAR, S., KAUL, R., WASIK, M. A., MIDDELDORP, J. & ROBERTSON, E. S. 2011. Epstein-Barr virus nuclear antigen 1 (EBNA1) confers resistance to apoptosis in EBV-positive B-lymphoma cells through up-regulation of survivin. *Virology,* 410**,** 64-75.
LU, S.-J., DAY, N. E., DEGAS, L., LEPAGE, V., WANG, P.-C., CHAN, S.-H., SIMONS, M., MCKNIGHT, B., EASTON, D., ZENG, Y. & DE THÉ, G. 1990. Linkage of a nasopharyngeal carcinoma susceptibility locus to the HLA region. *Nature,* 346**,** 470-471.
LUCCHESI, W., BRADY, G., DITTRICH-BREIHOLZ, O., KRACHT, M., RUSS, R. & FARRELL, P. J. 2008. Differential gene regulation by Epstein-Barr virus type I and type 2 EBNA2. *J. Virol.,* 82**,** 7456-7466.
LUNG, R. W., TONG, J. H., SUNG, Y. M., LEUNG, P. S., NG, D. C., CHAU, S. L., CHAN, A. W., NG, E. K., LO, K. W. & TO, K. F. 2009. Modulation of LMP2A expression by a newly identified Epstein-Barr virus-encoded microRNA miR-BART22. *Neoplasia,* 11**,** 1174-1184.
LUTZ, M. & KNAUS, P. 2002. Integration of the TGF-β pathway into the cellular signalling network. *Cell. Sig.,* 14**,** 977-988.
MACÍAS-SILVA, M., ABDOLLAH, S., HOODLESS, P. A., PIRONE, R., ATTISANO, L. & WRANA, J. L. 1996. MADR2 is a substrate of the TGFβ receptor and its phosphorylation is required for nuclear accumulation and signalling. *Cell,* 87**,** 1215-1224.
MACÍAS-SILVA, M., HOODLESS, P. A., TANG, S. J., BUCHWALD, M. & WRANA, J. L. 1998. Specific activation of Smad1 signalling pathways by the BMP7 type I receptor, ALK2. *J. Biol. Chem.,* 273**,** 25628-25636.
MAINOU, B. A., EVERLY JR., D. N. & RAAB-TRAUB, N. 2007. Unique signalling properties of CTAR1 in LMP1-mediated transformation. *J. Virol.,* 81**,** 9680-9692.
MARECHAL, V., DEHEE, A., CHIKHI-BRACHET, R., PIOLOT, T., COPPEY-MOISAN, M. & NICOLAS, J.-C. 1999. Mapping EBNA1 domains involved in binding to metaphase chromosomes. *J. Virol.,* 73**,** 4385-4392.
MARKIĆ, D., ĆELIĆ, T., ŠPANJOL, J., GRŠKOVIĆ, A., BOBINAC, D. & FUČKAR, Ž. 2010. Expression of bone morphogenetic protein-7, its receptors and Smad1/5/8 in normal human kidney and renal cell cancer. *Coll. Antropol.,* 34**,** 149-153.
MARTEL-RENOIR, D., GRUNEWALD, V., TOUITOU, R., SCHWAAB, G. & JOAB, I. 1995. Qualitative analysis of the expression of Epstein-Barr virus lytic genes in nasopharyngeal carcinoma biopsies. *J. Gen. Virol.,* 76**,** 1401-1408.
MARTIN, J. C., HERBERT, B.-S. & HOCEVAR, B. A. 2010. Disabled-2 downregulation promotes epithelial-to-mesenchymal transition. *British Journal of Cancer,* 103**,** 1716-1723.

MASSAGUÉ, J. 2000. How cells read TGF-β signals. *Nat. Rev. Mol. Cell Biol.,* 1**,** 169-178.
MASSAGUÉ, J. 2008. TGFβ in cancer. *Cell,* 134**,** 215-230.
MASSAGUÉ, J., BLAIN, S. W. & LO, R. S. 2000. TGFβ signalling in growth control, cancer and heritable disorders. *Cell,* 103**,** 295-309.
MASSAGUÉ, J. & GOMIS, R. R. 2006. The logic of TGFβ signalling. *FEBS Letters,* 580**,** 2811-2820.
MASSAGUÉ, J. & HATA, A. 1997. TGF-β signalling through the Smad pathway. *Trends Cell Biol.,* 7**,** 187-192.
MASSAGUÉ, J., SEOANE, J. & WOTTON, D. 2005. Smad transcription factors. *Genes Dev.,* 19**,** 2783-2810.
MASUCCI, M. G. & ERNBERG, I. 1994. Epstein-Barr virus: adaptation to a life within the immune system. *Trends Microbiol.,* 2**,** 125-130.
MATSUZAKI, K., KITANO, C., MURATA, M., SEKIMOTO, G., YOSHIDA, K., UEMURA, Y., SEKI, T., TAKETANI, S., FUJISAWA, J.-I. & OKAZAKI, K. 2009. Smad2 and Smad3 phosphorylated at both linker and COOH-terminal regions transmit malignant TGF-β signal in later stages of human colorectal cancer. *Cancer Res.,* 69**,** 5321-5330.
MATSUZAKI, K. & OKAZAKI, K. 2006. Transforming growth factor-β during carcinogenesis: the shift from epithelial to mesenchymal signalling. *J. Gastroenterol.,* 41**,** 295-303.
MAZERBOURG, S., KLEIN, C., ROH, J., KAIRO-OJA, N., MOTTERSHEAD, D. G., KORCHYNSKYI, O., RITVOS, O. & HSEUH, A. J. W. 2004. Growth differentiation factor-9 signalling is mediated by the type I receptor, activin receptor-like kinase 5. *Mol. Endocrinol.,* 18**,** 653-665.
MAZZIERI, R., MUNGER, J. S. & RIFKIN, D. B. 2000. Measurement of active TGF-β generated by cultured cells. *In:* HOWE, P. H. (ed.) *Methods in Molecular Biology.* Totowa, NJ: Humana Press Inc.
MCLAUGHLIN-DRUBIN, M. E. & MUNGER, K. 2008. Viruses associated with human cancer. *Biochim. Biophys. Acta,* 1782**,** 127-150.
MENDOZA, J.-A., JACOB, Y., CASSONNET, P. & FAVRE, M. 2006. Human papillomavirus type 5 E6 oncoprotein represses the transforming growth factor β signalling pathway by binding to SMAD3. *J. Virol.,* 80**,** 12420-12424.
MEULMEESTER, E. & TEN DIJKE, P. 2011. The dynamic roles of TGF-β in cancer. *J. Pathol.,* 223**,** 205-218.
MEYER, C., GODOY, P., BACHMANN, A., LIU, Y., BARZAN, D., ILKAVETS, I., MAIER, P., HERSKIND, C., HENGSTLER, J. G. & DOOLEY, S. 2011. Distinct role of endocytosis for Smad and non Smad TGF-β signalling regulation in hepatocytes. *J. Hepatol.,* 55**,** 369-378.
MICHEAU, C., BOUSSEN, H., KLLIANIENKO, J., CVITKOVIC, E., STOSIC, S., SCHWAAB, G., ESCHWEGE, F. & ARMAND, J.-P. 1987. Bone marrow biopsies in patients with undifferentiated carcinoma of the nasopharyngeal type. *Cancer,* 60**,** 2459-2464.
MILLER, C. L., BURKHARDT, A. L., LEE, J. H., STEALEY, B., LONGNECKER, R., BOLEN, J. B. & KIEFF, E. 1995. Integral membrane protein 2 of Epstein-Barr virus regulates reactivation from latency through dominant negative effects on protein-tyrosine kinases. *Immunity,* 2**,** 155-166.
MILLER, C. L., LEE, J. H., KIEFF, E. & LONGNECKER, R. 1994. An integral membrane protein (LMP2) blocks reactivation of Epstein-Barr virus from latency following surface immunoglobulin crosslinking. *Proc. Natl. Acad. Sci USA,* 91**,** 772-776.
MILLER, D. G., ADAM, M. A. & MILLER, A. D. 1990. Gene transfer by retrovirus vectors occurs only in cells that are actively replicating at the time of infection. *Mol. Cell. Biol.,* 10**,** 4239-4242.
MILLET, C., YAMASHITA, M., HELLER, M., YU, L.-R., VEENSTRA, T. D. & ZHANG, Y. E. 2009. A negative feedback control of transforming growth factor-β signalling by glycogen synthase kinase 3-mediated Smad3 linker phosphorylation at Ser-204. *J. Biol. Chem.,* 284**,** 19808-19816.
MINAROVITS, J., HU, L.-F., MARCSEK, Z., MINAROVITS-KORMUTA, S., KLEIN, G. & ERNBERG, I. 1992. RNA polymerase III-transcribed EBER 1 and 2 transcription units are expressed and hypomethylated in the major Epstein-Barr virus-carrying cell types. *J. Gen. Virol.,* 73**,** 1687-1692.
MISHRA, S. K., KEYEL, P. A., HAWRYLUK, M. J., AGOSTINELLI, N. R., WATKINS, S. C. & TRAUB, L. M. 2002. Disabled-2 exhibits the properties of a cargo-selective endocytic clathrin adaptor. *EMBO J.,* 21**,** 4915-4926.

MITCHELL, H., CHOUDHURY, A., PAGANO, R. E. & LEOF, E. B. 2004. Ligand-dependent and -independent transforming growth factor-β receptor recycling regulated by clathrin-mediated endocytosis and Rab11. *Mol. Biol. Cell,* 15**,** 4166-4178.
MIYAJIMA, A., ASANO, T., SETA, K., ASANO, T., KAKOI, N. & HAYAKAWA, M. 2003. Loss of expression of transforming growth factor-beta receptor as a prognostic factor in patients with renal cell carcinoma. *Urology,* 61**,** 1072-1077.
MIYAKI, M., IIJIMA, T., KONISHI, M., SAKAI, K., ISHII, A., YASUNO, M., HISHIMA, T., KOIKE, M., SHITARA, N., IWAMA, T., UTSUNOMIYA, J., KUROKI, T. & MORI, T. 1999. Higher frequency of *Smad4* gene mutation in human colorectal cancer with distant metastasis. *Oncogene,* 18**,** 3098-3103.
MIYASHITA, E. M., YANG, B., BABCOCK, G. J. & THORLEY-LAWSON, D. A. 1997. Identification of the site of Epstein-Barr virus persistence in vivo as a resting B cell. *J. Virol.,* 71**,** 4882-4891.
MIYASHITA, E. M., YANG, B., LAM, K. M. C., CRAWFORD, D. H. & THORLEY-LAWSON, D. A. 1995. A novel form of Epstein-Barr virus latency in normal B cells in vivo. *Cell,* 80**,** 593-601.
MIYAZAKI, H., WATABE, T., KITAMURA, T. & MIYAZONO, K. 2004. BMP signals inhibit proliferation and in vivo tumour growth of androgen-insensitive prostate carcinoma cells. *Oncogene,* 23**,** 9326-9335.
MIYAZAWA, K., SHINOZAKI, M., HARA, T., FURUYA, T. & MIYAZONO, K. 2002. Two major Smad pathways in TGF-β superfamily signalling. *Genes to Cells,* 7**,** 1191-1204.
MIYAZONO, K. 1998. Smad proteins: signal transducers for BMP and TGF-β/activin. *J. Bone Miner. Metab.,* 16**,** 133-138.
MIYAZONO, K., KAMIYA, Y. & MORIKAWA, M. 2010. Bone morphogenetic protein receptors and signal transduction. *J. Biochem.,* 147**,** 35-51.
MIYAZONO, K., KUSANAGI, K. & INOUE, H. 2001. Divergence and convergence of TGF-β/BMP signalling. *J. Cell. Physiol.,* 187**,** 265-276.
MIYAZONO, K., MAEDA, S. & IMAMURA, T. 2005. BMP receptor signalling: transcriptional targets, regulation of signals, and signalling cross-talk. *Cytokine Growth Factor Rev.,* 16**,** 251-263.
MOK, S. C., WONG, K.-K., CHAN, R. K. W., LAU, C. C., TSAO, S.-W., KNAPP, R. C. & BERKOWITZ, R. S. 1994. Molecular cloning of differentially expressed genes in human epithelial ovarian cancer. *Gynecologic Oncology,* 52**,** 247-252.
MORI, N., MORISHITA, M., TSUKAZAKI, T. & YAMAMOTO, N. 2003. Repression of Smad-dependent transforming growth factor-β signalling by Epstein-Barr virus latent membrane protein 1 through nuclear factor-κB. *Int. J. Cancer,* 105**,** 661-668.
MORI, S., MATSUZAKI, K., YOSHIDA, K., FURUKAWA, F., TAHASHI, Y., YAMAGATA, H., SEKIMOTO, G., SEKI, T., MATSUI, H., NISHIZAWA, M., FUJISAWA, J.-I. & OKAZAKI, K. 2004. TGF-β and HGF transmit the signals through JNK-dependent Smad2/3 phosphorylation at the linker regions. *Oncogene,* 23**,** 7416-7429.
MORRIS, M. A., DAWSON, C. W., WEI, W., O'NEIL, J. D., STEWART, S. E., JIA, J., BELL, A. I., YOUNG, L. S. & ARRAND, J. R. 2008. Epstein-Barr virus-encoded LMP1 induces a hyperproliferative and inflammatory gene expression programme in cultured keratinocytes. *J. Gen. Virol.,* 89**,** 2806-2820.
MORRIS, S. M. & COOPER, J. A. 2001. Disabled-2 colocalises with the LDLR in clathrin-coated pits and interacts with AP-2. *Traffic,* 2**,** 111-123.
MOSIALOS, G., BIRKENBACH, M., YALAMANCHILI, R., VANARNSDALE, T., WARE, C. & KIEFF, E. 1995. The Epstein-Barr virus transforming protein LMP1 engages signalling proteins for the tumour necrosis factor receptor family. *Cell,* 80**,** 389-399.
MOUSTAKAS, A. & HELDIN, C.-H. 2005. Non-Smad TGF-β signals. *J. Cell Sci.,* 118**,** 3573-3584.
MOUSTAKAS, A., SOUCHELNYTSKYI, S. & HELDIN, C. 2001. Smad regulation in TGF-β signal transduction. *J. Cell Sci.,* 114**,** 4359-4369.
MUNDY, G. R. 2002. Metastasis to bone: causes, consequences and therapeutic opportunities. *Nat. Rev. Cancer,* 2**,** 584-593.
MUNGER, J. S., HUANG, X., KAWAKATSU, H., GRIFFITHS, M. J. D., DALTON, S. L., WU, J., PITTET, J.-F., KAMINSKI, N., GARAT, C., MATTHAY, M. A., RIFKIN, D. B. & SHEPPARD, D. 1999. The integrin αvβ6 binds and activates latent TGFβ1: a mechanism for regulating pulmonary inflammation and fibrosis. *Cell,* 96**,** 319-328.

MURAKAMI, M., LAN, K., SUBRAMANIAN, C. & ROBERTSON, E. S. 2005. Epstein-Barr virus nuclear antigen 1 interacts with Nm23-H1 in lymphoblastoid cell lines and inhibits its ability to suppress cell migration. *J. Virol.,* 79**,** 1559-1568.

MURATA, M., MATSUZAKI, K., YOSHIDA, K., SEKIMOTO, G., TAHASHI, Y., MORI, S., UEMURA, Y., SAKAIDA, N., FUJISAWA, J., SEKI, T., KOBAYASHI, K., YOKOTE, K., KOIKE, K. & OKAZAKI, K. 2009. Hepatitis B virus X protein shifts human hepatic transforming growth factor (TGF)-β signalling from tumour suppression to oncogenesis in early chronic hepatitis B. *Hepatology,* 49**,** 1203-1217.

MURO-CACHO, C. A., ROSARIO-ORTIZ, K., LIVINGSTON, S. & MUÑOZ-ANTONIA, T. 2001. Defective transforming growth factor β signalling pathway in head and neck squamous cell carcinoma as evidenced by the lack of expression of activated Smad2. *Clin. Cancer Res.,* 7**,** 1618-1626.

MURPHY, S. F. 2010. *Modulation of innate immune responses in nasopharyngeal epithelial cells by the Epstein-Barr virus (EBV)-encoded latent membrane proteins LMP2A and LMP2B.* Ph. D. thesis, University of Birmingham.

MURRAY, P. G. & YOUNG, L. S. 2001. Epstein-Barr virus infection: basis of malignancy and potential for therapy. *Exp. Rev. Mol. Med.,* 3**,** 1-20.

NACHMANI, D., STERN-GINOSSAR, N., SARID, R. & MANDELBOIM, O. 2009. Diverse herpesvirus microRNAs target the stress-induced immune ligand MICB to escape recognition by natural killer cells. *Cell Host. Microbe,* 5**,** 376-385.

NAGARAJAN, R. P., ZHANG, J., LI, W. & CHEN, Y. 1999. Regulation of Smad7 promoter by direct association with Smad3 and Smad4. *J. Biol. Chem.,* 274**,** 33412-33418.

NAGASO, H., SUZUKI, A., TADA, M. & UENO, N. 1999. Dual specificity of activin type II receptor ActRIIb in dorso-ventral patterning during zebrafish embryogenesis. *Develop. Growth Differ.,* 41**,** 119-133.

NAGATA, H., HATANO, E., TADA, M., MURATA, M., KITAMURA, K., ASECHI, H., NARITA, M., YANAGIDA, A., TAMAKI, N., YAGI, S., IKAI, I., MATSUZAKI, K. & UEMOTO, S. 2009. Inhibition of c-Jun NH_2-terminal kinase switches Smad3 signalling from oncogenesis to tumour-suppression in rat hepatocellular carcinoma. *Hepatology,* 49**,** 1944-1953.

NAKANO, A., KOINUMA, D., MIYAZAWA, K., UCHIDA, T., SAITOH, M., KAWABATA, M., HANAI, J.-I., AKIYAMA, H., ABE, M., MIYAZONO, K., MATSUMOTO, T. & IMAMURA, T. 2009. Pin1 down-regulates transforming growth factor-β (TGF-β) signalling by inducing degradation of Smad proteins. *J. Biol. Chem.,* 284**,** 6109-6115.

NAKAO, A., AFRAKHTE, M., MORÉN, A., NAKAYAMA, T., CHRISTIAN, J. L., HEUCHEL, R., ITOH, S., KAWABATA, M., HELDIN, N.-E., HELDIN, C.-H. & TEN DIJKE, P. 1997. Identification of Smad7, a TGFβ-inducible antagonist of TGFβ signalling. *Nature,* 389**,** 631-635.

NAKAYAMA, T., GARDNER, H., BERG, L. K. & CHRISTIAN, J. L. 1998. Smad6 functions as an intracellular antagonist of some TGF-β family members during *Xenopus* embryogenesis. *Genes to Cells,* 3**,** 387-394.

NALDINI, L., BLÖMER, U., GALLAY, P., ORY, D., MULLIGAN, R., GAGE, F. H., VERMA, I. M. & TRONO, D. 1996. In vivo delivery and stable transduction of nondividing cells by a lentiviral vector. *Science,* 272**,** 263-267.

NASIMUZZAMAN, M., KURODA, M., DOHNO, S., YAMAMOTO, T., IWATSUKI, K., MATSUZAKI, S., MOHAMMAD, R., KUMITA, W., MIZUGUCHI, H., HAYAKAWA, T., NAKAMURA, H., TAGUCHI, T., WAKIGUCHI, H. & IMAI, S. 2005. Eradication of Epstein-Barr virus episome and associated inhibition of infected tumour cell growth by adenovirus vector-mediated transduction of dominant-negative EBNA1. *Molecular Therapy,* 11**,** 578-590.

NAYYAR, V. K., SHIRE, K. & FRAPPIER, L. 2009. Mitotic chromosome interactions of Epstein-Barr nuclear antigen 1 (EBNA1) and human EBNA1-binding protein 2 (EBP2). *J. Cell Sci.,* 122**,** 4341-4350.

NEMEROW, G. R., MOLD, C., SCHWEND, V. K., TOLLEFSON, V. & COOPER, N. R. 1987. Identification of gp350 as the viral glycoprotein mediating attachment of Epstein-Barr virus (EBV) to the EBV/C3d receptor of B cells: sequence homology of gp350 and C3 complement fragment C3d. *J. Virol.,* 61**,** 1416-1420.

NICHOLLS, J. M., AGATHANGGELOU, A., FUNG, K., XIANGGUO, Z. & NIEDOBITEK, G. 1997. The association of squamous cell carcinomas of the nasopharynx with Epstein-Barr virus shows geographical variation reminiscent of Burkitt's lymphoma. *J. Pathol.,* 183**,** 164-168.

NICKEL, J., SEBALD, W., GROPPE, J. C. & MUELLER, T. D. 2009. Intricacies of BMP receptor assembly. *Cytokine Growth Factor Rev.,* 20**,** 367-377.

NIEDOBITEK, G., AGATHANGGELOU, A., HERBST, H., WHITEHEAD, L., WRIGHT, D. H. & YOUNG, L. S. 1997. Epstein-Barr virus (EBV) infection in infectious mononucleosis: virus latency, replication and phenotype of EBV-infected cells. *J. Pathol.,* 182**,** 151-159.

NIEDOBITEK, G., AGATHANGGELOU, A. & NICHOLLS, J. M. 1996. Epstein-Barr virus infection and the pathogenesis of nasopharyngeal carcinoma: viral gene expression, tumour cell phenotype, and the role of the lymphoid stroma. *Semin. Cancer Biol.,* 7**,** 165-174.

NIEDOBITEK, G., YOUNG, L. S., LAU, R., BROOKS, L., GREENSPAN, D., GREENSPAN, J. S. & RICKINSON, A. B. 1991. Epstein-Barr virus infection in oral hairy leukoplakia: virus replication in the absence of a detectable latent phase. *J. Gen. Virol.,* 72**,** 3035-3046.

NISHIHARA, A., HANAI, J.-I., IMAMURA, T., MIYAZONO, K. & KAWABATA, M. 1999. E1A inhibits transforming growth factor-β signalling through binding to Smad proteins. *J. Biol. Chem.,* 274**,** 28716-28723.

NISHIMATSU, S.-I. & THOMSEN, G. H. 1998. Ventral mesoderm induction and pattern by bone morphogenetic protein heterodimers in Xenopus embryos. *Mech. Dev.,* 74**,** 75-88.

NONKWELO, C., RUF, I. & SAMPLE, J. T. 1997. The Epstein-Barr virus EBNA-1 promoter Qp requires an initiator-like element. *J. Virol.,* 71**,** 354-361.

O'NEIL, J. D., OWEN, T. J., WOOD, V. H. J., DATE, K. L., VALENTINE, R., CHUKWUMA, M. B., ARRAND, J. R., DAWSON, C. W. & YOUNG, L. S. 2008. Epstein-Barr virus-encoded EBNA1 modulates the AP-1 transcription factor pathway in nasopharyngeal carcinoma cells and enhances angiogenesis *in vitro*. *J. Gen. Virol.,* 89**,** 2833-2842.

OHASHI, N., YAMAMOTO, T., UCHIDA, C., TOGAWA, A., FUKASAWA, H., FUJIGAKI, Y., SUZUKI, S., KITAGAWA, K., HATTORI, T., ODA, T., HAYASHI, H., HISHIDA, A. & KITAGAWA, M. 2005. Transcriptional induction of Smurf2 ubiquitin ligase by TGF-β. *FEBS Letters,* 579**,** 2557-2563.

OSADA, H., TATEMATSU, Y., MASUDA, A., SAITO, T., SUGIYAMA, M., YANAGISAWA, K. & TAKAHASHI, T. 2001. Heterogeneous transforming growth factor (TGF)-β unresponsiveness and loss of TGF-β receptor type II expression caused by histone deacetylation in lung cancer cell lines. *Cancer Res.,* 61**,** 8331-8339.

OUSSAIEF, L., HIPPOCRATE, A., RAMÍREZ, V., RAMPANOU, A., ZHANG, W., MEYERS, D., COLE, P., KHELIFA, R. & JOAB, I. 2009. Phosphatidylinositol 3-kinase/Akt pathway targets acetylation of Smad3 through Smad3/CREB-binding protein interaction: contribution to transforming growth factor β1-induced Epstein-Barr virus reactivation. *J. Biol. Chem.,* 284**,** 23912-23924.

OUSSAIEF, L., RAMÍREZ, V., HIPPOCRATE, A., ARBACH, H., COCHET, C., PROUST, A., RAPHAËL, M., KHELIFA, R. & JOAB, I. 2011. NF-κB-mediated modulation of inducible nitric oxide synthase activity controls induction of the Epstein-Barr virus productive cycle by transforming growth factor beta 1. *J. Virol.,* 85**,** 6502-6512.

OWEN, T. J. 2010. *An investigation of the role of the Epstein-Barr virus-encoded protein, EBNA1, in the regulation of EBER expression.* Ph. D. thesis, University of Birmingham.

OWEN, T. J., O'NEIL, J. D., DAWSON, C. W., HU, C., CHEN, X., YAO, Y., WOOD, V. H. J., MITCHELL, L. E., WHITE, R. J., YOUNG, L. S. & ARRAND, J. R. 2010. Epstein-Barr virus-encoded EBNA1 enhances RNA polymerase III-dependent EBER expression through induction of EBER-associated cellular transcription factors. *Molecular Cancer,* 9**,** 241.

OWENS, P., PICKUP, M. W., NOVITSKIY, S. V., CHYTIL, A., GORSKA, A. E., AAKRE, M. E., WEST, J. & MOSES, H. L. 2011. Disruption of bone morphogenetic protein receptor 2 (BMPR2) in mammary tumours promotes metastases through cell autonomous and paracrine mediators. *Proc. Natl. Acad. Sci USA*.

PAGANO, J. S., BLASER, M., BUENDIA, M.-A., DAMANIA, B., KHALILI, K., RAAB-TRAUB, N. & ROIZMAN, B. 2004. Infectious agents and cancer: criteria for a causal relation. *Semin. Cancer Biol.,* 14**,** 453-471.

PANG, M.-F., LIN, K.-W. & PEH, S.-C. 2009. The signalling pathways of Epstein-Barr virus-encoded latent membrane protein 2A (LMP2A) in latency and cancer. *Cell. Mol. Biol. Lett.,* 14**,** 222-247.

PARDALI, K., KOWANETZ, M., HELDIN, C.-H. & MOUSTAKAS, A. 2005. Smad pathway-specific transcriptional regulation of the cell cycle inhibitor $p21^{WAF1/Cip1}$. *J. Cell. Physiol.,* 204**,** 260-272.

PARK, K., KIM, S.-J., BANG, Y.-J., PARK, J.-G., KIM, N. K., ROBERTS, A. B. & SPORN, M. B. 1994. Genetic changes in the transforming growth factor β (TGF-β) type II receptor gene in human gastric cancer cells: correlation with sensitivity to growth inhibition by TGF-β. *Proc. Natl. Acad. Sci USA,* 91**,** 8772-8776.

PARK, S. H. 2005. Fine tuning and cross-talking of TGF-β signal by inhibitory Smads. *J. Biochem. Mol. Biol.,* 38**,** 9-16.

PARK, S. H., LEE, S. R., KIM, B. C., CHO, E. A., PATEL, S. P., KANG, H.-B., SAUSVILLE, E. A., NAKANISHI, O., TREPEL, J. B., LEE, B. I. & KIM, S.-J. 2002. Transcriptional regulation of the transforming growth factor β type II receptor gene by histone acetyltransferase and deacetylase is mediated by NF-Y in human breast cancer cells. *J. Biol. Chem.,* 277**,** 5168-5174.

PARK, Y., KANG, M. H., SEO, H. Y., PARK, J. M., CHOI, C. W., KIM, Y. H., KIM, I. S., KIM, J. S. & OH, S. C. 2010. Bone morphogenetic protein-2 levels are elevated in the patients with gastric cancer and correlate with disease progression. *Med. Oncol.,* 27**,** 1192-1199.

PARK, Y., KIM, J. W., KIM, D. S., KIM, E. B., PARK, S. J., PARK, J. Y., CHOI, W. S., SONG, J. G., SEO, H. Y., OH, S. C., KIM, B. S., PARK, J. J., KIM, Y. H. & KIM, J. S. 2008. The bone morphogenesis protein-2 (BMP-2) is associated with progression to metastatic disease in gastric cancer. *Cancer Res. Treat.,* 40**,** 127-132.

PARKIN, D. M. 2006. The global health burden of infection-associated cancers in the year 2002. *Int. J. Cancer,* 118**,** 3030-3044.

PARKINSON, E. K. 1985. Defective responses of transformed keratinocytes to terminal differentiation stimuli. Their role in epidermal tumour promotion by phorbol esters and by deep skin wounding. *Br. J. Cancer,* 52**,** 479-493.

PARKINSON, E. K., GRABHAM, P. & EMMERSON, A. 1983. A subpopulation of cultured human keratinocytes which is resistant to the induction of terminal differentiation-related changes by phorbol, 12-myristate, 13-acetate: evidence for an increase in the resistant population following transformation. *Carcinogenesis,* 4**,** 857-861.

PARKINSON, E. K., PERA, M. F., EMMERSON, A. & GORMAN, P. A. 1984. Differential effects of complete and second-stage tumour promoters in normal but not transformed human and mouse keratinocytes. *Carcinogenesis,* 5**,** 1071-1077.

PARKINSON, K. & BALMAIN, A. 1990. Chalones revisited - a possible role for transforming growth factor β in tumour promotion. *Carcinogenesis,* 11**,** 195-198.

PATHMANATHAN, R., PRASAD, U., SADLER, R., FLYNN, K. & RAAB-TRAUB, N. 1995. Clonal proliferations of cells infected with Epstein-Barr virus in preinvasive lesions related to nasopharyngeal carcinoma. *N. Engl. J. Med.,* 333**,** 693-698.

PEGTEL, D. M., SUBRAMANIAN, A., SHEEN, T.-S., TSAI, C.-H., GOLUB, T. R. & THORLEY-LAWSON, D. A. 2005. Epstein-Barr virus-encoded LMP2A induces primary epithelial cell migration and invasion: possible role in nasopharyngeal caricnoma metastasis. *J. Virol.,* 79**,** 15430-15442.

PELLETT, P. E. & ROIZMAN, B. 2007. The Family Herpesviridae: a brief introduction. *In:* KNIPE, D. M. & HOWLEY, P. M. (eds.) *Fields Virology.* 5th ed.: Lippincott Williams & Wilkins.

PENG, H., SHINTANI, S., KIM, Y. & WONG, D. T. 2006. Loss of $p12^{CDK2\text{-}AP1}$ expression in human oral squamous cell carcinoma with disrupted transforming growth factor-β-Smad signalling pathway. *Neoplasia,* 8**,** 1028-1036.

PENG, R., MOSES, S. C., TAN, J., KREMMER, E. & LING, P. D. 2005. The Epstein-Barr virus EBNA-LP protein preferentially coactivates EBNA2-mediated stimulation of latent membrane proteins expressed from the viral divergent promoter. *J. Virol.,* 79**,** 4492-4505.

PENG, Y., KANG, Q., CHENG, H., LI, X., SUN, M. H., JIANG, W., LUU, H. H., PARK, J. Y., HAYDON, R. C. & HE, T.-C. 2003. Transcriptional characterisation of bone morphogenetic proteins (BMPs)-mediated osteogenic signalling. *J. Cell. Biochem.,* 90**,** 1149-1165.

PENHEITER, S. G., DEEP SINGH, R., REPELLIN, C. E., WILKES, M. C., EDENS, M., HOWE, P. H., PAGANO, R. E. & LEOF, E. B. 2010. Type II transforming growth factor-β receptor recycling is dependent upon the clathrin adaptor protein Dab2. *Mol. Biol. Cell,* 21**,** 4009-4019.
PENHEITER, S. G., MITCHELL, H., GARAMSZEGI, N., EDENS, M., DORÉ JR., J. J. E. & LEOF, E. B. 2002. Internalisation-dependent and -independent requirements for transforming growth factor β receptor signalling via the Smad pathway. *Mol. Cell. Biol.,* 22**,** 4750-4759.
PFEFFER, S., ZAVOLAN, M., GRASSER, F. A., CHIEN, M., RUSSO, J. J., JU, J., JOHN, B., ENRIGHT, A. J., MARKS, D., SANDER, C. & TUSCHL, T. 2004. Identification of virus-encoded microRNAs. *Science,* 304**,** 734-736.
PIEK, E., HELDIN, C.-H. & TEN DIJKE, P. 1999. Specificity, diversity and regulation in TGF-β superfamily signalling. *FASEB J.,* 13**,** 2105-2124.
POLVINO-BODNAR, M. & SCHAFFER, P. A. 1992. DNA binding activity is required for EBNA1-dependent transcriptional activation and DNA replication. *Virology,* 187**,** 591-603.
POULIOT, F., BLAIS, A. & LABRIE, C. 2003. Overexpression of a dominant negative type II bone morphogenetic protein receptor inhibits the growth of human breast cancer cells. *Cancer Res.,* 63**,** 277-281.
PROKOVA, V., MOSIALOS, G. & KARDASSIS, D. 2002. Inhibition of transforming growth factor β signalling and Smad-dependent activation of transcription by the latent membrane protein 1 of Epstein-Barr virus. *J. Biol. Chem.,* 277**,** 9342-9350.
PU, H., COLLAZO, J., JONES, E., GAYHEART, D., SAKAMOTO, S., VOGT, A., MITCHELL, B. & KYPRIANOU, N. 2009. Dysfunctional transforming growth factor-β receptor II accelerates prostate tumourigenesis in the TRAMP mouse model. *Cancer Res.,* 69**,** 7366-7374.
QIN, B. Y., LAM, S. S., CORREIA, J. J. & LIN, K. 2002. Smad3 allostery links TGF-β receptor kinase activation to transcriptional control. *Genes Dev.,* 16**,** 1950-1963.
QIU, W., SCHÖNLEBEN, F., LI, X. & SU, G. H. 2007. Disruption of transforming growth factor β-Smad signalling pathway in head and neck squamous cell carcinoma as evidenced by mutations of Smad2 and Smad4. *Cancer Letters,* 245**,** 163-170.
RAAB-TRAUB, N. 2002. Epstein-Barr virus in the pathogenesis of NPC. *Semin. Cancer Biol.,* 12**,** 431-441.
RAAB-TRAUB, N. & FLYNN, K. 1986. The structure of the termini of the Epstein-Barr virus as a marker of clonal cellular proliferation. *Cell,* 47**,** 883-889.
RABSON, M., GRADOVILLE, L., HESTON, L. & MILLER, G. 1982. Non-immortalising P3J-HR-1 Epstein-Barr virus: a deletion mutant of its transforming parent, Jijoye. *J. Virol.,* 44**,** 834-844.
RAVAL, P., HSU, H. H. T., SCHNEIDER, D. J., SARRAS JR., M. P., MASUHARA, K., BONEWALD, L. F. & ANDERSON, H. C. 1996. Expression of bone morphogenetic proteins by osteoinductive and non-osteoinductive human osteosarcoma cells. *J. Dent. Res.,* 75**,** 1518-1523.
RAZANI, B., ZHANG, X. L., BITZER, M., VON GERSDORFF, G., BÖTTINGER, E. P. & LISANTI, M. P. 2001. Caveolin-1 regulates transforming growth factor (TGF)-β/SMAD signalling through an interaction with the TGF-β type I receptor. *J. Biol. Chem.,* 276**,** 6727-6738.
REISMAN, D. & SUGDEN, B. 1986. *trans* activation of an Epstein-Barr viral transcriptional enhancer by the Epstein-Barr viral nuclear antigen 1. *Mol. Cell. Biol.,* 6**,** 3838-3846.
REISMAN, D., YATES, J. & SUGDEN, B. 1985. A putative origin of replication of plasmids derived from Epstein-Barr virus is composed of two cis-acting components. *Mol. Cell. Biol.,* 5**,** 1822-1832.
RENNE, R., BARRY, C., DITTMER, D., COMPITELLO, N., BROWN, P. O. & GANEM, D. 2001. Modulation of cellular and viral gene expression by the latency-associated nuclear antigen of Kaposi's Sarcoma-associated herpesvirus. *J. Virol.,* 75**,** 458-468.
RICKINSON, A. B. & KIEFF, E. D. 2007. Epstein-Barr virus. *In:* KNIPE, D. M. & HOWLEY, P. M. (eds.) *Fields Virology.* 5th ed.: Lippincott Williams & Wilkins.
RICKINSON, A. B., YOUNG, L. S. & ROWE, M. 1987. Influence of the Epstein-Barr virus nuclear antigen EBNA2 on the growth phenotype of virus-transformed B cells. *J. Virol.,* 61**,** 1310-1317.
RIGGINS, G. J., KINZLER, K. W., VOGELSTEIN, B. & THIAGALINGAM, S. 1997. Frequency of *Smad* gene mutations in human cancers. *Cancer Res.,* 57**,** 2578-2580.
ROBERTS, A. B., ANZANO, M. A., LAMB, L. C., SMITH, J. M. & SPORN, M. B. 1981. New class of transforming growth factors potentiated by epidermal growth factor: isolation from non-neoplastic tissues. *Proc. Natl. Acad. Sci USA,* 78**,** 5339-5343.

ROBERTS, A. B., FROLIK, C. A., ANZANO, M. A. & SPORN, M. B. 1983. Transforming growth factors from neoplastic and nonneoplastic tissues. *Fed. Proc.,* 42**,** 2621-2626.
ROBERTS, A. B., LAMB, L. C., NEWTON, D. L., SPORN, M. B., DE LARCO, J. E. & TODARO, G. J. 1980. Transforming growth factors: isolation of polypeptides from virally and chemically transformed cells by acid/ethanol extraction. *Proc. Natl. Acad. Sci USA,* 77**,** 3494-3498.
ROBERTS, A. B. & WAKEFIELD, L. M. 2003. The two faces of transforming growth factor β in carcinogenesis. *Proc. Natl. Acad. Sci USA,* 100**,** 8621-8623.
ROBINSON, J. E. 1982. The biology of circulating B lymphocytes infected with Epstein-Barr virus during infectious mononucleosis. *Yale Journal of Biology and Medicine,* 55**,** 311-316.
ROIZMAN, B. & BAINES, J. 1991. The diversity and unity of herpesviridae. *Comp. Immun. Microbiol. Infect. Dis.,* 14**,** 63-79.
ROJAS, A., PADIDAM, M., CRESS, D. & GRADY, W. M. 2009. TGF-β receptor levels regulate the specificity of signalling pathway activation and biological effects of TGF-β. *Biochim. Biophys. Acta,* 1793**,** 1165-1173.
ROSA, M. D., GOTTLIEB, E., LERNER, M. R. & STEITZ, J. A. 1981. Striking similarities are exhibited by two small Epstein-Barr virus-encoded ribonucleic acids and the adenovirus-associated ribonucleic acids VAI and VAII. *Mol. Cell. Biol.,* 1**,** 785-796.
ROSENZWEIG, B. L., IMAMURA, T., OKADOME, T., COX, G. N., YAMASHITA, H., TEN DIJKE, P., HELDIN, C.-H. & MIYAZONO, K. 1995. Cloning and characterisation of a human type II receptor for bone morphogenetic proteins. *Proc. Natl. Acad. Sci USA,* 92**,** 7632-7636.
ROTHHAMMER, T., POSER, I., SONCIN, F., BATAILLE, F., MOSER, M. & BOSSERHOFF, A.-K. 2005. Bone morphogenic proteins are overexpressed in malignant melanoma and promote cell invasion and migration. *Cancer Res.,* 65**,** 448-456.
ROUGHAN, J. E. & THORLEY-LAWSON, D. A. 2009. The intersection of Epstein-Barr virus with the germinal centre. *J. Virol.,* 83**,** 3968-3976.
ROVEDO, M. & LONGNECKER, R. 2007. Epstein-Barr virus latent membrane protein 2B (LMP2B) modulates LMP2A activity. *J. Virol.,* 81**,** 84-94.
ROWE, M., LEAR, A. L., CROOM-CARTER, D., DAVIES, A. H. & RICKINSON, A. B. 1992. Three pathways of Epstein-Barr virus gene activation from EBNA1-positive latency in B lymphocytes. *J. Virol.,* 66**,** 122-131.
ROWE, M., PENG-PILON, M., HUEN, D. S., HARDY, R., CROOM-CARTER, D., LUNDGREN, E. & RICKINSON, A. B. 1994. Upregulation of bcl-2 by the Epstein-Barr virus latent membrane protein LMP: a B cell-specific response that is delayed relative to NF-κB activation and to induction of cell surface markers. *J. Virol.,* 68**,** 5602-5612.
ROWE, M., YOUNG, L. S., CADWALLADER, K., PETTI, L., KIEFF, E. & RICKINSON, A. B. 1989. Distinction between Epstein-Barr virus type A (EBNA 2A) and type B (EBNA 2B) isolates extends to the EBNA2 family of nuclear proteins. *J. Virol.,* 63**,** 1031-1039.
RUF, I. K., RHYNE, P. W., YANG, C., CLEVELAND, J. L. & SAMPLE, J. T. 2000. Epstein-Barr virus small RNAs potentiate tumorigenicity of Burkitt lymphoma cells independently of an effect on apoptosis. *J. Virol.,* 74**,** 10223-10228.
RUF, I. K. & SAMPLE, J. 1999. Repression of Epstein-Barr virus EBNA-1 gene transcription by pRb during restricted latency. *J. Virol.,* 73**,** 7943-7951.
RUNYAN, C. E., PONCELET, A.-C. & SCHNAPER, H. W. 2006. TGF-β receptor-binding proteins: complex interactions. *Cellular Signalling,* 18**,** 2077-2088.
RUNYAN, C. E., SCHNAPER, H. W. & PONCELET, A.-C. 2005. The role of internalization in transforming growth factor β1-induced Smad2 association with Smad anchor for receptor activation (SARA) and Smad2-dependent signalling in human mesangial cells. *J. Biol. Chem.,* 280**,** 8300-8308.
RYU, B. & KERN, S. E. 2003. The essential similarity of TGFβ and activin receptor transcriptional responses in cancer cells. *Cancer Biol. Ther.,* 2**,** 164-170.
SADOWSKI, L., PILECKA, I. & MIACZYNSKA, M. 2009. Signalling from endosomes: location makes a difference. *Exp. Cell Res.,* 315**,** 1601-1609.
SAKAI, T., TANIGUCHI, Y., TAMURA, K., MINOGUCHI, S., FUKUHARA, T., STROBL, L. J., ZIMBER-STROBL, U., BORNKAMM, G. W. & HONJO, T. 1998. Functional replacement of the

intracellular region of the Notch1 receptor by Epstein-Barr virus nuclear antigen 2. *J. Virol.,* 72**,** 6034-6039.
SAMANTA, M., IWAKIRI, D., KANDA, T., IMAIZUMI, T. & TAKADA, K. 2006. EB virus-encoded RNAs are recognised by RIG-I and activate signalling to induce type I IFN. *EMBO J.,* 25**,** 4207-4214.
SAMPATH, T. K., COUGHLIN, J. E., WHETSTONE, R. M., BANACH, D., CORBETT, C., RIDGE, R. J., OZKAYNAK, E., OPPERMAN, H. & RUEGER, D. C. 1990. Bovine osteogenic protein is composed of dimers of OP-1 and BMP-2A, two members of the transforming growth factor-β superfamily. *J. Biol. Chem.,* 265**,** 13198-13205.
SAMPLE, J., HENSON, E. B. D. & SAMPLE, C. 1992. The Epstein-Barr virus nuclear protein 1 promoter active in type I latency is autoregulated. *J. Virol.,* 66**,** 4654-4661.
SAMPLE, J., LIEBOWITZ, D. & KIEFF, E. 1989. Two related Epstein-Barr virus membrane proteins are encoded by separate genes. *J. Virol.,* 63**,** 933-937.
SAMPLE, J., YOUNG, L., MARTIN, B., CHATMAN, T., KIEFF, E., RICKINSON, A. & KIEFF, E. 1990. Epstein-Barr virus types 1 and 2 differ in their EBNA-3A, EBNA-3B, and EBNA-3C genes. *J. Virol.,* 64**,** 4084-4092.
SÁNCHEZ, A., ÁLVAREZ, A. M., LÓPEZ PEDROSA, J. M., RONCERO, C., BENITO, M. & FABREGAT, I. 1999. Apoptotic response to TGF-β in fetal hepatocytes depends upon their state of differentiation. *Exp. Cell Res.,* 252**,** 281-291.
SANTÓN, A., CRISTÓBAL, E., APARICIO, M., ROYUELA, A., VILLAR, L. M. & ÁLVAREZ-CERMEÑO, J. C. 2011. High frequency of co-infection by Epstein-Barr virus types 1 and 2 in patients with multiple sclerosis. *Multiple Sclerosis Journal*.
SAVAGE, C., DAS, P., FINELLI, A. L., TOWNSEND, S. R., SUN, C.-Y., BAIRD, S. E. & PADGETT, R. W. 1996. *Caenorhabditis elegans* genes *sma-2*, *sma-3* and *sma-4* define a conserved family of transforming growth factor β pathway components. *Proc. Natl. Acad. Sci USA,* 93**,** 790-794.
SCHAEFER, B. C., PAULSON, E., STROMINGER, J. L. & SPECK, S. H. 1997a. Constitutive activation of Epstein-Barr virus (EBV) nuclear antigen 1 gene transcription by IRF1 and IRF2 during restricted EBV latency. *Mol. Cell. Biol.,* 17**,** 873-886.
SCHAEFER, B. C., STROMINGER, J. L. & SPECK, S. H. 1997b. Host cell-determined methylation of specific Epstein-Barr virus promoters regulates the choice between distinct viral latency programs. *Mol. Cell. Biol.,* 17**,** 364-377.
SCHLAGER, S., SPECK, S. H. & WOISETSCHLÄGER, M. 1996. Transcription of the Epstein-Barr virus nuclear antigen 1 (EBNA1) gene occurs before induction of the BCR2 (Cp) EBNA gene promoter during the initial stages of infection in B cells. *J. Virol.,* 70**,** 3561-3570.
SCHMIERER, B. & HILL, C. S. 2007. TGFβ-SMAD signal transduction: molecular specificity and functional flexibility. *Nat. Rev. Mol. Cell Biol.,* 8**,** 970-982.
SCHNEPP, R. & HUA, X. 2003. A Tumour-suppressing duo: TGFβ and activin modulate a similar transcriptome. *Cancer Biol. Ther.,* 2**,** 171-172.
SCHOLLE, F., BENDT, K. M. & RAAB-TRAUB, N. 2000. Epstein-Barr virus LMP2A transforms epithelial cells, inhibits cell differentiation, and activates Akt. *J. Virol.,* 74**,** 10681-10689.
SCHULTZ-CHERRY, S. & HINSHAW, V. S. 1996. Influenza virus neuraminidase activates latent transforming growth factor β. *J. Virol.,* 70**,** 8624-8629.
SEKELSKY, J. J., NEWFELD, S. J., RAFTERY, L. A., CHARTOFF, E. H. & GELBART, W. M. 1995. Genetic characterisation and cloning of *Mothers against dpp*, a gene required for *decapentaplegic* function in *Drosophila melanogaster*. *Genetics,* 139**,** 1347-1358.
SEKIMOTO, G., MATSUZAKI, K., YOSHIDA, K., MORI, S., MURATA, M., SEKI, T., MATSUI, H., FUJISAWA, J.-I. & OKAZAKI, K. 2007. Reversible Smad-dependent signalling between tumour suppression and oncogenesis. *Cancer Res.,* 67**,** 5090-5096.
SENGUPTA, S., DEN BOON, J. A., CHEN, I.-H., NEWTON, M. A., DAHL, D. B., CHEN, M., CHENG, Y.-J., WESTRA, W. H., CHEN, C.-J., HILDESHEIM, A., SUGDEN, B. & AHLQUIST, P. 2006. Genome-wide expression profiling reveals EBV-associated inhibition of MHC class I expression in nasopharyngeal carcinoma. *Cancer Res.,* 66**,** 7999-8006.
SEO, S. R., LALLEMAND, F., FERRAND, N., PESSAH, M., L'HOSTE, S., CAMONIS, J. & ATFI, A. 2004. The novel E3 ubiquitin ligase Tiul1 associates with TGIF to target Smad2 for degradation. *EMBO J.,* 23**,** 3780-3792.

SEO, T., PARK, J. & CHOE, J. 2005. Kaposi's sarcoma-associated herpesvirus viral IFN regulatory factor 1 inhibits transforming growth factor-β signalling. *Cancer Res.,* 65**,** 1738-1747.
SEOANE, J. 2006. Escaping from the TGFβ anti-proliferative control. *Carcinogenesis,* 27**,** 2148-2156.
SHAH, K. M., STEWART, S. E., WEI, W., WOODMAN, C. B. J., O'NEIL, J. D., DAWSON, C. W. & YOUNG, L. S. 2009. The EBV-encoded latent membrane proteins, LMP2A and LMP2B, limit the actions of interferon by targeting interferon receptors for degradation. *Oncogene,* 28**,** 3903-3914.
SHANMUGARATNAM, K. & SOBIN, L. H. 1993. The World Health Organization histological classification of tumours of the upper respiratory tract and ear. *Cancer,* 71**,** 2689-2697.
SHANNON-LOWE, C. D., ADLAND, E., BELL, A. I., DELECLUSE, H.-J., RICKINSON, A. B. & ROWE, M. 2009. Features distinguishing Epstein-Barr virus infections of epithelial cells and B cells: viral genome expression, genome maintenance, and genome amplification. *J. Virol.,* 83**,** 7749-7760.
SHANNON-LOWE, C. D., NEUHIERL, B., BALDWIN, G., RICKINSON, A. B. & DELECLUSE, H.-J. 2006. Resting B cells as a transfer vehicle for Epstein-Barr virus infection of epithelial cells. *Proc. Natl. Acad. Sci USA,* 103**,** 7065-7070.
SHEU, L.-F., CHEN, A., MENG, C.-L., HO, K.-C., LEE, W.-H., LEU, F.-J. & CHAO, C.-F. 1996. Enhanced malignant progression of nasopharyngeal carcinoma cells mediated by the expression of Epstein-Barr nuclear antigen 1 *in vivo*. *J. Pathol.,* 180**,** 243-248.
SHI, Y., WANG, Y.-F., JAYARAMAN, L., YANG, H., MASSAGUÉ, J. & PAVLETICH, N. P. 1998. Crystal structure of a Smad MH1 domain bound to DNA: Insights on DNA binding in TGF-β signalling. *Cell,* 94**,** 585-594.
SHIBATA, D., TOKUNAGA, M., UEMURA, Y., SATO, E., TANAKA, S. & WEISS, L. M. 1991. Association of Epstein-Barr virus with undifferentiated gastric carcinomas with intense lymphoid infiltration: Lymphoepithelioma-like carcinoma. *Am. J. Pathol.,* 139**,** 469-474.
SHIBATA, D. & WEISS, L. M. 1992. Epstein-Barr virus-associated gastric adenocarcinoma. *Am. J. Pathol.,* 140**,** 769-774.
SHIRE, K., CECCARELLI, D. F. J., AVOLIO-HUNTER, T. M. & FRAPPIER, L. 1999. EBP2, a human protein that interacts with sequences of the Epstein-Barr virus nuclear antigen 1 important for plasmid maintenance. *J. Virol.,* 73**,** 2587-2595.
SHIRE, K., KAPOOR, P., JIANG, K., HING, M. N. T., SIVACHANDRAN, N., NGUYEN, T. & FRAPPIER, L. 2006. Regulation of the EBNA1 Epstein-Barr virus protein by serine phosphorylation and arginine methylation. *J. Virol.,* 80**,** 5261-5272.
SIEBER, C., KOPF, J., HIEPEN, C. & KNAUS, P. 2009. Recent advances in BMP receptor signalling. *Cytokine Growth Factor Rev.,* 20**,** 343-355.
SIEGEL, P. M. & MASSAGUÉ, J. 2003. Cytostatic and apoptotic actions of TGFβ in homeostasis and cancer. *Nat. Rev. Cancer,* 3**,** 807-820.
SINGH, A. & MORRIS, R. J. 2010. The yin and yang of bone morphogenetic proteins in cancer. *Cytokine Growth Factor Rev.,* 21**,** 299-313.
SIVACHANDRAN, N., CAO, J. Y. & FRAPPIER, L. 2010. Epstein-Barr virus nuclear antigen 1 hijacks the host kinase CK2 to disrupt PML nuclear bodies. *J. Virol.,* 84**,** 11113-11123.
SIVACHANDRAN, N., SARKARI, F. & FRAPPIER, L. 2008. Epstein-Barr nuclear antigen 1 contributes to nasopharyngeal carcinoma through disruption of PML nuclear bodies. *PLoS Pathogens,* 4**,** e1000170.
SIXBEY, J. W., CHESNEY, P. J., SHIRLEY, P., BUNTIN, D. M. & RESNICK, L. 1989. Detection of a second widespread strain of Epstein-Barr virus. *Lancet,* 334**,** 761-765.
SKONIER, J., BENNETT, K., ROTHWELL, V., KOSOWSKI, S., PLOWMAN, G., WALLACE, P., EDELHOFF, S., DISTECHE, C., NEUBAUER, M., MARGUARDT, H., RODGERS, J. & PURCHIO, A. F. 1994. βig-h3: a transforming growth factor-β-responsive gene encoding a secreted protein that inhibits cell attachment in vitro and suppresses the growth of CHO cells in nude mice. *DNA Cell Biol.,* 13**,** 571-584.
SKONIER, J., NEUBAUER, M., MADISEN, L., BENNETT, K., PLOWMAN, G. D. & PURCHIO, A. F. 1992. cDNA cloning and sequence analysis of βig-h3, a novel gene induced in a human adenocarcinoma cell line after treatment with transforming growth factor-β. *DNA Cell Biol.,* 11**,** 511-522.

SMITH, S., GIRIAT, I., SCHMITT, A. & DE LANGE, T. 1998. Tankyrase, a poly(ADP-ribose) polymerase at human telomeres. *Science,* 282**,** 1484-1487.
SNUDDEN, D. K., HEARING, J., SMITH, P. R., GRÄSSER, F. A. & GRIFFIN, B. E. 1994. EBNA-1, the major nuclear antigen of Epstein-Barr virus, resembles 'RGG' RNA binding proteins. *EMBO J.,* 13**,** 4840-4847.
SOARES, A. F., XAVIER, R. L. D. F., MIGUEL, M. C. D. C., DE SOUZA, L. B. & PINTO, L. P. 2010. Bone morphogenetic protein-2/4 and bone morphogenetic protein receptor type IA expression in metastatic and nonmetastatic oral squamous cell carcinoma. *Am. J. Otolaryngology - Head and Neck Medicine and Surgery,* 31**,** 266-271.
SOMPALLAE, R., CALLEGARI, S., KAMRANVAR, S. A. & MASUCCI, M. G. 2010. Transcription profiling of Epstein-Barr virus nuclear antigen (EBNA)-1 expressing cells suggests targeting of chromatin remodelling complexes. *PLoS ONE,* 5**,** e12052.
SORRENTINO, A., THAKUR, N., GRIMSBY, S., MARCUSSON, A., VON BULOW, V., SCHUSTER, N., ZHANG, S., HELDIN, C. H. & LANDSTRÖM, M. 2008. The type I TGF-beta receptor engages TRAF6 to activate TAK1 in a receptor kinase-independent manner. *Nat. Cell Biol.,* 10**,** 1199-1207.
SOUCHELNYTSKYI, S., NAKAYAMA, T., NAKAO, A., MORÉN, A., HELDIN, C.-H., CHRISTIAN, J. L. & TEN DIJKE, P. 1998. Physical and functional interaction of murine and *Xenopus* Smad7 with bone morphogenetic protein receptors and transforming growth factor-β receptors. *J. Biol. Chem.,* 273**,** 25364-25370.
SPANO, J.-P., BUSSON, P., ATLAN, D., BOURHIS, J., PIGNON, J.-P., ESTEBAN, C. & ARMAND, J.-P. 2003. Nasopharyngeal carcinomas: an update. *Eur. J. Cancer,* 39**,** 2121-2135.
SPECK, P., KLINE, K. A., CHERESH, P. & LONGNECKER, R. 1999. Epstein-Barr virus lacking latent membrane protein 2 immortalises B cells with efficiency indistinguishable from that of wild-type virus. *J. Gen. Virol.,* 80**,** 2193-2203.
SPINELLA-JAEGLE, S., ROMAN-ROMAN, S., FAUCHEU, C., DUNN, F.-W., KAWAI, S., GALLÉA, S., STIOT, V., BLANCHET, A. M., COURTOIS, B., BARON, R. & RAWADI, G. 2001. Opposite effects of bone morphogenetic protein-2 and transforming growth factor-β1 on osteoblast differentiation. *Bone,* 29**,** 323-330.
SRINIVAS, S. K. & SIXBEY, J. W. 1995. Epstein-Barr virus induction of recombinase-activating genes RAG1 and RAG2. *J. Virol.,* 69**,** 8155-8158.
SRIURANPONG, V., MUTIRANGURA, A., GILLESPIE, J. W., PATEL, V., AMORNPHIMOLTHAM, P., MOLINOLO, A. A., KEREKHANJANARONG, V., SUPANAKORN, S., SUPIYAPHUN, P., RANGDAENG, S., VORAVUD, N. & GUTKIND, J. S. 2004. Global gene expression profile of nasopharyngeal carcinoma by laser capture microdissection and complementary DNA microarrays. *Clin. Cancer Res.,* 10**,** 4944-4958.
SRIVASTAVA, G., WONG, K. Y., CHIANG, A. K. S., LAM, K. Y. & TAO, Q. 2000. Coinfection of multiple strains of Epstein-Barr virus in immunocompetent normal individuals: reassessment of the viral carrier state. *Blood,* 95**,** 2443-2445.
STEWART, S., DAWSON, C. W., TAKADA, K., CURNOW, J., MOODY, C. A., SIXBEY, J. W. & YOUNG, L. S. 2004. Epstein-Barr virus-encoded LMP2A regulates viral and cellular gene expression by modulation of the NF-κB transcription factor pathway. *Proc. Natl. Acad. Sci USA,* 101**,** 15730-15735.
SUGDEN, B. & WARREN, N. 1989. A promoter of Epstein-Barr virus that can function during latent infection can be transactivated by EBNA-1, a viral protein required for viral DNA replication during latent infection. *J. Virol.,* 63**,** 2644-2649.
SUN, W., YU, Y., DOTTI, G., SHEN, T., TAN, X., SAVOLDO, B., PASS, A. K., CHU, M., ZHANG, D., LU, X., FU, S., LIN, X. & YANG, J. 2009. PPM1A and PPM1B act as IKKβ phosphatases to terminate TNFα-induced IKKβ-NF-κB activation. *Cellular Signalling,* 21**,** 95-102.
SUNG, N. S., KENNEDY, S., GUTSCH, D. & PAGANO, J. S. 1991. EBNA-2 transactivates a lymphoid-specific enhancer in the *Bam*HI C promoter of Epstein-Barr virus. *J. Virol.,* 65**,** 2164-2169.
TAKADA, K. 2000. Epstein-Barr virus and gastric carcinoma. *J. Clin. Pathol: Mol. Pathol.,* 53**,** 255-261.
TAKEUCHI, T., ADACHI, Y., NAGAYAMA, T. & FURIHATA, M. 2011. Nedd4L modulates the transcription of metalloproteinase-1 and -13 genes to increase the invasive activity of gallbladder cancer. *Int. J. Exp. Pathol.,* 92**,** 79-86.

TANG, J., GORDON, G. M., MÜLLER, M. G., DAHIYA, M. & FOREMAN, K. E. 2003. Kaposi's sarcoma-associated herpesvirus latency-associated nuclear antigen induces expression of the helix-loop-helix protein Id-1 in human endothelial cells. *J. Virol.,* 77**,** 5975-5984.
TAO, Q. & CHAN, A. T. C. 2007. Nasopharyngeal carcinoma: molecular pathogenesis and therapeutic developments. *Exp. Rev. Mol. Med.,* 9**,** 1-24.
TAO, Q., ROBERTSON, K. D., MANNS, A., HILDESHEIM, A. & AMBINDER, R. F. 1998. The Epstein-Barr virus major latent promoter Qp is constitutively active, hypomethylated and methylation sensitive. *J. Virol.,* 72**,** 7075-7083.
TATEISHI, M., KUSABA, I., MASUDA, H., TANAKA, T., MATSUMATA, T. & SUGIMACHI, K. 2000. The progression of invasiveness regarding the role of transforming growth factor β receptor type II in gastric cancer. *Eur. J. Surg. Oncol.,* 26**,** 377-380.
TEICHER, B. A. 2007. Transforming growth factor-β and the immune response to malignant disease. *Clin. Cancer Res.,* 13**,** 6247-6251.
TELLAM, J., SMITH, C., RIST, M., WEBB, N., COOPER, L., VUOCOLO, T., CONNOLLY, G., TSCHARKE, D. C., DEVOY, M. P. & KHANNA, R. 2008. Regulation of protein translation through mRNA structure influences MHC class I loading and T cell recognition. *Proc. Natl. Acad. Sci USA,* 105**,** 9319-9324.
TEMPERA, I., DENG, Z., ATANASIU, C., CHEN, C. J., D'ERME, M. & LIEBERMAN, P. M. 2010. Regulation of Epstein-Barr virus OriP replication by poly(ADP-ribose) polymerase 1. *J. Virol.,* 84**,** 4988-4897.
TEN DIJKE, P. & HILL, C. S. 2004. New insights into TGF-β-Smad signalling. *Trends Biochem. Sci.,* 29**,** 265-273.
TEN DIJKE, P., KORCHYNSKYI, O., VALDIMARSDOTTIR, G. & GOUMANS, M.-J. 2003. Controlling cell fate by bone morphogenetic protein receptors. *Mol. Cell. Endocrinol.,* 211**,** 105-113.
TEN DIJKE, P., YAMASHITA, H., SAMPATH, T. K., REDDI, A. H., ESTEVEZ, M., RIDDLE, D. L., ICHIJO, H., HELDIN, C.-H. & MIYAZONO, K. 1994. Identification of type I receptors for osteogenic protein-1 and bone morphogenetic protein 4. *J. Biol. Chem.,* 269**,** 16985-16988.
THAPA, N., LEE, B.-H. & KIM, I.-S. 2007. TGFBIp/βig-h3 protein: a versatile matrix molecule induced by TGF-β. *Int. J. Biochem. Cell Biol.,* 39**,** 2183-2194.
THORLEY-LAWSON, D. A. 2001. Epstein-Barr virus: exploiting the immune system. *Nat. Rev. Immunol.,* 1**,** 75-82.
THORLEY-LAWSON, D. A. & GROSS, A. 2004. Persistence of the Epstein-Barr virus and the origins of associated lymphomas. *N. Engl. J. Med.,* 350**,** 1328-1337.
THORLEY-LAWSON, D. A., MIYASHITA, E. M. & KHAN, G. 1996. Epstein-Barr virus and the B cell: that's all it takes. 4**,** 204-208.
THUN, M. J., DELANCEY, J. O., CENTER, M. M., JEMAL, A. & WARD, E. M. 2010. The global burden of cancer: priorities for prevention. *Carcinogenesis,* 31**,** 100-110.
TIAN, M., NEIL, J. R. & SCHIEMANN, W. P. 2011. Transforming growth factor-β and the hallmarks of cancer. *Cellular Signalling,* 23**,** 951-962.
TIERNEY, R. J., EDWARDS, R. H., SITKI-GREEN, D., CROOM-CARTER, D., ROY, S., YAO, Q.-Y., RAAB-TRAUB, N. & RICKINSON, A. B. 2006. Multiple Epstein-Barr virus strains in patients with infectious mononucleosis: comparison of ex vivo samples with in vitro isolates by use of heteroduplex tracking assays. *J. Infect. Dis.,* 193**,** 287-297.
TIERNEY, R. J., STEVEN, N., YOUNG, L. S. & RICKINSON, A. B. 1994. Epstein-Barr virus latency in blood mononuclear cells: analysis of viral gene transcription during primary infection and in the carrier state. *J. Virol.,* 68**,** 7374-7385.
TOBIN, S. W., DOUVILLE, K., BENBOW, U., BRINCKERHOFF, C. E., MEMOLI, V. A. & ARRICK, B. A. 2002. Consequences of altered TGF-β expression and responsiveness in breast cancer: evidence for autocrine and paracrine effects. *Oncogene,* 21**,** 108-118.
TOKUNAGA, M., LAND, C. E., UEMURA, Y., TOKUDOME, T., TANAKA, S. & SATO, E. 1993. Epstein-Barr virus in gastric carcinoma. *Am. J. Pathol.,* 143**,** 1250-1254.
TOMKINSON, B. & KIEFF, E. 1992. Use of second-site homologous recombination to demonstrate that Epstein-Barr virus nuclear protein 3B is not important for lymphocyte infection of growth transformation in vitro. *J. Virol.,* 66**,** 2893-2903.

TOMKINSON, B., ROBERTSON, E. & KIEFF, E. 1993. Epstein-Barr virus nuclear proteins EBNA-3A and EBNA-3C are essential for B-lymphocyte growth transformation. *J. Virol.,* 67**,** 2014-2025.
TONG, J. H., NG, D. C., CHAU, S. L., SO, K. K., LEUNG, P. P., LEE, T. L., LUNG, R. W., CHAN, M. W., CHAN, A. W., LO, K. W. & TO, K. F. 2010. Putative tumour-suppressor gene DAB2 is frequently down regulated by promoter hypermethylation in nasopharyngeal carcinoma. *BMC Cancer,* 10**,** 253.
TSANG, C. M., ZHANG, G., SETO, E., TAKADA, K., DENG, W., YIP, Y. L., MAN, C., HAU, P. M., CHEN, H., CAO, Y., LO, K. W., MIDDELDORP, J. M., CHEUNG, A. L. M. & TSAO, S. W. 2010. Epstein-Barr virus infection in immortalised nasopharyngeal epithelial cells: regulation of infection and phenotypic characterisation. *Int. J. Cancer,* 127**,** 1570-1583.
TSAO, S. W., TRAMOUTANIS, G., DAWSON, C. W., LO, A. K. & HUANG, D. P. 2002. The significance of LMP1 expression in nasopharyngeal carcinoma. *Semin. Cancer Biol.,* 12**,** 473-487.
TSUKAZAKI, T., CHIANG, T. A., DAVISON, A. F., ATTISANO, L. & WRANA, J. L. 1998. SARA, a FYVE domain protein that recruits Smad2 to the TGFβ receptor. *Cell,* 95**,** 779-791.
TSURUMI, T., FUJITA, M. & KUDOH, A. 2005. Latent and lytic Epstein-Barr virus replication strategies. *Rev. Med. Virol.,* 15**,** 3-15.
UCHIDA, J., YASUI, T., TAKAOKA-SHICHIJO, Y., MURAOKA, M., KULWICHIT, W., RAAB-TRAUB, N. & KIKUTANI, H. 1999. Mimicry of CD40 signals by Epstein-Barr virus LMP1 in B lymphocyte responses. *Science,* 286**,** 300-303.
ULLOA, L., DOODY, J. & MASSAGUÉ, J. 1999. Inhibition of transforming growth factor-β/Smad signalling by the interferon-γ/STAT pathway. *Nature,* 397**,** 710-713.
UOZAKI, H. & FUKAYAMA, M. 2008. Epstein-Barr virus and gastric carcinoma - viral carcinogenesis through epigenetic mechanisms. *Int. J. Clin. Exp. Pathol.,* 1**,** 198-216.
URIST, M. R. 1965. Bone: formation by autoinduction. *Science,* 150**,** 893-899.
VAES, B. L. T., DECHERING, K. J., FEIJEN, A., HENDRIKS, J. M. A., LEFÈVRE, C., MUMMERY, C. L., OLIJVE, W., VAN ZOELEN, E. J. J. & STEEGENGA, W. T. 2002. Comprehensive microarray analysis of bone morphogenetic protein 2-induced osteoblast differentiation resulting in the identification of novel markers for bone development. *J. Bone. Miner. Res.,* 17**,** 2106-2118.
VALENTINE, R., DAWSON, C. W., HU, C., SHAH, K. M., OWEN, T. J., DATE, K. L., MAIA, S. P., SHAO, J., ARRAND, J. R., YOUNG, L. S. & O'NEIL, J. D. 2010. Epstein-Barr virus-encoded EBNA1 inhibits the canonical NF-κB pathway in carcinoma cells by inhibiting IKK phosphorylation. *Molecular Cancer,* 9**,** 1.
VALERA, E., ISAACS, M. J., KAWAKAMI, Y., BELMONTE, J. C. I. & CHOE, S. 2010. BMP-2/6 heterodimer is more effective than BMP-2 or BMP-6 homodimers as inductor of differentiation of human embryonic stem cells. *PLoS ONE,* 5**,** e11167.
VAN BAARLE, D., HOVENKAMP, E., DUKERS, N. H. T. M., RENWICK, N., KERSTEN, M. J., GOUDSMIT, J., COUTINHO, R. A., MIEDEMA, F. & VAN OERS, M. H. J. 2000. High prevalence of Epstein-Barr virus type 2 among homosexual men is caused by sexual transmission. *J. Infect. Dis.,* 181**,** 2045-2049.
VAN DER VELDEN, J. L. J., ALCORN, J. F., GUALA, A. S., BADURA, E. C. H. L. & JANSSEN-HEININGER, Y. M. W. 2011. c-Jun N-terminal kinase 1 promotes transforming growth factor-β1-induced epithelial-to-mesenchymal transition via control of linker phosphorylation and transcriptional activity of Smad3. *Am. J. Respir. Cell. Mol. Biol.,* 44**,** 571-581.
VAN SCOY, S., WATAKABE, I., KRAINER, A. R. & HEARING, J. 2000. Human p32: A coactivator for Epstein-Barr virus nuclear antigen-1-mediated transcriptional activation and possible role in viral latent cycle DNA replication. *Virology,* 275**,** 145-157.
VASILAKI, E., SIDERAKIS, M., PAPAKOSTA, P., SKOURTI-STATHAKI, K., MAVRIDOU, S. & KARDASSIS, D. 2009. Novel regulation of Smad3 oligomerisation and DNA binding by its linker domain. *Biochemistry,* 48**,** 8366-8378.
VIGNA, E. & NALDINI, L. 2000. Lentiviral vectors: excellent tools for experimental gene transfer and promising candidates for gene therapy. *J. Gene Med.,* 2**,** 308-316.
VIVIEN, D., ATTISANO, L., WRANA, J. L. & MASSAGUÉ, J. 1995. Signalling activity of homologous and heterologous transforming growth factor-β receptor kinase complexes. *J. Biol. Chem.,* 270**,** 7134-7141.

VOO, K. S., FU, T., WANG, H. Y., TELLAM, J., HESLOP, H. E., BRENNER, M. K., ROONEY, C. M. & WANG, R.-F. 2004. Evidence for the presentation of major histocompatibility complex class I-restricted Epstein-Barr virus nuclear antigen 1 peptides to CD8+ T lymphocytes. *J. Exp. Med.,* 199**,** 459-470.

WANG, D., LIEBOWITZ, D. & KIEFF, E. 1985. An EBV membrane protein expressed in immortalised lymphocytes transforms established rodent cells. *Cell,* 43**,** 831-840.

WANG, F., GREGORY, C., SAMPLE, C., ROWE, M., LIEBOWITZ, D., MURRAY, R., RICKINSON, A. & KIEFF, E. 1990. Epstein-Barr virus latent membrane protein (LMP1) and nuclear proteins 2 and 3C are effectors of phenotypic changes in B lymphocytes: EBNA-2 and LMP1 cooperatively induce CD23. *J. Virol.,* 64**,** 2309-2318.

WANG, F., GREGORY, C. D., ROWE, M., RICKINSON, A. B., WANG, D., BIRKENBACH, M., KIKUTANI, H., KISHIMOTO, T. & KIEFF, E. 1987. Epstein-Barr virus nuclear antigen 2 specifically induces expression of the B-cell activation antigen CD23. *Proc. Natl. Acad. Sci USA,* 84**,** 3452-3456.

WANG, G., MATSUURA, I., HE, D. & LIU, F. 2009. Transforming growth factor-β-inducible phosphorylation of Smad3. *J. Biol. Chem.,* 284**,** 9663-9673.

WANG, S. & FRAPPIER, L. 2009. Nucleosome assembly proteins bind to Epstein-Barr virus nuclear antigen 1 and affect its functions in DNA replication and transcriptional activation. *J. Virol.,* 83**,** 11704-11714.

WANG, X., XU, K., LING, M. T., WONG, Y. C., FENG, H. C., NICHOLLS, J. & TSAO, S. W. 2002. Evidence of increased Id-1 expression and its role in cell proliferation in nasopharyngeal carcinoma cells. *Mol. Carcinog.,* 35**,** 42-49.

WANG, Y., FINAN, J. E., MIDDELDORP, J. M. & HAYWARD, S. D. 1997. P32/TAP, a cellular protein that interacts with EBNA-1 of Epstein-Barr virus. *Virology,* 236**,** 18-29.

WARD, M. H., PAN, W.-H., CHENG, Y.-J., LI, F.-H., BRINTON, L. A., CHEN, C.-J., HSU, M.-M., CHEN, I.-H., LEVINE, P. H., YANG, C.-S. & HILDESHEIM, A. 2000. Dietary exposure to nitrite and nitrosamines and risk of nasopharyngeal carcinoma in Taiwan. *Int. J. Cancer,* 86**,** 603-609.

WATANABE, Y., ITOH, S., GOTO, T., OHNISHI, E., INAMITSU, M., ITOH, F., SATOH, K., WIERCINSKA, E., YANG, W., SHI, L., TANAKA, A., NAKANO, N., MOMMAAS, A. M., SHIBUYA, H., TEN DIJKE, P. & KATO, M. 2010. TMEPAI, a transmembrane TGF-β-inducible protein, sequesters Smad proteins from active participation in TGF-β signalling. *Mol. Cell,* 37**,** 123-134.

WEN, X.-Z., MIYAKE, S., AKIYAMA, Y. & YUASA, Y. 2004. BMP-2 modulates the proliferation and differentiation of normal and cancerous gastric cells. *Biochem. Biophys. Res. Comm.,* 316**,** 100-106.

WILLIAMS, T. M. & LISANTI, M. P. 2005. Caveolin-1 in oncogenic transformation, cancer, and metastasis. *Am. J. Physiol. Cell Physiol.,* 288**,** C494-C506.

WILSON, J. B., BELL, J. L. & LEVINE, A. J. 1996. Expression of Epstein-Barr virus nuclear antigen-1 induces B cell neoplasia in transgenic mice. *EMBO J.,* 15**,** 3117-3126.

WIPFF, P.-J. & HINZ, B. 2008. Integrins and the activation of latent transforming growth factor β1 - an intimate relationship. *Eur. J. Cell Biol.,* 87**,** 601-615.

WOISETSCHLÄGER, M., JIN, X. W., YANDAVA, C. N., FURMANSKI, L. A., STROMINGER, J. L. & SPECK, S. H. 1991. Role for the Epstein-Barr virus nuclear antigen 2 in viral promoter switching during initial stages of infection. *Proc. Natl. Acad. Sci USA,* 88**,** 3942-3946.

WOISETSCHLÄGER, M., STROMINGER, J. L. & SPECK, S. H. 1989. Mutually exclusive use of viral promoters in Epstein-Barr virus latently infected lymphocytes. *Proc. Natl. Acad. Sci USA,* 86**,** 6498-6502.

WOISETSCHLÄGER, M., YANDAVA, C. N., FURMANSKI, L. A., STROMINGER, J. L. & SPECK, S. H. 1990. Promoter switching in Epstein-Barr virus during the initial stages of infection of B lymphocytes. *Proc. Natl. Acad. Sci USA,* 87**,** 1725-1729.

WOOD, V. H. J., O'NEIL, J. D., WEI, W., STEWART, S. E., DAWSON, C. W. & YOUNG, L. S. 2007. Epstein-Barr virus-encoded EBNA1 regulates cellular gene transcription and modulates the STAT1 and TGFβ signalling pathways. *Oncogene,* 26**,** 4135-4147.

WOZNEY, J. M., ROSEN, V., CELESTE, A. J., MITSOCK, L. M., WHITTERS, M. J., KRIZ, R. W., HEWICK, R. M. & WANG, E. A. 1988. Novel regulators of bone formation: molecular clones and activities. *Science,* 242**,** 1528-1534.

WRANA, J. L., ATTISANO, L., CÁRCAMO, J., ZENTELLA, A., DOODY, J., LAIHO, M., WANG, X.-F. & MASSAGUÉ, J. 1992. TGFβ signals through a heteromeric protein kinase receptor complex. *Cell,* 71**,** 1003-1014.

WRANA, J. L., ATTISANO, L., WIESER, R., VENTURA, F. & MASSAGUÉ, J. 1994. Mechanism of activation of the TGF-β receptor. *Nature,* 370**,** 341-347.

WRIGHTON, K. H., LIN, X. & FENG, X.-H. 2009a. Phospho-control of TGF-β superfamily signalling. *Cell Res.,* 19**,** 8-20.

WRIGHTON, K. H., LIN, X., YU, P. B. & FENG, X.-H. 2009b. Transforming growth factor β can stimulate Smad1 phosphorylation independently of bone morphogenic protein receptors. *J. Biol. Chem.,* 284**,** 9755-9763.

WRIGHTON, K. H., WILLIS, D., LONG, J., LIU, F., LIN, X. & FENG, X.-H. 2006. Small C-terminal domain phosphatases dephosphorylate the regulatory linker regions of Smad2 and Smad3 to enhance transforming growth factor-β signalling. *J. Biol. Chem.,* 281**,** 38365-38375.

WU, H., CECCARELLI, D. F. J. & FRAPPIER, L. 2000. The DNA segregation mechanism of Epstein-Barr virus nuclear antigen 1. *EMBO Reports,* 1**,** 140-144.

WU, H., KAPOOR, P. & FRAPPIER, L. 2002. Separation of the DNA replication, segregation and transcriptional activation functions of Epstein-Barr virus nuclear antigen 1. *J. Virol.,* 76**,** 2480-2490.

WU, J.-B., FU, H.-Q., HUANG, L.-Z., LIU, A.-W. & ZHANG, J.-X. 2011. Effects of siRNA-targeting BMP-2 on the abilities of migration and invasion of human liver cancer SMMC7721 cells and its mechanism. *Cancer Gene Therapy,* 18**,** 20-25.

WU, Y., MARUO, S., YAJIMA, M., KANDA, T. & TAKADA, K. 2007. Epstein-Barr virus (EBV)-encoded RNA 2 (EBER2) but not EBER1 plays a critical role in EBV-induced B-cell growth transformation. *J. Virol.,* 81**,** 11236-11245.

XIAO, J., XIANG, Q., XIAO, Y.-C., SU, Z.-J., HUANG, Z.-F., ZHANG, Q.-H., TAN, Y., LI, X.-K. & HUANG, Y.-D. 2010. The effect of transforming growth factor-β1 on nasopharyngeal carcinoma cells: insensitive to cell growth but functional to TGF-β/Smad pathway. *J. Exp. Clin. Cancer Res.,* 29**,** 35.

XIN, H., XU, X., LI, L., NING, H., RONG, Y., SHANG, Y., WANG, Y., FU, X.-Y. & CHANG, Z. 2005. CHIP controls the sensitivity of transforming growth factor-β signalling by modulating the basal level of Smad3 through ubiquitin-mediated degradation. *J. Biol. Chem.,* 280**,** 20842-20850.

XU, J., AHMAD, A., JONES, J. F., DOLCETTI, R., VACCHER, E., PRASAD, U. & MENEZES, J. 2000. Elevated serum transforming growth factor β1 levels in Epstein-Barr virus-associated diseases and their correlation with virus-specific immunoglobulin A (IgA) and IgM. *J. Virol.,* 74**,** 2443-2446.

XU, J. & ATTISANO, L. 2000. Mutations in the tumour suppressors Smad2 and Smad4 inactivate transforming growth factor β signalling by targeting Smads to the ubiquitin-proteasome pathway. *Proc. Natl. Acad. Sci USA,* 97**,** 4820-4825.

XU, J., MENEZES, J., PRASAD, U. & AHMAD, A. 1999. Elevated serum levels of transforming growth factor β1 in Epstein-Barr virus-associated nasopharyngeal carcinoma patients. *Int. J. Cancer,* 84**,** 396-399.

XU, J. & ROGERS, M. B. 2007. Modulation of *bone morphogenetic protein (BMP) 2* gene expression by Sp1 transcription factors. *Gene,* 392**,** 221-229.

YAJIMA, M., KANDA, T. & TAKADA, K. 2005. Critical role of Epstein-Barr virus (EBV)-encoded RNA in efficient EBV-induced B-lymphocyte growth transformation. *J. Virol.,* 79**,** 4298-4307.

YAMADA, N., KATO, M., TEN DIJKE, P., YAMASHITA, H., SAMPATH, T. K., HELDIN, C.-H., MIYAZONO, K. & FUNA, K. 1996. Bone morphogenetic protein type IB receptor is progressively expressed in malignant glioma tumours. *Br. J. Cancer,* 73**,** 624-629.

YAMAGATA, H., MATSUZAKI, K., MORI, S., YOSHIDA, K., TAHASHI, Y., FURUKAWA, F., SEKIMOTO, G., WATANABE, T., UEMURA, Y., SAKAIDA, N., YOSHIOKA, K., KAMIYAMA, Y., SEKI, T. & OKAZAKI, K. 2005. Acceleration of Smad2 and Smad3 phosphorylation via c-Jun NH2-terminal kinase during human colorectal carcinogenesis. *Cancer Res.,* 65**,** 157-165.

YAMASHITA, H., TEN DIJKE, P., FRANZÉN, P., MIYAZONO, K. & HELDIN, C.-H. 1994. Formation of hetero-oligomeric complexes of type I and type II receptors for transforming growth factor-β. *J. Biol. Chem.,* 269**,** 20172-20178.

YAMASHITA, H., TEN DIJKE, P., HUYLEBROECK, D., SAMPATH, T. K., ANDRIES, M., SMITH, J. C., HELDIN, C.-H. & MIYAZONO, K. 1995. Osteogenic protein-1 binds to activin type II receptors and induces certain activin-like effects. *J. Cell Biol.,* 130**,** 217-226.

YAMASHITA, M., FATYOL, K., JIN, C., WANG, X., LIU, Z. & ZHANG, Y. E. 2008a. TRAF6 mediates Smad-independent activation of JNK and p38 by TGF-β. *Mol. Cell,* 31**,** 918-924.

YAMASHITA, S., TAKAHASHI, S., MCDONELL, N., WATANABE, N., NIWA, T., HOSOYA, K., TSUJINO, Y., SHIRAI, T. & USHIJIMA, T. 2008b. Methylation silencing of transforming growth factor-β receptor type II in rat prostate cancers. *Cancer Res.,* 68**,** 2112-2121.

YAMATO, K., HASHIMOTO, S., OKAHASHI, N., ISHISAKI, A., NONAKA, K., KOSEKI, T., KIZAKI, M., IKEDA, Y. & NISHIHARA, T. 2000. Dissociation of bone morphogenetic protein-mediated growth arrest and apoptosis of mouse B cells by HPV-16 E6/E7. *Exp. Cell Res.,* 257**,** 198-205.

YANG, B. & KUMAR, S. 2010. Nedd4 and Nedd4-2: closely related ubiquitin-protein ligases with distinct physiological functions. *Cell Death and Differentiation,* 17**,** 68-77.

YANG, S., WEI, D., WANG, D., PHIMPHILAI, M., KREBSBACH, P. H. & FRANCESCHI, R. T. 2003. In vitro and in vivo synergistic interactions between the Runx2/Cbfa1 transcription factor and bone morphogenetic protein-2 in stimulating osteoblast differentiation. *J. Bone Miner. Res.,* 18**,** 705-715.

YATES, J. L., CAMIOLO, S. M. & BASHAW, J. M. 2000. The minimal replicator of Epstein-Barr virus oriP. *J. Virol.,* 74**,** 4512-4522.

YATES, J. L., WARREN, N. & SUGDEN, B. 1985. Stable replication of plasmids derived from Epstein-Barr virus in various mammalian cells. *Nature,* 313**,** 812-815.

YIN, Q., WANG, X., FEWELL, C., CAMERON, J., ZHU, H., BADDOO, M., LIN, Z. & FLEMINGTON, E. K. 2010. MicroRNA miR-155 inhibits bone morphogenetic protein (BMP) signalling and BMP-mediated Epstein-Barr virus reactivation. *J. Virol.,* 84**,** 6318-6327.

YIN, Y., MANOURY, B. & FÅHRAEUS, R. 2003. Self-inhibition of synthesis and antigen presentation by Epstein-Barr virus-encoded EBNA1. *Science,* 301**,** 1371-1374.

YIP, W. K., ABDULLAH, M. A., YUSOFF, S. M. & SEOW, H. F. 2009. Increase in tumour-infiltrating lymphocytes with regulatory T cell immunophenotypes and reduced ζ-chain expression in nasopharyngeal carcinoma patients. *Clin. Exp. Immunol.,* 155**,** 412-422.

YOSHIOKA, M., CRUM, M. M. & SAMPLE, J. T. 2008. Autorepression of Epstein-Barr virus nuclear antigen 1 expression by inhibition of pre-mRNA processing. *J. Virol.,* 82**,** 1679-1687.

YOSHIZAKI, T., HORIKAWA, T., QING-CHUN, R., WAKISAKA, N., TAKESHITA, H., SHEEN, T.-S., LEE, S.-Y., SATO, H. & FURUKAWA, M. 2001. Induction of interleukin-8 by Epstein-Barr virus latent membrane protein-1 and its correlation to angiogenesis in nasopharyngeal carcinoma. *Clin. Cancer Res.,* 7**,** 1946-1951

YOUNG, L. S., DAWSON, C. W. & ELIOPOULOS, A. G. 2000. The expression and function of Epstein-Barr virus encoded latent genes. *J. Clin. Pathol. Mol. Pathol.,* 53**,** 238-247.

YOUNG, L. S., LAU, R., ROWE, M., NIEDOBITEK, G., PACKHAM, G., SHANAHAN, F., ROWE, D. T., GREENSPAN, D., GREENSPAN, J. S., RICKINSON, A. B. & FARRELL, P. J. 1991. Differentiation-associated expression of the Epstein-Barr virus BZLF1 transactivator protein in oral healthy leukoplakia. *J. Virol.,* 65**,** 2868-2874.

YOUNG, L. S. & MURRAY, P. G. 2003. Epstein-Barr virus and oncogenesis: from latent genes to tumours. *Oncogene,* 22**,** 5108-5121.

YOUNG, L. S. & RICKINSON, A. B. 2004. Epstein-Barr virus: 40 years on. *Nat. Rev. Cancer,* 4**,** 757-768.

YOUNG, L. S., YAO, Q. Y., ROONEY, C. M., SCULLEY, T. B., MOSS, D. J., RUPANI, H., LAUX, G., BORNKAMM, G. W. & RICKINSON, A. B. 1987. New type B isolates of Epstein-Barr virus from Burkitt's lymphoma and from normal individuals in endemic areas. *J. Gen. Virol.,* 68**,** 2853-2862.

YU, J., PAN, L., QIN, X., CHEN, H., XU, Y., CHEN, Y. & TANG, H. 2010a. MTMR4 attenuates transforming growth factor β (TGFβ) signalling by dephosphorylating R-Smads in endosomes. *J. Biol. Chem.,* 285**,** 8454-8462.

YU, M. C., HO, J. H. C., LAI, S.-H. & HENDERSON, B. E. 1986. Cantonese-style salted fish as a cause of nasopharyngeal carcinoma: report of a case-control study in Hong Kong. *Cancer Res.,* 46**,** 956-961.

YU, M. C., NICHOLS, P. W., ZOU, X.-N., ESTES, J. & HENDERSON, B. E. 1989. Induction of malignant nasal cavity tumours in Wistar rats fed Chinese salted fish. *Br. J. Cancer,* 60**,** 198-201.

YU, M. C. & YUAN, J.-M. 2002. Epidemiology of nasopharyngeal carcinoma. *Semin. Cancer Biol.,* 12**,** 421-429.

YU, N., KOZLOWSKI, J. M., PARK, I. I., CHEN, L., ZHANG, Q., XU, D., DOLL, J. A., CRAWFORD, S. E., BRENDLER, C. B. & LEE, C. 2010b. Overexpression of transforming growth factor β1 in malignant prostate cells is partly caused by a runaway of TGF-β1 auto-induction mediated through a defective recruitment of protein phosphatase 2A by TGF-β type I receptor. *Urology,* 76**,** 1519.e8-1519.e13.

YU, P. B., BEPPU, H., KAWAI, N., LI, E. & BLOCH, K. D. 2005. Bone morphogenetic protein (BMP) type II receptor deletion reveals BMP ligand-specific gain of signalling in pulmonary artery smooth muscle cells. *J. Biol. Chem.,* 280**,** 24443-24450.

YU, P. B., DENG, D. Y., LAI, C. S., HONG, C. C., CUNY, G. D., BOUXSEIN, M. L., HONG, D. W., MCMANUS, P. M., KATAGIRI, T., SACHIDANANDAN, C., KAMIYA, N., FUKUDA, T., MISHINA, Y., PETERSON, R. T. & BLOCH, K. D. 2008. BMP type I receptor inhibition reduces heterotypic ossification. *Nat. Med.,* 14**,** 1363-1369.

YU, W. M. & HUSSAIN, S. S. M. 2009. Incidence of nasopharyngeal carcinoma in Chinese immigrants, compared with Chinese in China and South East Asia: review. *J. Laryngol. Otol.,* 123**,** 1067-1074.

YUAN, J.-M., WANG, X.-L., XIANG, Y.-B., GAO, Y.-T., ROSS, R. K. & YU, M. C. 2000a. Non-dietary risk factors for nasopharyngeal carcinoma in Shanghai, China. *Int. J. Cancer,* 85**,** 364-369.

YUAN, J.-M., WANG, X.-L., XIANG, Y.-B., GAO, Y.-T., ROSS, R. K. & YU, M. C. 2000b. Preserved foods in relation to risk of nasopharyngeal carcinoma in Shanghai, China. *Int. J. Cancer,* 85**,** 358-363.

YUAN, X.-L., CHEN, L., ZHANG, T.-T., MA, Y.-H., ZHOU, Y.-L., ZHAO, Y., WANG, W.-W., DONG, P., YU, L., ZHANG, Y.-Y. & SHEN, L.-S. 2011. Gastric cancer cells induce human $CD4^{+}Foxp3^{+}$ regulatory T cells through the production of TGF-β1. *World J. Gastroenterol.,* 17**,** 2019-2027.

YUE, J. & MULDER, K. M. 2001. Transforming growth factor-β signal transduction in epithelial cells. *Pharmacology & Therapeutics,* 91**,** 1-34.

ZAWEL, L., LE DAI, J., BUCKHAULTS, P., ZHOU, S., KINZLER, K. W., VOGELSTEIN, B. & KERN, S. E. 1998. Human Smad3 and Smad4 are sequence-specific transcription activators. *Mol. Cell,* 1**,** 611-617.

ZETTERBERG, H., STENGLEIN, M., JANSSON, A., RICKSTEN, A. & RYMO, L. 1999. Relative levels of EBNA1 gene transcripts from the C/W, F and Q promoters in Epstein-Barr virus-transformed lymphoid cells in latent and lytic stages of infection. *J. Gen. Virol.,* 80**,** 457-465.

ZHANG, F. & LAIHO, M. 2003. On and off: proteasome and TGF-β signalling. *Exp. Cell Res.,* 291**,** 275-281.

ZHANG, J. & LI, L. 2005. BMP signalling and stem cell regulation. *Develop. Biol.,* 284**,** 1-11.

ZHANG, W., ZENG, Z., ZHOU, Y., XIONG, W., FAN, S., XIAO, L., HUANG, D., LI, Z., LI, D., WU, M., LI, X., SHEN, S., WANG, R., CAO, L., TANG, K. & LI, G. 2009. Identification of aberrant cell cycle regulation in Epstein-Barr virus-associated nasopharyngeal carcinoma by cDNA microarray and gene set enrichment analysis. *Acta Biochim. Biophys. Sin.,* 41**,** 414-428.

ZHANG, Y., CHANG, C., GEHLING, D. J., HEMMATI-BRIVANLOU, A. & DERYNCK, R. 2001. Regulation of Smad degradation and activity by Smurf2, an E3 ubiquitin ligase. *Proc. Natl. Acad. Sci USA,* 98**,** 974-979.

ZHANG, Y., FENG, X.-H., WU, R.-Y. & DERYNCK, R. 1996. Receptor-associated Mad homologues synergise as effectors of the TGF-β response. *Nature,* 383**,** 168-172.

ZHANG, Y. E. 2009. Non-Smad pathways in TGF-β signalling. *Cell Res.,* 19**,** 128-139.

ZHENG, Y. M., TUPPIN, P., HUBERT, A., JEANNEL, D., PAN, Y. J., ZENG, Y. & DE THÉ, G. 1994. Environmental and dietary risk factors for nasopharyngeal carcinoma: a case-control study in Zangwu County, Guangxi, China. *Br. J. Cancer,* 69**,** 508-514.

ZHU, J. Y., PFUHL, T., MOTSCH, N., BARTH, S., NICHOLLS, J., GRASSER, F. & MEISTER, G. 2009. Identification of novel Epstein-Barr virus microRNA genes from nasopharyngeal carcinomas. *J. Virol.,* 83**,** 3333-3341.

ZILBERBERG, L., TEN DIJKE, P., SAKAI, L. Y. & RIFKIN, D. B. 2007. A rapid and sensitive bioassay to measure bone morphogenetic protein activity. *BMC Cell Biology,* 8**,** 41.

ZIMBER-STROBL, U. & STROBL, L. J. 2001. EBNA2 and Notch signalling in Epstein-Barr virus mediated immortalisation of B lymphocytes. *Semin. Cancer Biol.,* 11**,** 423-434.

ZIMMERMAN, L. B., DE JESÚS-ESCOBAR, J. M. & HARLAND, R. M. 1996. The Spemann organiser signal noggin binds and inactivates bone morphogenetic protein 4. *Cell,* 86**,** 599-606.

ZOU, H., WIESER, R., MASSAGUÉ, J. & NISWANDER, L. 1997. Distinct roles of type I bone morphogenetic protein receptors in the formation and differentiation of cartilage. *Genes Dev.,* 11**,** 2191-2203.

ZUO, W. & CHEN, Y.-G. 2009. Specific activation of mitogen-activated protein kinase by transforming growth factor-β receptors in lipid rafts is required for epithelial cell plasticity. *Mol. Biol. Cell,* 20**,** 1020-1029.

ZUR HAUSEN, H. 2001. Viruses in human cancers. *Curr. Sci.,* 81**,** 523-527.

ZUR HAUSEN, H., SCHULTE-HOLTHAUSEN, H., KLEIN, G., HENLE, W., HENLE, G., CLIFFORD, P. & SANTESSON, L. 1970. EBV DNA in biopsies of Burkitt tumours and anaplastic carcinomas of the nasopharynx. *Nature,* 228**,** 1056-1058.

ZWAAGSTRA, J. C., COLLINS, C., LANGLOIS, M.-J. & O'CONNOR-MCCOURT, M. D. 2008. Analysis of the contribution of receptor subdomains to the cooperative binding and internalisation of transforming growth factor-β (TGF-β) type I and type II receptors. *Exp. Cell Res.,* 314**,** 2553-2568.